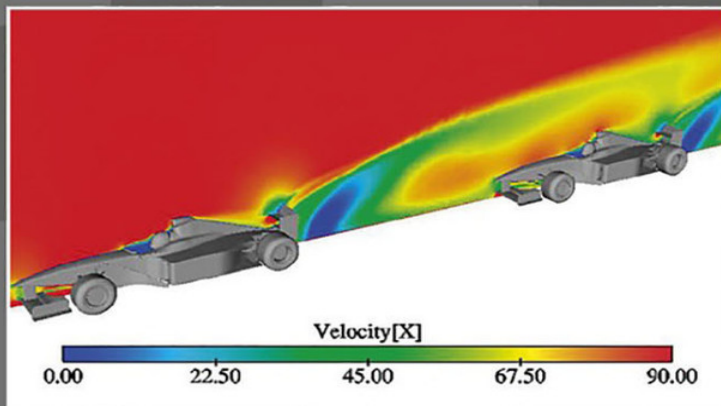


# COMPETITION CAR AERODYNAMICS



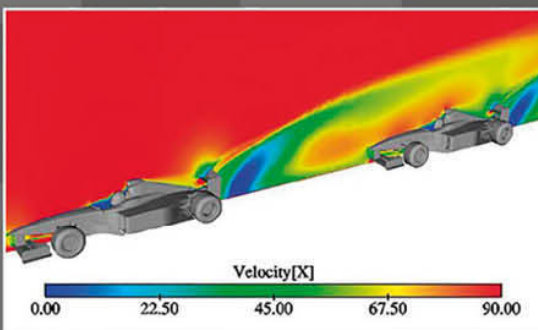
## A PRACTICAL HANDBOOK



Simon McBeath

**NEW! 3RD  
EDITION**

# COMPETITION CAR AERODYNAMICS



A PRACTICAL HANDBOOK



Simon McBeath

NEW! 3RD  
EDITION



First printed in hardback format in 2015.

First published in eBook format 2017 by Veloce Publishing Limited, Veloce House, Parkway Farm Business Park, Middle Farm Way, Poundbury, Dorchester, Dorset, DT1 3AR, England – Fax 01305 250479 – e-mail [info@veloce.co.uk](mailto:info@veloce.co.uk) – web [www.veloce.co.uk](http://www.veloce.co.uk) or [digital.veloce.co.uk](http://digital.veloce.co.uk).

eBook edition ISBN: 978-1-787110-86-1

Hardback edition ISBN: 978-1-845847-76-0

© Simon McBeath and Veloce Publishing 2017. All rights reserved. With the exception of quoting brief passages for the purpose of review, no part of this publication may be recorded, reproduced or transmitted by any means, including photocopying, without the written permission of Veloce Publishing Ltd. Throughout this book logos, model names and designations, etc, have been used for the purposes of identification, illustration and decoration. Such names are the property of the trademark holder as this is not an official publication.

Readers with ideas for automotive books, or books on other transport or related hobby subjects, are invited to write to the editorial director of Veloce Publishing at the above address.

All eBook design and code produced in-house by Veloce Publishing.

# Contents

## Preface & Acknowledgements

### Foreword by Willem Toet

## Chapter 1: Historical background

## Chapter 2: Out of thin air

## Chapter 3: Computational Fluid Dynamics (CFD)

## Chapter 4: Airdams, splitters and spoilers

## Chapter 5: Wings

## Chapter 6: Underbody aerodynamics

## Chapter 7: Miscellaneous devices

## Chapter 8: Removing (some of) the guesswork

## Chapter 9: A few case studies

## Chapter 10: Final thoughts

## Appendix 1: MIRA wind-tunnel test data

## Appendix 2: Some wing profile suggestions

## Appendix 3: Flow visualisation fluid

## Appendix 4: Commercially available full-scale wind tunnels

## Appendix 5: References

## Glossary of terms and abbreviations

## Further reading

# Preface & Acknowledgements

## Preface

My first effort on the topic of motorsport aerodynamics, *Competition Car Downforce*, was originally published in 1998. Then in late 2003, with help from Advantage CFD and under commission from *Racecar Engineering* magazine, I started writing a monthly column called ‘Aerobytes’. This not only provided some fascinating glimpses at the state of the art in computational fluid dynamics simulation but, at a more basic level, some incredibly useful graphical illustrations that explained how all the devices I had tried to explain in Downforce worked, and far better than I’d managed in mere words and sketches. Then during discussions, the idea of incorporating material from those ‘Aerobytes’ columns into a book was mooted (to my shame I forget exactly whose idea it was, bit if it wasn’t mine, thank you Rob Lewis, then at Advantage CFD, now at TotalSim Ltd, and Charles Armstrong-Wilson, then editor at *Racecar Engineering*). Anyway, it led to the publication of the first edition of Competition Car Aerodynamics.

In 2006 an arrangement between *Racecar Engineering* and MIRA came into being that saw ‘Aerobytes’ switch to being based on projects run in MIRA’s full-scale wind tunnel, an arrangement that is still going strong in late 2014. And it has provided rather different, more real world and practical but nonetheless invaluable knowledge on the aerodynamics of competition cars, albeit, like CFD, with its own peculiar shortcomings. One of the major reasons the second edition of this book came into being was to be able to make further good use of some of this material.

The ongoing arrangement at MIRA has produced regular new and fascinating projects, and some of the most interesting and more recent ones are brought together here in this new, third edition, along with additional CFD-based material, generated by the author using Ansys software, which adds further insights into why certain phenomena have the effects that they do.

As ever I’d like to apologise to academics about my random use of units throughout the book— you’ll find a mix of imperial and SI units, sometimes in the same equation, which will make you blanch. I hope it doesn’t spoil things too much.

## Acknowledgements

I need to thank a number of people who provided special help with this book, first and foremost the former staff of Advantage CFD (now defunct), in particular Philip Postle and the boss, Rob Lewis, now in charge at TotalSim. The assistance and guidance they provided was beyond the call of duty. I'm extremely grateful for that, as I am to Charles Armstrong-Wilson, former editor at *Racecar Engineering*, who enthused about Aerabytes from the start – his support to incorporate those columns, and subsequently MIRA wind-tunnel based material into the book was crucial. His successors, the late Graham Jones and Andrew Cotton, continued that enthusiastic support and my gratitude goes to them too.

A big thank you too to Willem Toet, professional Formula 1 aerodynamicist and fellow hillclimb enthusiast who has probably forgotten more than I'll know about this topic! For him to have taken the time to write the foreword was very gratifying, and I learn something from Willem every time I have the pleasure of talking with him.

Thanks to my late and much-missed friend Rob Barksfield, Graham Kendal (now retired), Dave Wain, Ivan Starkey, Ian Lindsay at MIRA, Angus Lock (formerly at MIRA), Rob Palin (formerly at MIRA and Williams F1, now at Tesla), James Key and Lucy Genon, formerly at Force India F1 Team, all at DJ Engineering Services, Wallace Menzies, Simon Farren at Reverie Ltd, Dr. Rob Dominy, Mick Kouros (previously at Fortec Motorsport, now at Team West Tec), Rupert Berrington Action Photography, Graeme Wight Junior, Martin Ogilvie, Dan Wasdahl, Kevin Mansell at Mansell Motorsport, Ian Dawson at Eco Racing, Paul Cundy, Adrian Winch, Richard Gould, Phil Brett, Alex Somerset, Franck Marie at Triple Eight Race Engineering, Borland Racing Developments, Mark Bailey Racing, Wiltshire College (Castle Combe), Alan Harding at AHS, Ben & Rob Willshire, Phil Jose and Mark Sumpter at Paragon Motorsport, Mike Topp and Mike Edmonds at MTECH Racing, Nick Reynolds and Barry Gates at RLR Motorsport, Steve Neal at Team Dynamics, Gavin Bennett, Russell Anderson, Phil Featherstone, Colin Paton, Roger Serrano, John Brooks plus Alan Mugglestone and Tim and Jacob Greaves at Greaves Motorsport, James Kmiecik, Mike Newton at Tiga Race Cars, Dave Beecroft at Orex Competition, Bjorn Arnils and Nadine Geary, Howard Ash and Gareth Williams at the University of Hertfordshire plus all the 2013 crew at the UH Racing Formula Student team, Kevin Robinson at the University of Bath plus Gemma Hatton, Dave Turton, Francisco Parga and all the crew on the 2014 Team Bath Racing Formula Student team, Mike Fuller at [www.mulsannescorner.com](http://www.mulsannescorner.com), Rennie Clayton at Dauntless Racing, Pepper

Bowe, Goodwood Festival of Speed, Castle Combe circuit, Thruxton circuit, Silverstone circuit, Gurston Down Hillclimb, Rockingham Motor Speedway, Santa Pod Raceway, Brands Hatch circuit, Donington Park circuit, and Sam Collins at *Racecar Engineering*.

I am also very much obliged for the support received from Ansys UK in the form of CFD-Flo, their latest ‘entry level’ CFD software, which has enabled me to produce yet more insightful material for this new edition.

And last but not least to my wife Tracey, who somehow puts up with my self-absorbed habits and provides much needed encouragement and support – ‘thank you’ just isn’t sufficient.

### **Publisher’s note**

Jurisdictions which have strict emissions control laws may consider any modifications to a vehicle to be an infringement of those laws. You are advised to check with the appropriate body or authority whether your proposed modification complies fully with the law. The author and publisher accept no liability in this regard.

While every effort is taken to ensure the accuracy of the information given in this book, no liability can be accepted by the author or publisher for any loss, damage or injury caused by misuse of, errors in, or omissions from the information given.

# Foreword

by Willem Toet

A PROFESSIONAL AERODYNAMICIST in Formula 1 for over 30 years, having run aero groups at Benetton, Ferrari, BAR Honda and (BMW) Sauber, Willem Toet is also an enthusiastic hillclimber in powerful open-wheeled single-seaters. He finished 4th in the 2004 British Hillclimb Championship and 2nd in 2005. Recently, he's become more directly involved in hillclimb car design (albeit just for fun!) with, for example, the Empire Wraith.

There are very few practical works on aerodynamics that are useful for road-car users wishing to make some small improvements and for club racers wanting to carve out some of that 'unfair advantage' we all want when we compete. A lifetime in F1 aerodynamics has taught me a lot, but, unless I'm forced to retire, I have no desire and no time to put it into a book and, even if I did, it probably wouldn't be of any use to those wishing to modify cars of a different type or run to different rules.

I've been giving advice on aerodynamics to club racers and in particular speed hillclimbers for many years, and while it's hard to beat having a professional giving you interactive advice on your specific problem, this book goes a long way to giving you the knowledge to tackle the first big steps towards achieving that 'unfair advantage'. Simon McBeath has taken advantage of some of our best development tools and put together a really useful practical explanation of how things work and how to get some important aspects of your car very close to an optimum, without needing the expense of models and wind-tunnel testing. One of the great aspects of the latest computational techniques is stunning visual imagery. Simon has taken full advantage of the latest methods to allow you to visualise airflow, as well as pressure and delta pressure plots.

Previous editions of this book already took readers to a reasonably high level of aerodynamic understanding using practical examples. This edition adds new data, both experimental and computational, which further enhances understanding. Simon has been given unprecedented access to some of the best tools and most experienced people in the business. This latest edition of

the book gives a revealing and visually clear insight into how some of the best racing cars have achieved the highest levels of aerodynamic efficiency.

I hope you enjoy and learn something new.

**Willem Toet**

# Chapter 1

## Historical Background

A COMPETITION CAR, like any vehicle, is a highly complex aerodynamic device. Unlike an aircraft in normal flight, a car is always in close proximity to the ground. This complicates the airflow around it, and makes understanding what's going on even more difficult. But aircraft and cars have one thing in common – in travelling through the air they both generate substantial forces. Both have to overcome aerodynamic drag, a force that opposes forward motion. An aircraft has to generate a lift force equivalent to its own weight in order to maintain level flight. A car however has no such prerequisite, and in fact it is greatly preferable that it stays on the ground so that its tyres can generate grip and provide tractive forces – that is, accelerative, braking and cornering.

This gives us our first clues as to how aerodynamic forces can influence vehicle performance. Drag opposes forward motion, and is a dominant factor in determining forward acceleration and deceleration at higher speeds, and maximum speed, but we'll look at this in more detail later. The earliest attempts at improving vehicle performance through considerations of aerodynamics involved trying to reduce drag by 'streamlining' vehicle shapes, and certainly speed records improved in no small part thanks to this approach. In conventional competition however, performance gains were made in the early years in all areas of vehicle dynamics, so it is difficult to pick out the level of influence brought to bear by reductions to vehicle drag when suspension, tyres, engines and so forth were all being improved.

However, the exploitation of aerodynamic lift forces can be seen to have had a sudden and dramatic effect on competition car performance. Aerodynamic lift, in the aeronautical sense of being directed upwards, lessens the tyres' grip and reduces the tractive forces that can be generated, again at higher speeds, and thus has a major influence on braking and cornering capabilities. Acceleration can also be affected, although because accelerative traction is at a premium in lower gears (especially with more powerful cars),

and aerodynamic forces are greater at higher speeds, acceleration is affected less by aerodynamic lift than are braking and cornering.

The opposite of aerodynamic lift, occasionally referred to as ‘negative lift’, or much more commonly as ‘downforce’, clearly adds to the tyres’ grip and, hence, a car’s ability to generate tractive forces. Now, this *can* be seen to have caused a rapid increase in lap speeds around the late 1960s, and again in the late 1970s, as two distinct methods of generating downforce were first exploited. There were also major developments in competition tyre technology during the 1960s too, which further contributed to performance hikes, and to this day the development of these two influential factors, aerodynamics and tyres, have gone hand in hand.

However, there is perhaps no other single aspect of competition car technology that has had such a big an influence on performance as the exploitation of downforce. In all the world’s current major single-seater championships, aerodynamic downforce is the most important single element in the performance of the cars. In sports prototype and GT cars, and saloon cars too, downforce has a large part to play. In rallying, drag racing, sprinting and hillclimbing, oval racing and a myriad of motorsport categories around the world, downforce is a crucial element in performance.

Downforce has become so significant that in most leading formulas, the governing bodies have seen fit to regularly review the regulations concerning downforce-inducing devices in an effort to try to keep things in check. In some cases this has involved drastic, sometimes almost panicky, changes to rules as lap times have tumbled to the extent that things seemed to be getting unsafe – cars were hurtling around corners at unimaginable speeds, producing driver-battering sideways forces. Braking distances were being cut to tens of metres where previously, hundreds of metres were required. In other categories, more regular reviews, in consultation with the racecar constructors and designers, has produced a more measured, on-going response to the problem. Other things being equal, this has helped to stabilise lap times in these categories, more or less.

Downforce plays such a large part in performance that devices to create it are expressly forbidden in some of the junior training formulae, like Formula Ford for example. The more senior training formulae permit only limited, and strictly controlled downforce creation so that drivers may learn in a gradual way how to handle it, how to exploit it, and how to ‘tune’ it to best advantage, before progressing to the top level where it is so crucial.

The use and knowledge of downforce has come a long way in half a century. The first known attempt to run an aerofoil on a racing car is generally believed

to have been made by a Swiss engineer, Michael May, on a Porsche Spyder as long ago as 1956. The car had an aerofoil mounted above the cockpit, acting through the centre of gravity of the car, which tilted from  $-3^\circ$  (at which angle the wing was nose-up) to  $+17^\circ$  (when the wing was distinctly nose-down). The scrutineers at both the Nürburgring and Monza, where he was hoping to compete, wouldn't permit its use, and it seems that he never actually raced with it.

During the early 1960s, designers and engineers made further attempts at gaining an advantage from aerodynamics, other than by reducing the drag. Drag reduction enabled faster top speeds to be achieved from a car with unchanged horsepower, but although this would improve the speed on the straights, it was only going to produce faster lap speeds if cornering speeds could be maintained or improved as well. In the special case of prototype sports cars for example, making a lower, more streamlined car may well have produced aerodynamic lift.

It would be difficult to tell if this was the case, because other areas of improved performance, such as suspension and tyre development, would contribute to higher cornering speeds, thus masking, or at least reducing the effect on lap time of any disadvantage caused by lift. The drivers would surely have noticed a loss of grip or steering feel at high speed, but there are documented cases of former aeronautical aerodynamicists insisting that the only parameter that mattered was low drag. But these cars had the biggest plan areas of all competition cars, and at places like Le Mans, top speeds were faster than in other competition categories. As we shall see in the next chapter, these two parameters, plan area and speed, are both related to the production of aerodynamic lift (and downforce...). As such, the problem was probably of greater significance to sports cars than any other category at the time. Thus, it was most likely in sports car racing that the first real attempts to lessen the problem of aerodynamic lift were made, with the fitting of 'spoilers' that disturbed the smooth, lift inducing flow over the large upper surface of these cars.



*Sports cars like the Ferrari 330 P3/4 were among the first to use 'spoilers'.*



*The Chaparral 2F – similar to the first 'winged racer', the 2E.*

Racers have continually and habitually experimented with ideas that seem to produce benefits to performance, and it wasn't long before spoilers started appearing on sports cars and saloon cars the world over. It was found that even though straightline speeds were coming *down*, through increases in drag, so too lap times were reducing. The inescapable conclusion was that cornering

speeds were actually increasing to the extent that overall lap speed was increasing, and this could only be happening because grip had increased between the tyres and the road. This meant that not only was lift being reduced, but that real *downforce* was starting to be generated.

Then a particularly innovative racer/engineer remembered again (everybody presumably had forgotten about – or had never heard of – May’s earlier experiments), that wings keep aeroplanes in the air by creating a lifting force at least as great as the weight of the plane. If that was the case, why couldn’t racers bolt wings onto their cars *upside down*, and create a force that pushed the cars more firmly onto the road to increase the available grip still further? That racer was American Jim Hall, whose Chaparral 2E CanAm racecar appeared with a wing at Bridgehampton, New York State in 1966, and it is Hall who is universally credited with being the first to actually race a car with aerofoils fitted.

It was the start of a revolution in racecar performance. Almost immediately, Formula 1 took up the idea, and simple aluminium fabrications mounted on struts little bigger than flamingo legs appeared like a rash. Regrettably, it would appear insufficient thought was put into the design of some installations, because a spate of accidents caused by structural failures of wings and wing supports led to the then current ruling body of F1, the CSI, to attempt to ban wings altogether. But after some rethinking and rapid talking by the constructors, some new rules were drawn up by the CSI, and wings were back, in modified and restricted form. Very soon they were in universal use on all Grand Prix cars, and it wasn’t long before they began to pervade in other formulas too. The 1970s saw gradual development and refinement of wings in single-seater and sports car categories, and saloon racers were doing their bit too. In Europe, the famous Group 2 saloons were sprouting more than mere spoilers, with ‘airdams’ and ‘splitters’ at the front end of the cars, and genuine aerofoil section wings at the rear.

The next mental leap that produced possibly the biggest performance advance of all came in the late-1970s, when another clever engineer, Peter Wright, working for Colin Chapman at Lotus Grand Prix (with Chapman’s encouragement) successfully introduced the concept of ‘ground effect’ into Formula 1 with the Lotus Type 78. The general concept however wasn’t new. A patent taken out in the 1930s described how a symmetrical wing created downforce when in proximity to the ground, and the designer of Sir Malcolm Campbell’s speed record vehicles found some downforce from the underbody too. Then Jim Hall showed what could be done with a car that created low pressure over its entire underside, with his Chaparral 2J in 1970. The effect

was to suck the car down onto the road really firmly, and Hall did it by using large fans powered by auxiliary motors to remove air from the underside, while ‘skirts’ (a term which became infamous in the late-1970s and early ’80s) did their best to seal the underside from the outside, and allow the creation of the low-pressure area below the car.



*The Chaparral 2J ‘sucker car’.*

In Formula 1 however, ‘aerodynamic devices’ were forbidden from moving relative to the car (a result of earlier frowned-upon attempts at making wings change their angles of incidence, from steep on the slow bits of circuits to shallow on the fast bits). This rendered the fan concept illegal, but there was an attempt at circumventing this rule in 1978 by the Brabham ‘fan car’, when the fan’s primary purpose was said by designer Gordon Murray, to be ‘engine cooling’, which enabled the car to win one race before it was then banned.

So Wright and Chapman’s great step forward was realising that it was possible to create substantial suction beneath the car by using only the car’s forward speed through the air, and the clever shaping of its underside. In crude terms, the whole centre structure of the car became an inverted wing which generated low pressure over a very large area. This enabled the production of hitherto unknown levels of downforce, and correspondingly greater cornering forces. The resultant increase in cornering speeds, and reduction in braking distances (and in some cases, the removal of the *need* for braking), saw rival designers begin to take the ‘wing car’ concept very seriously. It has to be said though, that the first ground-effect design, on the Lotus 78 car, was relatively inefficient. The following year’s Lotus 79 however, was a beautiful and highly effective refinement that enabled Mario Andretti to

dominate the 1978 Formula 1 World Championship, and Lotus to take the Constructors' title.



*The beautiful and highly effective Lotus 79.*



*Large plan areas help produce tons of downforce on Group C sports cars.*

The other teams played catch-up very rapidly indeed, and it wasn't long before Lotus were being beaten at their own game, so to speak, with Williams perhaps producing the most elegant ground-effect car of all in the FW07 series. The ground effect principle proceeded to pervade formulas all over the

world wherever downforce was permitted, and a number of other classic designs were born during this era, such as the ubiquitous Ralt RT2/3/4 series, which was so successful in Formulas 2, 3 and Atlantic/Pacific the world over. Sports cars exploited the principle too, and benefited from their huge plan areas to produce literally tons of downforce.

But then the ruling body produced one of its famous ‘rapid reactions’, and all of a sudden ground effect was banned in Formula 1 with the introduction of a mandatory ‘flat bottom’ between the front and rear axle lines. The axe fell on other categories somewhat later, but fall it did.

In Europe, Formula 1, Formula 3000 (the replacement for Formula 2 in the early 1980s and supplanted itself in 2005 by GP2) and Formula 3 had to pursue other means of regaining the downforce taken away by the changes in technical regulations. Formula 1 cars began a less than elegant looking development route involving extra ‘winglets’ attached to the outer, forward-most parts of the rear wings. It was around this period that some of Grand Prix racing’s most powerful engines were being used, during the so called ‘turbo era’, and every bit of downforce that could be won at the rear of the car was needed to assist in putting prodigious quantities of power onto the road. Drag became almost an irrelevance with four-figure brake horsepower levels being generated by turbocharged 1.5-litre engines. The less powerful single-seater categories had to rely on striking a balance between downforce and drag, with wing designs not as outrageous as in Formula 1. Sports cars continued for the time being along the ground effect route, exploiting the relative freedom that their rules permitted as well as the huge plan form area available to them for downforce generation.

Formula 1 returned to normally aspirated engines of 3.5 litres capacity in 1989, with a reduction to more modest power levels. The question of downforce versus drag had to be considered anew, and designers started looking at the underside of the car again as a potential downforce-inducer. It was realised that with a small ground clearance, and the right amount of nose-down attitude, a crude form of wing section could be created beneath the cars in spite of the flat bottom, and we were back to ground effect. It proved vital to allow the air from the underside to escape as efficiently as possible at the rear of the cars, and ‘diffusers’ came into being to do just that. A whole new aspect to downforce production had been discovered, and refinements continually appeared over the following few years.

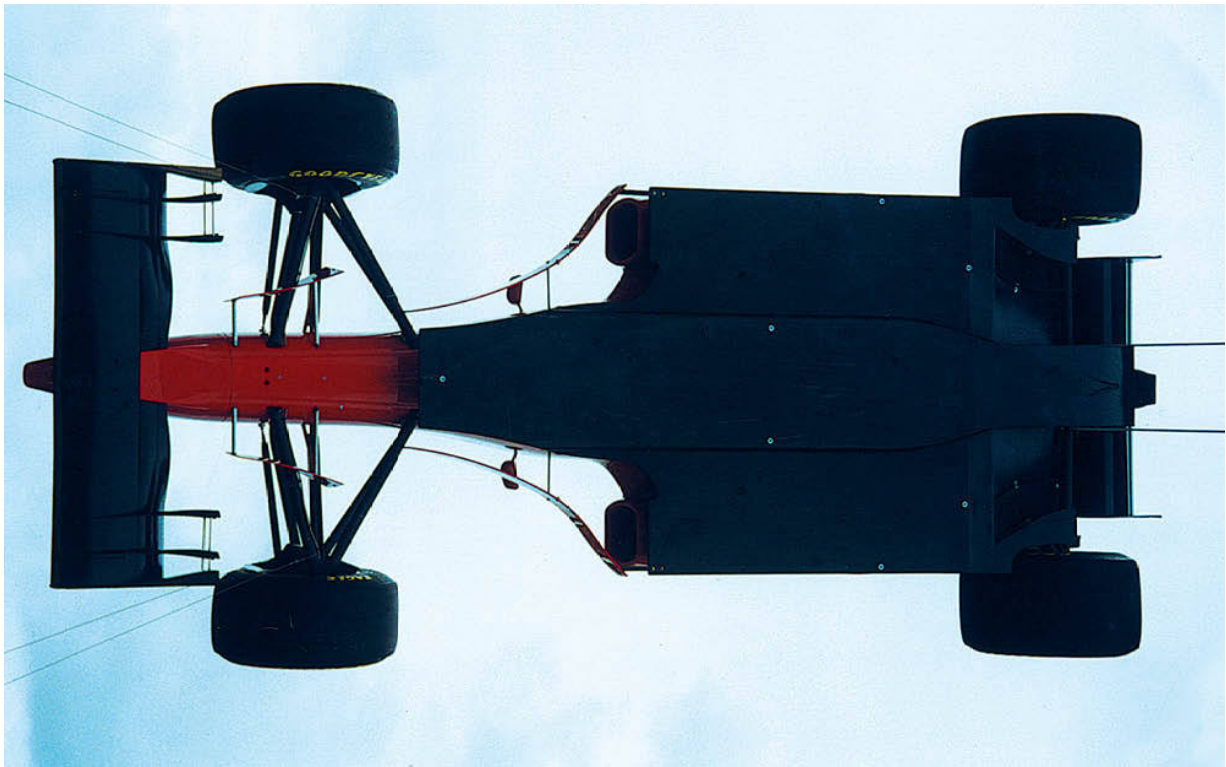
Formula 3000 and Formula 3 followed this route too, producing a generation of cars with incredibly low ground clearance and high spring stiffnesses to maintain as constant a car-to-ground gap as possible. Formula 1

went one better in this area of control, and produced so called ‘active suspension’ systems, which offered the ability to control the cars’ attitude as well as their ground clearance far better than a conventional mechanically sprung vehicle. The prime reason for doing this was quite clearly an aerodynamic one, rather than for any possible handling benefits, so in truth, active suspension was illegal – the cars were now themselves movable aerodynamic devices, with controls built in specifically to move things around for aerodynamic reasons. Presumably, the powers that be couldn’t separate this aspect from the fact that a car has to move, and as it does so it then becomes a movable aerodynamic device!

Other categories around the world wouldn’t allow the use of active suspension systems, and ultimately it was banned in Formula 1 as well, but development of the underside and diffusers continued. Wings too came in for more attention, and more complex shapes began to appear as designers started thinking in three dimensions, with ‘airflow management’ becoming a trendy phrase. Other attachments were bolted on which were all about gaining critical percentages of extra downforce, hopefully with little or no extra drag penalty.

Then, after that disastrous weekend at Imola in 1994, when Roland Ratzenburger and Ayrton Senna lost their lives in separate accidents, the FIA, the governing body of motorsport, produced some rapidly imposed rule changes which had the effect of reducing downforce in Formula 1 quite significantly. Some rule changes were immediate, and removed, perhaps, a few per cent of downforce. But a rule brought in for 1995, which was also applied in Formula 3000 and Formula 3, saw a large increase in the minimum permitted ground clearance over a large proportion of the underbody; the so-called ‘stepped floor’ was in. This produced a substantial reduction in downforce levels (maybe by as much as 40 per cent), and also lessened the cars’ sensitivity to their attitude relative to the ground, making them more predictable, safer and probably more enjoyable to drive.

Throughout this period of turmoil in the European administered formulas, the rule makers of IndyCar racing had been undertaking regular reviews of their technical regulations in the light of performance gains from the cars, and imposing almost annual rule changes. This approach seemed to ensure that really drastic changes were never actually necessary – the rule makers just chipped away at what was allowed in order to keep performance in check. Naturally, the designers and aerodynamicists always did their utmost to win back at least as much as was lost.



*Since 1995, Formula 1 cars have been obliged to run 'stepped underbodies' as on this 1996 Ferrari F310.*



*Prototypes are back in favour at Le Mans and in the related series in Europe and North America. (Lawrence Butcher)*

Sports cars meanwhile underwent a total change, and sports prototype cars were replaced, temporarily at least, with what were essentially road-going GT cars. Downforce inducing devices were permitted, including splitters, wings and profiled undersides, but in emasculated form compared with the technology permitted by the previous rules. However, after various metamorphoses, the prototypes came back again in several categories such as at Le Mans itself, the American Le Mans Series (ALMS) and the Europe-based Le Mans Series (LMS). Meanwhile, GTs continued on the international stage, running with the prototypes at their events and also in the various FIA GT Championships as well as in numerous national series.

Saloon car racing underwent changes during this period too, and in essence now at top level we have mildly modified ‘showroom’ specifications in a number of national categories as well as the World Touring Car Championship (WTCC) and the wilder, wackier machines in the German-based DTM series and the Australian V8 Supercar Championship. Meanwhile, good ol’ NASCAR stock car racing continued on its commercially highly successful but technologically pretty basic path. However, because of the speeds involved this category is an aerodynamically interesting area to study. NASCAR even flirted briefly with rear wings instead of the traditional rear spoilers following the introduction of the so-called ‘Car of Tomorrow’ in 2007, which featured a rear aerofoil instead of the long-serving spoiler. But a return to a large spoiler was made in 2010, seemingly at least in part because the teams and fans didn’t like the appearance of the wing!

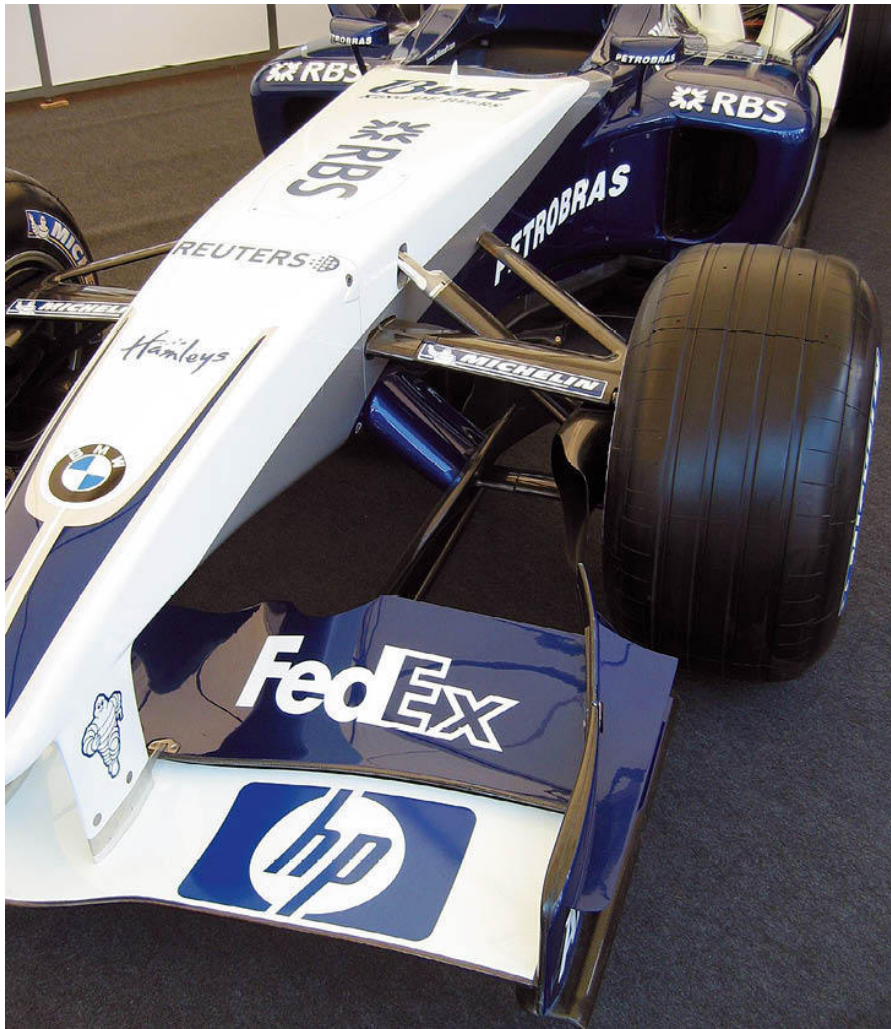
Throughout the whole of the period described briefly here, some formulas have come and gone, some have remained unchanged, others have adapted to rule changes and trends. But wherever its exploitation has been allowed, downforce has had a dominant influence on racecar performance. There are of course other important contributors to continually improving racecar performance, and these obviously include the tyres – the four little contact patches between the tyres and the ground ultimately defining and limiting how much grip a car can generate. In the case of racing categories where significant downforce is permitted, tyres have developed in response to the gains that the aerodynamicists have found.

It is interesting that the perpetual struggle of race car designers to make cars go faster is sometimes seen to be at odds with what might be said to be the main purposes of motor sport – to provide racing and entertainment for participants and spectators. Indeed, downforce itself is seen by some to be the main cause of the perceived lack of overtaking in many racing categories. (Is there less overtaking now than there used to be? I don’t know, but it sure

seems like summers used to be sunnier than they are now...) Drivers are often heard to complain that as soon as they attempt to get close behind another car in a corner, so as to slipstream past on the ensuing straight, their own car loses so much downforce at the front that significant grip is lost, and they cannot sustain the passing attempt. Further, the finger is pointed at downforce for reducing braking distances to mere tens of yards, which, it is said, also makes overtaking with the so-called 'out-braking manoeuvre' very difficult to carry out.



*Touring Cars were allowed limited downforce generation with wings and splitters in 2005.  
(Vauxhall)*



*Where would all the sponsors' names go if wings were banned. (Rob Barksfield)*

Undeniably these interactions between cars exist, as we shall see in a couple of fascinating studies later in the book, but whether they are the primary causes of this apparent difficulty to overtake is a moot point. Other factors such as track design, car dimensions, so-called 'driver aids' and even 'unsporting driver mentality' must all be to blame in some part as well. However, during 1996, the FIA commissioned studies into the aerodynamics of cars following each other closely, in an apparent attempt to find a general configuration that would enable close running and overtaking to occur.

Interestingly, the emphasis of these studies switched for a while from aerodynamics to tyres. It seemed that the studies indicated that if total downforce was reduced, far from making it easier for cars to follow each other, things actually got worse, and the adverse effect on the following car was, relatively speaking, greater in this guise. Other computer-based

simulations have come to the same conclusion. Ultimately, the FIA decided to introduce ‘treaded’ tyres in Formula 1 in 1998, in the hope that reducing the amount of rubber in contact with the road would reduce grip, and hence also, cornering speeds, with a commensurate increase in braking distances. At the same time, the cars were made 200mm (8in) narrower too, which effectively reduced the car’s ability to generate downforce in the underbody regions because of greater adverse interaction with the wheels. The change also simultaneously reduced frontal areas which, the theory went, should have increased straightline speeds. History now shows that performance was only temporarily held back, and certainly the status quo among the teams went largely unaffected. Subsequently, other measures to peg back downforce levels were introduced, even though this may not have been the logical or best method of slowing the cars and/or improving their ability to race with each other.

It is to be hoped that not too much technical freedom is taken away by the imposition of further rules banning wings, and other downforce inducing devices, as some observers seem to want. The science (and art) of producing aerodynamic downforce is far too fascinating to allow that to happen! And where would all those sponsors’ names go? But notwithstanding those slightly facetious arguments, there is also a legitimate case that can be put on safety reasons for the retention of downforce as an aid to keeping cars firmly planted on the ground. There are, mercifully, very few cases of competition cars in any category doing ‘back flips’ these days except in the most extreme and freakish of circumstances, so a unilateral ban on wings or other downforce generators has the potential to be most unsafe.

Indeed, following the much publicised flips that befell all three Mercedes CLK entries in the 1999 Le Mans 24 Hours, and a subsequent fatal testing accident that took the life of Michele Alboreto while preparing for the 2001 race with Audi, the FIA commissioned work to see what safety improvements could be made that lessened the likelihood of cars taking off at speed. The fact is that in a situation where a car such as this goes nose-up to the extent that it creates upward lift, the speeds and the large plan areas involved can create very large upward lift forces rather than large amounts of downforce. For example, Alboreto’s accident seemingly occurred following a rear tyre failure at speed, and the car started to spin. While partly broadside to its direction of travel, and with the trailing rear corner of the car lower than normal because of the tyre failure, this lifted the nose up higher than normal, and the car took off.

These occurrences saw the FIA commission a programme of work to identify where improvements could be made, and a range of measures was

introduced into the regulations for the 2004 race which reduced the risks of taking off in a variety of envisaged situations. Furthermore, the changes did not require totally new cars, only appropriate modifications that could be cost-effectively manufactured by the teams involved. The underlying and crucial point here is that the forces generated by the interaction of competition cars with the air they travel through are substantial, and any changes made to the regulations that could potentially affect those interactions needs to be very carefully considered if safety is not to be compromised.

Meanwhile in Formula 1 the FIA set up a new group, known as the ‘Overtaking Working Group’ (OWG), in 2007 to study why it had become increasingly difficult for F1 cars to run closely together, something that was demonstrably reducing the opportunities for overtaking to occur. The OWG comprised McLaren-Mercedes engineering director Paddy Lowe, Renault F1’s then director of engineering Pat Symonds, and was headed by Ferrari consultant Rory Byrne, assisted by renowned F1 aerodynamicist Jean-Claude Migeot. The brief was to define a technical concept that allowed more overtaking. Initial discussions defined objectives, which centred on increasing mechanical grip and reducing the role of aerodynamics, and we ended up with a new set of rules for 2009 that produced radically different-looking F1 cars that did, initially at least, have less downforce than the previous generation. The measures may have helped the cars run closely together without the car in front upsetting the stability and balance of the car behind, though whether this made any tangible contribution to the racing is debatable. But the process of involving the constructors in the necessary research to help improve ‘The Show’ at least helped avoid actually making things worse, so it has to be better than the way changes were implemented in previous years. That at least was a positive step forward.

In 2011, the Drag Reduction System (DRS) rear wing was introduced in Formula 1, which saw the nose of the second or flap element of the rear wing raised, under specified and controlled circumstances, to reduce drag, and give a following car a straight line speed advantage to facilitate overtaking manoeuvres. At least the idea was to make it easier, although in practice it seemed to provide a cast iron guarantee that a pass could be made, so perhaps the benefit was too great. However, the principle, whereby technical regulations allow moveable aerodynamic devices, was seized upon by more adventurous teams looking for lap time benefit. Clearly, from an engineering standpoint, there needed to be a failsafe mode which prevented the system from failing in the low drag, low downforce position. This was mandatory in Formula 1 and other FIA-regulated categories where DRS was used, yet even

with the high standards of engineering in F1, failures occurred which locked the wing in the low drag mode – potentially a very dangerous situation.

Meanwhile, LMP regulations underwent further modifications in ongoing efforts to reduce the risks of ‘flip overs’ with apertures in wheel arches (to reduce potential lift forces when a car got sideways) and engine cover fins (to add straight line stability and again to reduce lift when a car got sideways) among the measures mandated. These and other measures demonstrated an increasing need, and an increasing willingness on the part of the regulators, to remain involved in controlling aerodynamics to help maintain and improve levels of safety.

One of the most interesting advances in aerodynamics over the past 20 years or so has been the advent of computer modelling, and specifically computational fluid dynamics, abbreviated henceforth to CFD. The technique has only come into use in motorsport over about the last dozen or so years, but thanks to developments in computer hardware and CFD software it is available to many more people within motorsport, amateur and professional alike, either directly or from professional service providers. The technique enables simulations of fluid flow, airflow generally in our case, to be made around solid shapes using mathematical equations that are very rapidly solved by the software. There is no need here to go into the maths. We’ll even gloss over that side of it in the special chapter devoted to it later – after all, you don’t need to know how to make a spanner to undo a nut. But what the technology does provide us with is an amazing way of measuring and, more particularly here, visualising exactly what’s going on in the airflow around a competition car. For example, changes in flow velocity (including direction) and pressures around and on a competition car can be modelled and displayed; nuances of flow and pressure around detailed parts like wheels, wings and spoilers can be studied and the effect of changes to car configuration can be calculated. Also, it has given to this book the ability to illustrate – in ways that were not previously possible – how many of the devices that have been used in motorsport for years actually work! The power of this new tool is tremendous, and to say that its use is illuminating is to massively underestimate its benefits to our understanding.

So the rest of this book will look at the theory behind the generation of aerodynamic forces, and practical ways in which we can try to gain performance benefit from them. CFD will be used extensively to illustrate the aerodynamic effects involved. And data from competition cars tested in a full-scale wind tunnel will provide a real, practical appreciation of the effects of modifications and adjustments.

## Chapter 2

# Out of thin air

AERODYNAMIC THEORY IS based upon the basic laws of motion. There is nothing magical involved, but there are a great many facets to it, especially when dealing with competition cars. As an everyday example of the magnitude of the forces involved, a machine as vast and heavy as an airliner actually lifts off the ground solely because of its wings interacting with the thin air through which the plane moves. It seems equally incredible that, as is so often quoted, a current Formula 1 car can generate sufficient negative lift, or downforce as we prefer to call it, that it could drive across the ceiling of a large room, its own downforce holding it there (assuming the rule makers haven't radically cut back on downforce by the time you read this). Of course, it would need to be a pretty big room to allow for sufficient speed, and we'll gloss over just how it would get up there in the first place. However, the principle is valid even if the practicalities have to remain a little vague. So how is it that such large forces can be created out of thin air?

### **May the force be with you**

Intuitively we have a natural feeling for some aerodynamic forces. If we are travelling along in a car, and we stick an arm out of an open window, we can feel the quite substantial force exerted by the air impacting on the arm. If the palm of the hand is opened and tilted one way and then the other, we can feel upward and downward forces as well as the force that tries to drag the arm horizontally backwards.

These are of course, only the obvious manifestations of the forces involved. There are subtler, yet highly significant effects involved, which create forces that are at an angle to the airflow, rather than in the direction of the airflow. My school physics teacher demonstrated the following experiment, which graphically illustrates lift being created by air flowing over a surface. Take hold of an A4 or letter-sized piece of writing paper by the corners along one of the shorter edges, between the fingers and thumbs of each hand. Now hold the piece of paper up to just below your mouth, touching your lower lip, so that

the edge near to your mouth is horizontal, and the flexibility of the paper allows it to hang downwards from your fingers. Blow horizontally, across the top surface of the piece of paper; do you see what happens? The piece of paper bends upwards towards the stream of air blowing out of your mouth. Clearly, a force is being exerted on the piece of paper, causing it to flex upwards against the pull of gravity. It is the airflow that is causing this lifting force, yet the force is acting at right angles to the airflow. This is a manifestation of the ‘Coanda Effect’ which, though not the source of lift on wings, is nevertheless an example of how air flowing over a curved surface can generate forces.

### The sources of the forces

So, the two aerodynamic forces that we are perhaps most concerned about here are *drag* and *lift*, and as was stated at the beginning of this chapter, the study of aerodynamics is founded in the laws of motion. Perhaps it will be of benefit to briefly recap these fundamentals of physics. We’re all deeply indebted to Sir Isaac Newton (1643–1727) for defining his three laws of motion that, rather startlingly, describe how all manner of objects with appreciable mass, from grains of sand to planets and solar systems, behave when acted upon by forces, be they gravitational or otherwise caused. Competition cars fall somewhere in between these extremes and their dynamics and aerodynamics can be explained by consideration of Newton’s Laws of Motion, which are paraphrased below. It may not at first be obvious how aerodynamics can be explained by all this, but bear with it – air has mass and as such aerodynamic forces can be explained by these principles.

Newton’s First Law states that bodies or objects remain at rest, or continue moving in a straight line at unchanged velocity (that is, the same speed *and* direction), unless some other force acts upon them. Or if you like, a steady state will prevail unless something comes along to disturb it. Put the other way around, if you want to set a stationary body moving, or change its speed or its direction if it is already moving, then you have to exert a force upon it.

Newton’s Second Law says that the force required to achieve a given level of acceleration is directly proportional to the mass of the body that you want to accelerate. So, a heavy (strictly, ‘more massive’) competition car requires a greater force to accelerate it, or slow it, or corner it than a light (less massive) car. Greater mass creates greater ‘reluctance’ to a change in speed or direction, and this property is known as ‘inertia’. Inertia is the same as ‘mass’. So from Laws One and Two we now know that any change of a body’s speed or

direction requires a force to make it happen, and the force required depends on the body's mass.

Newton's Third Law says that for every action (or force) there is an equal and opposite reaction (force). What does this mean? Take the simple example of a car at rest. Gravity pulls the mass of the car onto the road, and as a result the road feels the car's weight acting upon it. The car's weight is equalled and opposed by the reaction from the ground. Another simple example is of a car travelling along at constant speed. The opposing forces of friction and air resistance (drag) exactly match the horizontal force exerted by the car's driven tyres to propel it along.

### **Resolving forces and reactions**

A force can be represented in diagrammatic form by a 'vector', which is an arrow that points in the direction the force acts, and whose length is proportional to the magnitude of the force. Figure 2-1 illustrates the balanced actions and reactions with a car travelling along at steady speed. The equal length vectors represent equal and opposed actions and reactions, and in this situation the car remains in a steady state. However, if that situation is altered, say with a reduction in the car's drag for example, then the tractive force needed to maintain that same steady speed is reduced, or conversely if the same tractive force were exerted then the car would be able to travel faster than it did before the reduction in drag (Figure 2-2). By the same token, if the car exhibited aerodynamic lift (and many do, as we shall see later) then this would reduce the effective weight felt by the tyres on the road surface, which would reduce the amount of available grip, as shown in Figure 2-3, and, vice-versa, if aerodynamic lift can be reduced or reversed then grip would be increased.

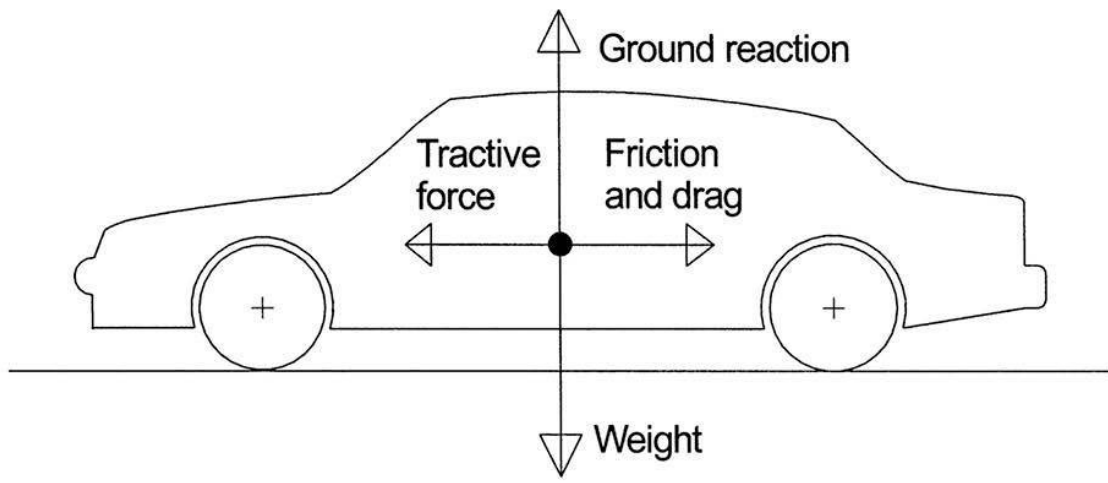


**Figure 2-1** Balanced actions and reactions, steady state prevails.

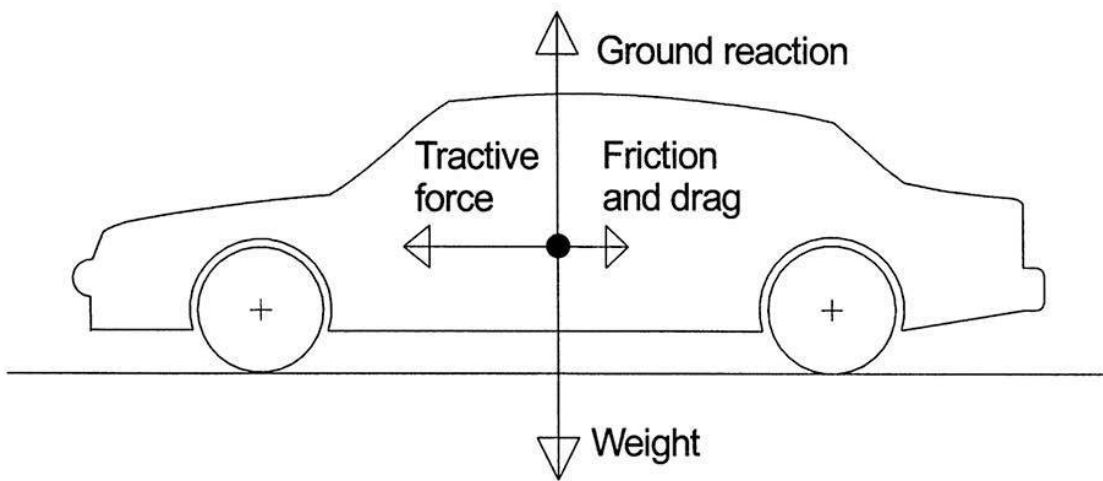


**Figure 2-2** Reduced drag means less tractive force is needed to maintain a constant speed.

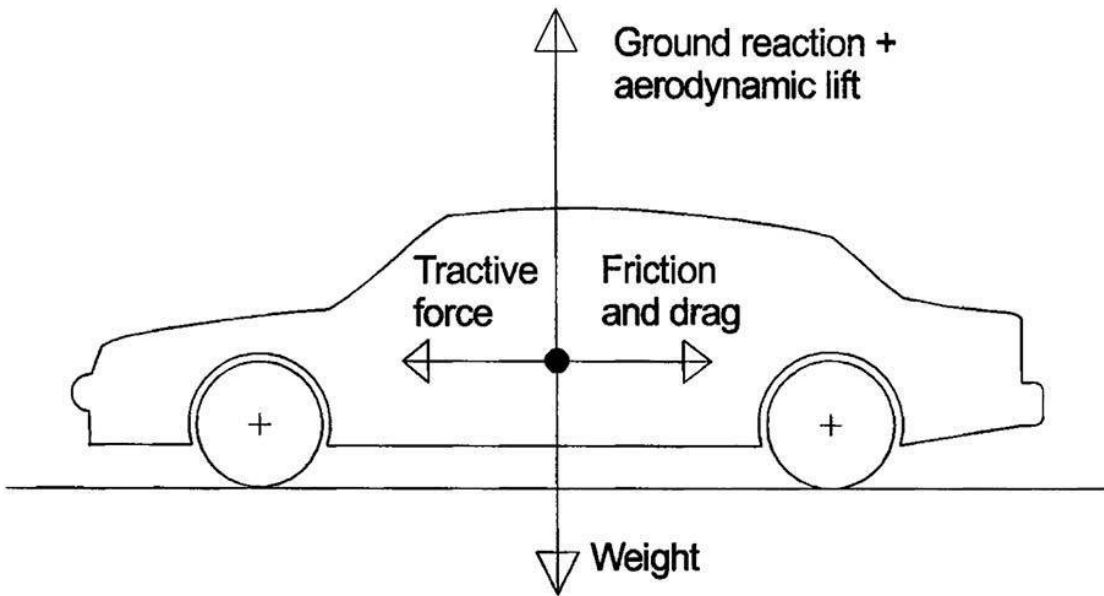


**Figure 2-3** Aerodynamic lift reduces available grip.

### Air properties

The forces that arise between a vehicle and the air surrounding it are the result of the properties of the air itself and the disturbance to the air caused by the vehicle's movement through it. It's invisible and it seems insubstantial, but air has mass. So, as a car passes through it, the air is accelerated and deflected around the car, and as we have seen from Newton's Laws of Motion, this sets up forces and reactions. The mass of air that is disturbed by the car's passage depends on three principal things:

- The size of the car (and its shape, but more on that later)
- The density of the air
- The speed of the car through the air

Examining these statements in turn, as far as size is concerned, it is fairly obvious that a larger car will disturb more air, and hence it will produce greater reaction forces from the air than a smaller car at the same speed.

The air's density is a measure of the number of molecules in a given volume, and its units of measure provide its mass per unit volume. For example, kilograms per cubic metre, or pounds per cubic foot. (There is another measure, 'slugs' per cubic foot, which is supposed to remove the confusion over pounds mass as distinct from pounds weight, but frankly it makes the

situation more confusing, so this is the last time slugs will get a mention in this book!) At a given temperature and air pressure, the air's density is something we cannot do anything about. An important aspect of this is that, although air is a gas, in the conditions in which we contemplate competition car aerodynamics, and in the relevant range of speeds involved, air is treated as an incompressible fluid, which is to say, its density is regarded as constant. There may be small variations in density as the result of temperature or atmospheric pressure changes (due to weather conditions or the altitude), but for all intents and purposes, air density does not change. The values for air density used in this book are  $0.00238\text{lb}/\text{ft}^3$  or  $1.225\text{kg}/\text{m}^3$ . Density is important because it tells us that in a given volume there is a given mass, which once again reminds us that air is 'massive', and as such is subject to the same laws of physics as anything with mass.

Just as size matters in aerodynamics, so too does speed for the simple reason that a car of given size creates greater disturbance to the air as it passes through it at higher speed than it does at lower speed.

So, it is now evident that the magnitudes of the reaction forces exerted on a car by the air will be related to car size, air density (which we can do nothing about), and car speed. There are however other properties of air that we need to go through in order to obtain a better understanding of why air does what it does around a vehicle. A useful note to add here is that aerodynamicists assume that what they call 'the principle of relative motion' applies, in which a body moving through the air is thought of as being the same as the air moving over a stationary body, such as with a car in a wind tunnel for example. This assumption can be very useful, partly because it allows aerodynamics writers to be sloppy in their references to whether it is the car or the air that is moving! However, the fact that cars move close to the ground means that there are times when the two situations are definitely not the same, as we shall see at various times later in this book.

## Viscosity

Air is a fluid, and as such it possesses a property known as viscosity, which can be thought of simplistically as being equivalent to 'stickiness'. It is not the same as density, however. For example, oil is more viscous than water, yet we know that oil is less dense than water because oil floats on water. The more viscous the fluid, the more force is required to push a body through the fluid, so in other words, viscosity resists a body's motion through a fluid.

Fluid often flows around a body as if it were in thin layers, or laminae. Because of viscosity, the layer immediately adjacent to the body surface

remains attached to the body. The layers of fluid adjacent to the attached layer are each held back slightly by the slower moving layer beneath, and as a result of the difference in their velocities they slide over each other. Then at some distance away from the body surface where the interaction with the static layer is no longer felt, there is no relative motion between the layers of fluid, and the fluid as a whole moves past the body at ‘freestream’ speed. This gives rise to a characteristic ‘velocity gradient’ in the fluid near the body surface, which is often diagrammatically represented as in Figure 2-4. The zone of slow moving air close to a body’s surface represented here is known as the ‘boundary layer’.

Where there is relative motion between the layers close to the body’s surface, ‘shear forces’ exist between them, and this is due to viscosity. These viscous shear forces are somewhat analogous to the friction forces between solid surfaces, certainly insofar as viscosity resists the motion of a body relative to the fluid it is passing through. But the real key here is that viscosity steals kinetic (movement) energy from the airflow near to a body surface and converts it into heat, and although the heat is insignificant in our context, the loss of energy from the airflow is not, as we shall soon see.

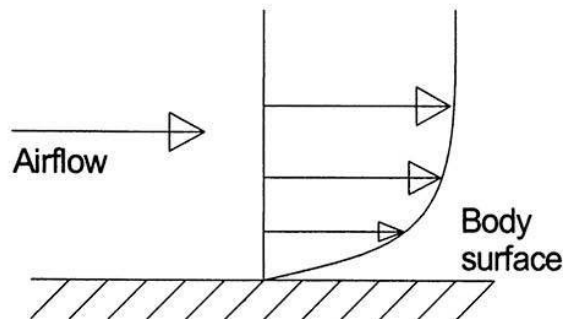


**Figure 2-4** Velocity gradient in the boundary layer.

### Laminar and turbulent flow

If all the particles within a parcel of air are moving in the same direction as the average air velocity, and the mean paths, or ‘streamlines’ traced by the air particles are parallel, then the flow is said to be laminar. If on the other hand, the air particles trace out erratic, non-parallel paths, even though the average velocity may be of the same magnitude and direction as in the laminar case, then the flow is said to be turbulent. These two types of airflow may be

visualised shortly after extinguishing a candle. The smoke just above the smouldering wick may be seen to rise in more or less straight streamlines, and exhibits laminar flow. However, as the smoke rises further, it starts to mix and swirl, and the streamlines cease to be parallel. The flow has become turbulent. The transition from laminar to turbulent occurs over distance as viscous effects remove energy from the flow, and the swirling and mixing of turbulent flow takes the place of laminar flow.

The transition from laminar flow to turbulent flow can also occur in the boundary layer. If the velocity differences between the sub-layers that make up the boundary layer are small, they will slide over each other with little interaction, so giving a 'laminar' boundary layer. But as energy is removed from the flow by viscous effects within the boundary layer, the flow within it starts to become more random and the transition to turbulent flow takes place even over a smooth body surface, as in Figure 2-5.

Boundary layers also tend to thicken further along a body as the viscous effects gradually remove energy from the fluid near to the surface, and the effects become felt further away from the surface. The non-parallel components of the velocity of the fluid particles within a turbulent boundary layer significantly increase the thickness of the boundary layer, causing it to grow more rapidly (and thicker boundary layers cause more drag). So the boundary layer may be thin and laminar over the front, upper parts of say, a saloon car, but it will gradually increase in thickness and at some point will become turbulent further back along the vehicle. It is also possible that something might disturb a laminar boundary layer, such as a change of curvature or surface 'roughness', and the boundary layer can become turbulent. How thick is a boundary layer on a competition car? Well, that depends on the distance along the body, and the speed at which it is moving relative to the airflow, but typically it may start off as laminar and a few millimetres thick at the front of the vehicle, gradually becoming turbulent and thickening to perhaps a few centimetres at the rear of the car.

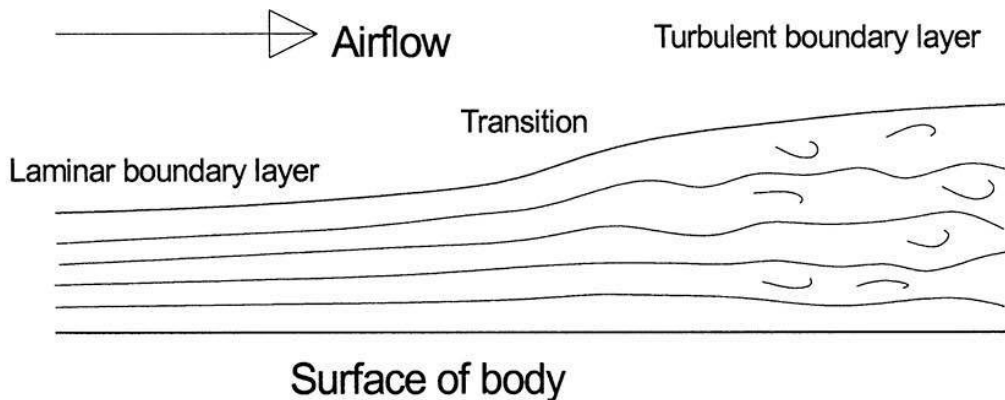


**Figure 2-5** Transition from laminar to turbulent flow; the boundary layer thickens as it becomes turbulent.

### From Aristotle to Bernoulli

So that's taken a brief tour of some of the relevant properties of air. From here we can go on to explain how aerodynamic forces arise, and also how to quantify them, and it is rather illuminating to first take a historical look back at how some potent brains have contemplated this topic before us. Aristotle, that well known Ancient Greek who lived from 384 to 322BC, a modest chap whose specialised subject was ‘the whole field of knowledge’, had a stab at it. He reckoned that as a body moved through air, a vacuum was formed ahead of it, which caused the body to continue moving. Well, you can see what he was getting at, although how he thought a body ever came to rest again isn’t clear... Then, in 1726 (AD) the aforementioned Sir Isaac Newton came up with some more plausible ideas when he realised that air and water moved in response to similar physical laws, and that these fluids were subject to the same laws as other objects and bodies with mass. This was getting much closer to what we know today, but sadly his first go at quantifying things was wide of the mark, and greatly underestimated the reality. He assumed that the forces on an object were caused by air particles rebounding from the object in a, well, Newtonian sort of way. In this case, the lift and drag forces were thought to be the result of momentum transfer between the air particles and the plate with which they collided. This clearly goes part of the way to explaining the cause of the forces involved – go back to the arm-out-of-the-window example, and you can *feel* that this is so. Drag can be partly explained by the Newtonian ‘collision’ effect, but his calculations for lift and drag did not agree with experimental results.

About 150 years later, another chap called Rayleigh likened aerodynamic lift to the flow set up by a plate planing on the surface of a body of water. There was still a large difference however, between this theory and the results from actual experiments, in which the lift force was measured at various angles of inclination.

It was not until the early 20th century, when engineers including a Russian by the name of Joukowski and a Briton called Lanchester turned their minds to the problem, that the flow patterns were correctly visualised, and the formulas derived for the lift force which very closely matched experimental results. It was realised that the influence of the inclined plate extended, by the effects of viscosity, into the air some considerable distance from the plate itself, and this is what enabled theory to match observed results. It is interesting to note that the Wright brothers had got their powered plane to remain in the air for a distance of 852 feet in 1903, some years before theory had fully explained the mechanisms – which goes to prove that you don't have to be fully versed in the theory in order to make something work in practice! Just as well, because this seems to be the basis on which much aerodynamic research is done in motorsport even nowadays...

We have to go back in history again, to the 18th century, to find the first explanations of the relationship between flow and pressure in a general fluid dynamics context. A Swiss mathematician by the name of Daniel Bernoulli is said to have understood the conservation of energy and hinted at a direct relationship between pressure and velocity. While professor of mathematics in St Petersburg he wrote a book called '*Hydrodynamica*', although this was not published until 1738, five years after leaving Russia. And he developed the equation that will perpetuate his name in fluid dynamic circles for evermore, which in simplified form is given by:

$$P_s + \frac{1}{2}\rho V^2 = \text{a constant} = \text{"Total Pressure"}$$

( $\rho$ , the Greek letter rho, is air density,  $V$  is flow velocity)

$P_s$  is the ‘static pressure’, and  $\frac{1}{2}\rho V^2$  is the ‘dynamic pressure’. So what does this tell us? Well, my physics teacher came to the rescue again, and paraphrased this mathematical formula as ‘Where the flow is fastest, the local pressure is least’. In other words, if the flow velocity is forced to increase, the local static pressure must decrease. Note that the equation is only valid along a given streamline, or mean flow path, and it does not take into account the effects of viscosity. Nevertheless, Bernoulli’s Equation is a powerful tool that enables us to explain many aerodynamic effects. It doesn’t matter what the

value of the constant is because the equation is used to compare velocity and pressure at two points along a streamline around a body. It is in fact a statement of the principle of Conservation of Energy, which tells us that in a given system such as the flow field around a car, energy can neither be created nor destroyed, it can only be converted from one form to another (possibly reversibly).

How does this help? you may ask. Well, the two parts of the equation represent two different forms of energy. The static pressure component,  $P_s$ , represents what is called ‘pressure energy’, which can be thought of as the potential energy within the fluid to do work, and the work it performs in our context is to exert forces on body surfaces. The dynamic pressure component,  $1/2\rho V^2$ , represents the kinetic, or movement energy of the fluid, and arises because the air is moving and therefore has velocity. (The kinetic energy of a given mass is usually given by  $1/2mV^2$  where  $m$  is mass, but in the case of a parcel of air of unit volume the mass is the same as the density.)

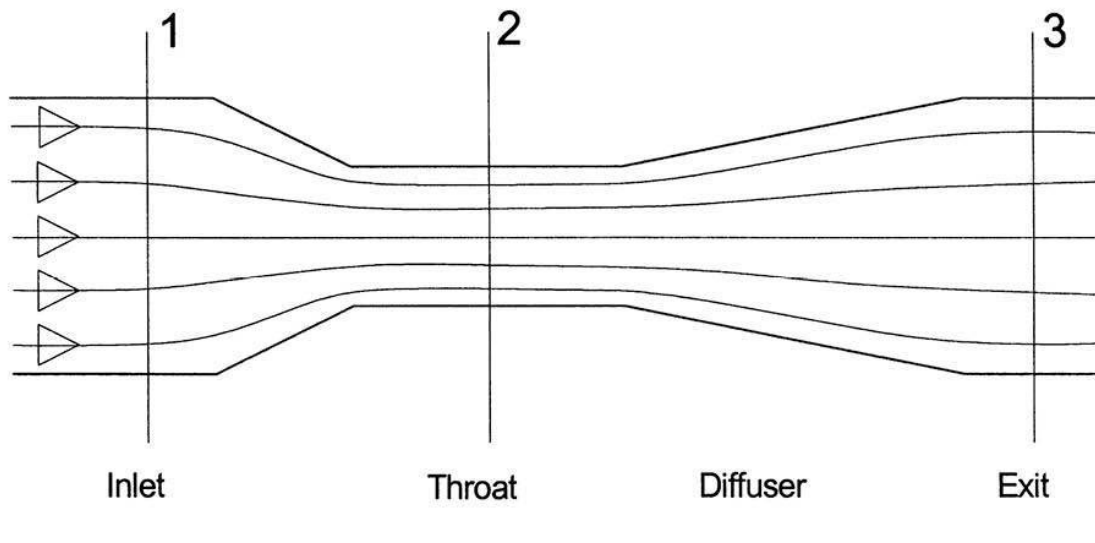
Bernoulli’s Equation tells us that, assuming there are no losses of energy, and the fluid in question is incompressible, the sum of these two components will be constant. Thus, if one of the components is altered, the other necessarily has to alter to maintain the energy total in the system. So, when the airflow is disturbed as it passes around a body like a car, changes occur to the local air velocity at different locations around the car. As the velocity is altered, the dynamic pressure (or energy) component  $1/2\rho V^2$  is altered, and so the local static pressure or pressure energy component must change too. In short, if the local velocity increases, the local static pressure will decrease, which is just what my physics teacher said.

The Bernoulli Equation, together with another important principle, that of Conservation of Mass, explains how a carburettor works. Figure 2-6 schematically shows a carburettor choke tube. This is an example of what is also known as a Venturi tube, after the Italian physicist, and we shall return to this in more detail later. However, in this instance, air is drawn through the carburettor choke tube by the induction stroke of the engine and it enters a reducing cross-sectional area as the inlet converges into the ‘throat’. Assuming the flow is incompressible, the law of Conservation of Mass requires that the mass flow through the narrow throat section is the same as that entering the inlet, and leaving the exit, thus:

$$\rho V_1 A_1 = \rho V_2 A_2 = \rho V_3 A_3,$$

where  $\rho$  = density,  $V$  = velocity and  $A$  = cross sectional area at each station indicated in the drawing, the product of  $\rho \times V \times A$  being the mass flow per unit time, in kg/second or lb/second.

Schematic of a venturi tube, for example as found in a carburettor choke tube



Air velocity accelerates through narrow throat,  
and so local static pressure drops

**Figure 2-6** A schematic diagram of a venturi tube.

Hence, where the cross-sectional area reduces, the flow velocity must increase to conserve the mass flow, and so there is a drop in static pressure in the narrow throat of the choke tube, and it is this local static pressure reduction which sucks petrol through the carburettor jet(s) and into the inlet charge to the engine. The flow velocity is then reduced again in the diffuser section of the venturi and returned to what it was at the inlet before the constriction, in order to recover the kinetic energy from the air, which of course results in an increase in static pressure again at line 3, which will be the same as it was at line 1, if there have been no losses.

It's easy to see how the flow can be accelerated, and the local static pressure reduced through the internal constriction of a venturi tube. But how do we

apply Bernoulli to a wing, and what causes the lift generating, or rather downforce inducing pressure changes around a wing?

It is apparent that as the airflow approaches our wing, the wing pushes the airflow out of the way, and the flow divides above and below the wing. This much is easily comprehended. But curiously, following its initial change of direction around the leading edge, the airflow then turns the other way, so to speak, to follow the rest of the curvature of the wing. Under ‘normal’ conditions, it continues to follow the wing’s profile above and below until it merges again at the trailing edge.

Let’s consider the more curved lower surface of the inverted, downforce-inducing wing in Figure 2-7. Newton’s First Law tells us that for the air to follow the wing’s curvature thus, there must be a force entraining it. If there were not, the air would simply carry straight on as soon as it passed the lowest point of the lower surface. Instead, the flow sticks to the surface, and this provides a clue to the source of this force, for it is viscosity – or perhaps more correctly, the fluid’s (in our case the air’s) ‘adhesive stickiness’ – that entrains the flow to follow the surface around the curvature.

However, there must also be a force that causes the air further away from the surface/air interface to follow the curvature too, and this is where Bernoulli gets involved again. It is the local reduction in static pressure, caused by the acceleration (turning) of the airflow near the surface that provides this force. The flow just outside the surface/air interface flows faster (turns more sharply) than the flow further away from the surface, and this ensures that the static pressure reduction is greatest near the wing surface. This provides the turning effect to the flow further away.

Referring back to Newton’s Third Law, the reaction to the turning force that pulls airflow towards and around the wing is that the wing is pulled in the opposite direction. And this is what causes lift, or in our case, downforce.

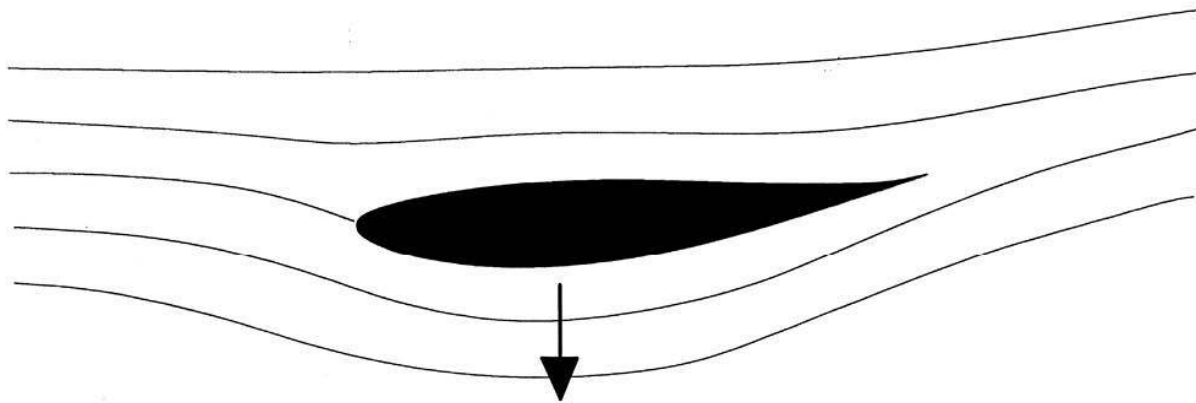


**Figure 2-7** ‘Stickiness’ entrains the airflow to follow the wing’s convexly curved surface; the Newtonian reaction to this manifests as lift, or in our case, downforce.

### Pressure distributions

We’ve seen how changes to local air velocity cause changes to local static pressures, but there’s another important concept to consider here which arises from the properties of air and the laws of physics. It will be apparent that, for example, as air encounters a body like our inverted wing, the changes in air velocity around the wing are not sudden step changes but reasonably gradual ones. This produces gradual changes in local static pressure around the body in question, and from this it will be evident that the distribution of pressure over the surfaces of the body will not be uniform. Let’s consider our inverted wing in more detail in order to contemplate the concept of pressure distributions.

Looking at Figure 2-7 again, it can be seen that the air passes above and below the wing, but one of the streamlines is shown meeting the wing near the leading edge. This is known as the ‘stagnation point’ because the air really does come to a halt at this point, which is to say, it stagnates. Because the air’s velocity here is zero, the dynamic pressure here is zero, and hence the local static pressure at the stagnation point is equal to the total pressure, which is as high as it can be around any moving body in the speed regime that’s relevant to competition cars. Thus, at this point on the wing, or any other body moving through the air, the static pressure is high.

Now let’s contemplate the air flowing below the inverted wing. As we have seen, the velocity is greater below the wing than above it, which creates the difference in static pressures below and above the wing. But clearly, as the air

divides around the leading edge it undergoes acceleration until at a point some way along the wing it reaches maximum velocity, where the local static pressure is at its minimum. Then the velocity will gradually decrease and, ideally, it should be back down to free stream velocity at the trailing edge, where the local static pressure will recover back up to the ambient value – indeed, this part of the regime is known as a region of pressure recovery.

So the static pressure has gone from ambient ahead of the wing, to high at the leading edge, to low part way along the underside of the wing, and back again to ambient at the trailing edge. This produces a static pressure distribution along the lower surface which could be graphically plotted, and which might look something like the one in Figure 2-8. An idealised static pressure distribution for the upper surface is also shown. (Note how these pressures are conventionally depicted with negative values above the zero line and with positive values below the zero line.)

It is important to appreciate that the static pressure changes brought about by the changes to the local air velocity do not just occur at the surface of the body in question. As those early 20th century engineers realised, the influence of a body on the airflow around it extends some way from its surface, and as such the changes to local static pressures also extend into the air well beyond the surface. We will see some amazing ways in which this can be visualised in subsequent chapters, but it helps when trying to understand how the low and high static pressure areas around a car interact with one another if you consider that their influence extends for some distance. Indeed, as we know just from travelling along a motorway, the influence of one moving car on the air around it extends far enough to cause interactions with cars ahead of, beside and behind it, and this has important ramifications in the competition arena too.



*Downforce comes partly from the reaction of the airflow with the upper surface of a wing...*



*...but it is the entrainment of the air to the lower surface of a wing that the major part of downforce comes from.*

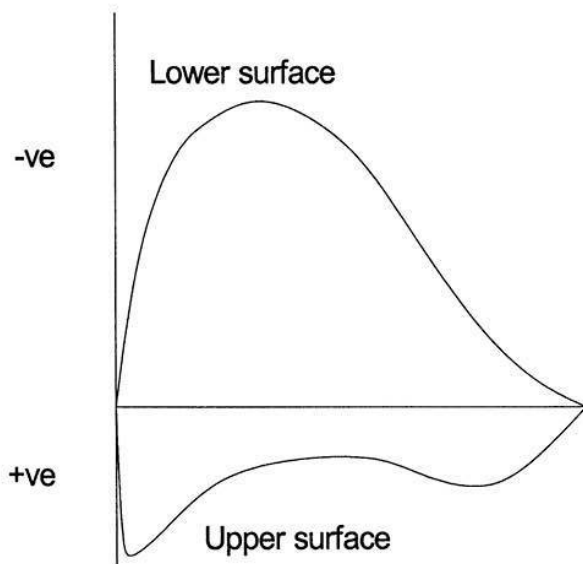


**Figure 2-8** A schematic plot of pressure distribution on the surfaces of a wing.

### Pressure gradients

As might be imagined, air flows quite naturally from a region of high static pressure to one of low static pressure, such as from ahead of the wing to the region of lowest static pressure, part way along it. For this reason this is known as a ‘favourable pressure gradient’. However, the air does not flow naturally from a region of low static pressure to a region of high static pressure, along what is known as an ‘unfavourable pressure gradient’. Why? Well, the use of the word ‘gradient’ might suggest an answer. This situation is somewhat analogous to a ball rolling down or up a hill. The ball will naturally and happily roll from the top to the bottom of the hill, where the gradient is favourable. But when it comes to rolling up the hill the situation is rather different, the gradient obviously being unfavourable. Indeed, the ball will only get to the top of the hill if it has sufficient kinetic energy (which is related to the square of its velocity of course) and if the gradient is not too steep. Exactly the same is true of airflow that encounters an unfavourable pressure gradient – it will only reach the ‘top of the hill’, which is to say, the trailing edge of the wing in our example here, if the airflow has sufficient kinetic energy and if the pressure gradient is not too steep.

If one or both of these conditions is not met then the airflow may not be able to remain ‘attached’ to the wing surface, in which event the flow is said to ‘separate’. This can happen with a wing, for example, if the velocity is too low, or if the angle of the wing is set too steep. In either case the airflow separates at some point along the lower surface, and in the worst case the flow can totally separate, a condition known as ‘stall’. With a competition car this is generally best avoided because it can cause a drop in efficiency, as we shall see in more detail later on. In the case of an aircraft, wing stall can have rather more drastic consequences...

In the real world of viscous flow regimes the effects of the boundary layer can add to the potential problem of flow separation. As air flows along a body and the boundary layer thickens, the air within the boundary layer loses kinetic energy because of viscous friction. And as we have just seen, towards the rear of a wing for example, the airflow is also losing kinetic energy as it slows down in the static pressure recovery region. This, together with the low energy in the boundary layer near the surface can cause the flow to separate. (Indeed, the flow immediately adjacent to the body surface actually reverses direction to form a recirculating ‘separation bubble’.) A similar situation can, for example, also prevail towards the rear of a production car roof. The flow is fast over the top of the roof and slows again towards the rear of the car. Boundary layer thickening also occurs along the roof, and so at some point towards the rear, especially where there is any kind of sharp lip or rapid change in the angle of the roofline away from the flow direction, the previously attached flow breaks down and separates, then going on to form the highly disturbed, turbulent region known as the ‘wake’, as shown schematically in Figure 2-9.

A laminar boundary layer creates less surface friction than does a turbulent one, and so drag is less as long as the boundary layer remains laminar. But a turbulent boundary layer may also delay the onset of flow separation in certain circumstances, or even cause the reattachment of a separated flow, as the velocity components in the turbulent layer which are non-parallel to the overall flow direction can actually re-introduce some ‘fresh’ energy into the boundary layer, effectively by stirring it up. This can have important positive benefits for drag reduction and downforce creation, and so it would be wrong to think that the laminar condition is what we are always aiming for. While a laminar boundary layer is beneficial in some circumstances, ‘vortex generators’ on a wing surface for example may be used to re-energise or even create a turbulent boundary layer to prevent separation.

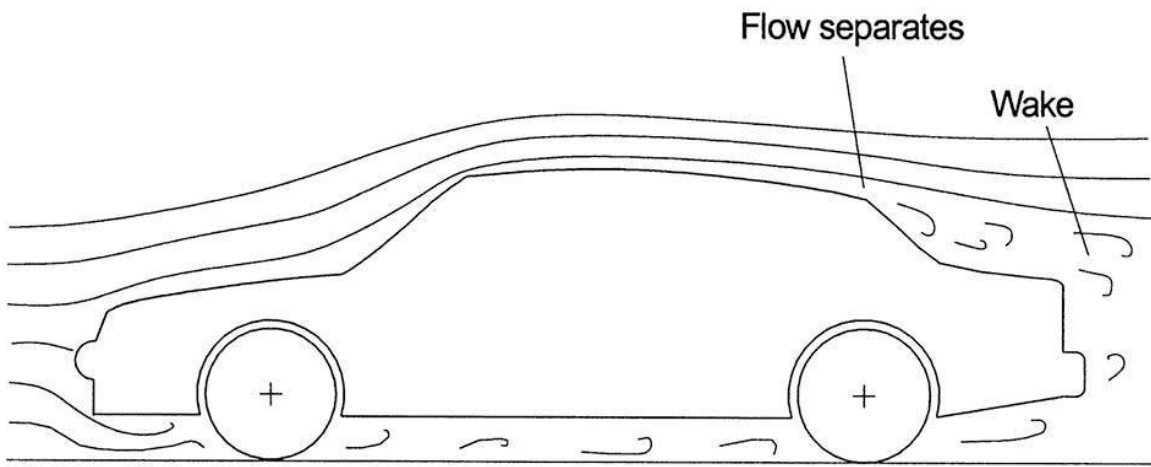


**Figure 2-9** The flow separates at the rear of this generic car, and forms the wake.

### Reynolds numbers

When cars are being aerodynamically developed one of the tools often used to aid the process is the wind tunnel. We shall look in detail at these in a later chapter, but competition car manufacturers frequently use scale models in suitably sized wind tunnels, mainly for reasons of practicality and economy of both model production, and tunnel manufacture and running costs. However, the properties of air that we have discussed mean that testing a model is not just a case of multiplying the measured forces by the appropriate scale factor.

We have seen how, at a given airflow velocity, the boundary layer thickens along a body. Consider a simple flat plate, with the air flowing parallel over one surface, the boundary layer thickens, as shown schematically in Figure 2-10. Obviously, the boundary layer is not as thick at a point  $L/2$  distance from the leading edge of the plate as it is at distance  $L$ , at the trailing edge, at a given flow velocity. From this it can be seen that the development of the boundary layer over a half-scale model will not be the same as it is on the full-sized body at the same velocity. We can also conclude that such important factors as boundary layer separation in the unfavourable pressure gradient region at the back of a vehicle body, for example, will not be the same on a half-scale model as on the full-size vehicle. In fact separation, if it occurs, is likely to occur further towards the rear of the model than on the full-size car.

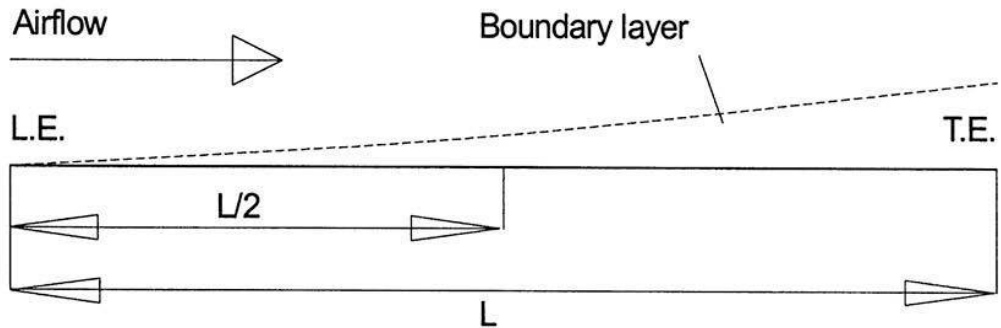


**Figure 2-10** Boundary layer thickness is not the same on scale models as on full-size cars.

To help with understanding the case when flows over models are likely to be similar to their full-scale counterparts, the Reynolds Number is useful. This is defined mathematically as

$$\text{Reynolds Number, } \text{Re} = \frac{\rho V L}{\mu}$$

where  $\rho$  is air density,  $V$  is air velocity,  $\mu$  is viscosity and  $L$  is an appropriate length to characterise the flow pattern, such as the length of a car (or model), or the chord (front to rear) dimension of a wing, or perhaps the length of the plate in our diagram. If we wish to calculate Reynolds Numbers then the following can be used:

For metric units the equation comes down to  
 $\text{Re} = 67778 \times VL$ , with  $V$  in metres/second and  $L$  in metres.

For imperial units use:  
 $\text{Re} = 6300 \times VL$ , with  $V$  in feet/second and  $L$  in feet.

Note that the Reynolds Number is another dimensionless quantity; that is, when the units of density, speed, length and viscosity are all resolved in the full equation, they cancel out and produce simply a number.

If the air's density and viscosity are assumed to be fixed, and we are looking at a particular velocity, then the Reynolds Number of a full-sized body of

length  $L$  will be double that of a half-scale model of length  $L/2$ . This difference in Reynolds Number tells us that the flow patterns for the two cases will not be the same. The aim is to test at similar Reynolds Numbers so as to obtain similar flow patterns. So, if  $L$  reduces to  $L/2$ , then to obtain the same Reynolds Number it would be necessary to test the half-scale model at double the air velocity. This is why there was a trend in Formula 1 towards larger scale models tested at higher velocities – the objective was to obtain a Reynolds Number as close as possible to those of full size.

Back in early 1998, the (then) Benetton Formula 1 team tried another approach to attaining representative Reynolds Numbers on the 50 per cent scale models it was running in its newly commissioned wind tunnel. The aim was to pressurise the tunnel to twice atmospheric pressure. Why? Because this would double the air density,  $\rho$ , which meant that at the same air velocity a half-scale model would have the same Reynolds Number as the full-size car at atmospheric pressure. It seems that technical problems precluded the tunnel's use at pressure, but the idea was valid (if costly), and indeed had previously been used in aeronautical wind tunnels for the same purpose.

## Pressure coefficients

Pressure coefficients are indicators of local static pressures at locations of interest around a body. If the pressure coefficients are known over the surface of a body they can be plotted to illustrate this, and if they can be calculated in the volume of air surrounding a body then it becomes possible to visualise the three-dimensional pressure distributions around a body like a wing, or an entire car. We'll be seeing a lot of this in later chapters. So, although this is going to get a bit mathematical for a while, it will help towards understanding many of the illustrations used later. You can of course, always come back to this section for reference as and when you need it. I'll type slowly to make things easier – for me, that is!

Pressure coefficients are calculated from Bernoulli's Equation, and it is useful to go through a mathematical derivation so we can understand what typical values might be around a competition car. Let's assume we have a body travelling along at speed  $V$ . Thus, the air velocity well away from the influence of the body is  $V_\infty$ . We will also say that the static pressure here is  $P_{s\infty}$ .  $V$  and  $P_s$  will represent the 'local' velocity and static pressure close to the body at any particular point of interest.

Now, Bernoulli's Equation says that the sum of the static pressure + the dynamic pressure (along a given streamline) is constant, so we can say that

$$P_{s_\infty} + \frac{1}{2}\rho V_\infty^2 = P_s + \frac{1}{2}\rho V^2$$

Or more simply, if we let  $\frac{1}{2}\rho V^2$  be represented by  $q$  we can say that

$$\begin{array}{lcl} P_{s_\infty} + q_\infty & = & P_s + q \\ \text{so} & & P_s - P_{s_\infty} = q_\infty - q \end{array}$$

$$\text{hence } \frac{P_s - P_{s_\infty}}{q_\infty} = \frac{1 - q}{q_\infty}$$

The term on the left-hand side of the equation is also written as  $\Delta P/q_\infty$ , and this is what is referred to as the pressure coefficient,  $C_p$ , where  $\Delta P$  (delta P) is the change in local static pressure,  $P_s$ , relative to the ambient (or barometric) pressure,  $P_{s_\infty}$  (that is,  $P_s - P_{s_\infty}$ ).

Substituting  $\frac{1}{2}\rho V^2$  for  $q$  back into the right-hand side of the equation  $1 - q/q_\infty$  becomes  $1 - (V/V_\infty)^2$

Thus

$$C_p = 1 - (V/V_\infty)^2$$

which is where we've been trying to get to! This tells us that if we know the local air velocity near a location of interest around the body in question, and we also know the freestream velocity, we can calculate the pressure coefficient,  $C_p$ , at that location of interest. We can also determine this if we know the local and freestream static pressures, but let's just stay with velocity for the moment because we can work out the sort of values we might expect at areas of interest around a competition car or a wing, for example.

In an earlier example we saw that at the stagnation point on the leading edge of a wing the local static pressure was equal to the total pressure because the air velocity at that point was reduced to zero. So, the pressure coefficient here would be

$$C_p = 1 - (V/V_\infty)^2 = 1 - (0/V_\infty)^2 = 1 - 0 = 1$$

This is as high, theoretically speaking, as Cp values go when the conditions are such that the air remains incompressible.

At a point some way away from the body, wing, car or whatever, where the airflow is not disturbed and the local air velocity is the same as the freestream velocity,  $V = V_\infty$  so  $V/V_\infty$  will be equal to 1, and hence the Cp will be  $1 - 1 = 0$ . From here we can see that where the local velocity is less than freestream, that is  $V < V_\infty$ , then  $(V/V_\infty)^2$  will be between 1 and 0, which means the Cp will be between 0 and 1.

Where the local velocity is higher than freestream, that is  $V > V_\infty$ , then  $(V/V_\infty)^2$  will be greater than 1, so the Cp will become less than 0, or negative. These ranges of values are set out in the table here for easy reference – they will help to interpret many of the graphics that will be used later on.

**Local velocity, V:** At stagnation point,  $V = 0$

**Pressure coefficient, Cp:** 1

**Local velocity, V:** In freestream,  $V = V_\infty$

**Pressure coefficient, Cp:** 0

**Local velocity, V:** Low local velocity,  $V < V_\infty$

**Pressure coefficient, Cp:** Between 0 and 1

**Local velocity, V:** High local velocity,  $V > V_\infty$

**Pressure coefficient, Cp:** Less than 0, i.e. negative

Let's just quickly look at a simple example to illustrate how a Cp can be negative. We'll go into the mechanisms involved in this example in more detail later, so just think of this as an appetiser. We're going to consider the airflow under a competition car that has been profiled to accelerate the air velocity in order to generate low pressure. Let's say the air speed is doubled under the car, and the car is doing 45m/sec (roughly 100mph).

So, the air under the car accelerates to 90m/sec, and thus  $(V/V_\infty)^2$  becomes  $(90/45)^2 = 4$ .

$$C_p = 1 - (V/V_\infty)^2 = 1 - 4 = -3$$

From this it is evident that where such negative Cp values are indicated, we know that the local air velocity has been increased quite considerably over the freestream velocity.

If we know what the velocity differences around a body are, we could then go back and use Bernoulli's Equation to calculate actual pressures, and it's then

just a step on to calculate actual forces, force being equal to pressure multiplied by area. Let's move on to doing just that, but first we'll consider the types of forces we're especially interested in.

### The forces involved

The two components of aerodynamic force that we are mainly interested in that relate to performance are *drag* and *lift* (see Figure 2-11). Drag and lift add together as vectors to give the resultant *total aerodynamic force*, and this is the net effect of all the pressures acting upon a body, such as a wing. Side forces can be important in relation to stability for example, but these are generally set up either by gusty winds or perhaps by other cars in proximity and as such are more transient and somewhat less predictable. They are important and shouldn't be ignored, but because of their transience they're hard to predict and model.

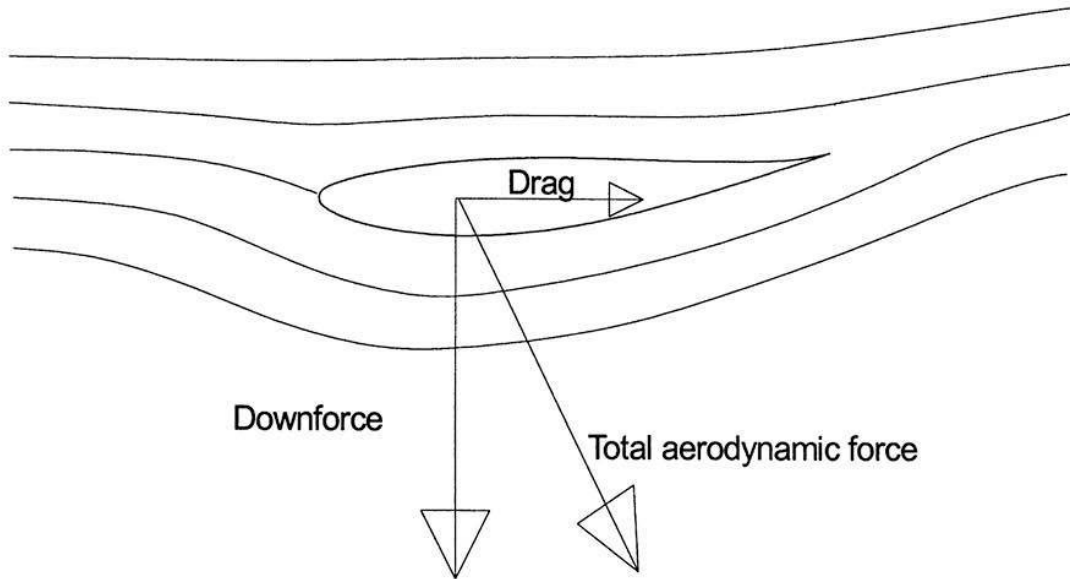


**Figure 2-11** The two main components of the aerodynamic force.

The local pressure differences felt by a body such as a wing can be expressed mathematically. From the earlier maths where we saw that  $C_p = \Delta P/q$  and  $q = 1/2\rho V^2$ , we can say that

$$\Delta P, \text{ the pressure differential} = C_p \times q = C_p \times 1/2\rho V^2$$

To calculate the force involved it is necessary to work out the sum of all the local pressures acting on the body, and of course it is necessary to multiply this by the area that the pressure is acting upon, since pressure = force/area. So we can say that:

$$\text{Force} = C_p \times 1/2\rho V^2 \times A$$

where A is the reference area upon which the sum of the pressure changes is deemed to act. In considering drag or lift forces, an appropriate coefficient is used that takes into account how the overall shape of the body in question affects the flow and distribution of velocities and local pressures. For drag,  $C_d$  is used, for lift,  $C_l$  is used. So from the equation above, we can establish equations for lift and drag as follows;

$$\text{Lift force} = C_l \times 1/2\rho V^2 \times A$$

$$\text{Drag force} = C_d \times 1/2\rho V^2 \times A$$

We'll refer to these fundamental equations quite frequently. (Note, by convention for vehicles the reference area is the frontal area of the vehicle, while for wings it is the plan area, as we shall see later.)

### Types of drag

In discussing pressure differences and viscous effects, it will be evident that all these effects contribute to aerodynamic forces. Let's consider the sources of drag for a moment. With many bodies, competition cars included, the dominant type of drag is referred to as *form* or *pressure drag*. This arises from the sum of all the pressure variations acting in the direction parallel to the motion of the body through the air, or the direction of the airflow over the body. With pretty well all non-streamlined bodies, like a competition car, there will be increased pressures on forward-facing surfaces, as well as flow separations which result in lower pressures at the rear compared to the front, and this is what creates form drag. Obviously, form drag is related to air velocity and the size of the body (car) in question. *Skin friction* or *viscous drag* arises from the viscous air interacting with surface roughness, and its magnitude is determined by the air's velocity next to the skin of the body in question. Form drag and viscous drag are often lumped together as they are both velocity dependent, especially when discussing wings when the sum of the two is called *profile drag*.

Another important source of drag is nowadays known as *vortex drag*. In our detailed look at wings later in the book we'll examine what used to be called *induced drag* more thoroughly, but in essence it is associated with rotating vortices that form behind any wing or body that generates an aerodynamic lifting force (upwards or downwards). Vortices thus generated have 'cores' which are at low pressure and which are sources of drag when they act on rearward facing surfaces.

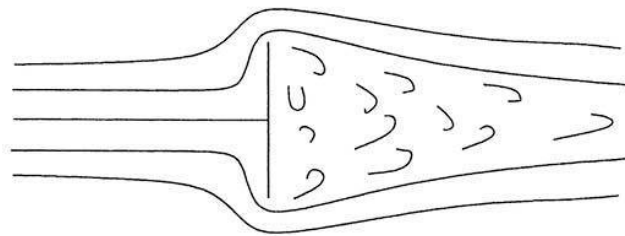
In the case of most competition cars viscous drag is a small contributor to overall drag. Form drag is the major source of drag for many cars, but where wings and other downforce-inducing devices are significant, vortex drag can also be significant. (Note that vortices are not all bad; there are occasions when they can be useful, as we'll see later in the book.)

Of more practical use is to contemplate the major causes of drag on a competition car, and put them into some sort of rough, if not strict, order of influence. They are:

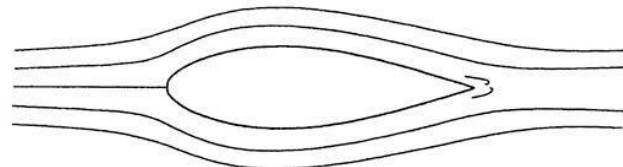
- The basic shape of the car
- The effects of wheels (and wheel housings, if relevant)
- The effects of external devices like wings, and spoilers
- The influence of internal flows for cooling, and ventilation
- Imperfections like door handles, mirrors, window seals, and panel fit

### Coefficient sizes

Lift and drag coefficients are relative measures of how much lift and drag a particular shape generates. If we look at drag first, intuition is surprisingly helpful, to the extent that we *know* that a flat plate turned perpendicular to an airflow will create more drag than a similar width tear-drop shaped object (see Figure 2-12). However, we cannot tell, just by looking, that the flat plate has a drag coefficient ( $C_D$ ) probably exceeding 1.1, and the tear-drop shape, if its length is four or five times longer than its width, has a  $C_D$  of about 0.04.



Flat plate,  $C_D > 1.1$



Tear drop shape,  $C_D \sim 0.04$

**Figure 2-12** Different shapes have different drag coefficients.

But we can usually tell by looking at a car whether it has a high or a low  $C_D$ , and we shouldn't be surprised that a land speed record attempt vehicle has a drag coefficient around 0.1 or so, and typical passenger cars these days have  $C_D$ s in the range 0.3 to 0.4. Typical competition cars however fall into the much broader range of around 0.4 to 1.4, depending on category and configuration. Let's look at a nice comparison between two McLarens of 1996 vintage. Though these cars are getting on a bit, the comparison works just as well now as it did then. The (road car-based) McLaren F1 GTR sports racing car looks to be an inherently less draggy shape than a McLaren Formula 1 single-seater racing car, principally because its wheels are shrouded and it has less downforce inducing devices evident, and some facts bear out this crude assessment.



*The 1996 McLaren F1 GTR looks less 'draggy' than...*



*... the 1996 McLaren Formula 1 car.*

When it comes to lift coefficients, subjective judgement is not so easy (unless you happen to be measuring such things on a regular basis), although some examples lend themselves to guesstimates. Taking these two McLarens again, the Formula 1 car just *had* to have a higher (negative) lift coefficient, with its multi-element aerofoils for generating downforce. The F1 sports car, in road trim had no aerofoils, and despite a profiled underbody designed to generate some downforce, by eye it simply didn't look to have a downforce-

inducing shape. Even in racing trim, as the F1 GTR, with front ‘splitter’ and rear wing, the sports car appeared to be a long way short of the single-seater in terms of lift coefficient, and hence, downforce production.

But what these assessments of coefficients do not take into account is, as Newton observed an awful long time before racing cars appeared, that *size* is just as important as shape when it comes to the magnitude of the aerodynamic forces created. Look back at the formulas for lift and drag again, and note that ‘A’, for area, is present in both equations. Clearly then, if the frontal area of one car is bigger than another it will produce more drag for the same  $C_D$  (at the same speed). For this reason some references quote  $C_D \cdot A$  values, that is, the drag coefficient multiplied by the frontal area, to allow direct comparison between vehicles of different sizes.

So let’s look at some numbers based on real racing cars, drawing on several sources for the data. A typical Formula 1 car of 1996 might have had a frontal area of roughly 14.5 square feet ( $1.35m^2$ ) (as estimated in the manner shown in Figure 2-13) and an average  $C_D$  of around 0.85, according to various references. Taking the density of air to be  $0.00238lb/ft^3$  ( $1.225kg/m^3$ ), then at 200mph, or 293.33ft/sec ( $89.4m/sec$ ) drag works out at

$$\begin{aligned} \text{Drag} &= CD \times 1/2\rho V^2 \times A \\ &= 0.85 \times 0.5 \times 0.00238 \times (293.33)^2 \times 14.5 \\ &\approx 1,262lb \text{ (574kg approx.)} \end{aligned}$$

At the same speed, a McLaren F1 GTR, with an estimated frontal area of about 17.0 square feet ( $1.58m^2$ ), calculated as width multiplied by height multiplied by a factor of 0.87 (to give a better approximation than just width times height), was said to have generated around 1,000lb (455kg) of drag at 200mph. Thus, the car with the larger frontal area produces significantly less drag, which implies that its  $C_D$  is lower. Doing the sums in reverse this drag coefficient works out at around 0.57 for the GTR GT. So our subjective appraisal of Gordon Murray’s sports car masterpiece *was* right, it was a less draggy shape than a Formula 1 car! Also, it is to be expected that the road-going version of the sports car had a much lower  $C_D$  again, because it didn’t have all the downforce-creating and drag-inducing appendages of the racing model.

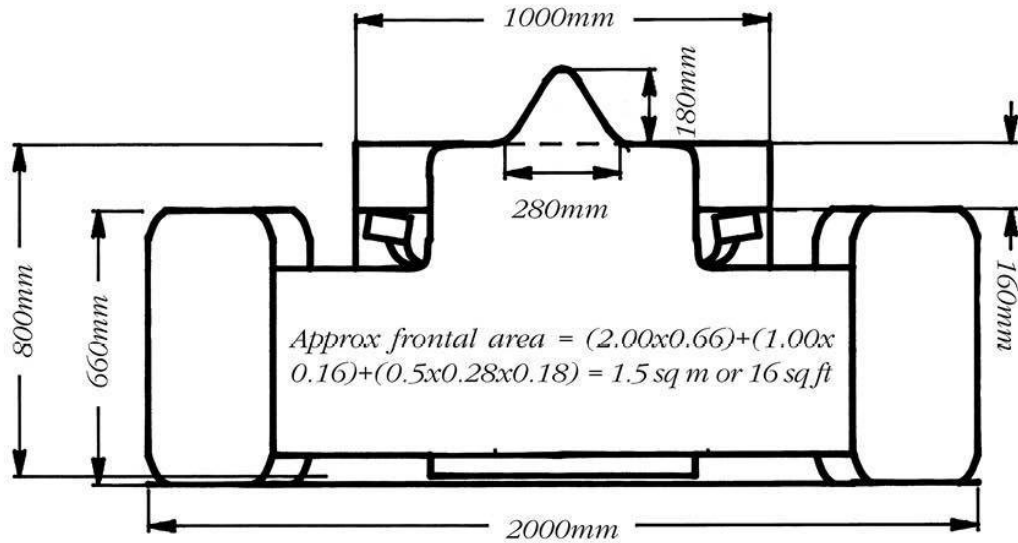


**Figure 2-13** A method for estimating frontal area.

It is interesting to do the same comparison with the downforce generated by the two types of car, and calculate overall  $-C_L$  values. It is reckoned that one 1996 Formula 1 car was producing a figure ‘approaching 4,000lb’ (1,820kg) of downforce at 200mph (320km/h) in the high speed circuit (‘low’ drag) configuration used at the Monza and (old) Hockenheim circuits, where speeds this high were not only possible, but regularly exceeded. Let’s take ‘approaching 4,000lb’ to mean 3,800lb (1,725kg) for the purposes of these calculations. The McLaren F1 GTR generated in the region of 600lb to 1,500lb (273kg to 682kg) of downforce, depending on configuration. For comparison we will use the lower value for the GTR, since it is presumably analogous to the high-speed set-up of the Formula 1 car we are using here. So, the sports racer was producing about 15 per cent of the downforce of the Formula 1 car at the same speed. Running the calculations in reverse again, we see that the respective overall  $-C_L$  values are 2.56 for the Formula 1 car and 0.34 for the sports racer. This is significant difference, and reflects, amongst other factors, the efforts of the technical regulators to cap downforce in the sports car category as well as the success of the Formula 1 aerodynamicists at defeating their regulators! Note that these  $C_L$ s should really have negative signs in front of them to demonstrate that downforce is being generated as opposed to positive lift.

The ratio of negative lift (that is, downforce) to drag -(L/D) is often quoted as a measure of aerodynamic efficiency. In the examples worked through here, the Formula 1 car has an -L/D ratio of 3.0:1, whereas the GT car's -L/D ratio is 0.6:1. The implication is that the single-seater is five times as aerodynamically efficient as the GT racer. This is a slightly simplistic way of looking at things though, since it doesn't take into account the purposes of the two vehicles, the aims of the competitions in which they take part, or the rules pertaining to each category. So -L/D ratios are interesting for comparing cars within a given category, and maybe for studying how a given manufacturer develops its cars over time, but perhaps they should not be used to compare cars in different categories.

### **Drag and power**

There is a direct mathematical relationship between top speed and available brake horsepower, which is based on the equation for calculating drag force. In simplified (Imperial units) form it is

$$\text{bhp absorbed by drag} = \frac{C_D \times A(\text{sq ft}) \times v^3(\text{mph})}{146,600}$$

For semi-metricated readers, who still use brake horsepower, the equation becomes

$$\text{bhp absorbed} = \frac{C_D \times A(\text{m}^2) \times v^3(\text{m/sec})}{1,225}$$

To convert bhp to kilowatts, multiply by 0.746. (The values of 146,600 and 1,225 are constants that take into account the value used for air density as well as the dimensional units used in each case.)

Notice that the velocity now has to be cubed (that is, multiplied by itself three times) in this equation. This is because force, as we have seen, is proportional to velocity squared, and power is proportional to force multiplied by velocity. Therefore, power absorbed by drag is proportional to the cube of the velocity. So it is evident that 'drag bhp' is a very velocity-sensitive parameter. Notice too the phrase 'available horsepower', which refers to the fact that the figure to use in this equation is the power available at the wheels. This is power that is available to accelerate the car, and to overcome air resistance. In his book *Race and Rally Car Source Book* the late and much missed

Allan Staniforth provides a handy table from which it is possible to estimate available horsepower if the bhp at the flywheel is known. The ‘correction factors’ quoted are said to take into account a range of variables such as alternator loads, fans, tyre rolling resistance and so forth. The corrections, in modified form, are quoted here for a selection of competition categories:

**Type of car:** Rear engined single-seater with cold or narrow tyres (eg Formula Ford, small hillclimb)

**Multiply flywheel bhp by:** 0.91

**Type of car:** Circuit single-seater with hot and wide tyres (eg Formula 1, Formula 3)

**Multiply flywheel bhp by:** 0.875

**Type of car:** Full race saloon/sports with engine at same end of car as driven wheels (eg Le Mans, Mini)

**Multiply flywheel bhp by:** 0.85

**Type of car:** Front engine, rear-wheel-drive competition car (eg Clubmans Supersports)

**Multiply flywheel bhp by:** 0.82

We can now make some top speed estimates for our two example cars, the generic Formula 1, and the McLaren F1 GTR, we get the following results; (see also Figure 2-14):

Car: McLaren Formula 1

$C_D$ : 0.85

A: 14.5

bhp: 700

Available bhp: 612.5

Theoretical max speed: 194.4mph (312.5km/h)

Car: McLaren GTR

$C_D$ : 0.57

A: 17.0

bhp: 600

Available bhp: 510

Theoretical max speed: 198.2mph (318.7km/h)

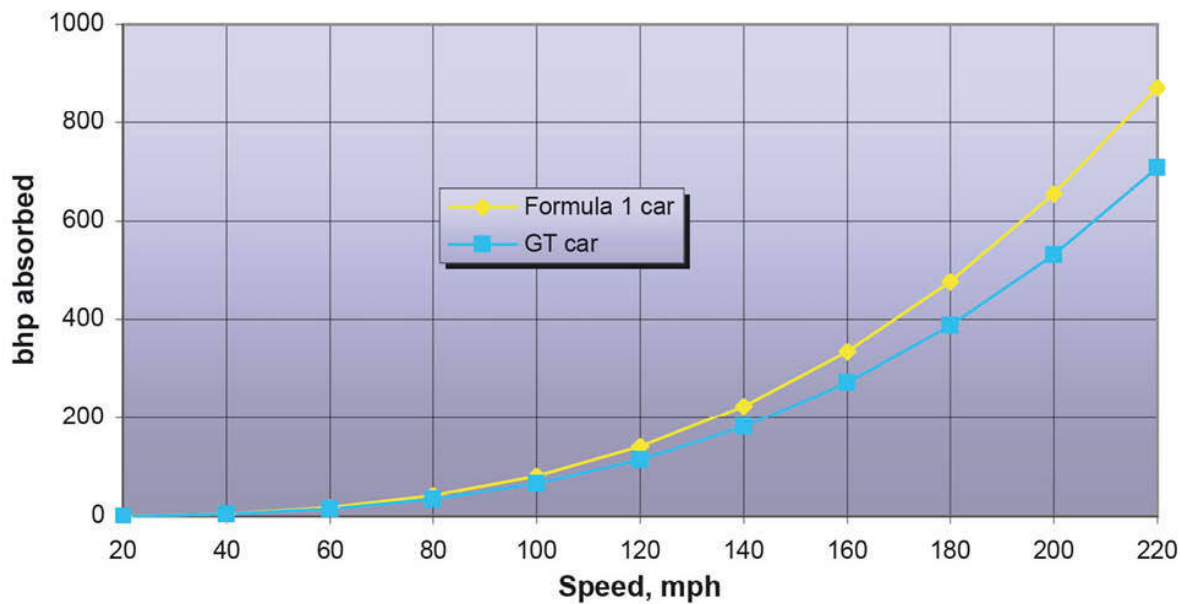


**Figure 2-14** Power absorbed by aerodynamic drag.

$A$  is frontal area in square feet, and the bhp values are ones bandied about in the motorsport press when the cars were current, and so they will serve to illustrate, even if they were not true! Available bhp figures have been corrected according to the previous table.

The vast majority of racers do not have the luxury of access to a wind tunnel, which means that, generally speaking,  $C_D$  values often have to be guesstimated. If, however, a test track with sufficient room to reach absolute maximum speed is available, and all the necessary gear ratios to attain that speed are also to hand, then it will be possible to estimate the  $C_D$ , once the frontal area has been measured. Alternatively, one of the straight line test methods described in Chapter 8 could be used. But while it is an academically interesting exercise, it has to be asked, does it really matter? Top speed is not usually of primary significance to lap or elapsed time in most forms of motorsport (the exceptions of high-speed oval racing and possibly Le Mans are obviously different). And yet, as we shall see in Chapter 5, it *is* of benefit to be able to estimate the  $C_D$  when it comes to calculating how much additional drag, induced by extra downforce creation, may be tolerated.

### Downforce, grip and balance

So why is downforce useful? Why does it make cars go quicker around a given bend, or circuit when clearly it creates a penalty in the form of extra drag? It's

all to do with friction, and grip. Imagine an object being pulled along by a piece of string across a surface at a constant speed. The friction generated between the object and the surface is given by yet another equation:

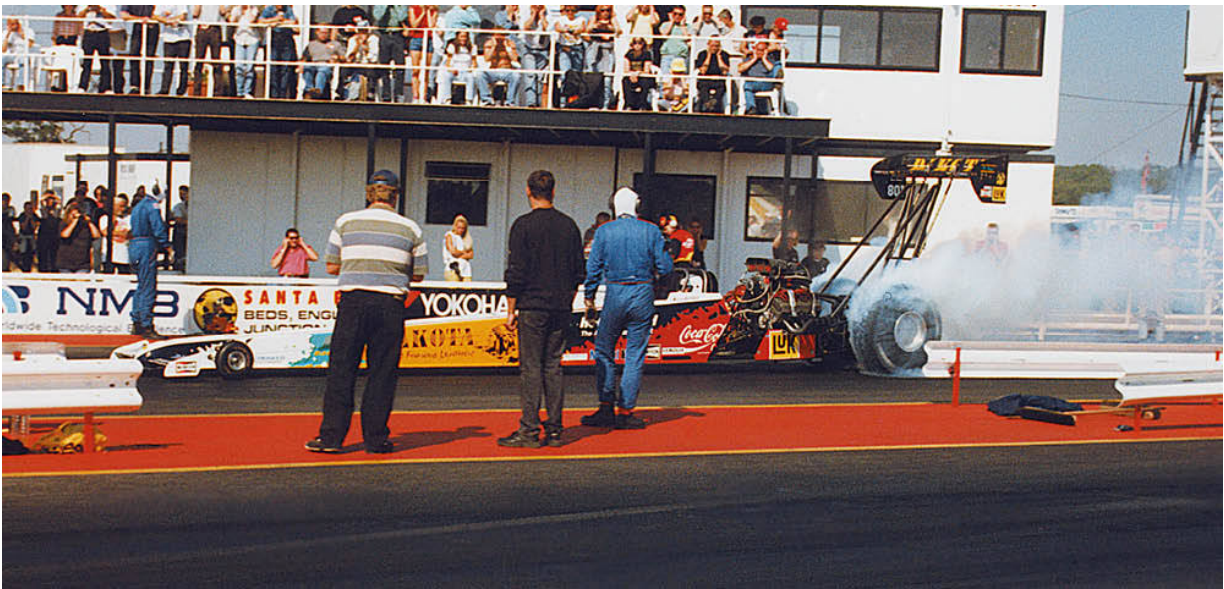
$$\text{The frictional force, } F = \mu R$$

where  $\mu$ , the Greek letter ‘mu’, now represents the coefficient of friction, and  $R$  is the ‘normal force’ (normal being a synonym for ‘perpendicular’) between the object and the surface, which, ordinarily, is the object’s weight (the earth’s gravity pulling its mass onto the surface). The coefficient of friction is governed by the nature of the object and the surface it rests upon. So for example, an ice hockey puck on wet ice exhibits a very low coefficient of friction, and the ice exerts practically no grip on the puck at all. In contrast, the driving tyres of a Top Fuel dragster on sticky asphalt generate an extraordinarily high coefficient of friction, and a correspondingly high level of grip exists between the tyre and the road surface. Notice that the area of contact between the body and the surface does not come into the equation. So why do wide racing tyres generate more grip than narrow ones? This is to do with matching the thermal and mechanical properties of the tyre to the car (and tracks) in question in order to generate just the right amount of heat and, hence, grip, a fascinating topic that is somewhat outside the scope of this book...

The normal force is, as stated above, usually the object’s own weight. So, an object weighing 5lb (2.27kg) exerts twice the normal force of an object weighing 2.5lb (1.13kg), and as such it generates twice as much friction when the string is pulling it along. Thus it requires twice the force to pull it along at a constant speed as does the lighter object. Now turn this concept around so that the object is a car, moving on an asphalt road. For the car to accelerate, or brake, or corner, the tyres must be able to utilise the friction between their contact patches and the road surface. The maximum limit of this friction is a function of the normal force, and the coefficient of friction between the tyres and the road, as defined by  $F = \mu R$ . In this case,  $R$  is the vehicle’s own weight, and so the maximum horizontal forces that can be generated are limited by the weight of the car, and how grippy the tyres are. (A complicating factor is that  $\mu$  actually drops slightly as  $R$  increases, but overall friction increases with  $R$ .)

This would be true on the Moon, or any other place where there is no air to speak of. But here on Planet Earth, where the air is dense and viscous, aerodynamics come into play, and interact with this simplistic view of vehicle dynamics. As we have already seen, it is possible for a car to create substantial

vertical forces by virtue of its passage through the air, and these add to or subtract from the vehicle's own weight to modify the normal force,  $R$ , and as such, alter the maximum frictional force that the car's tyres can generate. If a car creates positive lift, then the maximum frictional forces that can be generated are reduced, whereas if the car creates downforce, the maximum frictional forces are correspondingly increased. Thus, all other things being equal, a car with downforce can accelerate, brake and corner with greater force than a car with no downforce, or one with positive lift. Providing these increased limiting forces can be exploited, the car with downforce should be able to cover a given set of corners and straights in less time than one without downforce, because it will be able to accelerate and brake harder, and corner faster. And this, to coin a phrase, is what it's all about. Naturally, nothing ever comes free, and as we have already seen, downforce is no exception; the inherent drag penalties involved mean that the whole science (and art) is about trading off the gains against the losses to achieve a net benefit.



*It's all to do with friction and grip ...*

Let's work through a simplistic example for a hypothetical racing car travelling around a simple, constant radius corner to see the benefit of downforce. Assume the car travels around the corner in a steady state, neither speeding up nor slowing down, just with a perfectly balanced cornering force (not very realistic perhaps, but the maths is simpler!). The line taken by the car makes it a right angled ( $90^\circ$ ) 164ft (50m) radius corner. We have seen that the limiting force that can be generated is given by  $F = \mu R$ , and we'll assume  $\mu$  is

an average racing tyre value of 1.4. The car's mass is 1,100lb (500kg). The equation for the force which keeps a body moving in a circular path, known as the centripetal, or 'centre seeking' force, is given by

$$F = (mV^2)/r$$

where  $m$  is the body's mass, and  $r$  is the radius of the circle. So now, we can say that

$$\mu R = (mV^2)/r$$

because the limiting friction is exactly balancing the force required to maintain the circular path, and no other forces (acceleration or braking) are being fed in. This means our driver is very skilful indeed, and can balance the car precisely on the limit of adhesion available to him! Oh, if only that were possible...

Now let's indulge in a spot more algebraic jiggery-pokery, and rearrange this equation to make  $V$ , the velocity, the subject, vis:

$$V = \sqrt{[\mu R r / m]}$$

From this, we can feed in values for the coefficient of friction, the weight, or effective weight of the car, the corner radius and the car's mass, and calculate the maximum cornering speed possible in those conditions.

If we start with zero downforce generation, then  $R$  is equal to the car's weight, and the calculation becomes

$$V_{max} = \sqrt{[1.4 \times 1,100 \times 32.2 \times 164 / 1,100]}$$

which comes out to

$$V_{max} = 86.0\text{ft/sec (26.2m/sec)}, \text{ or } 58.6\text{mph (94.3km/h)}$$

Notice that the car's weight is expressed in this equation as its mass, which is what the 1,100lb really is, multiplied by the force due to gravity, of 32.2lb force per lb mass.

Using the equation for aerodynamic lift, and substituting the previously determined values for our generic Formula 1 car with a  $-C_L$  of 2.56, and a reference area,  $A$ , of 14.5 square feet ( $1.35\text{m}^2$ ), we can calculate how much downforce such a car would produce at this speed:

$$\begin{aligned}\text{Downforce} &= 0.5 \times 0.00238 \times 2.56 \times 14.5 \times (86.0)^2 \\ &= 326.7\text{lb (148.5kg, or 1,457N)}.\end{aligned}$$

This figure is then added to the vehicle's weight to produce an effective weight value because the car is now being pressed onto the ground with more force than just its own weight, and the value for R is the car's weight plus the downforce value. Thus, the maximum cornering speed now becomes

$$\begin{aligned}V_{\max} &= \sqrt{[1.4 \times (1,100 + 326.7) \times 32.2 \times 164 / 1,100]} \\ &= 97.9\text{ft/sec (29.9m/sec), or 66.8mph (107.6km/h)}$$

This is clearly a significant increase in cornering speed compared to the unassisted value, and to bring this gain into even sharper focus, we can calculate the time saving achieved by this gain in speed. Having said that the corner was a  $90^\circ$ , 164ft (50m) constant radius, the distance through it is one quarter of the circumference of a 164ft diameter circle, which distance would be given by  $2\pi r/4$ , or 257.6ft (78.5m).

$$\text{Time taken} = \text{distance/speed}$$

so in the unassisted case, the corner takes  $257.6/86.0 = 2.995$  seconds, and in the assisted case, the corner takes  $257.6/97.9 = 2.631$  seconds, a saving in this one short section of track of 0.364 seconds. Add to this the fact that the car now enters the next section of track 8.2mph (13.2km/h) faster than the unassisted car, and yet more gains are to be had from carrying that extra speed. Then one has to take account of the *extra* downforce created because the car is now able to corner faster than before! The process is an iterative one.

A key assumption here is that the downforce is 'balanced' front to rear so that the car's handling and cornering ability are also balanced. It is no simple matter to attain an aerodynamic balance during the infinite range of dynamic situations encountered on track, but it is an omnipresent "Holy Grail."

As mentioned earlier, the situation is not quite this simple because the tyres do not behave in a totally linear way. As the normal force on them increases, their coefficient of friction actually tails off, which means two things – first, the maths gets more complicated, and secondly, the gains are not quite as big as in our simple example here. Nevertheless, there are still significant benefits to be had, and, clearly, downforce has a major role to play in competition car performance.

## **Production cars and aerodynamic lift**

The case of the production car is, generally speaking, rather different, with modern shapes tending to generate *positive* lift. For the racers of production-based machines, the reduction or reversal, wherever possible and wherever permitted by the regulations, of this unfortunate propensity is a matter of considerable interest. What's more, this tendency for lift production has tended to worsen as car manufacturers have actively sought the lowest  $C_D$  they could achieve. The reason that so many production cars produce lift is, of course, tied up in their shape. Design trends have seen a general smoothing out of shapes, with raked back windscreens, and rounding of transitions to give much sleeker shapes, with the benefit, naturally, of low drag coefficients. But, the downside of this effort has been to ensure that the air flowing over the upper surfaces of vehicles is smoothly accelerated, and is kept as smooth, fast and undisturbed as possible. In fact, in side view, some modern saloon profiles bear more than a rough resemblance to a truncated aerofoil in the positive lift orientation (see Figure 2-15). This, of course, means that the low pressure is created above the vehicle, which causes an upward lifting force.

To put this effect into perspective, it is worth stopping to look at some more figures. Hard downforce values on current racing machines are always difficult to come by, but let's say a touring car produces around 110lb (50kg) of downforce at 100mph (160km/h). This doesn't sound a lot but when this figure is compared with the base production vehicles, which do not carry the front airdams, or the splitters, or the rear wings, and which are said to produce positive lift of up to +180lb (+82kg) at 100mph (160km/h), then 110lb (50kg) of downforce seems quite reasonable. This means, in fact, that the effective weight of the cars is up to 290lb (132kg) greater in racing trim than in road trim at 100mph as the result of the downforce. This represents about 13 per cent extra 'normal' force acting on the tyres at this speed, which simplistically translates to 13 per cent greater cornering forces being possible. In a racing category where hundredths of a second count, this is highly significant.

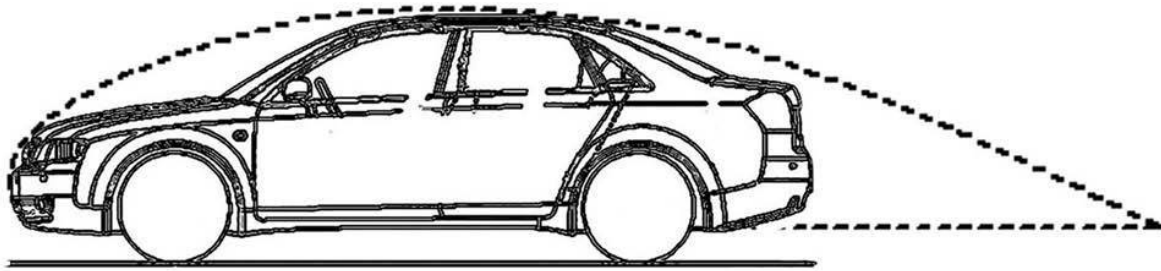


**Figure 2-15** Modern saloon car profile and a positive lift aerofoil shape.

### Non Bernoulli downforce?

Many of the explanations thus far used to describe the mechanisms that generate aerodynamic forces have relied heavily on Bernoulli's Equation. The limitations of this nevertheless incredibly useful equation were pointed out earlier, but it is also of some value to examine where Bernoulli does not describe the mechanisms at work.

It was stated earlier that Bernoulli's Equation in simplified form assumes there are no 'losses' in the system in question. This means it assumes no flow separations or viscous effects occur, which we have seen is not the case in most real situations. Where these effects do occur, there are losses in the energy of the airflow that can lead to reductions in static pressure in ways not described by the simplified Bernoulli Equation.

Take the wake of a car, for example. As was described earlier, the wake is a highly disturbed area of air at the rear of a body (car) where the airflow has lost kinetic energy through pressure recovery and because of viscous effects, and the flow separates from the body. So the air velocity relative to the car is low in this region. Yet we know that this is also an area of low static pressure because we can observe dust, leaves and so forth following the car along in its wake. We can also feel the suction effect of a car, or, more especially, a truck, when we drive up close behind it – this enables what's called 'slipstreaming' in racing, and it is a very real effect. So, the low static pressure in the wake is something that exists, yet it cannot easily be calculated by using the simple form of Bernoulli's Equation because it arises from energy losses that result in reduced total pressure. Nevertheless, it would be wrong to think of this as non-Bernoulli downforce, because Bernoulli's Equation is essentially a statement of the Conservation of Energy (in the simplified case, pressure energy and kinetic energy) in fluid flow. Thus, energy losses, or, more strictly

speaking, conversions into other forms of energy such as heat and sound in our context, are all a part of the whole.

## Chapter 3

# Computational Fluid Dynamics (CFD)

A RELATIVELY RECENT phenomenon to take a hold in competition car aerodynamics is a branch of science (or should that be engineering?) known as computational fluid dynamics, or CFD to give it its more manageable abbreviated name. As the title implies, it is a technique that benefits from the number-crunching capability of computers to provide simulations of fluid flow problems. This can involve all manner of fluids, or substances that behave like fluids, in a wide range of circumstances such as cooling airflows within a laptop computer, drugs in asthma inhalers, mud slides in a geological context, and winds blowing around buildings. Needless to say, the methods can be applied to air flowing around competition cars too.

CFD has only really been around since the 1970s, in large part because the requisite computing power only became available during that period. With the rapid increases we have seen in computer processor performance, and the cheapness of computer memory, the technique has rapidly become more accessible at reasonable cost. So as to avoid the need for too frequent updates to this book we won't even begin to mention the processor speeds or memory sizes currently available – they'd be out of date next week, if not tomorrow. Suffice it to say that at the start of the 21st century it had become possible to run pretty capable CFD software on a decent home computer. That is not to say that top race teams or professional providers of CFD services would do that – indeed, they have much greater power at their disposal, as we shall see later in this chapter. Nevertheless there is fully functional CFD software out there that will run on a home PC, which speaks volumes for the rate of progress in both hardware and software development.

CFD only really began to get a toehold in motorsport in the early to mid-1990s, and at the forefront in the field as a service provider set up in 1997 was a UK-based company called Advantage CFD. Originally a part of the Reynard Motorsport group, it was subsequently wholly absorbed into the Honda Formula 1 team (before that became Brawn GP and then Mercedes GP). It was in articles in the 'Aerobytes' series prepared for *Racecar Engineering*

magazine based on projects carried out by Advantage CFD that some of the highly instructive illustrations in this book originally appeared. Incidentally the founder of Advantage CFD, Dr Rob Lewis, went on to found another leading independent CFD service provider, TotalSim following Honda's absorption of Advantage CFD.

Subsequent to the association between *Racecar Engineering* and Advantage CFD that produced those early 'Aerobytes' columns, Ansys, one of the main vendors of commercial simulation software, also provided privileged access to the author to some of its fluid flow analysis software products, and further graphical illustrations generated with this software appear in this book. The insights that they collectively provide into the mechanisms and nuances of airflows around parts of competition cars are invaluable, and they frequently provide far greater clarity than would be possible with mere words and numbers.

Another interesting development in the world of CFD is 'open source' software. In particular a package known as OpenFOAM became available free of charge in 2004, and within a very few years it was being put to use by CFD service providers, OEM car manufacturers and motorsport teams (including Formula 1). While the software is free to download from OpenFOAM's website, some reasonably serious training would be needed for most people to be able to use it, and in round numbers it is reckoned that the costs in the first year of use would be comparable to the licence fees normally payable to the usual commercial vendors (generally a few thousand dollars/pounds/ euros per computer processor per annum). After that, though, no licence fees are payable, and the community that was building up around it, as with other open source products such as Open Office for example, will likely ensure the sustainability of the product, and indeed the concept of open source CFD. There have also been quite low-cost commercial products put on the market that provide a version of the normally free but not easy to use OpenFOAM, with a 'graphical user interface' (GUI) that makes it relatively easy to operate. Depending on your viewpoint, this could be seen as a pragmatic approach that increases access to a potentially very useful set of software tools for a much wider user base, or it could be viewed as a bit of a violation of the underlying principles of open source software sharing. Market forces will decide how all of this pans out, but it is probably a good thing for us all that the options to get into CFD are expanding.

## How does CFD work?

CFD is the analysis of systems involving fluid flow, heat transfer and associated processes such as chemical reactions through the use of computer-based simulations. It is a powerful modelling technique that has wide applications, but we're obviously focussing on its ability to solve what happens to the airflow around competition cars. Whereas the data and images produced as its end result make for insightful and comprehensible study, not to mention very pretty pictures, the mathematics that goes on in the background is highly complex. Fortunately, there is an increasing number of specialists whose task it is to understand the maths involved so that we don't need to! But, as in all things, it does pay to try to achieve a basic grasp of the fundamentals underpinning the process, so let's have a stab at doing that.

In Chapter 2 we saw that air is a fluid, that it possesses certain fluid qualities, and that when an airflow is disturbed around a moving body there are changes to the air's velocity which generate changes to the local pressures, which in turn create aerodynamic forces. And as we have seen, all of these occurrences obey the fundamental laws of physics, as they apply to fluids. In any specific case of a fluid flowing around a body there are the same 'unknowns':

- Fluid velocity in the three directions indicated as x, y and z\*
- Pressure
- Density
- Temperature

\*Typically the x-direction is horizontally fore and aft, the y-direction is horizontally side-to-side, and the z-direction is vertically up and down.

Generally speaking, density and temperature are thought of as invariables in competition car aerodynamics (although both may be relevant in some circumstances), and so in essence, CFD usually has to calculate what the changes in velocity will be around a given body. Solving the equations that represent the basic underlying principles, two of which were introduced in Chapter 2, achieves this. These principles are:

- The principle of Conservation of Mass
- The principle of Conservation of Momentum
- The principle of Conservation of Energy

The second of these principles, which we have not previously come across here is another nugget of wisdom from Sir Isaac Newton (essentially his Second Law of Motion) and says that the rate of change of a body's linear momentum is directly related to the force acting upon it. Momentum is the product of a body's mass and velocity ( $mV$ ), and so the principle of Conservation of Momentum can be stated as

$$F = (m_2V_2 - m_1V_1)/t$$

where  $F$  is the sum of all the resultant forces acting on a body,  $m_2V_2 - m_1V_1$  represents the difference between the final momentum and the initial momentum of the body brought about by this force, and  $t$  is time. Momentum can be transferred between masses, and so for example when air runs into an inclined flat plate, the air's direction, and hence its velocity, is altered, and the plate consequently feels a force. This represents a portion of the total aerodynamic load.

As we saw in Chapter 2, the principle of Conservation of Mass enables air velocity changes that result from changes to a body shape to be worked out, which then leads to calculations of pressure change from Bernoulli's Equation. The principle of Conservation of Energy underpins the whole process in a sense with the requirement that, unless circumstances dictate otherwise, no energy can be created or destroyed in a given 'system', it can only be altered into a different form.

Theoretically speaking, any fluid dynamic problem can be solved using the equations based on these principles. But, again, as we saw in Chapter 2, viscosity poses something of a problem, and effects like boundary layer development and flow separation complicate the issues. This is also true in CFD, and although certain types of 'ideal' flow can be very accurately predicted, it is not currently possible to obtain exact solutions for more complex flows. In fact the basic equations have to be bolstered by some simplifying assumptions and some additional calculations that do their best to simulate viscous complications, but which can be prone to a degree of error.

Nevertheless, as this is written, it is fair to say that the aerodynamic forces on, say, an entire Formula 1 car can be predicted to within a very few per cent of the real values, and in 2010 the first F1 car to be designed using only CFD, with no recourse to a wind tunnel, took to the track – the Wirth Research-designed Virgin. So we should not be over-concerned about accuracy in most cases. However, we should be aware that in situations where large scale flow separations and 'unsteady' flow occur, such as in the wakes of rotating wheels

for example – which is perhaps one of the more complicated cases to model – CFD may struggle to find an accurate solution. This is one of those cases where the ‘chaotic’ character of Mother Nature refuses to allow science to simplify and, hence predict, how She will behave.

There are in fact a number of different methods by which CFD can be used to reach a solution to a given case, and the most appropriate method to use will depend on the complexity of each case, and on the degree of accuracy required in the solution. For example, the simplest methods ignore the complications of viscosity altogether, and so the forces arising from surface friction and flow separation are just not taken into account. Such techniques are known as ‘panel methods’, and they can be applied quite usefully to streamlined bodies that exhibit attached flows, such as wings in some circumstances. Being relatively simple methods they are also the least time consuming to solve, and so relatively rapid solutions can be obtained, although realistically, they have limited engineering applications.

The methods that include the effects of viscosity and attempt to model boundary layer development and flow separations by applying what are known as Navier-Stokes equations that deal with fluid momentum, are inevitably a lot more complex. In fact, CFD uses simplified forms of these equations, which were originally derived in the early 1800s, together with equations relating to the conservation of mass and of energy. When considering bodies like whole competition cars, where substantial parts of the flow are turbulent, the situation becomes ever more complex. So-called ‘turbulence models’ to bolster the Navier-Stokes ‘solvers’ to attempt to deal with this real-life complication, but as there are various different turbulence models that are more or less appropriate for a given situation, you can see that the science is far from simple. Nevertheless, CFD is sufficiently mature now that it can provide pretty accurate and reliable simulations of real physical flows.

When you then consider the whole volume surrounding a complicated competition car, it is easy to see that there is a large complicated mass of moving air for which the calculations must be made. No wonder the computers of ten years ago took days to solve larger problems, or that even now solutions can take many hours, although probably to much greater accuracy than was previously attainable.

A way to generate a more rapid solution to a problem is to consider whether it needs to be examined in three dimensions (3D) or whether a 2D analysis will provide adequate information. We’ll look at some examples of 2D and 3D projects shortly, but while removing 3D effects clearly removes a substantial degree of realism from a simulation, certain types of comparison

can be satisfactorily explored first in 2D to examine trends before perhaps then using a 3D simulation to obtain some reliable data. But first let's look at the general process by which CFD analysis is performed.

### How CFD is done

There are in effect five steps in obtaining solutions from CFD. First a CAD (computer aided draughting) model must be generated, which essentially means that the component or the entire car has to be drawn on computer, in 2D if only 2D CFD is to be performed, or in 3D if maximum realism is required. This generates an electronic digital, or 'virtual', model that, as the second stage, is then imported into a 'pre-processing' package in which the relevant conditions are set up. Among the pre-processor functions, the size of the domain or volume in which the model is to be tested must have limits put around it, and this has to be large enough that the airflow at the edges of the domain remains undisturbed by the model within.

Then 'meshing' is performed in the pre-processor, the 'mesh' being a three-dimensional grid defining possibly millions of 'cells' (the tiny volumes bounded by the mesh points) in which the fluid dynamic calculations are carried out. The 'solver' then performs the CFD calculations on the meshed model. This process communicates information across all the cells in the mesh and goes ahead in an iterative way, balancing the forces and mass flows in every cell, and so across the whole flow 'domain', until a solution is reached.

Finally, 'post-processing' enables analysis of the various results such as pressures and velocities on and off the surfaces of the body being tested. The solver produces a substantial amount of data that, with the right post-processing tools, provides force calculations and enables 'visualisation' and analysis. Visualisation is without doubt a key benefit of CFD, making it possible to actually see flows, pressures, velocities, and moving 3D images of 'virtual air' flowing around a body.

Let's look at some of these aspects in a little more detail. The process of drawing by CAD obviously requires the use of a CAD software package that, in short, enables designers to lay out pretty much any shape they envisage, in 2D or 3D, using tools that generate lines, arcs, circles and so forth. CAD has been around for quite a while now, and in many design offices it has replaced drawing boards and pencils partly because of the ease with which drawings can be transmitted between designers, or directly to computer-aided manufacturing (CAM) centres which, for example, can mill or turn a product to the exact dimensions (theoretically) in the electronic drawing. There are of course other benefits to be derived from using CAD, but in our context the benefit is that a

CAD model can be imported into a CFD software package where it is treated as a solid body that can be aerodynamically tested.

The underlying physical principles by which CFD solves a particular case have been covered in the previous section. The way in which the software mathematically handles this is by constructing a mesh of cells over the surface and in the surrounding volume at which the fluid dynamic calculations are actually performed. Now it will be obvious why a 2D case will produce much more rapid solutions than a 3D one – in 2D there is but a single plane on which the mesh is laid out, but in 3D the entire volume around the body must be filled with cells in which calculations are done. For example, a typical 3D mesh around a complex case such as a whole Formula 1 car might comprise hundreds of millions of cells (the first commercial billion cell simulation was carried out on a field of 40 NASCAR stock cars in 2007). It's mind-boggling stuff, which is why it uses computers to do what they do best – crunch lots of numbers.

'Meshing' a model for CFD has traditionally been one of the more labour-intensive operations in this process, and required considerable expertise and judgement to know what density and type of mesh to use in a given situation. A denser mesh with its increased number of points will need more time to attain a solution, yet could offer increased accuracy, especially where there are steep pressure gradients around shape changes, for example. So there is a balance to be struck between accuracy and time-efficient processing. Frequently the mesh density will be increased near crucial shape details, but reduced in less critical areas.

It is also apparent from Figure 3-1 that different shape meshes are also used in different areas. Numerically speaking, the most accurate mesh type is what is called 'hexahedral', which is to say the cells are six-sided – cubic if you prefer. The CFD calculations that are performed on each cell have to balance the flow of mass, momentum and energy from one cell to another, and this is most accurately done if the cell walls are aligned with the primary flow direction, which with hexahedral cells they are. A wholly hexahedral cell mesh is known as a 'structured mesh'.

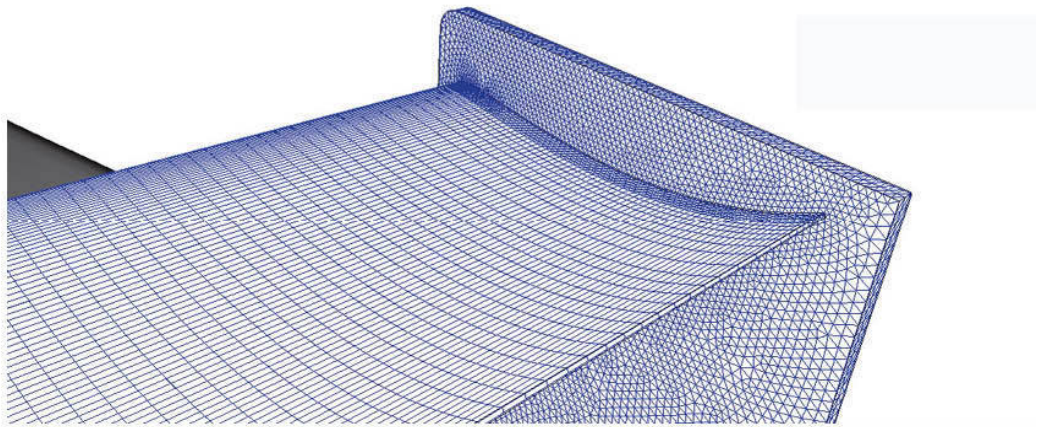


**Figure 3-1** Different-shaped meshes are used in different areas.

Cells that are ‘skewed’ from this ideal shape, and which are not therefore aligned as hexahedral cells can cause small errors during computation that accumulate into larger losses of accuracy, a process known as ‘numerical diffusion’. So while the cubic cell might be the ideal cell shape, complex body shapes obviously don’t always lend themselves to having cubic cells fitted around them, and this increases mesh complexity. Where hexahedral cells don’t fit the geometry of the body in question, tetrahedral (having four triangular shaped sides) cells are often used instead, forming an ‘unstructured mesh’. This can be fitted to complex shapes more easily and hence more rapidly, but is more prone to the type of computational errors mentioned above.

Hence, a mesh comprising hexahedral cells around critical areas, with (usually) tetrahedral mesh in less critical areas, will often be used to surround a model. Inevitably too there will be other odd-shaped cells linking the hexahedral cells with the tetrahedral cells, and any mesh comprising more than one type of cell is referred to as a ‘hybrid mesh’. It is all about an appropriate balance between achieving a solution in the right timescale, within budget, and to the desired accuracy. A ballpark quick solution can be achieved using purely tetrahedral mesh, but for optimum accuracy a hexahedral mesh would be used, albeit with a large increase in the time required to generate a solution. CFD providers have expertise in judging what is appropriate for a given case, both in terms of their direct experience with the CFD software they use, but also by being able to apply their innate knowledge of fluid mechanics to predict the types of flow regimes that will occur around a given object under study.

There are ‘auto-meshing’ software packages which are designed to take away some of the drudgery of this stage, and which may also mean, in some instances, that less expertise is needed to do a satisfactory job. There are also more user-friendly CFD packages becoming available that come with ‘templates’ tailored to a user’s particular field of interest that also facilitate this stage. All these methods will have their pros and cons, and as with so many computer-based operations, or any other task for that matter, it is a case of trying to select the best tool for the job to achieve the desired precision, in the requisite timescale, and to achieve targets.

After the model has been meshed, and other key parameters such as air density, viscosity, velocity and the requisite turbulence model, if appropriate, have been set up, and ‘boundary conditions’ have been applied to the various parts of the model to describe inlets and air speeds, outlets, whether parts are stationary or moving and so on, the solver is then set to work. Solvers work on an iterative basis until the conditions required meet the principles of conservation of mass, momentum and energy in all cells, at which point the solver is said to have converged to a solution. The time taken to reach a solution could, as has already been indicated, range from minutes in a very simple case to many hours for a complex case.

### **Post-processing**

As stated previously, CFD generates massive amounts of data from each model tested. The data is generally analysed, or post-processed, in two ways. The first and most obvious way is to calculate the quantitative values that were required in the first instance, such as lift and drag forces, or perhaps the pressure drop across a radiator. These can be compared to the values obtained in modified configurations in the quest for an optimum set-up, and this process can now be automated, as we shall see later. It is often possible to calculate the forces on individual components on a competition car model, such as the wings for example, as well as the sum of all the forces on the model.

The second way in which the data can be used is in visualisation. Flow visualisation techniques generate a range of different graphical illustrations of various aerodynamic parameters to help with analysis and understanding. For example, streamlines that show the direction and speed of flow at all points around a body (like smoke plumes in a wind tunnel only better) can be displayed; pressure or velocity distributions can be shown on the body surface with surface contours, or in the volume surrounding the body with what are

called ‘iso-surfaces’; and with some packages pressure or velocity differences between one configuration and another can be shown.

In the case of the simplest 2D CFD analysis methods the data generated is necessarily simpler, and the graphical output follows suit. For example, a 2D analysis of a wing profile might look at the wing working at a range of angles and calculate lift coefficients across that range. In addition, this type of tool can display pressure distributions from the leading edge to the trailing edge of the wing. Figure 3-2 is an example of a 2D CFD analysis plot showing pressure coefficients from the leading edge (on the left) to the trailing edge of a wing at a range of angles (referred to as ‘alfa’ here). Note, this particular software code uses negative ‘alfa’ values to indicate ‘nose down’ attitude, so -5 represents 5° nose down. Note also, that theoretical lift coefficient values are also given here, and we will come back to this type of plot again in the chapter on wings.

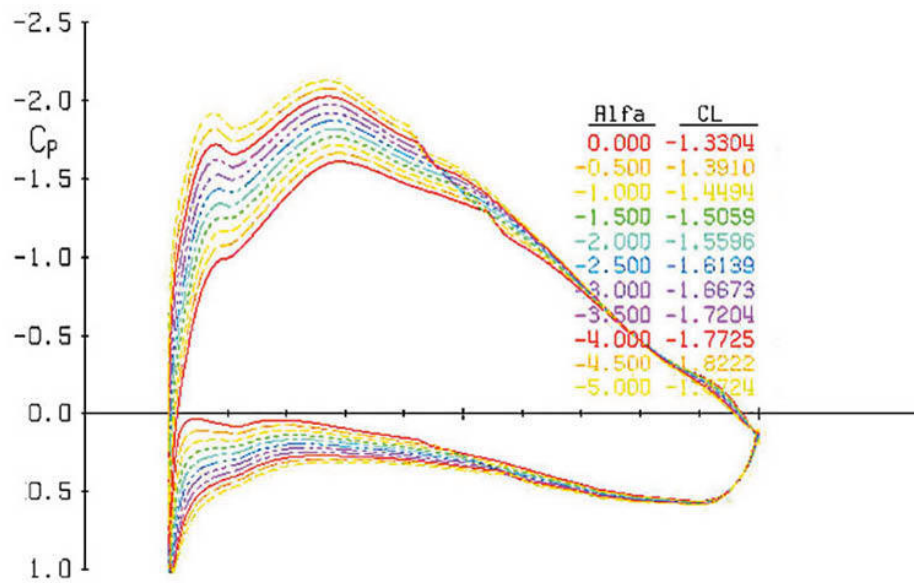


**Figure 3-2** Pressure coefficients on a wing, calculated by 2D CFD.

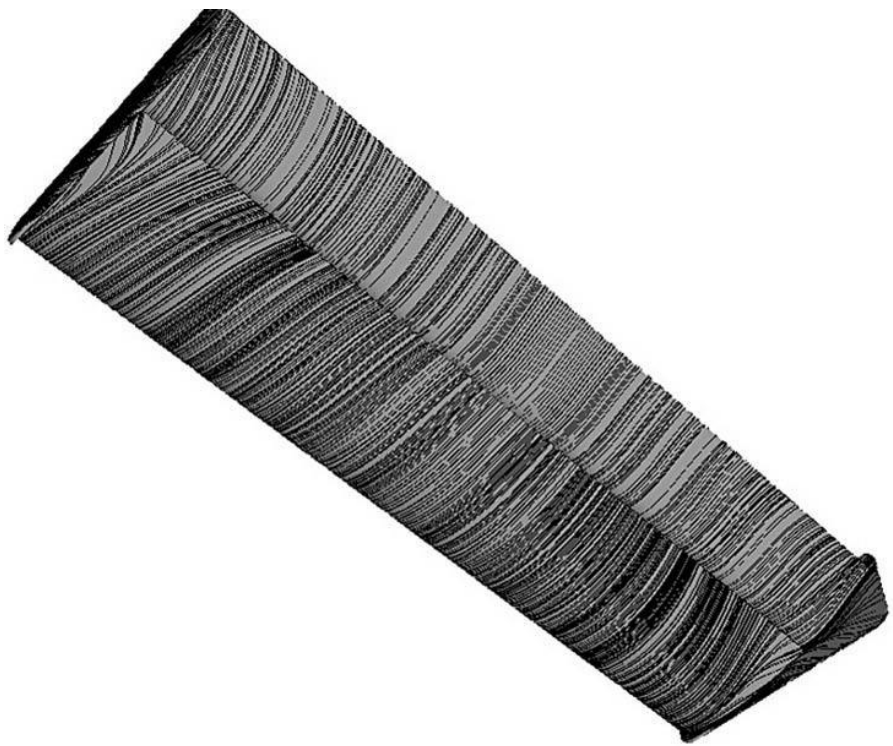
Such 2D analysis can be very useful for projects such as making rapid and cost-effective comparisons of wing profiles to determine which profiles show promise in generating greater downforce, or improved pressure distributions for example. However, flow is not two-dimensional. A wing, like any solid body, alters the airflow around it in all three dimensions, and this makes a big difference, for example, to calculations of drag because, as we saw in the

previous chapter, vortex drag is the result of a 3D flow change and therefore cannot be calculated by a 2D simulation.

Simulation in 3D provides a lot more information, but naturally involves a more complex CAD model, greatly increased meshing time, and longer processing time. However, the data generated bears much closer resemblance to real life. Lift and drag forces, including those components of drag attributable to vortex formation, can be calculated with considerable confidence. The forces on individual components can be calculated, such as the lift and drag generated by each separate element of a multi-element wing, and the percentage changes to forces as the result of set-up modifications or changing conditions can be calculated.

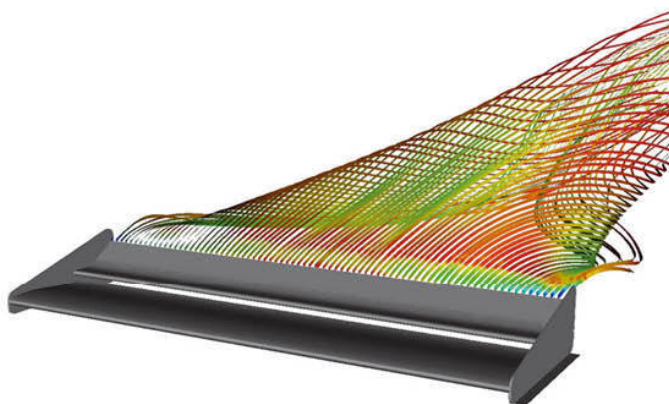
Something of at least equal interest is the ability to visualise what's going on. We'll take a brief tour of some fairly simple 3D examples to familiarise with the types of graphic plot of which we'll be seeing a lot more in subsequent chapters.

Figure 3-3 shows what's known as an 'oilflow plot'. In the real world, one of the techniques for visualising the flows on the surface of a body is to use an oily fluid such as paraffin, perhaps coloured with a suitable dye so it shows up clearly, sprayed or spotted onto the surface, and to then pass a representative airflow over the body. The oil drops, driven by the airflow, streak out and leave behind a record – 'streaklines' if you will – of the directions of the airflow over the surface. With competition cars, driving the car at an appropriate speed can obviously achieve a representative airflow, and the technique is also used in the wind tunnel. CFD can simulate the same thing by allowing surface streamlines to be plotted, and this gives an insight into the surface flow patterns that might prompt further probing. In Figure 3-3, without going into too much detail (we'll leave that until the chapter on wings) there are some areas of interest at the outboard ends of this dual element front wing.



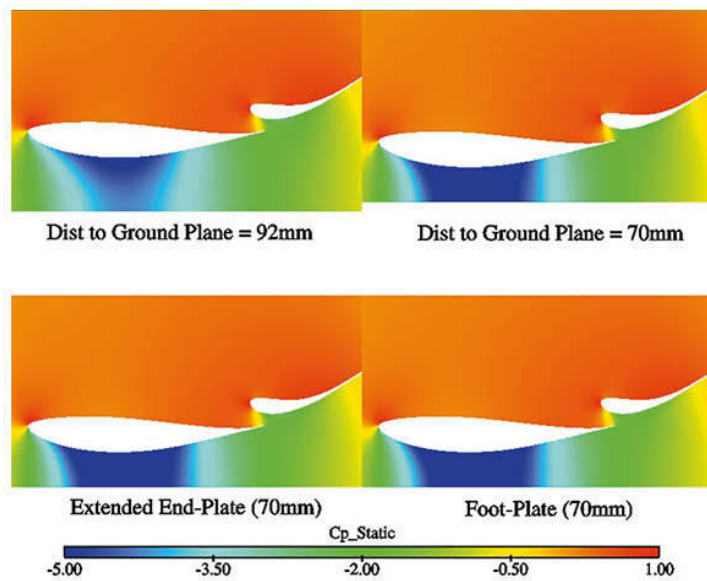
**Figure 3-3** An ‘oilflow plot’ shows surface flow directions.

Figure 3-4 shows streamlines over a portion of the same front wing profile, and the ability to visualise what is happening off the wing surface, to an extent in 3D, begins to reveal more detail about what is happening to the airflow, especially at the wing tip and downstream of that region. You probably won’t be able to avoid linking what you see in this image with what you saw in the oilflow plot above...



**Figure 3-4 Streamlines, coloured by velocity, leaving a wing.**

Figure 3-5 shows the same front wing in four different configurations and plots the static pressure coefficients ( $C_p$ -static) around the wing along a slice at the centreline of the wing's span (that is, halfway along it). The blue and green colours show low static pressure, the yellow and red show high static pressures. Thus, the low pressure under the wing and the high pressure above it are what generate the wing's downforce. If we were sitting in front of the computer with all the necessary data stored within, with these static pressure plots in front of us, we could look at any slice along the span of the wing, from the tip to the centreline shown here, and that would tell us quite a bit more about how the wing was working. We could also plot the static pressures on the wing surfaces too if we so desired.



**Figure 3-5 A  $Cp$ \_static plot shows the static pressure coefficients around a body.**

The four different configurations shown here produce different static pressure distributions, although it is not so easy to tell at first glance quite what the differences are between some of the cases. So while it is useful and fascinating to see what these pressure distributions are, it is of still more value to be able to plot how static pressures change as the result of a change in configuration. This is what a 'Delta\_Cp\_Static' plot does.

The Greek letter delta ( $\Delta$ ) is conventionally used to refer to the change in the value of a variable that results from a change to some influencing parameter. So a Delta\_Cp\_Static ( $\Delta C_p$ \_Static) plot shows how static pressure coefficients change as the result of, in this case, wing configuration changes. Figure 3-6 shows the change in static pressures (given by 'Del\_Cp\_Static' here) resulting from reducing the ground clearance on this same front wing. The picture is a lot clearer now. It is evident that reducing the ground clearance causes a greater reduction in static pressure under the main element, as shown by the blue colour here.

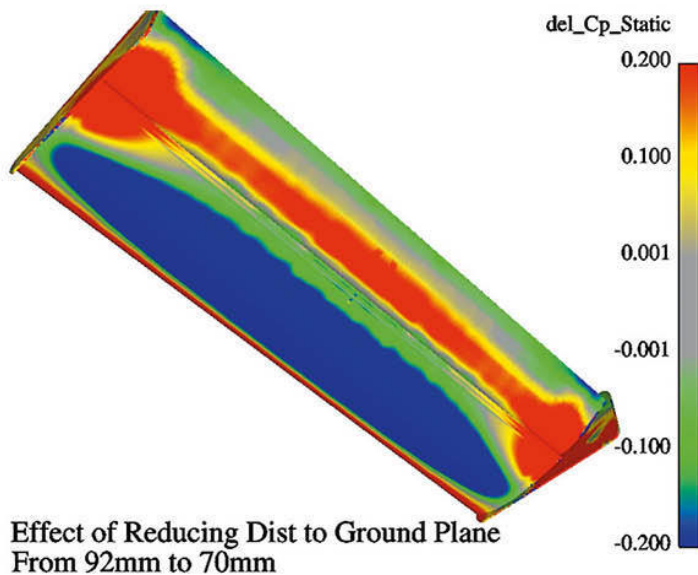


**Figure 3-6** A Delta\_Cp\_Static, or Del\_Cp plot shows the differences in static pressure on a model in two different configurations.

But what was not evident in the Cp\_Static slice was how the static pressure beneath the second wing element (the 'flap') was actually higher in the reduced ground clearance case than it was at the original ground clearance. Now, the red area under the flap in the Delta\_Cp\_Static plot tells us this quite clearly. The static pressure is still low here, but it is not as low as it was. We aren't going to get into the whys and wherefores now, but this does serve to show what a Del\_Cp\_Static plot is and what it can tell us.

Another type of plot that can be useful is the 'Cp\_Total plot'. In effect this plots the total pressure energy, which is to say, the sum of the static pressure and dynamic pressure energy around a body. If you recall how Bernoulli's

Equation was defined in the previous chapter, it was said that the sum of static pressure plus dynamic pressure should be constant, providing there are no losses. So, a more complete way of stating Bernoulli's Equation might be to say that the sum of static pressure plus dynamic pressure *plus the losses* is constant. In the real world there are always losses in energy in any system, or, more strictly, conversions of energy into other forms, such as heat and sound, and it is no different in aerodynamics. We saw in Chapter 2 how viscous effects contribute to losses in energy through skin friction, and the image in Figure 3-7 shows this happening.

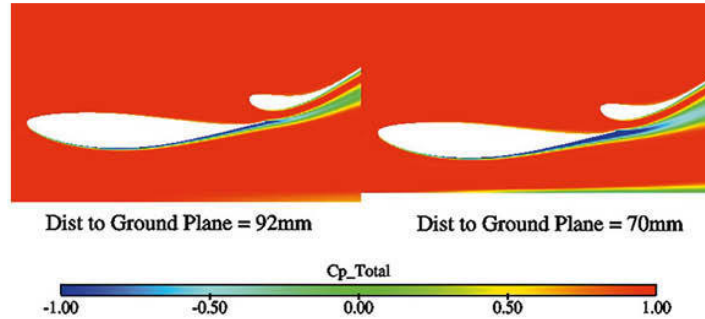


**Figure 3-7** A  $Cp_{\text{Total}}$  plot shows total pressure energy and reveals where losses occur.

For the most part in this slice through the volume surrounding our front wing, the red colour shows that the total pressure remains constant, as we would expect. It is evident however, that in the area adjacent to the lower surface of both the main element and the flap that there have been losses of total pressure. There have also been smaller losses along the upper surface too, and these areas of lost total pressure mark out the boundary layer along the two surfaces of the wing. The two boundary layers can be seen to merge at the trailing edge of the main element where they form its wake. So a  $Cp_{\text{Total}}$  plot can show where the airflow loses energy, and becomes 'tired'. We also discussed in the previous chapter how steep adverse pressure gradients can work against us, and how a tired boundary layer can add to the likelihood of flow separation. Well, a  $Cp_{\text{Total}}$  plot can indicate where this type of energy loss is likely to occur. It is interesting to see that the image on the right-hand side of this figure shows greater energy losses when the ground clearance is reduced. We'll ponder that some more later, but for now this example just serves to show what a  $Cp_{\text{Total}}$  plot can tell us.

## The practical benefits of CFD

As we have seen, to be able to perform CFD a CAD model is required of the component or car to be tested, but once that model is available, it is possible to run a large number of CFD simulations much more rapidly, and much more cheaply than making a real, physical model (or the full-scale, real thing) and running it in a wind tunnel or on a track. Overall concept and shape as well as myriad smaller details can be tested prior to manufacture, offering a much greater probability of getting a design right first time. Once a virtual model has been tested with CFD it is possible for the designer to analyse and visualise the flows around it at leisure, and to come back time and again to re-examine the data and visualisation plots to facilitate design optimisation. CFD thus provides an incredibly valuable and cost-effective tool that enables the designer to focus on the areas that are most in need of attention. This is something a wind tunnel cannot provide – flow visualisation is possible but is necessarily much more limited, and it is only possible to measure forces and moments exerted at the ‘attachment points’ of the model or vehicle to the tunnel force measurement equipment.

A further advance in CFD methods is provided by ‘auto-optimisation’. There are computational methods now available that mathematically assess the results obtained by changes to configuration or geometry (shape) of an object or an entire car, and which automatically select the most promising trends to explore. Of course, the constraints within which to operate, and the extent to which geometric parameters may be altered, are manually defined by the user, but the rest of the process happens automatically once the CFD engineer clicks on the ‘run’ button.

One of the key advances in auto-optimisation has been the arrival of so-called ‘mesh deformation’ software. Traditionally, the way in which a body’s geometry was optimised with CFD was to run a base case, then alter the CAD model to explore what might be perceived as a promising design modification, then re-mesh the model and run another CFD case. The results would then be compared and the process repeated until the best case that could be found was determined. This was all very time-consuming, especially the re-meshing phase. Now, by integrating computational optimisation methods with automatic mesh deformation, it is possible to explore geometry changes, within a set of constraints, and have the software alter the mesh along with the geometry. This precludes the need to re-mesh at every stage and has massively improved the efficiency of optimisation with CFD, enabling even more options to be explored in a given time.

It is impossible to resist the temptation to speculate on what might happen in the future with software like this. Will it be possible to tap in the dimensional constraints imposed by the technical regulations of any given category to define a starting shape for a CAD model, and then have the auto-optimisation software churn away until the absolute optimum aerodynamic solution is achieved? It sounds at first as though it ought to be possible, but just what *is* an optimum aerodynamic solution? And is there not going to be a different optimum solution for every track or venue visited? Thankfully, there are probably still too many variables for the entire human element in this part of the design process to be removed, and science will not totally supplant the part that art plays in competition car aerodynamics.

### **CFD limitations?**

As we have seen in this chapter, CFD is based on solving approximations of mathematical equations that are said to govern, but perhaps more accurately should be said to attempt to *describe* fluid flows. The ways in which viscosity and turbulence are modelled are of particular importance in determining how accurate CFD simulations are. Nevertheless, it would appear to be possible to estimate the forces on an object as complex as a racecar to within a very few per cent of actual physical measurements, although physical measurements themselves are also fraught with assumptions and practical difficulties. But in most cases where CFD is used, wind tunnel and track validations are still performed, and this may continue to be the case for some time to come.

However, in 2010 we saw the first Formula 1 car to take to the track the aerodynamics of which had been *entirely* developed in CFD without any wind tunnel validation. The Virgin F1 (Marussia, now defunct) car was designed by Wirth Research, the company that had previously used the same approach to design the Acura prototype sports racing car that did so well in the American Le Mans Series in particular. Initially at least the Virgin was just the quickest of the three new cars to hit the Grand Prix scene in 2010, the other two (Lotus, now Caterham, and HRT, now defunct) having been developed at least in part using more conventional scale wind tunnel models, and on that evidence it would seem that the two approaches had equal merit. This in itself was something of a landmark.

The underlying computational methods of CFD continue to be improved with time, and interested readers who research the topic further will find reference to numerous turbulence models that may be added to the ‘basic’ Navier-Stokes equations, as well as ‘hybrid techniques’ like ‘Large Eddy Simulations’ (LES) and ‘Detached Eddy Simulations’ (DES). All are attempts

at modelling better what actually goes on near the surfaces of the bodies under study. Thus, most CFD software will offer the user choices of turbulence models to select from.

At a basic level CFD has historically been used to produce ‘time averaged’ results using methods referred to as ‘steady state’, but in turbulent regimes it is well known that the flow is ‘unsteady’, and as such ‘transient’ methods have become more widespread, these attempting to provide real time simulations of the unsteady fluctuations in complex flow fields. The user of steady state CFD becomes aware of the unsteadiness in flows around bodies where large-scale separations occur, such as wheels, because it is sometimes harder to achieve a converged solution in such cases.

From the previous two paragraphs it is clear that as yet there is no single ‘Go’ button to be pushed to derive a comprehensive and definitive aerodynamic solution using CFD. To obtain the best results possible, not only is it preferable to have some understanding of the underlying fluid dynamics to be able to make the right choices in setting up simulations, it is also desirable to have an understanding of the way in which the software deals with these choices. Having said that, there are increasing numbers of products that are becoming available to engineers who want to be able to evaluate components early in the design cycle, and for whom the last word in leading edge software is not only unnecessary, it’s also inappropriate. These products can provide illuminating and invaluable insights into the general nature of internal and external flows around competition car components and even simplified whole car models, and some illustrations and data in this book were generated by the author using ‘entry level’ CFD software.

## Accessible software

Historically CFD software has been pretty costly for individuals and small teams to contemplate, but by 2010 there were signs of this situation changing. First, for those with high levels of computer literacy (think ‘capable of hacking’ level, not that this is recommended of course), OpenFOAM became available. This was actually first released in 2005, and is ‘open source’ software issued under the GPL (General Public License) arrangement. In short, this means it is free! But, and it’s quite a big but for most people, it’s not the kind of software that those who are more familiar with the typical graphical user interface personal computer environment, like Microsoft Windows or Mac OSX, will be able to open up and be immediately productive with. It also usually runs under the open source Linux operating system, and although that in itself is not a difficult environment to work within (if I can manage it then

pretty well everybody will be able to) it does require having either a separate PC or one that ‘dual boots’ to allow either Windows or Linux to be used. There are apparently versions of OpenFOAM, known as ‘distributions’, available for Windows and Mac OSX too. But if your last project was hacking into your government’s computer systems then OpenFOAM will pose few difficulties.

A number of independent CFD service providers, as well as automotive manufacturers and Formula 1 teams were using OpenFOAM by 2010, and with its freedom from the annual licensing costs usually associated with the commercial CFD software packages it’s easy to see why. There are initial costs in terms of adapting the software to suit your particular use, and of course training too, and it is reckoned that during the first year this typically costs about the same as a commercial licence would. After that though, its use is free.

There are also commercially available products that provide user-friendlier ways for the smaller team or individual to get their hands on some serious CFD software. One particular company in the USA called Symscape has developed an easy to use graphical user interface (GUI) that fronts what it calls a ‘custom version’ of OpenFOAM to provide the user with full 3D CFD capability in a package called ‘Caedium’, including geometry (CAD model) import and creation, automated meshing, a RANS solver and a range of post-processing tools. It has been suggested that I should point out that other open source software components are incorporated in Caedium too, namely ‘wxWidgets’ (a ‘cross-platform GUI’), OpenCascade (a ‘geometry engine’) and VTK (3D visualisation), so that’s all clear then! Windows, Linux and Mac OSX versions are available.

The principal of Symscape, Richard Smith, had this to say in May 2010: ‘My aim with Caedium is to offer 20% of the functionality of the big CFD vendors’ offerings, which hopefully covers 80% of most user needs, at less than 10% of their prices.’ This really did bring powerful CFD within the reach of many more motorsport users, from serious hobbyists and small teams up to semi-professional teams who might want to model wings, duct details and so forth, and maybe even ‘reduced detail’ car models too.

No doubt more and cheaper options will become available over time, possibly even entirely free, easy to use open source products too!

## **Computer clusters**

A single computer has a finite amount of processing power and memory available to perform numerically intensive tasks like CFD. But by connecting a

large number of PCs together into what's known as a cluster makes massive computing power available at a relatively very low price. Leading independent UK-based CFD service provider TotalSim did this by connecting arrays of essentially 'high street' but high-end PCs to provide super-computing power. In 2015, the company had multiple clusters with nearly 2000 cores. Within each cluster there was a master node which received and distributed the work to the other slave nodes. Additionally a single workstation hosted a queuing system that queued and distributed jobs to the various clusters. Jobs were scheduled according to size and priority. Within a cluster the CFD job was divided up across the nodes or slaves such that each node solved the flow in a region of space around the car. The nodes then communicated the results of their calculations with nodes working on the neighbouring space. The whole process was an iterative procedure working to minimise global error in the flow solution. Once a satisfactory level of convergence (which we can think of as 'solution accuracy') was reached the cluster then extracted forces and flow visualisation data before moving on to the next job. This all sounds pretty mind-boggling, but it gives an idea of how a high end service provider has to function to keep at the top of its game.

So, while it is true that a single PC can nowadays carry out CFD tasks, clearly the leading edge service providers are investing in ever greater number-crunching power to keep at the head of the field, and enable ever more complex problems to be solved. At a more basic level though, and on quite basic models, CFD will provide us with some terrific insights, in the forthcoming pages, into many aspects of competition car aerodynamics.

# Chapter 4

## Airdams, splitters and spoilers

AS WE DISCOVERED in Chapter 1, Michael May's ill-fated attempt at introducing real downforce to motorsport back in 1956 was either ignored, or more likely, perhaps, just not understood. Whichever it was, his efforts must have been completely forgotten about, because it was quite some time before racers once more 'discovered' downforce, and even then, it seems as if it was almost by accident.

It was during the 1960s that racers of closed-wheel production-based and sports GT cars got really concerned about aerodynamic lift at speed. By this time, top speeds had risen to the extent that the aerodynamic forces were pretty large, and drag-reducing streamlining was beginning to create shapes that could actually cause positive lift.

### **Years of instability**

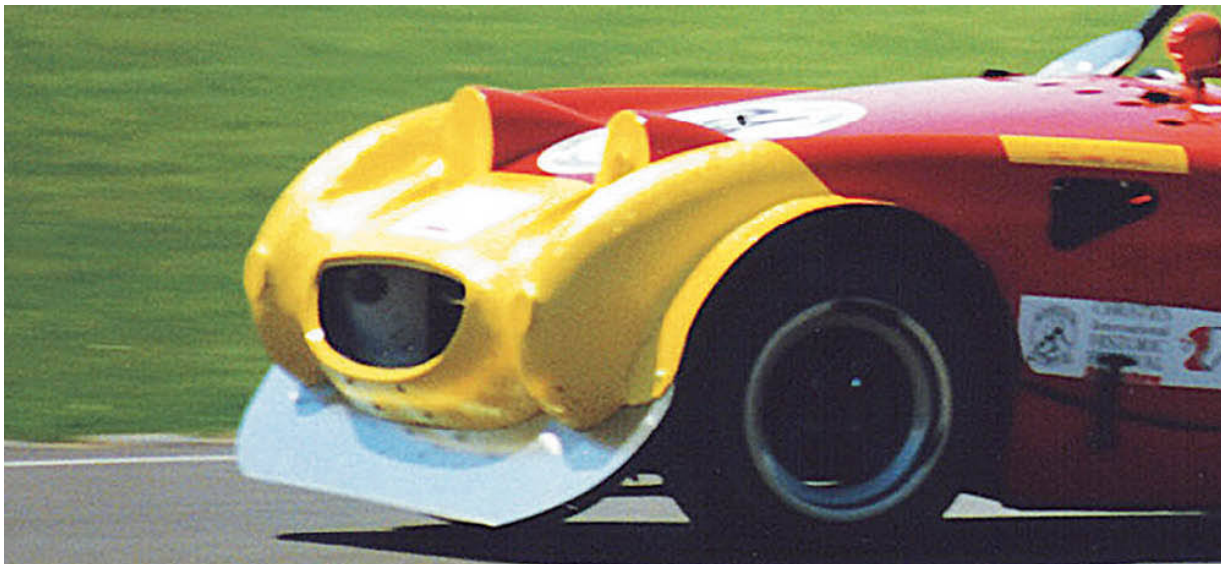
The effect of such lift was, literally, very unsettling, especially for the drivers, because cars became unstable at speed. Undoubtedly this problem would have attracted most attention in the faster sporting arenas such as Le Mans, and the Superspeedways of the USA. However, because their shape is intrinsically less lift-inducing, open-wheel single-seater racecars didn't experience this high-speed instability to the same extent as their closed-wheel brethren.

So, it was in the closed-wheel categories that lift reducing attachments first sprouted. 'Chin spoilers' and 'airdams' at the front, and 'ridge' spoilers at the rear were amongst the first anti-lift devices. Front 'splitters' later augmented airdams at the front, and over the years since the 1960s, as these items have been refined and developed, other variations have been added with the same lift-reducing purpose. This chapter will attempt to explain how these devices work, and what can be expected from them in terms of lift reduction or actual downforce production. Whether it was rear ridge spoilers or front airdams that appeared in motor racing first is a matter for the historians to argue over. In a practical sense, the end of the car that those 1960s racers would be most likely

to have studied first, aerodynamically speaking, would have been predominantly influenced by which end started to lose grip first at speed! But as far as we are concerned here, we have to start at one end or the other, and we will begin where the air (usually) strikes first – at the front.

### Front spoilers

Front spoilers vary in design complexity, from simple ‘chin’ spoilers, which are little more than a vertical or near-vertical piece of rigid, flat sheet bolted to the lower front panel of a car, to the beautifully shaped ‘airdams’ now integrated into road car designs, and extended in dimensions and effectiveness on competition cars. For the purposes of definition here, let’s assume that a front spoiler is something to be *added* to an existing car shape, whether or not some form of spoiler or airdam already exists.



*Front spoilers can be very simple but still very effective.*

In its simplest form, an ‘airdam’ extends downwards from the lower front panel of the car to reduce the car-to-ground gap. So how would this help? A CFD project on just such a device fitted to a virtual model of a NASCAR racecar reveals a lot about the mechanisms as well as the likely magnitude of the forces created by a simple airdam. Of course, such devices are strictly defined and limited by NASCAR rules, so the exercise shown here is an academic one to illustrate the general effect as well as the magnitude of force changes created by dimension changes.

Other textbooks tend to agree on the benefits of airdams to both downforce and drag, but explanations of the mechanisms involved are

somewhat mixed. The CFD exercise described and illustrated here used a full-scale model NASCAR racer that incorporated detail such as a ‘rough’ underside with exhaust pipes, chassis rails and cavities, and also a rear spoiler (see Figure 4-1). CFD simulations in 3D were run at 50m/s (180km/h or 112mph) air speed, and three different airdam depths.

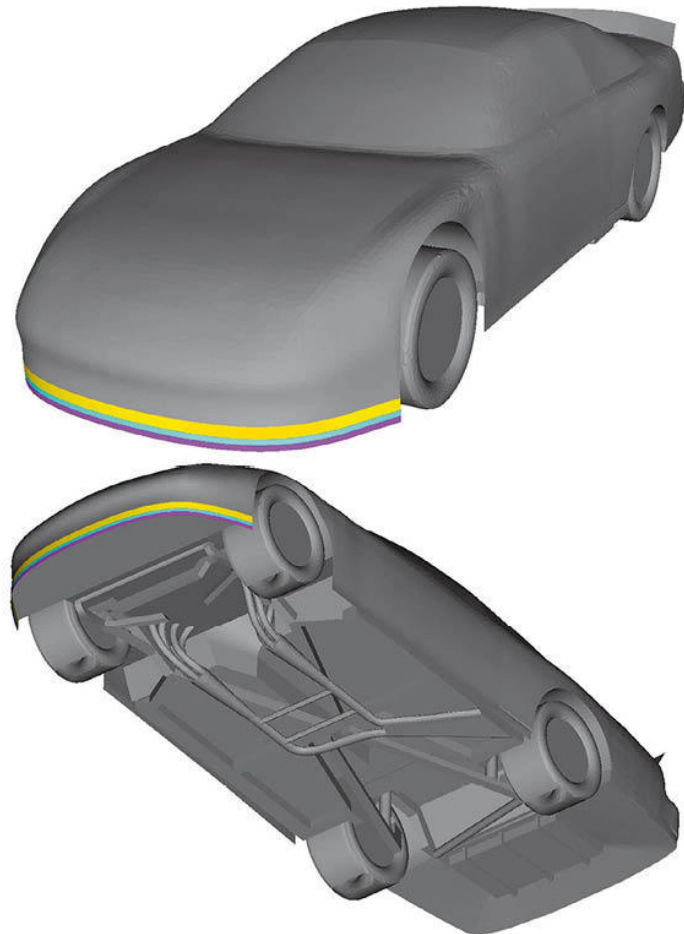


**Figure 4-1** A digital model of a generic NASCAR racer, with airdam depth variations shown.

The plots in Figure 4-2 show the results of downforce and drag (as dimensionless CDfA and CDA values, the product of frontal area and the relevant coefficient). We’ve ignored convention here for clarity; CDf values in this case represent a ‘coefficient of downforce’ that precludes the need (for now) for sometimes confusing ‘negative lift coefficients’. The plots show total downforce increasing and drag decreasing with increasing airdam depth. The downforce benefit dominates at the front end of the car. Furthermore, the rear

end actually loses some downforce. The trend is heading towards a more even front-to-rear balance and greater aerodynamic efficiency (increased downforce-to-drag ratio).

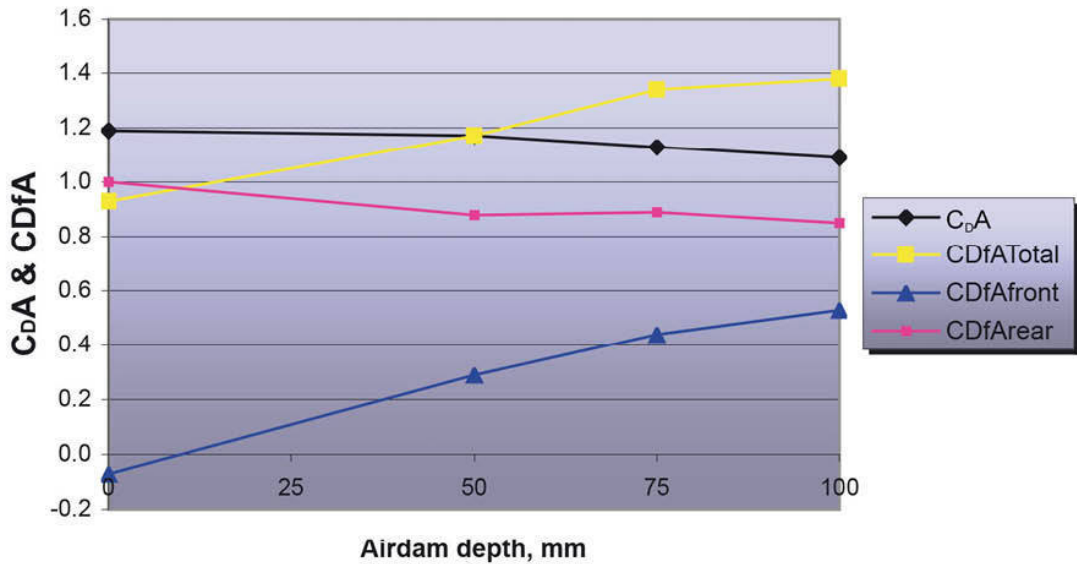


**Figure 4-2** The effect of airdam depth on downforce and drag.

As only three depths were evaluated it would be more than a little carefree to suggest these trends would continue beyond the deepest airdam measured here, and other references suggest that drag would actually start to rise again at some greater depth. However, the data and plots available here help to explain the effects.

Looking first at how the airflow is modified by the airdam, Figure 4-3 shows velocity coloured streamlines mapping the airflow at a height of 200mm above the ground; clearly less air passes beneath the car and more air is pushed around the sides with the 100mm airdam. In Figure 4-4 we can see there is a region of low velocity recirculation behind the airdam; furthermore the stagnation point, where the air hits the car ‘head on’, is lower when the airdam is fitted, so more air is also being pushed over the bonnet (hood), and therefore less under the car, when the airdam is present.

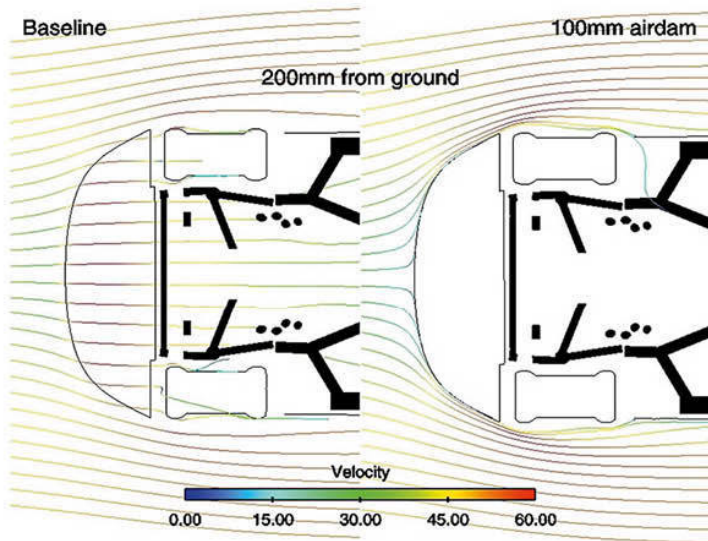


**Figure 4-3** A view from above of streamlines 200mm above the ground, with and without a 100mm airdam.

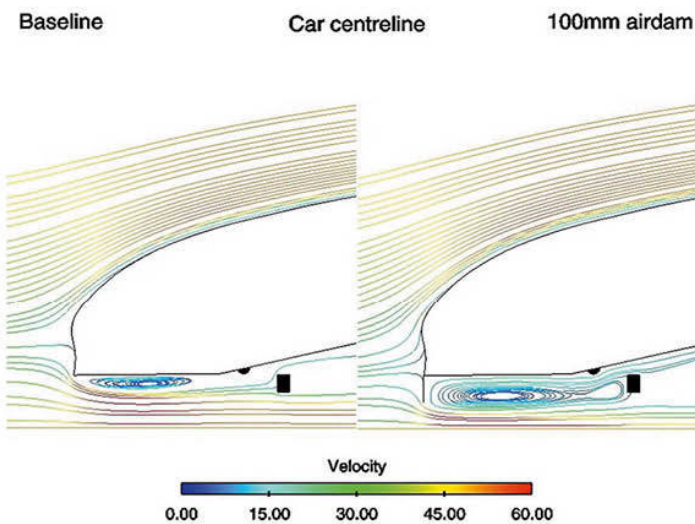


**Figure 4-4** A side view of streamlines with and without airdam.

Changes to the static pressure on the upper and lower body surfaces occur because of these flow modifications. Figure 4-5 shows the change in pressure coefficient, Delta\_Cp, plotted on the main surfaces, but only the vertical (Z-direction) component of the static pressure change is shown here, so that the

effect on downforce is isolated for clarity, hence the Delta\_CpZ designation. Thus reds and yellows indicate additional lift (upwards) while blues and greens indicate additional downforce.

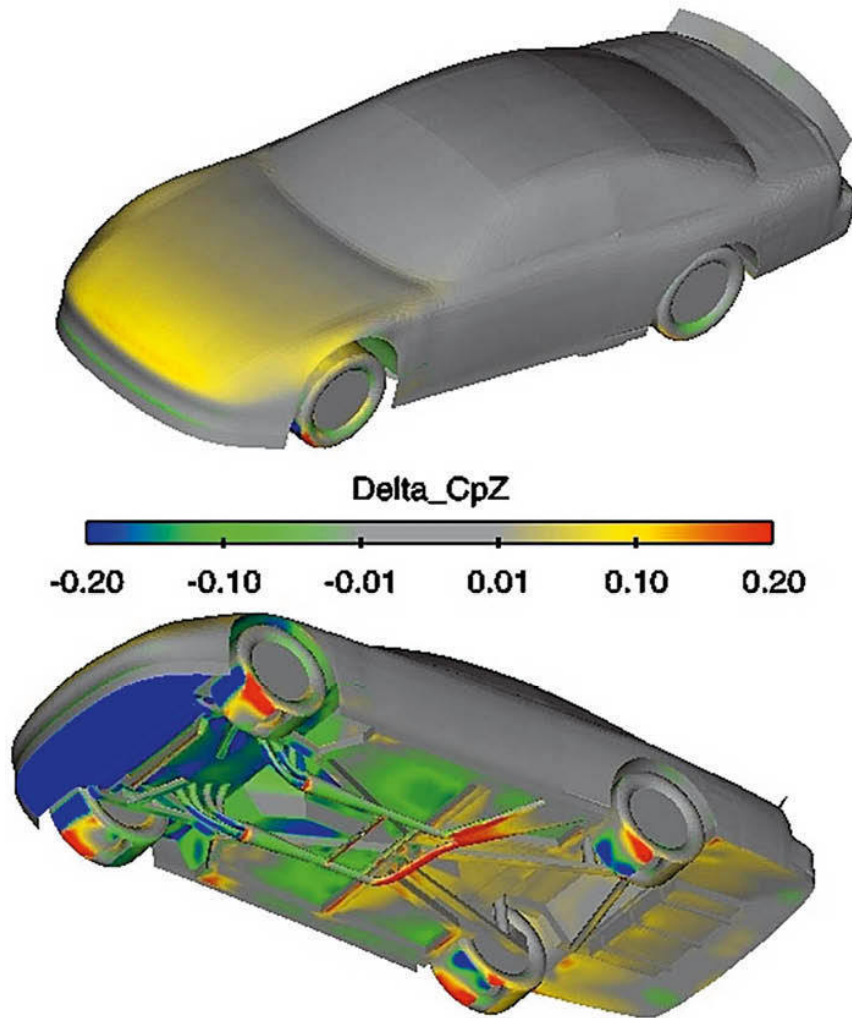


**Figure 4-5** Changes to static pressure affecting downforce.

The forward upper surface shows a small positive (upward) change in static pressure, indicating the airdam causes some additional lift over the bonnet. The underside however shows a large area of negative (vertically downward) change in static pressure, indicating additional ‘suction’ on the underside caused by the airdam. This extends roughly halfway along the car, and then

changes to a slight positive value, indicating some lift under the rear after the airdam was fitted. The net result is the gain in downforce we see, which is concentrated at the front. This will not be the last time that we see a design change to one end of a car causing a force change at the opposite end...

We can also see how the drag changes. Figure 4-6 shows the Delta\_CpX plot, indicating static pressure changes in the X-direction (parallel to the car's longitudinal axis), where positive (red and yellow) is an increase in rearward acting static pressure (more drag) and negative (blue and green) is a decrease in rearward acting static pressure (less drag). Clearly, the airdam itself is a source of drag where the air runs into it, but there is less drag on the forward part of the bonnet above it. There is also a reduction in drag from the wheels and significant areas of the underfloor and associated clutter. The net result is an overall decrease in drag.

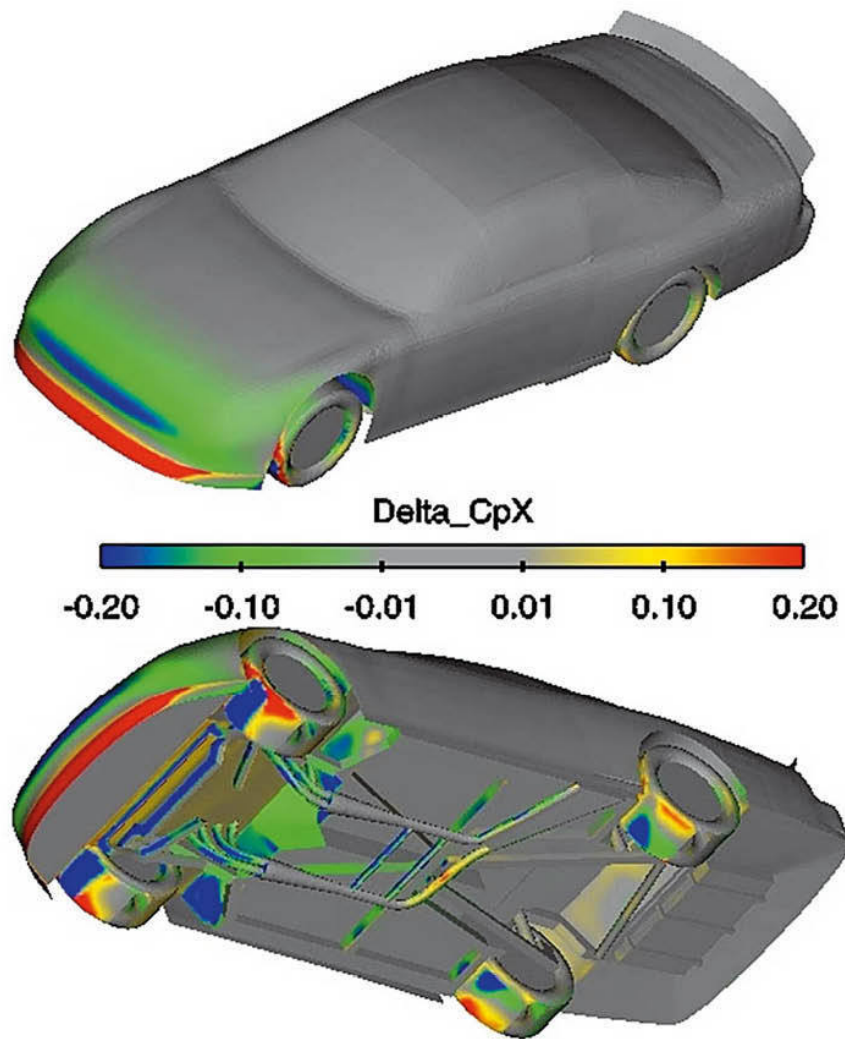


**Figure 4-6** Changes to static pressure affecting drag.

Can we explain these changes using Bernoulli's Equation? Well, the reduction in lift and drag over the forward part of the bonnet can both be explained by the increased flow over this area caused by the airdam, which leads to an increase in velocity, and a Bernoulli-type drop in static pressure. The slope of the bonnet means there are forward and vertical components to this static pressure reduction, leading to decreased drag and increased lift over this region. The additional drag on the airdam itself is also simply explained by Bernoulli, the airflow coming to a virtual stop here, leading to low velocity and therefore high static pressure acting rearwards.

The underside region behind the airdam is not so simple. As we saw in Figure 4-4, the air behind the airdam is recirculating and moving relatively slowly, and yet as we saw in Figure 4-5 the pressure is reduced behind the airdam. This seems to contradict Bernoulli, and this effect more readily falls into the category of apparently non-Bernoulli downforce as mentioned at the end of chapter 2.

Can CFD help to explain this? Figure 4-7 shows a Delta\_Cp plot that reveals the changes in static pressure along the car centreline that occurs when the airdam is fitted. This shows clearly that there is a very marked drop in static pressure behind the airdam, which is where our front-end downforce originates. We know that the velocity here is low, so we therefore know that the dynamic pressure is also low. So we must conclude that losses from the flow have increased here. Figure 4-8 shows a Delta\_CpT plot, which is the change to total pressure, and confirms that *total* pressure has indeed dropped behind the airdam. The reduction in static pressure has therefore actually been caused by *losses*. This might be expected to be inefficient and lead to excessive drag, but because of the inefficient nature of the flow under the car without an airdam the overall effect is actually beneficial.

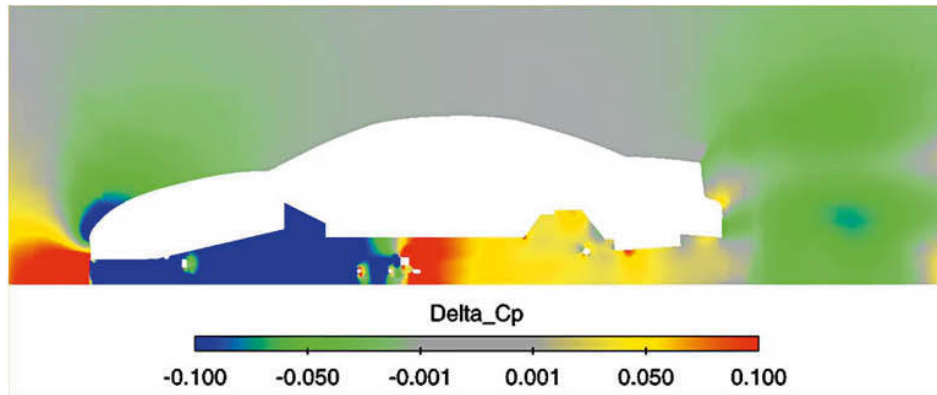


**Figure 4-7** The effect of adding an airdam on static pressure along the car centreline.

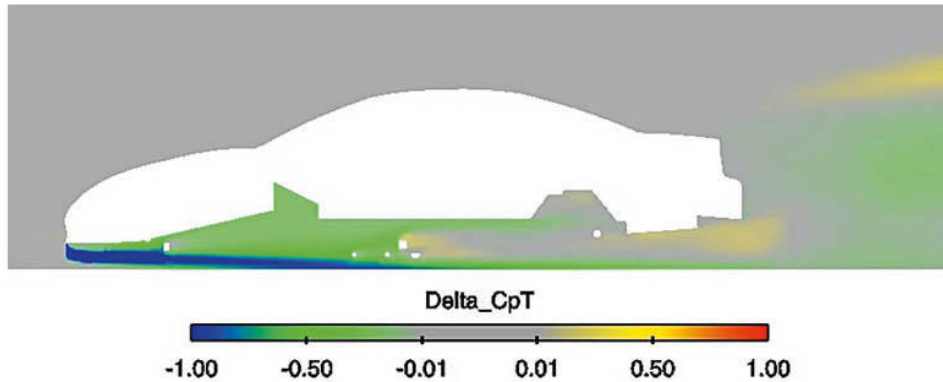


**Figure 4-8** The effect of adding an airdam on total pressure along the car centreline.

There are some qualifying remarks to be added to these observations, particularly relating to the reduction in drag discovered in this simulation. Clearly the air passing under a car with such a ‘rough’ underside like this pretty realistic model had, will not have a smooth passage, and it is easy to understand that this causes significant drag. So, if fitting an airdam reduces the mass airflow through this region then it follows that drag should reduce – less air interacts with all the lumps, bumps and cavities. However, for a car that has already been fitted with a smooth underside, perhaps partly in a search for reduced drag, a further drag reduction should not necessarily be expected from an airdam; in reality, an increase in drag may well occur in this case by virtue of the increased drag on the airdam itself. Nevertheless, the benefit of lift reduction/downforce may still be achieved, which helps improve the car’s on-track performance.

So, the airdam creates lift reduction, or downforce if we are lucky, by blocking off the flow to the underside. What magnitude of effect can we expect? The CFD simulations here produced the following results, relative to the baseline model with no airdam extension:

50mm airdam:  $\Delta CD_{FF} = 0.144$

75mm airdam:  $\Delta CD_{FF} = 0.204$

100mm airdam:  $\Delta CD_{FF} = 0.240$

These ‘ $\Delta CD_{FF}$ ’ values indicate the change in ‘downforce coefficient’ at the front of the car relative to the no airdam case, and each represents a gain in

front end downforce. In absolute terms, assuming a frontal area of, say, 2.5 square metres, and an air velocity of 50m/s (equal to 180km/h or approximately 112mph) the forces involved equate to an extra 551N (124lb) of downforce with the 50mm airdam up to 919N (206lb) with the 100mm airdam.

In order to determine the significance of these downforce values we need to assess them in relation to the static weight on the front axle of the car in question. Thus, 200lb (rounded off for convenience) represents 18% of the weight on the front axle of a 2,200lb (1,000kg) car with a 50/50 weight distribution, and if this much downforce is obtained, then the potential grip increase at this speed will be in direct proportion. You may recall, in Chapter 2 we said that typical production cars are said to produce around 160lb to 180lb (72.7kg to 81.2kg) of positive lift, overall, at 100mph. So an airdam could be expected to not only cancel this level of positive lift, but if it was a reasonably deep and effective device, to generate some genuine downforce as well. The danger here though is of over-generalising, and in reality the effect on any particular car will only be determined by appropriate testing, be it via CFD, a wind tunnel or on a track.

Remember, in order to calculate the forces at any other speed, that the force is proportional to the square of the speed, so at 25m/s (90km/h, 56mph), divide these figures by four, and at 100m/s (360km/h, 224mph) multiply them by four. At any intermediate speed of interest, say 75mph, multiply by the ratio of the speeds squared, that is,  $(75/112)^2 = 0.448$ .

There is a further important related issue to keep firmly in mind when considering a front airdam for your racecar – cooling. This is not just engine cooling, but brakes and transmission cooling too. Interestingly, by creating a low static pressure area below a car, the flow of cooling air through the engine compartment may actually be enhanced. At the risk of being thought slanderous, it always appears as if the designers of road vehicles create a nice big hole in the front of the car to channel air *to* a radiator matrix, but they then seem to forget about getting the air *from* the radiator. Somehow, the air is supposed to find its own way out, around and past the engine, and probably the transmission too, and into the turbulent, sluggish flow beneath the car. However, the fitting of an airdam, which we have seen causes a reduction in static pressure beneath the front of the car, can also create some suction on the air in the engine compartment. The effect of this can be to encourage more cooling air away from the radiator, and the engine may run cooler as a result. This in turn may enable a smaller air intake for cooling air to be used, with a further positive influence on drag – but this would have to be the result

of some cautious experimentation to avoid taking the notion to a reckless extreme that caused overheating.

A front-engined car relies on a flow of air over its crankcase to facilitate some of the heat rejection, so care must be exercised when contemplating an airdam. At the very least, it may be necessary to provide an appropriately sited cutout, ducted and radiused of course, to channel some air to where it is needed for this role. The same may apply to a front-wheel-drive vehicle if the transmission requires cooling in this way, and in the same vein, the airflow to auxiliary oil coolers must be maintained. Brake cooling will be ignored at your peril too, although the importance of cool brakes will of course depend on the particular competition category. As with the other aspects of cooling mentioned here, it is possible that installing an airdam will interfere with that part of the airflow that transports heat away from the front brakes (and possibly the rear brakes too, let's not forget). Once more, radiused ducts that channel air to the brakes may prove to be necessary. Track testing and actual competition may well be the only way you will find out what the ultimate requirements are going to be.



*A front splitter.*

## Splitters

We have seen that a basic, simple airdam reduces under-car static pressure by modifying the flow under the car. As Figure 4-4 shows, an airdam locally accelerates the velocity of the air which does flow under it, in the reduced car-to-ground gap, which also helps towards the local reduction in static pressure. So how can this be further exploited? We can add a 'splitter' to the airdam. In

its most basic form this is a horizontal extension of the lower lip of an airdam that protrudes forwards, although usually it would extend rearwards under the front of the car too, regulations permitting. Simple, and even crude though the splitter may appear to be, it is actually an extremely efficient aerodynamic device. A CFD study on the same NASCAR stock car model illustrates the mechanisms involved. Again, 3D runs were carried out at 50m/s air speed (180km/h or 112mph), and three different splitter lengths attached to the 100mm airdam modelled in the previous section were evaluated (see Figure 4-9).

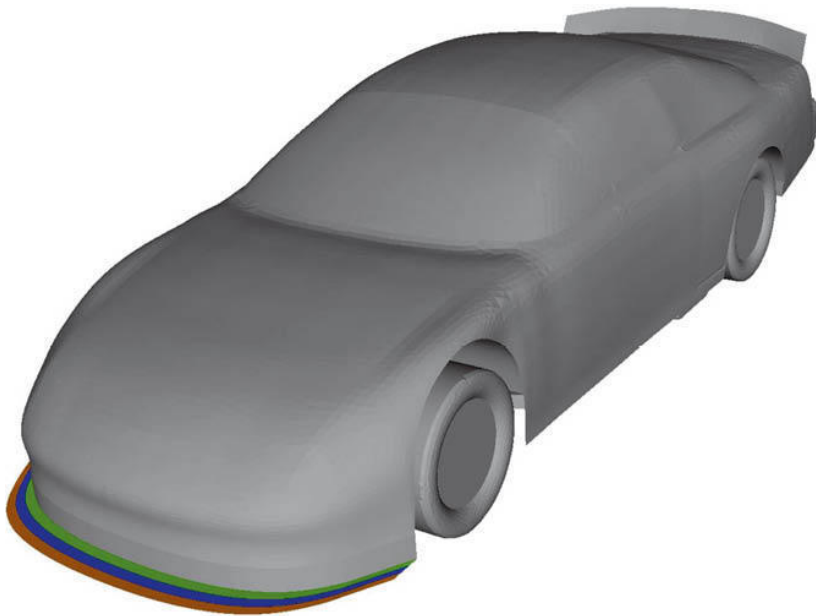


**Figure 4-9** Splitter variations tested.

The plots in Figure 4-10 show the results of downforce and drag (as dimensionless CDfA and  $C_D A$  values again) and show total downforce increased (by just over 10% compared to the baseline airdam only case) up to a splitter length of 100mm, while drag remained virtually unchanged (it actually increased by very little). As with the airdam, the gains in downforce were at the front end of the car, and in fact, once more the rear end actually lost some downforce. The front downforce peaked with the 150mm splitter length, but the further loss of rear downforce saw the total downforce slightly down compared to the 100mm splitter case.

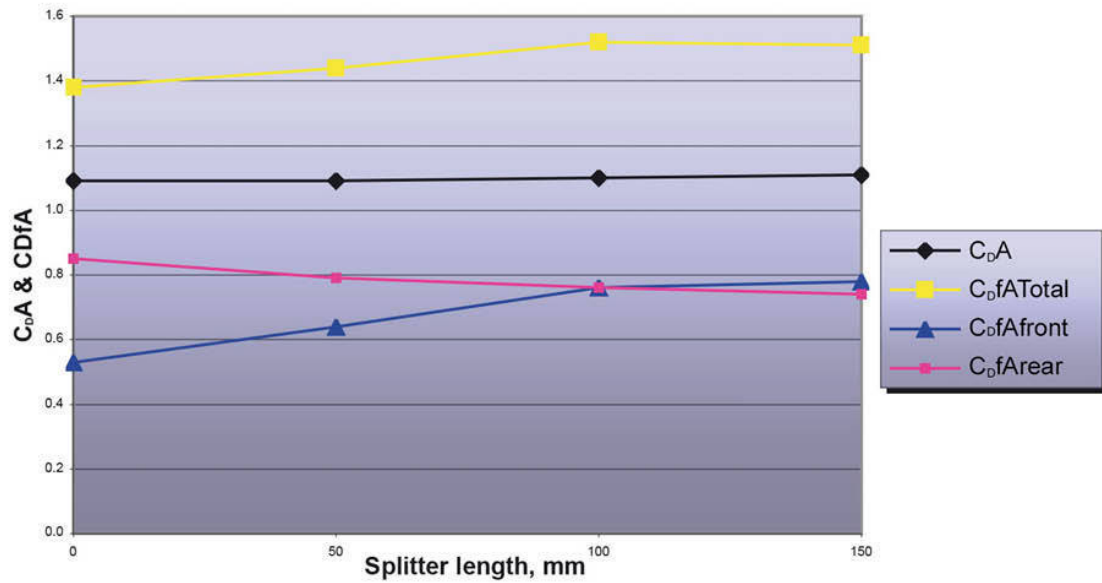


**Figure 4-10** The effect of splitter length on downforce and drag.

What mechanism is the splitter applying? Figure 4-11 helps explain what's happening, and actually agrees nicely with other textbook explanations of how a splitter generates downforce – and we get to *see* the evidence! It is very clear in this image of the static pressure distributions at the front of the car with and without the splitter, that the splitter 'taps' the zone of high static pressure ahead of the nose of the car, and furthermore that there is a very marked low static pressure zone immediately under the splitter. Thus, with high static pressure on the top of the splitter and low static pressure beneath it there is a large pressure differential that creates downforce.

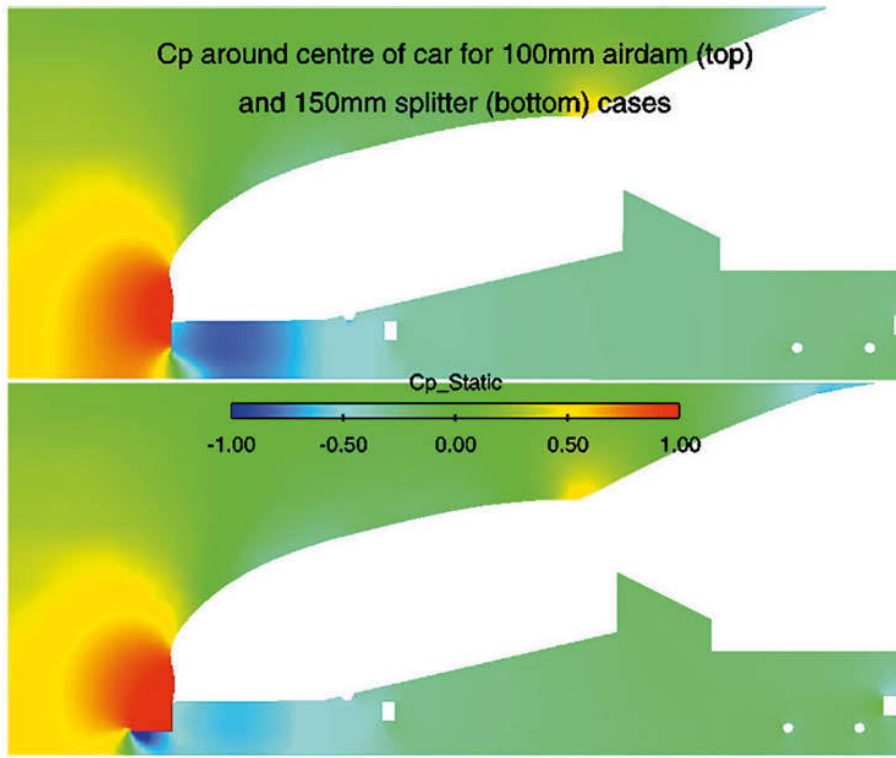


**Figure 4-11** Static pressures with and without a splitter.

It is also apparent that there would probably be little point extending the splitter further forward than the extent of the high pressure ‘bubble’, and this may be at least part of the reason why downforce peaks at 100mm splitter length in this case. This should not be regarded as a generalisation though, because the maximum splitter length that can be run will surely vary from car to car, depending on the car’s shape at the front end, and of course on the relevant rules.

Looking a little more deeply at what’s happening, it is also apparent in Figure 4-11 that the static pressure is not as low immediately behind the airdam when the splitter is fitted, as evidenced by the paler blue colour compared to the airdam-only case. The Delta\_Cp plot in Figure 4-12 indicates the difference in static pressures between the airdam-only and airdam-plus-150mm splitter cases. The marked static pressure reduction (blue) under the splitter is clear, as is the raised static pressure above the splitter, but there is also a rise in static pressure (red and yellow) behind the airdam and under most of the front of the car’s underside. Thus, although there is a very useful net benefit in front end downforce achieved by fitting the splitter, there is a

trade off in that the static pressure in the forward part of the underbody region has been slightly raised (although it is still negative), which counteracts some of the splitter-generated downforce. So it is a case of swings and roundabouts, but the swings win. This might also have implications for the venting of cooling air in some front-engined applications where this smaller pressure reduction works against air exiting the cooling system towards the underside. It might also just be an effect of the particular shape of the underbody behind the airdam in this very simple model, and we'll look into that in more detail shortly.

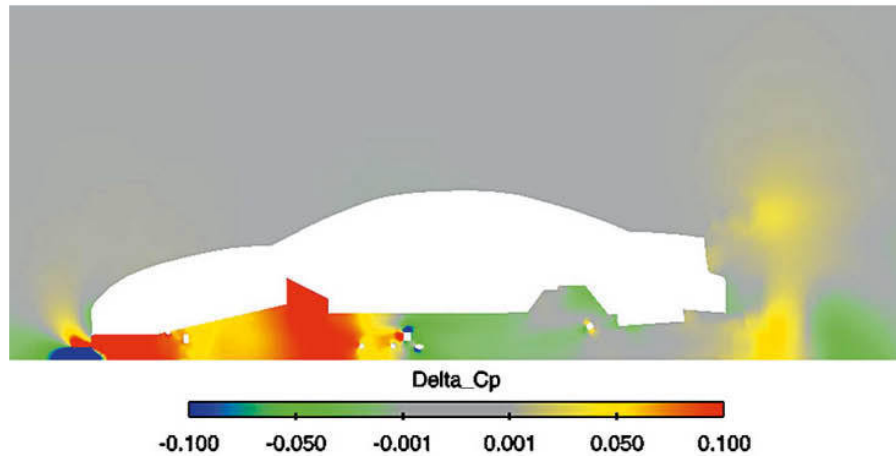


**Figure 4-12** Changes to static pressures caused by fitting a splitter.

The very small increases in overall drag are the result of some pluses and minuses too. The data generated by the CFD calculations (see the table) showed that there were modest reductions in drag felt by the car's body, wheels and the airdam, but these were offset by slightly less modest increases in drag felt by the underfloor and its tubes and protrusions, which result from the rearward component of the above mentioned increase in static pressure in that region acting on these components.

**Drag, N (lb):** Body

**Baseline with 100mm airdam:** 596 (134)

**With 150mm splitter:** 577 (129)

**Change caused by splitter:** -19 (-5)

**Drag, N (lb):** Wheels

**Baseline with 100mm airdam:** 213 (48)

**With 150mm splitter:** 196 (44)

**Change caused by splitter:** -18 (-4)

**Drag, N (lb):** Underfloor

**Baseline with 100mm airdam:** 194 (44)

**With 150mm splitter:** 238 (53)

**Change caused by splitter:** 44 (9)

**Drag, N (lb):** Underfloor pipes

**Baseline with 100mm airdam:** 56 (13)

**With 150mm splitter:** 111 (25)

**Change caused by splitter:** 55 (12)

**Drag, N (lb):** Rear spoiler

**Baseline with 100mm airdam:** 267 (60)

**With 150mm splitter:** 266 (60)

**Change caused by splitter:** -1 (0)

**Drag, N (lb):** Airdam

**Baseline with 100mm airdam:** 337 (76)

**With 150mm splitter:** 317 (71)

**Change caused by splitter:** -20 (-5)

**Drag, N (lb):** Splitter

**Baseline with 100mm airdam:** -

**With 150mm splitter:** 0.3 (0.1)

**Change caused by splitter:** 0 (0)

In practical terms the splitter is an uncomplicated device that can be a very useful, efficient generator and balancer (by adjustment, where permitted) of downforce. Its ability to function will be affected by the shape of car it is attached to – clearly a blunt front end as on our NASCAR model here will have a more pronounced high pressure zone to ‘tap’ ahead of it, than a sleek, low-line front end.

Another issue to keep in mind is that, being close to the ground to there is the likelihood that changes to ride height or the pitch angle of the car, for example when heavy braking compresses the front suspension, or when downforce compresses the suspension at the front and the rear, will cause changes to the magnitude of the downforce being generated by a splitter. This effect, often just referred to as ‘pitch sensitivity’, can cause inconsistent handling and a loss of confidence by the driver. One way of reducing this problem is to stiffen the car’s suspension, which reduces the amount of suspension deflection for a given input load, be it mechanical or aerodynamic. This can have disadvantages, both in terms of giving the driver a worse ride,

but also potentially by reducing the ability of the car to ‘mechanically’ grip the road, a condition which may make itself felt in slower corners where aerodynamics are not really helping. So the clever aerodynamicist will look for solutions that are less sensitive to changes in ride height, and which therefore allow the chassis engineers to retain a decent amount of suspension movement, and the chassis engineers will look for other ways of providing ‘platform control’, perhaps using additional elements in the suspension system that limit vertical travel or control its rate of change.

The preceding CFD exercise on splitters on the NASCAR model looked only at the forward extension of such a device from the bottom lip of the front panel. However, if the splitter panel was also extended rearwards under the front compartment, might we not expect to extend the region where fast, low pressure airflow could be encouraged? The author carried out just such an exercise on a simple saloon/sedan CAD model to study with CFD.

The CAD model for this investigation incorporated features intended to add realism, including an engine bay and related spaces and gaps around the engine, a radiator with inlet apertures in the front panel, and a rear axle unit and associated cavity, so that the major aspects of the complex airflows in these regions could be better simulated. The model’s modest 75mm (3in) forward-protruding splitter was extended rearwards in two increments of 485mm (19.1in) and 1200mm (47.2in), the longest of which is shown in figure 4-13. The former covered roughly half the underside of the front compartment (the engine bay in this front engine, rear drive model) and the latter effectively covered it totally. As the splitter was slightly below the car’s main floor level, there was a small vertical gap between the rear edge of the splitter and the main floor in the case of the large extension.

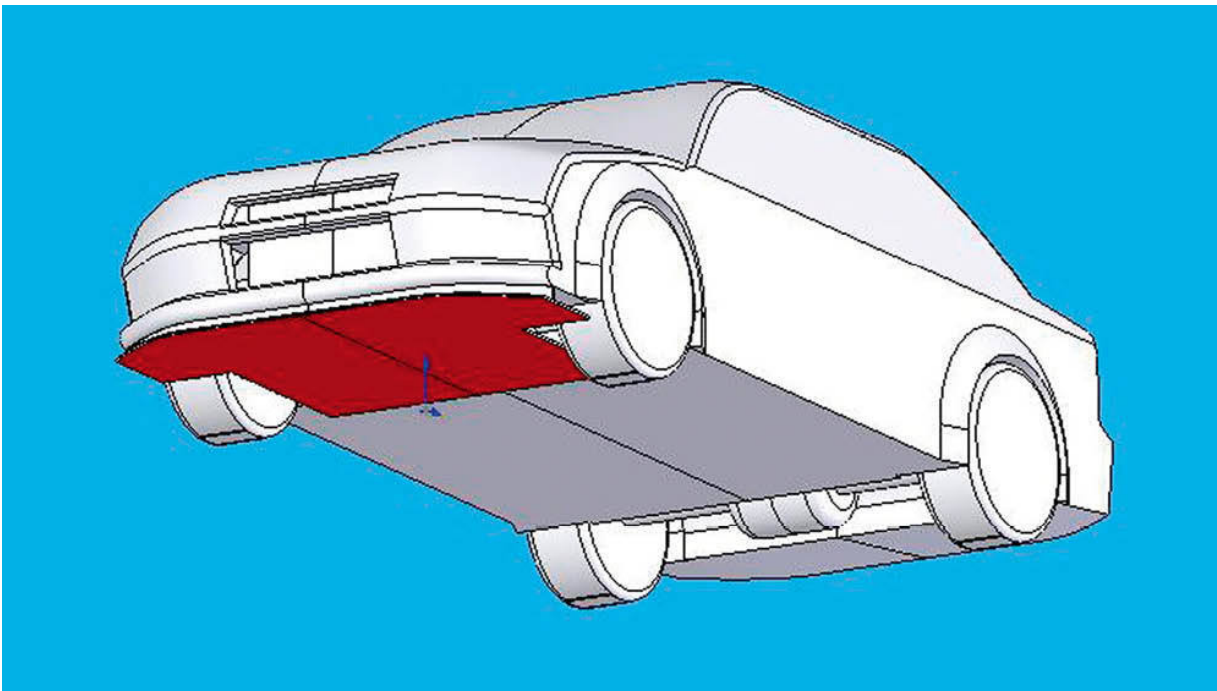


**Figure 4-13** Model of a saloon/sedan with a rearward extension of the splitter under the front compartment.

It will be apparent that even partial panelling under the engine bay would have other implications, too. The air that enters the front aperture either bypasses or passes through the radiator, which in our current model and on many production cars has to then find its way out beneath the car, and would have a reduced area through which to exit. This suggests that there would be some trade-offs. And note that in spite of attempts at adding some basic realistic features to the model, it was far too simplistic to represent reality, and hence the CFD simulations were only illustrative. But they do give us a qualitative idea and even a semi-quantitative hint at what the effects might be in reality.

The table below shows the results of the simulations in terms of changes to the car's drag and lift coefficients. Note that the model generated overall positive lift in this configuration, so negative changes to  $C_L$  values represent lift reductions. The changes are shown in 'counts', where 1 count equals a coefficient change of 0.001.

485mm rearward extension

Delta  $C_D$ , counts: +1

Delta  $C_L$ , counts: -19

1200mm rearward extension

Delta  $C_D$ , counts: -5

Delta  $C_L$ , counts: -118

So neither of the splitter extensions had much influence on drag, and both enabled lift reduction, modest in the case of the ‘half panel’, and fairly significant in the case of the full panel. If this is compared with the effect of fitting the forward protruding splitter only, which was to generate 145 counts of lift reduction and 22 counts of drag, then the gains from extending the splitter rearwards looked potentially worthwhile. However, this only tells a part of the story, and, in fact, the potential benefits are much better than this...

As we have already seen, one of the many incredibly useful facilities that CFD provides is the ability to measure the calculated forces on individual components. The following table shows the individual delta  $C_L$  values of the car body and splitter (including the rearwards extension in each case).

485mm rearward extension

Delta  $C_L$  body: +152

Delta  $C_L$  splitter: -170

1200mm rearward extension

Delta  $C_L$  body: +217

Delta  $C_L$  splitter: -336

It is now evident that the car body generated additional lift in each case, and that the splitter generated actual downforce each time, and almost double the downforce in the case of the longest rearward splitter extension. But it also becomes clear that two things were changing simultaneously each time the splitter extension was altered; both body lift and splitter downforce increased as the splitter was extended. This backed up the earlier premise that panelling under the engine bay, even partially, was likely to have consequences, and although the pros outweighed the cons here, it is apparent that the cons were negating some of the benefit that the splitters were providing.

So how, then, could the ‘cons’ be overcome, or at least mitigated in order to realise more of the benefit that the splitter was generating? Let’s consider why car body lift might have increased each time. By restricting the flow out of the engine bay, could it be that pressure within the engine bay had increased, which in turn produced an increase in the lift generated by the body?

Comparing figure 4-14 with figure 4-15 showing the pressure distributions along the centreline of the model with no rearward splitter extension and the full rearward extension, it is very clear that the magnitude of the low pressure

under the splitter, especially at the front, had greatly increased, but also the positive pressure in the front of the engine bay had also increased.

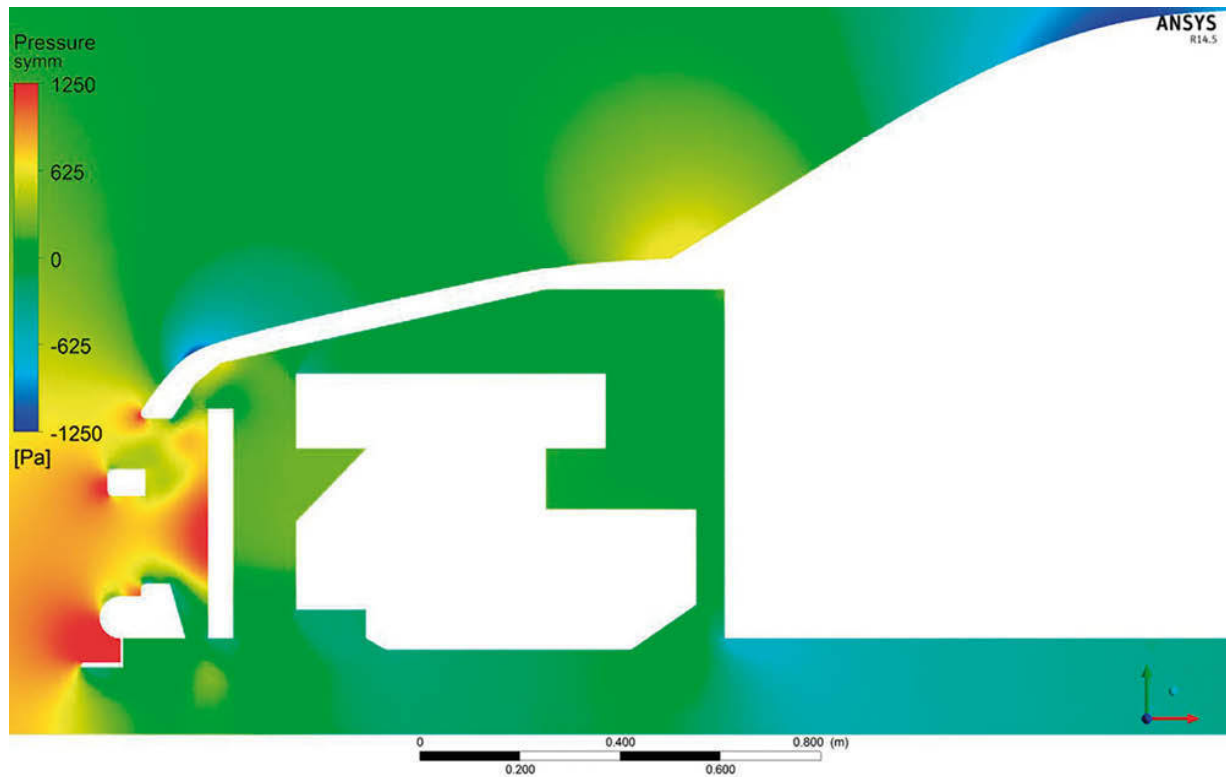


**Figure 4-14** Pressure distribution around and within the front end with no rearward extension of the splitter

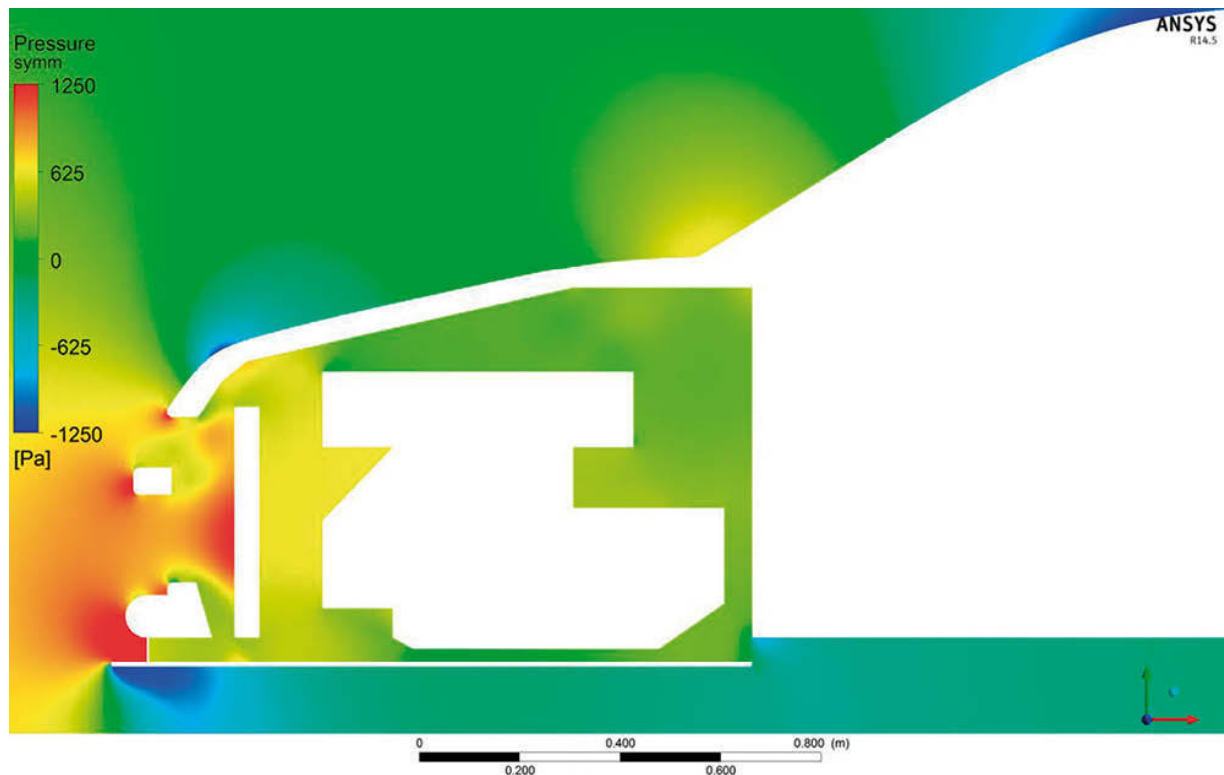


**Figure 4-15** Pressure distribution around and within the front end with a rearward splitter extension

What, then, if some of that pressure within the forward engine bay could be released by opening an aperture in the bonnet? To that end a simple slotted opening was created above the radiator exit, and the model was re-run to see how the results changed, and the tables below illustrate.

485mm rearward extension

Delta  $C_D$ , counts: +1

Delta  $C_L$ , counts: -19

1200mm rearward extension

Delta  $C_D$ , counts: -5

Delta  $C_L$ , counts: -118

1200mm extension + slotted bonnet opening

Delta  $C_D$ , counts: +33

Delta  $C_L$ , counts: -251

485mm rearward extension

Car body delta  $C_L$ , counts: +152

Splitter delta  $C_L$ , counts: -170

1200mm rearward extension

Car body delta  $C_L$ , counts: +217

Splitter delta  $C_L$ , counts: -336

1200mm extension + slotted bonnet opening

Car body delta  $C_L$ , counts: +47

Splitter delta  $C_L$ , counts: -298

So, this first attempt at mitigating the downsides of the panel under the engine bay saw some additional drag (probably because the first iteration of slotted opening was inefficient) but there was a substantial reduction in overall lift, much of which was because the earlier additional body lift from adding the longer splitter extension had been eradicated. There was also a small reduction in the downforce from the splitter, which, ironically, would also have come from the reduction in pressure in the engine bay (less downward acting pressure on top of the splitter panel). It was also evident that there was, indeed, reduced positive pressure within the forward engine bay, and that the pressures above the bonnet were also beneficially altered by the presence of the louvres.

This brief exercise demonstrated that the overall results of some aerodynamic modifications are about trade-offs. But it also showed the potential merits of extending splitter panels under the forward compartment. Needless to say, engine cooling and radiator exit air extraction would need careful thought, and the logical next step of an exercise like this might well be to examine the effects of radiator ducting – if there was physical space to do this – to improve cooling, but also to continue the process of minimising the negative effects of unwanted airflow entering the front compartment.

An important and often overlooked detail on splitters is that the leading edge either needs to have a radius on it, which means the splitter also needs to have reasonable thickness to enable this, or if it is made from thin sheet material then the leading edge needs to have an upturn on it. The reason for this can be seen in Figure 4-4, despite there being no splitter in this instance. Notice the pronounced downwards angle at which the airflow passes around the forwardmost lip. And notice too that flow separation is visible immediately aft of the forward lip in both cases. This has been caused by that forward lip being too sharp, and it causes losses in energy and velocity. With a splitter, a major part of the downforce comes from the reduction in pressure arising from the increase in velocity under the splitter (which usually extends rearwards under at least part of the front compartment, too). By easing the airflow under the splitter with a properly profiled leading edge, these flow

separations can be reduced or avoided altogether, to the betterment of downforce. This also has potentially important downstream benefits, because the airflow loses less energy if it is eased smoothly under the forward lip.

Another aspect of splitter design that can be overlooked is the strength and stiffness needed to support often very large forces. The pressure differentials between the upper and lower surfaces multiplied by the area over which they act need to be taken into account during manufacture. The precise forces depend on the size of the splitter and the speed of the car, of course, but a very rough rule of thumb for many applications is that if you can stand on your splitter without it unduly deflecting then it will probably be strong and stiff enough. From this it should be clear that thin aluminium sheet just won't do the job. Better to use quality plywood (probably 13mm or half inch minimum thickness) bolted solidly under the front of the car to some structural members, or lighter weight aluminium- or composite-skinned honeycomb panel if the budget stretches to that. Please note that making any aerodynamic parts structurally sound is your responsibility, not mine! I have fulfilled my responsibility by making you aware that aerodynamic forces can be BIG!

### **Wind tunnel data on splitters**

Clearly airdams and splitters are potent and useful devices, and to an extent we were able to get a feel for the kind of contribution they can make from the CFD cases illustrated earlier. But if wind tunnel data on a full-size, real car has a more practical, real world feel to it, then the case study here provides some confidence not only in the devices themselves, but also in the fact that the computer simulations are actually a pretty good guide to the general scale of things.

The MIRA full-scale wind tunnel in the English Midlands is an extremely useful facility, and provides data on real cars, complete with all the imperfections, lumps, bumps and cavities that are hard to accurately model on computers. However, as explained in more detail in Chapter 8, the MIRA facility does have two disadvantages that we need to be aware of because of the effect they can have on the results: it has a fixed floor, and the wheels of the test car do not rotate during tests. The former means that we need to be mindful of the results of components close to the ground, and the latter can certainly affect the airflow adjacent to and downstream of the wheels, even with closed wheel cars although more so with open wheelers. That said, what works in the wind tunnel works out on track, and trends and patterns in results obtained in the wind tunnel usually translate on to the track too.

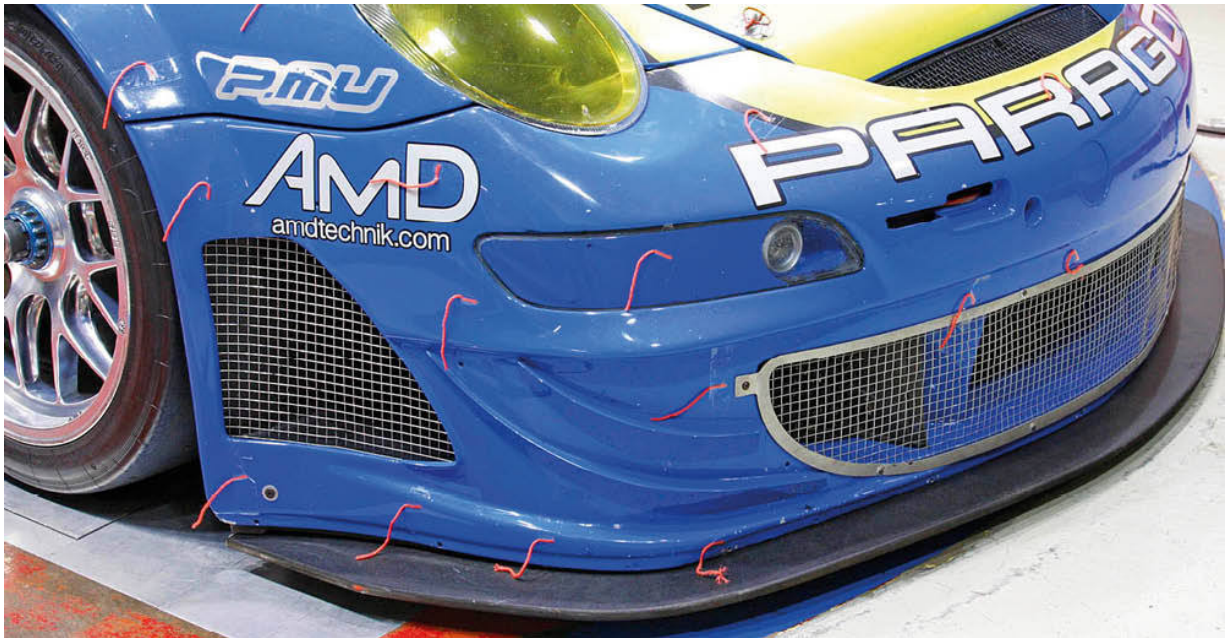
The wind tunnel actually measures the forces through load cells set under pads in the floor beneath the tyre contact patches. This data is then converted into coefficients using the lift and drag equations, and for ease of comparison with previously presented data we shall use CD.A and CL.A values here.

Another convention to introduce here is that of ‘counts’. One count is 0.001 in a coefficient value, coefficients typically being reported to three decimal places, so a change in drag coefficient from, say, 0.400 to 0.390 is a change of ‘10 counts’. This makes discussing changes to coefficients somewhat simpler.

The *Paragon* Porsche 997 was originally built to ‘GT2’ regulations for the American Le Mans Series (ALMS) but was brought to the UK to compete in more open GT racing categories. So the team was free to add aerodynamic appendages not allowed under the GT2 regulations it was designed for, and one option was to add a front splitter. The original car already featured a beautifully smooth underside, so the splitter extensions were attached from underneath, and were blended back into the main floor with a tapered trailing edge. So, the underside of the front compartment was already panelled over, and this perhaps gave a clearer idea of what a splitter alone can do. The Porsche’s frontal area was estimated at 2.1m<sup>2</sup> (22.6 square feet), and the changes are shown in ‘counts’.



*The Paragon Porsche 997 after various modifications had been made to its previous ALMS GT2 specification.*



*The longest splitter tried on the Porsche 997.*

Baseline, no splitter

CD.A: 0.914

CL.A: -1.098

CL<sub>F</sub>.A: -0.231

CL<sub>R</sub>.A: -0.867

%front: 21.0

Add 35mm splitter

CD.A: +4

CL.A: -120

CL<sub>F</sub>.A: -181

CL<sub>R</sub>.A: +61

%front: 33.8

Add 55mm splitter

CD.A: +2

CL.A: -158

CL<sub>F</sub>.A: -246

CL<sub>R</sub>.A: +88

%front: 38.0

Add 75mm splitter

CD.A: +0

CL.A: -189

CL<sub>F</sub>.A: -290

$CL_r.A$ : +101  
%front: 40.5

Note 1:  $-CL.A$  is the convention for expressing downforce but it means the same as  $CDf.A$  as used in the CFD examples earlier, where  $Df$  meant downforce. And  $-CLF.A$  and  $-CLR.A$  refer to front and rear downforce respectively.

Note 2: That for example where '+120' counts is shown next to a negative lift coefficient like ' $-CL.A$ ', this represents a gain in downforce.

So the baseline configuration produced a fair amount of downforce already. That downforce was clearly initially biased towards the rear though, and the Porsche had a roughly 40% front/60% rear static weight split. Perhaps not surprisingly the tendency was to understeer at higher speeds in baseline configuration.

Each splitter increment produced a significant change in front-end downforce and, again probably through mechanical leverage effects, reductions in rear downforce. The effect on drag was very small and could be said to be negligible. The longest splitter here was responsible for taking the aerodynamic balance from about 21% of the downforce on the front to around 40% on the front. Given that the proportion of static weight on the front was about 40%, to have the aerodynamics balanced in steady state cornering would require a similar proportion of the total downforce on the front, so this longest splitter would probably offer a reasonable balance, all other things being equal. Of course this is likely to be an oversimplification, because this is just one data point at one combination of ride heights, and ride height is a sensitive parameter when it comes to overall balance, and especially when discussing components that are near to the ground.



*Quite complex front diffusers were fitted to the Porsche 997 ALMS GT2.*

### **Front diffusers**

The simple splitter arrangement illustrated in the previous section is probably not very much like most splitters. Generally, though not always, a splitter will be seen to continue horizontally aft, behind the airdam and under the forward section of the car. A variation of that theme is to angle that rearward extension upwards to form a ‘diffuser’. This is a term that we briefly encountered in Chapter 2 when discussing venturi tubes, the diffuser being the region of expanding cross-sectional area aft of the narrow throat. We saw that as the airflow converged into the throat its velocity increased, the local static pressure decreased, and then as the airflow expanded into the diffuser, its velocity decreased again and the static pressure increased. So how could a diffuser aft of a splitter help?

Variations on the front diffuser that had been used on various saloon/sedan and sports racing cars, including a single, wide diffuser, a pair of separate narrower diffusers in line with the gap between the wheels and the chassis, and even four smaller diffusers. Our CFD model here features a single, wide front diffuser aft of the splitter on the NASCAR model, as shown in Figure 4-16,

and a simple ‘with versus without diffuser’ exercise was performed in 3D again at an airspeed of 50m/s (180km/h).

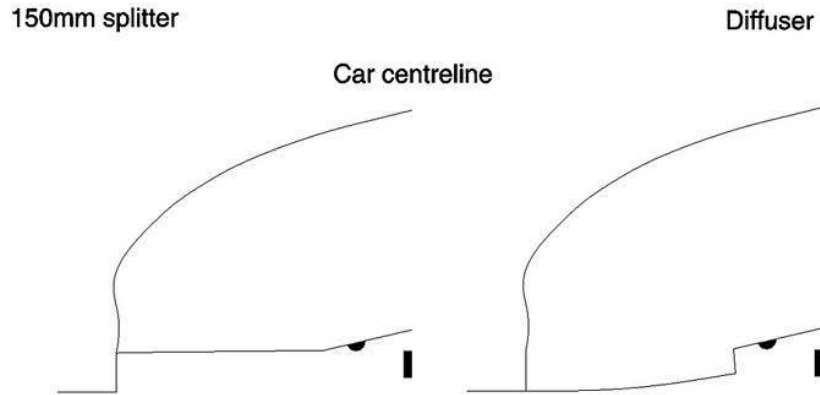


**Figure 4-16** The centreline profile showing the diffuser geometry tested on the generic NASCAR model.

The result of installing this simple diffuser on this model, with a 100mm deep airdam and a 150mm long splitter, was a 3.9% increase in overall downforce (the benefit was concentrated at the front, with rear downforce reducing slightly) and a 1.4% increase in drag. This represents a more modest benefit than either the airdam or the splitter achieved, but is nevertheless a worthwhile and reasonably efficient gain. Bigger gains could, no doubt, be achieved with optimisation, but the purpose here was to investigate why the benefit occurs.

Figure 4-17 compares the static pressure coefficients with and without the front diffuser, and it is apparent that after ‘fitting’ the diffuser the high-pressure zone (red) above the splitter has remained pretty much unchanged. However, there has been a significant decrease in static pressure under the splitter, evidenced by the larger zone of darker blue which also extends under the forward part of the diffuser. This creates more downforce.

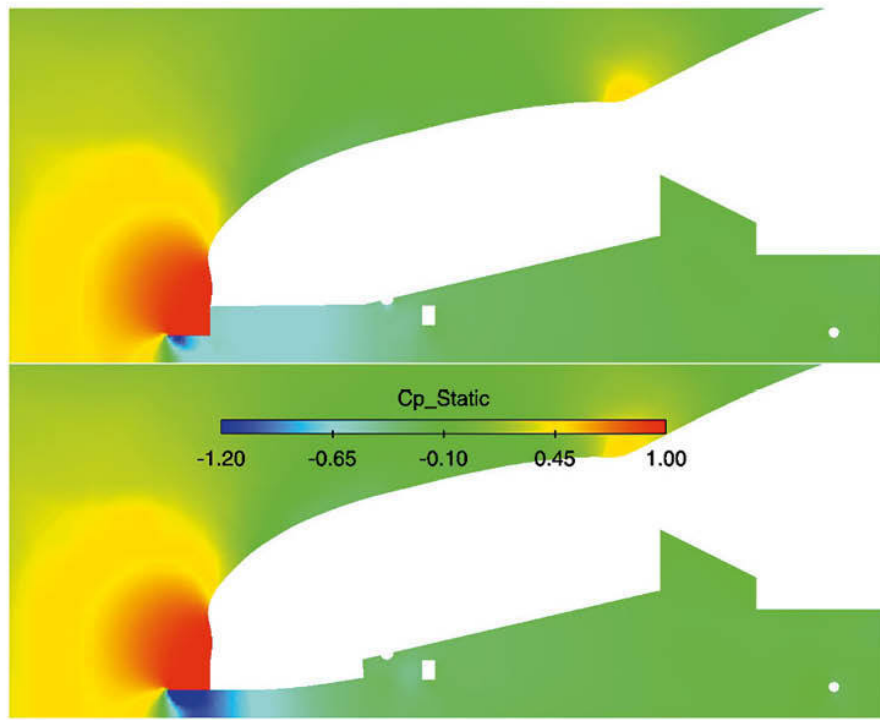


**Figure 4-17** Static pressures are different in the forward underbody with and without the diffuser.

However, the static pressure under the rearward part of the diffuser is now slightly *higher* (green rather than pale blue) than it was in the underbody here when there was no diffuser, which means less downforce is being created here than before. So as always, the picture is not a simple one.

Moving to Figure 4-18 which shows velocity coloured streamlines, a couple of things immediately become apparent. Most obviously, the large recirculation zone behind the airdam has now been eradicated, having nowhere in which to develop. Importantly, the diffuser allows the airflow to expand, where the recirculation zone previously acted as a barrier to this expansion. By facilitating expansion the diffuser promotes increased mass flow under the splitter. That this occurs is evident if you closely study the streamlines in Figure 4-18 – with the diffuser in place more streamlines can be seen to converge into the under-splitter region. This mass flow increase results in an increase in velocity under the splitter (of around 10% in this case), which contributes to the additional decrease in static pressure there, in true Bernoulli-fashion. There are also some small losses here resulting from the

sharp leading edge of the splitter on the model that caused a drop in total pressure and hence a further drop in static pressure, although this is not evident in the diagrams here.

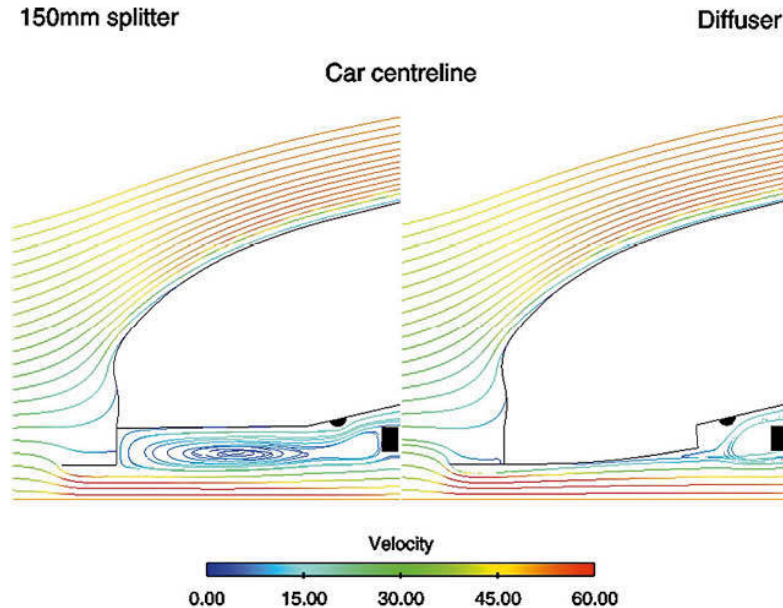


**Figure 4-18** Velocity coloured streamlines with and without the diffuser.

However, moving aft to the rear of the diffuser, a really close peer at the topmost streamline suggests the flow might have actually separated here. The oilflow plot in Figure 4-19 confirms much more clearly that this is the case. The change in the pattern of surface flow in the centre third, towards the rear of the diffuser is the result of flow separation. So why has this happened, and what are the consequences?

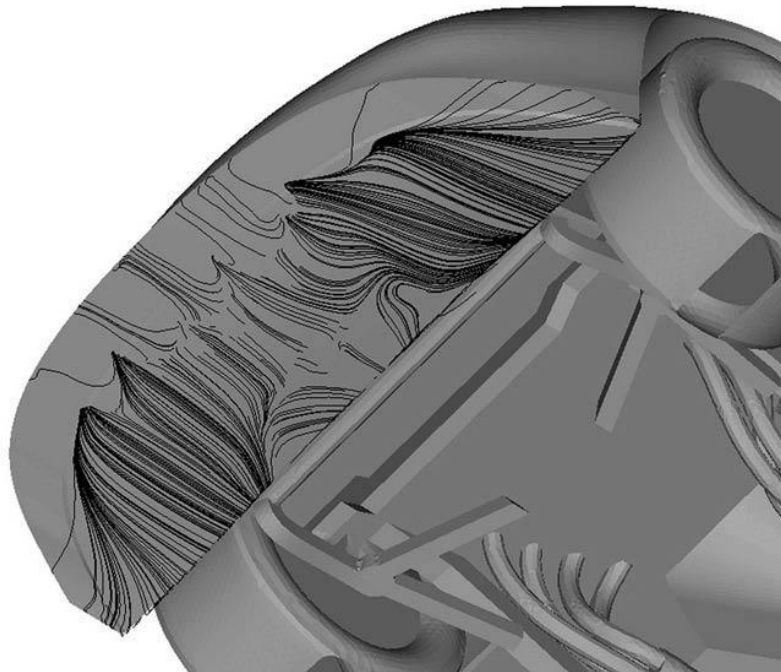


**Figure 4-19** The oilflow plot shows separation in the rear, the centre third portion of the diffuser.

We saw in Chapter 2 that separation can occur when air is flowing against too steep an adverse pressure gradient. In this instance the low pressure under the splitter has been amplified by the presence of the diffuser, but this has also created an increase in mass flow under the splitter which, when it expands again in the diffuser, rises to a higher static pressure (as shown in Figure 4-17), than it did without the diffuser. Thus the static pressure goes from lower than before to higher than before, the gradient has now become too severe, and so the flow has separated. This is an area where optimisation, perhaps of the angle of the central part of the diffuser or the ground clearance of the central part of the splitter could, no doubt, provide improvements.

Figure 4-20 is a CpX plot showing the static pressure components in the horizontal or X-direction only in the front underbody region. Positive (red and yellow) colours once again indicate drag. An area where drag occurs can be seen behind the airdam when there is no diffuser, but this shifts to behind the diffuser when it is fitted, and calculations showed that the magnitude of the drag in this region barely changes. Notably, the diffuser itself does not create any significant drag. There was, however, a slight increase in drag overall, and this was mainly due to the increased mass flow under the splitter/diffuser that runs into the underfloor protuberances and the rear of the front wheel wells. Design optimisation could again provide improvements here.

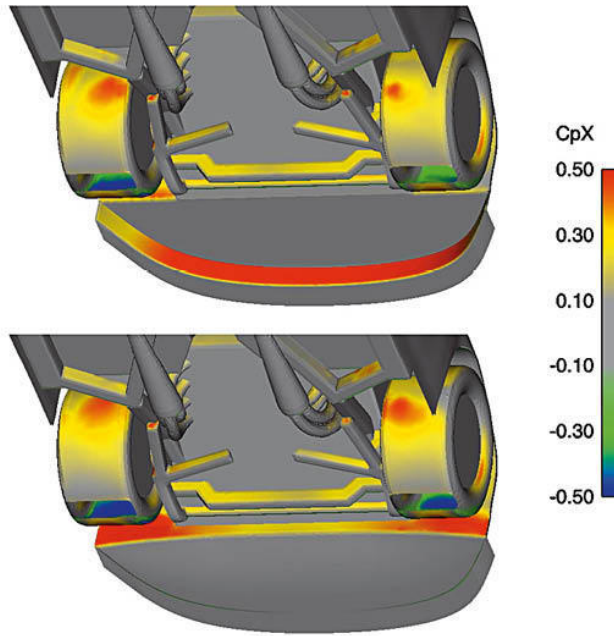


**Figure 4-20** A  $CpX$  plot shows how sources of drag have moved after fitting the diffuser.

This simple diffuser has provided an additional increment of reasonably efficient downforce to those substantial gains already achieved by the airdam and the

splitter. Improvements could be made, perhaps to the splitter, the shape and dimensions of the diffuser and other detail aspects, assuming technical regulations permitted, to provide further gains in downforce. Moreover, close study of where drag occurs would enable design changes that could further improve efficiency. One thing that is clear is that it would be pointless employing front diffusers if the air has nowhere to go, or is significantly blocked downstream, something we'll revisit in case studies in a later chapter.

One question that was raised about the splitter and diffuser arrangements tested in these two studies was whether using a flat, horizontal rearward extension of the splitter might be better than using a diffuser. The argument went that by maintaining a narrow cross-sectional area further back, the air velocity would remain high for longer, and so the low static pressure region would be extended, leading to more downforce. It is possible that this might be the case, but as we have seen, in order to get the increase in mass flow that led to the reduced static pressure we needed to allow the airflow to expand into a diffuser. This might suggest that it would be worth testing the extended throat idea, but that a diffuser would still be required, and no doubt further detailed optimisation work would be needed to get the best out of such an

arrangement. We'll revisit the concept of long throats and short diffusers in the chapter on underbodies.

### **Not just closed wheelers**

Splitters are sometimes thought of as devices whose use was limited to closed-wheel racecars such as saloons/sedans and sports GT cars, but this is not so. Splitters have been used successfully in some single-seater applications as well as the 'open-wheel' sports racer in the form of the Clubmans car, which includes categories such as Formula 750 in the UK. Single seaters in the late 1970s ran with what used to be rather vaguely called 'full width nose cones', as distinct from the narrow-nose-with-wings configuration, and cars like the March 782/783/793, Chevron B38/B40 and F2 and F3 racers of similar vintage were very successful with such noses installed. Most of them utilised a form of splitter which was sometimes adjustable, and there would appear to have been no problem balancing the downforce from the rear wing with this set-up, suggesting approximately equal amounts of downforce could be generated by a nose with a splitter and a rear wing.

This nose shape continues to find favour amongst the competitors in some categories, and it may well be that on some cars it offers a lower drag, more efficient source of downforce. There is a school of thought amongst Formula 750 racers, who have very little horsepower to play with, and certainly none to waste, that the full-width nose offers lower drag by diverting some of the airflow around the front wheels and tyres. Equally certain though is that cars in this formula with narrow noses and front wings have been very successful. You pays yer money and takes yer choice...



*The Formula 3 Dallara features a kind of splitter (the nibbled wooden plank, centre).*

It may not be immediately evident, but today's Formula 1, Formula 3 and other cars use a form of splitter, although not at the extreme front of the car. The regulations demand that these cars have a flat underside between the rearmost tangent of the front wheels and the front of the rear wheels. All current designs feature the so-called 'raised nose', with the underside of the nose significantly higher than the underside of the central chassis. So, on most, the flat underside juts ahead of and is below the rearward part of the nose underside, in much the same way as a splitter juts forward of an airdam. This under-chassis splitter therefore sees low pressure develop underneath it as the air accelerates into the underbody area. It also sees high pressure form on its upper surface, and if the chassis is high enough above it so that the high pressure acting on the chassis underside doesn't just cancel out the raised pressure on top of the splitter, there can be a net increment of downforce from this too.

Further rearward on F1 cars (and many other current single seaters) there are flat extensions of the underside that stick out, to the maximum permitted body width, ahead of the rear wheels. Again, these panels exploit the stagnation zone that exists immediately ahead of the rear tyres to create a pressure differential above and below them, and add to the car's overall downforce. In each case, these panels need to be rigid enough to resist

bending under the force applied, and to transmit that force to the chassis, and thence to the tyre contact patches.

A common mistake is to make a splitter that lacks sufficient rigidity to resist deformation under the considerable loads they can generate. A rough rule of thumb is that if you can stand on the splitter without it bending excessively then it is probably stiff (and strong) enough.

## Rear spoilers

Achieving an aerodynamic balance on a competition car is crucial. If we add devices such as those discussed in the foregoing sections to a car to increase front-end grip at speed then we're almost certainly going to want to add something at the rear to maintain a balance, unless we were just solving a shortage of front-end downforce in the first place. A rear spoiler is a simple way of attempting to achieve this.

Rear spoilers come in all shapes and sizes, from a simple inclined flat plate as defined by NASCAR or the European Late Model Series, to a three-dimensional, carefully integrated shape that smoothly follows the lines of the rear of a car. Whatever its shape, for our purposes here we shall consider the definition of a rear spoiler to be a device which is continuous with the upper surface of the car, with no gaps between itself and the car's bodywork. Spoilers with a gap to the bodywork will be regarded as wings, however crude they may be, and wings will be looked at in a separate chapter.



*The European Late Model Series mandates a simple, large rear spoiler.*

So how do rear spoilers provide aerodynamic benefit? The benefits to lift reduction/downforce creation, often with reductions or only small additions to drag are legend, but the mechanisms are perhaps not so well known. Once

more CFD simulations on the full-size virtual model of a NASCAR racer that we have seen in the previous sections help to evaluate and visualise the effects of changing spoiler angle and length. Figure 4-21 shows the racecar model, and the geometry of the spoiler variations tested (which for simplicity were modelled as thin flat plates).

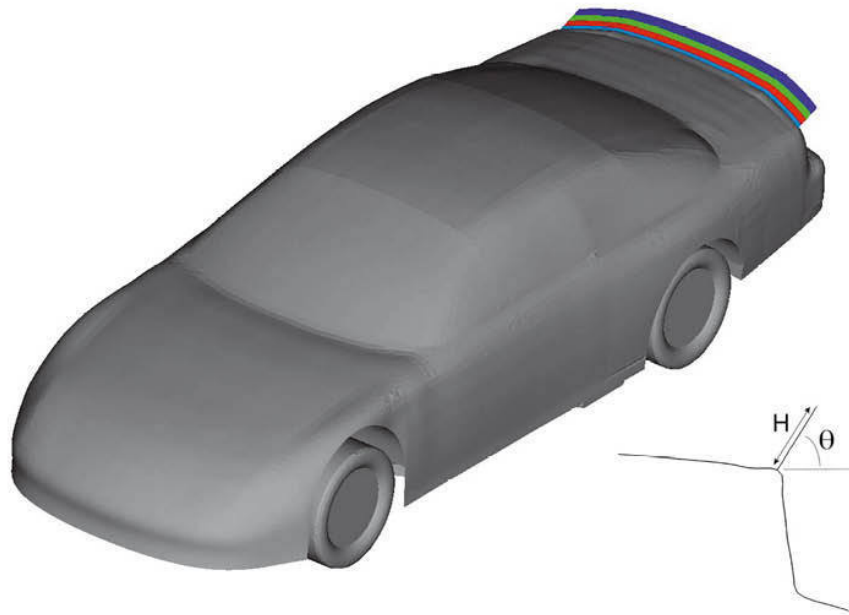


*Figure 4-21 Rear spoiler variations tested.  $H$  = length,  $\theta$  = angle.*

Figure 4-22 summarises the results in graphical form, with dimensionless coefficients multiplied by frontal area plotted versus spoiler angle at various spoiler lengths. Once more we've ignored convention here – positive CDfA values represent downforce, while negative CDfA values represent lift. Let's draw the obvious conclusions before proceeding to explanations:

- There was an increase in downforce (-CLA) when a rear spoiler was added. (This was felt at the rear; there was actually a slight decrease in front downforce.)
- There was a more or less linear increase in downforce with increasing spoiler length or angle.
- The downforce gain seemed to be tailing off at the steepest angle and longest length, although at shorter lengths the gains with increasing angle were still linear.
- In general, steeper angles and longer lengths led to greater drag.

- For any given length, increasing spoiler angle increased efficiency ( $CD_f A/CDA$ ), although once more, the gains were tailing off.

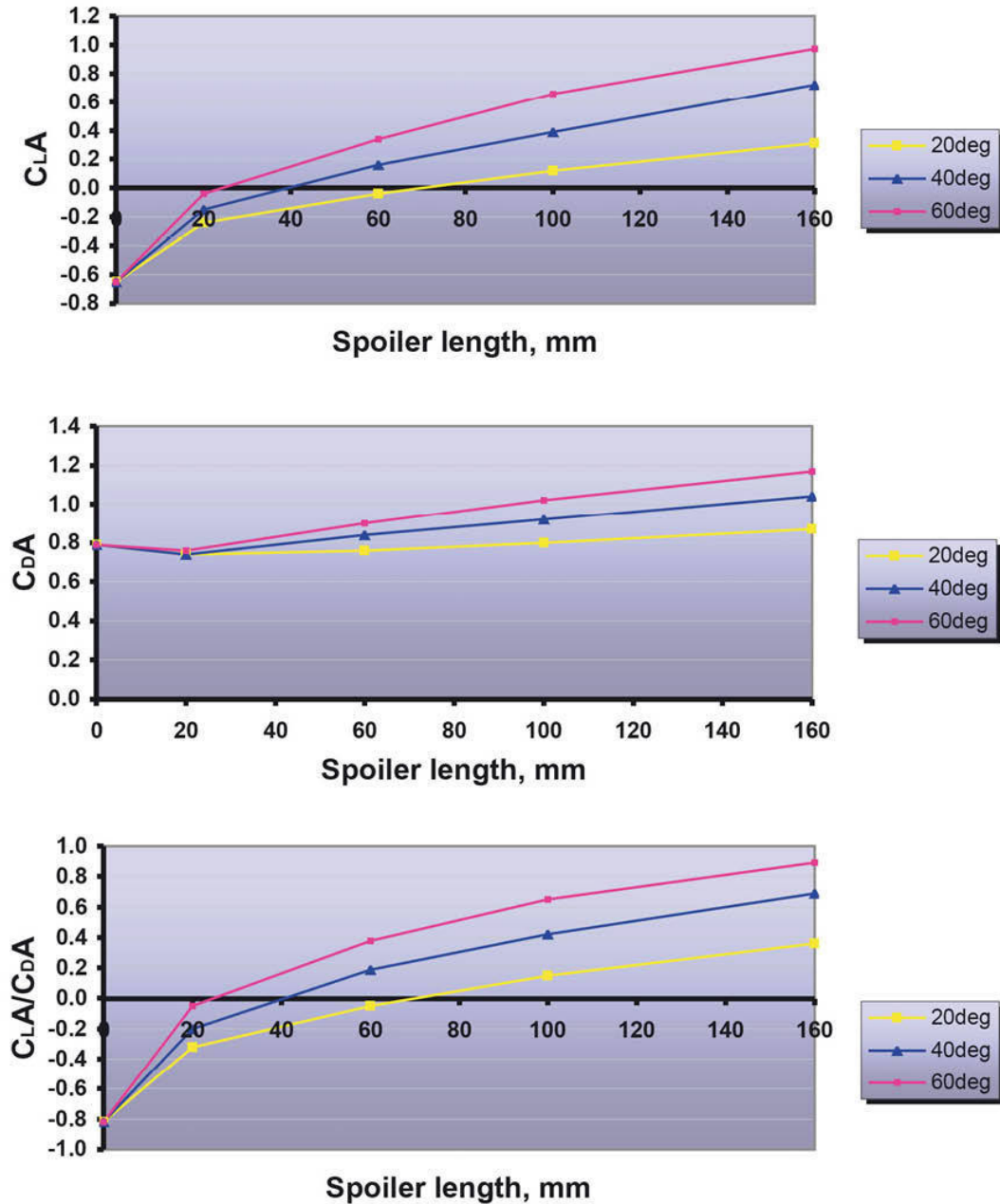


**Figure 4-22** Effect of spoiler length and angle on downforce, drag and efficiency.

There's no doubting the value of a simple rear spoiler on this type of generic production car shape then – substantial and perhaps surprisingly efficient gains in lift reduction/downforce creation are apparent. Indeed, a

shallow ( $20^\circ$ ) spoiler as long as 60mm is capable of actually reducing the car's drag while negating rear lift or creating modest downforce, and although it's likely that seeking maximum downforce will be the aim in many cases, clearly there are options to balance downforce and drag here, rules permitting. Note that different body shapes are likely to produce different results and therefore need individual evaluation.

How did the spoiler achieve these changes? Figure 4-23 shows the changes in static pressures ( $\Delta_{Cp}$ ) along the car's centreline that occurred with the steepest, longest rear spoiler. Clearly there was a substantial increase in static pressure over the rear deck of the car, extending quite a long way forward, which contributed to lift reduction/downforce generation. It is also clear that the static pressure behind the car reduced, which contributed to the increased drag in this configuration. There was also a notable reduction in static pressure beneath the car, which further contributed to downforce generation. Let's delve a little deeper into the mechanisms.

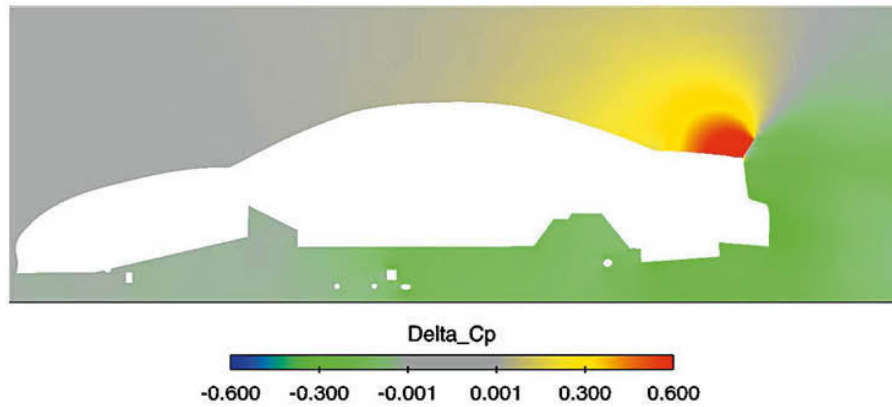


**Figure 4-23** The change to the static pressure from fitting the longest, steepest spoiler, compared to the no-spoiler case.

The change over the rear deck is relatively simple. Adding a spoiler has slowed the airflow over the rear deck, which has contributed to the increases in static pressure in this region. The airflow direction is also altered, the spoiler deflecting the flow upward, indicative of momentum transfer from the airflow

to the car, which further contributes to downforce. There is also a rearward static pressure component that contributes to extra drag.

Behind the car the situation is more complex. Adding a spoiler increases the size of the car's wake and the low total pressure region behind the car (see Figure 4-24). Increasing the spoiler angle leads to further increases in the wake size and the low total pressure region. It is the losses in total pressure that are significant here, more than any changes to air velocity. The losses in the car's wake are large and cause the static pressure to reduce. Any reductions in dynamic pressure as the result of decreases in flow velocity, which in a more ordered flow regime would cause *increases* in static pressure, are outweighed by the losses. This contributes to the general drag increase.

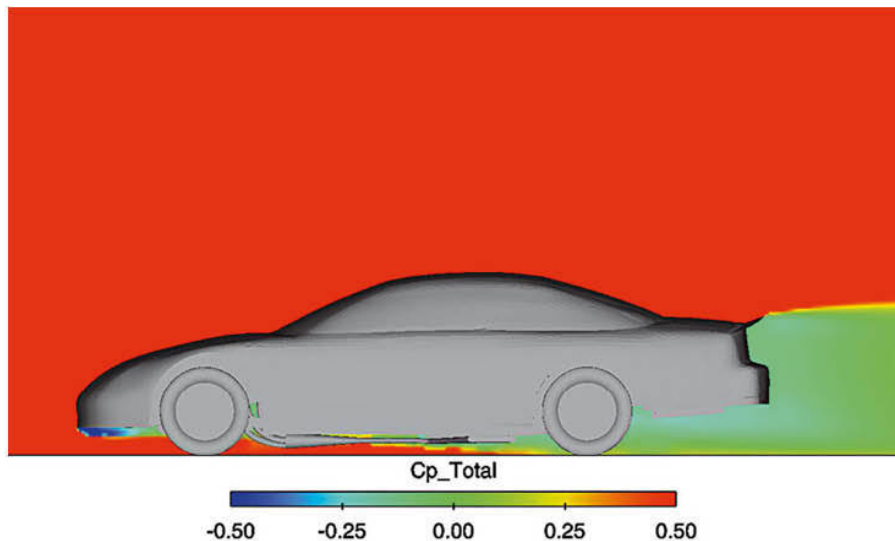


**Figure 4-24** The effect of the longest, steepest spoiler on total pressure.

Beneath the car a different situation prevails. The reduced static pressure region behind the car promotes an increase in mass flow under the car, air flowing happily into a low-pressure region. This has caused an increase in dynamic pressure and, in turn, a drop in static pressure under the rear of the car in classic Bernoulli style. However, although this adds to the generation of downforce, a drawback of this is that the increased mass flow that interferes with the pipes and chassis rails beneath the car also adds to the increase in drag already caused by the pressure differentials across the spoiler itself, and around the car as a whole. Increasing spoiler angle amplifies all these effects,

and Figure 4-25 shows the change in static pressures ( $\Delta C_p$ ) that occur when the longest spoiler is increased from  $20^\circ$  to  $60^\circ$  inclination.

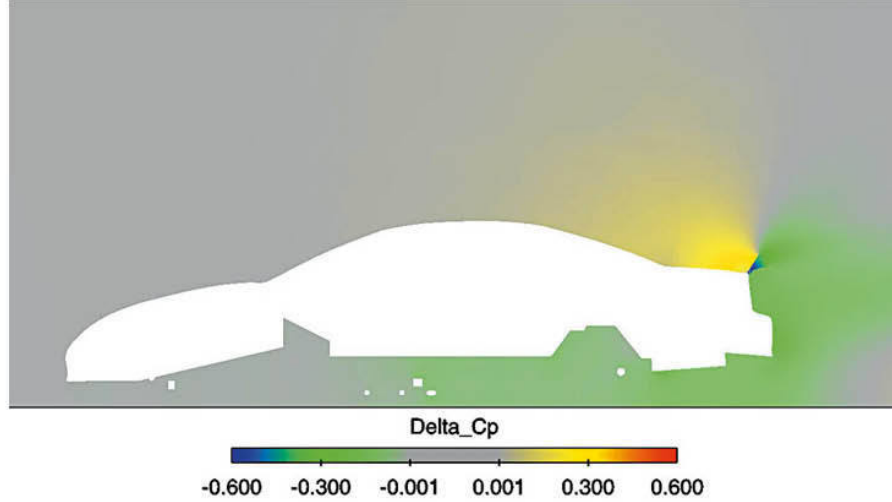


**Figure 4-25** The effect of increasing spoiler angle on static pressure; long, steep compared to long, shallow.

The change to the airflow behind the car from the no-spoiler case to the steepest, longest spoiler case is profound, as Figures 4-26 and 4-27 illustrate. Colour-coded velocity vectors in Figure 4-26 show that with no spoiler the airflow coming off the rear deck is fast and downward directed towards the rear, but the flow immediately behind the car is very slow and completely disordered. Contrast this with Figure 4-27, with the steep, long spoiler, and not only has the flow over the rear deck been slowed and redirected, but now the flow in the wake shows no recirculation under the car, and overall is pulled strongly upwards by the spoiler. The flow emerging from under the rear is also clearly smoother and faster.

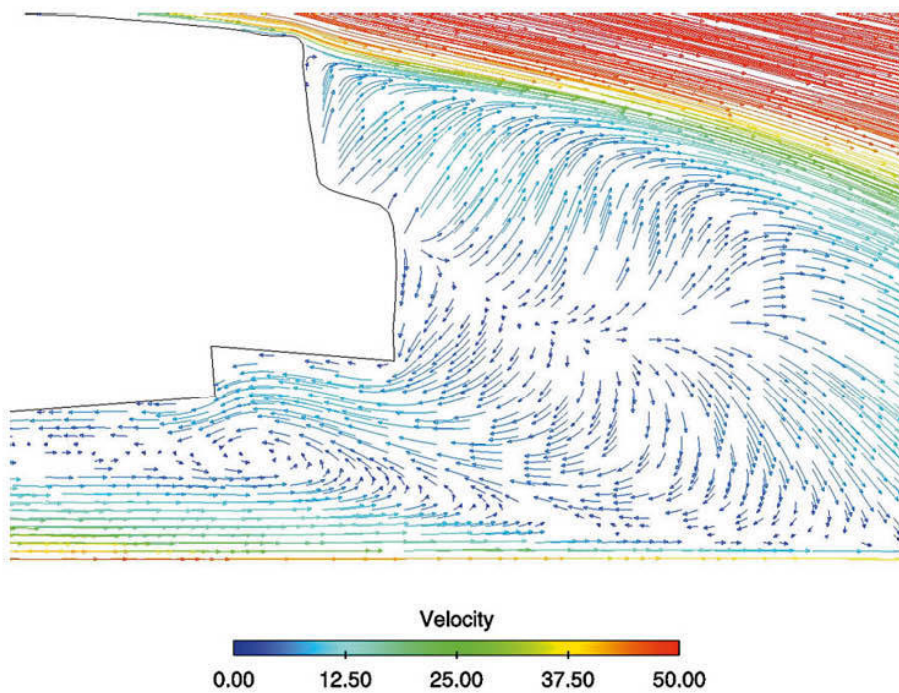


**Figure 4-26** Velocity coloured vectors with no rear spoiler.

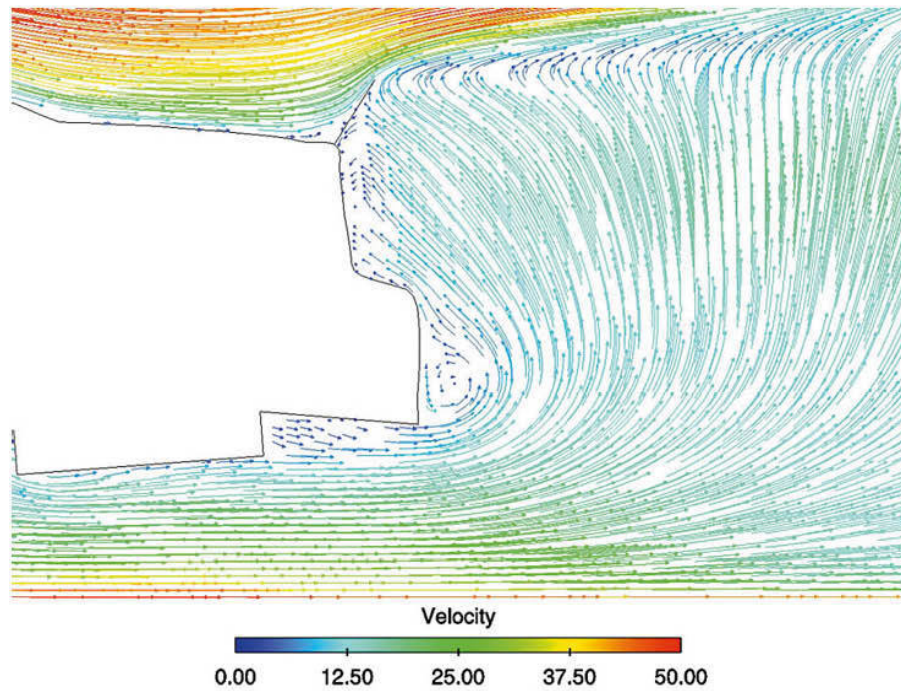
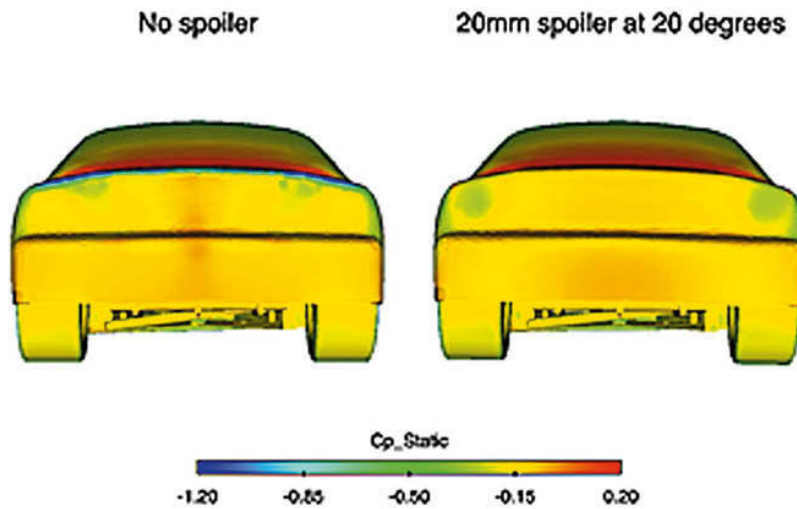


**Figure 4-27** Velocity coloured vectors with long, steep spoiler.

What magnitude of forces do these changes in lift coefficient represent? Using the same reference area (2.5 square metres) and velocity (50m/s or 180km/h, 112mph) as previously used in the airdam section, the forces generated by the longest spoiler would range from 1,470N (330lb) of downforce at a 20° angle up to 2481N (556lb) at the steepest angle tested here, compared to the baseline no-spoiler case where lift is generated. In relation to our typical car's weight of 1,000kg (2,200lb) these downforce values are significant, and we would certainly prefer to have them working for us in creating additional grip than against us by lifting the car at speed. The drag forces generated for this same long spoiler range from a very modest 123N (27lb) at 20° up to 583N (130lb) at 60°.

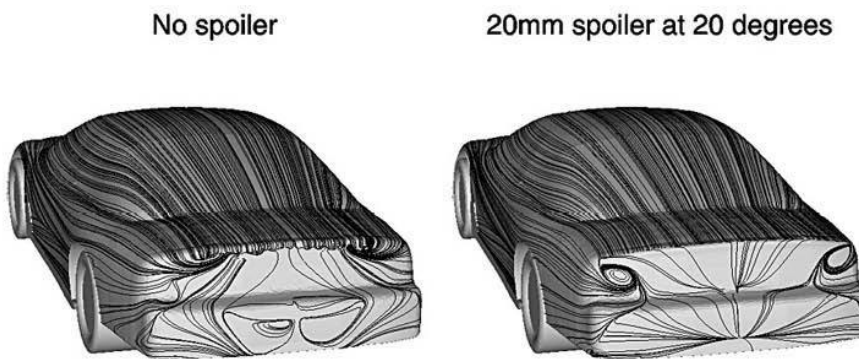
As we have seen, fitting a rear spoiler doesn't necessarily increase a car's drag. There are circumstances where a rear spoiler actually decreases drag. Those 1960s pioneers found that the height of the spoiler could be increased without initially hurting top speed, and indeed, in some circumstances, top speed did actually increase, demonstrating that drag reductions were a possibility. Then, at a particular spoiler height top speed did start to come down, but so too did lap times. This of course shows that although drag had increased, the overall net benefit was positive, and derived from increased stability and grip. Our CFD analysis mirrors these results exactly. It also gives us the opportunity to explain how the drag reductions with shorter and shallower spoilers actually occur.

Figure 4-28 plots the static pressure coefficients on the rear of the car for the baseline, no-spoiler case (left) and for the short, shallow spoiler case. Without the spoiler there is significantly lower static pressure (blue and green) on the upper part of the rear panel, just below the rear deck lip, than there is when the spoiler is fitted. Overall there is more area at lower static pressure without a spoiler, which of course creates more drag since it is acting on the essentially vertical rear panel, effectively sucking the car backwards. Fitting the small, shallow spoiler therefore increases the static pressure on the rear panel slightly and this leads to the reduction in drag. Those circular areas of low-pressure (green) in the case with the small spoiler are interesting, and we'll return to them very shortly.



**Figure 4-28** Static pressures on the rear panel, with and without the short, shallow spoiler.

So the net increase to the static pressure on the rear panel causes the drag reduction that occurs when the small, shallow spoiler is used, and Figure 4-29 supplies a clearer indication of how the flow is modified by the spoiler. In the no-spoiler case the air is flowing around the rear deck lip, and separation patterns can be seen along the upper part of the rear panel. When the spoiler is present these separation patterns are not seen, because the spoiler is causing the air to separate sooner. There are also pronounced circular patterns produced on either side when the spoiler is present, and these correspond to vortices formed by the spoiler.



**Figure 4-29** Oilflow plots with and without the short, shallow spoiler.

These flow patterns can be matched to the static pressures observed in Figure 4-28. In the no-spoiler case, the low static pressure on the uppermost part of the rear panel is associated with the airflow accelerating sharply around the radius here before separating slightly below the lip. This acceleration creates reduced static pressure here, and this in turn creates lift (on the horizontal part of the radius) and drag (on the rear facing part of the radius). Fitting the small spoiler eradicates the zone of flow acceleration, resulting in higher static pressure on the rear panel, and so less drag while the pair of vortices at the sides can be seen to align with the small circular regions of reduced pressure. However, these reductions (which actually add to drag) do not – in this case – outweigh the overall increase in static pressure on the rear panel caused by the spoiler.

This unusual short-spoiler case reminds us of several things: it never pays to over-generalise about competition car aerodynamics; that the devil is often in the detail; and that quite small changes to a competition car's set-up can have a pretty profound influence on its aerodynamic performance. It is also important to bear in mind that what works well on one car may not transfer straight over to another. A spoiler's effectiveness is clearly going to be dependent on the individual car it is fitted to, and on what has happened to the airflow on its way to the rear of the car. It is difficult to generalise, and we could for example, visualise an extreme case of a hatchback shape with a spoiler mounted at the bottom of the tailgate, where it is situated entirely in the wake and where it can do nothing for downforce production or lift reduction.

## Chapter 5

# Wings

THE DEVELOPMENT OF the various types of spoilers made it clear that lift reduction was only a part of what was possible with appropriately shaped and positioned aerodynamic attachments, and the search was on for greater quantities of downforce to press racecars ever more firmly onto the track, and enable higher cornering speeds. Following Jim Hall's resurrection of the use of the inverted aerofoil, the downforce revolution became really popular in the late 1960s, as Formula 1 cars sprouted wings front and rear, and we can now look back, 40 years later, to see where we have been. (If only we could see where we are going as clearly...) The wing designs used in those days look now to be pretty tame in comparison with the complex assemblages adorning each end of many of today's top-level single-seater racecars, and development continues at a furious pace at the sharp end of motorsport technology. Wings ain't what they used to be...

### **Definitions**

Before we go anywhere, we have to start off with some terms and definitions, if only so that we know we're all referring to the same things. It possibly goes without saying that the terminology of wings, as well as some of the technology, comes from the world of aeronautics and aircraft. Although the definitions start with 'A' they are listed not alphabetically, but rather as they came to mind. See also Figure 5-1.

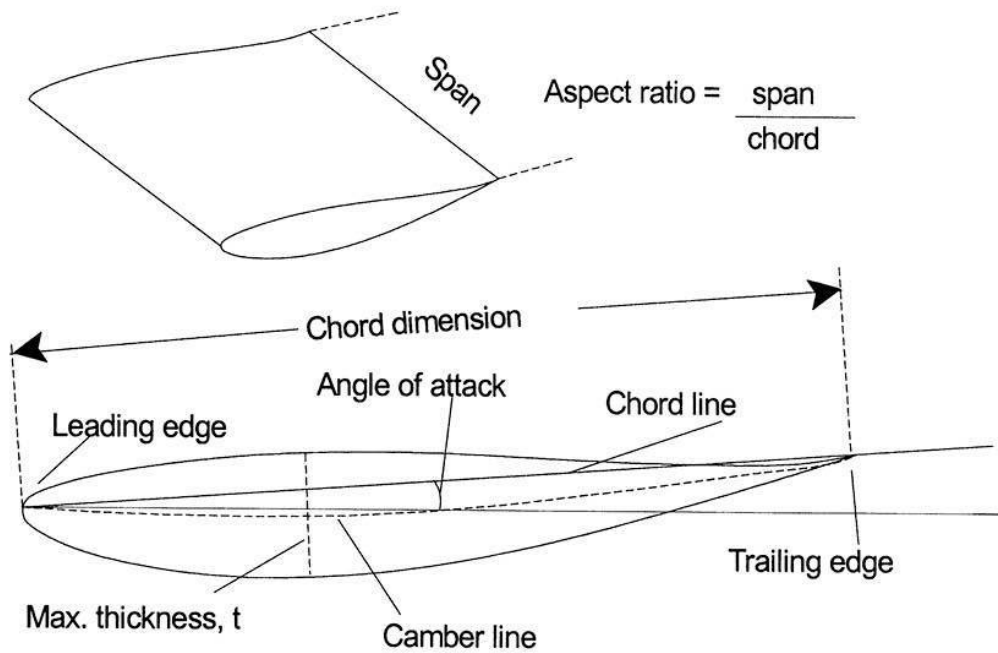


**Figure 5-1 Wing terminology.**

*Aerofoil* is generally just regarded as another word for a *wing*, which is a body so shaped that its motion through the air creates lift, or in our case, downforce, without causing excessive drag. An *airfoil* is the two-dimensional profile which defines the shape of a wing or aerofoil section. Since wing shapes can be quite complex, it follows that a wing may have various airfoil sections along its length.

The *leading edge*, or L.E., is rather obviously the front part of the wing, and is usually a more or less blunt, radiused shape. The *trailing edge*, or T.E., is just as obviously the rearmost part of the wing, and is generally thin and tapered. The imaginary straight line joining the L.E. to the T.E. is the *chord line*, and the distance along this line from the L.E. to the T.E. is the *chord dimension*, denoted by the letter 'c'. The maximum *thickness* of the wing is denoted by the letter 't', and is expressed as a percentage or decimal fraction of the chord dimension. Thus, if a wing has a chord dimension of 12in (305mm), and  $t = 18\%c$  (or  $0.18c$ ), the maximum thickness is  $12 \times 0.18 = 2.16$ in (54.9mm). The maximum thickness position is also usually stated as a decimal fraction of the chord, measured from the L.E., so if  $t_{max}$  is said to be at  $0.3c$ , it will be 3.6in (991.4mm) from the L.E. of a 12in (305mm) chord wing.

A wing section can be symmetric or asymmetric, and if it is the latter it is referred to as having *camber*, meaning that its lower (in the racecar context) surface is more curved than its upper surface. Racecar wings generally possess camber these days, although those early efforts were practically symmetrical. The line drawn through the midpoints of a wing, from the L.E. to the T.E. is known as the *median line* or *camber line*. The amount of camber present is sometimes defined as the maximum distance between the camber line and the chord line, expressed once more as a percentage or decimal fraction of the chord dimension,  $c$ . The location of maximum camber is defined in the same way as maximum thickness, also as a fraction of  $c$ .

The width of a wing is known as its *span*, and the ratio of span to chord is the *aspect ratio*. Aircraft generally have high aspect ratios while racecars, especially single-seaters, have very low aspect ratios. The *angle of attack* of a wing is the angle between the freestream airflow and the wing's chord line. It is tempting sometimes to think of the airflow approaching a racecar wing as being horizontal, parallel to the ground. This may be true of front wings (although not necessarily), but is almost certainly never true of a rear wing. Hence, the flow onto a wing may be at an angle that is locally different from parallel to the ground. It has to be admitted that for convenience, racers often quote wing angle relative to horizontal simply because it's easier to make measurements that way, but it pays to keep in mind that the airflow onto a wing is rarely parallel to the ground. Racecar wings are no longer allowed to have adjustable angle while on the move in most competition categories. Changes to angle may generally only be made in the pits or paddock. Jim Hall's Chaparral 2E and 2F in 1966 and 1967 had variable angle rear wings, which were adjusted by the driver via a third pedal (the cars had auto transmission).

The point (or line) at which the forces on a wing or other body appear to act is known as the *aerodynamic centre*. In reality this effect is the sum of the pressure distribution over the whole of the wing, both lower and upper surfaces, caused by the wing's influence on the local air velocities and the resultant local static pressure changes. As we saw in Chapter 2, the effect of a wing is to reduce the static pressure below the *suction side*, the more cambered lower surface (in the racecar context), and to raise the static pressure of the air over the upper, *pressure side* of the wing. The result of this is that both downforce and, unfortunately, drag are produced, and there will be much more on this as we go through this chapter.

In the case of wings, downforce (or negative lift) and drag coefficients,  $-CL$  and  $C_D$ , are quoted with reference to the *plan area* of the wing, that is, the span multiplied by the plan view chord for a simple rectangular wing, rather than

the frontal area which is the reference area for a whole car. The *lift to drag (L/D) ratio* is once more used as a measure of aerodynamic efficiency.

### Downforce and wing design criteria

Before we start to look in detail at the influence of wing design criteria, mention must first be made of the NACA wing profiles. The National Advisory Committee for Aeronautics (NACA) was an American body, the forerunner of NASA, (that country's current aerospace agency), which developed a system of defining and cataloguing aerofoil shapes during the 1920s and '30s, following on from earlier post World War One work in Germany and elsewhere. The book by Abbott and von Doenhof (see Appendix 2) entitled *The Theory of Wing Sections* gives a great many of the NACA wing profiles, and this catalogue still serves as a valuable source of shapes that could be applied to motorsport. Yes, the profiles were created for aeronautical applications, and yes, the teams at the forefront of motorsport research may now have progressed beyond the need for this type of information, but that still leaves an awful lot of constructors and competitors, amateur and professional, for whom such a reference book, however ancient and whatever its original application, is a real boon. Of course, the actual choice of profile still has to be made, but hopefully we can derive some guidelines here. Further valuable sources of similar information are also given in Appendices 2 and 5.



*The Chaparral 2E and 2F (seen here) had driver-adjustable wing angles.*

Competition car wings can be single-element, dual-element or multi-element devices, depending on the racing category and the configurations permitted by the rules, as well as the demands imposed by the particular track and the tolerance of a given car to downforce and drag. Some cars run simple wings because they have to, while others run them because they cannot tolerate large amounts of drag. Other cars carry multi-element devices because their tolerance to drag is greater, and the need for large amounts of downforce is paramount. One crucial point to remember is that the environment a wing has to work in on a racecar is totally different to that in which an aeroplane wing has to work. So, although a lot of the basic information available on wings comes from the world of aircraft, keep in mind that things happen differently, and usually a lot less efficiently on racecars (just why that is so will be picked up as we go through this chapter).



*Some cars use single-element wings because they don't have the power to tolerate lots of drag.*



*And some cars carry large multi-element wings to maximise downforce with little concern over drag. (Rupert Berrington Action Photography)*

### **Single-element wings**

The downforce generated by wings is influenced by a number of fundamental parameters including the number of wing elements, overall dimensions, the angle of attack at which the wing is set, camber and thickness, to name but a few. We're going to start by looking at varying some of those parameters on single-element wings before moving on to multi-element wings, and other influential aspects.

### **Angle of attack**

The simplest wing parameter to change on a racecar is the angle of attack, often designated by the Greek letter alpha ( $\alpha$ ). Changing other parameters, such as span, chord, thickness or camber, requires re-manufacture and maybe a re-design, but changing angle does not.

What happens to the airflow around a wing as the angle of attack is increased? In particular, what goes on as the angle gets to critical higher angles? To show what is really going on, here are some data from some simple two-dimensional CFD runs on a wing section similar to that in Figure 5-1 (based on NACA profile designation 63<sub>2</sub>-615). Note that real world three-

dimensional aerodynamic effects, and in particular, the location of a wing on a racecar, naturally conspire to complicate the whole issue, but 2D provides a useful model for exploring the basic effects.

A virtual airflow of 50m/s (180km/h or 112mph) over the wing section in question was set up, and runs were performed at a range of angles (between wing and freestream airflow) from 0° to 16°. Downforce values at a notional wing area were then calculated from the basic lift equation (Lift, or downforce =  $1/2 \rho A C_l V^2$ ), as were surface pressure coefficients and streamline velocities off the wing surface, to provide the illustrations herewith.

Figure 5-2 shows the basic relationship for this wing section between downforce and angle of attack. A number of conclusions are apparent. First, the maximum angle of attack to run in this instance would appear to be 12°, this yielding maximum downforce here (although don't take this as too indicative of a maximum angle in reality – such a wing could possibly run steeper on a competition car, as we shall see later). Second, the initial linear increase in downforce with increasing angle had already begun to tail off after 8°, which begs the question: 'What is happening here?' And third, it is evident that downforce was already being generated at zero angle of attack; how can this be?

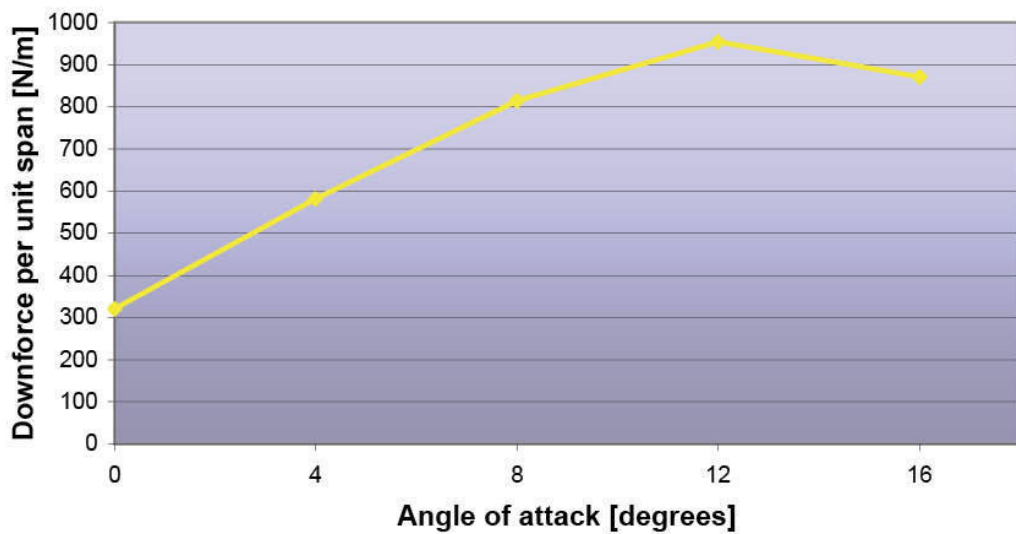


**Figure 5-2** Downforce versus angle of attack calculated on our wing profile by 2D CFD.

Starting with the last point first, many people seem to think that a wing needs a visibly positive angle on it to provide downforce. Yet if the graph line of Figure 5-2 was extrapolated to the left it would be evident that downforce

would still be generated at small *negative* angles, that is, with the nose higher than the tail, and that the ‘aerodynamic zero’, the angle at which no downforce is generated, would be about  $-5^\circ$ , that is,  $5^\circ$  nose up. This is because this wing is not symmetrical in profile, but is ‘cambered’, having more curvature below the chord line than above it. This creates the difference in the velocities over the upper and lower surfaces even at zero or small negative angles of attack, which generates the difference in pressures above and below that creates downforce.

Figures 5-3 and 5-4 illustrate the zero angle case. Figure 5-3 is a surface pressure plot for this wing, and shows not only a negative pressure coefficient on the convex lower (‘suction’) surface of the wing, but also a positive pressure coefficient on the rearward portion of the concave upper (‘pressure’) surface (and at this angle the negative pressure on the forward portion of the upper surface). Figure 5-4 shows the streamlines coloured by static pressure, and demonstrates even more clearly the distribution of low and high pressures in the air around the wing. The stagnation point can be seen at the leading edge, where the streamlines divide above or below the wing. The pressure coefficient is high here, as would be expected.

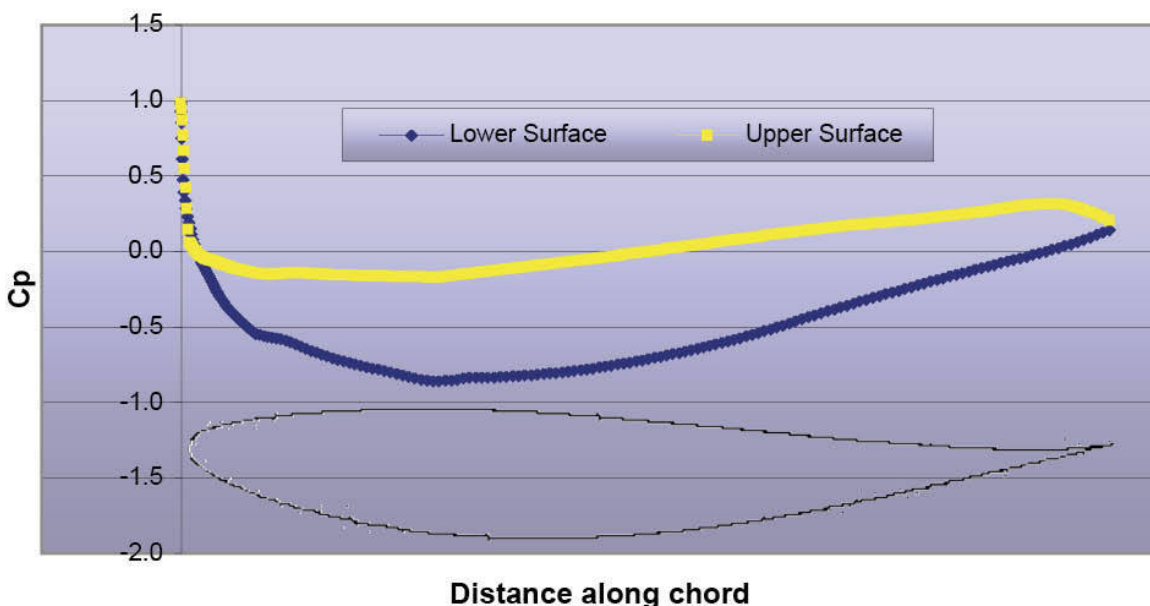


**Figure 5-3** Surface pressure distributions at  $0^\circ$ . The wing profile is shown for reference.

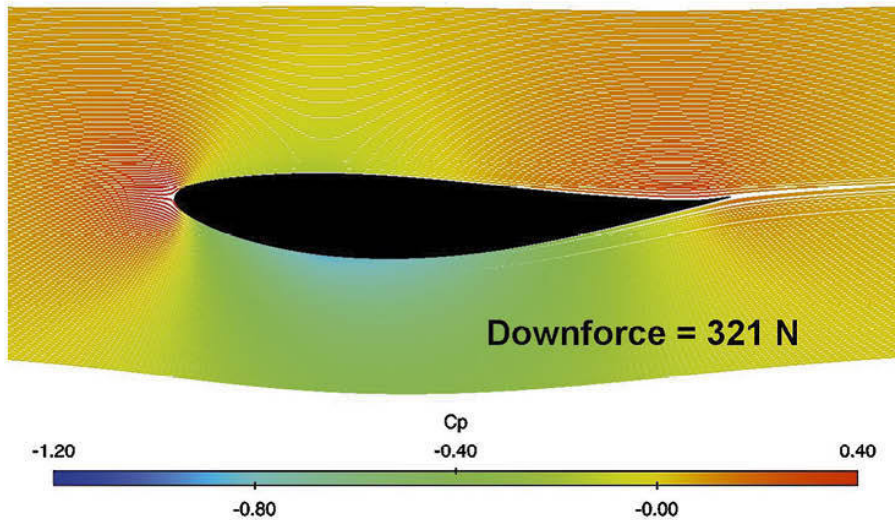


**Figure 5-4** Pressure coloured streamlines around the wing at  $0^\circ$ .

Figures 5-5 and 5-6 represent the  $12^\circ$  case. As the angle of attack increased the suction side of the wing developed ever-lower pressures, and there was also a general forward shift in the low-pressure region. The stagnation point actually shifted to the upper surface, and the static pressure on the upper surface was positive all the way along. The airflow was accelerating right around the leading edge, contributing to that forward shift in the low static pressure region. Furthermore, because of the increasing magnitude of the low pressure, an increasingly adverse pressure gradient developed towards the trailing edge of the wing.

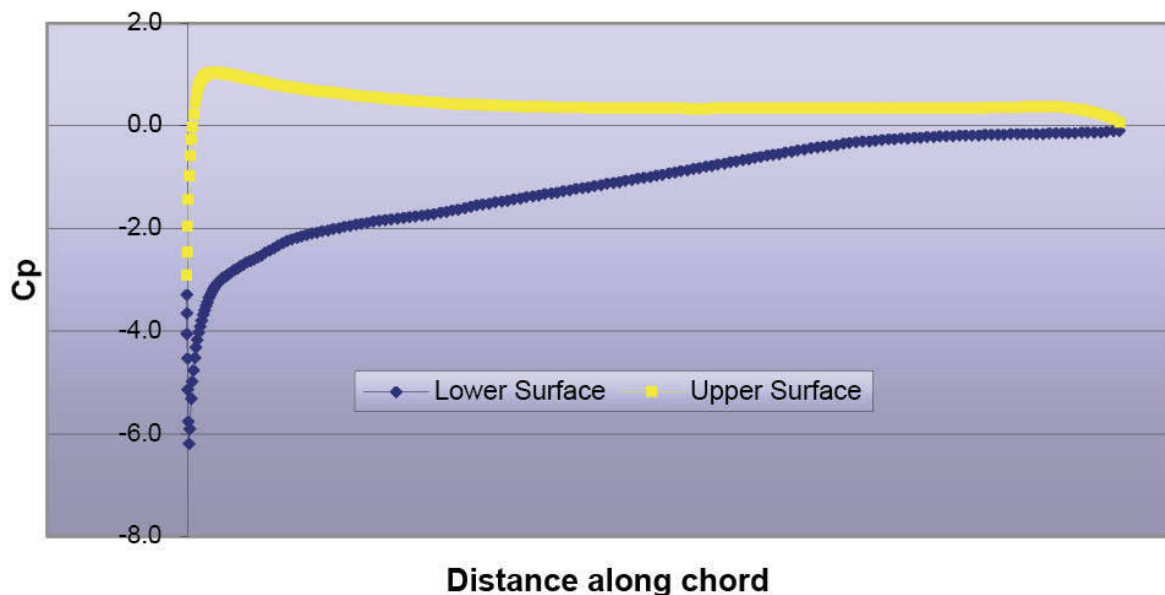


**Figure 5-5** Surface pressure distributions at  $12^\circ$ .

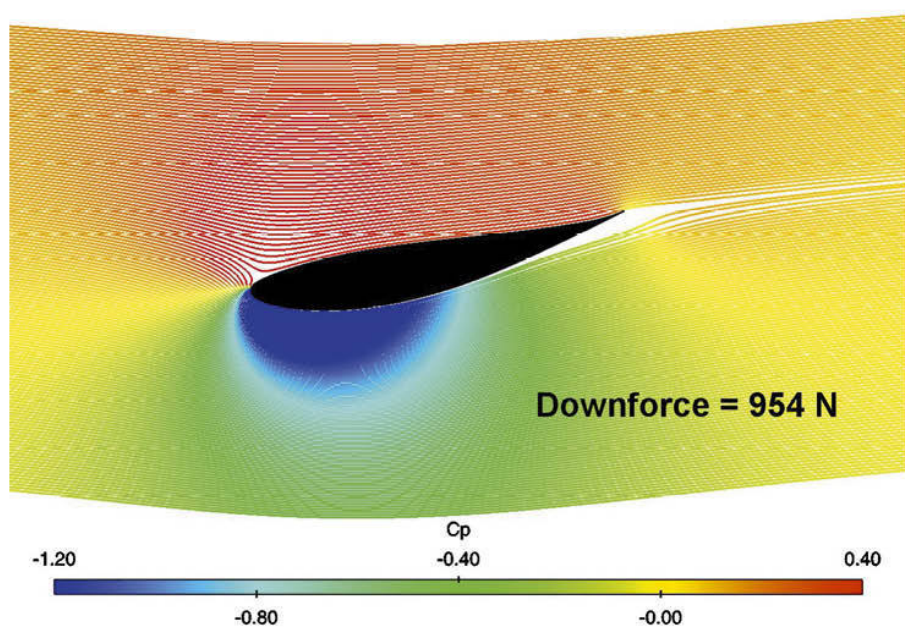


**Figure 5-6** Pressure coloured streamlines around the wing at  $12^\circ$ .

As we have seen previously, if the adverse pressure gradient becomes too steep for the level of momentum the air possesses then separation can occur, and this can be seen developing at  $12^\circ$  in Figures 5-5 and 5-6. The surface

pressure plot shows a flattening of the suction side pressure curve at about two thirds chord, and some separation is clearly shown by the streamlines at this point. However, as the  $12^\circ$  case generates maximum downforce in this instance, we can conclude that some flow separation is not necessarily too detrimental. Figure 5-7 shows very clearly what happens when things are pushed too far. Although high downforce was still being generated at  $16^\circ$ , it reduced compared to the  $12^\circ$  case, and major flow separation occurred under the wing. This amounts to wing stall.

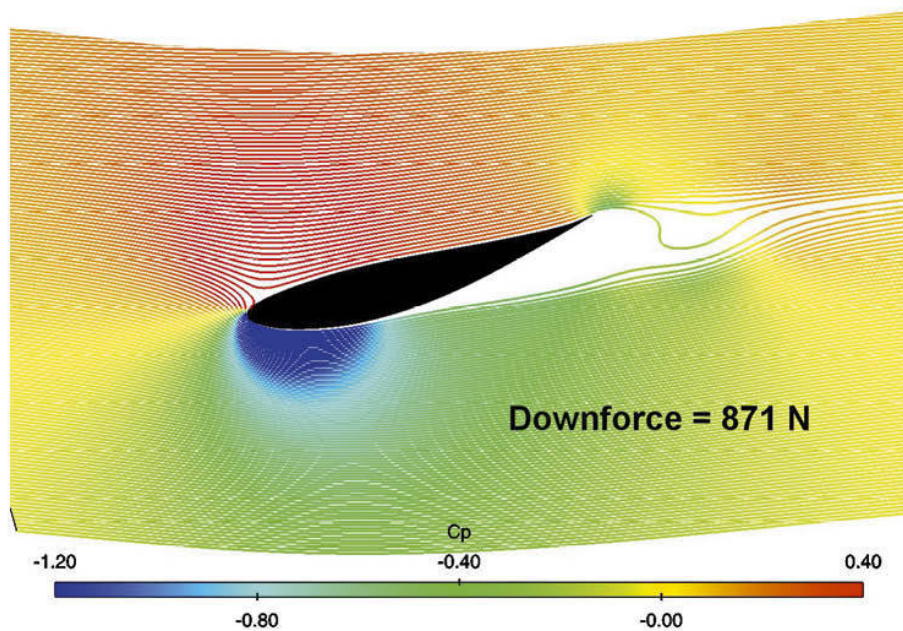


**Figure 5-7** Pressure coloured streamlines around the wing at  $16^\circ$  showing flow separation.

## Camber

Changing camber is another way to manipulate a wing's lift coefficient, although caution should be exercised to ensure you don't go outside any relevant dimensions specified in the regulations.

The accepted wisdom in the aeronautical texts is that more camber gives more lift (downforce in our context) at a given angle, although the suggestion in some references is that stall may occur at lower angles. Traditional texts however, don't make it clear whether *maximum* downforce should be expected to change with camber.

So how much camber is good, and what happens to the airflow around a wing as camber is increased? A range of wing models was set up once again using the NACA 63<sub>2</sub>-615 profile as a starting point. The shape was then

manipulated to put more or less camber into it, maintaining the location of maximum camber at the same position along the wing chord in all cases. Then, a set of two-dimensional CFD runs at a virtual air speed of 50m/s (180km/h) was performed at a range of angles of attack, and over a range of cambers from 4% to 12%.

Downforce versus angle of attack for the range of cambers studied is plotted in Figure 5-8. (Note: the missing point indicates that ‘unsteady’ flow conditions in the extreme camber cases prevented a solution being calculated. It might be wise to assume that the failure to solve this data point indicates a configuration to be avoided...). The first noticeable relationship is that, for a given angle of attack, downforce did increase with greater camber, at least up to camber values of 9% applied to this particular ‘family’ of wing profiles. Secondly, peak downforce also increased with camber, again up to the 9% camber value at least. Thus, the whole downforce curve was translated vertically as camber was incrementally increased, but the stall angle appeared to be about the same, 12° to 14°, in three out of the four cases up to 9% camber.

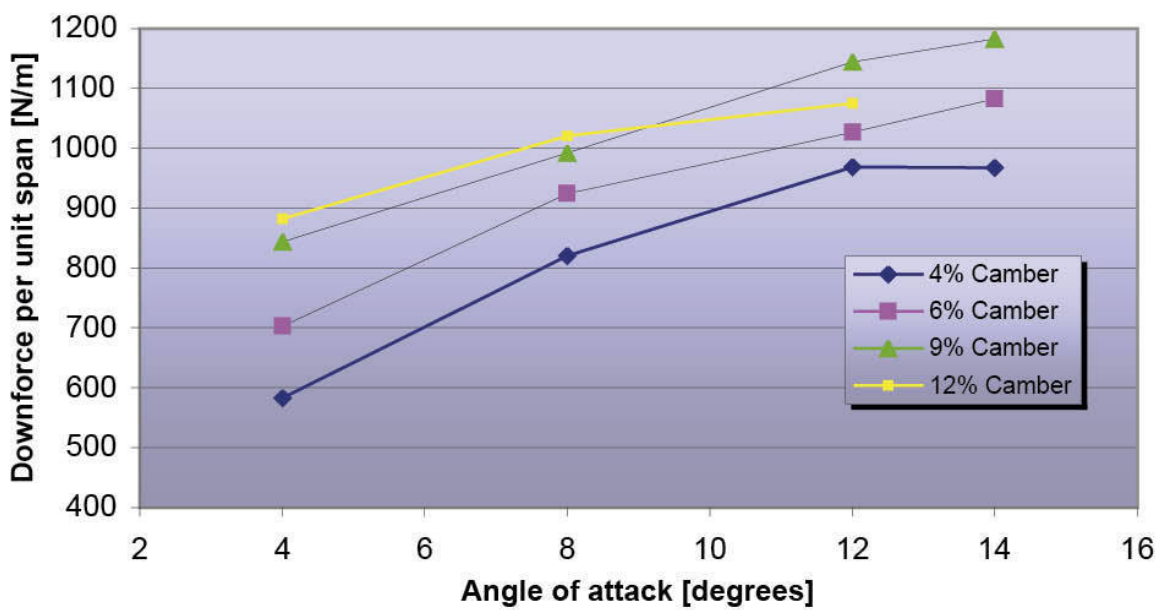


**Figure 5-8** Downforce versus angle for a range of camber values.

However, the highest camber value studied here behaved differently from the others. While it followed the same slope up to an angle of attack of  $8^\circ$ , performance tailed off sooner than with the lower camber wings. The 12% camber wing peaked at just  $12^\circ$ , with a lower downforce value than that achieved by the 9% camber wing at this angle. The obvious conclusion is that the geometry generated by giving this wing profile 12% camber pushed things too far, and 9% camber looks to be optimum here for maximum downforce.

Figures 5-9, 5-10 and 5-11 show pressure-coloured streamlines from three of the runs performed, these all being at  $8^\circ$ , but at cambers of 6%, 9% and 12%. The flow around the wings changed as camber was increased, with almost fully attached flow on the underside of the lowest camber wing here, flow separation developing at 9% camber, while substantial flow separation had developed at 12%. Thus, although downforce increased with each additional increment of camber, it is clear that the airflow was struggling to remain attached to the wing as higher values of camber were applied. Steeper angles demonstrated more separation developing with only small additional increments of downforce.

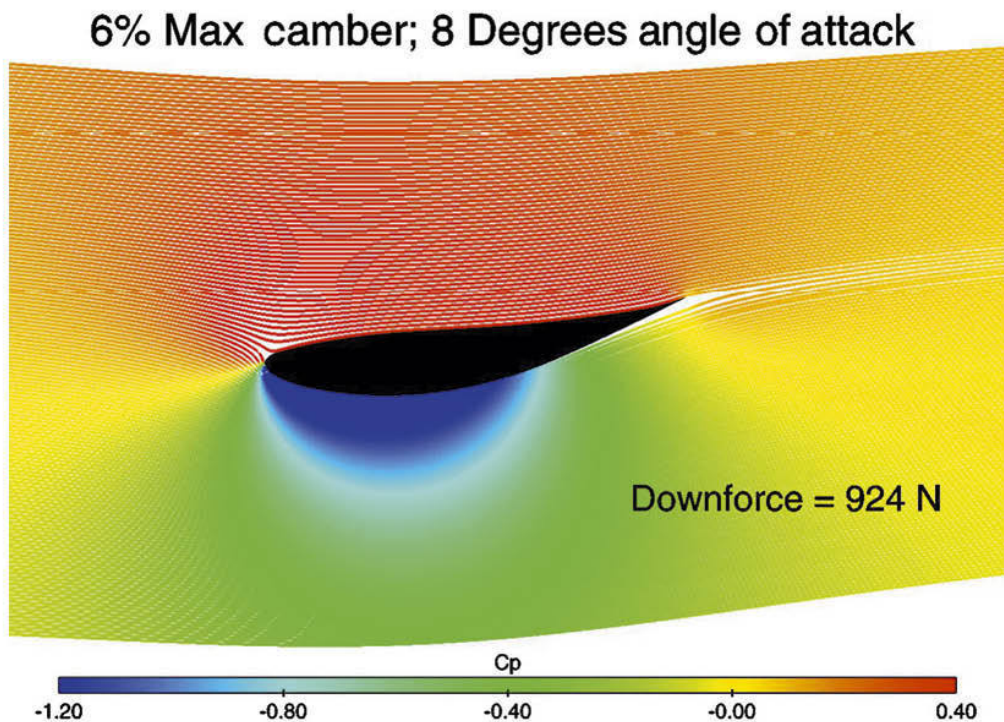


**Figure 5-9** At 6% camber flow was fully attached.

9% Max camber; 8 Degrees angle of attack

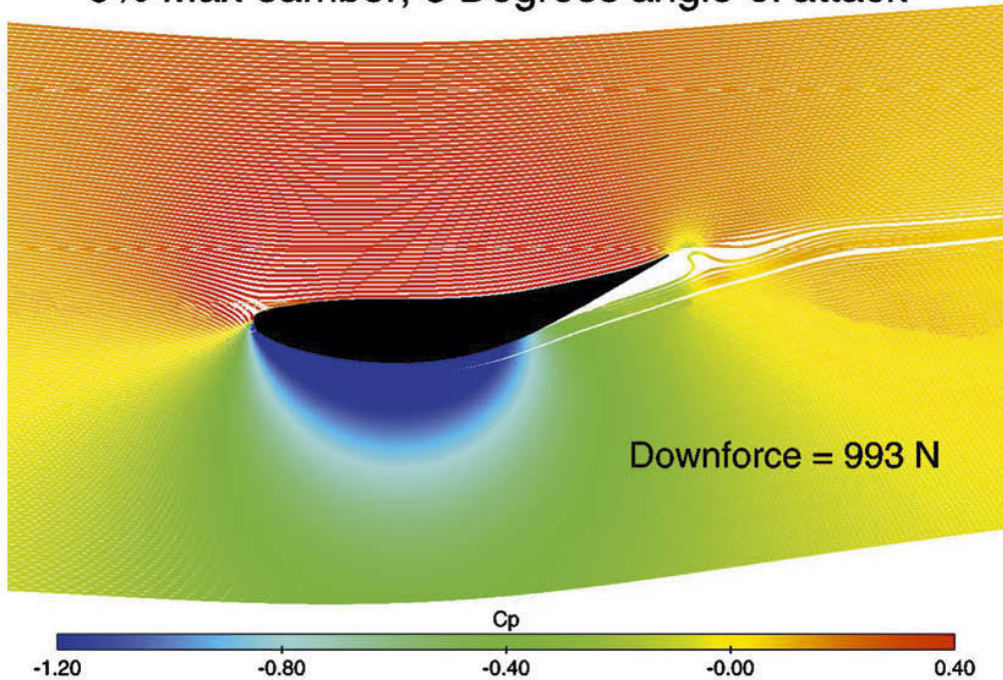


**Figure 5-10** At 9% camber separation was beginning to develop.

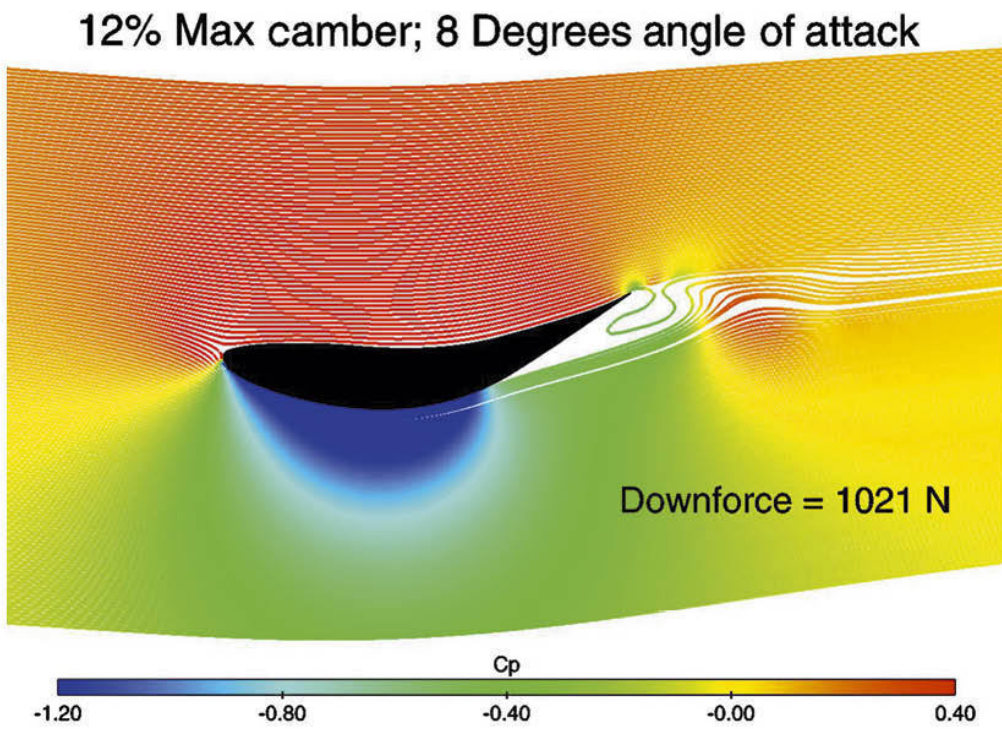


**Figure 5-11** At 12% camber substantial separation occurred.

So, the lesson here is that you can generate considerably more downforce from a single-element wing if you add more camber, but only up to a point. The optimum value found in this study should not be taken as a generalised figure though, but rather as an indicator that there will be a maximum camber value that any particular wing profile can be ‘morphed’ to.

Again, as this was a 2D CFD study, 3D effects like the vortex drag created by the generation of downforce were not evaluated. The profile drag can be calculated using 2D techniques, and profile drag, like induced drag, does change with angle of attack. Basically, profile drag increased with camber in this exercise. Thus, efficiency ( $L/D$ ) decreased as more downforce was generated, in a diminishing returns relationship with increasing angle of attack, although 4% and 6% camber demonstrated similar  $L/D$  values. Put another way, the best efficiency figures occurred at the lower camber values.

This exercise only looked at one location for maximum camber, 50% along the chord. It is possible that the effect on wing performance would be different if the location of maximum camber were different. There are

suggestions in some references that shifting the point of maximum camber forwards is appropriate to low drag set-ups at low angles of attack. Conversely, rearward-biased camber is said to have a greater effect on downforce generation with a more progressive stall. Indeed, by changing the rearward geometry of a wing the downforce characteristics can be significantly altered, and this is most easily done with adjustable flaps, of which more shortly.

### **Wing thickness**

Section thickness is another parameter that has an influence on wing performance, but different aeronautical references give different views on its effect. For certain symmetrical wing profiles (such as the NACA 0006, 0009 and 0012, having zero camber, and thickness from 0.06c to 0.12c) the stall was said to become more ‘abrupt’ as thickness was increased, while for other non-symmetrical sections (eg the NACA 2412, 2415 and 2418, each having 2% maximum camber at 0.4c, with thickness from 0.12c to 0.18c), increased thickness seemed to lead to a more gentle stall, but a lower peak lift coefficient. When the thickness of these profiles was increased beyond 0.12c, the maximum  $-C_L$  value actually tailed off slightly again, and the implication of this is that if a wing is intended to remain as a single-element device, a maximum thickness of 0.12c could be construed as a design parameter. However, very thin wing profiles seem to be associated with an abrupt stall, caused by ‘leading edge separation’, a phenomenon caused by too rapid acceleration of the airflow around the leading edge of the wing.

In contrast to this, information from Abbot & von Doenhof and McCormick (see Appendix 2) showed that at Reynolds Numbers of 2 million and less, increasing thickness over 12% of chord (0.12c) had little effect on  $-C_{L_{max}}$ , and this could have significance for a great many competition categories, except perhaps the very fastest. The implication of this is that thickness doesn’t really matter in our speed regime. But is this really the case? Using CFD to take a new look at thickness using similar basic 2D methods to those used in the previous sections, the results were rather different to what either of those textbooks stated...

A range of wing models was again drawn using the NACA 63-615 profile as a generic starting point. This gave maximum thickness ranging from 8% of chord to 24% of chord, all with maximum thickness located at the same point along the chord. The CFD evaluations were again run at 50m/s (180km/h) at angles of attack ranging from 0° to 16°. In a slight variation of our plots, downforce versus thickness at various angles in this range are shown in Figure 5-12, and a number of conclusions may be drawn.

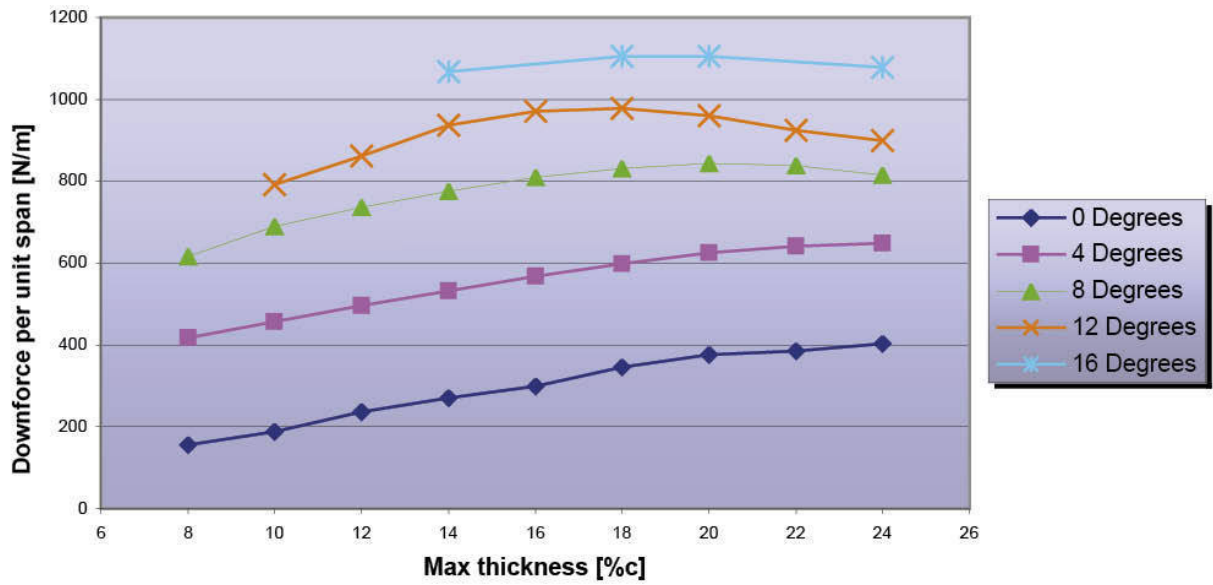


**Figure 5-12** Downforce versus thickness for a range of angles.

First, it is very evident that in this exercise maximum downforce did not peak at 12% thickness. In fact, downforce continued to climb with increasing thickness, but peaked at values that were dependent on angle of attack. At the shallowest angles tested,  $0^\circ$  and  $4^\circ$ , peak downforce occurred at the maximum thickness evaluated, although gains had begun to tail off at around 20% thickness. At  $8^\circ$  maximum downforce occurred with 20% thickness, while at  $12^\circ$  maximum downforce was achieved with 18% thickness. What initially seemed to be a trend towards slightly lesser thickness producing best downforce at steeper angles had, however, reversed by the  $16^\circ$  plot, which showed almost identical peak downforce values at 18% and 20%.

From this we might reasonably conclude that we could expect downforce to increase with increased thickness, up to a practical top limit of around 18% to 20% thickness if angles of attack up to  $16^\circ$  are likely to be run.

It is apparent that some data points have been left off this graph, and the reasons are significant when it comes to choosing an appropriate wing thickness. Specifically, the thinner sections did indeed exhibit leading edge separation at the steeper angles of attack of  $12^\circ$  and  $16^\circ$ . This had the effect of causing early, abrupt stall, and highly unsteady flow conditions aft of the leading edge. In other words, thin wings, in this family of profiles at least, cannot be run at steeper angles. 2D CFD *may* make this potential problem appear worse than it actually is; nevertheless, it is a real phenomenon. It can be

avoided in a number of ways, obviously one of which is to use a thicker section, which tends to generate a more generous leading edge radius that gives the air an easier passage around this part of the wing.

So, thicker sections appear to be a way to increase downforce, but what about drag? Clearly, increases in downforce will lead to increased drag anyway. What can be illustrated from these evaluations is that the thicker wing sections, not at all surprisingly, generate greater ‘profile drag’, and we can get an idea of how profile drag changes by looking at the drag calculated by 2D CFD (although as we have seen this is not the full drag picture).

Figure 5-13 plots L/D (lift to *profile* drag ratio here) against wing thickness. Again it is evident that efficiency changed according to angle of attack and thickness. Clearly L/D was highest at the shallower angles where lower drag was generated, but of more interest here is that in general, peak L/D occurred with a wing section of 16% thickness from 4° to 12° angle of attack. Intriguingly, at the steepest angle of attack, 16°, maximum L/D occurred with 20% thickness, this obviously due to the higher downforce generated in this case.

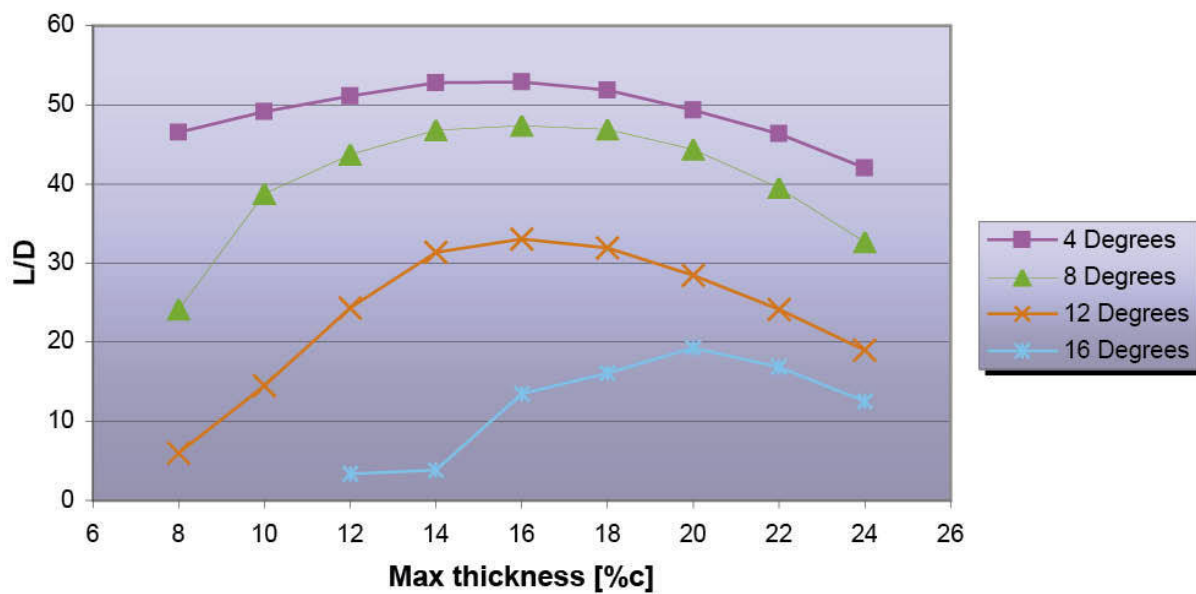


**Figure 5-13** Lift to (*profile*) drag ratio versus thickness.

Thus, with this ‘profile family’ best efficiency occurred using a thickness of 16% although again, if it was anticipated that the wing would be run at its steepest angle most of the time a thickness value of 20% might be more

efficient. Taking this, and the earlier conclusions on achieving maximum downforce, a good compromise between maximising downforce and efficiency might be to run a wing of this kind of section profile with around 18% thickness, inclining slightly one way or another depending upon the principal aim.

Clearly, as with camber, there are tunes to be played when juggling the requirements of maximising downforce and efficiency.

### **Leading edge radius**

Another parameter of interest was mentioned in passing above – leading edge radius. This is the radius of the circle that fits into the profile of the extreme foremost part of the wing section. To an extent this parameter is defined by the other main parameters, including in particular the maximum thickness, its location along the chord of the wing. However, it is also possible to vary thickness without altering the other basic parameters.

Leading edge radius is another parameter on which contradictory references may be found. We have seen that a sharp leading edge, especially on a thin wing section, can cause leading edge separation, creating an abrupt and possibly early stall. However, at a shallow angle of attack it may also be the case that a sharp leading edge helps to maintain a thinner boundary layer over the first part of a wing, leading to improved efficiency. Both these effects may occur on the same wing at different angles of attack. Furthermore, in the case of high downforce, multi-element wings, the high suction developed on the main element can cause very rapid acceleration around the leading edge, and in order to prevent leading edge separation a change to the leading edge shape may be required. This might mean a profile with more forward camber that turns the leading edge more into the oncoming flow direction, or perhaps a more rounded, thicker profile. Historically, leading edge profiles in the major single-seater formulas have changed from blunt, large radius designs to much sharper shapes nowadays, perhaps in the order of 1–3% of chord. Applying these numbers, a 300mm (11.8in) chord wing might have a leading edge radius of 3mm to 9mm ( $\frac{1}{8}$ in to  $\frac{3}{8}$ in) radius. This evolutionary design shift reflects the improvement in the knowledge of flow directions from techniques like CFD that have in turn enabled this kind of device optimisation. But if a wing is likely to be used across a wide angle range it would make sense to err towards the upper end of the leading edge radius range. But if a wing is likely to be used across a wide angle range, it would make sense to err towards the upper end of the leading edge radius range.

## Single element selection criteria

So for a single element wing, the selection parameters might include:

- Low angle of attack for low downforce and low drag, high angle of attack, up to a maximum of around  $14^\circ$  to  $16^\circ$  *relative to the airflow* for greater downforce, with inherent drag penalty.
- Camber in the range 4% to 6% for low downforce, low drag and high efficiency around 9% or so for maximum downforce.
- Thin section thickness for a very low downforce, low drag set-up, 14% to 16% thickness for best efficiency across the widest range of angles, and 18% to 20% thick for maximum downforce.
- A leading edge radius probably in the range 1% to 3% of chord.

There is still an endless choice of thickness and camber distributions to pick from, but this general four-point plan may help to draw up a short list of candidate profiles to suit a particular competition category, and the venues visited – it may not be possible to pick just one profile that suits all the venues to be visited, but the decision on whether to compromise on just one wing, or have a selection available is *yours!*

## Quantifying downforce from single-element wings

The graphs in the foregoing sections have given downforce in Newtons per metre of span, but clearly, downforce depends on the plan area of the wing, which is span multiplied by chord. The chord dimension used in these trials was 400mm (15.75in approx.), so we can read directly off the graphs what levels of downforce these wings at this chord and 1 metre (39.4in approx.) span would generate at the airflow velocity used here (50m/s, or 180km/h). To calculate levels of downforce for bigger or smaller areas, simply multiply by the ratio of the area you have in mind, in square metres, and to calculate at different speeds multiply by the ratio of the speeds *squared* (eg at 33.5m/s, equivalent to 75mph, multiply by  $(33.5/50)^2 = 0.45$ ). Be careful when extrapolating the forces at different speeds and at different wing chord measurements too far – as we have seen, the Reynolds Number is related to both of those parameters, and the airflow does not behave the same at markedly different speeds and body sizes. And when altering dimensions the wing's aspect ratio also changes, which as we shall see later also affects performance.

Just to expand on these downforce values, peak downforce values, depending on camber and thickness, have been roughly in the range of 970N to 1,180N for these single element wings. For 'imperialists' this corresponds to

about 217lb to 256lb. Re-calculating at 44.65m/s (100mph) makes this range about 774N to 940N (173lb to 204lb). These are probably somewhat optimistic values, and this is down to the fact that the CFD analysis was done in 2D, which did not take into account 3D effects that would tend to yield somewhat lower lift coefficients. While 2D is great for comparing the relative effectiveness of different aerofoils the data generated should not be used too literally.

By way of comparison, the aeronautical data given in Abbott & von Doenhof suggests that the maximum lift coefficients of single-element wings range from about 1.2 to 1.6 just before they get to the stall angle, and a typical value for a 12% thickness (0.12c), moderately cambered wing (say 4% camber at 0.4c), such as the NACA 4412 is a maximum  $C_L$  of about 1.5 at 13°.

However, all of these  $C_L$  values are at Reynolds Numbers of  $Re = 3$  million (or  $3 \times 10^6$ ), and stall angles tend to reduce at lower Reynolds Numbers, leading to lower  $C_L$  values. In the case we are using for our example here, the wing had a chord of 0.4m, and speed was 50m/s. Going back to Chapter 2 briefly, we said that the Reynolds Number could be calculated thus when using metric units:

$$Re = 67,778 \times \text{speed} \times \text{'length'}$$

length in this case being the chord dimension.

Thus, our Reynolds Number here is  $67,778 \times 50\text{m/s} \times 0.4\text{m}$ , which comes out to 1,335,560, or  $1.335 \times 10^6$ . This is a lot lower than the value at which the above lift coefficients are quoted, and we can safely assume therefore that the lift coefficient at this lower value will also be lower, maybe of the order of 1.3 to 1.4 at the maximum angle of around 12° to 13°.

Other factors will also conspire to produce a lower  $C_L$  than we might desire, such as turbulence from the rest of the car ahead of the rear wing, and the fact that the wing has a small aspect ratio (span divided by chord, dealt with in more detail later) – but let's not get too pessimistic! To make the sums slightly easier in this instance, we will just assume that the effective  $C_L$  has declined by around 25%, and is going to be exactly 1.0. So we can now calculate a realistic value for the negative lift or downforce that our single-element wing might produce at 100mph (44.65m/s):

$$\begin{aligned} \text{downforce, } N &= 1/2\rho A C_L V^2 \\ &= 1/2 \times 1.225 \times (1 \times 0.4) \times (44.65 \times 44.65) \\ &= 488.4\text{N (109.5lb)} \end{aligned}$$

So, even if the wing is operating in ‘dirty’ air at the back of the car, and due allowance is made for the loss of achievable downforce as a result of this, around 100lb+ of downforce could be expected from this size single-element wing running at close to its maximum angle at 100mph.

### Dual-element wings

If considerably more downforce than is attainable with a single-element wing is required, we might contemplate the use of a multi-element wing. The simplest multi-element design is, of course, the dual-element wing, where the *mainplane* is supplemented by a *flap* (see Figure 5-14). If a flap is added to an existing single element wing in the appropriate position, a number of things happen. First, the plan area is increased, which as we have seen, enables the creation of more downforce. Secondly, the effective camber of the dual element device is increased, which again will supplement downforce at a given angle of attack. Thirdly, a crucial interaction between the mainplane and the flap is brought about by their positions relative to each other, which assists in the creation of more downforce by modifying the airflow over the whole wing.

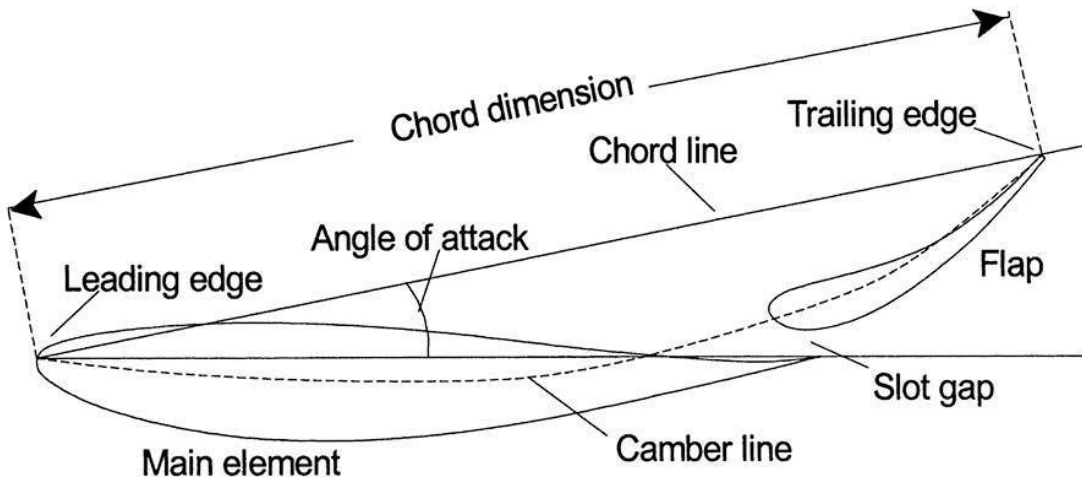


**Figure 5-14 Dual-element wing terminology.**

There are a number of criteria relating to the flap size and, especially, position that are important. The size of the flap, that is, the flap chord dimension, is generally of the order of 25% to 30% of the *overall* (mainplane plus flap) chord,  $c$ . Bigger flap chords of 30% to 40%  $c$  are used, and can produce higher increments in downforce coefficient. The actual shape of the flap is frequently a scaled down version of the mainplane, but it may just be a simple NACA profile and still function effectively. It may need to be

somewhat thicker than the mainplane, relative to its own chord dimension in order that it can be made stiff enough.

The most important consideration however is the relative positioning of the flap in relation to the mainplane. The key here is that a narrow slot is formed between the mainplane trailing edge and the flap leading edge. This necessitates an overlap between the two elements, with the flap being positioned above the mainplane trailing edge (in a downforce inducing application). The size of the gap between the mainplane and the flap is said to be best at around 1% to 2% $c$  if you consult the aeronautical texts, and the overlap between the flap leading edge and mainplane trailing edge, although not so critical, is usually said to be best at around 1% to 4% $c$ . However, trials the author has done on a dual-element rear wing profile on a single-seater racecar at full scale in the MIRA wind tunnel in the UK suggested a somewhat bigger gap and overlap were best for maximum downforce; 3.8% $c$  and 5.2% $c$  respectively (15mm gap and 20mm overlap on a 385mm chord wing, to save you the trouble working it out) produced the best figures. The most critical criterion is said to be that the shape of the slot must be convergent, that is, narrowing from its opening to its exit. In reality, the only way to optimise the geometry of a given wing and flap is to test, preferably with CFD or in a wind tunnel so reliable data can be generated. The figures above, however, will get you in the ballpark

It is frequently said that the function of a flap is to not only add area (possibly) and camber to increase downforce, but ‘to allow some air from the upper, pressure side of the wing to bleed through the slot into the suction side. By forcing this air to pass through a convergent slot, it is accelerated, and as such enters the flow on the suction side with increased energy, and lower pressure. This helps to control the boundary layer, and delay flow separation, which in turn ought to enable a higher angle of attack to be used before stall occurs.’ However, to put the record straight on this popular misconception, this is *not* the fundamental mechanism by which a flap augments lift. The effect of fitting a flap is too large for this to be a primary lift enhancing mechanism.

The reality is that, not surprisingly, a number of interactions occur. First, the flap has the effect of turning the airflow at the mainplane trailing edge, thereby effectively increasing the angle of attack of the whole wing. In so doing it increases the air velocity over both surfaces of the mainplane. In the case of the suction surface of the mainplane this is beneficial because it raises the velocity at the trailing edge, which in turn reduces the severity of the adverse

pressure gradient here and this enables the wing to be ‘pushed harder’ because the likelihood of separation on the mainplane is reduced.

There is also an interaction between the mainplane and the flap that benefits the flow around the flap. This in part relates to keeping the mainplane wake separate from the flow field around the flap. By using a sufficiently wide slot gap the mainplane wake is prevented from interfering with the formation of the flap boundary layer. This ensures that the boundary layer on the flap is ‘fresh’ and therefore thin at the start of its adverse pressure gradient, and as such flow separation is less likely to occur on the flap.

This combination of interactions enables much greater pressure differentials between the upper and lower surfaces to be withstood by multi-element wings than single-element devices. So the amalgamation of additional area (maybe), increased camber, and the beneficial modification of the flow field around the wing all add up to produce a very significant increment of extra downforce.

What then are the general design criteria that should be employed for a two-element wing? Well, some of the basic criteria for a single-element wing will still be applicable to the mainplane design. However, it is said that thicker mainplane sections with more rounded leading edge radii can work better with flaps, and if the flap chord is at the higher end of the preferred range, say 30% to 40% chord, then a mainplane thickness as high as 20% is said to give a significant increase in downforce compared to a mainplane of around 10% thickness. The amount of camber in the mainplane will depend on the application, and is likely to be in the range of 5% to 15% $c$ , and quite possibly 20% or more for high downforce applications, positioned perhaps slightly forward of or around halfway along the chord. The adjustment to the angle of the flap will have the effect of altering the rearward bias of the camber of the overall wing.

As for the flap itself, as has already been stated, the flap chord will most likely be around 30% $c$ , and the flap thickness may need to be, relatively speaking, slightly thicker than the mainplane thickness. The position of the flap’s maximum thickness is often fairly well forward, say at around 0.20 $c$  – this can help to create the converging slot shape between the flap and the mainplane by producing fairly rapid curvature from the flap’s leading edge onto its lower surface. The flap profile does not seem to be critical in order that it will perform a useful function, but logic dictates that the same criteria that apply to a single-element mainplane ought to be applicable to the shape of a flap. So it would seem to be a reasonable assumption that a more cambered flap will help to generate more downforce than a less cambered one. Furthermore, the use of a flap with more camber can make it easier to achieve

the convergent slot shape than if the flap has a flatter profile. The maximum angle of inclination of the flap relative to the mainplane chord line will be determined by testing, but will probably not exceed 40°. While downforce will increase with steeper flap angles, the increments become smaller, and the increases in drag become larger, so efficiency drops off.

Once more we can use a CFD study to put some quantities on the likely magnitude of the gains we can expect from a dual-element wing over a single-element device, and also see some of the effects that provide benefit. The model set-up on this occasion used, as the main element, the generic wing profile on which the single-element analyses of the previous sections were based. A flap with a chord approximately 40% that of the main element was located near the trailing edge of the main element at the relative position referred to earlier, that the author had established (on a different wing...) in wind tunnel testing.

To enable direct comparison with the data to be made, the overall chord dimension of the dual-element device was made the same as that of the single-element. A virtual airflow of 50m/s (180km/h) was once again used in these 2D simulations.

The two parameters that were altered in this set of trials were the angle of attack, and the overall camber of the dual element device. Camber values of 9%, 12%, 15% and 18% were investigated, where this value represents the maximum deviation of the camber line (the line joining the midpoints between upper and lower surfaces) from the chord line (leading edge to trailing edge). Figure 5-14 shows the base model used. The slot gap between the two elements was kept constant throughout in order to maintain the same flow incidence between them.

Figure 5-15 plots the results of all the variously cambered dual-element wings against angle of attack. Figure 5-16 displays the results of the cambered single-element wings, also against angle of attack, but this time scaled to the same chord value as the dual-element wing, and plotted on the same downforce scale for direct comparison.

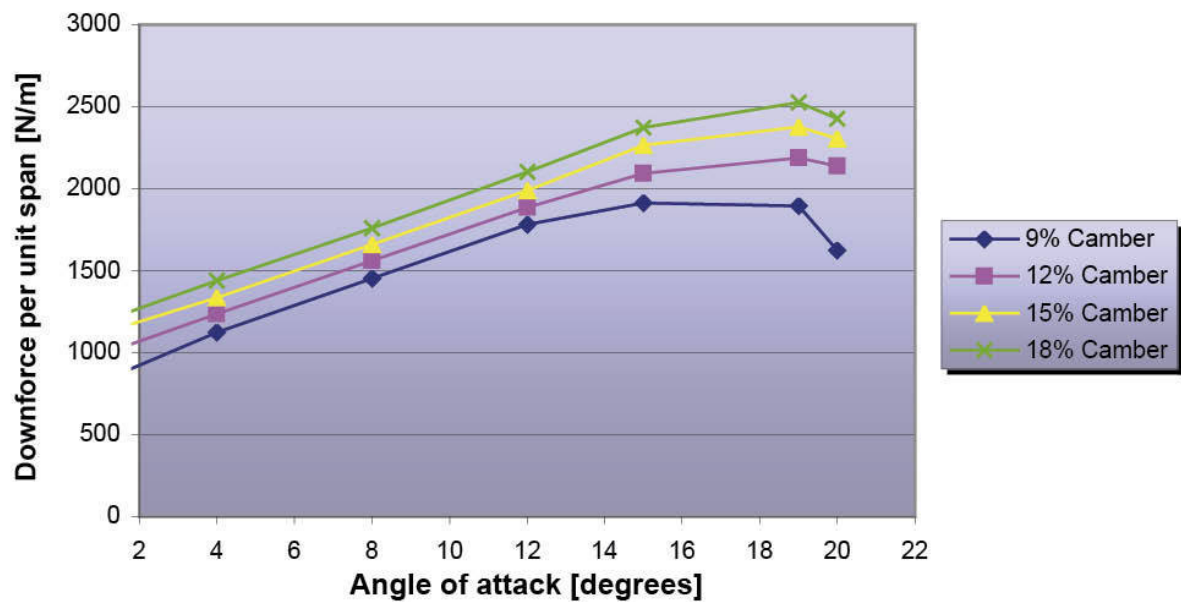


**Figure 5-15** Downforce versus angle for various camber values for a dual-element wing.

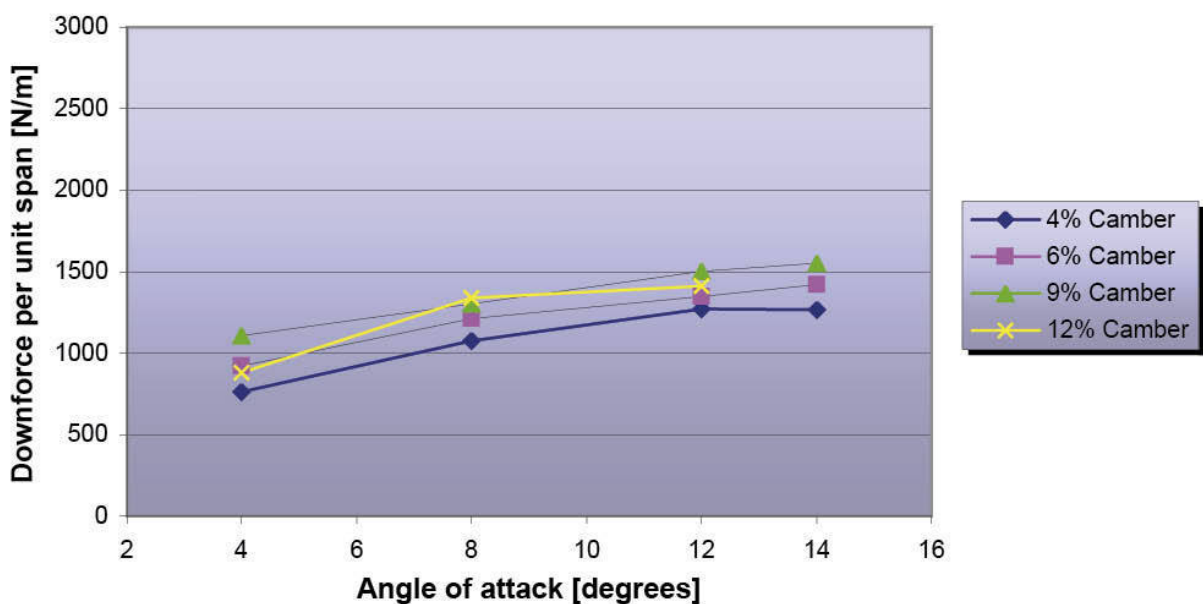


**Figure 5-16** Downforce versus angle for various camber values for a single-element wing of the same chord as the dual-element wing.

A number of observations relating to the dual-element configurations are apparent. First, downforce was higher than that generated by the single-element wings right across the range of angles (except the lowest) and the cambers studied. Secondly, the stall angles were higher, enabling more peak downforce to be generated, and thirdly, higher camber values could be used, gains still accruing at 18% camber in the dual-element case, this again enabling increases in downforce to be generated. The table gives some comparative results at the same angles and camber values, scaled to the same chord value. (Where permitted, if a flap were added to a main element so that chord actually increased, then downforce would also increase in proportion to the increase in chord as well as the increase in lift coefficient.)

Angle of attack, degrees: 4

Camber, %: 9

Single-element downforce, N: 1107

Dual-element downforce, N: 1122

Increase, dual over single, %: 1.4

Angle of attack, degrees: 8

Camber, %: 9

Single-element downforce, N: 1302

Dual-element downforce, N: 1452

Increase, dual over single, %: 10.3

Angle of attack, degrees: 12

Camber, %: 9

Single-element downforce, N: 1501

Dual-element downforce, N: 1784

Increase, dual over single, %: 15.8

Angle of attack, degrees: 4

Camber, %: 12

Single-element downforce, N: 1158

Dual-element downforce, N: 1237

Increase, dual over single, %: 6.4

Angle of attack, degrees: 8

Camber, %: 12

Single-element downforce, N: 1339

Dual-element downforce, N: 1560

Increase, dual over single, %: 14.1

Angle of attack, degrees: 12

Camber, %: 12

Single-element downforce, N: 1410

Dual-element downforce, N: 1886

Increase, dual over single, %: 25.3

Figure 5-17 shows how the mainplane and the flap helped to generate all this extra downforce. As we have seen, the single-element device was exhibiting flow separation at  $8^\circ$  and 12% camber, whereas at the same angle and camber the dual-element device showed a much more extensive low static pressure (blue) region beneath the whole main element and the flap. Figure 5-18 shows how far this particular set-up could be pushed. At 18% camber and  $20^\circ$ , which is just past the downforce peak of  $19^\circ$ , the flow was still fully attached to the lower surface of the main element, and substantially attached to the flap, with considerable downforce being generated.

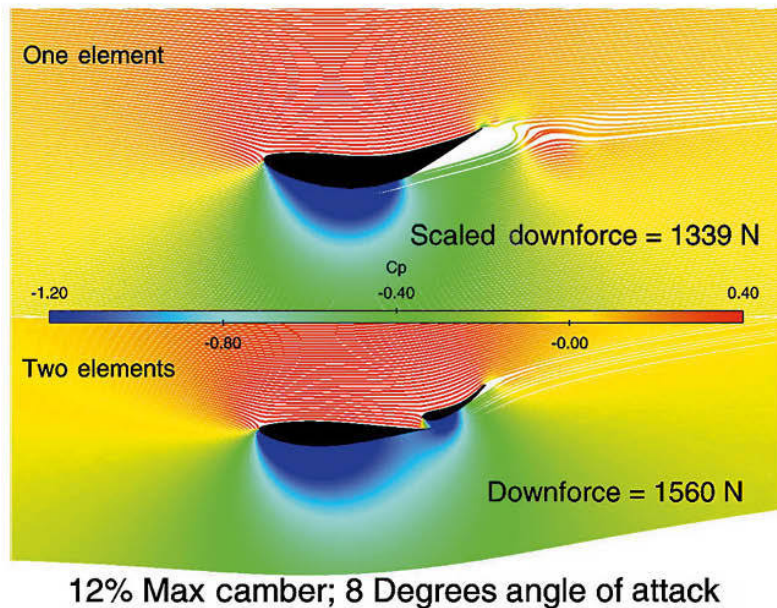


**Figure 5-17** Single- and dual-element wings exhibit very different flow patterns and pressure distributions.

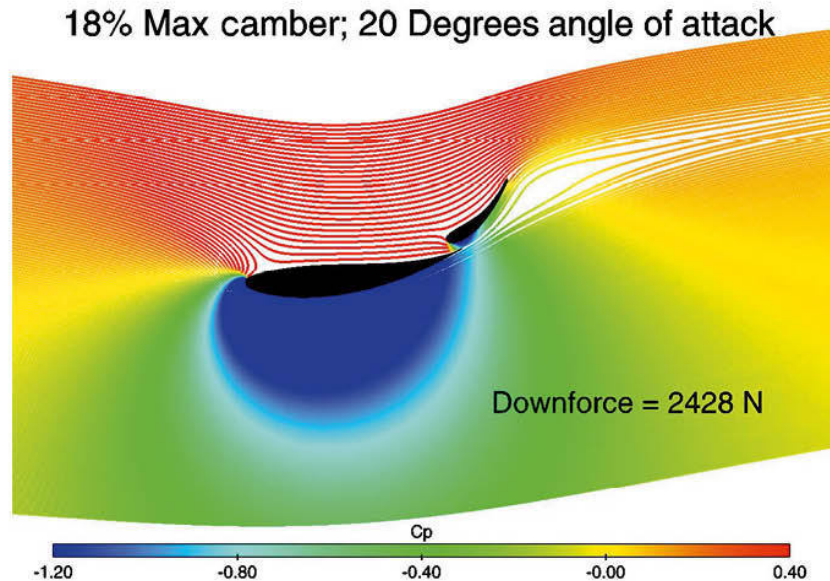


**Figure 5-18** The dual-element wing can be operated at much steeper angles.

In terms of the actual forces the maximum downforce per metre of span from the dual-element wing was 2,525N, or 566lb at 50m/s, which would equate to 2,018N or 452lb at 44.7m/s (100mph). At the same chord the best single element wing here produced 1,260N (282lb) at 100mph, so the two-element wing produced 60% more downforce. If the flap had been added to the single-element wing so that an increase in chord was also realised then the downforce could reasonably be expected to more than double, and although the actual numbers here might not be translated into practical reality, the relative changes most probably would. Thus we could expect lift coefficients of  $-C_L = 2$  and above from a dual-element wing.

It will be no surprise though, that there's no free lunch here. Drag increases as a wing is worked harder, and 'efficiency', as defined by the lift-to-drag ratio, tends to suffer. But notwithstanding increases in drag, it is apparent that large increases in downforce are available through the use of a dual-element wing instead of a single-element device. Clearly though, 3D CFD, or some other form of testing would be required in order to determine the efficiency of any wing configuration in relation to its potential use, and such a study follows here.

### Wing performance on a car

To glean a better idea of how much a wing's performance changes when on the back of a car, compared to when evaluated in isolation, a brief CFD exercise to measure a dual-element rear wing's downforce was carried out. First the wing was run in isolation, but at the height it would have been if mounted on the car; then it was evaluated on the car, which in this case happened to be a single seater model. The results showed a 6.5% decline in downforce, and it was apparent that the upstream 'clutter' of car, driver and roll-hoop sapped energy from the airflow and changed its angle of attack to the centre of the wing, and also that the wing mountings had a local deleterious effect. Other types of car, wing and relative locations of the two would see different comparisons, but in all cases a wing will perform differently on a car to how it performs in isolation.

### **3D CFD wing comparisons**

A 3D CFD study by the author compared a 400mm chord variant of one of his designs, designated '183', versus two dual-element variants that utilised the same main element but at 300mm chord supplemented by a 120mm chord flap deployed at 20° and 30° to the main element respectively. The overall chords of the dual element wings were thus approximately 400mm too. The CAD models are shown in Figure 5-19. The wings were each evaluated across the same angle range and downforce and drag values were extracted from the CFD post-processing module. The data are shown in the plots in Figures 5-20 and 5-21.

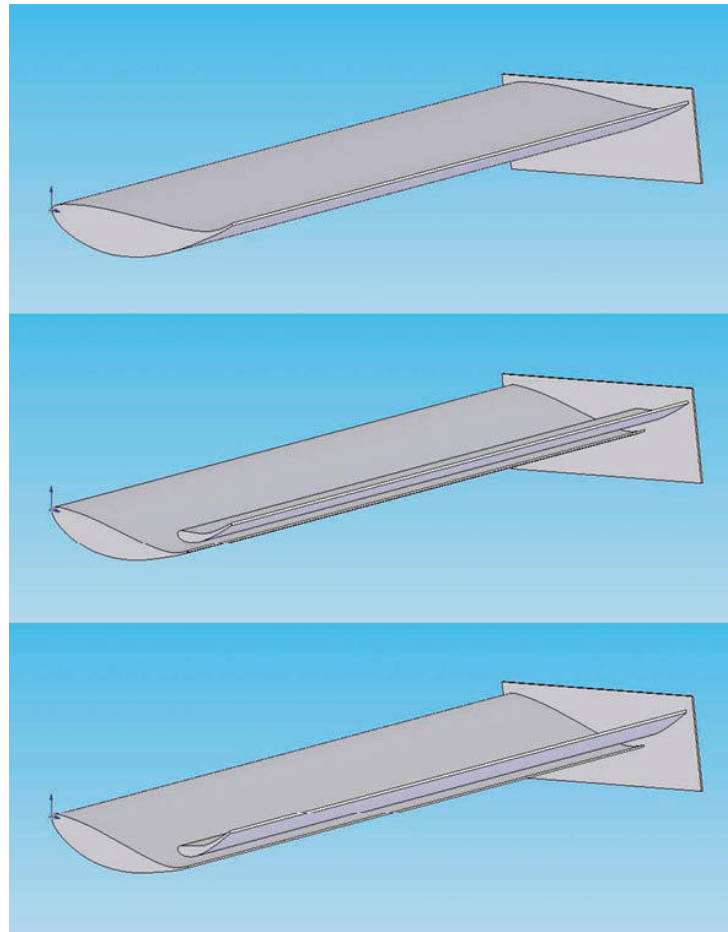


**Figure 5-19** CAD models of three 400mm chord wing variants evaluated in CFD.



**Figure 5-20** Downforce versus angle of attack on the three wing variants.

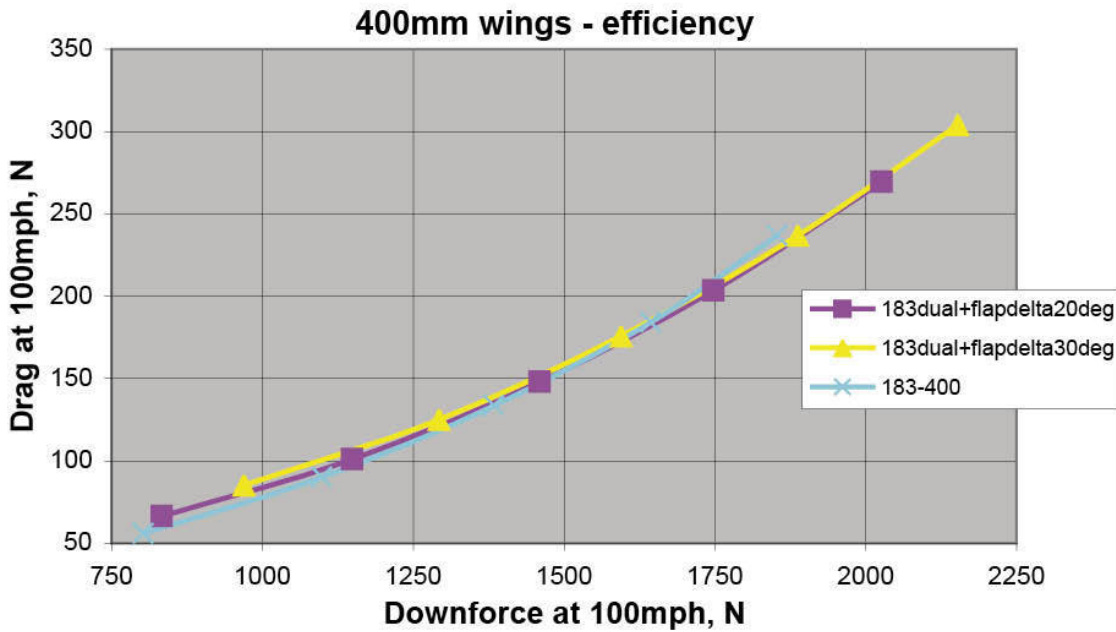


**Figure 5-21** Downforce versus drag shows how the efficiency of each wing configuration here changes through their working ranges.

In the downforce versus angle of attack plot (Figure 5-20) it can be seen that the dual-element wings produce more downforce at a given angle than the large chord single element wing, and the wing with the steeper flap angle is the most potent device here at any given overall angle by virtue of its greater camber. Also apparent is that the single element wing's downforce has started to level off at the steepest angle shown here, whereas the dual element wing plots are still linear, implying they would go on to steeper angles still before their performance began to level off. This is all in line with the 2D data presented in the previous section.

However, moving on to the drag versus downforce plot for these wings in Figure 5-21, more subtle performance differences can be seen. At the lower downforce end of the plots on the left-hand side of the graph it can be seen that the single element wing creates slightly less drag than either of the dual element wings at any given downforce level, and that the dual element wing with the 20° flap produces less drag at the same downforce levels than the one with the 30° flap. Move to the high downforce, right-hand end of the graph, though, and this situation reverses, although there isn't much to choose

between the two dual-element configurations. And of course the dual-element wings go on to produce more total downforce.

This would seem to indicate that for a given chord dimension, if lower downforce levels are to be run then a single element wing might be the more efficient choice, but as soon as higher levels of downforce are required then a dual element wing can be just as efficient in ‘downforce to drag’ terms, and at steeper angles can yield still higher downforce if required. Naturally every case will be different and it would warrant an exercise such as this to be able to make an informed choice before committing to wing manufacture or purchase.

### **Multi-element wings – more flaps, and slats**

Still greater  $-C_L$  values are attainable if further flap sections are added. The ‘double-flap’ arrangement, where two flaps are positioned above the mainplane trailing edge is a logical extension of the single-flap set-up, and effectively increases the wing camber even more. The geometries of the two flaps are often shown in aeronautical texts as being quite different from each other, with the first flap perhaps being smaller and thicker than the second, and some racecars adopt this principle. However, the all-important relative positioning between the wing elements still matters, and double-flap set-ups on racecars are just as likely to be made up with similar if not identical shapes and sizes for the two flaps.

The size of the slot gap between the mainplane and the foremost flap, and that between the fore flap and the secondary flap may be similar, or the former may be bigger than the latter. Aeronautical data gives a mixture of information here, but this may be because the geometry of deployed flaps on aircraft can be altered in flight, and the gaps will be different at different deployed flap angles. On a racecar however, generally speaking the flaps must remain fixed once the car leaves the confines of the pit lane or paddock, and the flap positions and gaps must therefore be chosen beforehand for each adjustable angle that can be set. Frequently it can be seen that the second slot gap is smaller than the first, and if avoiding interference from the boundary layer of the element in front is a key issue, then the gap behind a small flap perhaps only needs to be small compared to the gap behind a larger mainplane. The best arrangement will only be ascertained by testing, but in the absence of any better information, as a fair starting point set the first gap to somewhere in the range suggested for a dual-element wing, with the second gap similar, or perhaps slightly smaller than the first.



*A triple-element rear wing.*

The combined chord dimension of the two flaps would appear from the aeronautical texts to be ideally set in the range 30% to 40% of the overall wing chord, so in relative terms, the flaps here are individually smaller than in the dual-element case. However, looking at different racing categories it is clear that the respective rules governing each formula have a marked effect on the designs that have evolved. In the days when triple-element wings were allowed on Formula 1 cars they evolved to relatively very short mainplane chords relative to the flap chords, and this resulted from the restriction on overall chord. This suggests that as long as you are prepared to optimise a set-up for the circumstances in which it is to be used, there are no hard and fast rules on this aspect.

In terms of performance gains, the addition of a second flap adds a further substantial increment to the  $-C_L$  value, and figures of well over  $-C_L = 3.0$  are frequently cited for this kind of arrangement. In general terms, additional flaps add smaller additional downforce increments. Overall angles of attack (mainplane and flaps considered) well in excess of  $20^\circ$ , and approaching  $30^\circ$  are common. Angles of flap inclination might be in the region of  $25^\circ$  to  $30^\circ$  for the fore flap, and between  $30^\circ$  and  $70^\circ$  for the secondary flap, all angles measured relative to the mainplane chord line. Some configurations leave the fore flap fixed, with the secondary flap being adjustable, while others have both flaps adjusted as a pair, the flaps remaining fixed relative to each other. In both cases, this means that only one of the two slots is altered, and if nothing else, this makes engineering the attachment and pivot points for the flaps a lot easier!

For more downforce, yet more flaps can be added, and an extreme case, known as the ‘Venetian blind’ flap arrangement, is variously reported with three or even four flaps in addition to the mainplane. Clearly, optimising such a set-up will be a time consuming task. As an indication of what is possible though, in some IndyCar configurations to pre-1997 rules, the rearmost flap was inclined at an angle steeper than  $90^\circ$ , with the trailing edge actually pointing towards the front of the car! This was a ‘maximum downforce, don’t worry about the drag’ configuration if ever there was one.

Earlier it was mentioned that high downforce wings can suffer from leading edge separation, and that a change to the forward geometry of the wing may be required to prevent this from happening. One way this can be achieved, without altering and re-manufacturing the mainplane profile itself, is to use a leading edge *slat* (see Figure 5-22). This has the effect of adding ‘downwash’ to the front of the wing, which reduces the acceleration of the airflow under the forward-most part of the suction side of the main element, and this reduces the likelihood of leading edge separation, such as might occur on wings with heavy rearward camber bias and steep angles of attack. The benefit of a slat only really starts to be seen at steeper angles where its presence may delay the onset of leading edge separation. Thus, the wing assembly can obtain a substantial increase in downforce. That leading edge slats are not more frequently seen is probably down to two factors; first, many categories now limit the number of elements that may be used; and secondly, it is possible that a similar benefit may be obtained by optimising the shape of the mainplane, such as by turning its leading edge upwards into the incident airflow.



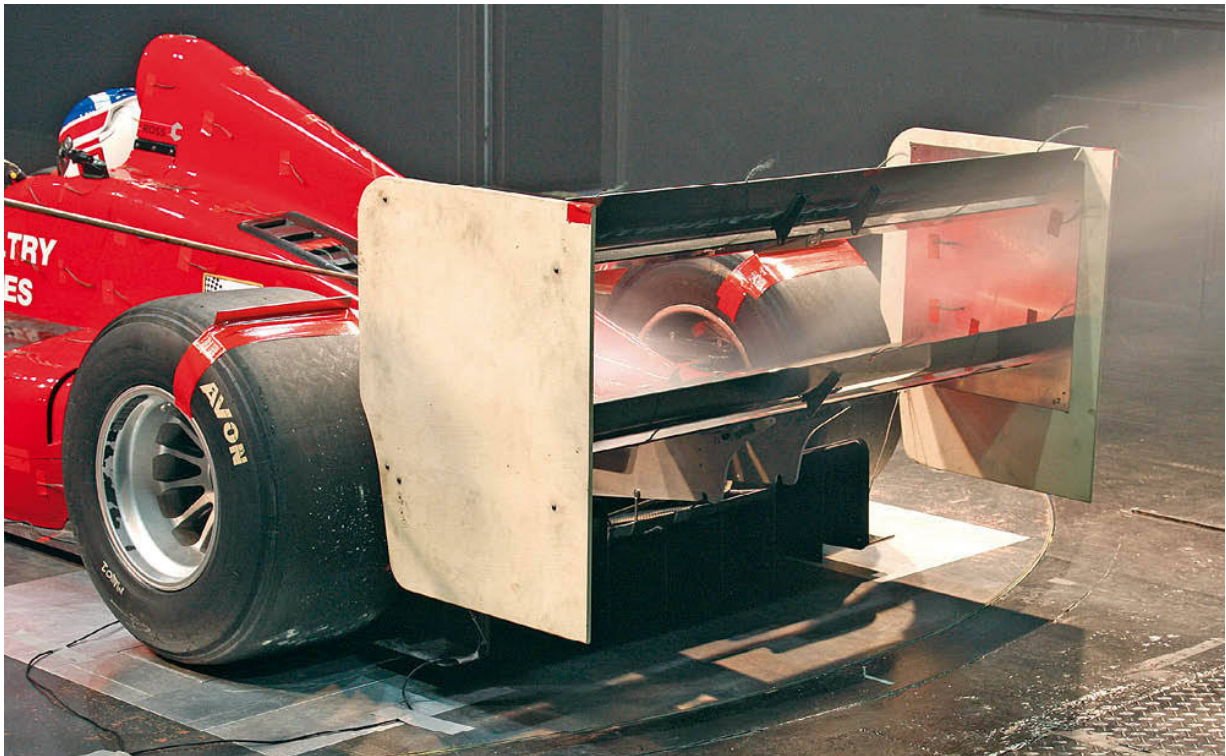
**Figure 5-22** A triple element wing with leading edge ‘slat’.

Data on the  $-C_L$  values that were obtained with these extreme wings is rather sparse. Somewhat theoretical sounding figures of 4, 5 and even 6 are mentioned, but perhaps a more realistic value can be obtained indirectly from a paper which was actually about the structural loadings imposed on the chassis of a late 1990s Williams Formula 1 car. The maximum loading from the rear wing was said to be in excess of 6,000 Newtons (612kg, or 1,346lb), and putting this figure into the lift equation, together with an assumed maximum speed of 200mph, and an approximate area of 3.28 by 0.98 feet (1.0 by 0.3 metres) produces a  $-C_L$  value of 3.7. So we can safely assume that rear wing lift coefficients in excess of 3.5, and maybe as high as 4.0 were actually achieved from the multi-element, multi-tier devices previously seen in that category.

### Multi-tier wings

That brings us nicely on to the subject of multi-tier wings. The first powered aircraft to actually fly was a biplane, so the multi-tier concept is not exactly new. The apparent benefit of increased wing area is the obvious reason for using a biplane or multi-tier configuration, especially when there are limited locations in which the wings can be attached. There is a distinct disadvantage that arises from such an arrangement however. Consider that the upper tier produces low pressure beneath its under surface. Now envisage what happens when another wing is located beneath the upper tier. The low-static pressure area beneath the upper tier acts upon the positive pressure upper surface of the lower tier, and this sounds about as rewarding as trying to lift yourself off the ground by pulling up on your bootlaces! So why do some racecars persist with multi-tier wings? Because it's not as bad as that. There is interference between the tiers, and the net result is that you don't get twice as much downforce from two tiers as you do from one when they are relatively close together. However, the combined effect can still be of net benefit, with more downforce being achieved than with just one tier. Indeed, with a vertical separation equal to the chord dimension, the suggestion is that two identical tiers will produce at least half as much downforce again as one tier alone. There are also other possible benefits from a multi-tier arrangement. The first is that, although wing efficiency may become unfavourable with three or four tiers, the effect on the airflow is such that an increase in the overall angle of attack may become tolerable, allowing more downforce to be generated before stall occurs. Secondly, the lower tier(s) may be positioned so that it (they) interact(s) favourably with the underbody airflow, assisting and augmenting the production of low pressure in the underbody region. Thus, a large gain in

overall downforce may be achieved through careful design and development of this aspect.



*Dual-tier rear wing on a hillclimb single seater.*

### **Wing twist**

Some categories mandate simple, straight wings but others permit wings with varying profiles across their span. In one sense these complex profiles have become possible thanks to modern manufacturing techniques, including computer aided manufacture of patterns and moulds coupled with composite moulding techniques. But the driving force has been aerodynamic benefit. So what are the benefits?

There are two sources of potential benefit. The first is that a wing's performance can be tuned using complex spanwise profiles to attain a specific aerodynamic target, for example best lift to drag ratio, from a given set of regulatory (usually dimensional) constraints. To meet such a target a wing might have a shallower angle applied, or a smaller chord, or less camber (or even more than one of these features) near the wing tips in order to reduce tip vortex strength and the inherent induced drag. And it might also feature characteristics that increase the potency of the centre section, using the opposite of those characteristics that might be applied at the tips, in order to

bring overall downforce up to the level of a plain wing but with (hopefully) less drag.



*The wind tunnel smoke plume shows how the angle of the airflow approaching the GT3 Ferrari F430's rear wing changes across the wing's span.*

The second way in which benefit can be gained from spanwise profile changes arises from something that was mentioned earlier in the chapter, which is that the airflow incident upon a rear wing is rarely parallel to the ground, and indeed varies across the span in a way that depends on the car shape ahead of it. For example, the rear screen region of a GT car produces a

local airflow direction that approaches a rear wing at an angle several degrees downwards, whereas the airflow that approaches the outer portions of a car-width wing does so more or less parallel to the ground, depending on other protuberances like mirrors and suchlike. So sometimes you see wings that have the angle of the profile in the centre section of the span reduced to match the angle of the ‘onset’ flow. This means that the whole wing is operating at much the same effective angle *relative to the local airflow direction* right across the span, and this can make for a very efficient wing.



**Figure 5-23** Evaluating a straight-section wing on this simple GT car model produced the static pressure plot shown in the next figure.

Then again, the airflow that has passed over the upper body of even something as sleek as a GT car loses energy through interaction with the car’s body surface, and even a simple straight wing generates reduced downforce from its centre section than it does from the outer sections onto which flows air with higher energy, as shown in Figure 5-24. So obtaining good downforce from the centre section can require that the profile’s potency be strengthened here...

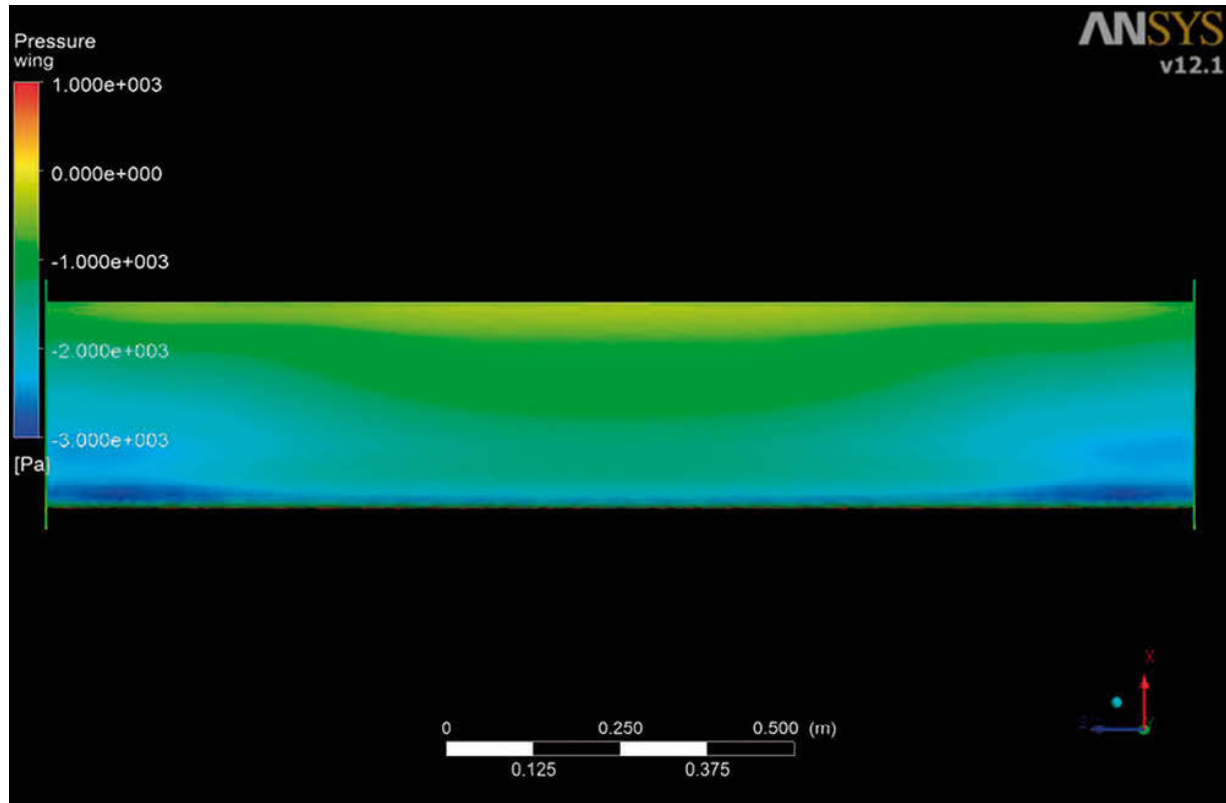


**Figure 5-24** The static pressure plot shows how the centre section of a straight wing on this GT car model achieved less pressure reduction than the outer sections (the airflow is coming from the bottom of the page here).

So the manner in which spanwise profile changes are applied really does depend on the aerodynamic aims, and what might be seen on a given car at one track might be different to what is seen at another.

### End plates

End plates are not just used to hide the precise shape of the wing profile you are using, or to put a sponsor's name on. They serve a valuable purpose, which is to increase a wing's downforce. They can also reduce the drag at the same time. It is well known that without end plates, or 'spill plates' as they are sometimes more usefully known, the difference in air pressure between the lower and upper surfaces of a wing prompts the air on the high pressure side to migrate to the low pressure side. This causes a loss of downforce. Fitting end plates significantly reduces this 'spillage', and helps to maintain the pressure differential above and below the wing. End plates do need to be reasonably large to be effective, although generally, there is not much scope to have too much end plate above a rear wing if the wing trailing edge is already

as high as the rules allow (and it probably should be). However, that generally leaves plenty of room for end plates to extend below the wing, and often the end plates actually constitute the primary wing mounts, or at least, the secondary, stabilising supports. Front wings tend not to allow much end plate below the lower surface because of ground proximity, so other tricks are employed there, as we shall see shortly.

Let's have a look at a couple of CFD studies on end plates, first on a rear wing. The regulations in many categories provide at least some limitations on the size of wing end plates that can be utilised at the front or rear. The maximum height is usually restricted, and if the rules don't limit minimum height too then other practical constraints such as the ground or other parts of the racecar will. There is also the dictum of minimum weight, of some importance with parts that are generally well beyond the wheelbase and, at the rear, high up as well.

The question remains – how big, aerodynamically speaking, is good? The important variable is said to be the height of the end plate,  $h$ , relative to the span,  $b$ , of the wing (see Figure 5-25). Bigger end plates have the effect of increasing the effective aspect ratio, AR, of the wing by reducing spillage, and this benefits both the downforce and induced drag (the portion of drag directly resulting from downforce generation, and the dominant cause of drag generated by most racecar wings).

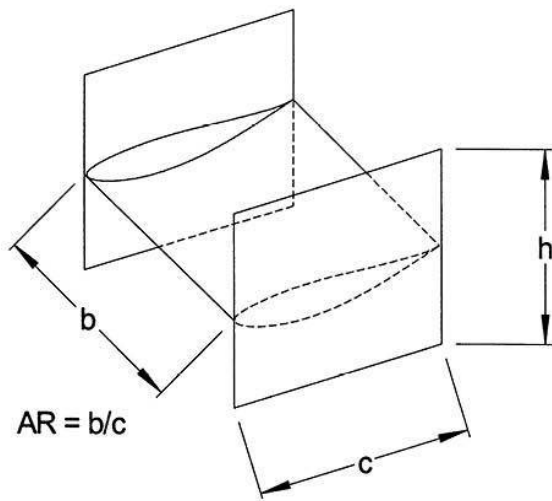


**Figure 5-25** Variables affecting end plate performance.

One reference tells us that the effective aspect ratio is proportional to  $h/b$  up to values of  $h/b \sim 0.6$ , when the gains begin to tail off. In other words, bigger (taller) is better, up to a point, but we need to get a bit more practical. For one thing, as stated above end plates rarely protrude the same distance above a racecar rear wing as below it, because of maximum height restrictions, and the general desire to run the wing as close to maximum height as possible to try to find some ‘clean’ air above and behind the racecar.

So one CFD study looked at the effects on a three-dimensional two-element wing in ‘free stream air’ of some more realistic-looking end plate variations compared to the no end plate case – see Figure 5-26. The force results are shown in the table, and do indeed show a trend to more downforce and lower drag.

Case: ep0

Downforce (N): 769.2

Drag (N): 194.8

Case: ep1

Downforce (N): 786.7

Drag (N): 188.3

Case: ep2

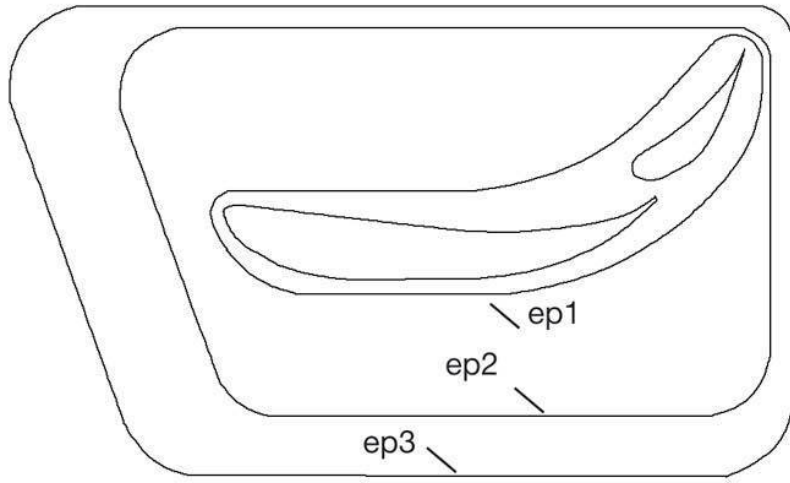
Downforce (N): 873.4

Drag (N): 183.8

Case: ep3

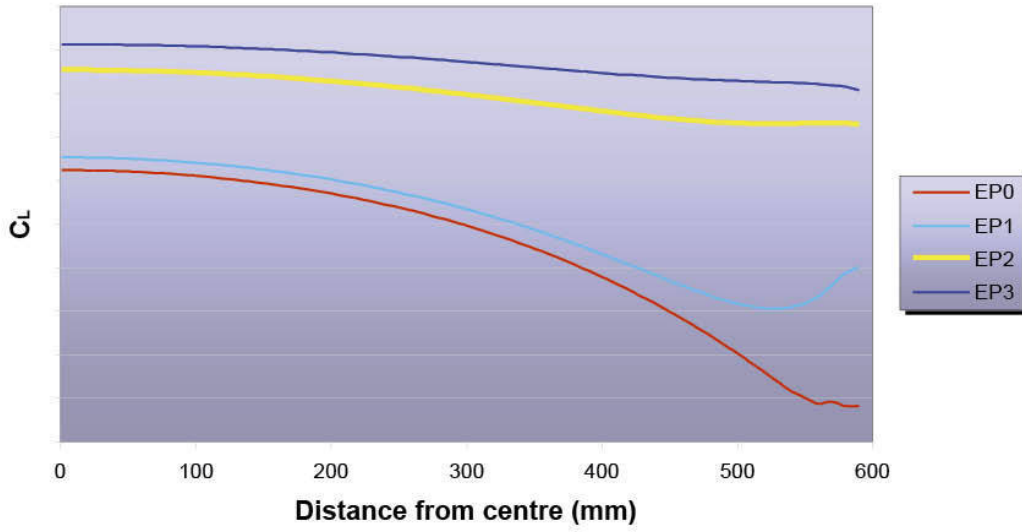
Downforce (N): 900.1

Drag (N): 178.1



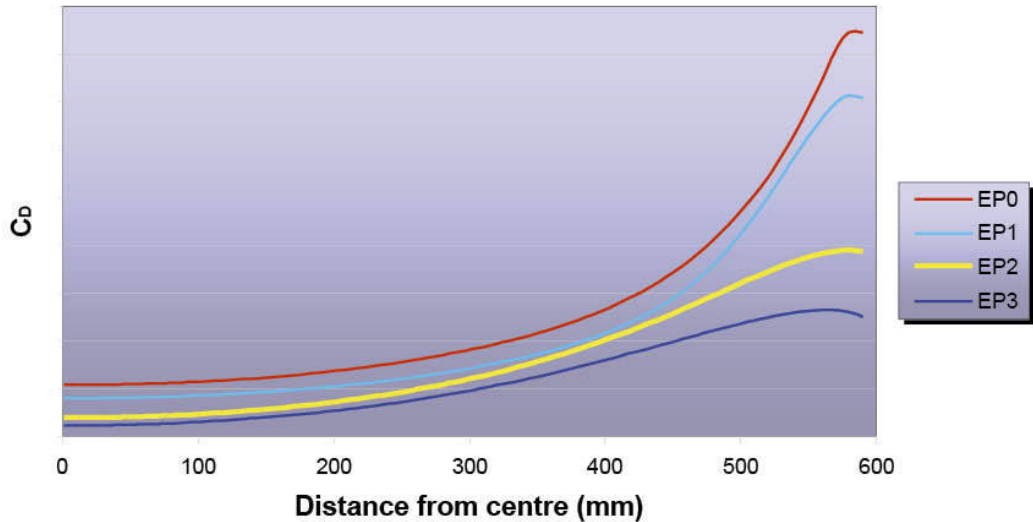
**Figure 5-26** End plate variations tested here.

The graph in Figure 5-27 plots the lift coefficients across the wingspan, from the wing centreline on the left of the graph to the wing tip on the right. The downforce generated near the tips declines far more drastically with no end plate or just the small end plate compared with the medium and large end plates. Thus, with decent sized end plates fitted the lift coefficients near the wing tip are more akin to the values they would be at a similar distance from the centreline of a much wider wing without end plates. This confirms the notion that end plates effectively increase the aspect ratio, which for a given chord dimension is the same as saying that end plates have effectively increased the wingspan.



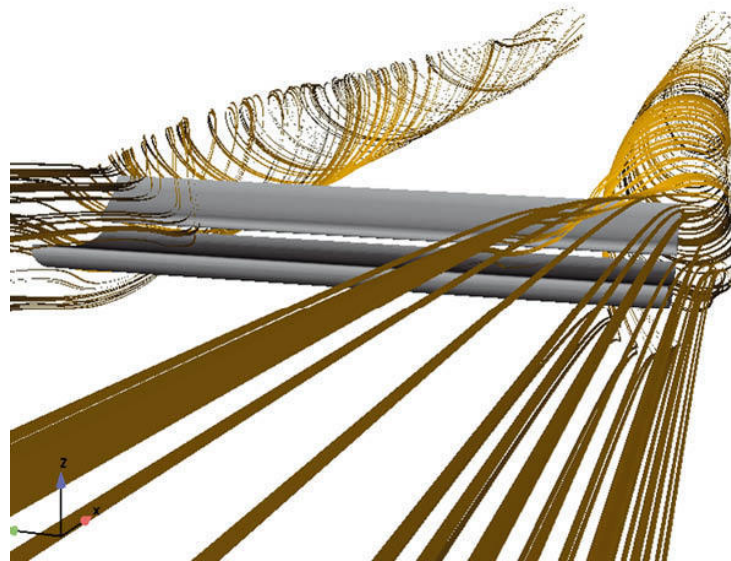
**Figure 5-27** Lift coefficients across the wingspan with the different end plates.

Figure 5-28 plots the drag coefficients across the wingspan in a similar way, and again it is evident that drag increases near the wing tips far more with no end plate or the small end plate than it does with the medium and large end plates. Not surprisingly, efficiency ( $L/D$ ) declines more rapidly near the tips with smaller end plates.



**Figure 5-28** Drag coefficients across the wingspan with the different end plates.

The streamlines in Figure 5-29 spectacularly show the wing-tip vortices in the no end plate case. Figure 5-30 shows the situation with the large end plate installed. The vortices are now produced at the rear tips of the end plates, moving their influence away from the wing itself. Furthermore, pairs of vortices have formed, at the top and bottom of each end plate, and these merge downstream into a single vortex. Thus, taller end plates move the vortices further from the wing where they have less detrimental effect on its performance.



**Figure 5-29** Vortex formation with no end plates.

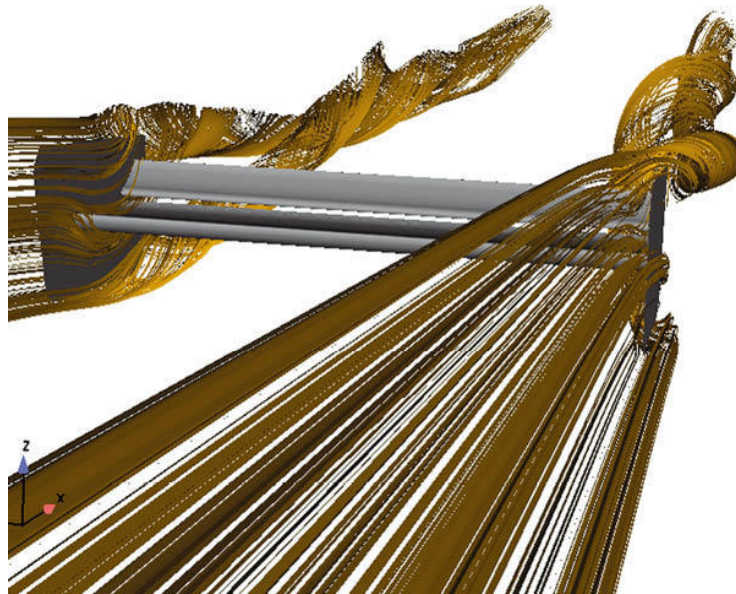


**Figure 5-30** Vortex formation with the large end plates.

There are various reasons for thinking that we should have more end plate below the wing than above it, given that this will be inevitable anyway. The static pressures above and below the wing also suggest this is a good idea. The static pressure increase above the wing is much smaller than the static pressure decrease below it. Thus, the influence of the wing extends further below it than above it, and simply put, this means we need more end plate below the wing. Extending this notion, the ideal size of end plate will also therefore depend on the downforce level of the wing. Lower downforce wings create smaller pressure changes, and hence the wing's influence on the pressures in the air around it extends less far, meaning smaller end plates can be used, and vice versa for higher downforce wings.

A CFD study carried out by the author attempted to cover a range of reasonably practical end plate variants on a single element wing of 300mm chord operating at an angle of 16° throughout. The end plates all stood above the wing by the same minimum amount in order to meet the assumption that the wings would be run at or near to a regulated maximum permitted height. So the only parameter that was altered was the depth of end plate below the lowest point of the wing's suction surface. This ranged from (effectively) zero depth to two chords' depth, or 600mm, and some of the CAD models are shown in Figure 5-31.

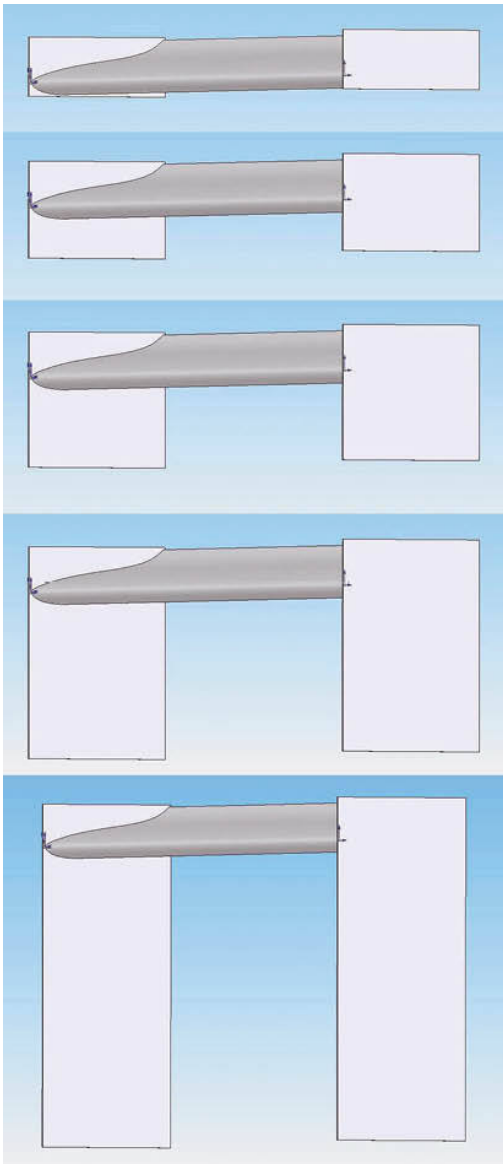


**Figure 5-31** A realistic range of end plate depths was evaluated in another CFD project.

The results obtained using Ansys FloWizard are shown in Figures 5-32, 5-33 and 5-34. ‘Trend lines’ have been added to iron out the lumps and bumps in the results, and it certainly looks clear enough that downforce did indeed increase with end plate depth, though in a diminishing returns way. The range represented almost 10% of the minimum downforce value, or in other words a gain of nearly 10% in downforce was achieved with the deepest end plate compared to the shortest.

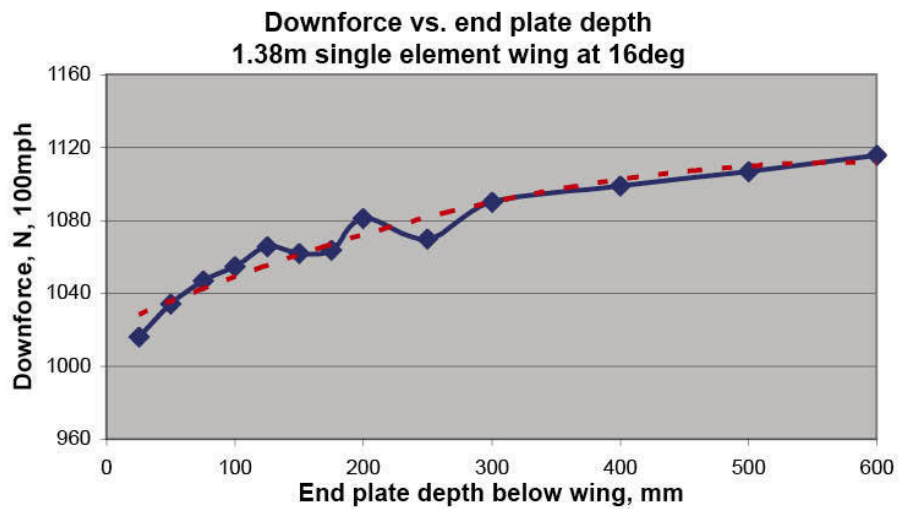


**Figure 5-32** Downforce versus end plate depth showed diminishing gains.

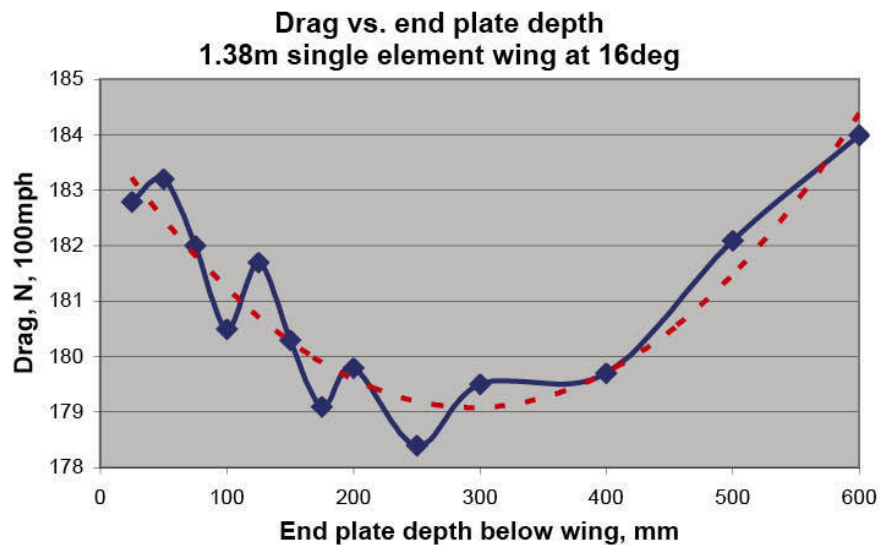


**Figure 5-33** Drag versus end plate depth showed a drag minimum at around one wing chord's depth.

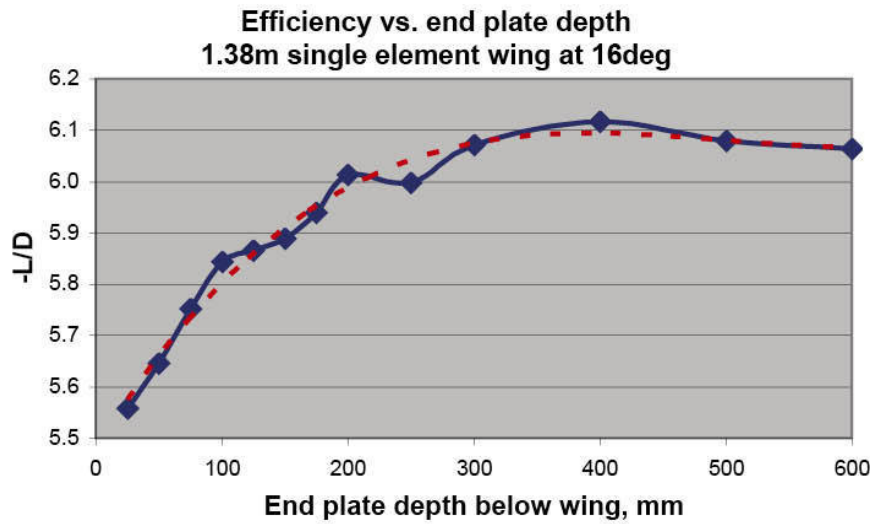


**Figure 5-34** Efficiency versus end plate depth seemed to confirm that one chord's depth was sufficient.

On the other hand drag showed a quite different pattern, with minimum values in the 250mm to 350mm range before it increased again at greater end plate depths. To explain this we might reasonably suppose that increasing the end plate depth reduced vortex drag, but then as end plate size was increased, the viscous drag component increased sufficiently to reverse the trend. Note that the changes in drag were relatively small, the range representing 3% of the peak drag value. Finally the  $-L/D$  ‘efficiency’ graph seemed to peak at around 400mm end plate depth for this set-up, which would be quite a practical sized end plate to run in many cases, technical regulations permitting. The gain in efficiency compared to the ‘worst case’ at zero end plate depth was just over 10%, most definitely worth exploiting.

### Front wing end plates

Front end plates are, of necessity, a very different case to rear end plates, but simplistically their job is the same – to enhance the effectiveness of the front wings. However, the complex designs used in the top categories like Formula 1 are also shaped to help the airflow downstream of the front wing, which can obviously have influence on the flow field over the entire car. We will look at a couple of pretty simple front wing end plate projects to get an idea of what’s going on, and then speculate on some of the more complex end plate shapes.

Formula 1 designs feature wide ‘foot plates’ that incorporate quite complex shapes. Clearly, trading off quite large amounts of the wingspan permitted by

the maximum width regulation and replacing it with foot plates must be beneficial – they wouldn't do it unless it was worthwhile. (Actually, since 2008 there has been less choice in the front end plate width, but prior to that the choice of trading off wingspan against end plate width was free.) The CFD exercise reported here was carried out a few years ago as a quick 'look-see' on a wing being used on a hillclimb single-seater. F1 designs have now progressed way beyond the very simple device tested here, but the data is available from this trial.

The two-element front wing was analysed in 3D with and without the foot plate, at a virtual air velocity of 33.5m/s (120km/h, or 75mph) in freestream air (not attached to a car model) but in 'ground effect', with the ground moving at the same velocity as the air. The foot plate was modelled as a thin plate with a 'span' of just 25mm, added to the existing 1,400mm wingspan. Figure 5-35 illustrates half the wing to show the geometry involved.

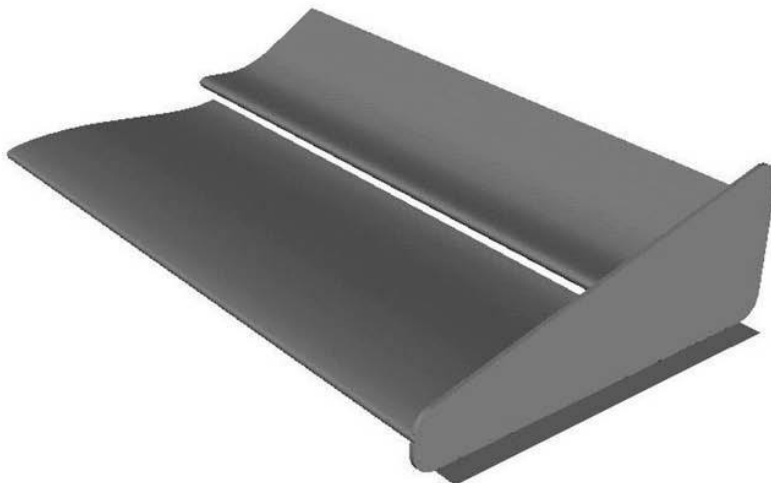
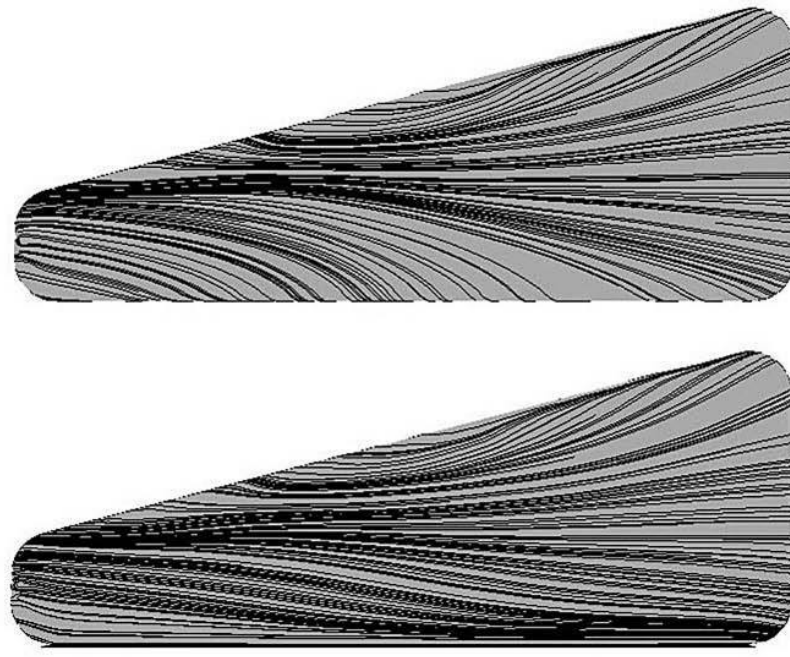


**Figure 5-35** Two element front wing with small 'foot plate'.

The baseline case without the foot plate produced 653.8N (146.6lb) of downforce, and adding the foot plate increased this by 7.0% to 699.3N (156.8lb). If instead the span had been increased by 50mm overall we might have expected at best a downforce increase in proportion to the span increase of 50/1,400 or 3.6%. So the footplate seemed to work better than simply adding extra wingspan.

Figure 5-36 shows oilflows on the outer face of the end plates from which it can be seen the foot plate is preventing air from spilling under the end plate. Figure 5-37 demonstrates the change to the static pressures on the end plate

brought about by the foot plate (shown in magenta). Most significantly there has been a marked increase in static pressure at the bottom of the end plate (red region), and this raised pressure will be acting on the top surface of the foot plate. This is where at least some of the additional downforce is accruing.



Oilflow - Top without footplate, bottom with footplate

**Figure 5-36** Oilflows on the outer surface of the end plates, with and without foot plates.

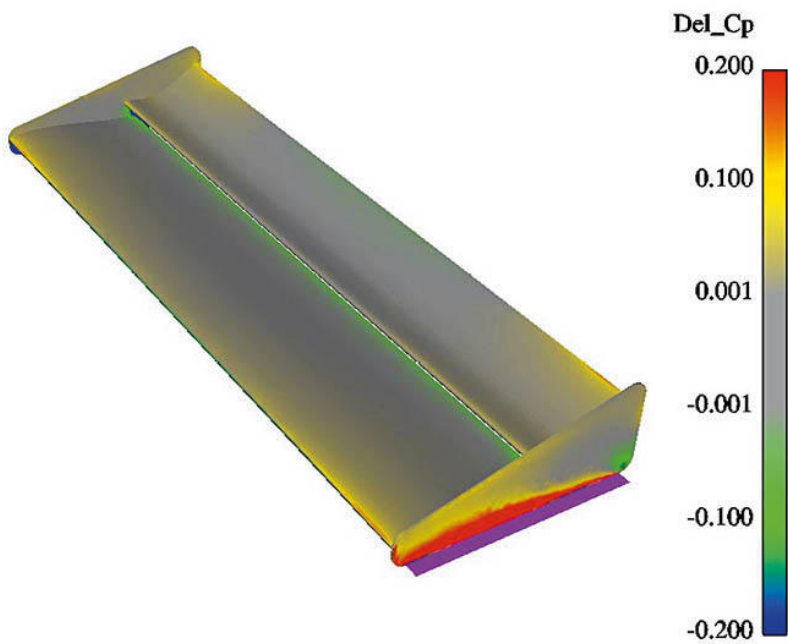


**Figure 5-37** Static pressure rose on the lower edge of the end plates, so would have risen too on the foot plate.

Figure 5-38 shows the changes in static pressures on the lower surface after fitting the foot plate. Clearly more suction (blue and green) is developed on almost the whole lower surface of the mainplane and to a lesser extent on the central portions of the flap. This is where the bulk of the downforce increase accrues.

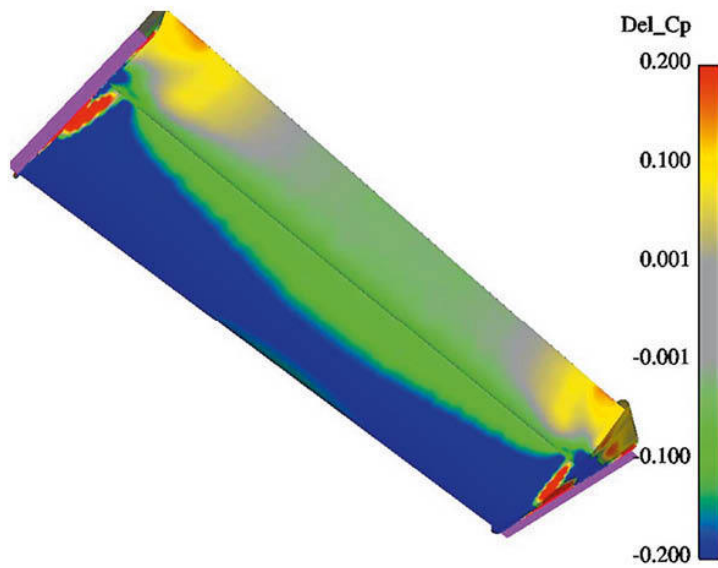


**Figure 5-38** Static pressure changes on the wing underside after fitting the foot plates.

A small but important detail is also revealed in this Del\_Cp plot. At the outer extremities of the mainplane and on the adjacent inside surface of the end plates there are small regions of markedly increased static pressure (red), aft of which are similar small regions of decreased static pressure (blue). This is where the vortex that is formed as the airflow rolls in under the end plate has been moved slightly rearward by the foot plate. Thus, there has been an increase in static pressure in its old location and a decrease in its new location.

But how do any of the above effects explain the significant overall increase in downforce and, especially, the increased suction over most of the under surface of the wing? Although not shown here, there has in fact been an incremental increase in the lift coefficient right across the span of the wing as the result of fitting the foot plate. This is very similar to the effect we saw arising from increasing a rear wing end plate from ‘medium large’ to ‘large’. The benefit there arose from bigger end plates preventing more air from leaking from the pressure surface to the suction surface, and effectiveness was increased across the whole span. So we can conclude that foot plates have a similar effect to larger end plates. Also, if the front wings of pre-2009 Formula 1 cars are any indicator, considerably larger foot plates than those tested here must provide useful benefit.

There are other complex modifications and additions to front wing end plates where the rules permit, such as ‘flip ups’ ahead of the front wheels and integral ‘cone-shapes’ at the rear, lower extent of the end plates. Without data

to hand, in the case of the former we can speculate that air is being deflected upwards to the benefit of front wing downforce, but also possibly to reduce front wheel lift and drag. The latter are apparently devices that control and steer the inevitable wing ‘tip’ vortices so that they have less adverse effect on the rest of the car downstream. Pre-2009 Formula 1 cars could also frequently be seen to converge towards the rear wheel when viewed from above and this clearly was about steering the airflow between the front wheels, presumably again to improve the front wing performance as well as to manage the flow to the rest of the car. With the adoption of very wide wing assemblies in 2009, though, the end plate design emphasis appeared to switch essentially to deflecting airflow outboard of the front wheels, though as ever the detail design variations are myriad and often perplexing without inside knowledge!

To evaluate one of the concepts mentioned in the previous paragraph, a front wing end plate incorporating a large footplate with ‘quarter cones’ at the rear was tried in the MIRA wind tunnel on a hillclimb single seater, the DJ Firestorm. The technical regulations in UK hillclimbing offer a great deal of latitude in aerodynamic design. However, one regulatory constraint on single seat racing cars is maximum bodywork width ahead of the front wheels, which is limited to 1500mm. The overall width across the front wheels of the Firestorm was approximately 1680mm, so the wing width was roughly 180mm narrower than this. The new front end plate for the Firestorm was based on a prototype made by the author in 2005 that essentially copied the key elements seen in F1 front end plates of that period

When DJ Engineering made and fitted a pair of these end plates to the car, the owner/driver Wallace Menzies reported the difference immediately and insisted they stay on the car henceforth, suggesting a worthwhile gain in downforce. The wind tunnel revealed the differences, as shown in the table below.

CD:	+0.5% Change
-CL:	+20.1% Change
-CLfront:	+31.1% Change
-CLrear:	+12.5% Change
%front:	+9.2% Change
-L/D:	+19.5% Change

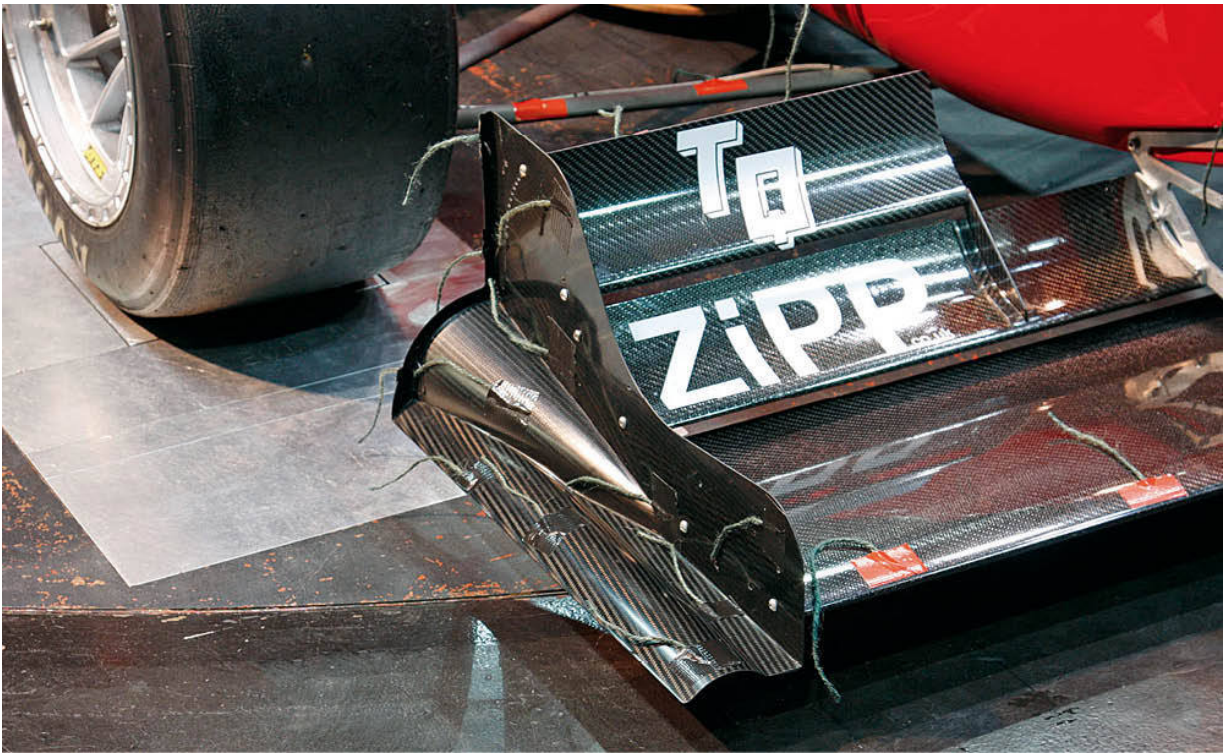
For a seemingly fairly small alteration, the change from a simple flat plate to this more complex front end plate produced a very significant change in the numbers, with a sizeable increase in downforce for a negligible change in drag.

As expected, there was a downforce gain at the front end, although an increase of over 30% was unexpected, if very welcome! So too was the increase in downforce at the rear, which was a definite bonus. Let's speculate on some mechanisms here.

First, the span of the front wing elements was made to accommodate the new, wider end plates while remaining within the regulation front bodywork width, so with the simple flat sheet end plates that the car started with here, the front wing was approximately 200mm narrower than it could have been, at just under 1300mm. However, even if that extra span were present and gave a downforce increase commensurate with the increase in plan area of the front wing that would still not have amounted to 30%, even allowing for the overall chord dimension of the outer portions being larger than the central portion. In other words, these new end plates were worth more than the equivalent extra span of wing would have been.



*Flat front end plates were compared with...*



*... front end plates with more complex features.*

We have seen that horizontal ‘footplates’ act like deeper end plates and enable a front wing to generate more downforce. The footplates also see reduced pressure beneath and raised pressure on top, and so generate an increment of downforce themselves. Being located just ahead of the front wheels can also see the raised pressure that occurs on the front face of the tyres exerting its influence on the top of the footplate too.

But what of the inverted semi-circular section channel running fore and aft along the footplate, and the hollow quarter cone shape let into the rear, lower part of the vertical face of the end plate? CFD shows that the former entrains the first stage of the tip vortex so that it passes along the channel, adding to the effect of a deeper end plate by reducing flow under the wing. The latter entrains the second stage of the tip vortex that rolls in under the wing, thus allowing more of the full span of the wing to function ‘normally’, less impaired by the presence of the vortex, while also adding its own low pressure to the underside of the cone. Again, both of these would add to front wing downforce.

Then there’s the gain in rear downforce to explain. It seems fair to say that, as there was effectively no change in drag, this rear downforce increment did not arise from the new front end plates somehow improving the flow to the

rear wings, because rear wing downforce increments invariably come with an increase in induced drag. The most probable alternative explanation is that the flow through the underbody was enhanced or improved in such a way that it developed more downforce with the new front end plates, and because the underbody was designed to concentrate its downforce contribution in line with the centre of gravity, this increment was spread between front and rear. Thus some of the additional front-end downforce probably also came from the underbody too, and not just the front wing. More on underbodies in the next chapter...

### End plate louvres

A feature widely seen on Formula 1 and other top level racecars, and equally widely copied elsewhere, is end plate 'louvres'. When these features first appeared on F1 rear wing end plates the initial reaction was that they would probably be losing a small amount of downforce by bleeding away some of the high pressure above the wing's upper surface, but that this was presumably being traded against a reduction in vortex drag in a quest for improved efficiency. The table below shows what happened when tape was stuck over the outside flat surface of these louvred slots on a 2007 Honda RA107 F1 car evaluated in the MIRA wind tunnel for Aerobytes.

$\Delta$ CD with louvres open: -9

$\Delta$ -CL with louvres open: +5

$\Delta$ -CLfront with louvres open: -1

$\Delta$ -CLrear with louvres open: +6

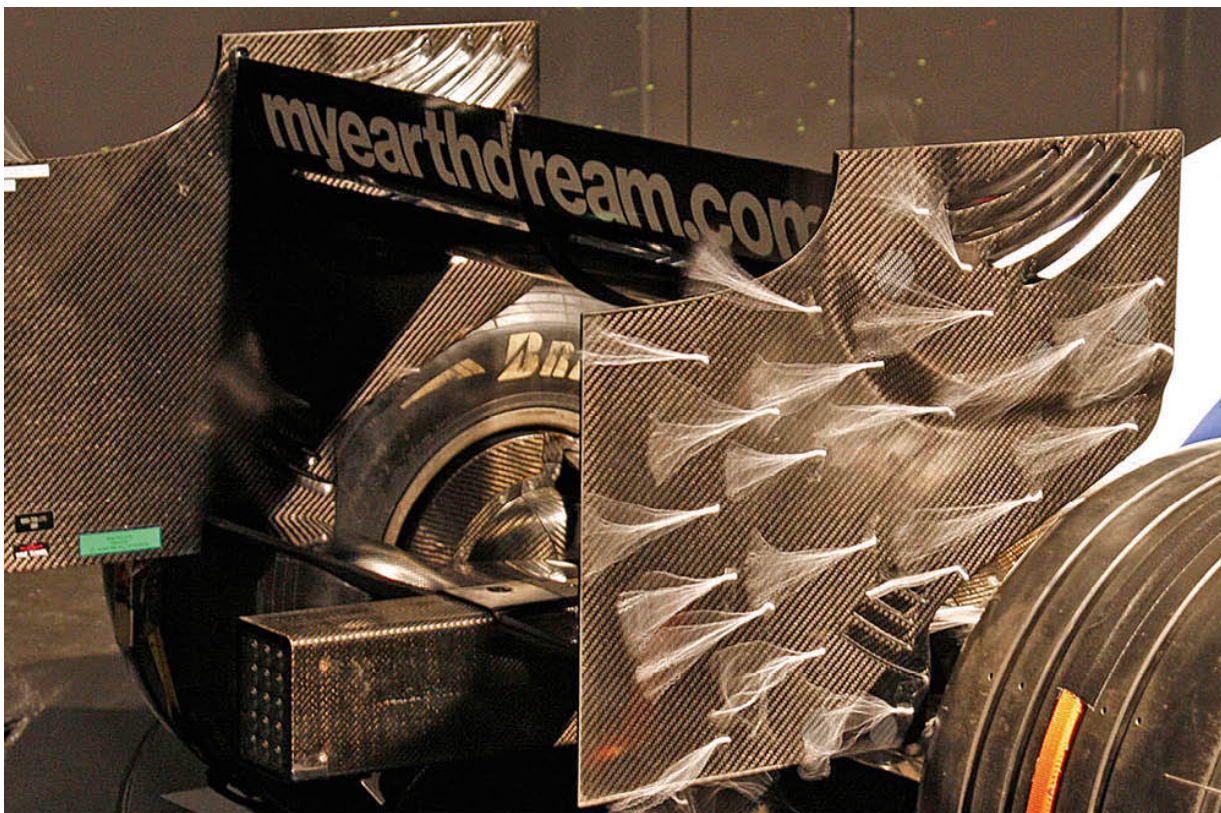
$\Delta\%$ front with louvres open: -0.16%

$\Delta$ -L/D with louvres open: +18

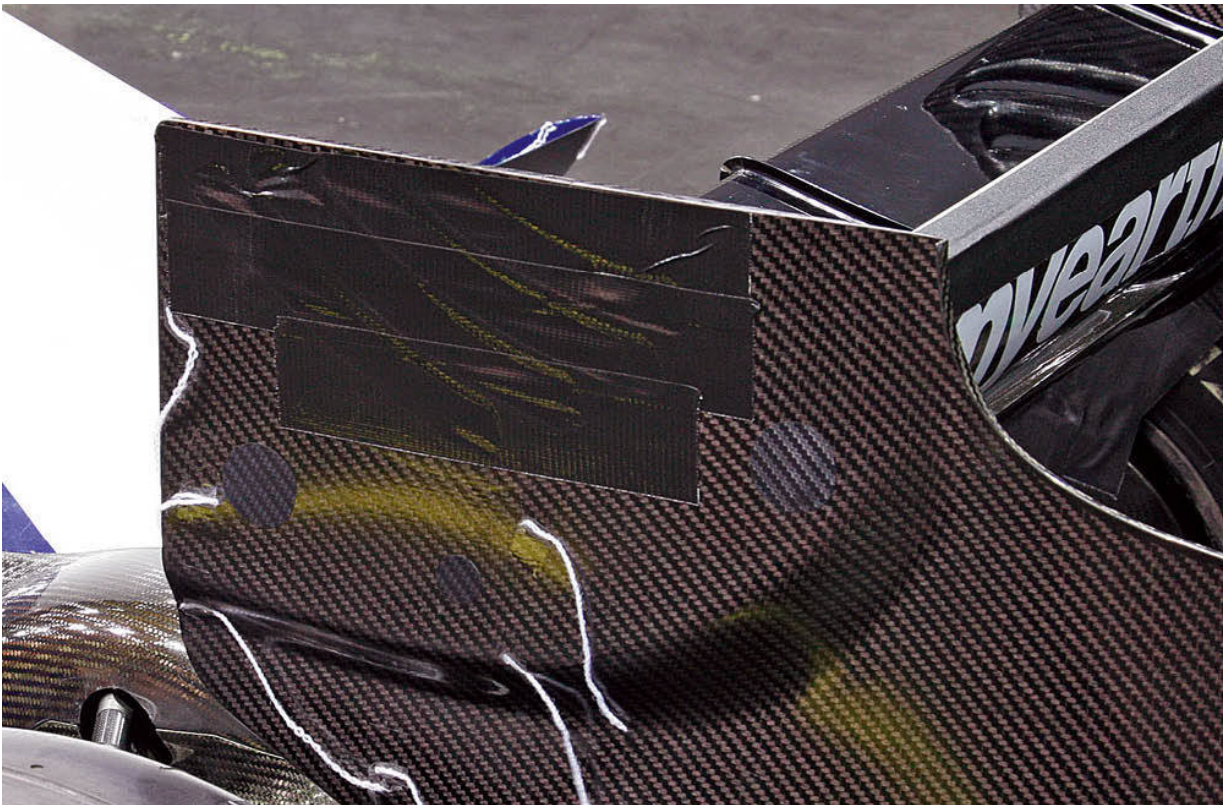
Note:  $\Delta$ , the Greek letter 'delta' represents the change brought about by a modification

In reality what the louvres did was to provide the expected drag reduction, but they also generated a small increase in rear downforce, not the expected decrease. How could this be? It would appear that the sectional profile of the 'blades' between the louvred openings is of a simple aerofoil shape obviously designed to minimise drag from the air passing through the louvred openings. But it seems that these also generated a small downforce component sufficient to offset and indeed reverse any loss of downforce that would have arisen from bleeding away positive pressure from above the upper wing surface. Overall the magnitude of the louvres' effect was modest, but in percentage

terms drag reduced by just under 0.9% and rear downforce increased by just under 0.6%, resulting in a net gain in efficiency (-L/D) of 1.21%. Though these effects seem relatively very modest, they would no doubt be cause for a small party in the aerodynamics department of the F1 team that first came up with the idea! Whether they would justify the additional man-hours in pattern-making, moulding and trimming for the rest of us would depend how far down the development road we were...



*The local airflow was certainly modified when the end plate louvres on the Honda RA107's were 'open'; notice the near-vertical angle of the upper wool tuft.*



*'End plate louvres had a very modest but beneficial effect'*

### **Gurneys (or 'wickers')**

The 'Gurney' is a small right-angled strip attached to the trailing edge of the rearmost element of a wing. The device was first used by American Dan Gurney, who reportedly told the competitors who asked, that it served only a structural purpose, in a hopeless attempt to avoid giving the game away. It was in fact a means of adding downforce for surprisingly little drag penalty, in spite of its apparent crudeness. The Gurney flap has the effect of adding a vertical component to the velocity at the trailing edge. This deflects the flow upwards, and increases the downforce; a similar effect to adding more camber to a wing (or indeed, a spoiler). The Gurney also slows the flow down ahead of itself, which increases the static pressure above the wing here, also adding an increment of downforce. Research has shown that the Gurney adds a pair of counter-rotating vortices to the wake immediately behind it. This is probably associated with a drop in total pressure (as in other wakes), which will contribute to a drop in the static pressure here that in turn helps to keep the flow attached at the trailing edge of the suction surface. This is borne out by references showing that wings can be pushed to slightly higher angles with a Gurney than without, so generating more downforce before stall occurs.

Primarily, the Gurney has been shown to add downforce across the range of angles in the same way that adding camber does.

One of the main practical advantages of the Gurney is that it is easily fitted and removed, or replaced with one of a different size or span, or one with more complex shapes, and it is thus an important part of the fine-tuning kit that racers take to the track. Small Gurneys give rise to quite substantial increases in downforce for a small extra drag component, while larger ones add smaller extra increments of downforce, but bigger chunks of drag. Thus there are sensible limits to work to here, and Gurneys are usually less than 5% of chord in height. Smaller sizes than this will be most efficient, and a Gurney of around 2% of chord can add as much as 0.30 to the  $-C_L$  with a very small additional drag increment. An experiment by the author with a 20-inch (500mm) chord three-element rear wing on a hillclimb single-seater in the MIRA full scale wind tunnel showed that a  $\frac{3}{8}$ in (9mm) Gurney gave an extra 8.2% downforce for only 2.8% extra drag.

Some wind tunnel data from other cars makes interesting reading, too, as the table below reveals.

Car / Gurney: Benetton B199 / 12mm

$\Delta CD(\%)$ : +3.9

$\Delta CL(\%)$ : +2.0

$\Delta \% front$ : -2.11

$\Delta L/D(\%)$ : -1.8

Car / Gurney: Honda R107 / 15mm

$\Delta CD(\%)$ : +11.8

$\Delta CL(\%)$ : +11.6

$\Delta \% front$ : -6.08

$\Delta L/D(\%)$ : -0.2

Car / Gurney: Ligier JS49 / 12mm

$\Delta CD(\%)$ : +9.3

$\Delta CL(\%)$ : +7.6

$\Delta \% front$ : -5.80

$\Delta L/D(\%)$ : -1.6

Note: the change in ‘% front’ is the absolute change, not the relative change.

The first thing to note is that all these Gurneys were quite big relative to their wing chord dimensions, and this is reflected in the results, which saw the percentage drag gains exceeding the percentage downforce gains. However, in

each case the Gurney shifted the balance quite significantly and in this respect they are very useful tuning tools.

In general it is probably best to only use Gurneys when running a rear wing at or near its steepest angle, when the Gurney can help keep the flow attached, enabling a slightly steeper angle to be run to increase the maximum downforce available. At lower angles more efficient gains can usually be found simply by increasing the angle of the Gurney-less wing. Figure 5-39 shows a comparison of CFD simulations on a single element wing running at an angle of  $14^\circ$  with (on the right) and without a 10mm Gurney. The region of flow separation in the centre has reduced slightly with the fitting of the Gurney, and the magnitude of the suction, as shown by the intensity of the blue colour on the underside) has also been increased by the presence of the Gurney.

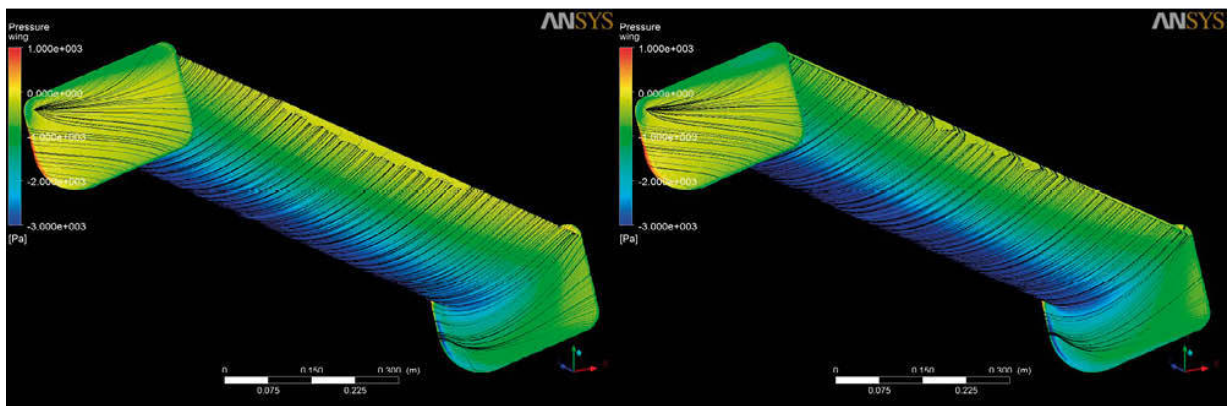


**Figure 5-39** With a 10mm Gurney (right) this wing at  $14^\circ$  is able to produce more downforce thanks to delayed flow separation and increased suction on its lower surface.

### Ground effect and front wings

Many of the above influences on wing performance are essentially negative, and detract from the downforce that a wing actually creates, as distinct from the theoretical downforce that it should produce. However, there are influences that, up to a point, can have a marked positive effect on the downforce produced by front wings, one of which is ‘ground effect’. The downforce produced by a wing well clear of the ground actually increases as the wing is brought nearer to the ground. The cause can be explained by thinking of the wing-ground system as being analogous to a venturi system – the acceleration of the airflow, and thus the static pressure reduction under the wing, becomes more marked between the wing and the ground than it would have been below the wing in freestream air. The effect is said to become more marked the nearer it gets to the ground, until it is very close to the ground,

when the adverse pressure gradient on the wing's suction surface becomes too steep, *and* the reducing gap to the ground begins to choke off the mass flow of air that can physically pass under the wing; the flow under the wing then starts to separate and ultimately stalls, and downforce declines rapidly. Fig 5-40 shows the results of a 2D CFD trial on a three-element front wing close to the ground.

Putting some numbers on this, a wing operating in the region of  $0.136c$  (2.5in or 63mm in this case) ground clearance might be expected to produce up to double the downforce it would in freestream air: that is, at ground clearances greater in magnitude than the chord dimension. This becomes very relevant when selecting a front wing profile to balance a rear wing, as we shall see in a later section. A further interesting observation from Figure 5-40 is that the magnitude of the  $-C_L$  at 2.5in (63mm) may be as much as 33% greater than that produced at  $0.283c$  (5.2in or 131.6mm) ground clearance. This demonstrates the sensitivity of the  $C_L$  to proximity to the ground, and leads onto a brief look at a further aspect of 'pitch sensitivity' with respect to front wings.

In a dynamic situation, a car is constantly rolling, pitching and yawing on its suspension in response to the mechanical loads being fed through it, and as its speed rises and falls, the downforce it produces also goes up and down. These effects combine to produce changes in ride height and pitch attitude (nose up or down) that can have a marked influence on the actual proximity of the front wing to the ground, and its angle of attack. This in turn creates varying amounts of downforce, with the net result that a car can become unpredictable, and even unstable, as the generation of inconsistent levels of downforce serve to confuse the driver and dent his confidence in the car. There is a further, even worse manifestation of pitch sensitivity, which can occur when the front wings are run too close to the ground. In this situation the wings can stall at low dynamic ride height. This then causes the downforce to fall off rapidly, so the front of the car rises again, only to allow the airflow to re-attach, which creates more downforce which sucks the nose down again... This creates an oscillation known as porpoising, which was a particular problem in the era of underbody ground effect-generated downforce in Formula 1 in the 1980s. Thus, pitch sensitivity and methods of lessening its effects, once using active suspension systems are often right at the top of designers' priority lists. Nowadays additional springs or dampers or other 'third elements' in the suspension that control ride height changes, and damping systems that enable the independent adjustment of high and low damper

piston speeds so as to isolate and control the slower vehicle attitude changes from the faster wheel movements are used.

Further improvements in pitch sensitivity reduction have also arisen from the use of complex spanwise front wing shapes. In part this is tied up with managing the airflow to the car's underside and to the radiators within the sidepod ducts. A further benefit is that pitch sensitivity is reduced because the wing-to-ground gap is variable across the span of the wing. Thus, the situation where the flow beneath the wings completely stalls at very low ground clearance doesn't arise. Such a wing will probably not produce as much downforce as one with constant, very low ground clearance, but it should be more consistent.

We can see the effects of reducing ground clearance on a front wing in the following brief CFD study on front wing sensitivity. A two-element front wing was analysed in 3D at two different ride heights at a virtual air velocity of 33.5m/s (120km/h, or 75mph). The wing was tested in freestream air (that is, not attached to a car model) but a moving ground plane was included in the model. Just two ground clearances were tested because this was another quick 'look-see' trial related to application on a hillclimb single-seater. The static ground clearance as installed on the car measured 92mm (3.6in) from the ground to the wing leading edge, and a 70mm (2.75in) setting represented the ground clearance to the leading edge with what was thought to be a typical amount of front suspension compression. In the context of Figure 5-40 these values represent about 0.22c and 0.16c where c equals the overall chord dimension of 425mm (see Figure 5-41 for the wing geometry).

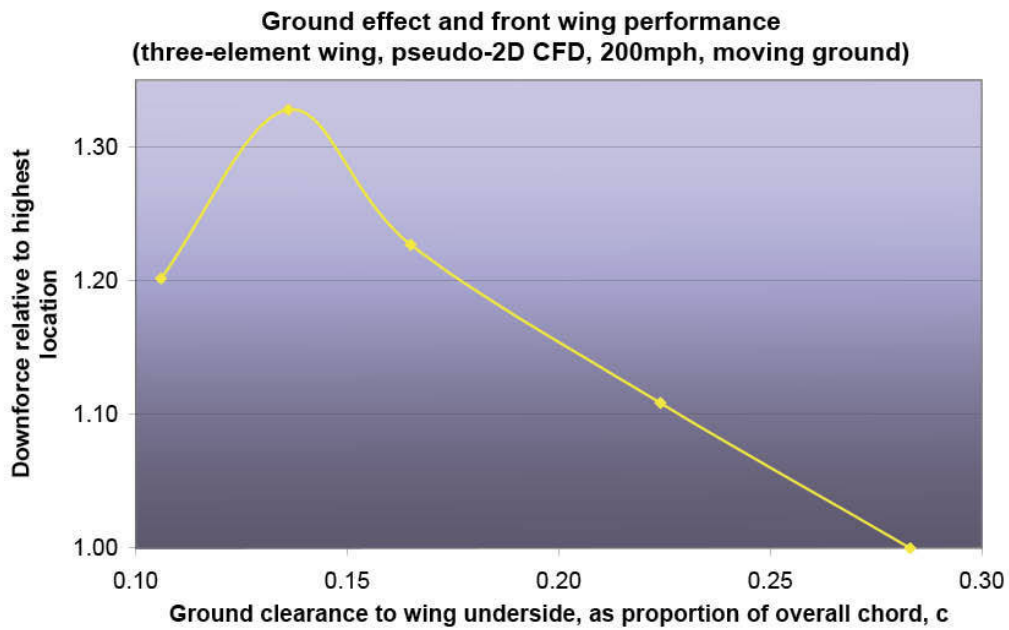


**Figure 5-40** Downforce from a front wing increases as ground clearance decreases, but only up to a point.



**Figure 5-41** A two-element front wing in ground effect.

The result showed a downforce jump of 4.5% from 625.2N (140lb) at 92mm to 653.8N (147lb) at 70mm. This was perhaps a smaller increase than would be expected from Figure 5-40 (which might suggest a 10% or so increase), but was in line with the general expectation of a significant increase.

The Del\_Cp\_static plot in Figure 5-42, showing the changes to the static pressures on the wing underside as the result of decreasing the ground clearance, is most instructive. It is very evident from this plot that the suction

under the mainplane has been increased by dropping the ground clearance, but that the suction on the flap has been lessened – the static pressure here is higher at 70mm ground clearance than it was at 92mm. So the mainplane is working harder, but the flap is producing less downforce.

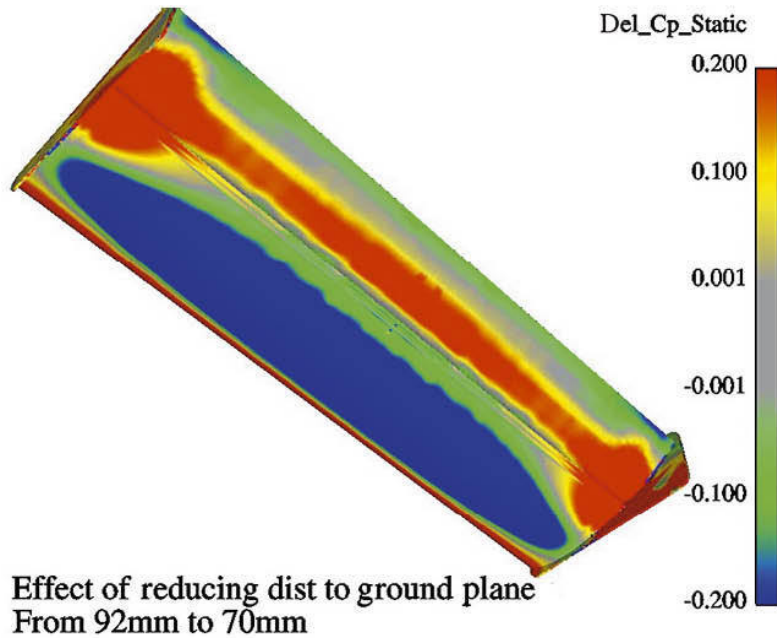


**Figure 5-42** Changes to static pressures caused by reducing ground clearance.

Figure 5-43 shows the total pressure in each case. The additional area of blues and greens under the rear of the 70mm ground clearance mainplane and in its (larger) wake show increased total pressure losses, meaning the air reaching the region under the flap has ‘become tired’ and lost energy compared with the 92mm ride height case. As such, the static pressure under the flap has not been reduced as much, even though lowering the wing’s ground clearance did reduce the static pressure under the mainplane more.

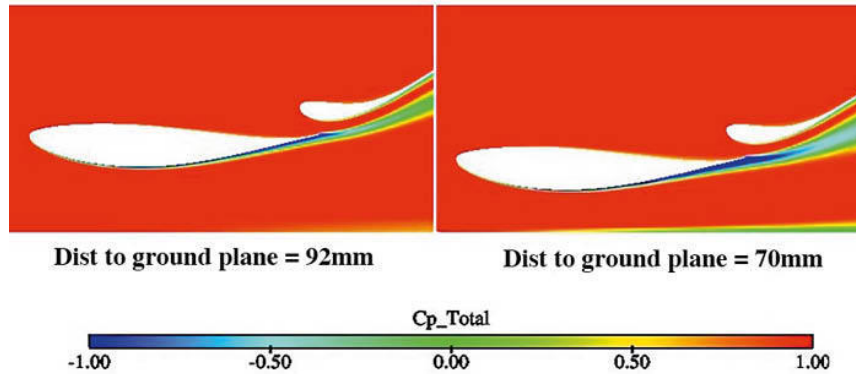


**Figure 5-43** Total pressures at the two ground clearances.

From this we can see that the adverse pressure gradient (from the lowest pressure region to the trailing edge) under the wing with less ground clearance has become steeper. Were this situation to be made more extreme, then the possibility of flow separation and, ultimately, stall exists. In other words, running the wing still closer to the ground could lead to stalling.

Such a situation can indeed occur, but there are a number of possible remedies. Obviously, maintaining a sufficiently high ground clearance is one method, and various suspension control devices are used to minimise reductions in front ground clearance partly for this reason. Optimising the profile of the wing can lessen the likelihood of separation or even stall occurring in this way throughout a practical range of ground clearances too – running a wing that generates less flow convergence between itself and the ground, for example, would make the air work less hard and again, lessen the likelihood of separation. Such a wing, which would incorporate less camber and probably a more rounded leading edge, generates its downforce by virtue of a low ground clearance rather than through an intrinsically high lift coefficient. Clearly, there are various tunes to be played here, but the important point is that you can run into problems of front wing sensitivity, and if possible counter-measures are probably best introduced at the design stage.

### How to select and design a wing set-up

What follows may look mathematical, but don't let that fool you! It is, in all honesty, highly empirical, and just happens to contain a few calculations that might make it look more complicated on first glance than it really is. For the competitor who wants to fit wings to his or her car for the first time, or who perhaps wants to figure out if the set-up already fitted to their pride and joy is

somewhere in the right ballpark, then hopefully, the principles outlined here, full of assumptions and estimates though they are, will provide a better first approximation than blind guesswork on its own. The basis of the scheme is that you have to figure out how much drag you are prepared to accept from a wing set-up, and that having determined that, you can then select appropriate wings for your car. The scheme is outlined here for a single-seater racecar, but could be applied to other categories, at least in part, as well.

The eight-point plan to a first approximation of a wing set-up is as follows:

1. Calculate the theoretical top speed without wings – this needs values for the frontal area, the power at the wheels, and the  $C_D$ .
2. Decide how much you are prepared to knock off that top speed by the addition of wings. An implicit principle here, based on experience and hard measurements, is that the front wings add relatively little drag, whereas the rear wing contributes tangibly to overall drag.
3. Calculate the difference in power absorption figures between the top speed without wings and the top speed you are prepared to accept with wings.
4. The difference between these two power absorption figures is what you are going to ‘donate’ to the rear wing in the quest for downforce.
5. Calculate the maximum wing  $C_D$  value that this represents. This requires values for the wingspan and chord dimensions to work out the *plan* area of the wing.
6. Using an estimated value for the lift-to-drag ratio, work out what  $-C_L$  figure corresponds with the  $C_D$  value, figure out a corresponding basic configuration (that is, single-, dual- or possibly multi-element), and then consult the wing catalogues to seek a specific profile that will provide this  $-C_L$  value, and at what approximate angle of attack. A couple of profiles are provided in Appendix 2, but the choice is from a vast range of possibilities (see the catalogues and websites in Appendix 5).
7. Calculate the theoretical downforce figure that the rear wing will give, then calculate the downforce required at the front to balance this value. The front wing dimensions will be needed here, as will the wings’ ground clearance so that ground effect can be allowed for in determining the requisite  $-C_L$ (front) figure.
8. Determine a suitable configuration, profile and approximate angle of attack for the front wings.

The guesstimate as to what you are prepared to drop your maximum top speed by is going to have to be based on the best knowledge you have got

about the speed regimes of the tracks on which you compete. For example, you will probably have a good idea of the maximum speed you achieve on each track. You will also be able to at least estimate the time you spend at various speeds, and if your car is equipped even with just a rudimentary data acquisition system such as a rev counter with a memory, you will be able to work out exactly how long you spend in the various speed brackets. With a more sophisticated data acquisition system, you will be able to let a computer work these things out for you, and plot out how long you spend in each sector of the track too. All of this will facilitate a reasonable judgement to be made as to how critical top speed is at a given track. Further analysis, objective wherever possible (but subjective will do if data isn't available), has to take into account how much time is spent accelerating, braking and cornering, and at what speeds. This will all help, firstly, to cause lots of confusion (!), but secondly, to get a handle on the nature of each track, and to help decide whether it's a 'downforce track' or not. Naturally, there are no black and white decisions here. Even the pros, equipped with lap time simulation software on powerful computers are actually working on assumptions and guesstimates at least as much as hard data and past experience. So get to it and start analysing!

Perhaps the hardest thing of all to take into account is that the rear wing will not give you as much downforce as you hope it will from this method. Without the benefit of wind tunnel testing, or actual measurements on the real car, it is impossible to say just how much the rear wing is going to suffer from the mess that the rest of the car makes of the airflow. All that can be said is that whatever this approximation throws up as a solution, it will be hard pressed to achieve the theoretical results predicted, and you may need a steeper angle of attack, or perhaps even an additional wing element if the results suggest fitting something which is marginal between, say, a single-element and a dual-element wing. Anyway, it's instructive as well as fun to attempt a numerical solution to this vexing problem, so let's work through an example to see what comes out.

### **Wing configuration calculation**

Taking a hillclimb single-seater with which the author had intimate experience (having co-assembled and developed it), the frontal area without wings was 12.6 square feet ( $1.17\text{m}^2$ ), the wingless  $C_D$  was 0.65 (measured in MIRA's full-scale wind tunnel). Power at the flywheel was around 295bhp, leaving about 260bhp left to overcome aerodynamic drag (the 12% or so deduction is intended to account for powertrain losses and rolling resistance for a car of this nature, with its normal footwear of wide, but cool tyres). This power

figure will correspond exactly to the power absorbed at the vehicle's maximum speed in this wingless state, which from the equation we first saw in Chapter 2 would be:

$$V_{max} (\text{mph}) = \sqrt[3]{[(\text{bhp} \times 146,600) / (C_D \times A \text{ in sq ft})]}$$

so

$$\begin{aligned} V_{max} &= \sqrt[3]{[(260 \times 146,600) / (0.65 \times 12.6)]} \\ &= 167.0 \text{ mph} (268.4 \text{ km/h}) \end{aligned}$$

This is way in excess of the maximum speed on any track visited. The fastest speed recorded at any hillclimb venue the car competed on was 118mph (190km/h). Therefore, for the sake of the example, and for our first iteration, let's assume that we decide that a maximum speed of, say, 135mph (217km/h) is going to be more than enough to leave some top end acceleration at the fastest part of the fastest course visited. How much power would be absorbed at this speed? This would be calculated by rearranging the power equation, thus:

$$\text{bhp absorbed} = \frac{C_D \times A \text{ in sq ft} \times (\text{max. speed selected, mph})^3}{146,600}$$

so

$$\begin{aligned} \text{bhp absorbed} &= \frac{0.65 \times 12.6 \times (135)^3}{146,600} \\ &= 137.5 \text{ bhp} \end{aligned}$$

The difference between this and the 260bhp absorbed at the absolute maximum speed is the value that we are going to 'donate' to the rear wing drag = 260 - 137.5 = 122.5bhp. So what wing  $C_D$  does this correspond to? To figure this out, we need to know the wing dimensions, and in this case they are 42.1in span x 21.7in chord (1.07m x 0.55m), so plan area is 6.34 square feet ( $0.5885\text{m}^2$ ). Using the re-arranged power absorption equation again, we can say that the maximum wing  $C_D$  will be:

$$\text{Wing } C_{D\max} = \frac{\text{'wing bhp' } \times 146,600}{\text{Wing plan area in sq ft } \times (\text{selected speed, mph})^3}$$

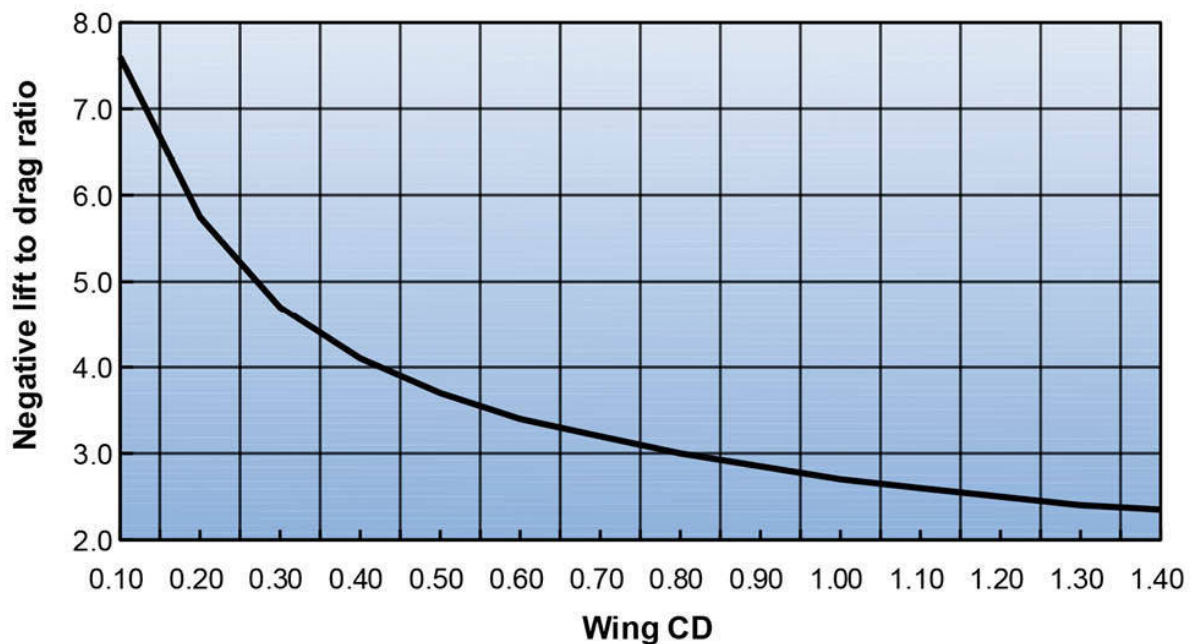
so

$$\text{Wing } C_{D\max} = \frac{122.5 \times 146,600}{6.34 \times (135)^3} = 1.15$$

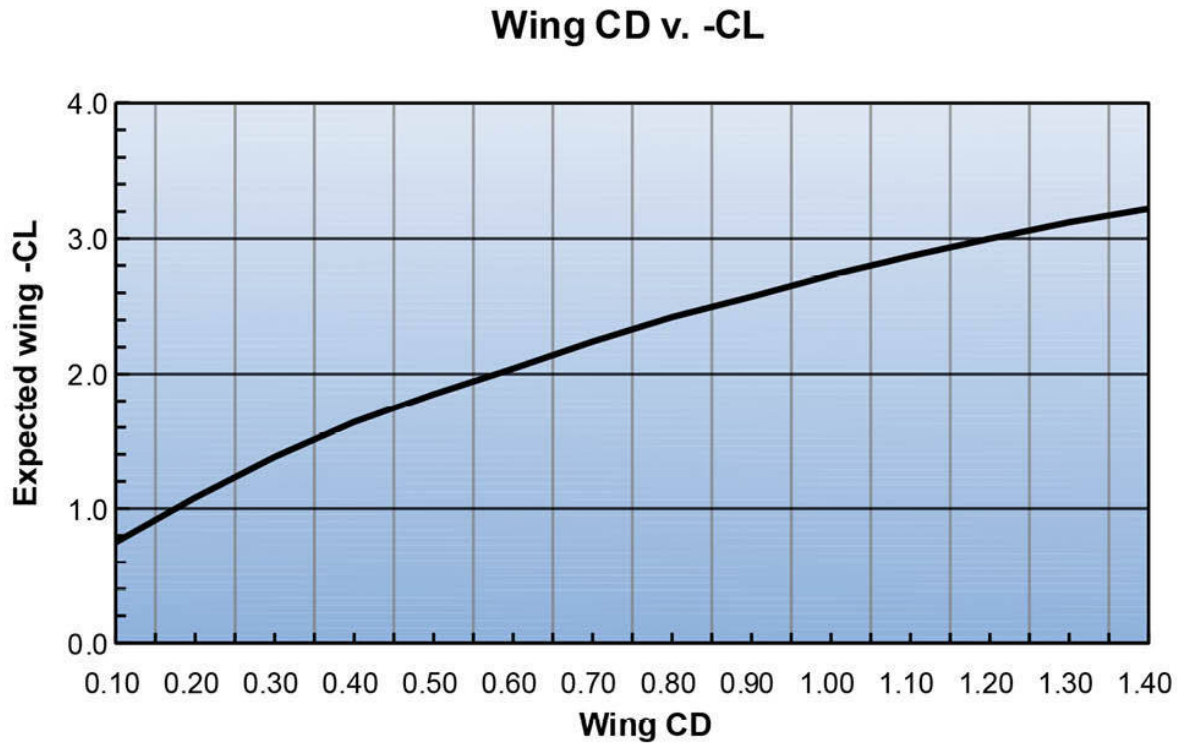
So what kind of wing will have a  $C_D$  of 1.15? Unfortunately we can't just look this up in the wing catalogues. A short cut to finding out what sort of wing will correspond to a particular  $C_D$  is to use a lift-to-drag ratio, based on real data on wings trawled from the literature, to determine the likely  $-C_L$  that this will correspond to, and then use the catalogues (listed in Appendix 5) to seek out a configuration and possible profile that would produce this  $-C_L$ . It is possible to work this out from theory, but somehow, hard data simply has a more secure feel to it ...

Figure 5-44 shows an approximate correlation based on published data points of wing lift-to-drag ratio versus  $C_D$ , and Figure 5-45 shows the  $-C_L$  values, versus  $C_D$  figures, derived from this. Once again, this should get you in roughly the right area. In our example, a  $C_D$  of 1.15 should correspond to a  $-C_L$  of about 2.95 (the lift-to-drag ratio is therefore around 2.57:1).

**-L/D ratio versus wing CD**



**Figure 5-44**  $L/D$  versus wing  $CD$ .



**Figure 5-45 Wing CD versus CL.**

But what configuration wing does this correspond to? Figure 5-46 is a rough guide to typical lift coefficients of competition car wings – the reader should consider that each line represents only a typical average value – and from this we can see that a  $-C_L$  of 2.95 would correspond to a three-element wing. A potent two-element design could, with optimisation, perhaps achieve this  $-C_L$  value, but a three-element, double-flap arrangement could be set at a low angle, or with low flap deflection to achieve a lower downforce level, or a higher angle to obtain a higher coefficient, so providing more tuning options. Thus, the likely best first estimate of a rear wing configuration to suit this car, on the basis of the assumptions made here, is a three-plane rear wing. Curiously, or perhaps not so curiously, this is what the car was fitted with at the time.

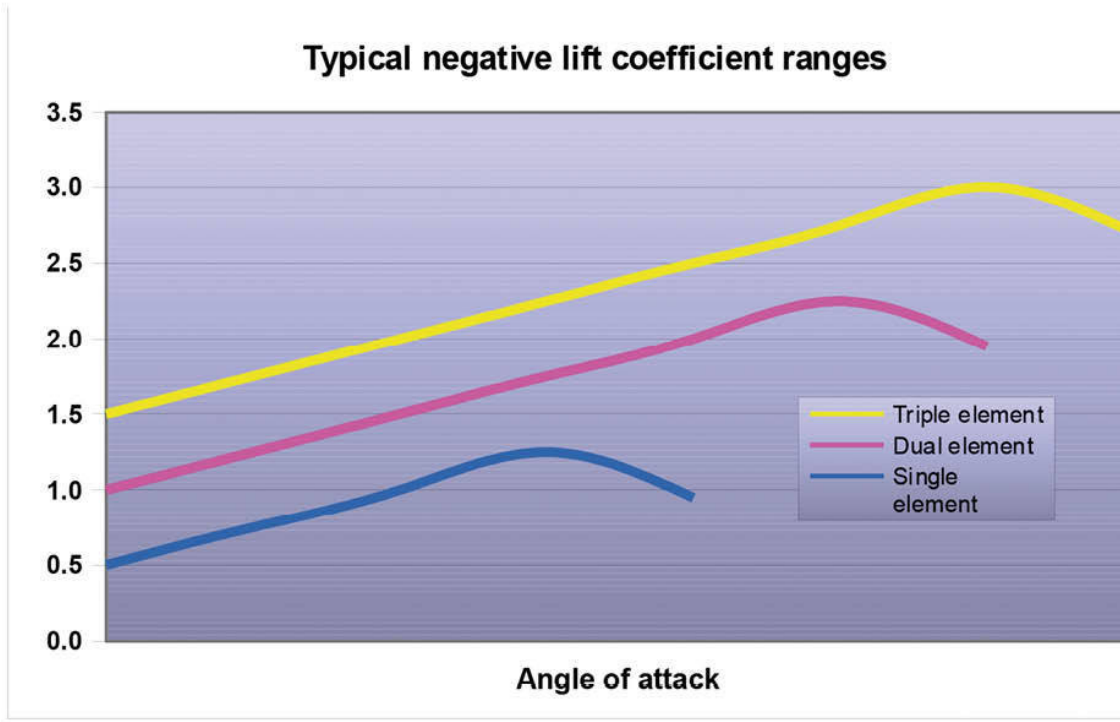


**Figure 5-46** *Typical lift coefficient ranges.*

However, as we will see shortly and as has been stated previously, it is better to run a wing as wide as the rules allow, and subsequently a two-element wing built to the maximum span allowed of 55in (1.4m), and with a smaller chord to achieve a higher aspect ratio, but a similar plan area to the original wing was fitted. With no analytical or measurement facilities available the only option for this team was to build the wing, fit it, and see if it helped performance in absolute terms (against the clock) or relative terms (against the opposition). And it did help, seemingly producing at least as much downforce but also permitting higher top speeds, suggesting better efficiency too.

We have yet to work out the front wing configuration that should, theoretically, balance the original rear wing. To do this, let's assume equal mechanical cantilever effect front and rear (they weren't equal, but it makes the calculations easier!), and an aerodynamic balance in proportion to the weight distribution, which with the driver aboard was about 38:62 front:rear. The front wing area was about 4.34sq ft ( $0.4\text{m}^2$ ). Thus, to keep the aerodynamic balance the same as the static weight split front to rear, we can say that the downforce at the front needed to be 38/62 times the downforce at the rear,

which, putting in the relevant values for area, means we can say the following, using the basic downforce calculation:

$$\text{downforce}_{\text{rear}} \times 38/62 = \text{downforce}_{\text{front}}$$

$$\text{so } \frac{1}{2}\rho A_{\text{rear}} - C_{L\text{rear}} V^2 \times 38/62 = \frac{1}{2}\rho A_{\text{front}} - C_{L\text{front}} V^2$$

the  $\frac{1}{2}\rho$  and  $V^2$  on both sides of the equation cancel each other out

$$\text{which means } A_{\text{rear}} \times -C_{L\text{rear}} \times 38/62 = A_{\text{front}} \times -C_{L\text{front}}$$

$$\text{so } -C_{L\text{front}} = \frac{A_{\text{rear}} \times -C_{L\text{rear}} \times 38/62}{A_{\text{front}}}$$

Put in the value for the  $-C_{L\text{rear}}$  of 2.95, together with the figures for the front and rear areas, and the answer is that the  $-C_{L\text{front}}$  needs to be 2.67.

But, we have yet to take into account ground effect, which, by making the front wings produce more downforce by being close to the ground means we don't need a section with this high a  $-C_L$  value in order to achieve the level of necessary downforce. Figure 5-40 showed how downforce increases as a wing gets closer to the ground. Let's assume that the front wings are going to be about 5in (125mm) clear of the ground. The wing chord is 13.75in (350mm), so the ground clearance is about 0.36c relative to the chord. Figure 5-40 indicates that we can perhaps expect an increase in  $C_L$ , relative to the wing in freestream air of about 1.37, or 37%. So, we only need to use a wing configuration that produces a  $C_L$  of 2.67/1.37, or 1.95. This corresponds to a two-element wing, perhaps at moderate overall angle of attack.

The important thing is that we have determined that this car could have run with a three-element rear wing of the dimensions specified, which would be balanced with a two-element front wing. Precise installation angles would have to be determined by testing. Interestingly, the car in this example was balanced with a pair of two-element front wings, although the angle of attack at the front is somewhat steeper than the calculations suggest. This may be because the car had a fairly narrow front track, with reasonably wide tyres not far behind the trailing edge of the front wing flaps. This would tend to reduce the effective working area of the front wings, and require a steeper angle of attack

to make the effective portion work that much harder in order to balance the rear wing.

What none of this takes into account, of course, is the downforce that might be generated by the underside of the car. *If*, and it is a big if, the underside happens to produce its downforce with a convenient front-to-rear split matching the weight distribution (there or thereabouts), then the wing configuration calculations here will still be valid with regard to working out a balanced set-up. If the underside produces, say, rear biased downforce, then the implications are that the rear wing may not have to produce as much downforce, and also that the front wing(s) may have to work harder to balance the rear. This would appear to be the case with the current crop of Formula 3 cars, for example; with their tiny regulation rear wings and relatively large front wings, it has to be concluded that the underbody and diffuser must be making a significant contribution to rear downforce. Furthermore, the interaction between rear wings, especially of the multi-tier type, and the underside cannot be taken into account by the empirical approach. This is something that can only really be solved with appropriate testing

### **Wing mountings**

No mention has so far been made of some of the practicalities involved with choosing a wing set-up. The manner of attachment of front and rear wings can have an effect on their efficiency. For example, at the front of a single-seater, a pair of wings either side of a nose cone will have a plan area limited by the maximum width permitted, minus the width of the nose. Thus, the narrower the nose is, the bigger will be the available plan area, and the larger will be the aspect ratio, which combine to produce more downforce, more efficiently. Even better is if the front wing is a single device, with a span dimension equal to the full width permitted, creating the maximum possible aspect ratio. This can be achieved either by mounting the wing above the nose, or below it. Mounting above the nose isn't a good idea because the central portion of the wing's suction surface will lose effectiveness by its proximity to the nose cover, and the whole wing will, most probably, be so far above the ground that it will lose the benefit of ground effect. On the other hand, mounting the wing below the nose puts the whole underside of the wing into ground effect, and utilises the wing's width to the maximum. Thus, the current phase of high nose designs in so many single-seater formulas at present is exploiting these advantages to the full.

Rear wings have two options for attachment, which are sometimes combined; the 'centre post' and 'end plate' mount variations are both used

across a wide range of racing categories. With either method, it is important to consider the effect that the mounting structure can have on the flow on the all-important underside of the wing. If the mounting is to be of the centre post type, then the post, or twin plates as are sometimes used, should be shaped and faired so as to interfere as little as possible with the wing's airflow. However, consideration of the effects of the air interacting with the wing mountings is often overlooked.

In the case of the end plate mounting, since the thickness of the end plates has a controlling influence on their rigidity, it follows that they are likely to eat into some of the available wing area (if span is restricted by regulations, which it usually is), and also exert an effect on the airflow at the outer edges of the wing. Again, the leading edges (at least) of the end plates should be shaped so as to disturb the airflow onto the wing as little as possible. Structural considerations are outside the scope of this book, so suffice to say that at maximum speed wings can generate substantial loads, and mountings need to be able to cope with these loads with a suitable margin of safety.

### **Aspect ratios again**

It has already been mentioned in passing that a larger aspect ratio makes for a more efficient wing. Figure 5-47 shows in general how the lift coefficient versus angle of attack alters with aspect ratio. It is clear that a low aspect ratio yields a lower lift coefficient. But, on the positive side, the stall angle is delayed, ironically by the very 'leakage' of air around the tips and end plates that reduces the  $-C_L$ , which reduces the expansion of the airflow aft of the lowest static pressure region, and delays separation, with stall becoming less abrupt. This leakage affects a bigger proportion of the span of a low AR wing, making such a wing a less sensitive device.

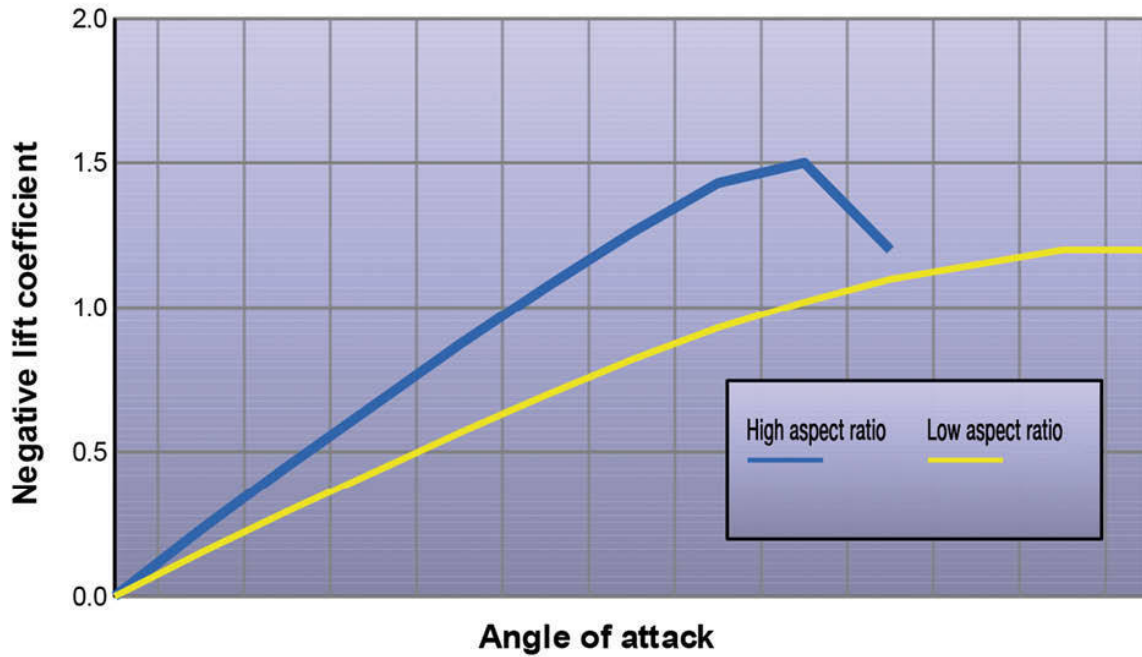


**Figure 5-47** Generic effect of aspect ratio.

This is not a good reason for selecting a low AR wing though! Better to maximise the span in order to achieve the best aspect ratio, and hence the highest -CL possible. Referring back to the sample calculations on the rear wing of the hillclimb car, the maximum span allowed in this competition category is 1.4m, and there really is no good technical reason for *not* having a wing of this span, so as to maximise the possible AR. There is a formula used for estimating the lift coefficient of an aerofoil, which in simplified form tells us that

$$C_L \text{ is proportional to } \frac{1}{1 + (2/\text{AR})}$$

This means that increasing the aspect ratio does indeed lead to an increase in the lift coefficient at a given angle of attack. Feeding in some AR values into this formula over the typical range of competition car aspect ratios, and plotting them on a graph, relative to the lift at AR = 1, yields the plot shown in Figure 5-48. If the wing on the hillclimb car in the earlier example had its 1.07m by 0.55m (AR = 1.95) wing replaced with one of 1.40m by 0.42m (AR

$= 3.33$ , with the same plan area), then this graph suggests that its lift coefficient will increase by over 25%, if all other things remain equal.

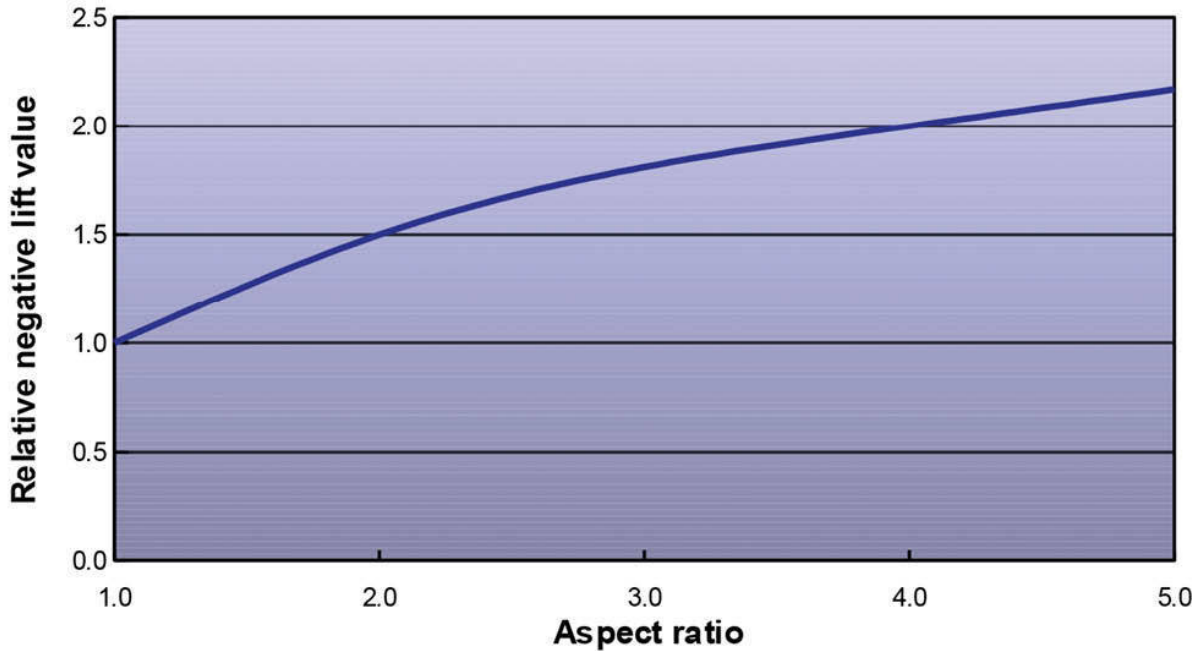


**Figure 5-48 Lift and aspect ratio.**

But the news gets even better! There is also an approximation for calculating the induced drag component of the total drag caused by a wing. As we have seen, the induced drag gets greater with increased downforce. It is also affected beneficially by an increased aspect ratio, and a formula for approximating a value for induced drag is

$$C_{D,i} \approx \frac{C_L^2}{\pi AR} \quad (\pi = \text{Greek letter "pi"})$$

If we look at the two configurations for the hillclimb rear wing, one with  $AR = 1.95$ , producing a  $C_L$  of 2.80, and the other with  $AR = 3.33$ , which theoretically will create a  $C_L$  25% greater, that is, 3.50, then the induced drag coefficients work out at 1.28 for the former, and 1.17 for the latter. Thus, not only has the theoretical lift increased, but also the theoretical induced drag has

reduced in spite of the extra lift! This is too good a bonus not to be exploited. It also indicates that the earlier correlation put forward for deriving -CL values from lift to drag ratios, which was based on reported data, can only really be applied with any confidence to the aspect ratios of the wings that the data were measured on, which were in the range 1.5 to 2.0. Larger AR wings will perform better.

Wings are the most obvious manifestation of the use of downforce to improve competition car performance. Perhaps it is because of this that they often come under attack as the cause of what is seen as reduced overtaking and a decline in ‘proper’ racing in a range of racing categories around the world. Whether or not you agree with this, it is indisputable that wings have, and will probably continue to have, an important role to play in motorsport – even if it’s only to carry the sponsors’ names!

### The ‘global’ effects of wing angle changes

One of the things that becomes almost immediately apparent when making configuration changes in the wind tunnel is how changes at one end of the vehicle affect not just that end but the whole vehicle, as we saw in the previous chapter when looking at airdams and splitters in the wind tunnel. The same is true of rear wing angle changes, and the data below come from the British GT3 specification Ferrari F430 Scuderia of championship contenders MTECH Racing.

Wing angle: 0°

CD.A: 0.972

-CL.A: 1.539

-CLf.A: 0.851

-CLR.A: 0.691

% front: 55.25%

-L/D: 1.583

Wing angle: 4.5°

CD.A: 1.058

-CL.A: 1.701

-CLf.A: 0.800

-CLR.A: 0.903

% front: 47.04%

-L/D: 1.608

Wing angle: 6.0°

CD.A: 1.079

-CL.A: 1.726  
 -CLf.A: 0.781  
 -CLR.A: 0.945  
 % front: 45.26%  
 -L/D: 1.600  
 Wing angle: 7.5°  
 CD.A: 1.109  
 -CL.A: 1.781  
 -CLf.A: 0.785  
 -CLR.A: 0.995  
 % front: 44.10%  
 -L/D: 1.606  
 Wing angle: 9.0°  
 CD.A: 1.134  
 -CL.A: 1.798  
 -CLf.A: 0.769  
 -CLR.A: 1.031  
 % front: 42.76%  
 -L/D: 1.586

We can see how adding wing angle adds to both total downforce and drag. It's also evident how the balance changes, not just through adding downforce at the rear but also by removing it from the front, again probably through mechanical leverage effects though possibly also from modifications to the airflow over, under and around the car. It isn't possible to tell from the data what the contribution of each of these effects actually was.

Note that the car's efficiency ( $-L/D$ ) was worst at either end of the wing adjustment range in this case. At zero degrees the smaller total downforce value was responsible for this whereas at the steepest wing angle tested here it appears that the downforce gains tailed off more rapidly than the drag increments.

## **Wing location**

An oft-recurring question is: at what height should a rear wing be mounted, especially if the racecar in question has a diffuser? Two seemingly contradictory factors come into play when trying to decide the answer to this question. The simple answer in many cases is that the wing will work best if you mount it as high as the rules of your category permit. That way the airflow reaching the wing is as little affected by the rest of the car as possible, and the

wing will perform as well as it can in what is still, usually, a highly compromised location.

However, in *Race Car Aerodynamics*, Joseph Katz cites a number of examples in which wing locations below the permitted maximum height proved beneficial. A dual element wing on a closed sports prototype style racecar apparently gave the greatest vehicle downforce when its height was slightly less than half the wing's chord dimension above the rear deck, measured to the wing's trailing edge, with the downforce tailing off at heights either side of this. And a single element wing on a sedan-based racecar showed best vehicle downforce when at about 0.7 of its chord above the rear deck, again with downforce reducing at higher or lower positions. In other examples Katz illustrates how the presence of a rear wing on various racecar shapes helped to augment the static pressure reductions in the underbody to the betterment of vehicle downforce. So clearly there were some interesting interactions here that make it worth studying wing height in more detail.

So when the opportunity arose to take a race modified Lotus Exige into the MIRA full-scale wind tunnel the chance to try some different wing heights was too good to miss. This particular Lotus Exige S2 belonged to Phil Peek and had been modified by Reverie Ltd with a number of components that were suitable for GT3 and Britcar-type applications. Featured were a complex front splitter that essentially led into a smooth, flat underside; front dive planes; the standard rear diffuser arrangement was still fitted at test time; 40mm wider wheel arches were installed at front and rear; and a new, more aggressive wing profile than the standard road item at nearly full car-width span and incorporating planform curvature was also installed. The wing's chord dimension was 230mm.



*The Lotus Exige used in this wing height trial.*



*The lowest wing height tested.*



*The intermediate wing height.*



*The highest wing position evaluated.*

A set of alternative height wing support plates was manufactured prior to the test to facilitate rapid configuration changes to be made. The highest setting corresponded with the maximum permitted height under the FIA GT3 regulations prevailing at that time, which required the maximum height of any part of the wing assembly to be at least 100mm below the roof height. The data derived are plotted in Figure 5-49.

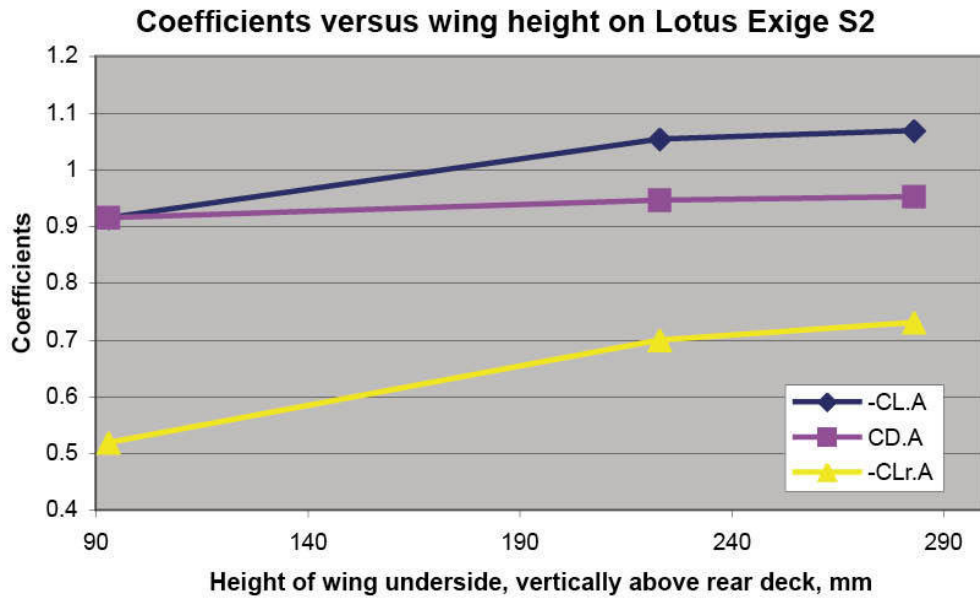


*Figure 5-49 Overall car coefficients versus wing height on a race-modified Lotus Exige S2.*

Although only three data points were obtained here, the relationship seems pretty clear at the wing angle of 10° tested – downforce increased with wing height until its height was slightly greater than its own chord dimension, the gain then appearing to flatten off. Katz plotted data at wing heights up to 5.5 times the wing chord, but regulations prohibit the wings to be run that high in most categories, academically interesting though this might have been. However, although the experiment on the Exige didn't go down to very small wing-to-deck gaps, there did not seem to be the peak in vehicle downforce in the 0.5 to 0.7 times the wing chord region that Katz had shown. What could have been the reasons for the difference in this case?

It could simply be that the particular shape of rear deck and the profile of the rear wing produced a downforce peak at a somewhat greater height than Katz had shown, and that downforce could then have declined again if greater heights had been tested, thus matching the type of relationship shown by

Katz. Or it could have been that there wasn't the same degree of interaction between the wing and the rest of the vehicle in this case, and that moving the wing away from the rear deck simply proved to be more beneficial.

Two observations might bear out this hypothesis. Firstly, with a wing above a surface, it follows that as the wing is brought closer to the deck surface the wing's suction acts on that surface, and as well as the wing sucking itself downwards, it also sucks the deck surface upwards. This would naturally tend to lessen the overall force felt by the tyres. And the region below a wing in which the static pressure is substantially reduced extends very roughly one chord's distance below the wing. Thus, we might anticipate that overall downforce would decline appreciably as the wing to deck gap reduced to below this distance. Eventually the gap would become so small as to choke off the flow under the wing and downforce would reduce further, the wing then serving only as a spoiler.

However, another observation was made later on in this test session that would also undoubtedly have influenced this experiment. As it transpired, the diffuser on this car appeared from smoke plume tests to be running stalled because of the presence of the twin exhaust tail pipes protruding into the central diffuser channel (the outer channels were also apparently fully stalled, although this is not uncommon). This could have precluded the possibility of any beneficial interaction between the wing and the diffuser, which might otherwise have seen greater downforce generated at a lower wing height, as shown by Katz.

Clearly it would have been beneficial to rerun this trial with a diffuser that was working effectively. But we might reasonably conclude here that in the absence of beneficial underbody interaction, or where little interaction might be expected, it would indeed seem that putting the wing as high as the rules allow maximises downforce. Were the wing to be allowed to overhang the rear of the vehicle too, which it was not in this instance, the picture might be different again because the wing's low-pressure region would almost certainly interact more strongly with the airflow exiting the underbody.

Another wind tunnel study, this time on the ADR3 sports racing car revealed further interesting interactions. The car was evaluated with the rear wing in its stock position, which saw the wing set back from the rear deck and the maximum permitted height being exploited, and then the wing was moved to some different locations. Initially, it was lowered in 33mm increments until it was 100mm lower than standard. It was then moved forward by 135mm, and the results are summarised in the table below.

Rear wing: 1. Stock position

CD: 0.582

-CL: 1.065

-CLfront: 0.360

-CLrear: 0.705

%front: 33.80

-L/D: 1.830

Rear wing: 2. 33mm below stock

CD: 0.573

-CL: 1.041

-CLfront: 0.373

-CLrear: 0.668

%front: 35.83

-L/D: 1.817

Rear wing: 3. 66mm below stock

CD: 0.566

-CL: 1.015

-CLfront: 0.390

-CLrear: 0.625

%front: 38.42

-L/D: 1.793

Rear wing: 4. 100mm below stock

CD: 0.555

-CL: 0.983

-CLfront: 0.400

-CLrear: 0.582

%front: 40.69

-L/D: 1.771

Rear wing: 5. 100mm below + 135mm forward

CD: 0.556

-CL: 1.058

-CLfront: 0.437

-CLrear: 0.620

%front: 41.30

-L/D: 1.903

Rear wing: 6. 66mm below + 135mm forward

CD: 0.572

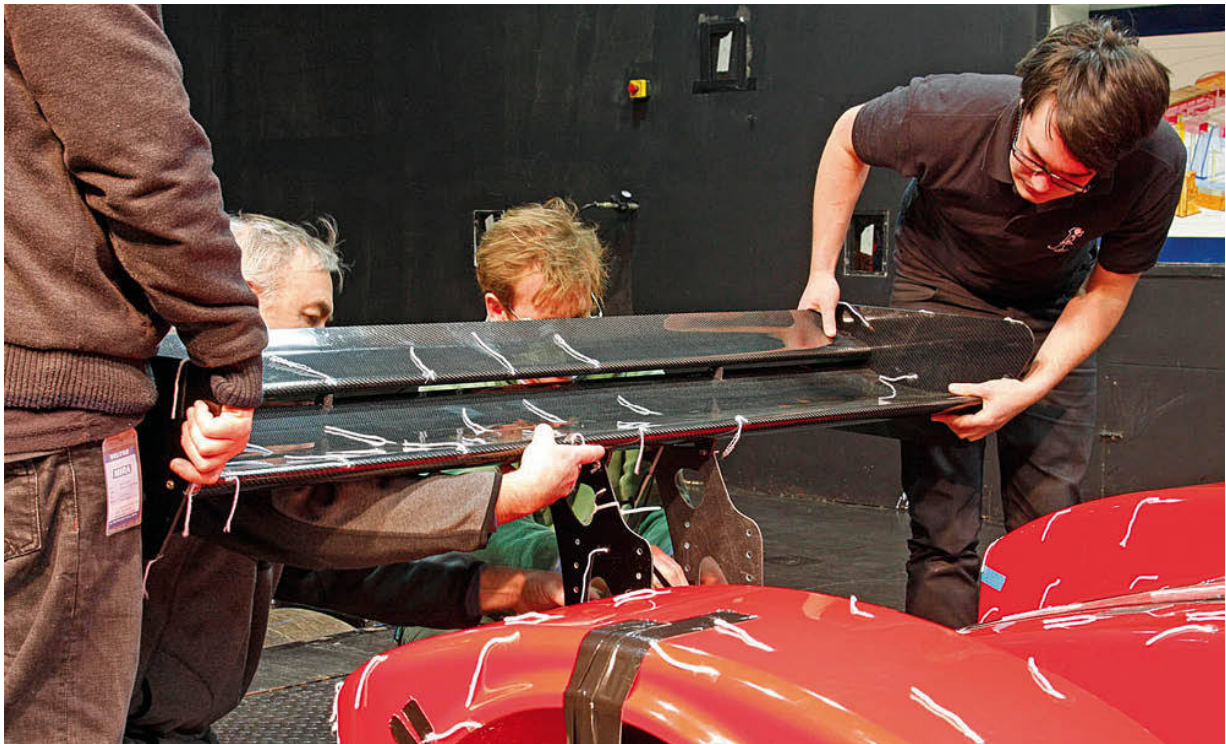
-CL: 1.069

-CLfront: 0.429

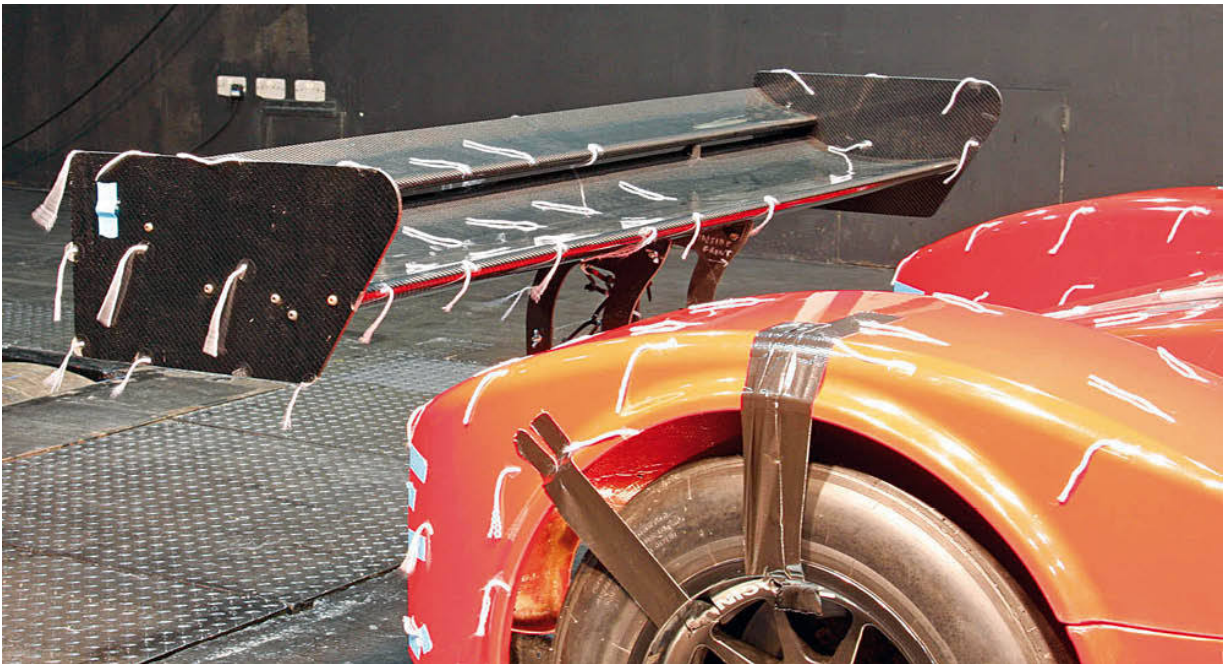
-CLrear: 0.640  
%front: 40.13  
-L/D: 1.869

From rear wing position number 1 (stock) to number 4, as the wing was lowered there was a simple trend of reducing drag and reducing downforce, together with a significant, almost linear reduction in rear downforce, and a concomitant, though possibly non-linear, increase in the forces felt by the front wheels. Despite the drag reductions, efficiency also reduced at each step.

However, when the wing was then moved forward by 135mm, while being retained at this new, 100mm lower height, to position number 5, total downforce jumped up again to almost the same level it was before the wing was moved. It also increased by roughly equal amounts at each end of the car, with virtually no change in drag with the forward shift. Efficiency thus also improved markedly, and balance was now over 41% front. The obvious conclusion here was that the wing's interaction with the underbody had improved, hence the roughly equal downforce jumps front and rear with no drag increase.



*The ADR's rear wing in its stock position, and about to be moved.*



*The ADR's overall aerodynamic performance benefitted from moving the wing lower and further forwards than its stock location.*

The wing was then raised to the 66mm below stock height at this new, more forward position (position number 6), but although total downforce increased slightly, drag and efficiency changed for the worse, so position number 5 was selected as the best available. This raised the obvious question about whether position 5 was actually ‘the sweet spot’ for the rear wing, but with a tight timescale there wasn’t the opportunity to explore this further.

The exercise did demonstrate the point, though, that a car with a downforce-generating underbody can benefit from running the rear wing at lower than maximum height, and with a fore/aft location that brings the wing into more intimate interaction with the underbody diffuser’s exit. We’ll explore this phenomenon further in chapter 9, but there’s an important general point to be made here, and that is that a competition car’s aerodynamic package is not – or should not be – a disjointed collection of devices, but an integrated whole. This should be borne in mind as we necessarily work our way through the various devices in turn.

### **Alternative strategy for improving wing effectiveness**

Wing location clearly has important global effects on a car’s aerodynamic performance, as we have seen in the two foregoing wind tunnel examples, but sometimes technical regulations limit the possible alterations, for example

changing wing location or design. To explore another possible strategy, an exercise on a simple saloon/sedan model was carried out with CFD. A wing with a span of about 80% of the car's overall width was placed in a fairly typical stock location on the car, with the trailing edge directly above the rearmost part of the rear deck, and with the leading edge at about half the height of the rear screen. The wing was a modestly cambered single element device set at 4° relative to the horizontal. Figure 5-50 shows the streamlines (coloured by velocity) arriving at and departing from the wing, and the different angles at which the airflow encountered the wing across its span are evident. Notice too that something seemingly odd was going on in the centre of the wing's suction surface, and this becomes more evident in the close up, lower angle view in figure 5-51. It is evident that the flow was separating from the central part the wing's suction surface.

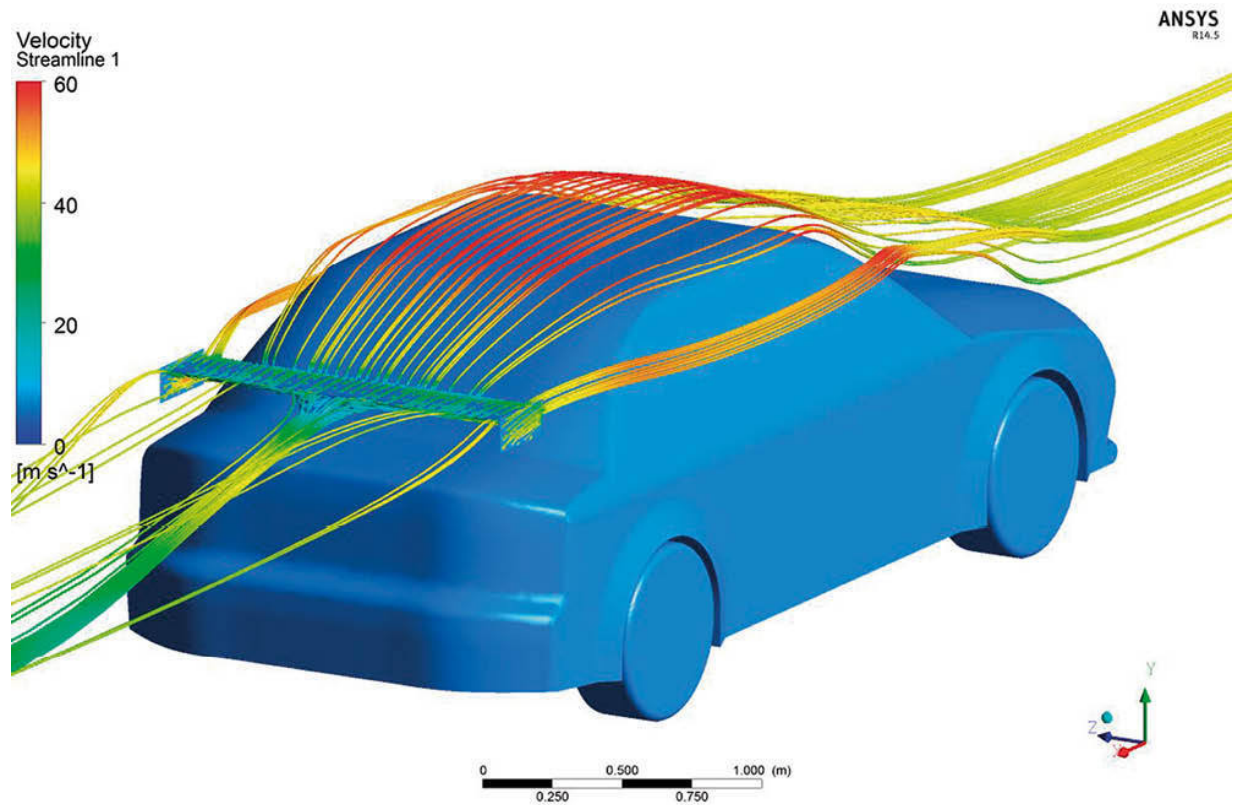


**Figure 5-50** Streamlines, coloured by velocity, arriving at and departing from the rear wing on a simple saloon/sedan model.

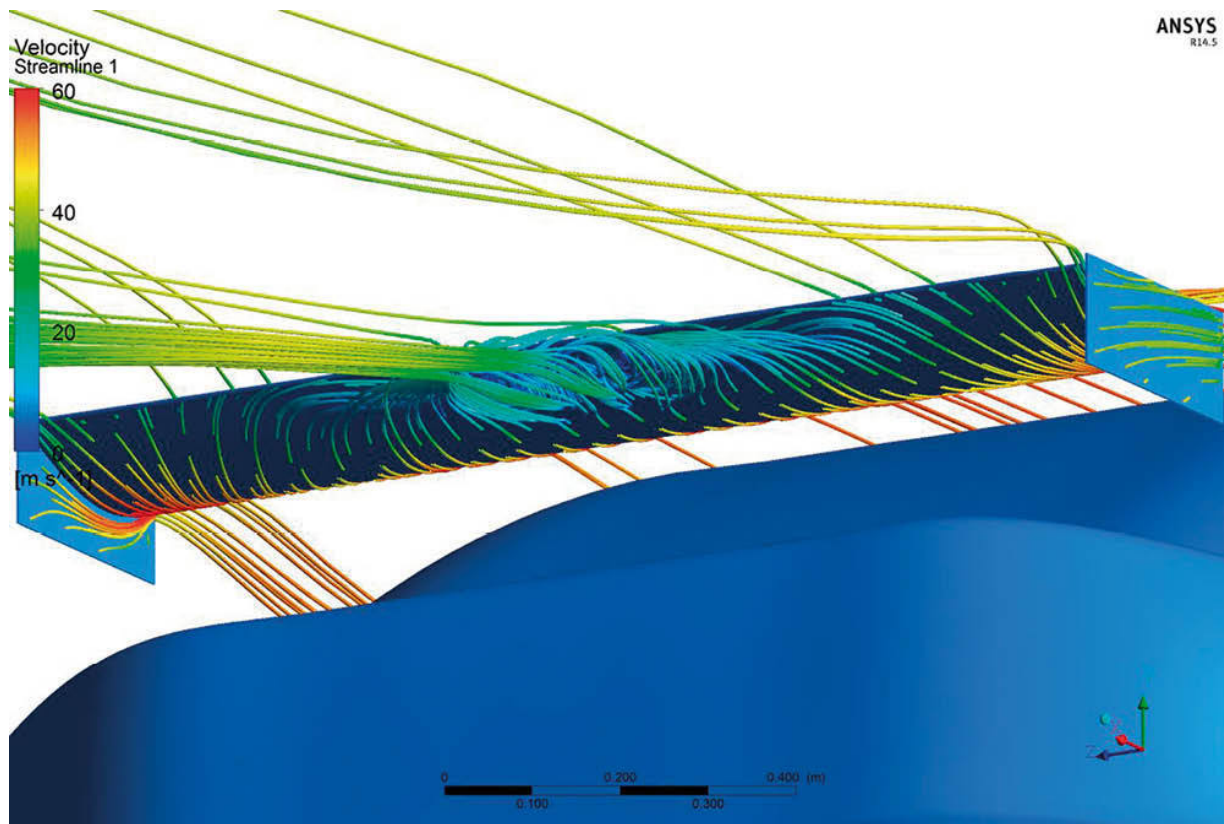


**Figure 5-51** From a lower viewpoint it is clear that there is flow separation in the centre of the wing.

There might be several ways of dealing with this, but if the wing cannot be moved or changed in design, perhaps another method could be employed? So a very simple spoiler was added to the rear lip of the trunk to attempt to help to turn the airflow under the centre of the wing, and it produced an interesting result. Figure 5-52 reveals that the flow separation visible in figure 5-51 had totally disappeared. And although the wing's downforce contribution was reduced compared to the initial test (possibly because of proximity to the spoiler), the spoiler added sufficient downforce of its own that this combination actually generated considerably more (rear) downforce. The idea is far from new, as the photo of the 2006 RJD Motorsport Nissan 350Z GT2 demonstrates, and it's easy to imagine that varying the spoiler's height and angle would be an effective (and cost-effective) means of specifically tuning the wing to the airflow on a given car.

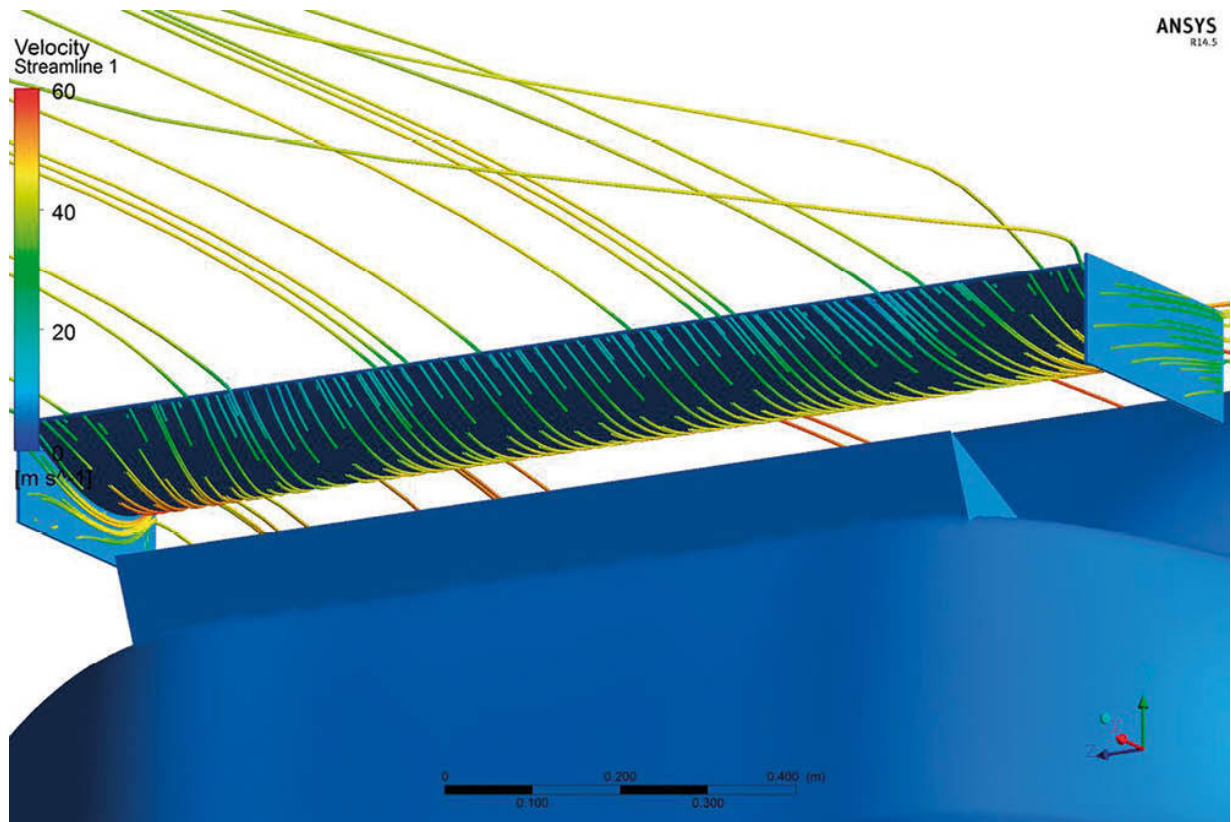


**Figure 5-52** The fitment of a simple rear spoiler re-attached the wing flows and also added overall downforce.



*This GT2 Nissan 350Z sported just such a rear spoiler, rear wing arrangement.*

## Chapter 6

# Underbody aerodynamics

IF WINGS ENABLED a step forward in competition car performance, then historically speaking the exploitation of underbody airflow to generate downforce facilitated the proverbial giant leap. It had long been realised that the airflow under a car was affected by the close proximity of the ground, but only the disadvantages seemed to be noticed at first, and effort was put into reducing the airflow beneath the car in order to reduce drag; early examples of this approach include the MG speed record attempt vehicles in the 1950s. However, during the heated debate on the wings of Formula 1 cars during 1968/69, when it looked likely that wings would be banned for evermore, BRM did some work on designing a car body that used its own ‘wetted’ surfaces to create downforce. Peter Wright, working under Tony Rudd, had been running some tests during 1969 in the wind tunnel at the Imperial College, London, and the results were sufficiently good for BRM to set about, very secretly, building a car to exploit the new found effects. Sadly perhaps, the legendary BRM politics intervened, and the car never reached a racetrack. Rudd and Wright departed, Wright to Specialised Mouldings, where he designed the very simple inverted wing-shaped sidepods for the March 701 F1 car, which, while using the inverted wing principle to create a modicum of downforce, were not really exploiting ground proximity.

Around this time that famous American racer/innovator, Texan Jim Hall, burst into the limelight again producing the latest variation on the Chaparral sports racer theme, the 2J. This had a supplementary motor, actually a snowmobile engine, powering two large fans that sucked away at the underbody region in order to reduce the pressure there. To maximise the effect, virtually the entire under car region was sealed by flexible Lexan plastic rubbing strips, so that the car became a hovercraft in reverse, so to speak. Estimates of the downforce that the car achieved vary from 1,300lb to 2,000lb (590kg to 910kg), substantial enough to make the rather heavy (2,000lb/910kg) car extremely competitive in the skilled hands of Vic Elford against the all-conquering McLarens in the CanAm series of 1970, although the unreliability

of the auxiliary engine kept the 2J from being consistently effective. The special thing about the fan car concept of course is that its downforce is not speed dependent – it can develop as much downforce at rest as it can at race speeds, so the Chaparral's starts and slow corner performance were said to be nothing short of devastating.

Almost immediately, the storm of protest over the fan car concept led to it being banned by the governing body, and to this day the ‘movable aerodynamic device’ rule has been used in many mainstream motorsport categories to prevent any such scheme from appearing again, or at least, to attempt to prevent similar ideas from reappearing – more of this shortly. The way forward from here was a little time in coming, and once more Peter Wright and Tony Rudd were intimately involved, by then at Team Lotus, in Norfolk, England, in 1975. Rudd had been given a list of crucial development issues to address by Colin Chapman, and since most were aerodynamic in nature, Peter Wright was brought in.

Wright and his team were again using quarter-scale models in the Imperial College wind tunnel, which was equipped with a ‘moving ground’ conveyor belt to simulate the car moving over the road. They noticed that the sidepods, designed to carry radiators and fuel, on the model were sagging, and producing inconsistent results. So, after wiring them up more securely, they also sealed the bottom edges of the sidepods with ‘skirts’, and started to get some unbelievable results! In fact, they repeated the tests several times to convince themselves of what was happening. Chapman wanted to know what would happen if the sidepods were shaped like inverted wings, whereupon Wright produced his photos of the never-raced 1969 BRM ‘wing car’, and in fairly short order, a new Lotus F1 car was drawn, a model made, and during the latter part of 1976, Mario Andretti tested, what was designated the Lotus Type 78. The car was immediately two seconds a lap faster than the admittedly tardy Type 77, and Andretti’s scarcely contained enthusiasm was picked up by sponsors John Player, who apparently insisted on the car being renamed the JPS Mark III. At the car’s glitzy press launch, the designers were sworn to say only that they had found ‘something for nothing’, a reference to the substantial gain in downforce for little or no drag penalty, and thus was made the biggest single leap in race car performance – ever.

The Lotus 78 won races during 1977, but Wright and the R&D team spent all year perfecting a reliable sliding ‘skirt’, which sealed the underbody from unwanted sideways migration of air into the low static pressure region, the function of the skirt being crucial to the underbody’s effectiveness. The lessons from the 78 were carried over to the superb Type 79, which was

effectively the first no-compromise ground effect car, and this proceeded to dominate the World Championships for drivers *and* constructors during 1978. However, there was one small hiccup for Lotus that year – the Brabham ‘fan car’. Earlier attempts at regulating against the use of fans to create suction beneath the car had reckoned without the ingenuity of Gordon Murray, then Brabham’s chief designer. His current charge, the Alfa Romeo flat 12 powered BT46 needed a new cooling system to replace the unsuccessful surface cooling concept tried in early 1978. Murray decided on a large air/water heat exchanger mounted above the engine, fed by cool air from a large fan – which happened to draw its air supply from the Brabham’s underbody area. The car just happened to have two transverse and two longitudinal skirts sealing the underbody region, so that the fan sucked the car down onto the road surface very firmly indeed. The car won its first race in Sweden, with Niki Lauda at the helm, but the protests from the other teams led the governing body to ban any further use of fans for creating downforce. They allowed the win to stand, however, perhaps by way of apology for giving the idea tacit approval at the concept stage! There are still some sporting categories where fan-induced downforce has not been banned, but most formulas and classes no longer allow this kind of downforce generation.

However, the development of ground effect ‘tunnels’, as profiled underbody channels became known, continued, despite various attempts by the regulators to contain the incredible cornering speeds that resulted. Major single-seater and sports racing categories all around the world were affected at all levels of motorsport. Come 1982/83, the FISA had had enough, and banned profiled undersides in F1 (and subsequently other categories), and the next phase of development was concentrated on the ‘flat floors’. In The States, the then IndyCar World Series, among others, continued with tunnels, although year by year their effect was mollified by dimensional changes in order to contain cornering speeds. Tunnels also came and went in top-level sports racing categories, and that is pretty much how things stand today – most racing categories insist on a ‘flat floor’, although there are some that still allow tunnels. However, even where flat floors have to be used, there is still a degree of freedom with respect to underbody shape ahead of the front wheels, and behind the rear wheels, and as we shall see, this is significant.

The rather lengthy, if incomplete historical prelude to this chapter is quite deliberate, because there is no question that the development of underbody aerodynamics has been the most significant as far as downforce production and performance gains are concerned. Once the Lotus 78 paved the way, *all* competition car categories had to at least look at the concept to see if there

was benefit to be gained, and although many formulas now severely restrict design freedom in this area, the exploitation of ‘ground effect’ is not going to go away as long as competition cars run in close proximity to the ground.

## Back to basics

All cars, by definition, operate in ‘ground effect’. This means that there *will be* interference with the airflow underneath the car arising from the proximity of the car and the ground. This has a large bearing on the overall behaviour of the airflow over, under and around a car, and as such, the influence on performance can be considerable. Interestingly though, the effects may be beneficial or adverse, depending on the exact nature and design of a car. We saw in Chapter 5 that the downforce produced by a front wing in ground effect was greater than that produced by the same wing in freestream air, and the effect increased the closer to the ground the wing was moved, until at a certain close distance reductions in downforce occurred again. Similarly, keeping attached flow is central to the ability of the underbody airflow to produce downforce.

A typical passenger car has a very rough underside, with such items as the exhaust system, suspension, transmission, drive train and fuel tank all protruding into the underside region, and cavities such as those around the engine and transmission and wheel wells adding to the ‘roughness’. Chapter 4 discussed how this roughness contributes to drag; this type of underside creates a thick boundary layer, which tends to haul the air below the car along with it. Thus, the boundary layer will extend right to the ground, and at the rear of the vehicle, it merges with the wake, which now will also reach the ground (look at Figure 4-21 again). The flow along the underside is generally slow and turbulent, if not blocked off completely by this interference, and although total pressure, and thus static pressure *may be* low, it would be far better to have a fast flow through the underbody region and so produce much lower static pressure without losses. This way there is a chance of reducing, cancelling or hopefully reversing the usual positive lift that a passenger car creates.

There are three main factors here to be considered for a given car: the ground clearance; the underside ‘roughness’; and the shape of the underside. The impact that each of these factors has is related to each of the others. For example, if a car has a very rough underside, then one method of decreasing the positive lift that it produces will be to actually *increase* its ground clearance. Conversely, reducing the ground clearance in an effort to lower a car’s centre of gravity for competition use, a basic and essential aim to improve cornering

and handling, may actually make the positive lift worse if the car's underside is rough. As we saw in Chapter 4, blocking off some of the airflow from going under the car is one way to improve this situation, but the general message is that rough undersides are not good! In fact, it is pretty self-evident that fitting a smooth under panel is bound to enable the air to move faster along the underside, and it is equally obvious that drag will be reduced as well if the lumps and bumps can no longer interfere with the smooth passage of the air under the car.

The shape of the underside has a marked influence on the under car airflow too. If static pressure under the car is positive, which may still be the case even with a smooth undertray, then the airflow can be improved by shaping the undertray. If some lateral curvature is incorporated, involving the rounding of the sill areas, then any high pressure air under the car will be encouraged to bleed out sideways into the faster, unobstructed flow passing down the sides of the car, which will help to relieve the high static pressure under the car. This would be a rather unimaginative remedy however, treating the symptom but not curing the cause of the problem. It would be far better to create a low static pressure region under the car.

So how do we create low static pressure beneath a competition car? It becomes necessary to start thinking in terms of longitudinal shaping of the underside to create a form of venturi system. By making the gap between the ground and a car like a venturi tube, where the ground is one side of the tube and the car undertray is the other side, we can cause the air to accelerate under the car to decrease the static pressure there. A small drop in pressure can add up to a large force because of the large plan area available (a one percent reduction in ambient pressure is equivalent to approximately  $1000\text{N/m}^2$ , roughly  $100\text{kg/m}^2$  or  $21.2\text{lb/ft}^2$ ).

As in a venturi tube, it is necessary first to channel the airflow into a narrowing section so that, in accordance with the Conservation of Mass, its velocity increases through the narrow 'throat'. This creates the low static pressure that generates our downforce, and then it is necessary to slow the flow back down to ambient again, but in a gradual, controlled way that doesn't cause flow separation. The venturi system uses a diffuser to fulfil this role. Raising the rear section of a competition car's undertray forms a diffuser. It can now be seen that the primary function of the diffuser is not to create downforce, as many people believe. It is in fact the essential final part of a venturi system, and its main job is actually to allow the velocity to slow down again (by virtue of the increasing cross-sectional area, the principle of Conservation of Mass still applying), to recover the kinetic energy as efficiently

as possible (that is, hopefully without flow separation occurring). This allows the static pressure to rise back up to ambient again so that the airflow exits the venturi as close to freestream pressure and velocity as possible. Having said that, the static pressure in the diffuser, on average, is lower than ambient so as a secondary effect, some downforce will be generated here.

Another misconception is that ‘a diffuser expands the air to produce low pressure’ but this is not the case. That mechanism would require the air’s density to change, which a diffuser in an open, unsealed system like this cannot bring about.

Another important issue relating to diffusers is boundary layer development along the underside of a car. As with any of the surfaces over which the air is flowing, the boundary layer along the underside thickens towards the rear. This reduces the effective angle of a diffuser, and is something to be borne in mind when we look at this particular aspect shortly.

It will be apparent that air will try to leak in from the sides into a low static pressure region under a car, and skirts were devices that acted like wing end plates to try to prevent this, and maintain the lowest static pressure possible. Now with skirts banned in most categories it is not possible to attain such low static pressures under a competition car. However, various clever ‘tricks’ have been employed that attempt to do the same job as a skirt and we will pick up on a few of those along the way.

The next questions obviously centre on the precise shaping required. How much do we need to contract the area through which the air will flow? What ground clearance should we run? What shape and angle should the diffuser be? We can draw on some of the reference books and also on some more CFD trials to gain some insights, although the hard fact is that, as with any aerodynamic topic we might choose to examine, every case is different and requires optimisation to get it right. However, if we treat the information we can draw on here as guidance then hopefully we can at least head in the right design and development directions.

The general aim of a venturi style underbody then is first to reduce the cross-sectional area into the throat region to accelerate the airflow; then we have to decide how long to make the throat to maintain that fast, low static pressure airflow. We then have to decide on how to expand the cross-sectional area again, all within the physical constraints of the car and, of course, the dimensional constraints of the rules. This design effort may relate to the entire plan area of the car or, say in the case of a single-seater, it may be that only the sidepod underbody regions can be venturi shaped. Either way, the general principles will be the same.

## Ground clearance

The shape of the car and its ground clearance will govern the effective contraction of cross-sectional area. Clearly, unless some form of airdam totally seals the gap between the front of the car and the ground, and providing it has a clear passage downstream, air will converge into the car-to-ground gap at the front and it will accelerate. The precise ground clearance that a car should run at in order to create beneficial ground effect conditions is specific to any one vehicle and it is difficult to generalise. It will be evident however, that a smaller ground clearance will, in theory and up to a point, cause more airflow convergence, hence more airflow acceleration and hence a faster flow under the car. But cast your mind back to the section on front wings operating in ground effect in the previous chapter, and in particular the topic of ground clearance sensitivity. Not surprisingly, this is an issue that effects car underbodies as well as wings near the ground, and it needs to be borne in mind in this context too, as we shall see...

If we look at some figures based on experiments done on road vehicles of average underbody roughness we can perhaps start to get a feel for things here. Scibor-Rylski (see Appendix 2) tells us that at ground clearances of between 0.125 and 0.600 times the wheelbase, ‘conventional’ cars produced negative lift coefficients, as the ‘venturi effect’ assisted the underbody flow, but at ground clearances of less than 0.125 times the wheelbase, the lift coefficients became decidedly positive. Consider that an average ground clearance-to-wheelbase ratio will be of the order of 0.05, and we again can see why conventional cars with rough undersides can often be operating in a highly unsatisfactory positive lift regime. The conclusion to be drawn once again is that it is imperative at the very least to fit a smooth undertray if *positive* under-car static pressure is to be avoided.

Clearly, if common practice is anything to go by, competition cars are able to run close to the ground without generating the positive pressure that the conventional, rough underbodied vehicles referred to above apparently developed. A further reference, Katz (see Appendix 5) gives some hope here, and suggests that a  $1/5$ -scale model with a smooth underbody produced a minimum lift coefficient at 1.38in (35mm) ground clearance, which corresponds to 6.9in (175mm) at full scale (if we ignore Reynolds Number differences). However, the tests that gave this result were measured in a wind tunnel with a fixed floor that would have developed its own boundary layer, and it is likely that the result over a moving floor wind tunnel would have shown the minimum CL to have occurred at a smaller ground clearance than this. But this is getting nearer the order of ground clearance that might be seen

on competition cars, which is useful, and means we can start to think about the *benefits* of running close to the ground, rather than any possible disadvantages.

During the early 1990s, extremely small ground clearances were in common use in some of the FIA's single-seater categories, Formula 1 included. Gut feel suggests that the ground clearances were impossibly small to allow significant, smooth, fast flow along the underbody, and this seems to have been the case. The extremely low ground clearance was more about maximising mechanical grip by lowering the centre of gravity. At speeds where downforce mattered though there was a 'working gap' through which air could flow. Remember too that the underbody and diffuser solutions in these categories were derived in the large majority of cases from wind tunnel development in moving ground test facilities (and later with the help of CFD), where the criticality of running so close to the ground could be evaluated under carefully controlled conditions. Thus, the designers were able to optimise their cars at very low ground clearances to generate high downforce. The obvious risk here was that the cars were very sensitive to tiny changes of ground clearance or 'pitch angle' (nose-down attitude), which could lead to rapid and apparently inconsistent changes in downforce levels – not good for driver confidence!

So let's look at a CFD model that explored the effects of changing the ground clearance of an idealised competition car venturi system. Although just a two-dimensional study, this trial also compared the theoretical levels of downforce calculated by Bernoulli's Equation with those calculated by the CFD model taking viscous effects into account. The model used here was a 2m long section representing a very much simplified and isolated sidepod underbody profile. The downforce values relate to a nominal underbody width and should not be taken as anything other than indicative of trends.

As we have seen, air is accelerated into the throat of a venturi by being channelled into a reducing cross-sectional area. The 'area ratio', that is, the ratio of the inlet area to the throat area, tells us by how much the velocity will increase, since velocity varies inversely with the area (simplistically, if you halve the area you should double the velocity). Clearly, the cross-sectional area of the throat of a profiled underbody close to the ground depends very much on ground clearance, and the area ratio will increase more rapidly with ever-decreasing ground clearance. Thus, using Bernoulli-based calculations we might expect to see downforce predicted to rise rapidly with decreasing ground clearance, and the relevant line in the graph in Figure 6-1 confirms this, with a classic inverse relationship curve.

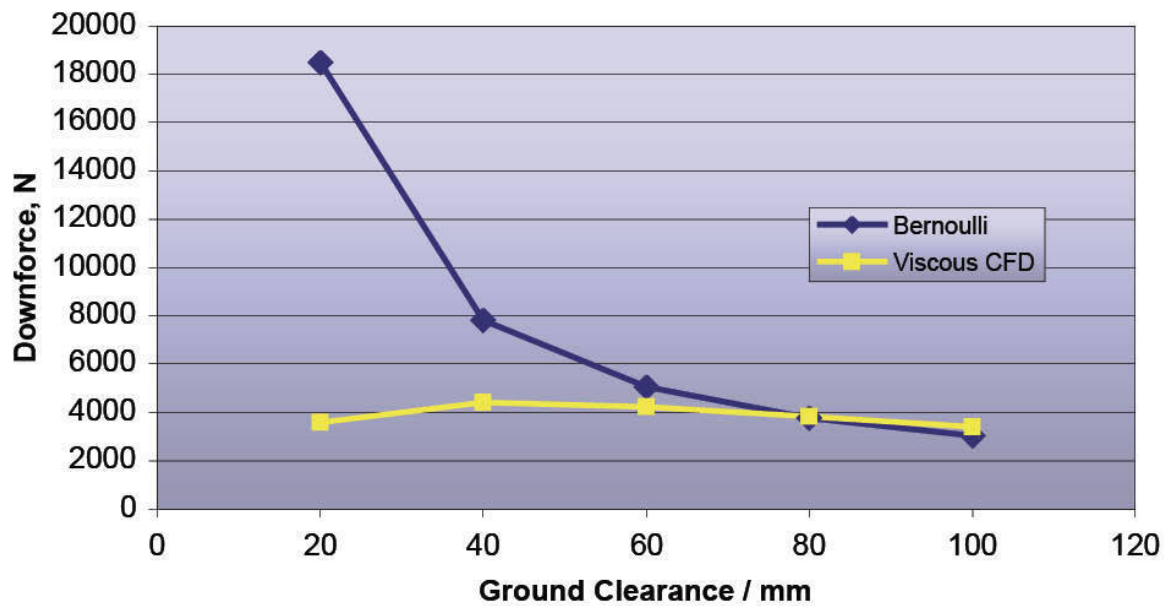


**Figure 6-1** Underbody downforce versus ground clearance, calculated via Bernoulli and viscous CFD for our simple model.

The results predicted by viscous CFD are also plotted on this graph, and the picture is obviously very different in this case, most significantly at the smaller ground clearances. At the larger ground clearance end of the scale, where the volume of air affected by the viscous effects of the underbody surfaces is small relative to the overall airflow, the Bernoulli predictions and CFD predictions are actually very close. However, at ground clearances of around 70mm or less, the viscous effects are becoming ever more significant. By 20mm the air is being asked to flow through such a small gap that the viscous effects are dominant, reducing the downforce by about 80% relative to the figure predicted by Bernoulli, and the downforce attains its maximum at 40mm ground clearance with this model. (In case you're wondering, the reason that the viscous CFD downforce value is slightly higher than the Bernoulli value at 100mm ground clearance is because of necessary slight variations in the models, which meant that a defined radius was required on the inlet of the CFD model and so its effective inlet size was slightly bigger. Elsewhere, viscous effects masked this difference.)

Figure 6-2 shows plots of static pressure coefficients in the underbody at three of the ground clearances tested using viscous CFD (the black silhouettes show the sidepod profile used here, which had inlet and diffuser angles fixed

respectively at  $10^\circ$  and  $5^\circ$ , topics we'll examine separately in later sections of this chapter). Looking first at the 100mm case the pressure plot shows an evenly distributed, moderately low static pressure along the venturi throat (flat section). At 40mm ground clearance significantly lower static pressure is attained in the throat, and this gap achieves the highest overall downforce figure. In the case of the 20mm ground clearance model the flow steadily accelerates through the throat, attaining similarly low static pressure to the 40mm case only at the rear of the throat. It appears that 'viscous blockage' at this low ground clearance makes its effect felt right at the start of this downforce inducing device with a 20mm gap.

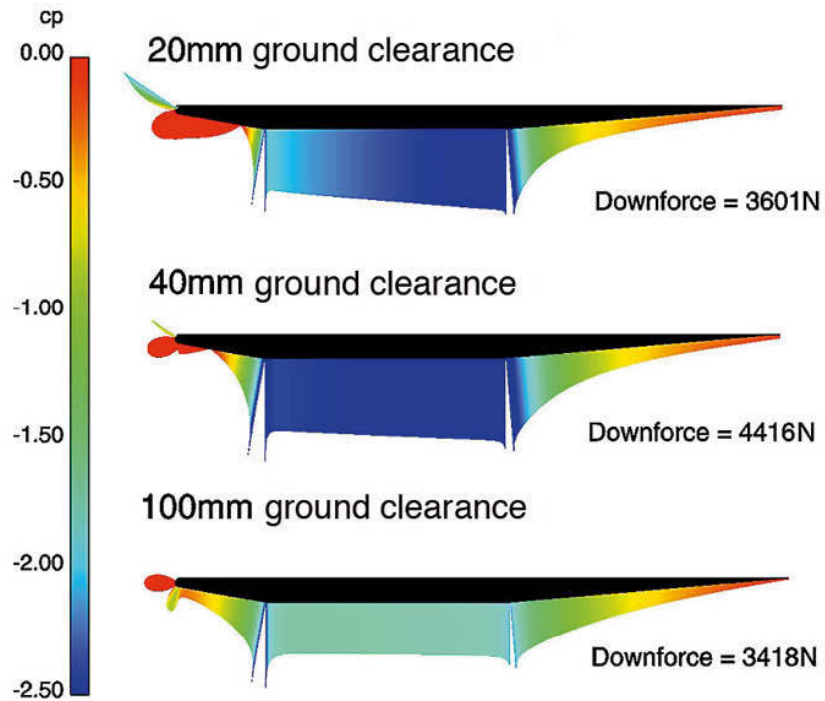


**Figure 6-2** Static pressures in the model underbodies at three different ground clearances.

There is another interesting effect of reducing ground clearance, and it is analogous to something we saw in the case of a front wing in ground effect. Just as the area ratio becomes more extreme at the inlet as ground clearance is reduced, so it does at the diffuser end of the venturi. The diffuser is a region of adverse pressure gradient anyway (the flow is trying to go from a low to a high pressure region – which we know it will only do if asked very nicely!), and the consequence of working the airflow too hard in the throat at just 20mm

ground clearance is that this gradient is now too steep, and flow separation occurs. This can be seen in the velocity streamline diagram in Figure 6-3, where at 20mm ground clearance a distinct recirculation region where the flow has separated can be seen adjacent to the diffuser roof. Taking all these effects into account, the result at 20mm ground clearance is a downforce figure some 18.5% lower than that achieved at 40mm. Figure 6-4 shows the flow separation to be much smaller, and the general airflow velocity to be much higher at 40mm. At ground clearances above this there is no separation apparent.

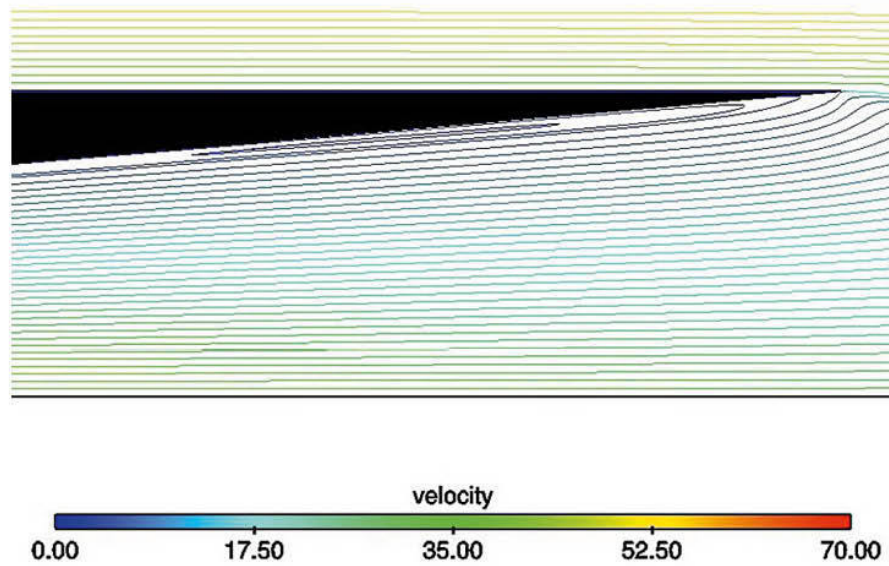


**Figure 6-3** Flow separation and generally low velocity in the diffuser at 20mm ground clearance.

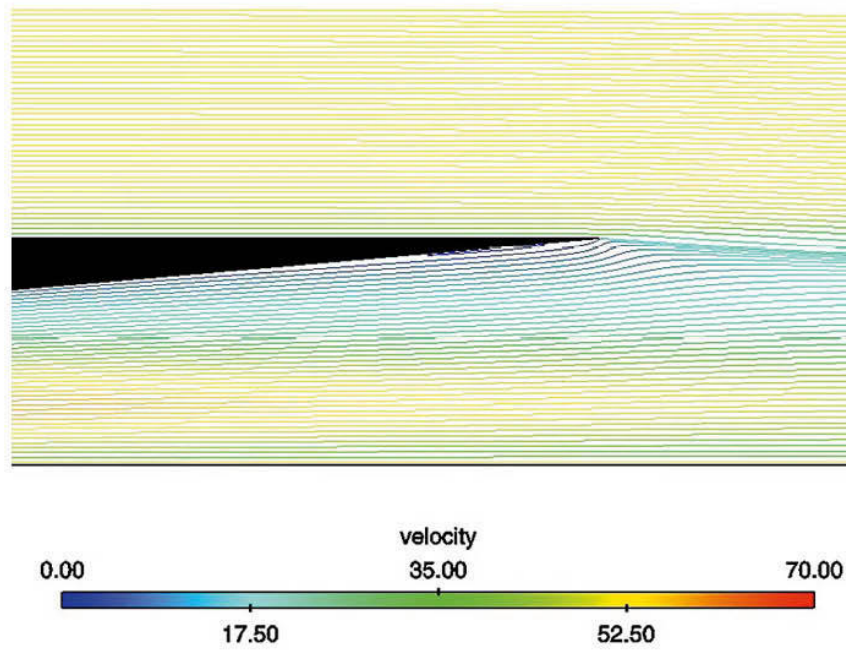


**Figure 6-4** At 40mm ground clearance flow separation is much reduced and velocity generally higher.

So, while initially a decreasing ground clearance does produce the expected increase in underbody downforce, too small a gap leads to a reduction in downforce because of viscous effects. A further note of caution though; because this model was run in 2D, and because it modelled a very simple sidepod in glorious isolation from other parts of a competition car, it would be very unwise to use these ground clearance values literally. The general aim would appear to be to run the smallest ground clearance possible that maintains ‘unblocked’ flow and no diffuser separation. In the case of our sidepod model here, optimum downforce occurred at 40mm ground clearance, but fully attached flow with only a 4.3% loss of downforce occurred at 60mm, which might suggest a suitable operating range – for this model at least.

Before we move on to tweaking other underbody parameters it is worth just stopping to look at what else these visualisations can tell us about the low static pressure region in a profiled underbody. Referring to Figure 6-2 again, it is apparent that the lowest pressures are formed in the throat, and also that as ground clearance is reduced the lowest pressure zone shifts rearwards somewhat. This is likely to be rather important in relation to the aerodynamic

balance of the car, especially if there was significant compression of the car's suspension due to aerodynamic loading – there would be a relative increase in rear grip compared to the front as speed increases, possibly enough to shift the handling balance towards (increased) understeer at high speeds, which may or may not be deemed desirable.

The sharp static pressure 'peaks' at the junctions of the inlet and throat, and the throat and diffuser, are caused by the rapid acceleration of the airflow around these sharp corners. It is interesting, in fact, that the airflow does not appear to separate at the sharp transition into the diffuser, when gut feel says sharp changes of direction should be avoided. In circumstances where the underbody is being worked much harder however it may be that separation could be triggered here.

### **Diffuser angle**

Using the same Bernoulli-based and CFD-based models as above, the effects of modifying the angle of the diffuser can be examined. The maximum height of the diffuser remains fixed so that changes to its angle have the effect of changing the diffuser length. In some racing categories technical regulations often define diffuser start points and lengths, but there is some flexibility, to a greater or lesser degree, in other categories.

Figure 6-5 illustrates the static pressure distributions along the underbody, calculated according to Bernoulli's Equation, at the extremes of the diffuser angle range studied here,  $3^\circ$  and  $11^\circ$ . It is clear that this model predicts that low pressure would persist for longer where the venturi throat, the flat underbody section, is longer. Thus, more underbody area is maintained at low pressure with the shorter, steeper diffusers, and that produces a greater theoretical downforce value. Figure 6-6 plots all the diffuser angles versus the Bernoulli-calculated downforce values (the blue line) and shows downforce increasing with increasing diffuser angle in this model. The gains tail off because the lengthening of the venturi throat is not linear with changing angle.

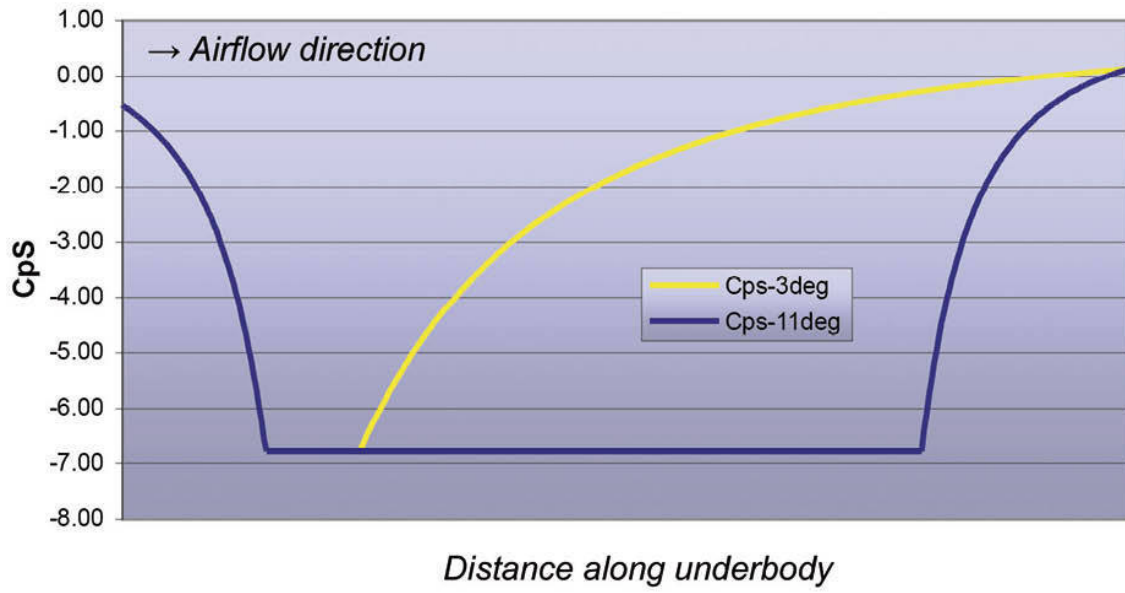


**Figure 6-5** Static pressure distributions at two diffuser angles, calculated via Bernoulli for our simple model.

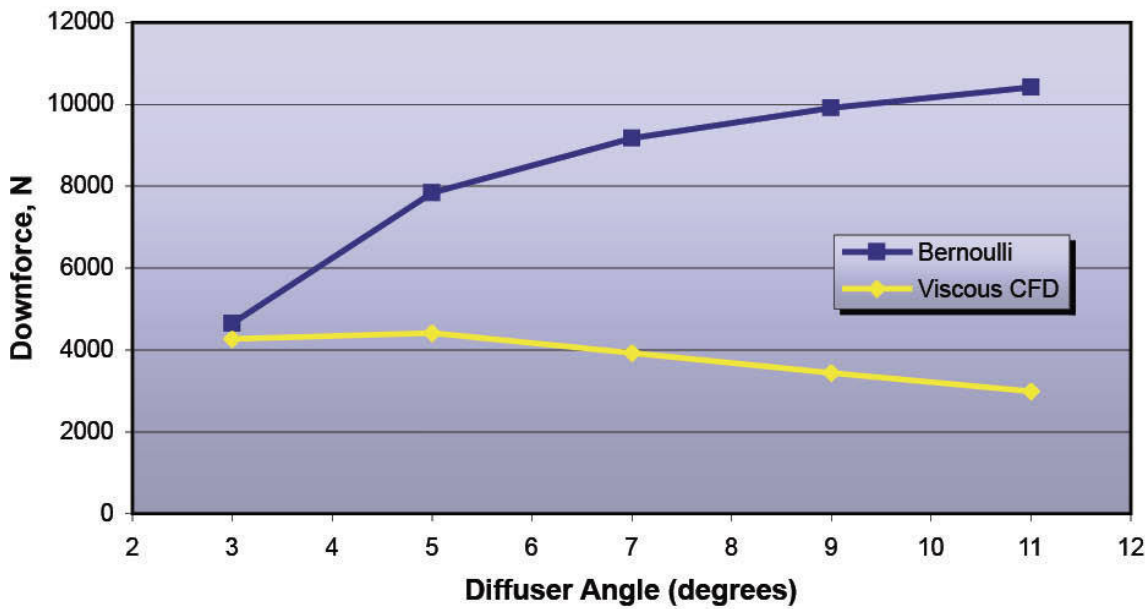


**Figure 6-6** Underbody downforce versus diffuser angle, calculated via Bernoulli and viscous CFD for our simple model.

However, when viscous computational fluid dynamics was applied the story was rather different, as Figure 6-6 shows (the yellow line). If the diffuser angle

is too steep, the pressure gradient becomes too ‘steep’ and flow separation results. Thus, downforce in our simple model tops out at just  $5^\circ$ .

Figure 6-7 shows how substantial the flow separation in our particular model is at  $11^\circ$ , and how the region of high velocity flow in the diffuser is greatly reduced when this much separation has occurred. Figure 6-8 goes further, and shows the magnitudes and static pressure distributions along each of three of our underbody configurations. It can be seen that the static pressure differential between the inlet and throat, which is what drives the flow through the underbody, is markedly reduced in the  $11^\circ$  case because of the separation in the diffuser. This separation has caused a reduction in mass flow through the throat, which in turn reduces the velocity increase in the throat and so the pressure reduction is much smaller in magnitude, leading to less downforce generation.

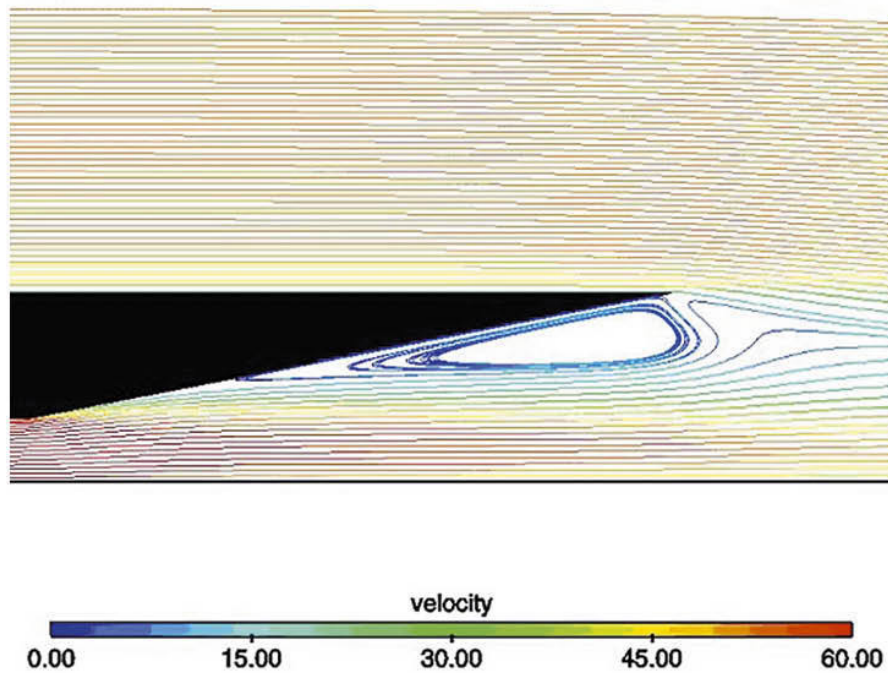


**Figure 6-7** Substantial flow separation at  $11^\circ$ .

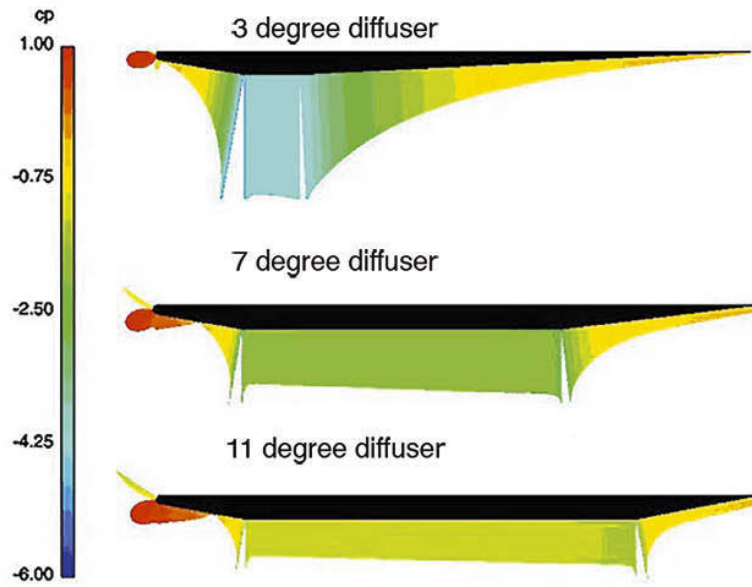


**Figure 6-8** Static pressures in the model underbodies at three different diffuser angles.

So the trick to maximising downforce appeared to be to have the longest throat section with the shortest, and therefore steepest possible diffuser that maintains attached flow. Again, this 2D CFD study does not take into account 3D flow effects, such as the sideways leakage of air into the low-pressure region that would occur in the real world, and which actually permit steeper diffuser angles without separation. Components like wheels and underbody protrusions all serve to complicate the problem, as could the presence of a rear spoiler or wing, which might beneficially interact by reducing or delaying separation in steeper diffusers. And importantly, this simple model did not generate a low ‘base’ pressure, such as is found in the wake of so-called ‘bluff bodies’ like competition cars, which plays a significant role.

### Inlet angle

Having seen the results of the previous sections, applying Bernoulli physics to changes in underbody inlet angle we might expect that the shortest possible inlet, which provides the longest possible throat in which the lowest static pressure will occur, will generate the maximum downforce. The gains would tail off as increasing the inlet’s angle makes less and less difference to its length. Figure 6-9 shows that this is the case, and downforce, calculated by Bernoulli’s Equation, has virtually peaked at 20° inlet angle.

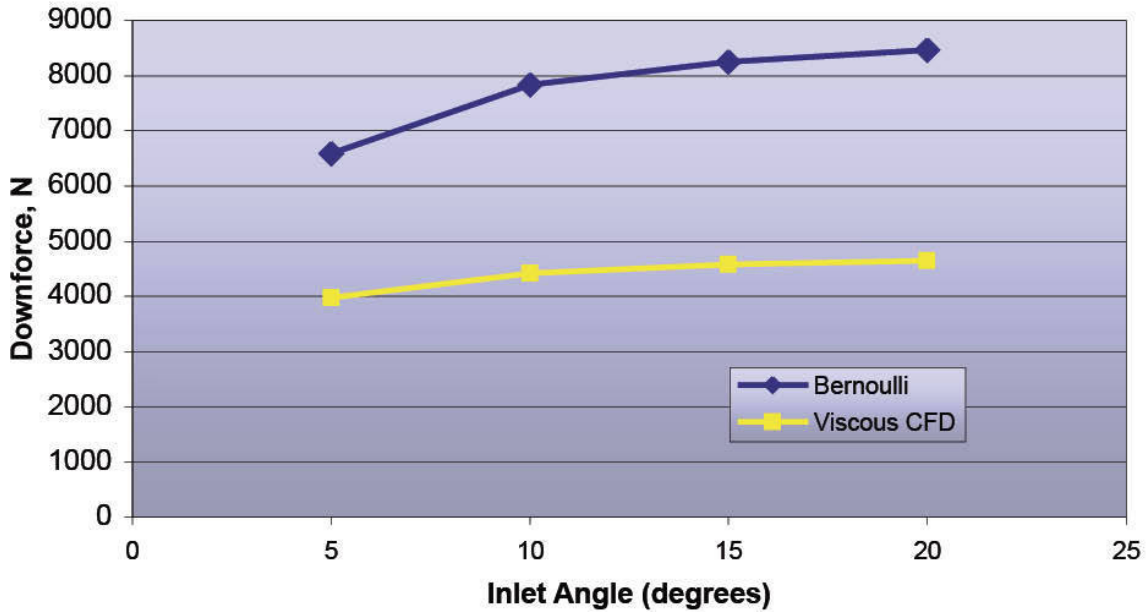


**Figure 6-9** Underbody downforce versus inlet angle, calculated via Bernoulli and viscous CFD for our simple model.

Taking viscous effects into account once more changes things however. Figure 6-9 also shows the downforce calculations from a viscous 2D CFD simulation on this model again. Interestingly, the relationship between downforce and inlet angle is similar to that calculated by Bernoulli's Equation, except that the values are much lower. Viscous effects have reduced the airflow's velocity, which means the static pressure reductions along the whole underbody are not as great, which in turn means downforce is less.

Over the range of inlet angles tested here, the underbody does seem to behave generally as Bernoulli might have expected even when viscous effects are applied, insofar as downforce increases with inlet angle. Figure 6-10 shows a plot of static pressure coefficient at the two extremes of inlet angle tested. It is evident that the static pressure decreases more rapidly with the steeper inlet and although, significantly, the minimum static pressure is not quite as low as in the shallow case, the low pressure region is indeed longer because the throat is longer, which explains the greater downforce.

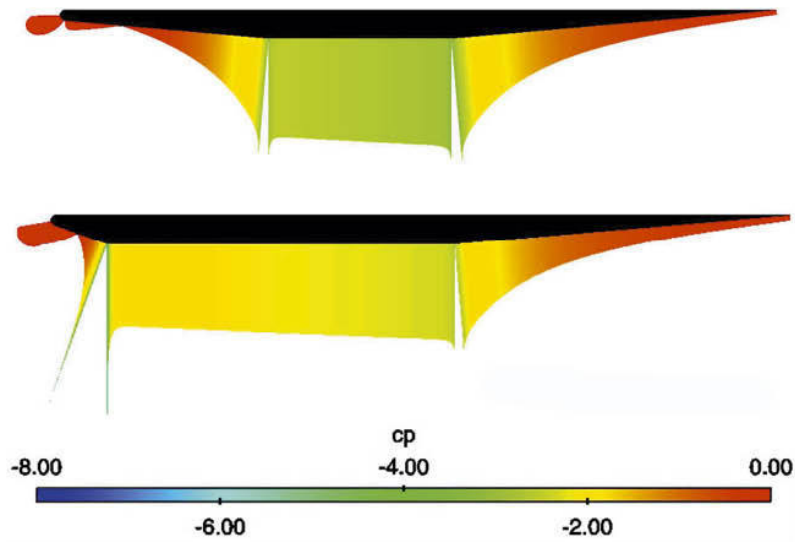


**Figure 6-10** Static pressures in the model underbodies at the shallowest and steepest inlet angles tested.

An additional significant point is that the aerodynamic centre may be further forwards at steeper inlet angles because of the aforementioned earlier (more forward) drop in static pressure, and because the flat throat extends further forwards at steeper angles. This could again have an effect on the balance of a car at ‘aero speeds’.

Downforce appears to have almost flattened out at  $20^\circ$  inlet angle, and there are reasons to think, with this model at least, that this might be the maximum angle worth running. It was pointed out above that with the  $20^\circ$  inlet the static pressure in the throat did not get as low as in the  $5^\circ$  case. Why should this be? Because viscous effects are again at work.

It is the vehicle’s passage through the air that promotes the acceleration of air through our venturi, but it is viscous effects that transfer that acceleration to the air that is not immediately adjacent to the vehicle surface. With a  $5^\circ$  inlet angle the acceleration of the airflow through the inlet is very gradual, and viscous forces are sufficient to pull the air nearer the ground along at a very similar acceleration to the air near the underbody.

However, at the  $20^\circ$  inlet angle, the air is accelerating so rapidly adjacent to the underbody surface that it seems that the viscous forces are not large enough to accelerate the air nearer to the ground at the same rate. The result is

as shown in Figure 6-11, which shows the vertical velocity profiles in the venturi at the inlet-throat transition. The velocity profile at  $5^\circ$  inlet angle is almost linear through most of this vertical section, but in the  $20^\circ$  case the more rapid flow at the underbody surface is evident, as is the lag in velocity through most of the rest of the section. Thus the velocity through the whole of the throat becomes lower, as Figure 6-12 shows, and the ensuing static pressure reduction along the whole throat becomes correspondingly lower in magnitude at steeper inlet angles.

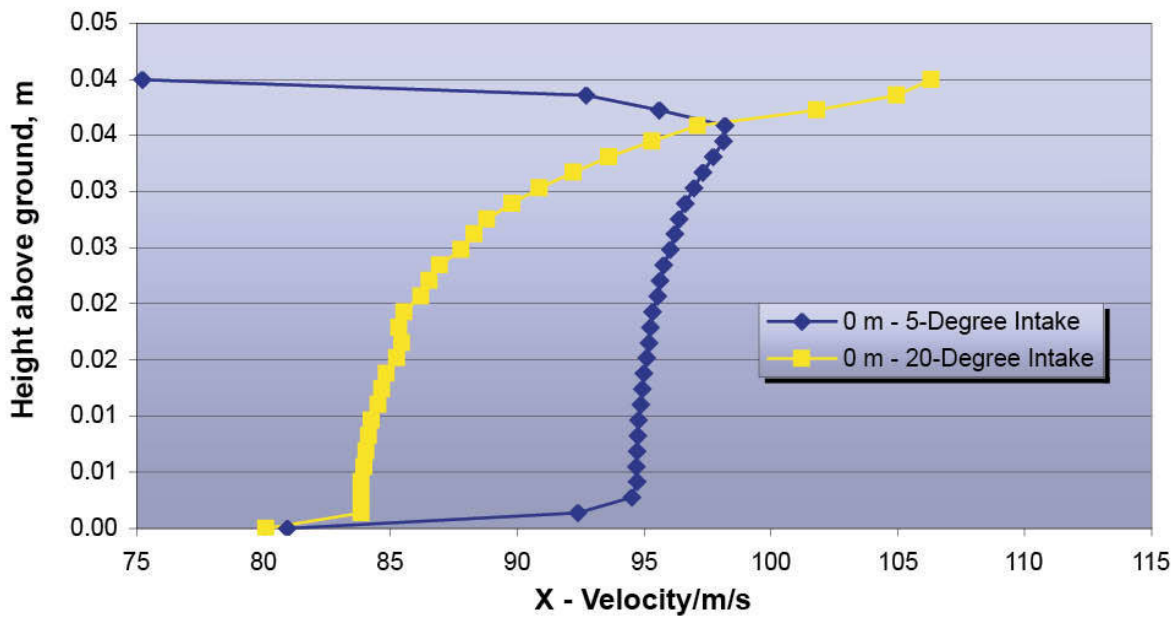


**Figure 6-11** The vertical velocity profile at the start of the underbody throat.

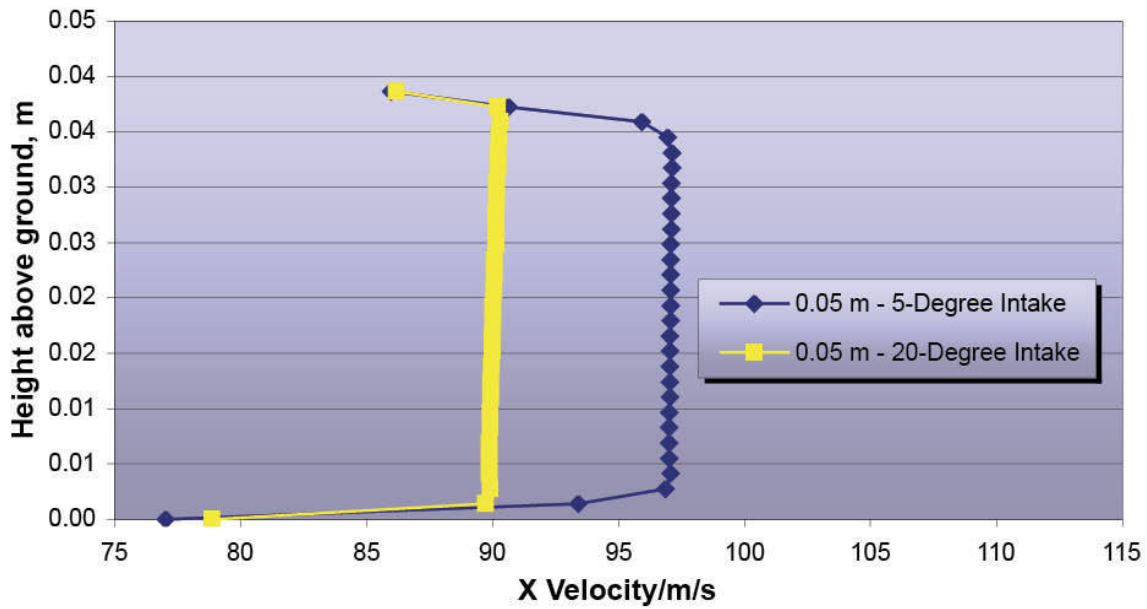


**Figure 6-12** The vertical velocity profile 50mm into the underbody throat.

So, as with the diffuser, to maximise underbody downforce run the shortest, steepest inlet possible, but only up to a point. In the case of the 2m long sidepod underbody model used here that maximum angle would appear to be 20°, although this should not be taken literally as an applicable generalisation.

These three simple CFD studies illustrate that the shape of a venturi underbody, combined with its ground clearance, define how much downforce can be generated. It will be pretty clear that as we are trying to maintain a constant mass flow of air through the venturi system that we need to try to match the effective inlet and diffuser areas. This is never going to be easy, especially given that air also enters the venturi system from the sides as the low static pressure in the throat and forward parts of the diffuser actually suck in more air from the sides. Nevertheless, through computational or track-based tests, making the underbody work effectively will probably focus on optimising details to ensure rapid flow from the inlet, through the throat and minimal separation in the diffuser.

It will be apparent that these parameters also govern where the downforce is concentrated, and it is the job of the aerodynamicists to juggle the distribution of downforce to match what the vehicle dynamicists require while trying to maximise aerodynamic grip, efficiency and consistency. We'll return to look at other aspects, this time in 3D, at the end of this chapter.

## Flat floors

Not all categories permit profiled underbodies. Some allow diffusers and radiusued inlets with flat floors in between, such as most of the FIA-regulated categories including Formula 1 at the time of writing. Others allow strictly controlled profiled underbodies. But in some categories you're not allowed to put any shape into the floor. Nevertheless, it is still important to try to exploit this situation to achieve any possible aerodynamic gain, and just as important to avoid the potential for adverse interactions.

As was mentioned briefly at the start of this chapter, one of the basic things to do is to ensure the underbody is smooth, and a quick glance at another CFD study on the NASCAR model we saw earlier shows how the removal of some of the underbody clutter helped matters. Figure 6-13 shows the two configurations tested here, with pipework and chassis tubes ‘removed’ in the latter case. Obviously the practical solution to smoothing out this underbody, if the regulations permitted it, would be to panel in the clutter as far as possible, but this theoretical exercise helps illustrate the type of gains to be found.

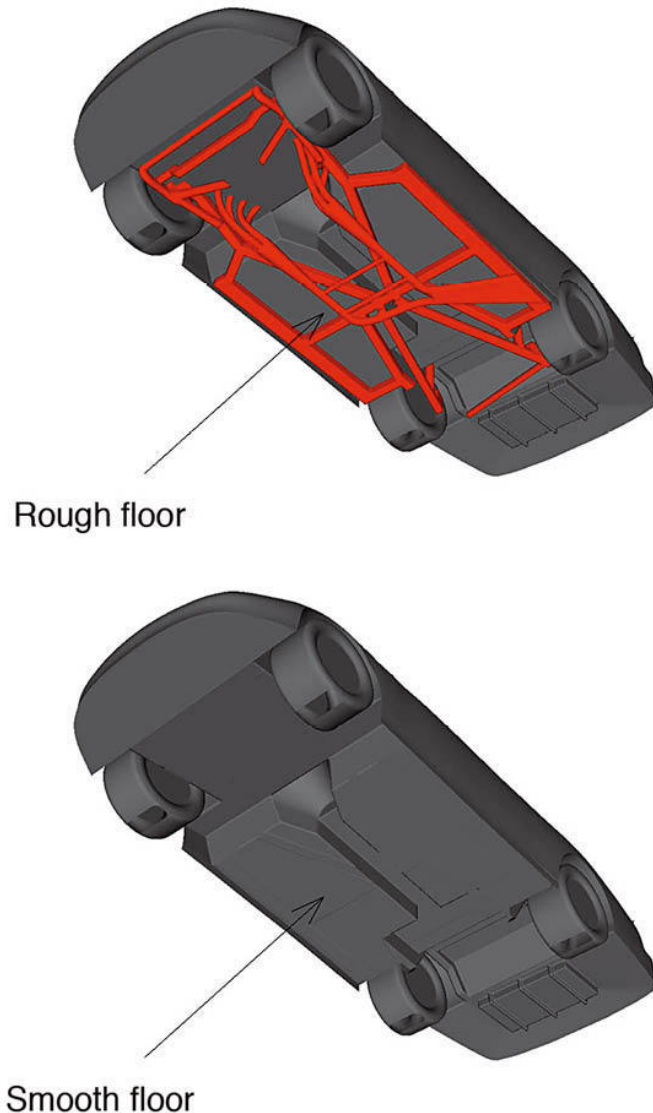


**Figure 6-13** 'Rough' and 'smooth' underbody configurations.

Moving on to Figure 6-14 it is very evident that the static pressures have changed, and lower static pressure is being developed under the forward most and rearmost parts of the underbody after the clutter has been removed. Furthermore, downforce increased by about 6.5%, and the table shows where these gains came from.

#### Rough floor, N

Body: -1,752 (lift)

Wheels: -183 (lift)

Underfloor: 3,232 (downforce)

Rear spoiler: 133

TOTAL: 1,430

Smooth floor, N

Body: -1,682

Wheels: -190

Underfloor: 3,262

Rear spoiler: 133

TOTAL: 1,523

Difference, N

Body: 70 (less lift)

Wheels: 7

Underfloor: 30 (more downforce)

Rear spoiler: 0

TOTAL: 93 (6.5% more downforce)

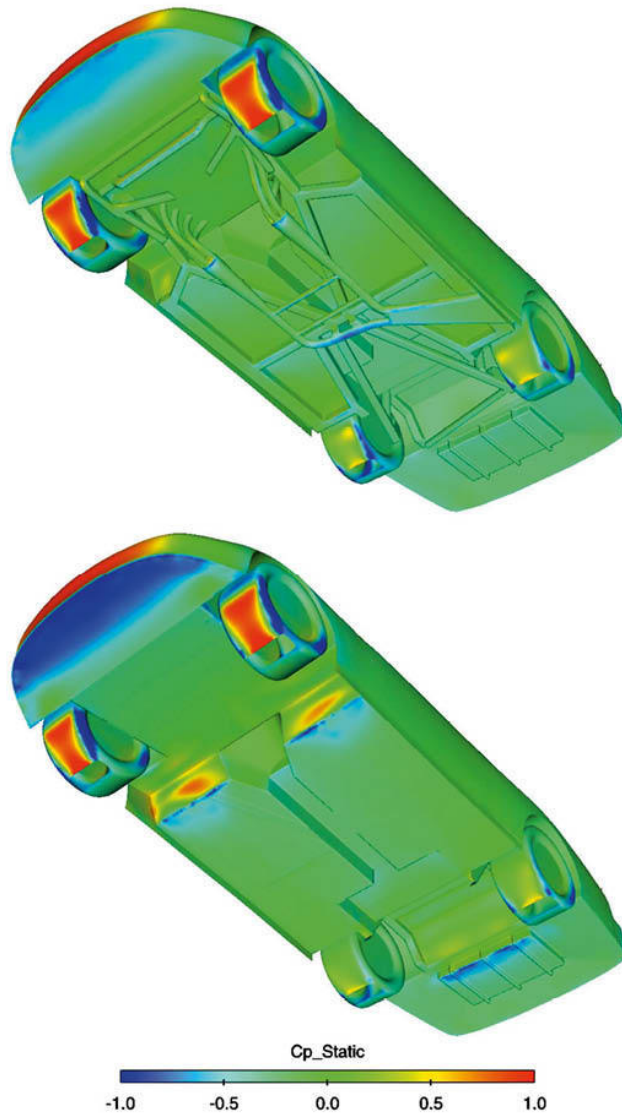


**Figure 6-14** Comparison of static pressures in ‘rough’ and ‘smooth’ underbody configurations.

Note that although some of the downforce gain came from the underbody, nearly three quarters of it actually came from reduced lift *over* the body. However, both these changes were the result of less underbody clutter encouraging increased mass flow beneath the car, which of course reduced the mass flow over the car. The change to drag was very small – a 1% reduction – and reflected the gain arising from reduced underbody clutter that the air encountered being balanced by the increase in mass flow that interfered with the underbody roughness still present. Probably a smooth underbody panel would provide even better gains in downforce and a greater decrease in drag.

Note that none of these benefits could be expected if an airdam blocked off the flow to the underbody.

There is another important aspect to flat floors too, and that is ensuring that the floor has a negative incidence angle, or rake. In other words, the front of the undertray *must* be lower than the rear. This is common sense really, and it is blindingly obvious, hopefully, that if the reverse was true, and the front was higher than the rear, then air would pack under the car at speed and give it very unhealthy, and potentially very unsafe upwards lift. Ensuring a car has this negative incidence angle is therefore vitally important.

At the very least, a significant reduction in a vehicle's (positive) lift coefficient can be expected from a correctly raked underbody panel, and references suggest that only a small angle of one or two degrees is enough to make a big difference. In essence, the entire underside of the car then becomes a simple venturi section, with a very short inlet and throat under the front of the car, through which the air will be accelerated, producing low pressure there. The rest of the underbody becomes a long diffuser, which, being smooth, allows the air to continue flowing rapidly, although gradually decelerating towards the rear. Thus, low static pressure is attainable under a car with a smooth, flat, raked floor.

When car manufacturer VW briefly ran a race series called Formula Volkswagen it used a 1,600cc single-seater that ran with dual-element wings front and rear, but in common with many 'training' formulas, it had a flat underfloor. VW Motorsport published some aerodynamic set-up data in 2002. Part of this data related to the effect of changing the chassis rake, and while altering the rake angle has an effect on the wing angles, the underbody aerodynamics also obviously change. Two graphics show what happens to overall downforce, and to aerodynamic balance (see Figures 6-15 and 6-16). The total downforce plot shows the change to overall lift coefficient, and dropping the front or raising the rear increases total downforce. The aerodynamic balance plot shows that dropping the front or raising the rear shifts the balance of downforce towards the front as well as increasing total downforce. It is easy to see why these effects occur by referring back to the basics of venturi underbodies, so this flat floor was behaving as if it were a simple venturi. Clearly, altering the chassis rake provides a potent tool for downforce and balance adjustment, even with a flat floor.

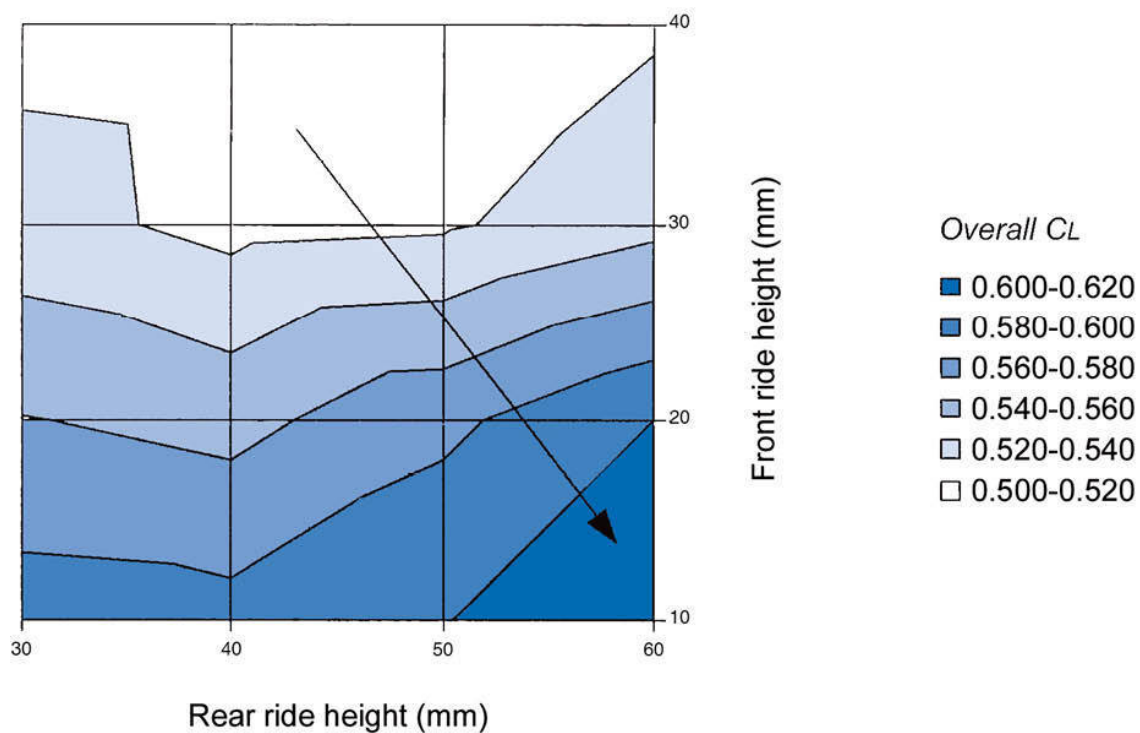


**Figure 6-15** Influence of chassis rake on total downforce on a flat-bottomed single-seater.  
(Volkswagen Motorsport)

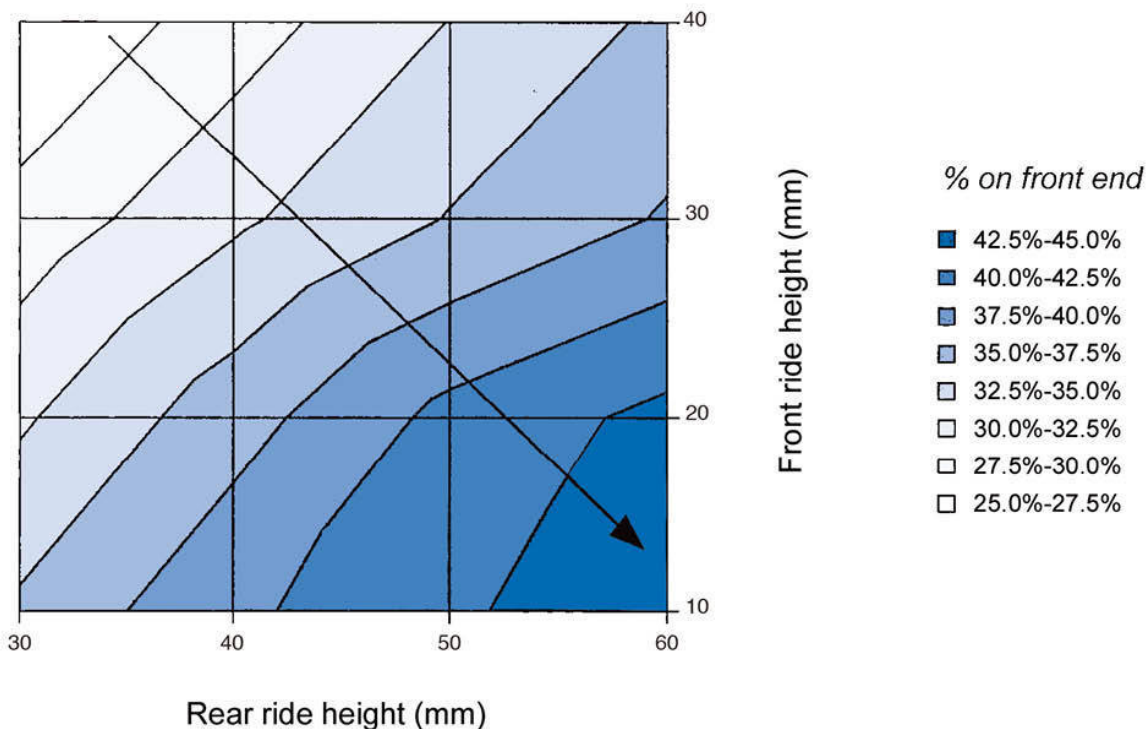


**Figure 6-16** *The influence of chassis rake on front-to-rear aerodynamic balance on a flat-bottomed single-seater. (Volkswagen Motorsport)*

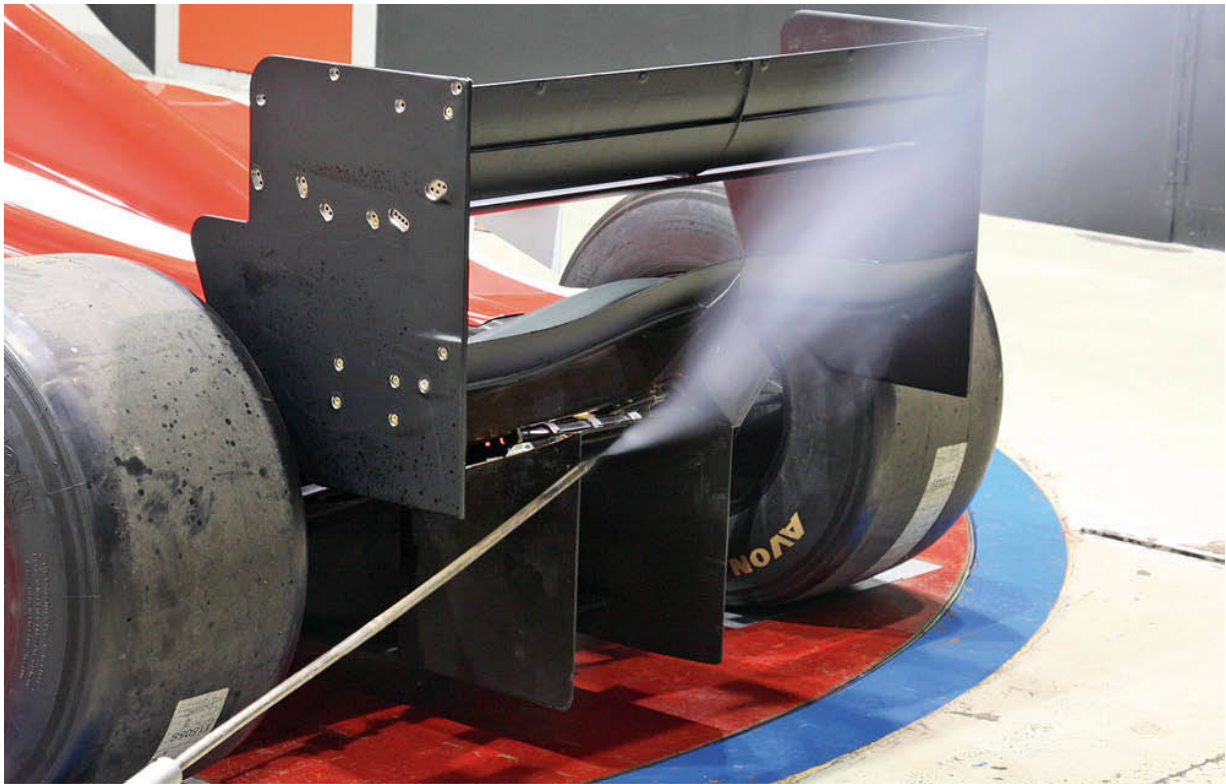
Remember that rake and front ground clearance are inextricably related, and there may be circumstances (which might be arrived at through static set-up or through dynamic changes out on the track) where the car is low enough to cause separation or stall. Both of which we are trying to avoid. The rake must be sufficient though, to ensure it does not become positive, that is, rear down during normal suspension movement, and preferably under any other circumstances such as cresting a rise at speed.

In some categories ground clearances are, or at least were, very small indeed, and it is easy to see that with a flat floor, even with a rear diffuser, such an arrangement could be very sensitive to ground clearance and rake angle. The small ground clearances that used to be seen in Formula 1 and Formula 3 for example are no longer permitted because of the 'stepped floor' rule mentioned in Chapter 1. It will also now be apparent that a stepped bottom will be less sensitive to changes of ground clearance or rake because there will be relatively less change in underbody cross-sectional area, at least to the raised outer sections of the underbody, with a car's vertical movement.

## More on diffusers

A car which is required to have a flat section to its underbody between the front and rear wheels and a limited overhang behind its rear axle line will not have very much room for a gently sloping diffuser. Clearly, Formula 1, and indeed Formula 3 diffusers, which are very short because of regulations, seem to have outrageously steep angles. However, they manage to keep the flow attached in part because the rear wing, and especially the lower tier if used, has a marked impact on the performance of the underbody region. Generally speaking, rear wings do not overhang the back end of competition cars by very much, depending on specific regulations. There is, therefore, an interaction between the low static pressure created under the rear wing, and the airflow in the diffuser(s), and this effect applies to just about any category you care to think of that uses a rear wing, and where attempts are made to exploit the underbody flow. In fact, it has been said that the rear wing actually ‘drives’ the diffuser.

Katz gives examples of a variety of vehicle types from passenger car based racecars to single-seaters, on which pressure distribution plots were carried out with and without rear wings. In all cases the rear wing had a profound beneficial effect on the under car static pressure, and the effect extended well forward in each case, so that integrated over the underbody area, the enhancement of total downforce was very significant. The effect is clearly analogous to the positioning of a flap at the appropriate place to augment the effect of a single-element aerofoil.



*Rear wings help to 'drive' steep diffusers.*

The flat-floor configuration is prevalent in many competition car categories, and has been developed to a level where, for example, Formula 1 cars are able to generate almost as much downforce as when they used ‘tunnels’ (see below). Estimates put the amount of downforce attributable to the underbody alone on a Formula 1 car at around 250lb to 300lb (114kg to 136kg) at 100mph (160km/h), or perhaps just less than one third of the car’s total downforce, depending on configuration.

### Tunnels

The precursor to the flat underbody-with-diffuser configuration was the ground effect ‘tunnel’ design, which in later refined forms produced the largest downforce figures ever seen in motorsport. Instigated, as we have seen, by Team Lotus in what now looks to have been the relatively simplistic Lotus 78, tunnels swept through motorsport and caused a step change in lap times the world over. That first ground effect car (ignoring ones with auxiliary power that preceded it) used inverted wing section sidepods attached to the chassis between the front and rear wheels to generate its underbody downforce. The proximity of the wing sections to the ground was seen to enhance their beneficial effect, and their very low aspect ratio, which would ordinarily lead to

low efficiency, ceased to be a problem when ‘end plates’ that reached to the ground all but totally sealed the underbody from sideways leakage of air into the underside region.

To accommodate vertical movement of the car on its suspension the lower parts of these end plates were allowed to slide up and down within the outer side panels of the wing sections so that they maintained contact with the road surface. ‘Sliding skirts’ in general are not fondly remembered. They massively increased the available downforce when they slid up and down freely, but an equally massive reduction in downforce occurred when they stuck in the ‘up’ position. They were far from 100% reliable, and many a wide-eyed driver had to walk back to the pits when the sudden loss of grip from a stuck skirt pitched his car off the track. Skirts were eventually banned on safety grounds, but not before several years had passed.

The Lotus 79 that followed on from the trend-setting 78 was a superb refinement of the basic wing car idea, and was the first true, no-compromise ground effect car. Pretty much all other detail aspects of the car’s design, including to an extent even the basic positioning of the engine, gearbox, wheels and driver were secondary to the effectiveness of the tunnels. The whole concept of ground effect was refined on this car, and its success on the track is testimony to its superiority over the opposition at the time. Lotus had truly found Chapman’s desired ‘unfair advantage’.

The concept of twin venturi tunnels either side of the centre section was dictated by the positioning of the engine and gearbox behind the driver in mid-engined single-seater and sports prototype and GT cars. Undoubtedly, a front-engined, front-wheel-drive car could, if permitted, utilise a single tunnel virtually the whole width and length of the car, but whatever the configuration of the car, the basic design parameters for the venturi tunnels were the same. The profile had to consist of a convergent inlet section, followed by a throat, which led into a diffuser section. The overall shape, in three dimensions, was determined on the one part by the ground, and on the other by the chosen profile and the specific packaging of the fundamental components of the car. The inlet and throat sections were generally fairly easy to shape and position, and a wide front track ensured that the front wheels were as far out of the way as possible. It was necessary for the diffuser sections to be routed through to the rear of the car, past the engine and its ancillary components and exhausts, and preferably not impinging on the adverse effects of the rear wheels.

The importance of the expanding diffuser sections of the tunnels can be gathered from the lengths that designers went to try to attain as uncluttered and clean a shape in this region of the car as possible. It all sounds

commonplace at this level of motorsport now, but for the first time especially close attention was paid to this aspect of aerodynamics. Gearboxes were made especially narrow, exhausts were re-routed, engine ancillary components such as fuel and oil pumps were relocated, and in one particularly famous example, that of the Porsche-built TAG turbo engine destined for John Barnard's McLaren MP4/2 in 1984, the shape of the engine was designed from the outset, to Barnard's specific criteria, to optimise the rear of the tunnels. The governing body pulled the carpet out from under the feet of this project when it banned profiled undersides in F1, but in all probability the careful packaging exercise that was done allowed aerodynamic advantages even on the flat-bottomed car that the engine ultimately powered.

Peter Wright, the man responsible for the design and development of those early Lotus ground effect cars, wrote a paper in 1983 (see Appendix 5) in which he presented graphically the effect of ground clearance, pitch angle and skirt-to-ground gap on downforce levels. He found that the greatest downforce, and the best lift-to-drag ratio were achieved at 2.56in (65mm) ground clearance, with a nose down angle of around  $0.7^\circ$  to  $0.9^\circ$ . Lift coefficient, with respect to frontal area was about  $-2.25$ , with a lift to drag ratio of 3.3:1, representing a drag coefficient of 0.68, but these are whole car figures and include the contribution of front and rear wings. The underbody was said to contribute 80% of the 3,600lb (1,636kg) total downforce at 180mph (290km/h). The effect of the skirt-to-ground gap was interesting, with a 0.4in (10mm) gap creating a 26% reduction in downforce, and a 0.8in (20mm) gap almost halving the whole car's downforce. Obviously, these numbers applied only to the car from which the data was derived, but they must have been fairly representative of late 1970s ground effect cars in Formula 1.

Ground effect tunnels between the front and rear axles created an aerodynamic centre which was fairly well forward on a car, and the business of attaining a front-to-rear aerodynamic balance was rather different to the flat bottom-with-diffuser case. Indeed, as a rather obvious generalisation, the further forward the throat of the venturi, the further forward will be the centre of pressure. This had the advantage that in order to attain a front-to-rear balance, very little, and sometimes no front wing needed to be run, which in turn meant that the airflow into the tunnels was cleaner. This situation seemed to last as long as sliding skirts, but with the overall reduction in downforce, and shift in balance brought about by the banning of sliding skirts, front wings reappeared and grew larger again. However, it was still crucial that the front wings did not impede the airflow into the tunnels, or for that matter, into the

radiators, which were now generally housed in, and fed by ducts in the leading edge of, the sidepods. Current ‘tunnel’ cars (and flat-bottom cars come to that) benefit from the use of asymmetric front wings, such that the portion of the front wing or flap ahead of the tunnel entrance/sidepod duct is less extreme than the outer portions.

Rear wings never disappeared from ground effect cars, and this can be put down to two factors: first, the rear wing provided a means to balance the aerodynamics, and if front wings were absent, it was the *only* method of doing that at trackside, since tunnels were non-adjustable; and secondly, the aforementioned interaction between the rear wing and the tunnels meant the effect of the rear wing reached well forwards of its actual location.

A well-designed tunnel was very much a three-dimensional device, and not just a two-dimensional venturi shape in side elevation. Although consisting of a ‘roof’ which was essentially at right angles to the ‘walls’ in order to maximise the effective cross-sectional area of the tunnel, and hence the mass flow of air through it, the roof to wall joins needed to be generously radiused to help prevent flow separation. Conversely, in the case of skirt-less tunnels, the lower joins from the bottom of the tunnel wall to the outer portion of the floor were beneficially left sharp. This had the effect of creating a vortex within the diffuser as the inevitable sideways flow migrated into the tunnel, which further lowered the static pressure and assisted with maintaining attached flow. Figure 6-17 shows a simple, wide tunnel model, with the low static pressure zones (blue) caused by the vortices spilling in on each side.



*Asymmetric front wings aid the flow to the radiators and underbody.*

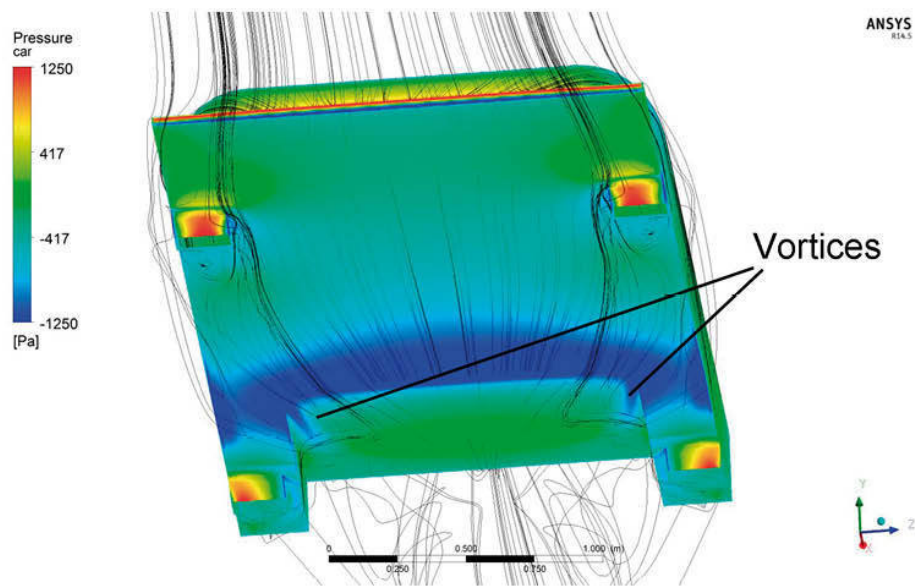


**Figure 6-17** The blue-coloured low static pressure areas in this 'wide tunnel' reveal the influence of vortices, and the streamlines show the inflow at the sides that create the vortices.

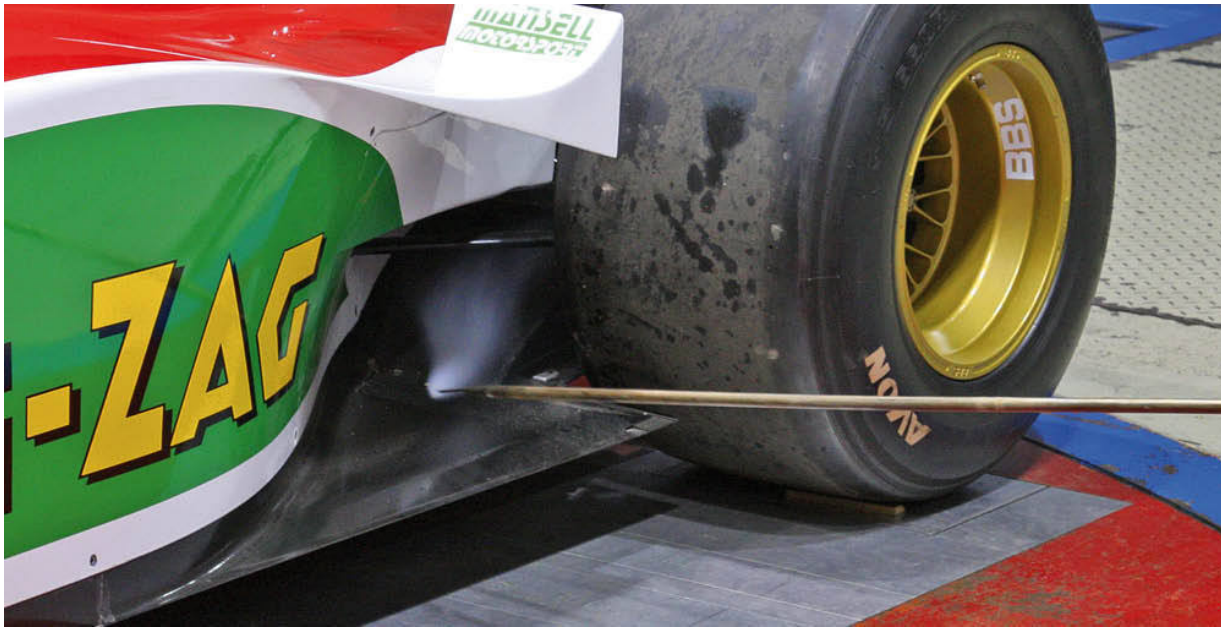
The tunnels were rarely straight from front to rear, but instead, angled inwards to direct the airflow inboard of the rear wheels. Allowing the airflow to impinge on the rear wheels caused major turbulence in the diffuser, seriously affecting the efficiency of the tunnels. The leading edge of the inlet to the underbody region was radiused to ease the air into this region of accelerating flow.

It was imperative that the tunnels be made as rigid as possible, so that the static pressure differentials did not distort the structure and give inconsistent downforce. Obviously, the mounting structures needed to be adequate to carry the very large downloads too. Just as important as the attempt to seal the outboard edges of the tunnels from the flow beyond, so it was to seal the inboard edges against the chassis – the low pressure in the tunnels could just as easily pull air in from around the engine bay for example, if such leakage was allowed.

The lowest pressures occurred in the throat of the tunnels and at the transition between the throat and the diffuser, and by using a longer throat more downforce could be achieved. The downside of this was greater sensitivity to ride height and rake angle. Once again it was a case of the designers trying to find a compromise that the drivers could live with. However, this did not stop a ludicrous phase in development that saw spring stiffnesses climb to almost unbearable levels (for the driver) in order to maintain a consistent aerodynamic platform. While the aerodynamics might have benefited from incredibly stiffly sprung racecars, the drivers – and ‘mechanical grip’ at low speeds – certainly did not.

Once skirts were banned and a minimum ground clearance was specified, there was a drop in downforce levels for a time, but various ploys were tried in order to win back the losses. Some were patently silly, such as the short-lived fashion for driver-controlled devices that altered ride height, allowing the cars to run right down on the deck out on the track, but on the way back to the pits, the car would be re-set to a legal level again. There were more clever, subtle and legal ideas tried, such as the ‘splitters’ located ahead of the rear wheels on some single-seaters. These not only exploit the high static pressure ahead of the wheels, they also act like horizontal skirts, on a similar principle to the foot plates on the lower edge of front wing end plates seen in the previous chapter.

All of the above has been written in the past tense, but of course much still applies to those categories that permit tunnels still.



*The 'tyre shelf' acts like a splitter, and also as a horizontal skirt.*

### Turning vanes and exhaust blowing

Turning vanes, sometimes also known as strakes, can be seen in the majority of diffusers. Their purpose is to control the lateral element to the airflow that inevitably exists in the throat-to-diffuser region, especially where that region is located at or near the rear axle line. The low pressure in the throat and forward part of the diffuser sucks air in from the sides, and because the air also has to funnel in between the rear wheels, there is bound to be a convergence in the flow in this area. Turning vanes, vertically mounted in the diffuser, are positioned so as to channel this lateral flow and help maintain attached flow in the diffuser. Helpful vortices that aid attached flow can also be initiated, these also contributing to reductions in static pressure.

'Exhaust blowing' originally referred to the practice of routing the engine exhaust outlets into the rear diffuser. The principle was that the high-speed gas emerging from the exhausts was 'injected' into the flow in the diffuser, which re-energised the boundary layer to reduce separation. This sounds like a good use of energy that would otherwise go to waste, until you remember that the effect varies with throttle opening and engine rpm. The benefit is therefore not consistent, being at its greatest when the engine is at high rpm with the driver pressing the throttle firmly, a set of circumstances not always coincident with travelling around a corner, and certainly not when braking hard.

However, some drivers learned to exploit the effect better than others, using left-foot braking, which enabled them to keep the right foot on the throttle,

and so keep the flow of exhaust gas into the diffuser at, or near its maximum. Two-pedal layouts and hand clutches made their appearance in Formula 1 and assisted with this aspect of driving. The gain in downforce from exhaust blowing was said to be relatively small. Some cars still route their exhausts to blow over the top of the diffuser, and small gains in downforce with reductions in drag have been reported. That the effect is relatively small and inconsistent, would seem to make it a pretty unattractive concept, although it became one of Formula 1's 'must haves' again in 2010. Perhaps this implied that development to the new rules introduced in 2009 had begun to slow, or else the gains found there were more worthwhile.

This latest fad for exhaust blowing was outlawed again in 2014 when a whole raft of new engine and drivetrain regulations were introduced in F1. However, while it was permitted, it was one of those developments that some teams made work well and with which others struggled. Bearing in mind the resources that even the tail end of the grid teams have at their disposal, this ought to be enough to put off the rest of us from even trying to emulate what was being done! For the record, though, it's believed that, in essence, exhaust gases were being routed so as to diminish the adverse and disruptive effect on the diffuser of the air that 'squirts' off the forward, lower, inboard part of the rear tyres. The 'Coanda Effect' was employed, wherein a jet of gas (the exhaust plume in this instance) tends, if properly directed, to adhere to a surface, and at the same time also pulls with it a generally increased mass flow of air. So, as well as acting like a kind of 'air skirt' to better seal the diffuser from the disrupted flow around the rear tyres, it may also have been that the mass flow through the diffuser was being amplified to the betterment of underbody downforce.

### **Front wing interactions**

Wing and underbody interactions have been mentioned several times now, and clearly can be adverse or beneficial. The effect of an ill-designed or badly deployed front wing can be very negative, not just on the underbody flow, but the flow over the whole car. However, the impact can be minimised with care, and the attention to detail paid by the top professionals is an object lesson for all. Front wings are not made complex just to give the pattern makers and composite laminators job satisfaction!

The most obvious thing that a front wing must not do is stall. If so much front downforce is needed that the front wing is anywhere near stall, then better to balance the car by using *less* front wing and taking off rear wing, because the disturbance caused by a front wing working this hard is likely to be

to the detriment of flow to the rest of the car. An alternative, and perhaps longer-term fix would be to use a larger chord front wing, or to make the car's nose narrower and increase the span of the front wings, each of these adding wing area, and hence, downforce, all other things being equal, or giving equivalent downforce at a smaller, and less flow-disturbing angle of attack. Secondary front wing elements on top racecars are often steeper at their outer extremities than at the inner part of their span. This again allows a better flow to the radiators, but also to the first part of the underbody.

The trend was initiated in rather extreme form by the Tyrrell Formula 1 team with the 'anhedral' front wing design on the Type 019, which led to the first of the now almost ubiquitous 'raised nose' configurations. The aim was, and is to improve the flow to the underbody. It also made the front wing, and indeed the whole car less sensitive to changes of ride height and pitch, because the flow beneath the wing did not get entirely blocked off when the car's nose dipped groundwards.

### Low drag

As mentioned earlier, when Lotus announced the Type 78 they used the phrase 'We've found something for nothing'. Although it has to be said that Lotus did *not* manage to break the laws of Nature here, what they had done was to manage the airflow around the car in a much more efficient way, so that the large increase in downforce was achieved at very modest drag penalty. By creating a means for the air to flow smoothly underneath the car, in order to maintain high flow velocity, and hence low pressure, they also created a low drag regime too, with relatively little disturbance where once before there was aerodynamic mayhem! Furthermore, by raising the underbody at the rear of the car, and maintaining the smooth flow right back to the rear of the diffusers, the effective base area of the car was reduced, the wake was made smaller, and the form drag was cut as a result. However, there would have been some increase in the induced drag as the result of creating the downforce, but overall the gains were at very small cost in terms of drag. So 'something for nothing' was overstating it a bit, and however appealing that notion is, you rarely if ever get anything for nothing. The illusion came from making the aerodynamics work much more efficiently.

While ground-effect tunnels were banned from Formula 1 from the start of 1983, the use of tunnels was still permitted in Group C sports prototypes, up until that category's demise in 1992. The basic configuration of the sports prototype permits a very large underbody area, and the enclosed wheel nature of the cars also permits low-drag designs to be built. Thus it was in this

general sports prototype group that the most efficient downforce-producing designs *ever* were made. Cars like the Jaguar XJR series, the Porsche 956 to 962, the Peugeot 905, the Nissan P35 and the Mazda RX7-792 were all developed to such a degree that  $-CL$  values of nearly 4.0 were quoted, with  $C_{DS}$  of around 0.7, lift/drag ratios therefore approaching 6:1!

### **The effects of underbody changes**

The underbody of even tightly regulation-restricted racecars is worthy of close attention, and can provide a powerful tool for tuning overall downforce, as well as its front to rear distribution. Wind tunnel trials on the 2006 RJS Motorsport Nissan 350Z GT2 racecar yielded some interesting data on this topic.

We saw earlier in this chapter how diffuser angle affects downforce. It was apparent that downforce increased with increasing diffuser angle, up to the point where flow separation in the diffuser became significant. Being just a simple 2D model in that instance, we were unable to see what happened to drag, or to aerodynamic balance, or indeed to the flow itself when 3D flows are taken into account. Had we studied a full 3D digital racecar model we could have derived this information with CFD of course. Instead we can now see how these parameters could be assessed in the MIRA wind tunnel on a real 3D racecar. Keep in mind that the tunnel in question has a fixed floor, and that boundary layer growth along the floor will have an effect on underbody flow. Nevertheless, trends can be examined and acted upon with reasonable confidence.



*An adjustable diffuser on this Nissan 350Z GT2 car produced some interesting data.  
(MIRA)*

Figure 6-18 summarises the effects of changing the diffuser angle on four parameters; drag, downforce (negative lift,  $-L$ ), efficiency ( $-L/D$ ) and rear downforce as a proportion of total downforce ( $-LR/-L$ ). The changes have been expressed as percentages relative to the values measured at the baseline of  $8^\circ$  diffuser angle (for confidentiality reasons force and coefficient values are not available).

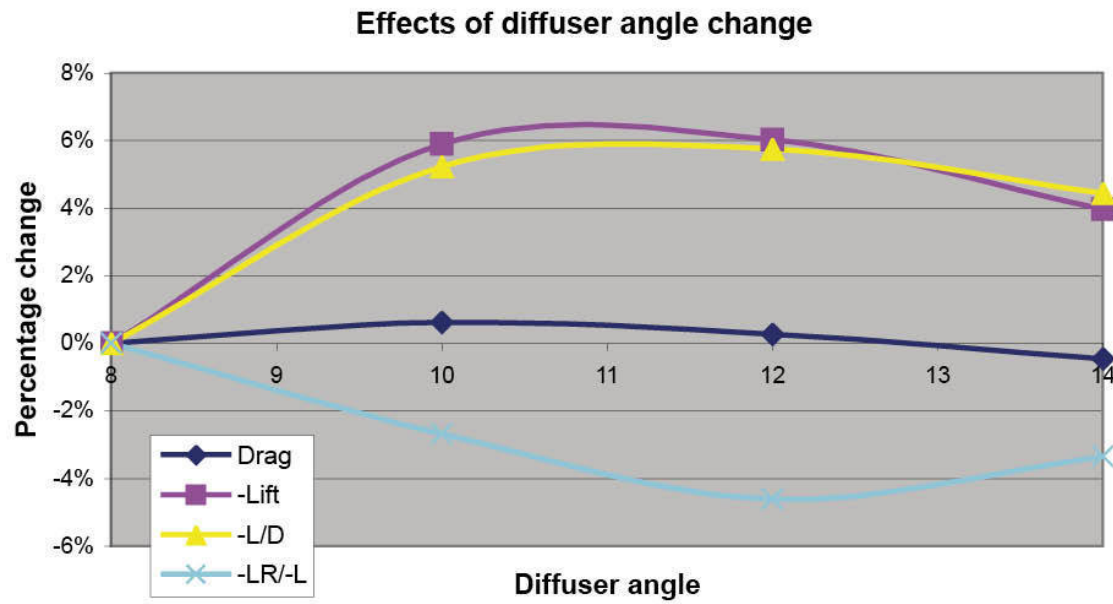


**Figure 6-18** Altering diffuser angle affected downforce, drag, balance and efficiency.

Looking first at drag, it is apparent that there were very small changes across the range of angles measured here, and after an initial small rise the drag then fell until at  $14^\circ$  it was slightly less than at  $8^\circ$ . The highest overall downforce value was measured at  $12^\circ$  although the value at  $10^\circ$  was almost identical.

What isn't shown here is that *rear* downforce peaked at  $10^\circ$  and then gradually decreased from there. This might tend to suggest that flow separation started to become significant in the diffuser once  $10^\circ$  had been exceeded. And it isn't obvious whether an angle somewhere between  $10^\circ$  and  $12^\circ$  might have yielded slightly greater downforce. The line illustrating the car's efficiency,  $-L/D$ , pretty much follows the downforce curve, given that drag doesn't change much with changing diffuser angle. Of course, with the car running over a track surface there would be no ground boundary layer to alter the effective diffuser angle, and the actual maximum diffuser angle may differ somewhat from the wind tunnel optimum.

The changes to the rear downforce proportion follow a rather different and very interesting pattern though. There is a forward shift of the aerodynamic centre with each diffuser angle increment, this shift being at its maximum at the peak downforce setting of  $12^\circ$ . This was of particular value in this development because the team was looking to move the aerodynamic centre forwards. This may seem like a counter-intuitive result, given that it is often –

and erroneously – thought that the diffuser generates the downforce. But clearly what we're seeing here is that the increases in diffuser angle have generated more forward-biased underbody downforce. This results from incremental increases in mass flow, and hence velocity, through the underbody 'throat' *ahead* of the diffuser. With a flat-bottomed racecar like this, the throat could be said to extend from the front of the car to the diffuser's leading edge. Hence the underbody-generated downforce tends to be forward biased, and additional increments arising from diffuser angle increases amplify this shift until the diffuser reaches its optimum.

Another underbody adjustment tool available to the racecar engineer is chassis rake, and RJD Motorsport also mapped a small number of settings, viz  $0.3^\circ$ ,  $0.9^\circ$  and  $1.3^\circ$  overall chassis rake (with a fixed diffuser angle of  $10^\circ$  in this case). The results, again expressed as percentage changes compared to the baseline value ( $0.3^\circ$ ) are shown in Figure 6-19.

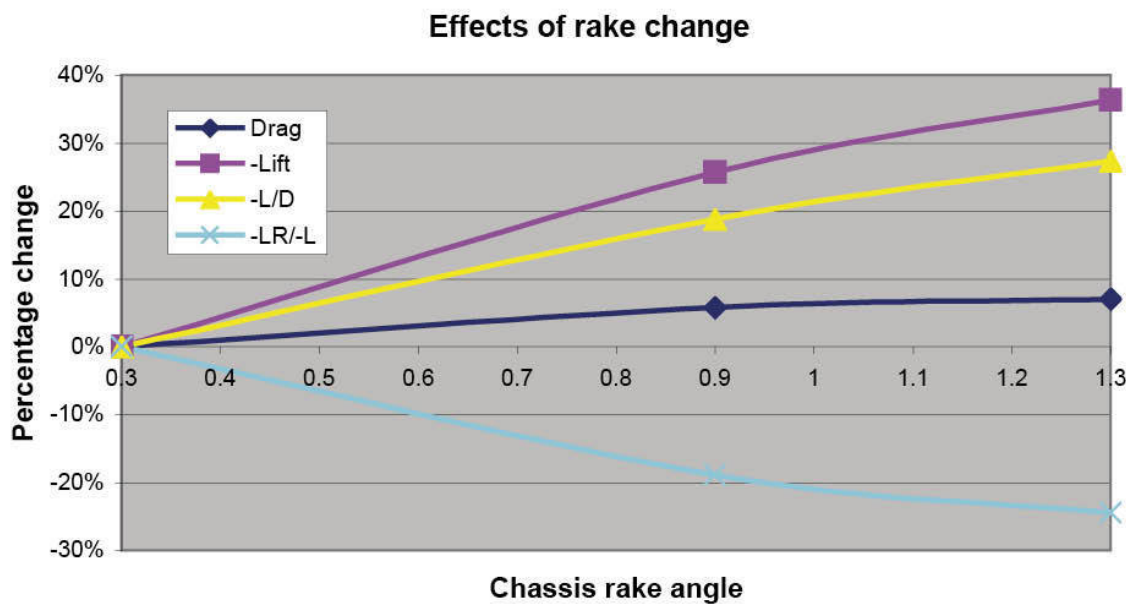


**Figure 6-19** Altering chassis rake also affected downforce, drag, balance and efficiency.

The first observation to make here is that the changes of angle represent quite large differences in height along the car. For example, the height difference between  $0.9^\circ$  and  $1.3^\circ$  is around 30mm along the entire car length, or 18.5mm difference in height at the axles (length = 4,310mm, wheelbase = 2,650mm). But with the quite large minimum ride height mandated for this

class (50mm), pretty coarse adjustments were made in order to obtain clear results. And the results were indeed clear-cut. In short, as rake angle increased downforce increased significantly, drag increased but much less so, and so efficiency also increased quite markedly. There were also marked forward shifts in downforce balance, this again being of benefit to this particular project.

Increasing the overall chassis rake is analogous to increasing the diffuser angle, in that it opens up the rear underbody cross-sectional area. Providing the ground clearance at the throat entry isn't so small that choking occurs, this increases mass flow through the underbody, causing a bigger velocity increase in the throat region, which in turn creates a greater reduction in static pressure there. Also, as rake is increased the narrowest part of the throat is moved forwards, which promotes a forward shift in downforce, seen here as reductions in rear downforce percentage.

It seems reasonable to assume that racecars that run smaller ground clearances than this GT2 car would demonstrate greater sensitivity to diffuser angle and chassis rake, but the principles would be similar.

### **The effect of the rear wing on the underbody**

The rear wing can significantly influence the performance of the underbody, especially when that underbody generates a large proportion of a racecar's downforce.

This 1991 vintage IMSA GTP Jaguar XJR-16 produced high lift coefficients in the MIRA wind tunnel ( $> -3.0$ ) and high efficiency (downforce over drag, or  $-L/D > -3.5$ ), with drag coefficients being relatively low ( $< 0.9$ ) for the lift coefficients seen. The designers of these late 'Group C' and IMSA GTP type cars were allowed considerable freedom to exploit the underbody region, and long diffuser tunnels – the transition of which was roughly halfway along the wheelbase – were complemented by large flat forward floor areas and protruding splitter extensions. This not only generated substantial downforce, it also put the aerodynamic centre of the underbody fairly well forwards on the car, the potent rear wing assembly then helping achieve the desired balance and overall high lift coefficient values.



*Adjusting the lower rear wing on this 1991 vintage IMSA GTP Jaguar XJR-16 altered downforce and efficiency but changed the balance very little. (MIRA)*



*The lower rear wing tier was just higher than the rear bodywork. (MIRA)*

The Jaguar XJR-16 seen here in original IMSA GTP specification carried a two-tier rear wing assembly, as other contemporary cars did, each tier having

dual-element configuration although the upper tier featured a smaller chord dimension and less camber. It was also located higher and therefore saw higher energy airflow, which would help it to perform better. However, the lower tier fulfilled more than just the obvious role of generating its own contribution to total downforce, as the following study reveals.

Figures 6-20, 6-21 & 6-22 show the effects of altering the angle of the lower rear wing flap on the overall lift coefficient and efficiency ( $-L/D$ ), the drag coefficient, and the aerodynamic balance, the last expressed as a percentage of the total downforce exerted at the front wheels. We can see that increasing the angle of the flap increased the car's lift coefficient (3.6% variation across this range, relative to the maximum value here) and the drag (5.6% variation across the range tested). So although there was a gain in downforce, there was, proportionately, a larger increase in drag, and this led to the 1.9% decrease in efficiency across this lower wing flap angle range, relative to the best value.

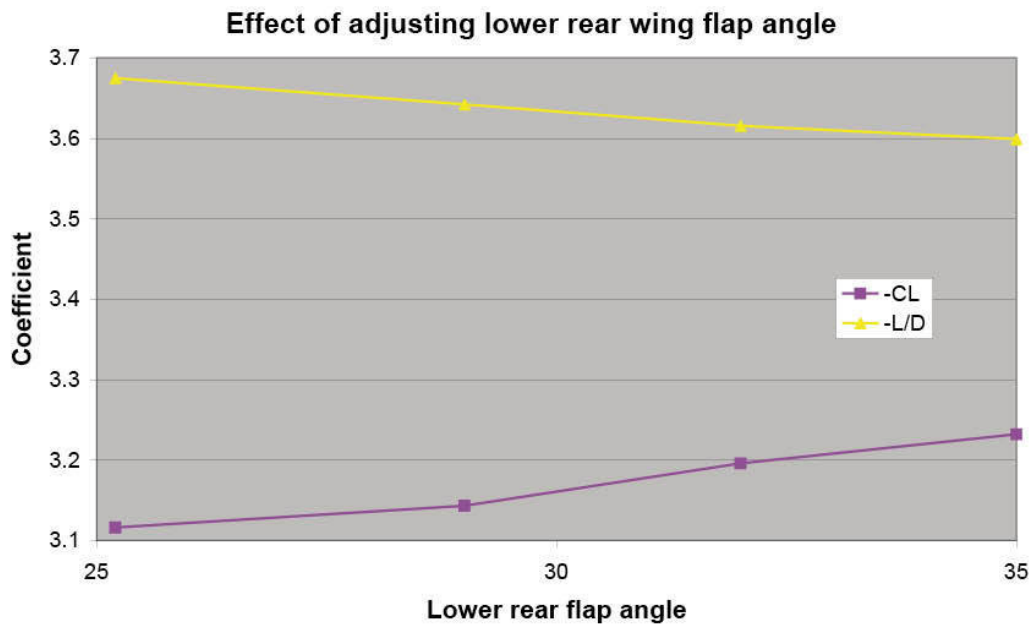


**Figure 6-20** Downforce went up but efficiency came down with increasing lower wing angle.

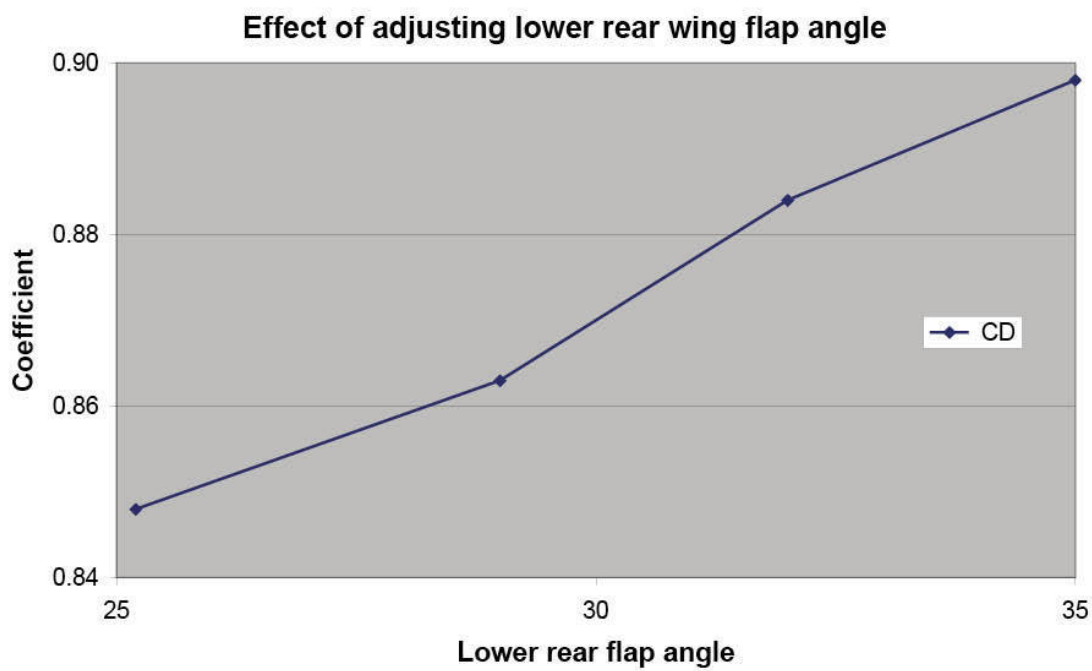


**Figure 6-21** Drag increased with increasing lower rear wing angle.

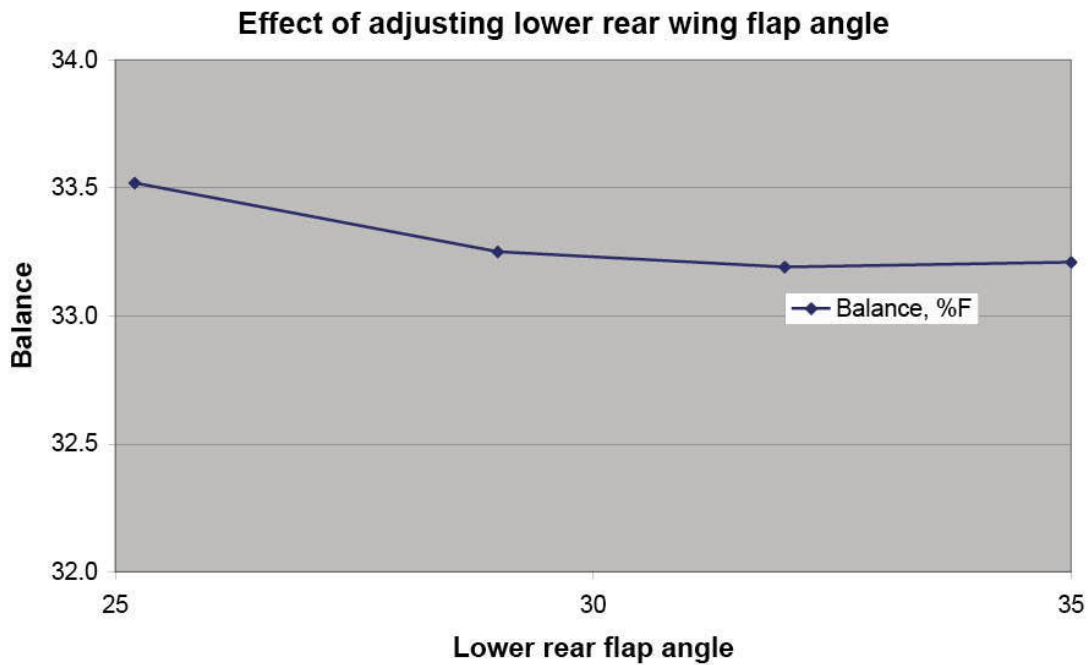


**Figure 6-22** Balance scarcely altered with increasing lower rear wing angle.

We'll come back to the reasons for this particular mix of trends later. But looking at figure 6-22, it is apparent that while adjusting the lower rear wing flap had a significant effect on downforce and drag, the car's balance changed very little, only moving from 33.52% front maximum to 33.21% front minimum as the flap angle was increased. Had these increases in flap angle merely led to an increase in the downforce contribution of the rear wing assembly we would have expected a rearward shift in aerodynamic balance. But the fact that the balance barely altered is evidence that increases to the lower rear wing flap angle also had an influence further forward, specifically by helping the underbody to develop more downforce. Not unexpectedly, adding Gurneys to the lower rear flap had a similar effect to increasing flap angle.

But although these configuration changes produced increases in downforce, both saw a decrease in efficiency, so let's consider the mechanisms at work here to figure why this is so. The underbody of a ground effect racecar is very sensitive to the base pressure, which is the pressure immediately behind the car. Air naturally flows into regions of low pressure, whereas the air in the underbody is flowing from a region of very low pressure in the flat portion of the underbody, and the pressure is then, ordinarily, rising through the diffuser tunnels to their exits. This is another example of an 'adverse pressure gradient', so called because it goes from low to high pressure, and the airflow only follows an adverse pressure gradient if it has enough energy and momentum to do so and the gradient is not too steep.

However, a racecar is an example of a 'bluff body', which is to say one with a chopped off, blunt rear end behind which a wake exists. Although the wake is a low energy, turbulent region, it is at somewhat reduced static pressure, and this can actually assist the flow from the underbody to emerge, helping to draw it out of the diffuser(s). If we then position a rear wing in close proximity to a diffuser exit, the very low static pressure under the wing means we can develop considerably reduced static pressure behind the car, and this exerts a much stronger pull on the airflow emerging from the underbody. The result is considerably greater mass flow and higher velocity, and hence lower static pressure through the primary downforce generating 'throat' region of the forward underbody. It also enables much lower ground clearances to be run, which in turn help to further speed up the airflow in the underbody, again adding to potential downforce.

However, as we have seen from the data here, the downside of generating reduced low pressure immediately behind the racecar is that drag also increased. Pressure drag can be a significant proportion of the drag of a racecar, and in this instance the presence of a low-mounted, potent wing

would add to the car's pressure drag as well as the wing generating its own pressure drag. Given that the generation of increased downforce creates increased vortex drag too, it isn't surprising perhaps that increasing the angle of such a low-mounted wing as in this example added significant drag as well as downforce. As in all quests for optimum aerodynamic performance, the settings to be used will inevitably be a compromise that quite probably would vary from track to track.

### **Visualising flows emerging from diffusers**

It's all too easy to imagine smooth, organised airflow emerging from diffusers, but the wind tunnel smoke plume gives a more realistic view, even though having an aerodynamicist (and a photographer) in the tunnel to hold the smoke wand limits air speed to 25–30mph for safety reasons. However, the following photographs are quite revealing. With both cars it is apparent that the flow emerging from the centre of the diffusers is as one might imagine, or at least hope – essentially smooth and parallel to the roof of the diffuser; therefore the flow was attached even at this low speed. (The Exige had an aftermarket exhaust system that sat above the diffuser rather than the OEM one that was located in this central diffuser region and which disrupted the flow in the area where it should have been at its best.) However, outboard the flow in the Lotus Exige's diffuser appears to be reversed (stalled) and thoroughly turbulent, and the images of the Ferrari's diffuser show the flow becoming less organised outboard of the centre, and thoroughly turbulent again as it emerges from the outermost section.



*The flow emerging from the centre of this modified Lotus Exige's diffuser looks to be fast and smooth.*



*The flow in the outer section of this Exige's diffuser looks to be going in the wrong direction!*



*As with the Lotus, the flow emerging from the centre of this GT3 Ferrari's diffuser centre is fine.*



*Move outboard and the flow begins to look less organised.*



*In the outermost section of the diffuser the flow is highly disorganised.*

Clearly this shows that reality does not match the ideal picture, and it isn't difficult to imagine that the flow around the wheels (especially their wakes), the wheel wells and the suspension is largely responsible for helping to make a mess of things here. It is equally clear that anything that can be done to isolate or at least reduce the influence of the disrupted flow around the wheel and so forth from the diffuser would be beneficial, so strategically located panels and fences can all help.

### 3D CFD studies

We have run through various underbody cases and examples from two-dimensional CFD studies to wind tunnel projects. We'll round off this chapter with a glimpse at some basic 3D CFD studies on aspects of underbodies using a 'bluff body' bearing a slight resemblance to a simplified sports racing car.

The CAD model (see figure 6-23) was without any complicating design features, with the exception that partial cylinders representing the wheels and tyres were included as these clearly have a major influence on the flows under a racecar. Thus, while our simulations cannot be directly related to an actual racecar, nevertheless they enable us to see how things changed, semi-quantitatively and qualitatively, with alterations to the geometry. Having looked at diffuser angle and rake angle in the wind tunnel, the 3D model was used to examine diffuser length.

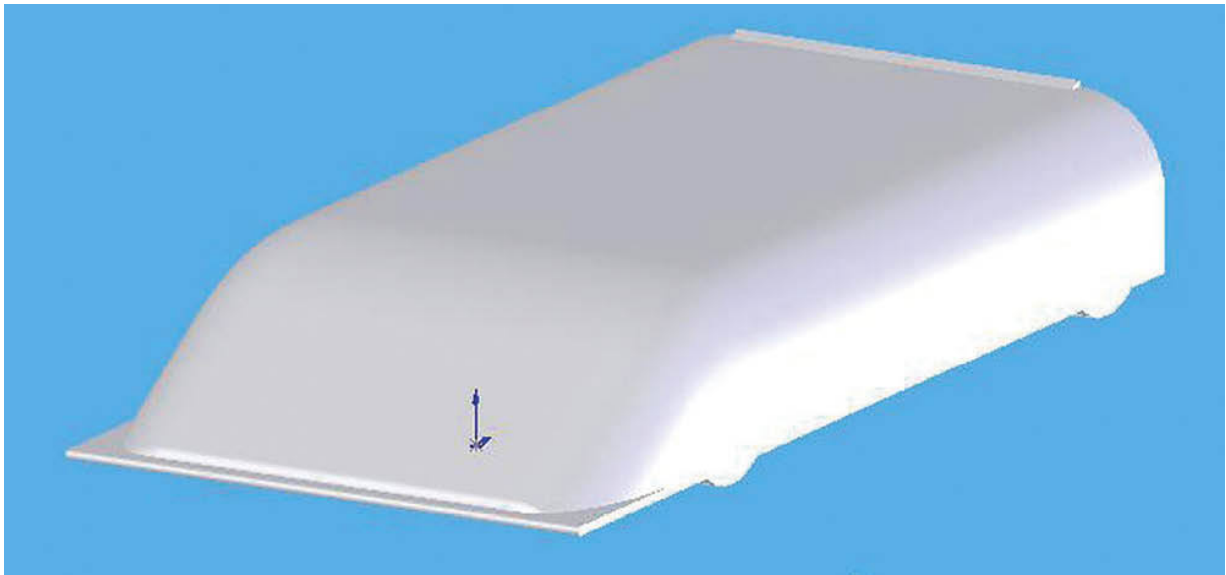


**Figure 6-23** The model used for generic 3D CFD underbody studies.

One of the most often asked about basic parameters, diffuser length, isn't always one over which technical regulations allow any freedom. However there are still categories where the freedoms do exist as well as those historical ones, such as Croup C and IMSA sports prototypes where long diffusers, or more accurately long tunnels were de rigueur and which are therefore of great interest. So the diffuser in our simple model was modified to incrementally increase diffuser length and height while retaining the same roof angle, with the shortest and longest diffusers shown in figure 6-24. The results are shown in figures 6-25 and 6-26.

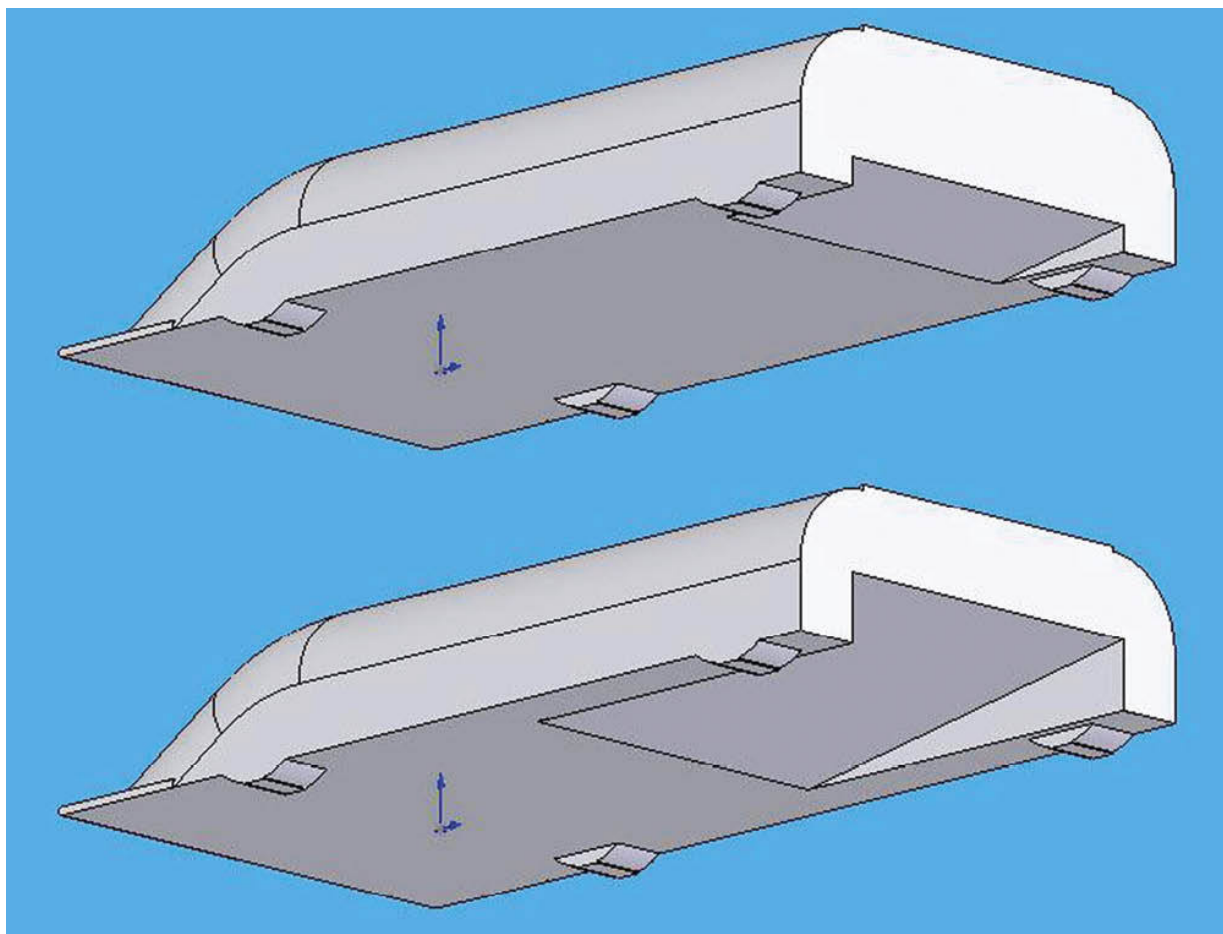


**Figure 6-24** The longest and shortest diffusers.

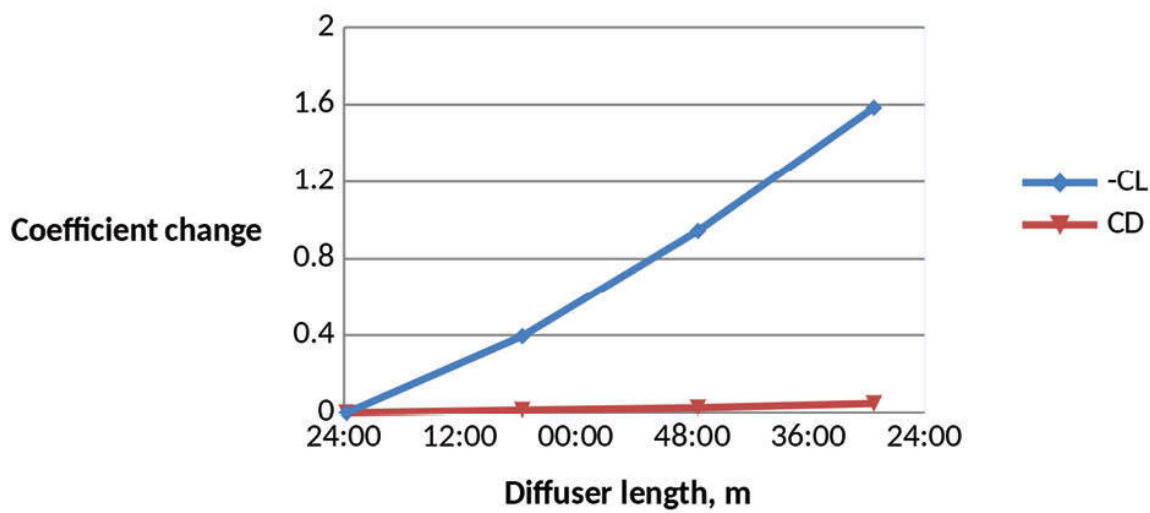


**Figure 6-25** The effects of diffuser length on downforce and drag.

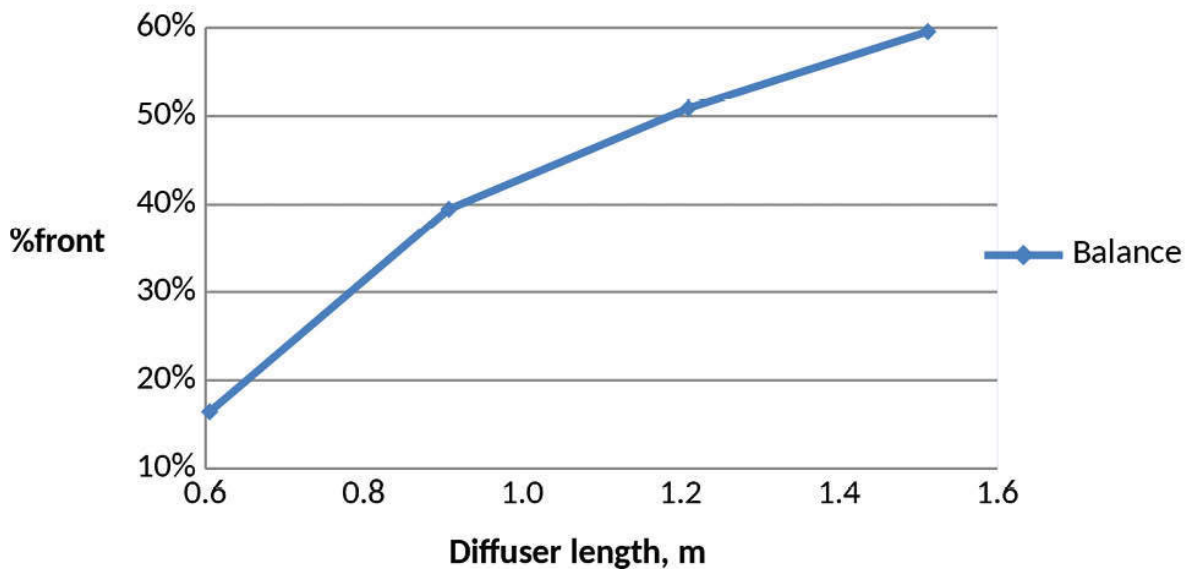


**Figure 6-26** The effects of diffuser length on aerodynamic balance.

The increases in downforce here were enormous compared to the relatively modest gains obtained with changing diffuser angle and chassis rake. In light of this, it's perhaps easier to see how the aforementioned Group C/IMSA prototypes generated such high downforce figures, and also that diffuser length was the obvious parameter for the regulators to target in order to reduce downforce! Drag can be seen to have increased slightly with increasing diffuser length as well here, but the efficiency (-L/D) of the model rose from 1.022 to 5.973!

Figure 6-27 shows the pressure distributions on the lower surface of the shortest and longest diffusers tested. Not only did the suction peak at the diffuser transition move forwards, it also became much more extensive, and pressure was lower in the case of the longest diffuser as far forward as the splitter. There was also a pronounced low pressure 'jet' visible in the diffuser itself, the result of the aforementioned potent vortices that formed as the convergent flow passed over the sharp edge on the outer wall of the diffuser. Overall then it's easy to see how the aerodynamic balance shifted significantly forwards with increasing diffuser length.

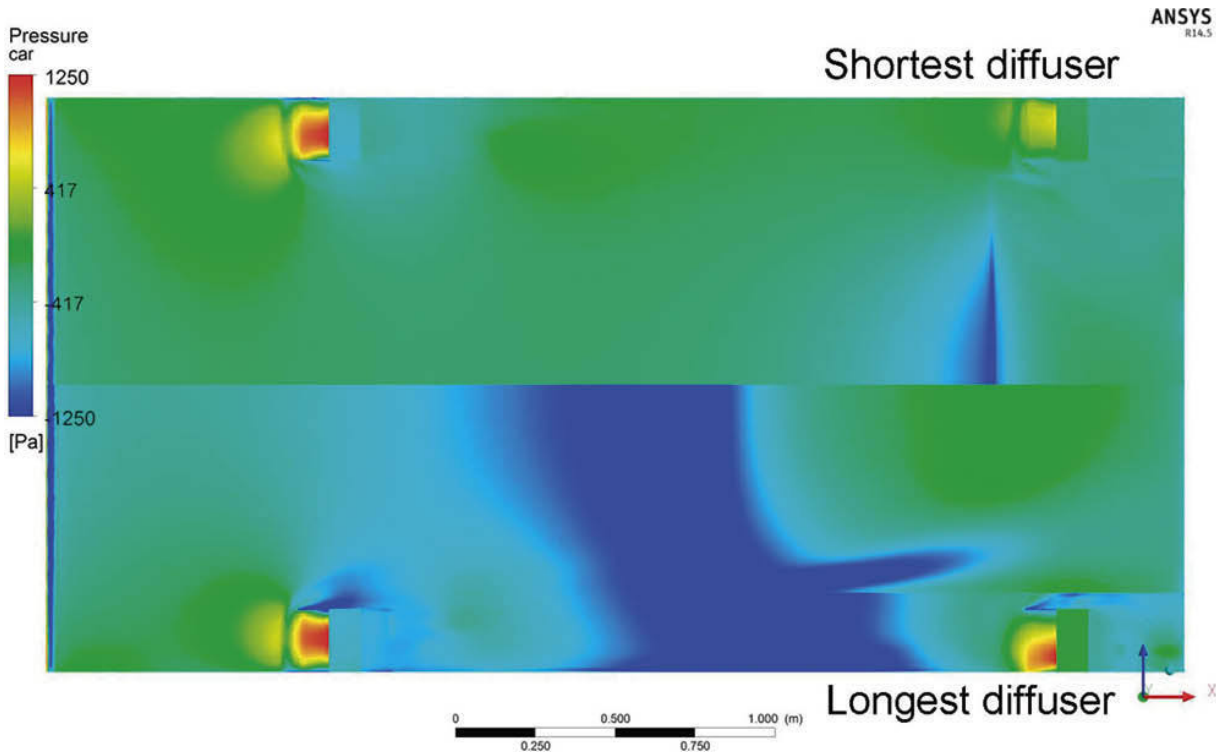


**Figure 6-27** Static pressure distributions on the lower surface of the shortest and longest diffusers.

Of all the parameters we have looked at, this one seems superficially to clash with the findings of the 2D CFD trials at the start of this chapter. Yet the reason seems clear enough when considering the extra diffuser volume that the air has to fill. The air's density cannot change so as to magically cause a partial vacuum in the diffuser, and so the mass flow increases to fill the bigger diffuser, both from ahead of the model and from the sides. The additional velocity increase this creates through the throat and the sides of the underbody is what produces the increased area and magnitude of the low pressure regions.

Few diffusers are seen without vertical, more or less fore-aft aligned fences or 'strakes' located within them, so what would they be worth on our model? In this case the baseline model was the short diffuser at  $0.2^\circ$  rake to provide a model that had a reasonable aerodynamic balance with which to begin. Then one, two and finally three strakes were added to each side of the diffuser, at 150mm (5.9in), 300mm (11.8in) and 475mm (18.7in) respectively from the outer walls (see figure 6-28 showing all the strakes in place). Figures 6-29 and 6-30 illustrate the results.

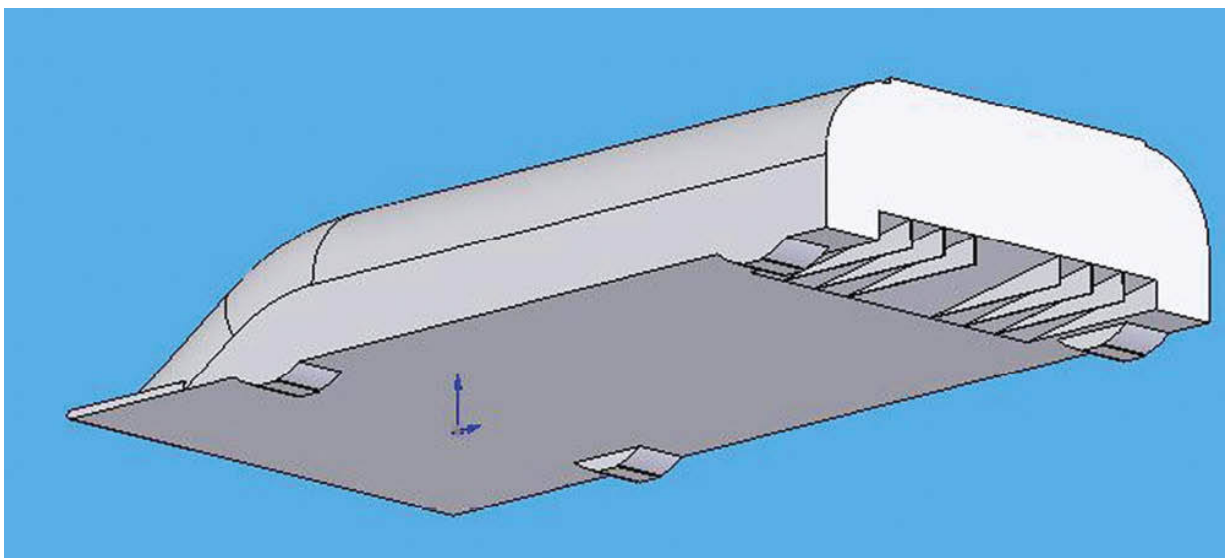


**Figure 6-28** The short diffuser with three pairs of strakes in place.

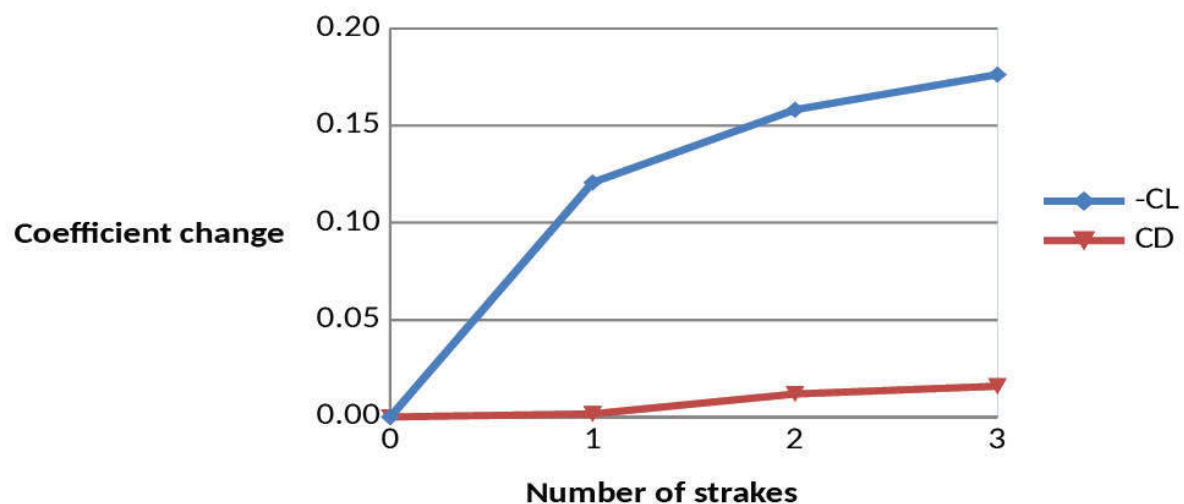


**Figure 6-29** The effects of adding strakes to the short diffuser on downforce and drag.

## Effects of strakes

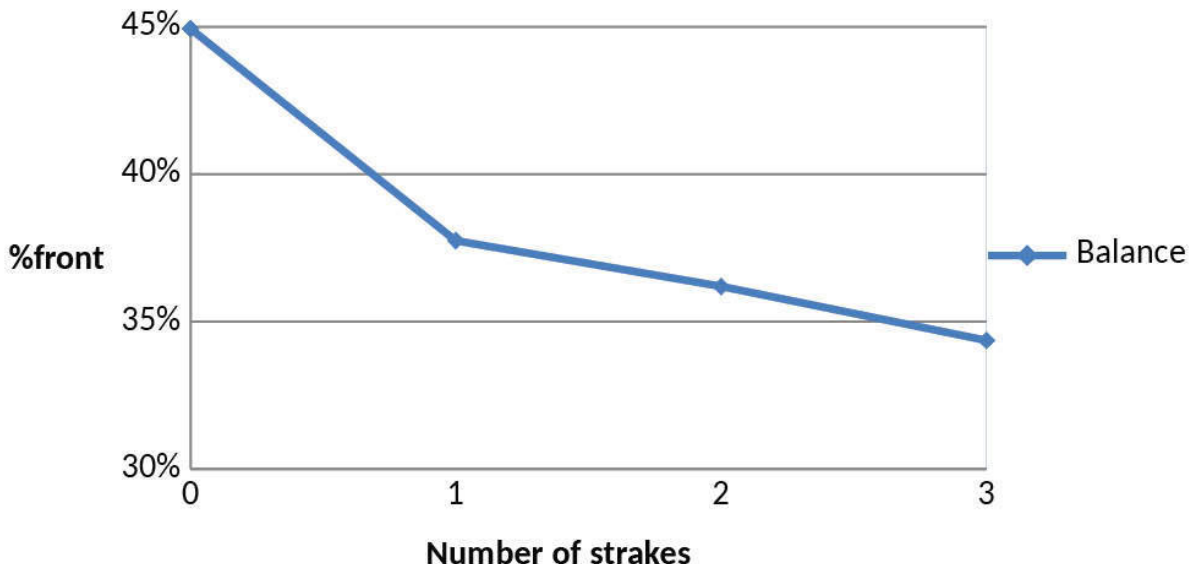


**Figure 6-30** The effects of adding strakes on aerodynamic balance.

In figure 6-29 we see a classic ‘diminishing returns’ downforce plot, the first pair of strakes producing a moderate gain, with successively smaller gains thereafter. Drag barely changed initially but then seemed to jump slightly with the second and third pairs of strakes. Nevertheless the overall efficiency gains were significant,  $-L/D$  rising from just over 1.0 to just over 1.6. Constrained to a short diffuser, on the strength of this data strakes looked well worthwhile. Figure 6-30 shows that aerodynamic balance shifted rearwards in this case as extra strakes were installed, again with the initial effect being quite marked, followed by a lesser but linear effect.

Figure 6-31 once more shows the underside pressure distributions, this time with surface streamlines also plotted. The suction peak ahead of the diffuser transition can be seen to have strengthened with the fitment of the first pair of strakes, and the formation of a pair of small vortices was also evident in the blue ‘jets’ that started just inboard of the leading edge of the strakes. Generally the pressure in the diffuser was lower. The surface streamlines show the flow to be better organised in the outer part of the main diffuser inboard of the strakes, with less of the flow from in front of the rear tyres reaching the central diffuser. With four strakes the main suction peak was strengthened, but very evident here was the pair of additional, even stronger vortices just inboard of the second pair of strakes, which contributed to further reduced pressure in the diffuser. Finally the inner pair of strakes appeared to have less effect on the

main suction peak but another pair of low pressure vortices was set up. The overall flow direction was also more significantly influenced by this third pair of strakes.

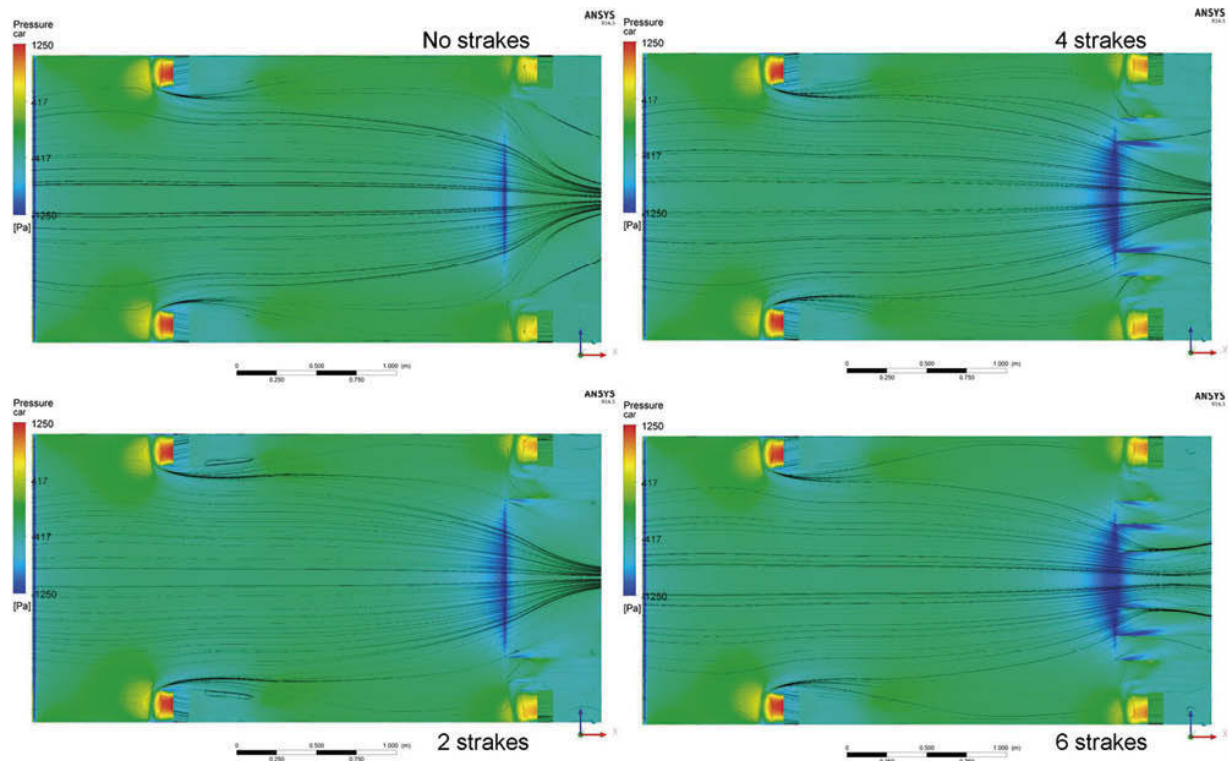


**Figure 6-31** Static pressure distributions on the lower surface, with surface streamlines also plotted, with no strakes (top left) to six strakes (bottom right).

So, these very simple strakes markedly increased overall downforce and caused a rearward shift in aerodynamic balance. An obvious further area to study would be strake curvature to see, for example, what would be the effect of aligning the leading edges of the strakes with the local airflow direction. Would vortex formation be reduced, in which case would the attendant low pressure regions diminish and produce less downforce? Or would the flow become better organised, leading to increased mass flow and lower pressures in the diffuser, producing a gain in downforce? Always, more work is needed!

## Summary

We have seen that the underbody of a vehicle can be shaped or modified to produce a large amount of downforce, and that the components upstream and downstream of the underbody region can have a marked influence on the efficiency of the underbody aerodynamics. Unfortunately there is just not the

large database of information available on designs and shapes to use, as there is with aerofoils for example, nor indeed is it really practical to try to deal with specifics because every new design is going to be different. But hopefully, this chapter has offered some general if necessarily conservative guidelines on the key parameters to consider for an underbody design.

The professionals meanwhile have computational fluid dynamics to model myriad configurations in order to hone in on an optimum solution, and then wind tunnels in which to validate the solutions. We'll look in more detail at the tools that are used by the pros, and also at those that can assist the amateur in the search for an aerodynamic solution to going faster, in a later chapter.

## Chapter 7

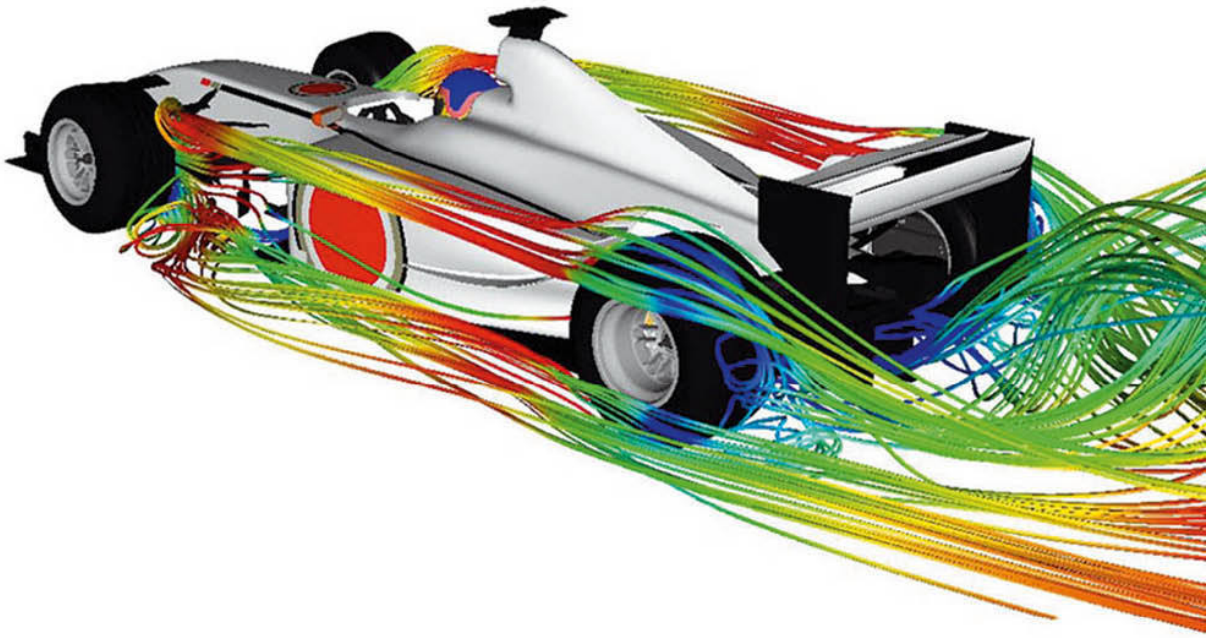
# Miscellaneous devices

QUITE A BIT of time and space has been devoted so far to some of the most obvious and best-known devices for generating beneficial aerodynamic effects around competition cars. This chapter is a brief survey of some of the other devices that have been used to increase downforce or reduce drag – or both – where possible, or which can't be avoided, yet still influence aerodynamics, like wheels!

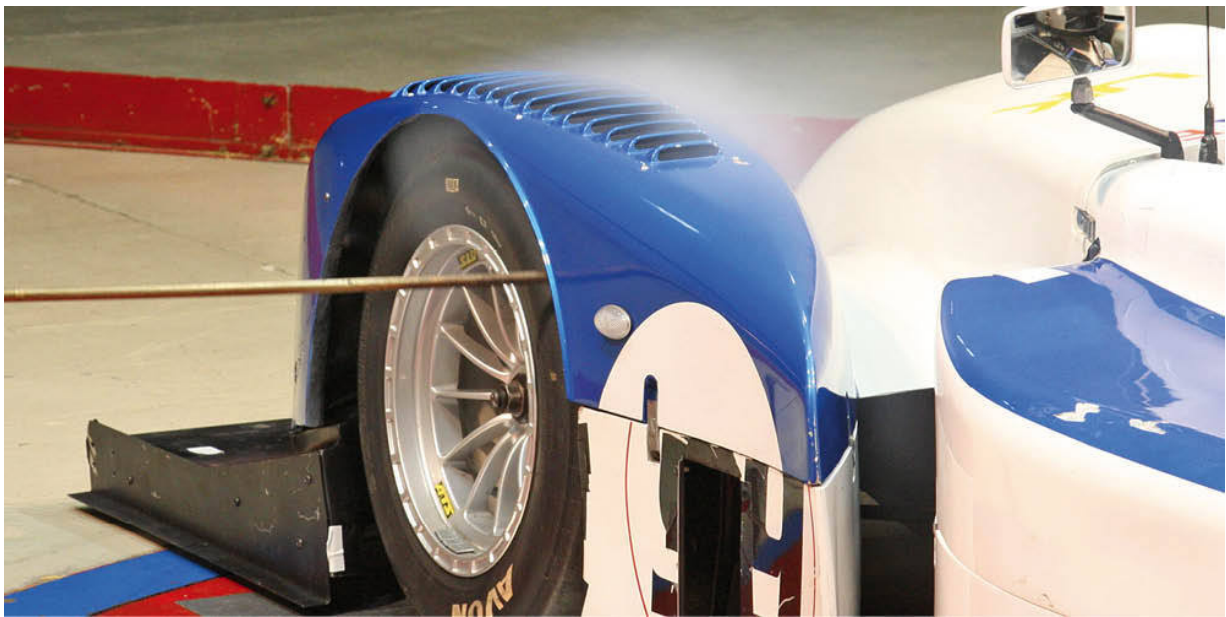
### **Wheels**

There's no getting away from the need for wheels (and tyres) in our type of motorsport. Also, there is no getting away from the aerodynamic havoc that wheels create either, especially on open-wheel competition cars. For example, the wheels apparently create a third or more of the total drag of a Formula 1 car. Keeping in mind that Formula 1 wheel widths are relatively narrow these days, certainly compared to some less restrictive racing categories, it is likely then that other types of single-seater will see an even bigger proportional drag contribution from their wheels. Of course, in the case of wingless racecars the wheels' drag contribution will represent an even bigger proportion of total drag. Adding to the drag that wheels create, they also very often generate positive lift (although as we'll see later in this chapter, this can be reversed, even on an open-wheeler...).

One of the problems with wheels is that the flow over, around and, especially, behind them is extremely difficult to model or predict, complications arising largely from the flow separations that occur over the top and around the perimeter of rotating wheels. The combination of factors such as their design and shape, rotation, contact with the ground; variable yaw angles (and steering angles at the front) all add to the complexity of trying to assess how they affect the airflow. Wind tunnel models ideally need to have rotating wheels if reliable measurements are to be made, and the same applies to CFD models too.



*The flow around the wheels is complex, as this BAR Honda CFD model demonstrates.*



*Smoke emerging from the wheel arch louvres of the Ligier JS49 sports racer. Notice how the smoke has travelled forwards in the wheel arch, even with non-rotating wheels.*

But what can be done to alleviate the adverse effects of wheels? One of the most basic approaches would be to examine the size of wheel to use, since

wheel drag is obviously proportional to wheel frontal area. Usually this factor is tied down in the regulations, but if it isn't, and this part of the aerodynamics of the car is likely to be significant to performance, then it is probably worth considering, especially as the wheels can be such a big contributor to overall drag. After that it is a case of trying to 'manage' the airflow around the wheels to lessen their adverse effects. Obviously, solutions depend fundamentally on whether the car is open-wheeled or closed-wheeled, as well as technical regulations.

Open-wheeled cars have been using various deflectors to try to tidy up the airflow in the vicinity of the wheels for some time now. Much effort is concentrated at the front of the car, the wake of the front wheels being likely to heavily influence the aerodynamic performance of everything else downstream. Bargeboards and similar deflectors exist at least partly to try to improve conditions behind the front wheels. 'Flip ups' on the front wing end plates and some of the devices on front wings ahead of the front wheels, and on the sidepods ahead of the rear wheels obviously deflect air over and around the wheels, potentially inducing some downforce in the process as well as modifying the airflow ahead of and behind the wheels so that drag is reduced. Making the central body at the front and the rear as narrow as possible is also at least partly about giving the air somewhere to go between the wheels.

With closed-wheelers the situation might appear to be simpler, but can in fact be more complex than with open-wheelers. Enveloping bodywork obviously shrouds the wheels from much of the air that they would otherwise encounter, and this is the basic reason we expect a lower drag coefficient from a closed wheeler, but air still enters the wheel wells from in front, underneath and out to the sides, and how it is dealt with can have significant effects. It is also the case that rotating wheels can act as pumps in semi-enclosed wheel wells, an effect that increases with vehicle speed to the extent that air can be drawn into the wheel wells from the rear and pumped out at the front, according to one former wind tunnel operator writing to *Racecar Engineering*.

Often, such efforts to improve things will involve ducts, cutaways and louvres that in general help air to escape from wheel wells. The louvres on top of sports prototype wheelarches are present to help reduce the differential that can exist between the low static pressure over such a curved wheelarch compared to the static pressure in the wheel well, a potential source of undesirable positive lift. The cutaways often present on the vehicle sides behind the front wheels also assist air to escape not only from the wheel wells, but also from under the entire front of the car. As such these features often

work in concert with front splitters and diffusers, providing an exit for air that has been exploited further forwards on the car.

## Ducts

A number of the systems around a competition car, such as oil and water radiators, brakes and even electronic systems, are air-cooled, and the induction system of the engine needs a feed of air for the purpose of producing brake horsepower. Diverting air to these systems – or worse, just sticking a radiator matrix out into the airstream – can cause drag, and if we're unlucky or careless, aerodynamic lift as well. Ducts allow us to utilise the energy of the airflow to do the jobs we want with the minimum of aerodynamic losses.

Three types of ducts have been categorised on competition cars according to their type of inlet; the ‘straight through or ram air inlet’ (as in the front or side-mounted radiator for example); the high-mounted ‘scoop’, such as that used to feed air to a competition car engine, and the ‘flush duct’ or ‘NACA submerged inlet’ duct. Each has different but well-established design characteristics that are present for good reasons. Very many competition cars seem to ignore some of the basic principles here, undoubtedly at some cost to aerodynamic efficiency. A little extra care will help to minimise penalties.

### Straight through ducts

The straight through duct is the type most often used to feed air to and from engine (and other) radiators. But why bother with a duct? After all, it's lighter and cheaper just to bolt a radiator to the side of a single-seater, for example, than to mess around shaping metal or glass fibre panels. The reasons are very simple and have been known for a long time, as the late Carroll Smith showed us in *Tune to Win* in 1978, quoting pre-Second World War experiments on ducted and unducted heat exchangers. The drag coefficient of a radiator just hung on the side of an aircraft (or vehicle) was between seven and 13 times higher than nicely ducted systems. Furthermore, the heat exchanging efficiency of a radiator thus ducted was higher. Both thermal and aerodynamic efficiency are improved if we slow the air down ahead of the radiator, and to do this we need a proper duct.



*A nicely radiused duct inlet, with a nicely radiused 'reducer' being installed.*



*A nicely radiused duct inlet, with a horrible taped reducer in place.*

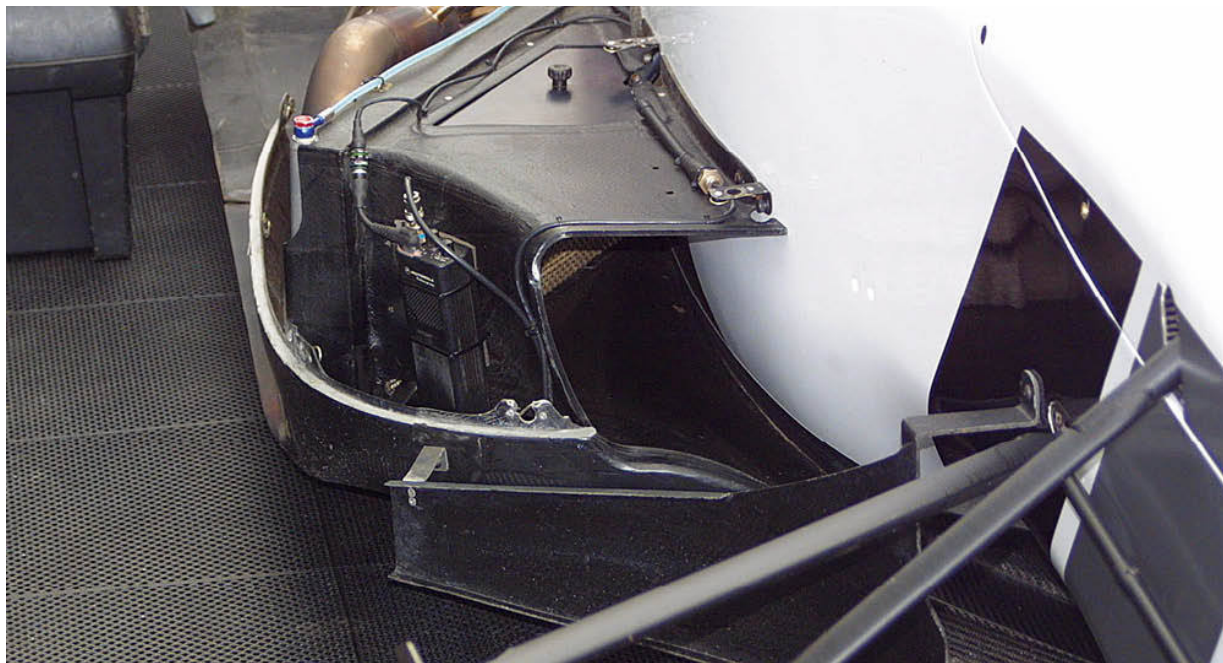
How do we design a 'proper duct'? First there must be a pressure drop that actually drives air through the system, so the inlet needs locating where the air's energy is high so that this can be converted to high static pressure, and the exit must be positioned where the static pressure is lower than at the inlet. The inlet itself must have radiused lips all round so that when our vehicle is

even at a quite modest angle to the approaching airflow, that airflow does not separate as soon as it enters the duct. Then the air needs to be slowed down to increase the dwell time for heat exchange within the radiator, and to reduce the pressure drop, and hence the drag, across it, so there must be as gentle a diffuser section as space (and rules) permit immediately after the inlet. All of the air must pass through the radiator matrix, with as even a velocity across the radiator face as possible, so the diffuser (and the section aft of the radiator) must be sealed to the radiator matrix (foam strip is often used for this purpose). The air then needs accelerating up to or near to freestream velocity again, so the duct cross-sectional area must gradually contract after the radiator matrix. Finally, the exit needs to feed the air back into the airstream with as little disruption to the external flow as possible. Ideally, like the top professionals, we should have a range of inlet and/or exit duct panels to select from so that we can change the area of one or both to optimise and adjust the system to the prevailing conditions. This is a lot better than the age-old and horrible technique of blanking off either the inlet or the exit with race tape. How do you think the designer of your car feels after he has provided you with a nicely radiused inlet feeding into a diffuser, and you slap a flat piece of tape across the inlet, thus negating much of the benefit all his effort brought you, and for which you paid him!

Those are the generalities, and there are many possible solutions. It helps to look at how cars that have been designed with the help of CFD and/or wind tunnel programmes have achieved these aims. However carefully a radiator duct system appears to have been designed, there is one awkward, unavoidable fact that applies to all cars. There is but one ideal speed for a given radiator system to function at best efficiency, which means that at all other speeds it is operating at less than optimum efficiency. The best you can do is to discuss with your radiator supplier the power of the engine you are cooling (which will pretty much dictate how much heat needs to be disposed of) and the speed regime in which you most often operate the car. If he knows what he is doing he will then help you to select the correct radiator matrix area and thickness to provide adequate cooling, probably with some reserve to take account of unusually hot conditions. He will hopefully, then be able to advise on the preferred inlet and exit areas which, references suggest, will be somewhere in the rather broad range of 25% to 65% of the radiator area, depending on system efficiency and radiator location. Again, a look at common practice on cars you know have been designed well, and which operate in a similar competition environment to yours, will help here too.



*Reducer panels enable the radiator airflow to be optimised, as on this Reynard 011 ChampCar's 'flugelhorn' duct exit.*



*The diffuser section ahead of the Dallara F305's radiator.*

It is apparent from doing such an exercise that, for example, with space constraints ever-present, diffuser and contractor section shapes can't be all that critical, but it has to be worth at least trying to decelerate air in the diffuser gradually so as not to induce separations. Carroll Smith reckoned keeping the angle of diffuser wall divergence under 15° ought to keep you out of trouble

here, and if space dictates that greater angles are unavoidable then internal vanes may help prevent separation occurring.

A common mistake is to assume that a large (or larger) inlet size will benefit cooling, but trying to force too much air through a duct and radiator with a restricted capacity can actually cause reverse flow, which does nothing useful for drag or cooling efficiency, and can also cause external flow separations. The author has seen this effect in the wind tunnel on numerous occasions, and being able to witness the air flowing in the wrong direction, that is, forwards, in front of a side-mounted inlet duct, is definitely thought-provoking.



*The brake duct on this Williams F1 car seemed to align with the front wing end plate. (Rob Barksfield)*

A duct that can also fall into the ‘straight through’ category is the brake-cooling duct. These come in a wide range of shapes and sizes, depending on category and the demands involved. Clearly, the extent to which these, like any other ducts, protrude into the airstream has a large bearing on how effectively they do their primary job, but also on how drag (and downforce) can be affected. Such is their influence that, where permitted, different configurations might be run in qualifying and race trim. The risk of overheating the brakes on a single lap qualifying run has to be weighed up against the cost in lap time of the extra drag of ‘race sized’ ducts. Thus, smaller ducts could be used for qualifying, reverting to larger ones to ensure proper cooling in the race, or more simply (and crudely) part of the duct inlets might be blanked off. At an even more basic level, in categories where few braking applications are made, such as hillclimbing in the UK where the courses are pretty short, brake-cooling ducts are absent altogether.

## Scoops

The scoop inlet is so-called because it is raised above the car’s surface to ‘scoop’ fresh, high-energy freestream air. The distance it needs to be above the surface depends on where it is located on the car, the idea being that it is raised sufficiently to be clear of the boundary layer on the car’s adjacent surface. Thus, a front-mounted bonnet scoop may only need to protrude slightly above the surface to be able to draw in a good supply of freestream air. Similarly roof-mounted ventilation intake scoops protrude only a little. However, if located further back on the car a scoop would have to be raised higher to clear the inevitably thicker boundary layer.

Some of the same generalities apply to this type of duct as to the straight-through duct described above. Radiused inlet lips are still required, and in most cases the duct will need a diffuser section, it will need sealing to the system it is feeding, and if appropriate it will need a contractor section and a properly integrated exit. There is of course one typical application of the scoop duct that doesn’t require the contractor and exit, and that is the engine inlet scoop, often called the airbox. This has some of its own particular requirements since it needs to be matched as far as possible with the engine’s working rpm range and with the car’s speed regime, as the study below demonstrates.

Assuming technical regulations do not mandate an engine inlet restrictor, how big, and what shape should an airbox inlet be? Gut feel immediately suggests engine capacity and rpm are critical factors, but where do we go from there? A race engine, like any internal combustion engine, is a pump. The amount of air it shifts depends on its swept volume, rpm and volumetric

efficiency (the ability to pump more or, perish the thought, less than its actual capacity). It is relatively simple to calculate the volume (or mass) flow rate of air that enters the engine for a given engine size and across a range of rpm. Figure 7-1 illustrates this for a four-stroke engine of three litres capacity, and over a rev range representative of a 2005 Formula 1 engine, with the simplifying assumption that volumetric efficiency is 115% across the rev range.

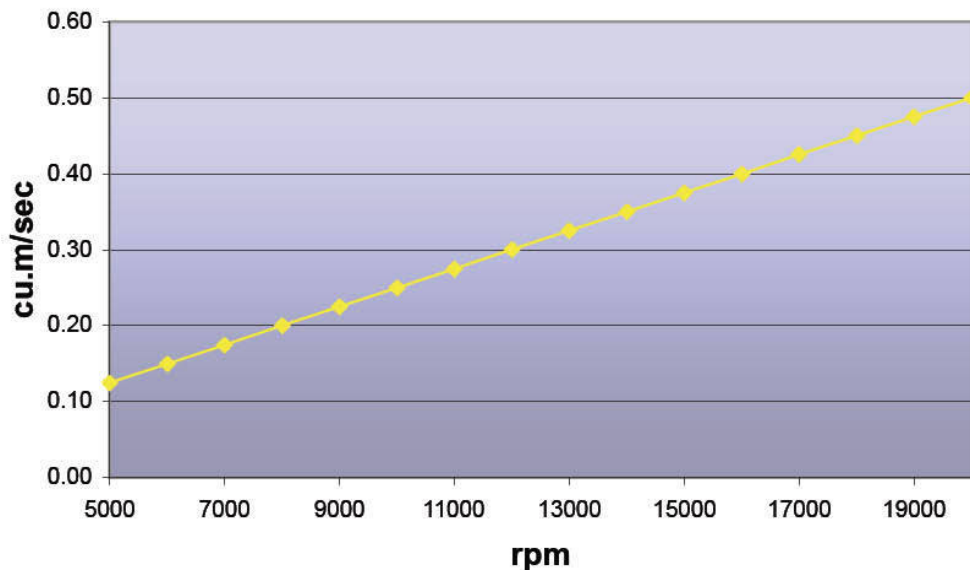


**Figure 7-1** Volume flow rate of a three-litre engine, 5,000rpm to 20,000rpm, assuming a constant 115% volumetric efficiency.

A reasonably large airbox volume is generally deemed necessary so that the engine has an adequate reservoir of slow moving, ‘clean’ air to inhale. For external aerodynamic efficiency the entry to the airbox inlet, and indeed the whole airbox should be small and, ideally, properly matched to the engine’s needs so that it scoops in just the right amount of air. A quick glance at Figure 7-1 will show that this engine has a wide range of volumetric flows across such a working rev range, while clearly, any engine with a reasonably broad rev range will have a variety of breathing requirements.

To determine how big the inlet needs to be, the following concept, suggested by Dr Rob Lewis of TotalSim (and formerly of Advantage CFD), relates the vehicle’s forward speed to the volume flow rate of air inhaled by the engine at various rpm levels, and considers the air being sucked in as a column

of air entering the airbox inlet. By dividing the volume flow rate by the car's speed it is possible to calculate the theoretical cross-sectional area of this column at the inlet, over the relevant range of car speeds and engine rpm. For clarity this can then be calculated as if it were the diameter of a cylindrical column, and this data is graphed in Figure 7-2.

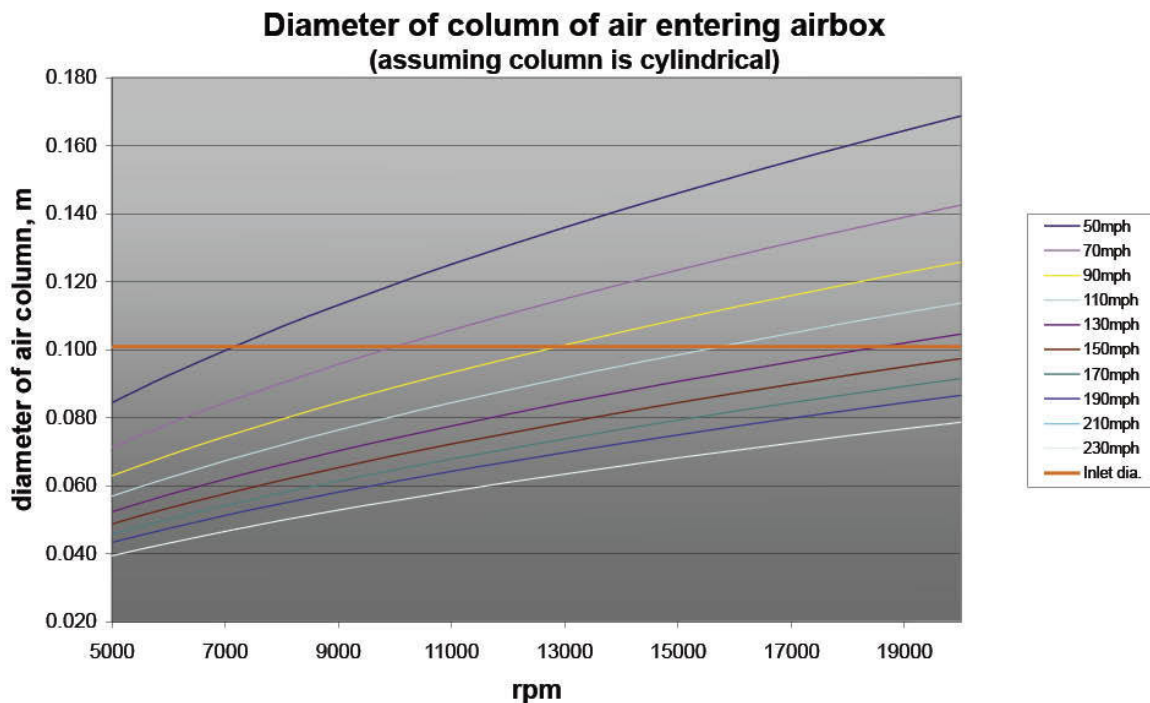


**Figure 7-2** The diameter of the column of air entering an airbox across a range of car speeds and engine rpm, assuming the column is cylindrical.

So, in short, the size of the column of air approaching and entering the inlet varies considerably with car speed and engine rpm, and yet, pretty obviously, the actual inlet orifice size is fixed on a racecar. Take a typical 2005 Formula 1 airbox inlet area, said to be  $0.008\text{m}^2$ , equivalent to approximately 0.1m in diameter if the orifice were circular, and is depicted in Figure 7-2 as the horizontal line marked 'inlet dia.'. Thus, when the column of air approaching the inlet is smaller than this the column will expand at the inlet, and when the column of air is larger than the inlet area then it must contract at the inlet. In either situation the inlet design must try to prevent unwanted flow separation using properly radiused edges and careful shaping.

Figure 7-3 shows this data calculated as the 'expansion ratio' of the air column by dividing this actual inlet area by the air column area at each combination of speed and rpm shown here. An 'expansion ratio' less than

100% means the column has to contract at the inlet, and a ratio greater than 100% means the column will expand at the inlet. The intersections of the line marked '100%' with the other graph lines shows the limited number of rpm/speed combinations at which the air column diameter actually matches the inlet size. (Obviously, if gearing was taken into account it would be apparent that many of these speed and rpm combinations will not actually be encountered, but disregarding those there are still many relevant combinations.)

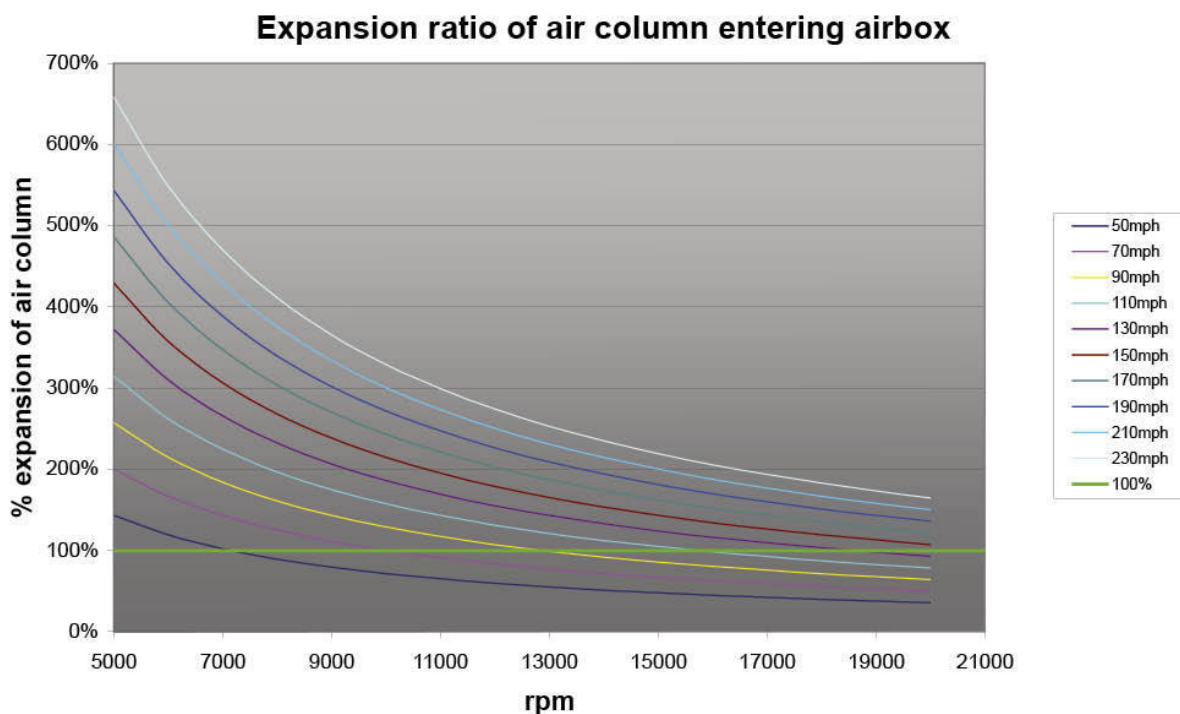


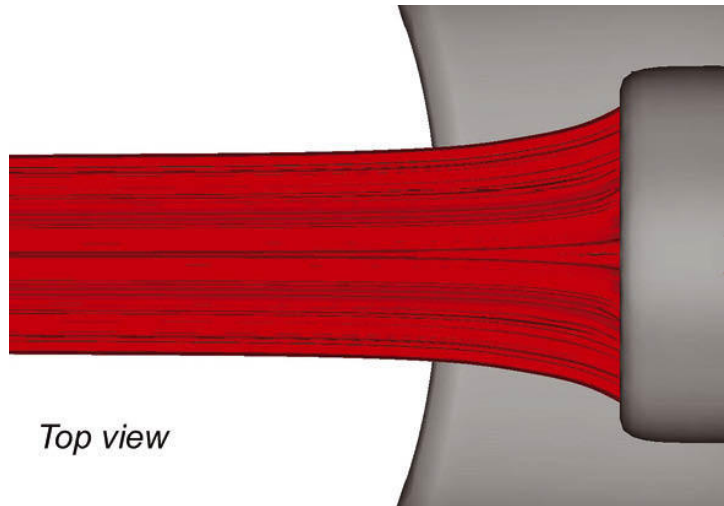
**Figure 7-3** The expansion ratio of the air entering the airbox inlet, as a percentage of the inlet area.

Contraction, it seems, loses more energy than expansion of the column, and would probably lead to less efficient power production. However, contraction occurs mostly at low car speed and high rpm combinations, where the likelihood is that power will exceed grip anyway so some losses would be tolerable. Nevertheless, the contracting airflow needs a smoothly radiused lip on the inlet to minimise the risk of flow separation here, which would increase those losses. In circumstances where the air column expands (see Figure 7-4) at the inlet (above the 100% line) clearly, the emphasis will be on designing an inlet that enables the initial expansion here to be smooth and efficient, again

requiring radiusd lips and smooth-shape transitions. The trick though is going to be to size the inlet orifice so that the airflow into the airbox is at its most efficient, which we might reasonably assume is when there is neither contraction nor expansion, at the rpm and speed combinations that matter most ...

In all cases the airbox then needs to expand the flow further and gradually towards the engine inlets so as to recover static pressure while avoiding flow separation. This requires a diffuser section, the length of which will possibly be dictated by regulations as well as practicalities (that is, available space). In the 1970s, when F1 rules permitted extremely tall airboxes, the thinking was that inlets needed to be high in order to grab 'clean' air. But often, the inlets were oddly shaped (tall rectangles for example) with sharp edges, neither characteristic being at all efficient. A round orifice is likely to be the most efficient since it has the greatest area relative to the length of its entrance periphery, at which boundary layer development, and hence losses commence.\* That these airboxes worked was possibly more because their height provided a long, gradual diffuser to slow the air down efficiently before it entered the engine.

\* For an area of  $0.008\text{m}^2$  a circle has a circumference of about  $0.317\text{m}$ , a square's four sides add up to about  $0.358\text{m}$  and a triangle's three sides add up to about  $0.380\text{m}$ .



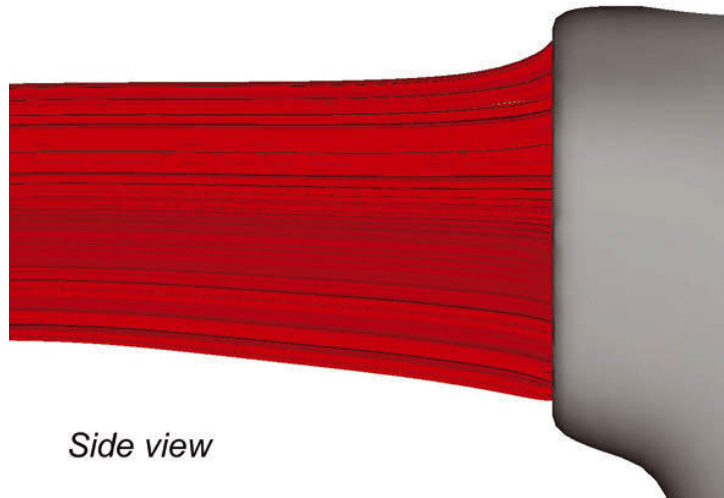


**Figure 7-4** CFD plots of an expanding air column entering a Formula 1 airbox.

Another interesting issue is the exploitation of ‘ram effect’, where an airbox inlet faces directly into freestream air. However, although reasonably significant at high speeds, this effect is smaller at motorsport speeds than is often thought. Figure 7-5 shows what can be achieved if the inlet catches and ‘stagnates’ (ie stops) the airflow and converts all its dynamic pressure (kinetic energy) into static pressure (potential energy) from which the engine can benefit. The graph is based on calculating the dynamic pressure ( $\frac{1}{2}\rho V^2$ ) at each speed, and then working out the increase in effective air density if all of that dynamic pressure was converted to static pressure, and then added to the absolute (ambient) air pressure. If we assume that engine power is proportional to inlet air density then Figure 7-5 suggests that at speeds over 200mph a gain in power of 5% or 6% *might* be possible (about 45bhp for a 2010 F1 engine) if the airbox is 100% effective.

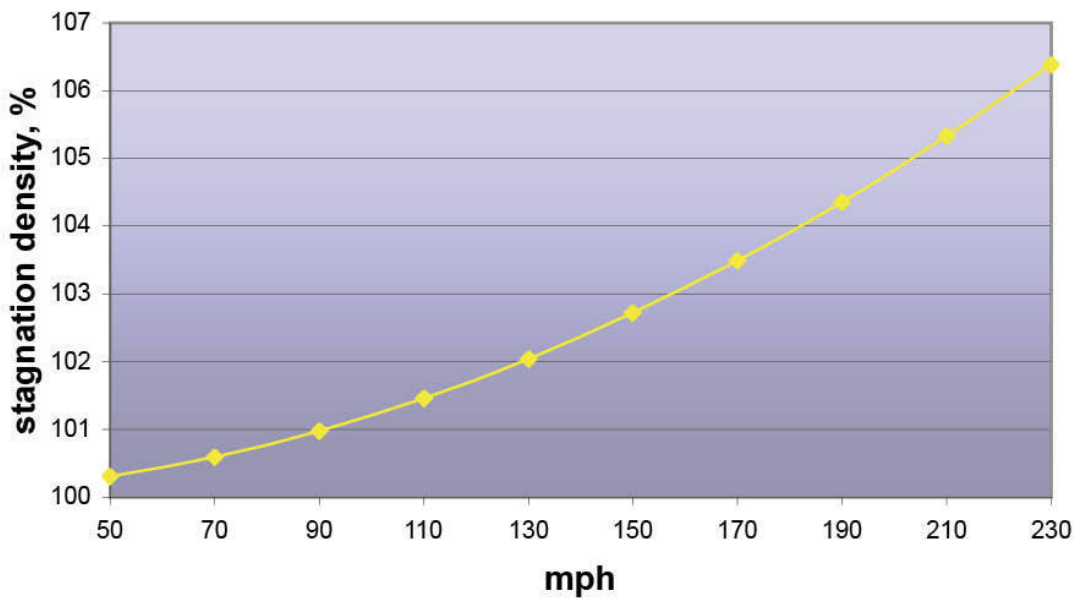


**Figure 7-5** Ram effect across a racecar speed range, assuming dynamic pressure is all converted to static pressure.

Perhaps of more significance, is feeding the engine with cool air since this provides the highest available air density right across the speed range. So the inlet needs to be positioned away from on-board sources of heat, and also well above ground level – air adjacent to the track surface can be much hotter than just a few inches above ground.

### NACA ducts

Otherwise known as a ‘flush’ or ‘submerged inlet’ duct, a NACA duct enables air to be directed, for example, to a cooling system with high efficiency and very little additional drag (other than that caused by the cooling system itself). However, to function effectively such a duct ideally needs locating in an area where the boundary layer is thin, and it should be orientated parallel to the local airflow direction. As such, these ducts are usually best located on the forward part of a competition car, although they can be seen in more rearwards locations.

The curious shape of the NACA duct exists for very good reasons. The idea is that air flowing towards the narrow opening of the duct flows down the gently sloping ramp (probably between  $6^\circ$  and  $10^\circ$ ), but the air that approaches from outside this central inlet flows over the edges of the diverging duct walls. As in any situation where the air flows over an edge at an angle, it forms a

vortex. In this case, two counter-rotating longitudinal (low static pressure) vortices are formed, one on each duct wall, and these induce more ‘outside’ air to flow down into the duct. It follows that the outer edges of the NACA duct need to be sharp to encourage this vortex formation. There are some obvious similarities between the NACA ducts and underbody diffusers in the way that vortex formation is encouraged and exploited to further reduce static pressure and enhance the flow through the system. Indeed, as we saw in Chapter 4, NACA ducts have been used to supplement front splitters to further accelerate the airflow under the splitter and so generate more downforce.

The duct ‘inlet’, in the conventional sense, is the area between the ramp floor and the lip on the forward-facing, upper, rearmost lip. Thus, as with other types of duct inlet, it is imperative that this lip is radiused to prevent flow separation occurring, and all the previously mentioned requirements for duct features downstream of the inlet still apply. Figure 7-6 shows the basic shapes and rules involved.



*A NACA duct on the top of the rear wheelarch of the Ferrari F550 GTS.*

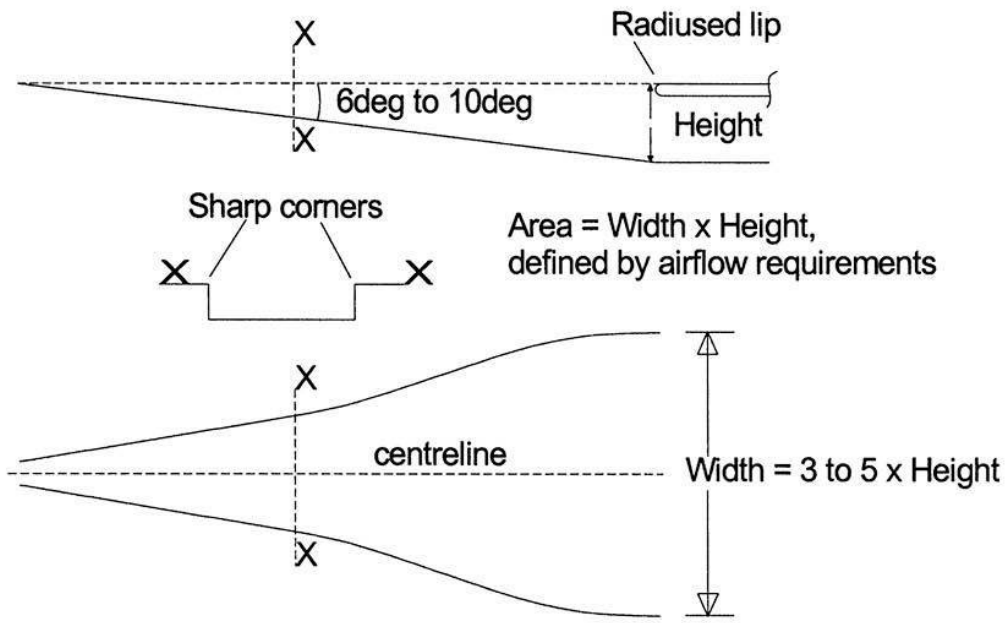


**Figure 7-6** The basic requirements of a NACA duct.

Allan Staniforth, in Race and Rally Car Source Book, provided a neat explanation of how NACA duct dimensions are actually derived. The method involves deciding first what the inlet area of the duct needs to be. This may be something that can be worked out, as he did with an example of an engine's inlet requirement at maximum rpm and speed (he calculated the volume flow rate required to feed the engine at maximum rpm, then worked out the area that this corresponds to at the car's maximum speed, echoing in part the study we looked at in the section above on scoops). In other circumstances it may be something that needs estimating (or guessing).

If you start with a required area you can then apply the rule of thumb for the width-to-height ratio (between 3 and 5 to 1, as shown in Figure 7-6), and calculate the requisite height (depth) of the duct. If you then apply the rule of thumb for the ramp angle you can use trigonometry (or a ruler and a protractor, if you prefer to draw this out) to work out what the overall length of the duct needs to be. Clearly, a steeper ramp angle will give a shorter duct, which is not necessarily a good thing – a typical ramp angle is likely to be 7° to 8°. Use the following table to help work out the required length of the duct:

Ramp angle: 6°

$$\text{Length} = \text{Depth} \times 9.5$$

Ramp angle: 7°

Length = Depth x 8.1

Ramp angle: 8°

Length = Depth x 7.1

Ramp angle: 9°

Length = Depth x 6.3

Ramp angle: 10°

Length = Depth x 5.7

A set of coordinates that define a NACA duct in plan view is given here which, in conjunction with the guidelines above and in the drawing in Figure 7-6, will enable a duct to be drawn which matches what millions of dollars worth of aeronautical research figured out for us. It would be rude, careless even, to not utilise the fruits of all *that* effort. The coordinates given should be multiplied by the length (L) and width (W) figures worked out using the above method, and will define one of the duct sides, in plan view. This should then be mirrored about the centreline to produce the other side. The ‘origin’ or ‘zero point’ if you will, is at the narrow, upstream end of the duct.

X/L: 0.0

Y/W: 0.083

X/L: 0.1

Y/W: 0.158

X/L: 0.2

Y/W: 0.236

X/L: 0.3

Y/W: 0.312

X/L: 0.4

Y/W: 0.388

X/L: 0.5

Y/W: 0.466

X/L: 0.6

Y/W: 0.614

X/L: 0.7

Y/W: 0.766

X/L: 0.8

Y/W: 0.916

X/L: 0.9

Y/W: 0.996

X/L: 1.0

Y/W: 1.000

Take note that there are plenty of ‘off-the-shelf’ moulded ducts now available whose manufacturers do not appear to have taken this valuable information, or the generalised requirements of this type of duct, into account, and whose products may not, therefore, be all they’re cracked up to be.

### Front wing strakes

A truism of racecar aerodynamics might be ‘what happens at the back of the car affects what happens at the front, and vice versa...’ Another maxim might be that one can rarely make reliable assumptions about the likely benefits of a modification, and in particular the overall effects, however small the modification may be. This is why the ability to model the effects of changes is so valuable. The following CFD study illustrates the surprising ramifications of a very small change at the front of a Formula 1 car.

A frequently seen feature on open wheel racecars is the front wing strake, a vertical fence attached to the underside of the wing a little way inboard of the end plate, probably at some small angle to the centreline of the car and most likely curved in plan view. Figure 7-7 shows the geometry of one strake set-up evaluated by CFD on a 2001 BAR Honda F1 car.

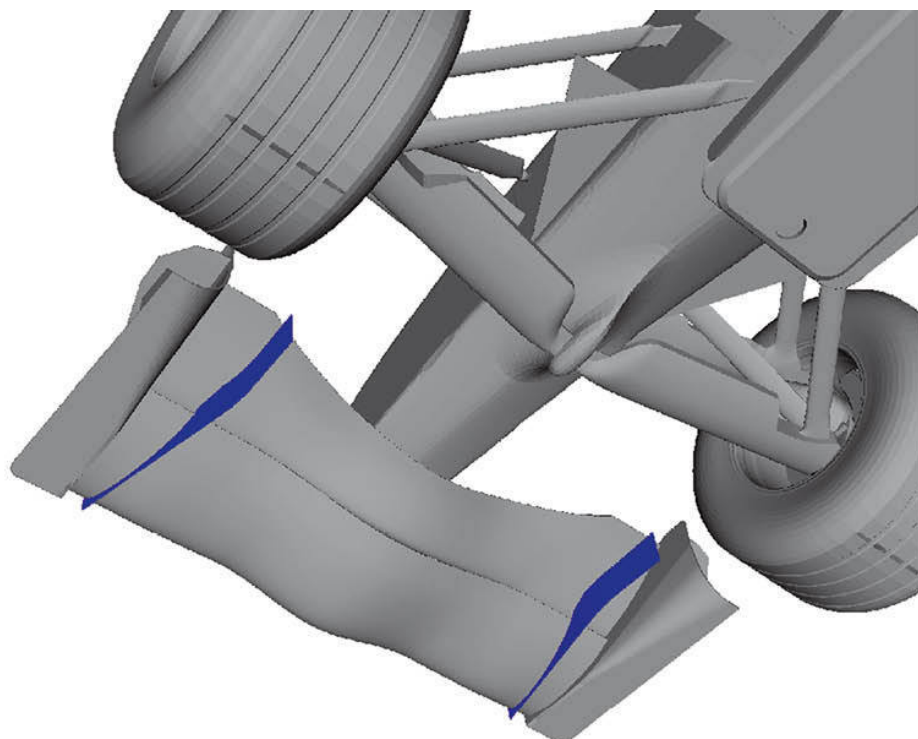


**Figure 7-7** Front wing strakes tested on a digital model of this 2001 BAR Honda.

What benefit would have been sought from the fitment of devices like this? The strake is one of a family that Milliken & Milliken (see Appendix 2) describe as ‘flow control devices’ that are capable of exerting a greater influence on the overall aerodynamic forces (and their distribution) than the forces the devices themselves experience. More specifically, the role of such a device is ‘locally guiding the flow’. The obvious inference to draw from this is that steering the flow with strakes under the front could have a local benefit to the front wing. However, the Millikens also suggest that there might be changes to static pressure distributions, velocity (speed as well as direction) and vorticity (flow rotation), and given that the devices are installed at the front of the car, it might also be reasonable to expect changes to manifest themselves some distance downstream.

This study produced some expected results and some unexpected ones. Front wing downforce did indeed increase, but only by around 0.3%, while intriguingly, rear wing downforce increased by 3.1%. This result immediately affirms both our opening statements, and also points to the surprisingly ‘global’ effect that these small plates had on the airflow. Other results bear this out too, as the table shows. (We can only relate percentage changes, not absolute forces, for confidentiality reasons.)

#### Total

Downforce change: +0.5%

Drag change: +0.1%

#### Body (excl. wheels)

Downforce change: -0.4%

Drag change: +0.7%

#### Front body

Downforce change: -1.7%

Drag change: -

#### Rear body

Downforce change: +0.5%

Drag change: -

#### Front wheels

Downforce change: +50.6%

Drag change: +1.5%

#### Rear wheels

Downforce change: +8.7%

Drag change: -2.6%

Front wing

Downforce change: +0.3%

Drag change: +0.1%

Rear wing

Downforce change: +3.1%

Drag change: +1.9%

Front mainplane

Downforce change: +1.0%

Drag change: -0.7%

Front flap

Downforce change: +1.0%

Drag change: +0.7%

Front end plate

Downforce change: -3.9%

Drag change: -6.9%

Rear top mainplane

Downforce change: +4.1%

Drag change: +3.3%

Rear top flap

Downforce change: +2.7%

Drag change: +2.6%

Rear upper forward

Downforce change: +1.0%

Drag change: -10.2%

Rear lower

Downforce change: +1.0%

Drag change: -2.6%

The overall result of fitting the strakes was a 0.5% gain in downforce for a 0.1% increase in drag, a small but efficient benefit, but there was also a rearward shift in overall balance, further emphasising that changes at the front have effects at the back. The dominant producers of change were actually the rear wing, which created more downforce but also as a result more drag; the lift generated by the wheels, which changed significantly, especially at the front, as shown in the table as a downforce increase; and as suggested by the reduction in ‘body’ downforce at the front (where the ‘body’ is everything except the wheels) there was also a loss of downforce from the underbody, particularly in the forward section.

So why did these strakes cause these changes? The first point to make is that a reduction in mass flow under the car was determined, and this would explain the reduction in underbody downforce (less air flow = less flow contraction = less velocity increase = less reduction in static pressure). A decrease in mass flow under the car would probably mean increased flow over the car, hence the rear wing receives faster flowing air so it generates more downforce (and drag).

But how could such a small pair of devices as these wing strakes alter the flow pattern to this extent? It seems that a vortex formed on the inside face of each strake, which had the effect downstream of deflecting more air over the car and less beneath it. Figure 7-8 is a simulated oilflow comparison showing how the flow across the underside of the front wing and especially the flap was subtly altered by the strakes. This superficially minor change to the flow pattern at the wing surface near the strake is evidence of this vortex formation.

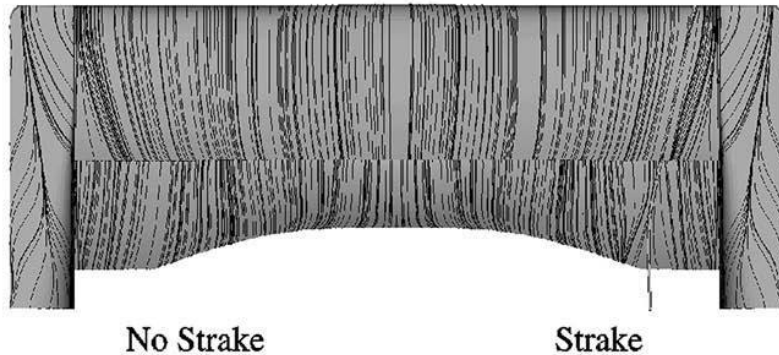


**Figure 7-8** The flow across the lower surfaces of the front wing and flap, with and without the strake.

Figures 7-9 to 7-12 are Delta\_Cp plots from various viewpoints of the car, and these show the differences in the static pressure coefficients ( $C_p$ ) over the car's surfaces as the result of fitting the strakes. Blues and greens show where static pressure decreased, and reds and yellows where it increased. An increase on an upper surface indicates an increase in downforce, as does a decrease on a lower surface, and vice versa. Similarly, an increased  $C_p$  on forward-facing surfaces shows more drag, as does a decreased  $C_p$  on a rearward-facing surface, and vice versa.

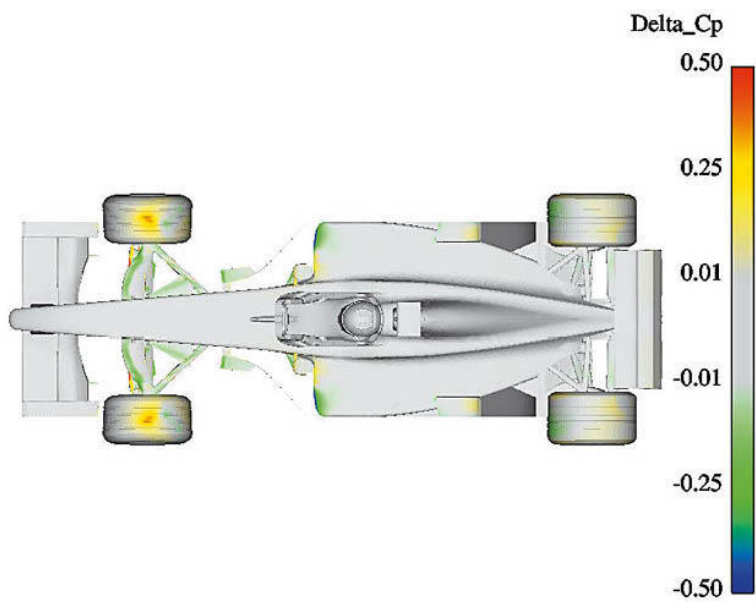


**Figure 7-9** Static pressure changes on the upper surfaces.

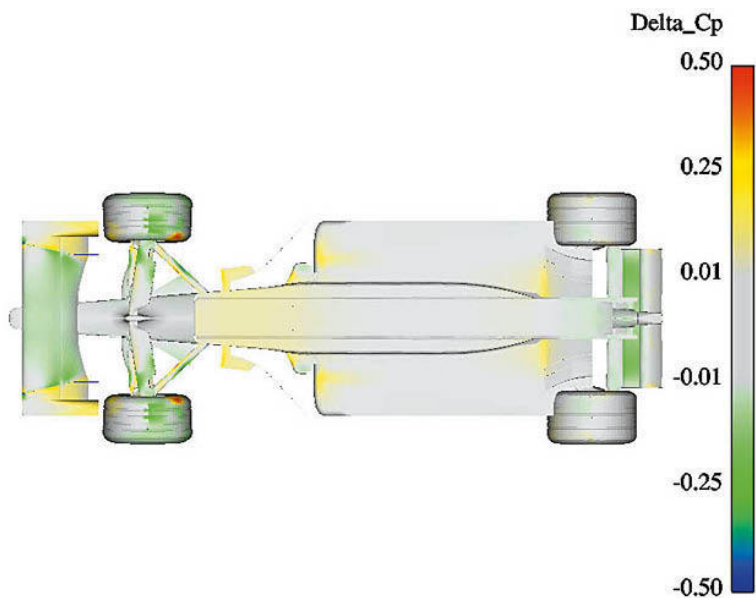


**Figure 7-10** Static pressure changes on the lower surfaces.

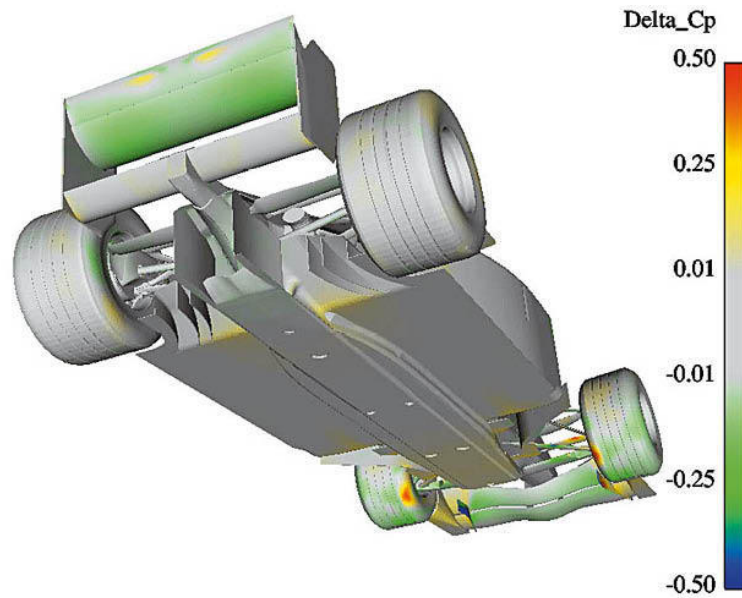


**Figure 7-11** Static pressure changes on the lower and rear surfaces.

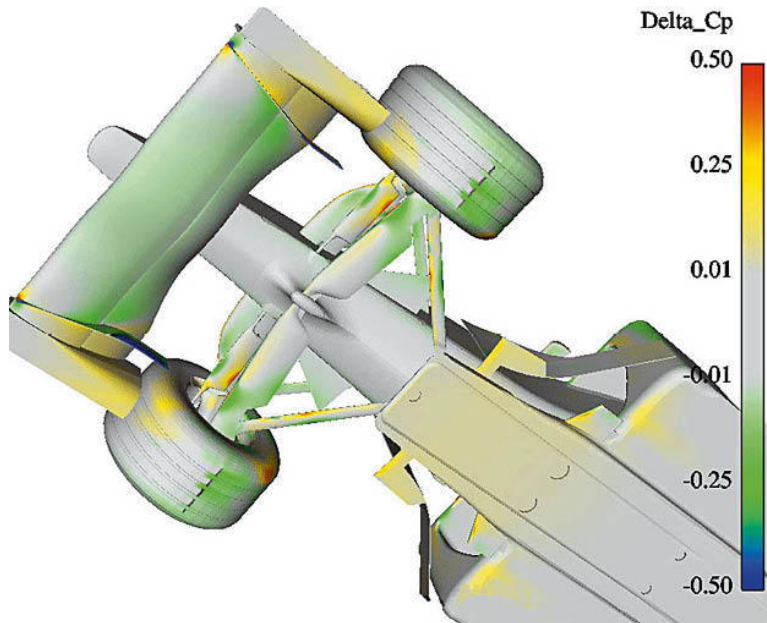


**Figure 7-12** Static pressure changes under the lower half of the car.

Figure 7-9 shows an increased  $C_p$  on the front tyre tops, which corresponds with the drop in front wheel lift. Figure 7-10 illustrates the areas under the front wing and the rear wing that produced lower pressure (= more downforce), and also that the front of the underbody and the transition into the diffuser developed an increased  $C_p$ , corresponding with reduced

downforce here. Figure 7-11 shows that not just the rear mainplane underside developed lower pressure but also the flap. The gains and losses at the front of the car can be seen in Figure 7-12, with less downforce from the outboard sections of the front wing, but by virtue of the large portion of its span at lower pressure, there is more downforce from the span between the strakes, and the front wing overall. The decreased  $C_p$  visible on the inside face of the strakes (the blue area arrowed) is further evidence of the above-mentioned vortex.

So, there have been gains and losses from areas all over the car, some surprising, some not, with a small, net overall benefit in downforce and a rearward shift in balance. That the overall gains were at the ‘wrong’ end of the car should make us wary of presumptions and keener to check things out carefully. Of course, a different strake configuration may have yielded a quite different result.



*These strakes on the Dallara F308's front wing had a modest but beneficial effect in the MIRA wind tunnel*

A wind tunnel study on front wing strakes makes for interesting comparison with the foregoing CFD study. It was, apparently, often hard to obtain sufficient front downforce on the pre-2012 Formula 3 Dallara F308 to be able to optimally balance the car. One of the devices used to address this situation

was the front wing strake. In a MIRA wind tunnel session on the Fortec Motorsport F308 and its (then) brand new F312, the front wing strakes of the F308 were evaluated by removing them from under the front wing main element. There were two pairs, outer and inner, and the outer ones were removed first and the inner ones second. The table below shows the results in counts of adding the inner ones first followed by the outer ones.

+ inner

$\Delta CD$ : +2

$\Delta Cl$ : +5

$\Delta CL_f$ : +1

$\Delta CL_r$ : +4

$\Delta\%_{front}$ : -0.3

$\Delta L/D$ : +1

+ outer

$\Delta CD$ : +1

$\Delta Cl$ : +53

$\Delta CL_f$ : +38

$\Delta CL_r$ : +15

$\Delta\%_{front}$ : +1.4

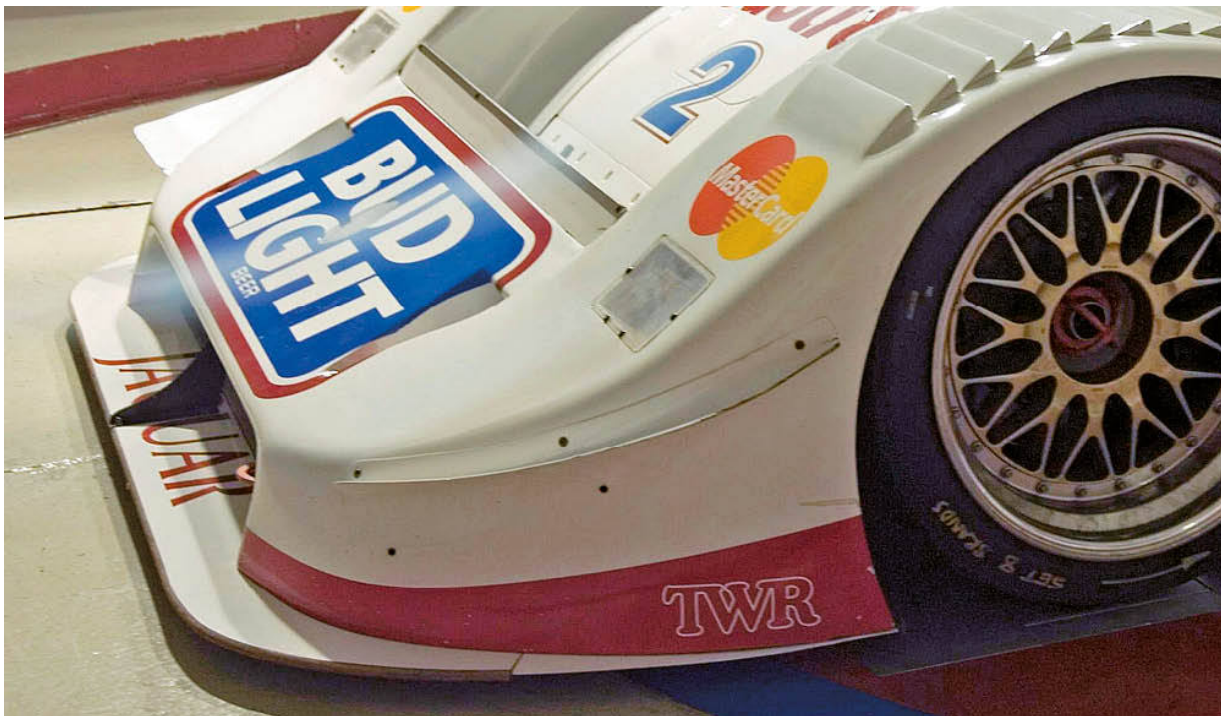
$\Delta L/D$ : +87

The inner strakes alone had a very small effect, adding a little rear downforce but having almost negligible effect at the front. The outer turning vanes were quite another matter though, adding a decent downforce increment (about 0.4% total) for negligible extra drag, and they provided a forward balance shift in the process. Because of the methodology we cannot tell if the inner and outer turning vanes were acting jointly or whether the outer ones were doing all the work and would have done just as much on their own. If their mechanism was to control and exploit the wing tip vortex, and perhaps steer it in a way that helped the wing and other downstream components, then one suspects that the outer ones on their own would have done most of the job, but perhaps not as well as the combination did. Nevertheless, the benefit of having them both there was clear.

## Dive planes

Another device frequently seen on closed wheel competition cars is the dive plane, or dive plate if you prefer, so called because of the resemblance to the devices on the bows of submarines that assist those vessels to dive. They are

also frequently but improperly referred to as ‘canards’. In their simplest form on competition cars they are flat or curved plates, inclined downwards at the front, and they are generally attached low on the forward corners of saloon/sedan, GT and sports racing cars. Such inclined plates would be expected to create an increment of downforce, but as with most things aerodynamic their overall effects can be surprising and varied.



*Dive planes on the 1991 IMSA GTP Jaguar XJR-16. (MIRA)*



*This Noble M400 also featured steep dive planes.*

One of the more surprising reported examples was on a Nissan sports prototype in the mid-1980s, where overall downforce increased considerably to levels that, it was said, could not possibly have arisen from the dive planes alone. In this case it was postulated that the dive planes set up a vortex that ran down each side of the car that acted like an invisible skirt to help the profiled underbody – which featured large diffuser tunnels – to generate more downforce. However, in the examples below we'll see more modest results, and furthermore that the effects differed in detail between each case examined.

Looking first at a MIRA full-scale wind tunnel study of a 1991 IMSA GTP specification Jaguar XJR-16, the photo shows the dive planes fitted to the car at the start of this test session. It also shows the attachment holes for a much more aggressively angled set that was also evaluated. The car was baseline tested with no dive planes, and the table shows the results from these three configurations as coefficient changes relative to the ‘no dive planes’ case.

Change, counts: Shallow dive planes

CD: +18

–CL: –52  
–CL front: +36  
–CL rear: –89  
% front: +1.61% absolute  
–L/D: –88

Change, counts: Steep dive planes

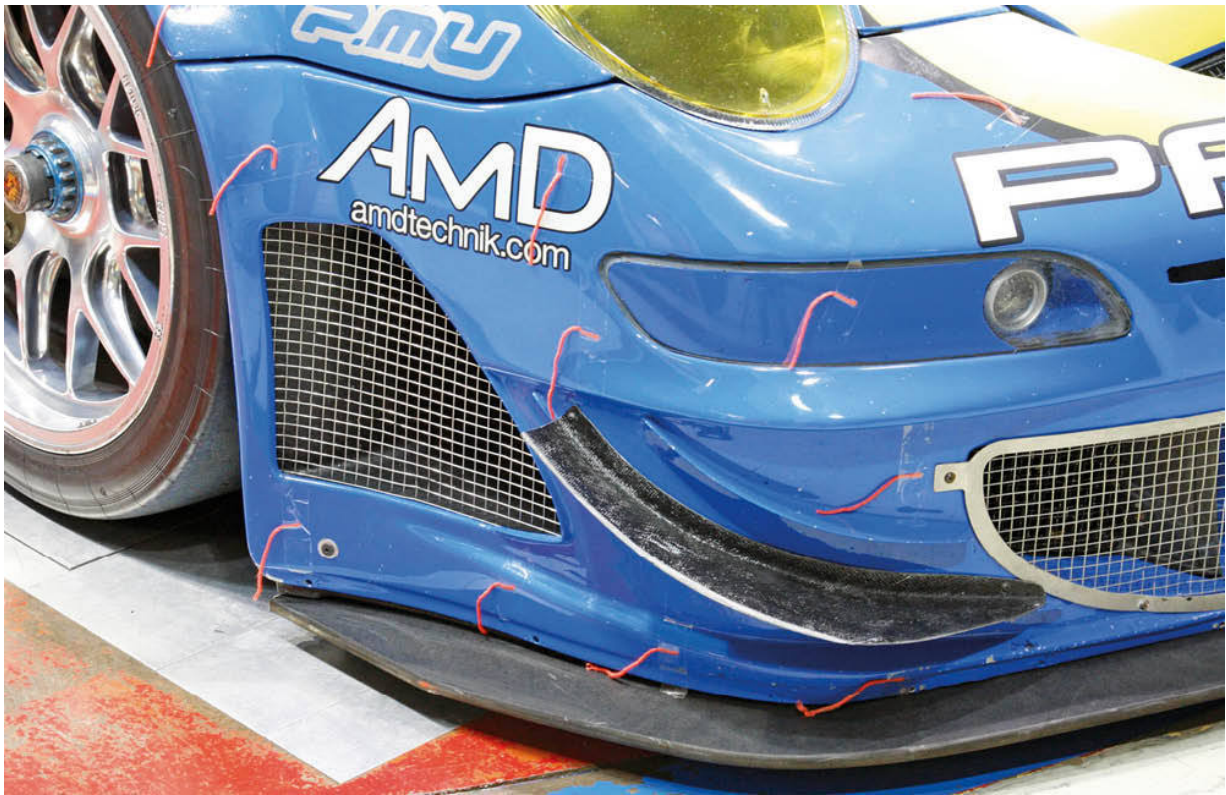
CD: +21  
–CL: –23  
–CL front: +102  
–CL rear: –124  
% front: +3.32% absolute  
–L/D: –107

The first surprise here was that fitting the shallow dive planes knocked 52 counts off the total downforce (a change in –CL of 0.052). However, it is apparent that the balance was more to the front, and in fact the front lift coefficient went up by 36 counts with the shallow dive planes fitted. However, the rear lift coefficient decreased by some 89 counts.

Comparing this to the steeper dive planes, the total downforce still decreased relative to the no dive planes configuration, but by just 23 counts. And the balance was shunted significantly more to the front as the front lift coefficient increased by 102 counts while the rear lift coefficient decreased by 124 counts over the no dive planes case. So, while both types of dive plane added front downforce, they also knocked off rather more at the rear. Note too that drag increased with either type of dive plane, and efficiency decreased in both cases. So these dive planes were useful but inefficient balance shifters.



*The Radical SR10 LMP1 car's dive planes proved rather more efficient.*



*The modified ALMS GT2 Porsche 997's modestly extended dive planes also worked quite efficiently.*

On the Britcar Noble M400 of Paul Cundy, the dive planes were of roughly similar plan area to those on the IMSA Jaguar above. However, they were set at a pretty steep angle, though at similar height to the Jaguar relative to the front upper bodywork. The coefficient changes 'with' dive planes relative to 'without' dive planes on the Noble are shown in the table below.

Change, counts: With dive planes

CD: +11

-CL: -6

-CL front: +66

-CL rear: -73

% front: +12.95% absolute

-L/D: -34

In this instance, drag increased by 11 counts with the fitting of dive planes, and overall downforce reduced by 6 counts, the combination dropping efficiency by 34 counts, or over 3%. However, the effect on balance was very

marked in percentage terms, this of course being the result of a significant change in the front  $-CL$  value, which itself was quite a modest value compared to the Jaguar GTP car.

Common factors here were that all the dive planes examined were quite large, and all terminated above the wheel centres. And smoke visualisation on the Noble showed the wake from the dive planes merged with that from the side mirrors and impinged on the outer portions of the rear wing.

The results on the Eco Racing Radical SR10 LMP1 racer were rather different to the previous two cases, in both of which we saw front-end downforce increase as expected, but also rear downforce decreased, seemingly because the dive planes adversely affected the airflow to the outer portions of the rear wings on those cars. Efficiency ( $-L/D$ ) also reduced in both those previous cases. The table below shows the results of fitting a second pair of dive planes to the Radical SR10.

#### Change, counts

$CD$ : +17

$-CL$ : +50

$-CL$  front: +48

$-CL$  rear: +2

% front: +2.1% absolute

$-L/D$ : +10

So in this instance the dive planes produced the expected gain in front downforce but also a gain in efficiency ( $-L/D$ ), this partly arising because of no loss of rear downforce, enabling a pretty efficient gain to be made overall. What distinctions are there in the way these dive planes were deployed compared to the other two cars? In the case of the Noble GT we saw very steep dive planes located quite high on the front body sides, and using smoke visualisation their wakes were observed to impinge on the rear wing's outer portions. The IMSA Jaguar on the other hand ran shallower dive planes that were also quite low-mounted, not dissimilar in fact to the Radical's. The difference between the two sports prototypes, though, was the presence of the dual element lower wing tier on the IMSA car, upon which the dive planes' wake could impinge. However, the LMP1 Radical could only use a single wing tier and it was mounted high, seemingly above the path of the dive planes' wake and as such 'out of harm's way'. Nevertheless, it is unusual for a gain in front-end downforce that is achieved by using a device ahead of the front axle

not to take off some rear downforce, so there must have been other interactions going on here as well.

One last example reinforces the variation that arises with dive planes but also

helps to better understand them. On the ‘Paragon’ Porsche 997 ALMS GT2 car the effects of adding a pair of modest dive plane extensions to the tiny ‘works’ dive planes were as follows:

Change, counts

CD: +20

-CL: +36

-CL front: +44

-CL rear: -9

% front: +5.03% absolute

-L/D: +14

So here we had a modest front-end gain, a small rear-end loss, and overall a reasonably efficient balance shift.

What general conclusions can we draw about dive planes, then? We can perhaps say that by adding dive planes like those featured here:

- Drag increases
  - Front downforce increases
  - Rear downforce might decrease
  - The aerodynamic balance shifts to the front
  - Efficiency ( $-L/D$ ) might decrease if rear downforce reduces but might increase if not.
  - The effects will depend on the dive plane size and its steepness
- In short, dive planes can be very useful but need to be deployed with care.

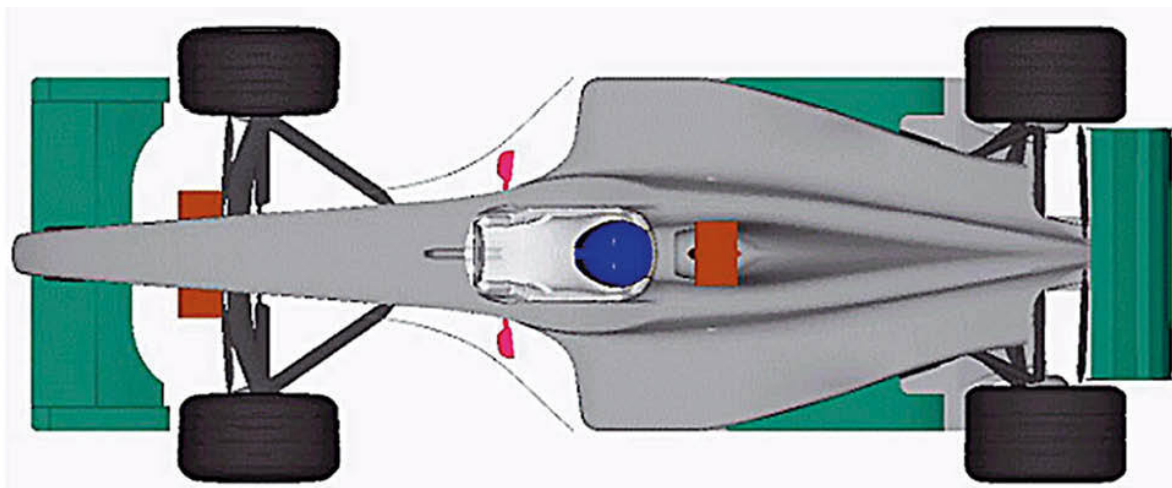
## Bargeboards

Much has been said and written about the purpose of bargeboards, but one thing we can confidently say is that they fall in the same class of device as front wing strakes, which is to say they are another ‘flow control device’.

Coming in a wide range of shapes, sizes and specific locations, bargeboards can simplistically be described as more or less vertical plates, curved in plan view, located close to the chassis sides, usually though not always aft of the front wheels, and ahead of the sidepods. Superficially, one might reasonably assume they ‘manage’ the airflow in the region between the front wheels and

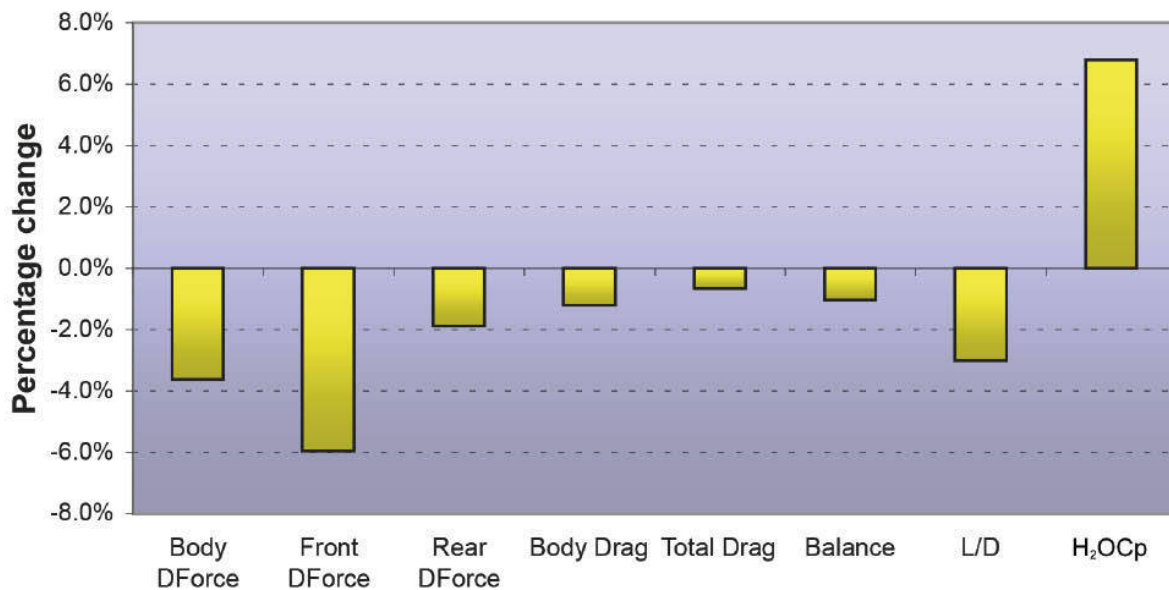
the chassis, in particular ‘steering’ the front wing and wheel wakes. But as they have developed, their increasingly three-dimensional shape, the appearance of ‘saw-tooth’ lower lips and so forth, suggest they may be exerting other influences. As always the story is complex.

The project highlighted here was carried out on a bargeboard configuration on the 2001 BAR Honda, but nicely illustrates the overall effects in this case (see Figure 7-13). The aim was to investigate the changes in the flow around the car, and the redistribution of aerodynamic forces caused by removing the bargeboards. Once again, actual force measurements cannot be quoted, but we are privy to the percentage changes that were determined. As a footnote, this exercise was also correlated with the physical model in the BAR (later to become the Honda, then the Brawn GP and then the Mercedes GP) wind tunnel, and trends and force magnitudes were very closely matched between tunnel and computer.



**Figure 7-13** The plan view of the BAR Honda and its bargeboards, as tested here.

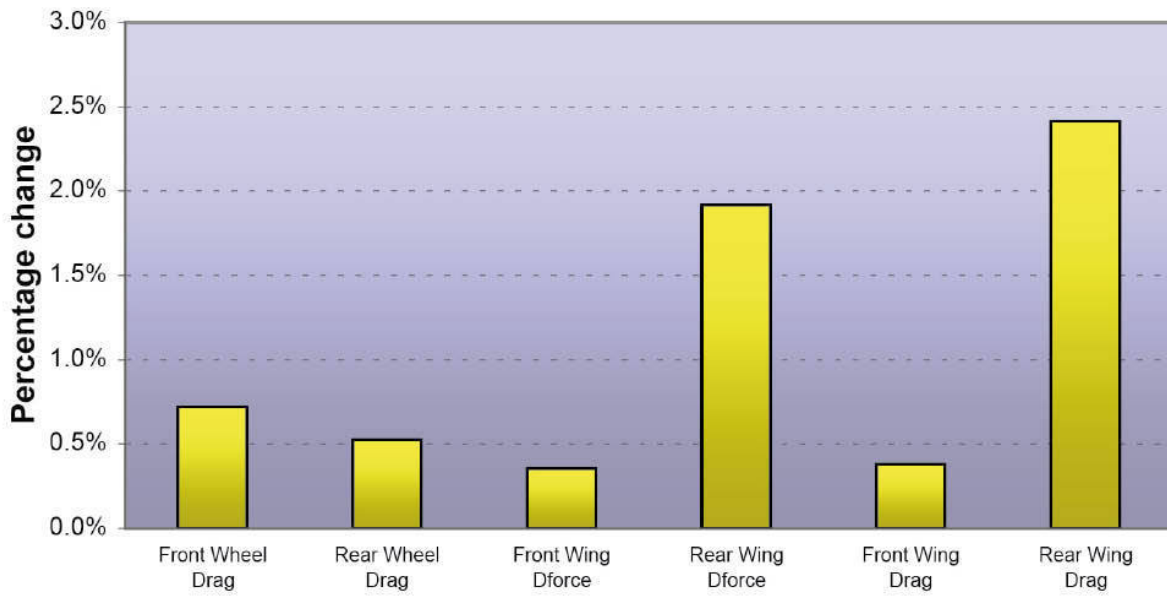
Figure 7-14 summarises the percentage changes to some major aerodynamic parameters following removal of the bargeboards. Evidently, the bargeboards had a significant effect on downforce, drag and efficiency (L/D). In short, removing the bargeboards reduced the overall downforce by 3.6% while also reducing drag by 0.6%. Interestingly, cooling efficiency, shown as ‘H<sub>2</sub>OCP’ (pressure coefficient on the radiator), actually improved by 6.8% when the bargeboards were removed.



**Figure 7-14** Percentage changes to overall forces following removal of the bargeboards.

Of more value perhaps is to look at these results the other way around, in other words, to look at the effects of fitting the bargeboards, and obviously, increases would approximate with the decreases shown in the graph, but with negative and positive signs reversing. Thus, there was a 3.6% or so increase in overall downforce (given as ‘body downforce’ which omits wheel lift/downforce) and a forward shift in the distribution of downforce when these bargeboards were fitted. Although there was also a gain in drag of around 0.6% when the bargeboards were fitted, L/D improved by 3%.

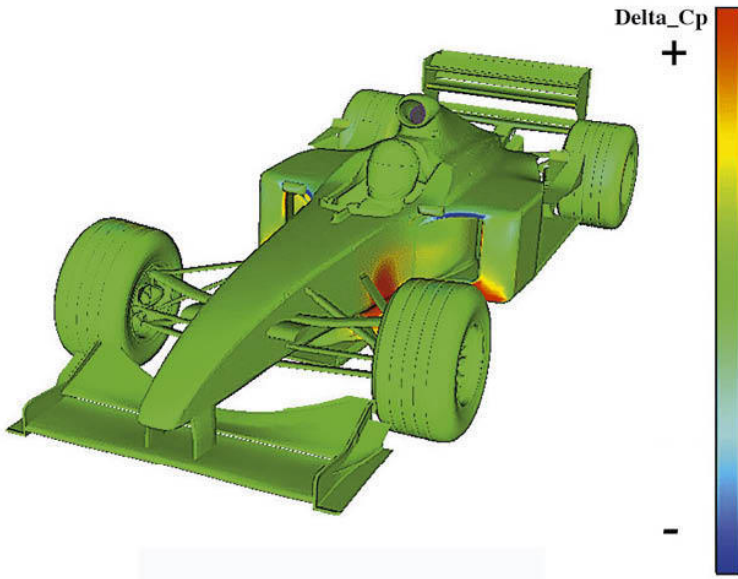
Breaking down the force redistributions further helps to work out where the changes were taking place. For instance, Figure 7-15 shows the percentage changes to wheel and wing forces when the bargeboards were removed. There were small increases in front wing forces, but more significant increases in rear wing downforce and drag. Since these increases, when bargeboards were removed, would equate to decreases when bargeboards were fitted, clearly the overall gain in downforce achieved by fitting the bargeboards must have come from somewhere other than the wings – we must therefore look to changes around the body.



**Figure 7-15** Percentage changes to the forces on wheels and wings.

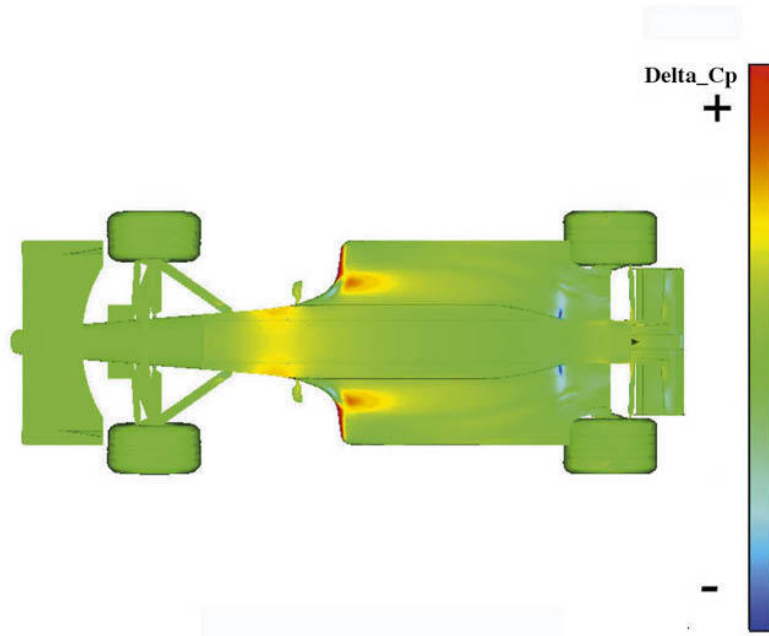
The wheel drag also increased in the absence of the bargeboards, equating to drag decreases with bargeboards, and since wheel drag is a significant proportion of overall drag these apparently small changes should not be overlooked. This comment could also be applied to the rear wing, also a major contributor to overall drag, so the change in rear wing drag here could be important.

Further visualisation of changes caused by the removal of the bargeboards is required to begin to see the mechanisms at work. Figure 7-16 is a Delta\_Cp plot that shows the changes to surface static pressures when the bargeboards were removed. Reds and yellows indicate removing the bargeboards caused increases in static pressure, while pale and dark blues show decreases in static pressure. The influence of the bargeboards can be clearly seen on the chassis sides and leading edge of the sidepods.



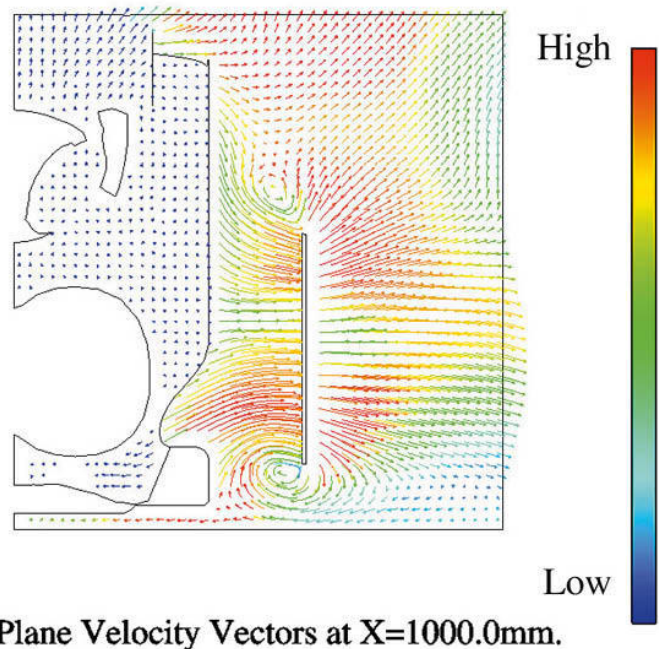
**Figure 7-16** Static pressure changes caused by removal of the bargeboards.

Figure 7-17 shows the change to static pressures on the underbody. Although the magnitude of the changes was not disclosed, there was a static pressure increase at the front of the underbody and a decrease in the diffuser when the bargeboards were removed. Turned the other way around, fitting the bargeboards created a decrease in static pressure at the front of the underbody and an increase in the diffuser, with an overall reduction in underbody static pressure that produced the increase in (forward-biased) downforce with bargeboards fitted. Also just apparent in this plot is the reduction in static pressure on the rear wing's lower surfaces when the bargeboards were removed, equating to the loss of rear wing downforce when the bargeboards were fitted. So, this plot explains the change to overall downforce and its distribution. But what has caused this pattern of change?



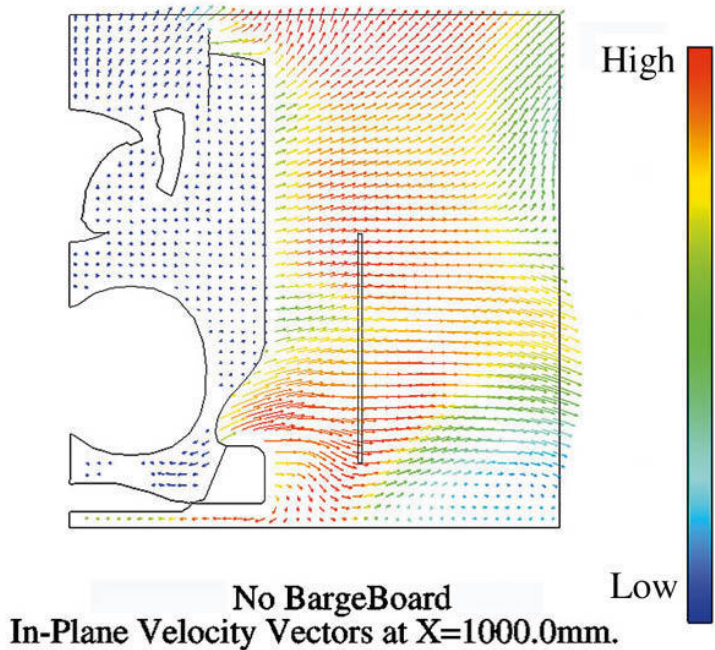
**Figure 7-17** Static pressure changes to the underbody caused by removal of the bargeboards.

Figures 7-18 and 7-19 show a slice taken 1m back from the front axle along the left-hand side of the car. Velocity vectors in the transverse, vertical plane of the slice are shown. Figure 7-18 illustrates the airflow pattern with the bargeboard, and Figure 7-19 without the bargeboard. It is apparent that by turning the airflow the bargeboard has initiated a pair of vortices, one from its top edge and one from its bottom edge. This lower vortex subsequently travels downstream (Figure 7-20 is a slice 200mm further on) causing the decrease in static pressure in the forward section of the underbody, and its influence is what we saw ‘in reverse’ in Figure 7-17.



In-Plane Velocity Vectors at  $X=1000.0\text{mm}$ .

**Figure 7-18** *Vortices set up by a bargeboard; the plot shows velocity vectors in the transverse plane 1m back from the front axle line.*



No BargeBoard  
In-Plane Velocity Vectors at  $X=1000.0\text{mm}$ .

**Figure 7-19** *No bargeboard, no vortices.*

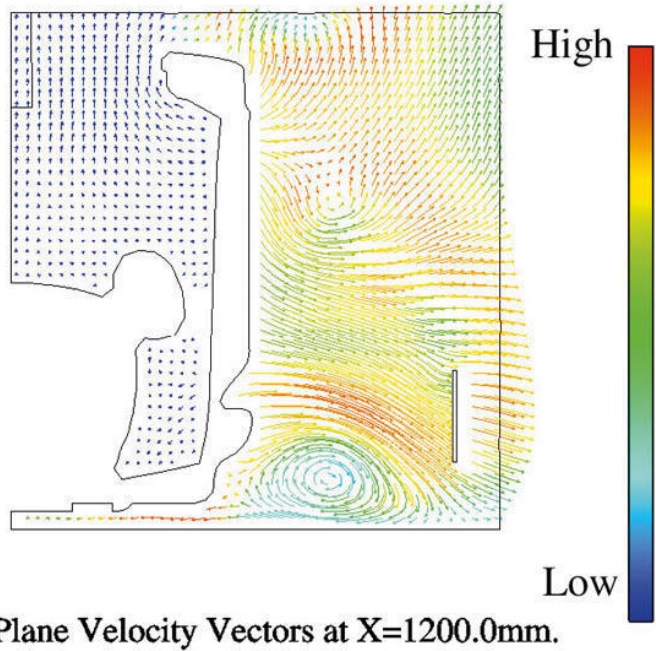


**Figure 7-20** The lower vortex 200mm further downstream, heading for the underbody.

Why is there an increase in static pressure in the diffuser with bargeboards fitted? Probably because by being worked harder in the forward part of the underbody the airflow has lost energy here compared to the no bargeboard case. Thus the velocity here is less, and so the static pressure is slightly higher.

So that's what these bargeboards really did. Obviously, different cars with different shape bargeboards in different locations will be exploiting the airflow in slightly different ways, but it is likely that similar mechanisms will be at work.

A wind tunnel study on a later car to come out of the Honda F1 factory, the 2007 RA107, once more makes for interesting comparison and shows how important bargeboards and related devices had become. The RA107 was not exactly one of the most competitive cars of its era, and the results in the MIRA wind tunnel will have been affected by the tunnel's stationary floor and the car's non-rotating wheels during testing. But nevertheless what follows gives an idea of how potent bargeboards and related devices can be.

Prior to the major bodywork regulation changes of 2009, Formula 1 cars had sprouted all manner of 'off-body' aerodynamic devices. One of the longstanding devices to have been in use though was and still is the bargeboard. The Honda RA107 featured two pairs of these, which we'll refer to as the forward and rearward pairs, though both pairs were located well forward on the car. First the forward pair (fp) was removed, and then the

rearward pair (rp), and the results are set out in the table below, which shows delta values or changes expressed in counts when the bargeboards were added.

with fp

ΔCD: +14  
Δ-CL: +127  
Δ-CLfront: +77  
Δ-CLrear: +50  
Δ%front: +1.50%  
Δ-L/D: +95

with rp

ΔCD: +25  
Δ-CL: +489  
Δ-CLfront: +292  
Δ-CLrear: +197  
Δ%front: +7.74%  
Δ-L/D: +438

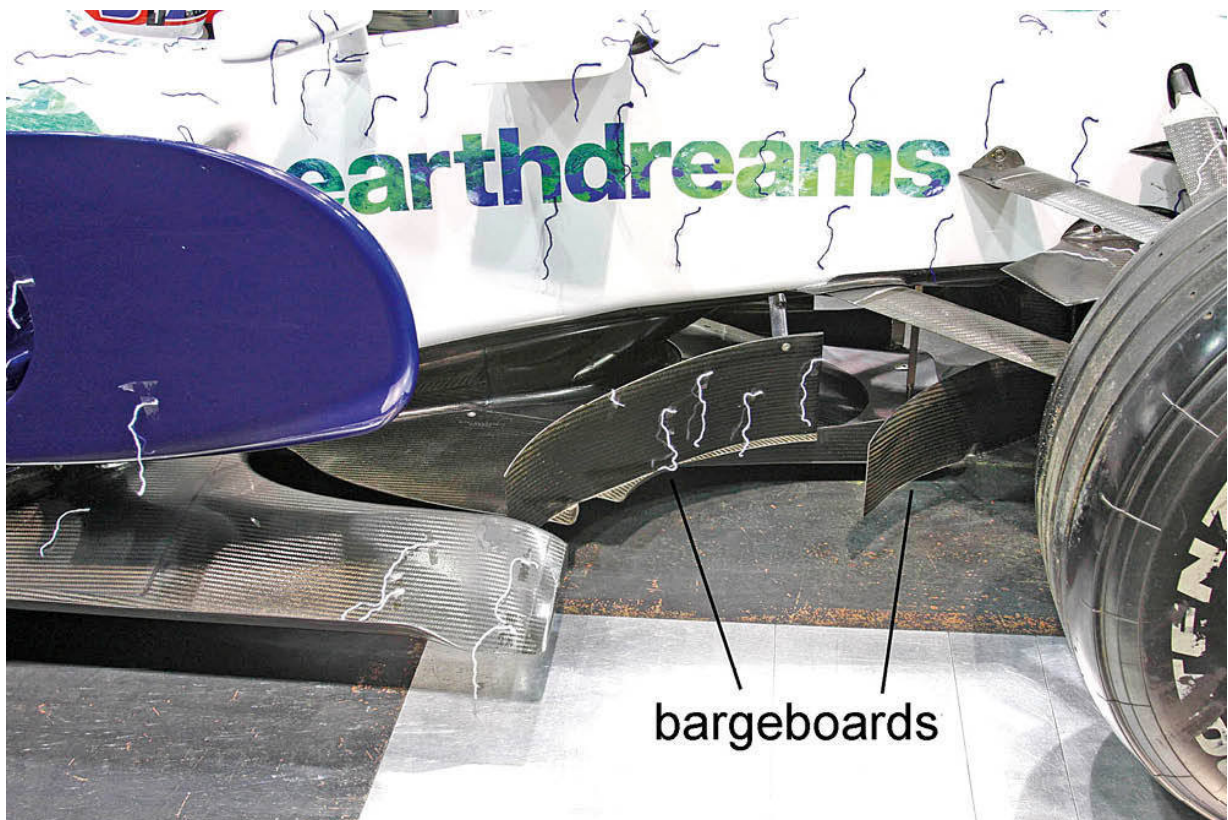
Total with

ΔCD: +39  
Δ-CL: +616  
Δ-CLfront: +369  
Δ-CLrear: +247  
Δ%front: +9.24%  
Δ-L/D: +533

The first and most obvious conclusion from this data set is that these bargeboards were extremely powerful devices, especially the rearward ones. We must include the usual caveat here, which is that although ‘trip strips’ were attached to the wheels to simulate the effect of wheel rotation, the MIRA wind tunnel floor is stationary so our downforce data, especially with respect to ground proximity devices, will have been underestimated. However, it might also be that the bargeboards, which we have seen act as vortex generators, may also have served to ‘refresh’ the near-ground airflow to mitigate the fixed floor issue to some extent.

But just taking the data at face value, the bargeboards together produced an increase of 39% to the total downforce of the bargeboard-less car, with 86% more front downforce and 21% more rear downforce. And these substantial downforce increments came for just 3.9% more drag, meaning that efficiency (-L/D) increased by more than 33%. This seems extraordinary for what are

little more than two pairs of well-located curved plates with small horizontal lips and serrations on their bottom edges... But such is the potency of the combined effect of turning the wakes of the front wheels and front wing outwards so that they do not adversely affect downstream components, and also generating vortices with low pressure cores that enter the underbody and augment the downforce generated there.



*The Formula 1 Honda's bargeboards were extremely potent devices.*

### Vortex generators

The previous section showed how two different types of essentially simple, curved, vertical plates located at different points on a Formula 1 car both caused significant modifications to the airflow downstream, at least partly by setting up vortices. Other devices are also used to generate beneficial vortices. A vortex can have quite strong effects. As we have seen, the rotation within a vortex can induce changes in velocity (speed and/or direction) some distance away from the vortex centre that may be used to alter the flow downstream beneficially. The vortex core has reduced static pressure within, which in some circumstances, can be beneficially exploited too.

Why do vortices form? If a plate or a vane, for example, is at an angle to the airflow, there will be a static pressure differential between the windward (raised  $C_p$ ) and leeward (reduced  $C_p$ ) sides. This induces the air to spill over the edges, from the higher to the lower pressure region. The air starts to make the turn but, because of the sharpness of the edge, it cannot remain attached. Nevertheless, the attempt at making the turn adds an angular component to its velocity that results in rotating flow – a vortex – being established. The additional velocity imparted to the vortex causes a reduction in static pressure in its core. A vortex tends to dissipate downstream as viscosity reduces the kinetic energy within. So, vortices might usefully be exploited by helping with static pressure reductions that provide downforce, or by altering the direction of flow.

One of the better known uses of vortices is in the generation of lift at high angles of attack on delta wing aircraft (think Concorde or Space Shuttle for example). Though superficially irrelevant to our cause, bear with this because it will soon become apparent that there is overlap with racecar aerodynamics.

The simplest manifestation of a delta wing at high angle of attack is a triangular plate pointing into the airflow. A model of just such a device with an aspect ratio of 1 (that is, length and width were equal, at 300mm in fact) was set at a range of angles from 10 degrees to 40 degrees and run through CFD to simulate and visualise how such a device generates lift. The devices were placed at negative angles of attack (nose down) in order to generate downforce and make us feel more comfortable!

Figures 7-21 and 7-22 are front and rear views of the delta wing inclined at 20°, and show the leading edge vortices that have been created. The streamlines are coloured by velocity, and those in the forward part of the vortices are at raised velocity (freestream was 44.7m/s or 100mph) while towards the rear the streamlines are showing reduced velocity, and the vortices have expanded in size. Figure 7-23 has had the streamlines removed to reveal the pressure distributions on the lower surface. It is clear that the proximity of the vortices has produced lowered pressure on the underside of the delta wing, which coupled with the inevitably raised pressure on the inclined upper surface has generated downforce. The data from the four models is summarised in table below.

Angle, degrees: 10

Downforce, N: 24.9

Drag, N: 5.4

-L/D: 4.63

Angle, degrees: 20  
 Downforce, N: 49.6  
 Drag, N: 18.6  
 -L/D: 2.67  
 Angle, degrees: 30  
 Downforce, N: 63.1  
 Drag, N: 36.6  
 -L/D: 1.72  
 Angle, degrees: 40  
 Downforce, N: 57.8  
 Drag, N: 48.6  
 -L/D: 1.19

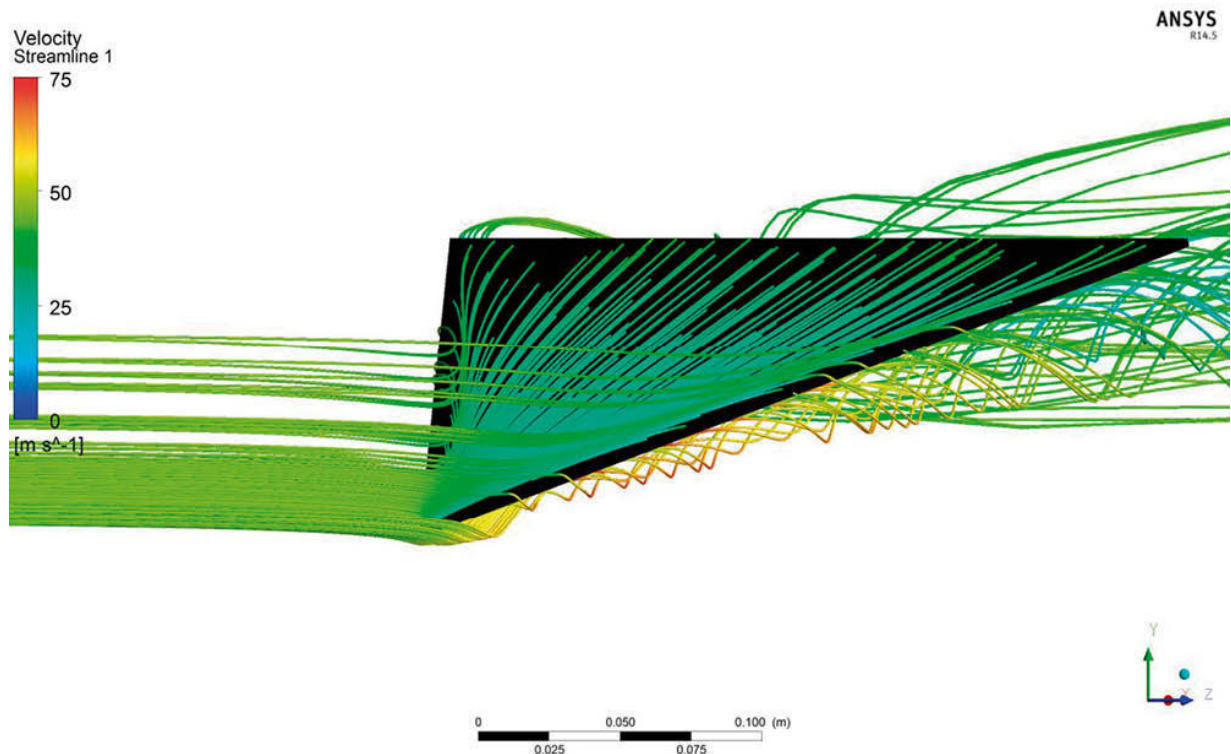


**Figure 7-21** A 'delta wing' comprised of a simple flat, triangular plate inclined at 20° nose down

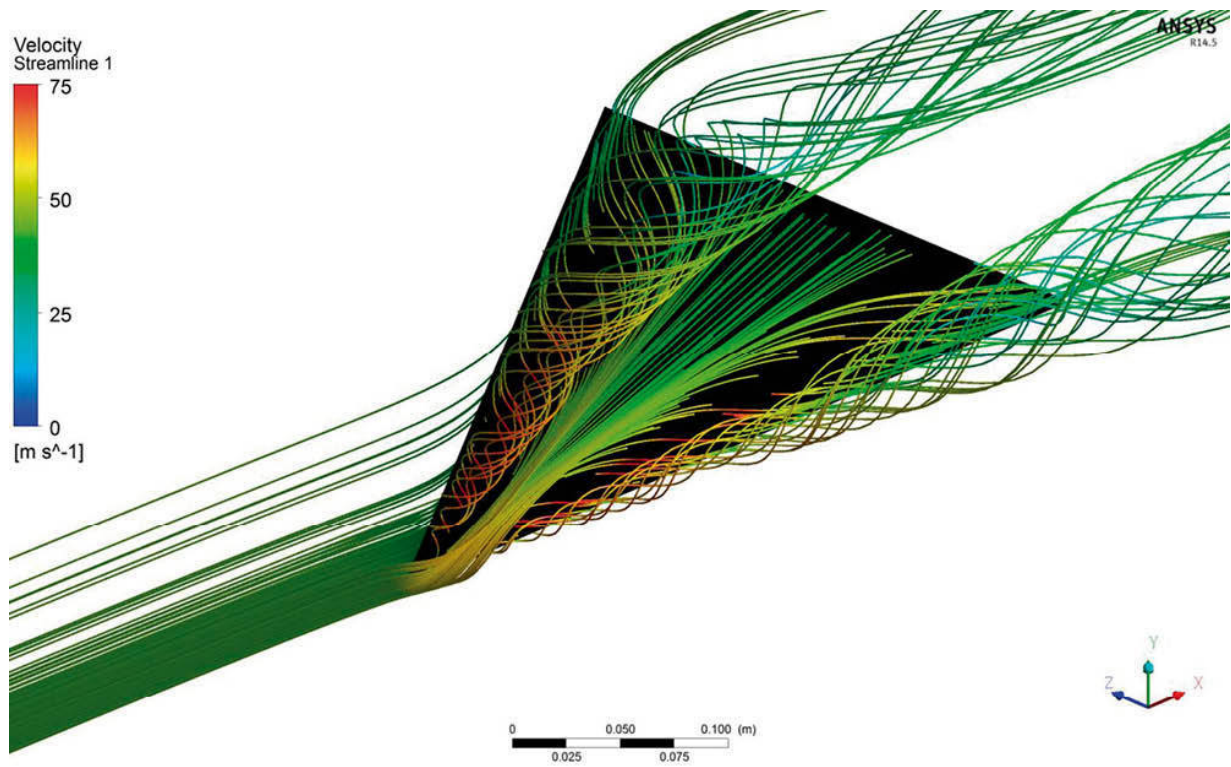


**Figure 7-22** Viewed from below and behind, the vortices set up by the delta wing are very evident

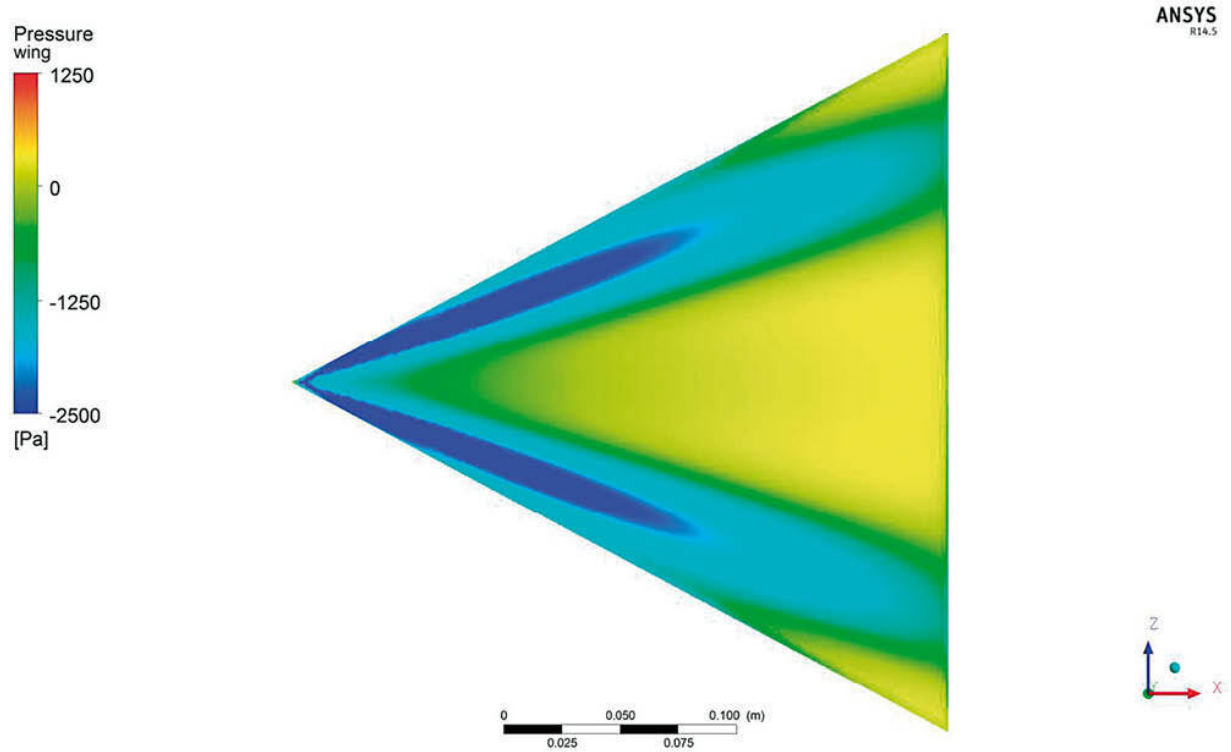


**Figure 7-23** *Viewed from directly below, with the streamlines removed the reduction in static pressure caused by the vortices on the lower surface (blue areas) is very obvious.*

So a device that sets up vortices can itself generate downforce, and in the case of the shallower angled delta wings, efficiency (lift over drag, -L/D) was actually not bad when compared with a high downforce wing, for example. But the absolute values of these forces were modest relative to total car downforce. However, when this principle is applied creatively, as we have seen with bargeboards, and as we see in a few other examples here, greater benefits can accrue.

The devices shown here on this 2010 Dallara F310 Formula 3 car show that the category was permitted more complexity in this area than Formula 1 was at this time. It would be reasonable to surmise that the purpose of the large triangular protrusion ahead of the lower, forward-most part of the sidepod would be to set up a vortex along the side of the car to act as an invisible skirt (akin to the dive plane example highlighted earlier) to help the underbody to produce more downforce. Note too the saw-tooth bottom edge to the aft bargeboard, which would again be there to set up or enhance vortex formation in the forward underbody. An experiment by the author a few years ago during a wind tunnel session on a hillclimb single-seater saw a very crude triangular vortex generator fixed just ahead of the venturi-shaped underbody tunnel inlets on the car. This achieved about a 1% downforce gain with little shift in balance. The significance of such a gain depends on how well optimised the car is. If you were desperately looking for the odd fraction here and there then 1% might have been worth celebrating! As it was, 1% seemed negligible, which probably says how far from fully sorting the car we really were ...



*A selection of vortex generating devices on the 2010 Dallara F310 Formula 3 car.*



*Vertical vortex generators in the underbody inlet of the 2001 Reynard 01I ChampCar. The Lola ChampCar used similar devices.*



*A vortex generator (bottom centre) towards the rear of the sidepod on this Lola B1/00 ChampCar.*

The Reynard 01I ChampCar, like its Lola counterpart, used curved, vertical vortex generators in its underbody inlet, these resembling bargeboards in both location and purpose.

The Lola B1/00 ChampCar featured what were apparently vortex generators located ahead of, and below the rear tyre flip ups (the white triangular device, bottom centre). Their location, and the design of the flip up, suggests that their role was to assist the flow on the flip ups, either by using the vortices they generate to modify the flow direction on the flip ups or, more likely perhaps, to assist the flow in remaining attached to the underside of the flip ups. This latter conclusion is backed up by the obvious additional efforts made to maintain flow attachment on the underside of the flip ups, namely the separate flap and the Gurney on the flap trailing edges. There may also have been an influence on the forces felt by the horizontal 'skirts' ahead of the rear wheels. The vortex generators were supported by small struts connected to the floor (barely visible in the photo), which suggests that it was

important to prevent the devices from flexing under aerodynamic load, or perhaps vibrating due to buffeting.

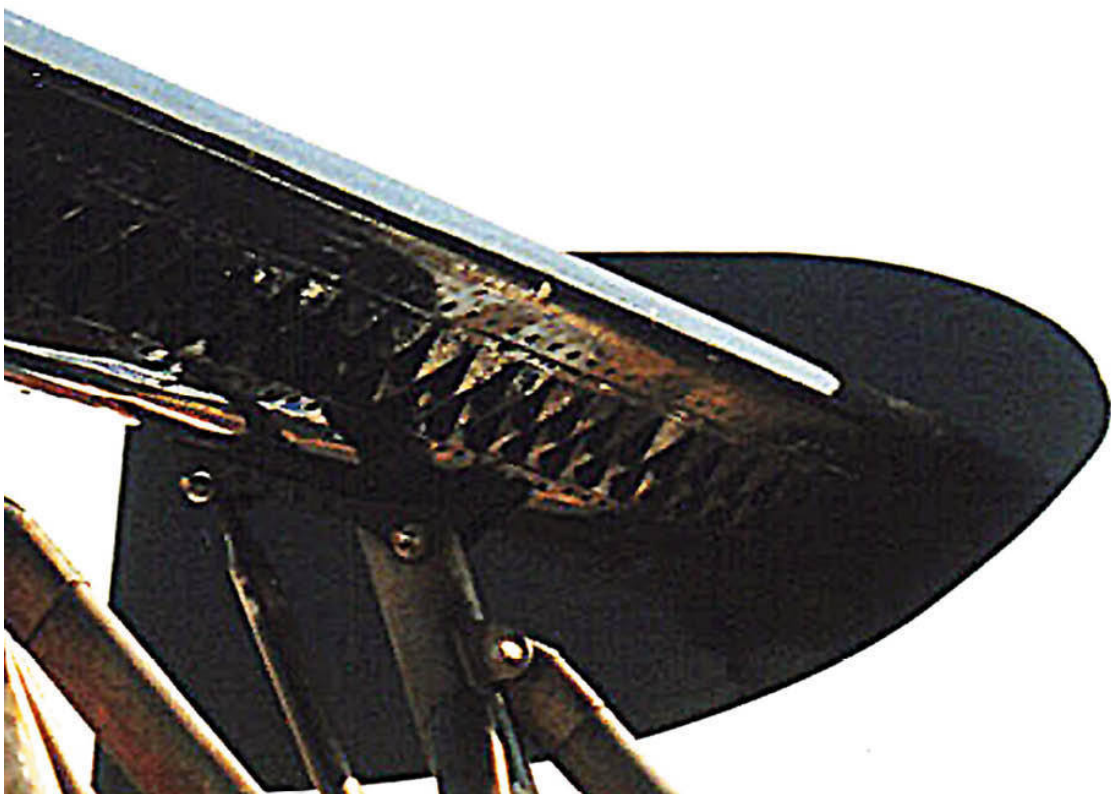
The manipulation of vortices to enhance pressure reductions is seemingly not without its risks. A chance remark during a conversation with an ex-Formula 1 aerodynamicist about the phenomenon of ‘vortex bursting’ highlighted one such. As a vortex travels downstream it weakens and increases in size. Eventually, if the rotational velocity within becomes low enough, the vortex structure breaks apart, and the vortex bursts. The effect can be sudden, and not only leads to a loss of effectiveness but also to potential disruption downstream.

A device mentioned in the chapter on wings was the so-called ‘turbolator’ which, by various means, forces the transition from laminar flow to turbulent flow on a wing’s suction surface, thereby re-energising the boundary layer and helping to delay or prevent flow separation. One method by which this is done on aircraft is to fix small vortex generators that protrude perpendicularly (into or through the boundary layer) from the surface about a third the way back on the wing. These set up small vortices that trail back along the wing and stir up and add energy to the boundary layer. We can just make out such vortex generators on the suction surface of this Top Fuel dragster’s rear wing. The devices were attached in two rows across the whole span of the main element, about a quarter to a third of the chord back from the mainplane leading edge. It is often said that vortex generators like these are used to cure a flow problem. Perhaps in this instance they were a ‘fix’, either for a wing profile that could have had a better pressure distribution, or because of the manufacture technique that, for example, saw surface joins and lines of rivets across the span just ahead of where the vortex generators were, as shown in the magnified view. But some aeronautical references now claim they are not simply ‘fixes’ but are able to offer enhanced performance from proven wing profiles in terms of peak lift coefficient and increased stall angle.

Such a brief survey of a few miscellaneous aerodynamic devices must surely have some important omissions, but hopefully, this examination of some of the more common devices has provided explanations of – or at least clues to – the principles by which other devices operate.



*Vortex generators on the suction surface of this Top Fuel dragster's rear wing mainplane.*



*Vortex generators on the suction surface of this Top Fuel dragster's rear wing mainplane, in digitally enhanced close up.*

## Chapter 8

# Removing (some of) the guesswork

VEHICLE AERODYNAMICS MIGHT be a branch of engineering, but that doesn't stop it from being an art form at the same time. If it was simply a precise engineering discipline, the chances are that all cars would be virtually identical in appearance, and quite possibly (within a given category) in performance too. Thankfully that is not the case, and there is still scope for individualism. This goes on to mean that the amateur aerodynamic stylist has just as much chance of making his or her ideas work as not, but in order to increase the likelihood of success it does help to be able to determine what is going on in the air moving around your creation, and what the actual effects on the vehicle are. There are various ways of doing this, some more precise than others, and there are some that the amateur competitor can only admire from the comfort of the armchair. However, as we have seen, some techniques that were once the sole preserve of the professionals are becoming increasingly accessible to the rest of us. Nevertheless, with careful observations and perhaps some prudent investment, even those of us on micro-budgets can divine a surprising amount of aerodynamic information that can help with the design and development of a competition car.

### Flow visualisation

When asked to explain why he lived in New York City, comedian Woody Allen apparently once said: 'I never trust air I can't see'. He probably didn't realise it at the time (or since, come to think of it...), but he had hit upon one of the problems faced by amateur and professional aerodynamicists alike – they cannot see the medium they are dealing with until they contaminate it with something, or use some means of revealing the direction it is flowing in, and the state it is in – that is, smooth or disturbed, attached or separated.

It is sometimes possible to see brief glimpses of evidence of flow patterns around cars from the sidelines or even on television. For example, on particularly humid days, Formula 1 and Indycars can generate visible rear wing-tip vortices. The vortices are always there, of course, when the car is in

motion, but the special nature of the humid atmospheric conditions means that the low static pressure in the core of the vortex causes the water vapour to condense and become temporarily visible. In wet conditions, the extraordinarily high ‘upwash’ from rear wings can be seen as tall rooster tails of fine spray that continue way above the spray thrown up by the tyres. On other occasions, more general flow patterns show up, for example, when one of these cars blows an engine in a cloud of oily smoke. The engine owner’s loss is our gain, as the smoke gets caught up in the larger scale circulatory patterns created by the car, and rather than just being able to see the core of the rear wing tip vortices, the whole rotating flow at the rear is, again briefly, visible. A car’s influence on dust, leaves and other detritus may also make certain aspects of the airflow around it visible temporarily. Even muddy streaks left on body surfaces in wet weather, if they aren’t cleaned off immediately, can be revealing as we’ll see, but all of these instances, fascinating though they are, are transient, and not much use for serious study. More controlled methods of revealing airflow patterns are needed.

Flow visualisation is not really a primary technique used by professional aerodynamicists in the world of motorsport, but it does tend to be used as a means of checking out the cause of a particularly interesting or crucial result arising from a change or a modification. For example, during a set of wind tunnel trials, gradually increasing a wing angle may yield positive gains in downforce up to a point, at which drag continues increasing, but the downforce gains start to tail off. The obvious assumption is that the flow is beginning to separate. Using a means of flow visualisation around the wing in question could help in determining whether the flow over just a part of the wing has in fact separated. If that has proved to be the case, the span-wise wing twist, for example, could be altered so that the flow across the entire span remains attached for longer, allowing more downforce to be generated before large-scale separation and stall occur.

However, for the enthusiast aerodynamicist, being able to see what is happening to the air around our competition cars – and in particular, around and near crucial areas like wings, spoilers and diffusers as well as cooling intakes and outlets and so forth – can help greatly in understanding what is going on. It can also provide much food for thought, and pointers for areas to improve and develop in order to make a more aerodynamically efficient vehicle. There are various ways of doing this, which for the most part can be used out on the track, either during testing, or in competition if test time is hard to come by.

The best known and perhaps most often used means of showing up the flow patterns near a car's surfaces is the 'wool tuft' method. Pieces of wool yarn about 3in to 4in (75mm to 100mm) long are stuck to the 'wetted surfaces' of the vehicle, that is the bodywork, wings, spoilers and all the parts of interest (including the driver's crash helmet possibly) with self-adhesive tape (make sure the tape is stuck down flush with the body) so that they can trail along in the expected direction of flow. The car is then driven along, perhaps at a set of pre-determined speeds, while observers look on and take photographs or video footage. This might be done from trackside, or from another car running along with the car under test, assuming the venue and the occasion will permit such liberties! Care must be exercised to ensure that the 'chase car' does not get so close that it affects the airflow over the test car though. The images yielded by this exercise can be somewhat startling, with the flows over and around parts of the car being rather different from what might have been imagined! For example, the flow coming off a single-seater's front wing can be seen to be very non-uniform, especially if the span of the wing extends in front of the front wheels. Similarly, the flow over the bonnet area of a passenger-based car can be seen to be remarkably complex. This is where this kind of study can begin to really help in the understanding of what air does as it passes around, over and under a competition car – the general effects and influences can actually be seen, and gathering this information is perhaps the first step on the way to being able to direct and manage the flow in a way that eases its passage past your vehicle in the most efficient and productive way – or should that be 'in the least damaging and performance sapping way'?



*Wool tuft testing the GWR Predator hillclimber. Notice the flailing tufts on the top of the rear end plate, evidence of the tip vortex.*

Wool tufts can show up the flow directions near important details like the trailing edges of rear wings, or over the rear deck ahead of a rear spoiler, and near cooling inlets or NACA ducts which feed air perhaps to an oil cooler or the engine inlet system. It is also possible to see whether the flow is smooth or unsteady sometimes. If the car is being watched or videoed, it will be seen that some of the wool tufts trail back smoothly in the direction of flow, while others are flailing wildly about, and maybe lifting above the surface instead of lying back along it. In photographs, the tufts in smooth flow regions will show up just as they are seen, while those that were flailing about are likely to appear as fan-shaped blurs, providing the camera shutter speed is not too fast (some experimentation may be necessary here). Clearly, these are indicators of disturbed and separated flow in the regions concerned – it may or may not be possible or even desirable to do something about it, but at least you'll know the situation exists. Longer tufts will give more movement to amplify this effect.

It has been suggested that an ordinary workshop compressor airline or a leaf blower (one of those devices for blowing fallen leaves into your neighbour's garden) could be used to provide the airflow for static wool tuft tests. However, neither of these devices is capable of providing sufficient airflow over a substantial enough area of a car to enable the various flow interactions to occur when the car is moving through the air. Furthermore, the quality of the airflow emerging from either of these sources is very unlikely to be similar to the airflow over a car. It would also be difficult to be certain about the direction in which to point either device in order to try to simulate real conditions. In short, this is an interesting idea but with little merit – better to stick to the real thing and accept that if you don't have access to a wind tunnel you just have to drive the car along to derive use from wool tuft testing.

The wool tuft technique does have its shortcomings. For one thing, in common with some other flow visualisation techniques, only the flow immediately adjacent to the surfaces is shown up, which means that a mental picture still has to be built up of the three-dimensional flow above the surfaces, but at least this will be a bit easier once the surface flows have been visualised. For another, it is, of course, impossible under normal circumstances to see what is happening underneath wings, splitters and the entire underbody. However, with some ingenuity it would be possible to attach a remotely operated camera with a secure fixing to, say, the rear wing mounts in order to photograph or video the wing underside, or perhaps the flow at the rear of the diffuser. More determined efforts could probably provide images of

underbody flow too. Just make sure the image capture device isn't so big or located such that it affects the flow in the regions you want to study!

Another method of visualising the flow directions over a car's surfaces is to look at the streak marks left by liquids which land, either by design or otherwise, on your car. As mentioned earlier, this can happen on a wet and dirty day, when rain and dust combine to leave muddy streak marks over parts of the body, or when one car has been following another which is losing fluid, such as oil, and depositing it on the car behind, whereupon it too leaves tell-tale marks all over the bodywork. On these occasions it is most instructive to take a close look at these marks when the car returns to the paddock, and even to make sketches and take photos. The 2005 Le Mans-winning Audi R8, shown here as it left the track, tells a few aerodynamic stories. At the front, grime has deposited densely on areas where high static pressure develops, notably on the near vertical surfaces above the splitter while streak marks in line with the local flow directions can be clearly seen in the recesses that lead to the side radiators.



*Twenty-four hours of oily grime on the 2005 Le Mans-winning Audi R8 reveals some information on surface flows and pressures. (Rob Barksfield)*

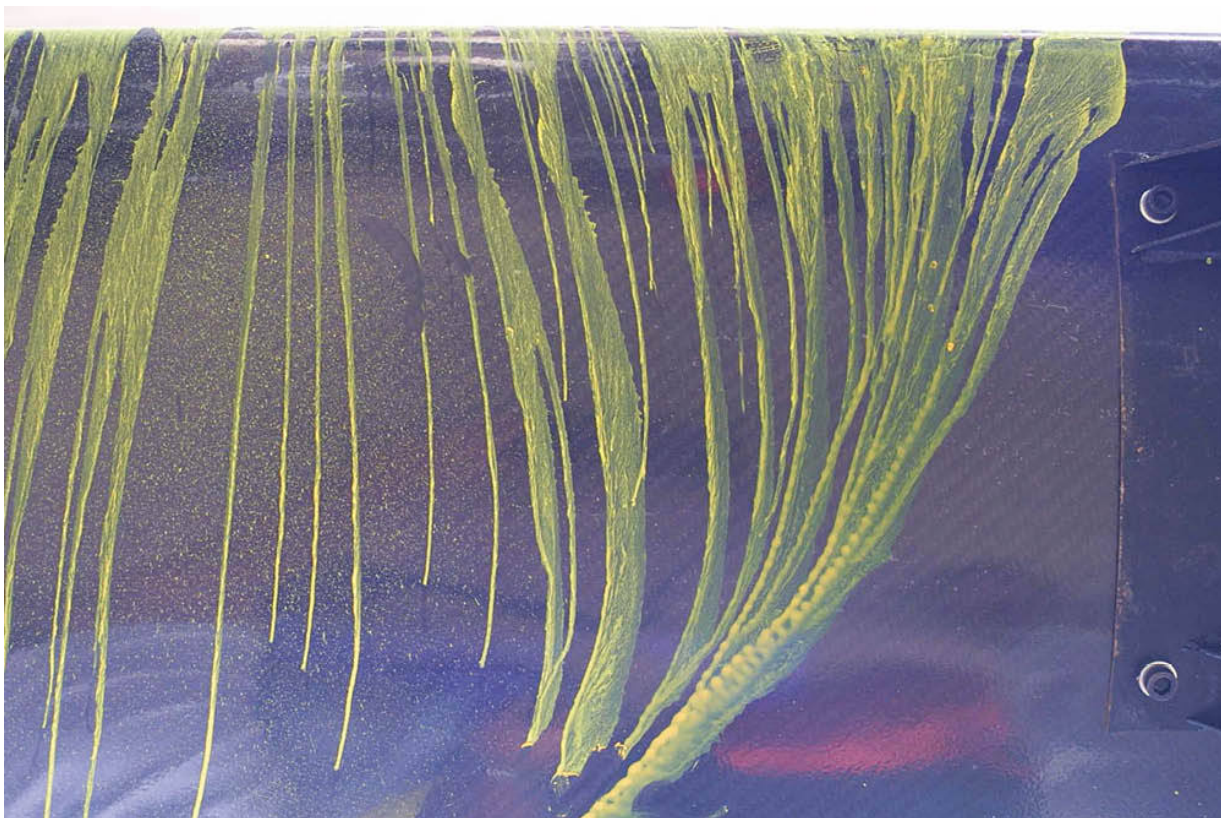
It isn't necessary of course to wait for a wet day, or for an unfortunate fellow competitor running on a circuit ahead of you to be losing oil. You can apply droplets of suitable liquid to areas of interest prior to going out on track, and then take a look at the results on returning to the paddock. Fluids that can be used for this exercise need to be relatively low viscosity and not so volatile that they evaporate too quickly, especially on a warm day. Paraffin (kerosene), diesel engine fuel and thin lubricating oil have all been found excellent for this purpose. Don't for goodness sake, use anything corrosive towards paint or any of the other surface finishes on your car! In order for the streak marks to show up, some form of colouring pigment needs to be added, although often, there is enough dust around to adhere to the oily marks. A small amount of 'Copperslip' has also been used to colour paraffin for this purpose. A professional's recipe can be found in Appendix 3.

The idea is that the liquid will actually evaporate during the test run, so leaving behind a kind of printed record of the flow pattern. If the liquid is insufficiently volatile, it may not evaporate, and will run back down to the low points of surfaces once the car slows or stops, possibly confusing or even obliterating the record of what happened at speed. Note that the fluid should be applied immediately before the test run, and the car should be accelerated fairly smartly so as to record the flow at the chosen speed. It may be that the application of a little ingenuity could see the rigging up of a pump, a fluid reservoir and some piping, so that the driver could release the fluid, over the chosen parts of the vehicle, once up to a pre-selected speed. If the run speed were then maintained for a few moments while the fluid dried out, leaving behind the coloured dye, the streak patterns left would be a record of that particular speed.

As mentioned previously, professional race teams use this general form of flow visualisation during wind tunnel (and sometimes track) test programmes, when checking out a particularly interesting condition or configuration.

Having spent some time with a top single-seater team in a scale wind tunnel, it was fascinating to watch the methodical collection of downforce and drag data as increasing increments of front wing angle were worked through. At a reasonably steep angle of front wing incidence, the downforce gains started tailing off, and so the technicians applied their own particular liquid brew (diesel fuel-based) to the front wings, dashed out of the tunnel, and wound up the wind speed again. After the run, they then slid a large mirror beneath the car to examine and record the flow patterns on the lower surface of the wings, and further back in the underbody region. The information that they discovered resulted in a phone call to the production department to see if the

wings could be made with a modified amount of spanwise twist. This highlights two of the special advantages of using fluid markers for flow visualisation; an observable record is left on the car, which can be studied, sketched and photographed; and because of this, it is relatively easy to study flow patterns on the under surfaces of components, and the main body. Some wind tunnel technicians use fluorescent dyes such as fluorescein in the test fluid so that under ultra-violet illumination the streak marks show up particularly vividly.



*Coloured streak lines using 'flow vis fluid' indicate the substantial wake of an obtrusive central wing mount on the bottom surface of this rear wing (the flow was from the top of the picture).*

Still though, with the exception of those transient cases mentioned at the beginning of this section, it has only been possible so far to examine the flow at the surfaces of a car. There is one technique however, that enables the flow in the regions off the body of a car to be examined, and that is smoke-plume flow visualisation. The major shortcoming of this technique is that you really need access to a wind tunnel in which to carry out the trials, and probably a full-scale one at that since a scale model is unlikely to be available to most of

us. But as we shall see in a later section, the ‘luxury’ of a full-scale wind tunnel may not be totally unattainable.

The generation of a smoke plume is done by heating a suitable oil like paraffin, and passing the smoke down a tube to a probe, which can be positioned so as to direct the plume in the airstream at any area of interest. A mobile probe can be used for rapid visualisation of the flow all around the car, or multiple probes can be used for simultaneous study of the flow at various positions. This form of flow visualisation makes the three-dimensional nature of the passage of the air around a car much easier to comprehend and envision. It becomes all too easy, especially when looking at two dimensional photographs and drawings, to allow the mind to restrict itself to thinking just in 2D, but that would be a dangerous habit to get into. With a smoke plume, it is possible to see how far above or beyond the car’s surface changes of shape and contour exert an influence on the airflow, whereas the previous two visualisation methods only show what is happening at the very surfaces themselves. Such things as vortex formation, for example, can be seen at the trailing edge tips of a rear wing, or down the sides of sculpted sidepods. Airflow turning under the lower edge of ground effect sidepods; the marked influence of the front wings on the airflow to the rear of the car can be seen, and flow separation zones over rear screens and ahead of spoilers – all of these can be seen. This helps one get a better three-dimensional perspective on what actually happens to the air around a car, and can assist in determining the existence of specific effects such as wing stall.



*Smoke plumes can reveal flows off the surface, and in three dimensions. (MIRA)*

One final word of caution on flow visualisation: the medium, and indeed the equipment being used to show up the flow can affect the flow pattern ... Nobody said this would be easy!

### **Data gathering**

One aspect of competition car technology that has grown and developed rapidly in recent years is data acquisition. It is now possible for any competitor to buy much the same kind of data logging electronic wizardry that professional race teams use, and amass mountains of information about

chassis (and engine) related parameters. But gathering useful data need not be expensive. The important thing is to make careful observations, and equally careful records of everything relevant that you can measure. If your budget stretches only to the ubiquitous stopwatch, then just make sure you get all the really relevant times that you can – total elapsed as well as split times in critical parts of the tracks for example. If improving cornering speeds by adding downforce is what you are interested in, then time your car through corners where that is going to make a difference. If it's drag that you are worried about, look at straight-line segments, and then relate those values to elapsed times to check out the overall impact of the tests you are running. This kind of thorough, disciplined approach does not need huge expenditure, and yields some very useful information.

Supplementing records of stopwatch times with objective visual observations can often prove very helpful. A trustworthy team member who knows what they are looking for, positioned at important parts of a track, can come back with invaluable feedback on car behaviour, and can compare that to other cars in your class or category too. So if your new 'barn door' rear wing allows you to go faster through a particular corner, that much might be evident from split timing, but it will be even more useful to know the split times of your competitors through the same section too. If, then, that knowledge is supplemented by your observer's remark that the car 'looked really planted through Turn 2 compared to all the others' then that all helps in the interpretation of your development progress.

Detailed observations can sometimes provide surprises, and photographs taken with a telephoto lens of your car on track can provide all sorts of information. For example, a photo of a single-seater that the author once drove showed the car on the fastest straight just prior to entering the fastest corner on one particular course. It is very evident that the car's suspension had been compressed through a fair proportion of its available travel, and since the track is reasonably smooth, and there was little if any cornering load yet developed, the conclusion was that the suspension had been well compressed by aerodynamic downforce. It is small wonder that the following corner, which was taken with only a slight reduction in speed and which has a change of camber running across it just after the apex, was frequently the scene of a disconcerting sideways lurch in this car. The chances are that the combination of downforce compression, coupled to cornering load, and with the bump thrown in, used up all the available suspension travel, and thrust the car onto its bump stops. The car was fitted with slightly stiffer springs and the lurching problem much reduced, but it could be that without the photographic

evidence, we'd have spent longer trying to find a solution to that particular problem.

Driver feel and feedback is vital too, and comments need to be recorded alongside all the objective information that you can collect. While the stopwatch will tell you the impact of an aerodynamic change on elapsed time (and therefore speed), unless the car is equipped with the very best of data logging gear, only the driver will be able to tell you how, or whether, the change affected the car's behaviour. Now that so much information can be logged objectively while a car is performing, the often-maligned driver seems to have come in for an even harder time from race engineers and team directors. This should not be the case, because without the driver, the team has no way of knowing what's really going on. It is up to the engineers and driver to learn how to communicate effectively with each other so that the hard data and the subjective feedback can be put together to give a complete picture. This particular difficulty doesn't occur, of course, if you're a one-man band who engineers, prepares, drives and develops the car, so chances are you will have less arguments! But that doesn't mean you shouldn't try to measure everything you can and record it all alongside your remarks about subjective feel.

If yours is a one-person team – or at least, one with a small complement – you will probably benefit greatly from some form of data logging, given that there may not be any spare people to go out and do split times and the like. Once again, though, this does not mean spending huge sums of money if you are prudent, and prepared to spend some of your spare time at the track, and at home between events, squeezing as much information from a simple data logger as you can. Don't be misled into thinking that unless you can monitor speed, lateral G forces, longitudinal G forces, steering angle and throttle position that you won't be able to learn anything of value. It is actually possible to learn a great deal from a simple rpm or speed versus time graph, such as is provided by one of the more basic data loggers now widely available. The information is downloaded to a computer, to be analysed and studied with the software that the manufacturer will provide for that express purpose. Thus, you need to be reasonably familiar with computers, but you do not need to be an expert. However, you do need a computer, quite probably a portable one so you can download runs at the track. So the cost of obtaining this capability may be somewhat more than the relatively modest cost of the data logger and the software, if you don't already own a computer. However, once you have bought the kit, the information you can obtain and build up never wears out, which just has to be a unique achievement in motorsport!

The surprisingly varied information that can be gleaned from just a trace of rpm or speed versus time, and which can be used for assessing aerodynamic aspects of performance includes corner and straight speeds (calculated from the speed per 1,000rpm each gear, if relevant), the elapsed time of a run (if other forms of timing are not available), the split times between various sections of the track, and braking deceleration rates (calculated from the rate of change of speed in a braking zone). Thus all other things being equal, it becomes possible to measure gains in corner speed from increasing downforce, perhaps with a related drop off in straight-line speed, and this can be set against overall elapsed time as a measure of net gain or loss. Simplistic though this type of analysis might be, it has to be better than just stopwatch timing, and furthermore, a permanent printed record of each and every lap or run you ever do can be kept for more thorough inspection, if you ever get the time.

### **Practical track test methods**

With a disciplined approach and perhaps some more serious data logging kit, track testing can be used to derive some serious aerodynamic data, and it can be a sensible alternative – if not a necessary supplement – to wind tunnel or CFD time for any team.

A big advantage of track testing, be it on a circuit, a disused runway, a drag strip or whatever venue is available to you, is that you test the actual racecar itself. So you measure real straight-line speeds, real cornering speeds, real sector times and real forces. You also evaluate the realities of less than perfect bodywork fit, protruding fasteners, warts and all. While some of this is also true of full-scale wind tunnel testing (and could be of CFD if your digital model included such detail), another plus of track testing is that the vehicle moves over the track as well as through the air. This means the wheels rotate, and that there is no need to simulate ‘moving ground’, or to develop means of controlling the slow moving boundary layer of air that develops over the floor of a wind tunnel ahead of the test model. CFD allows these benefits too, but you need – or must create – a 3D CAD model first, and that facility is often unavailable or unaffordable. So there are positive benefits to using track time to gather aerodynamic data. As with any simulation techniques though, there are shortcomings too, as we shall see.



*If you're reasonably rich and famous you need at least nine people to analyse all the data you generate!*

So what kind of aerodynamic knowledge can you obtain on track? This depends fundamentally on what level of data acquisition is available. As we've already discussed, 'traditional' testing enables parameters affected by aerodynamics such as lap times; sector times; higher speed corner entry, apex and exit speeds (>60mph or 100km/h probably, though dependent on downforce levels); and straight-line speeds to be recorded or logged when you visit the actual racetrack. With a racecar that has an optimised mechanical set-up it is then possible to run aerodynamic configuration changes and generate a lot of useful information about the effects of those changes, supplemented by driver feedback on aerodynamic handling balance.

For a practical methodology we could do a whole lot worse than follow the advice of the late Carroll Smith in *Engineer to Win*, where he documents a test in which two different wings were compared. Each configuration was run over five laps, and only wing configuration changes were made. Averages of lap times were recorded, with what were called 'abnormally high or low times' being discarded (perhaps a crude but nevertheless an effective statistical approach!).

The data revealed much useful information about the effects on the car's handling balance and its performance in various sectors of the track. With the relatively low-cost basic data loggers available nowadays, this type of test is very easy to execute – but it does need a disciplined approach, as outlined by Carroll Smith, to generate meaningful results. And – especially if weather or track conditions change during the session – it is also crucial to return to the baseline set-up periodically during the session. Ideally conditions will be consistent, but some variables can always be relied upon to change the baseline, such as tyre deterioration.

### Measuring drag

Indirect measurements of the effects of configuration changes are very valuable on sector or lap times and speeds, and are often all we really need to know. But what about directly measuring aerodynamic forces? It is possible to begin to do this with surprisingly little investment in instrumentation. And again you don't need a racetrack – but you do need a long, straight, flat and smooth piece of road. And in terms of the minimum tools needed, drag is the easiest to measure of the two forces in which we are most interested.

There are various ways to measure drag on track, though one method is more commonly used than all the others. Two of the more sophisticated techniques require measurement of either suspension loads in the horizontal plane or driveshaft strain (torque). In both cases the sensors and the data acquisition systems required to log and enable analysis may be beyond budget. Nevertheless, both methods provide the ability to measure total vehicle drag. A third option, available space, gearing and reliable at-the-wheels brake horsepower and frontal area figures permitting, is to measure the car's maximum speed, and calculate the drag coefficient using a form of the equation we saw in an earlier chapter:

$$\text{BHP absorbed} = \frac{C_D A V^3}{1225}$$

(A, frontal area in square metres, and V, vehicle speed in metres/second). Rarely are all the required elements to do this available though...

Probably the most widely used technique to measure drag is the deceleration or coastdown technique, something *Racecar Engineering* columnist

Paul van Valkenburgh wrote of in that journal, and also his book *Race Car Engineering and Mechanics*. This provides a measurement of the total drag force. Observant readers will have spotted the drawback of these methods though – that the total drag force includes a mechanical resistance component as well as an aerodynamic one. We'll come back to that shortly.

First, how is the coastdown method used? Simply put, the vehicle is taken up to a reasonably high speed, put into neutral, and allowed to slow down. The rate of deceleration, which is proportional to the total drag force as defined by Newton's Second Law of Motion, is either measured by accurately timing between two reference speeds, or calculated from logged speed versus time data. Thus the simpler data logging systems that measure speed via wheel rotations or by using GPS technology could be utilised. It sounds simple, but it is a method prone to various drawbacks. For example, if absolute drag forces or coefficients are required, then some means of measuring or estimating the mechanical resistance (mostly rolling resistance, plus transmission losses) and the rotational inertia of wheels, brakes, gears and so on are also required.

There are methods detailing the mathematical treatment of these aspects, such as that within the standard SAE J1263 'Road load measurement and dynamometer simulation using coastdown techniques'. Other more practical suggestions include van Valkenburgh's walking speed coastdown to give an indication of the rolling resistance (though transmission losses are speed dependent). And then there's Joseph Katz's idea of towing the car at the relevant speeds in a 'sealed' bottomless trailer and measuring the total non-aerodynamic towing force, suggested in his book *Race Car Aerodynamics*. More practically, rolling road chassis dynamometers can be used to measure mechanical resistance forces, including tyre and transmission resistance, over a wide range of wheel speeds. And there are entirely mathematical approaches to factoring out the rolling resistance component from coastdown test data, such as that highlighted by Hitoshi Takagi and Yutaka Narita at the 2004 MIRA Aerodynamics Conference.

But if it's the incremental changes arising from alternative configurations that you're interested in, it isn't actually necessary to factor out the mechanical resistance component. Changes to the total drag that arise from changes to the aerodynamic configuration can be safely assumed to be aerodynamic in nature in our context, unless the magnitude of changes so dramatically increases the vertical forces that rolling resistance is affected too. Even then, it's better that we measure it!

But one of the evident drawbacks of outside track testing, assuming a sufficiently long, flat road or section of test track is available, is environmental

fluctuations, otherwise known as wind. SAE J1263 includes some mathematical and measurement corrections that can be applied to cater for wind fluctuations, although criticism has been levelled at this approach. But the obvious, practical remedy is to test in still or near still conditions, which usually means sometime between sunset and sunrise. And run the car several times in opposite directions, if necessary applying some statistics to the results to smooth out data fluctuations.

Another important factor is the actual level of drag. A high drag car will decelerate more rapidly than a low drag car when coasting down, and thus will require less measurement precision to obtain a reasonable result. The corollary of this is that low drag, and small drag changes, require higher measurement precision. And drag increments from configuration changes may either not be sufficiently large to be detected, or they may not exceed the levels of environmental fluctuations, with the same result – they will not be picked up. So, the coastdown method could be relatively easily employed to attain a baseline drag force figure, from which a  $C_D$  value could then be calculated. But its use to obtain incremental drag changes arising from configuration changes could be pushing the limits of precision in many cases.

### **Measuring surface pressures**

It is possible to map the local static pressures over and under a racecar's surfaces, and to monitor the effects of configuration changes, using what we might call 'pre-data logging' methods, and again Paul van Valkenburgh covers this approach in Race Car Engineering and Mechanics. Whole body surface pressure plots could be produced, or study could be confined to areas of particular interest, such as underbodies and diffusers, or wings. And you actually only need enough space to run the car safely at the chosen test speeds, so the track requirement is as basic as it can be.

The measurements are carried out by drilling small holes through the surface(s) of interest and fitting tubes, flush with the outside surface of these holes. The tubes can then be connected to a set of traditional U-tube manometers, probably half filled with dye-coloured water, and with the other end open to atmosphere. The levels in the manometers will respond differently to the different local static pressures at different locations on the car as it is driven along at the relevant test speed. This enables information on pressure distributions to be compiled (recording may usefully be done photographically), and differences between configurations could be determined.

If you wish to calculate actual static pressures, pressure coefficients and so forth, it is necessary to compare static pressure readings on the body surfaces with a reference static pressure in air that is undisturbed by the car's motion. With a closed car this could be measured inside the car, but with an open car the reference static pressure can only really be measured a few feet above or ahead of the car with a Pitot tube (see Figure 8-1). This device also enables the total pressure to be measured, and the difference between the total pressure and the reference static pressure can be used to calculate dynamic pressure, as defined by Bernouilli's Equation. And, from that, the true speed through the air, including any environmental airflow (wind) can be calculated (dynamic pressure, remember, is defined as  $1/2 \times \text{air density} \times \text{air velocity squared}$ , or  $1/2\rho V^2$ , where  $\rho$ , the Greek letter rho, represents air density).

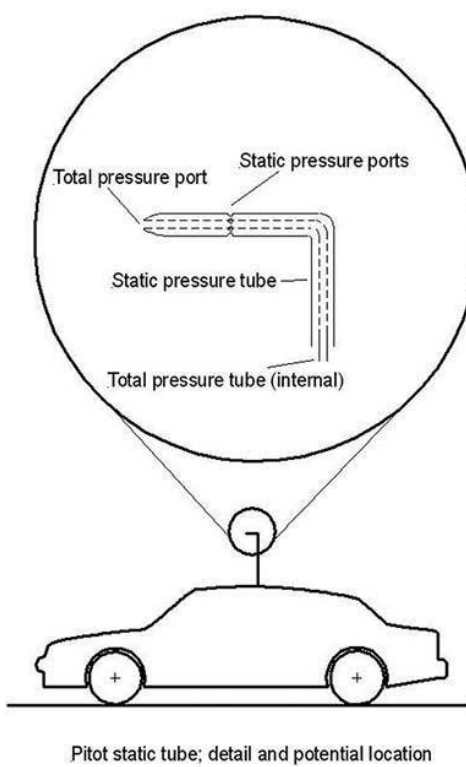


**Figure 8-1** A Pitot Static tube, and a suitable location for measuring speed through the air.

If a suitable data logging system is available, it is obviously possible to purchase electronic aerodynamic pressure sensors that replace the manometer(s), and which enable data recording. Multi-port sensors are available, as are so-called 'scanning valves', each of which enables the rapid

acquisition of pressure data from multiple points of interest. Such sensors still require connecting via narrow-bore plastic tube to the surface ‘ports’ where pressures are to be sampled. Alternatively, surface-mounted pressure transducers are also available for the same purpose, which may not require the drilling of myriad small holes in your racecar.

In reality, measuring static pressures at a large number of locations over a racecar’s surfaces will require quite a number of runs even if a multi-port pressure scanner is available. The mapping process is therefore likely to be adversely affected by environmental fluctuations. On a practical level then, this technique could perhaps be more usefully deployed to measure more localised pressure profiles, such as wing or underbody surfaces, as suggested above. But such information can provide very useful insights into the effects and interactions of configuration changes. For example, as Katz shows us in a number of illustrations in *Race Car Aerodynamics*, the effect of the presence of a rear wing or its location on underbody pressures can be plotted from a relatively small number of pressure measurements.

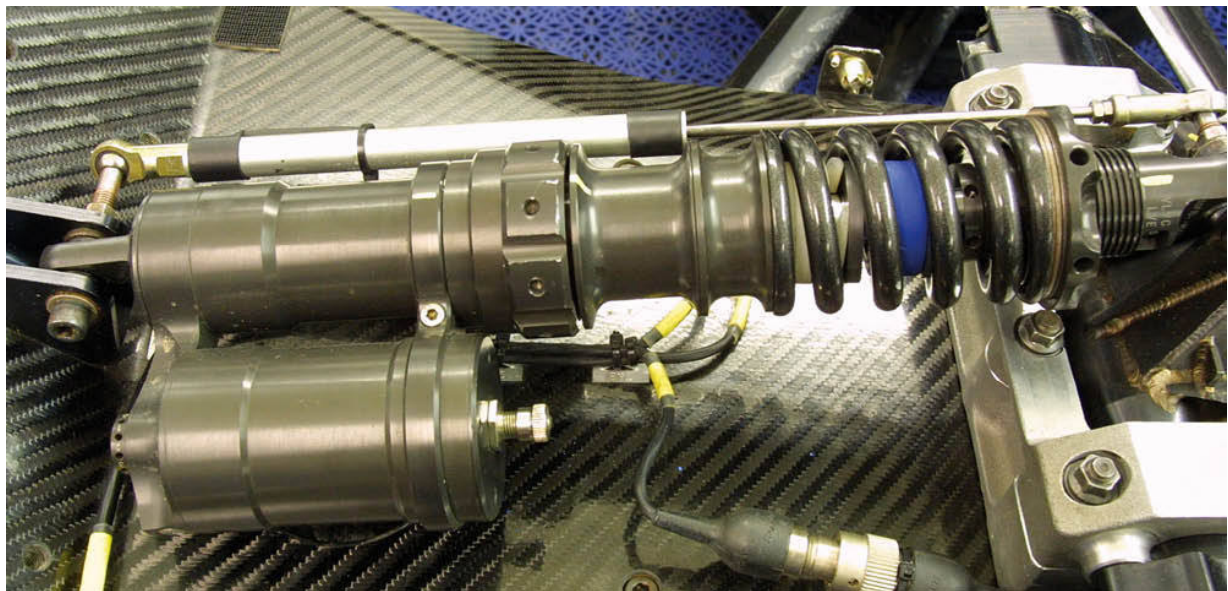
## **Measuring downforce**

When it comes to aerodynamic forces, we’re often far more interested in downforce than drag, usually for good reason. And it can be easier to measure downforce in many cases because the forces involved can be larger than drag, except in categories where downforce is limited by regulations. As with drag force measurement, downforce can be measured in a number of ways. And again, you just need an adequately long, flat, smooth straight that allows you to accelerate up to and run safely at reasonably high speed.

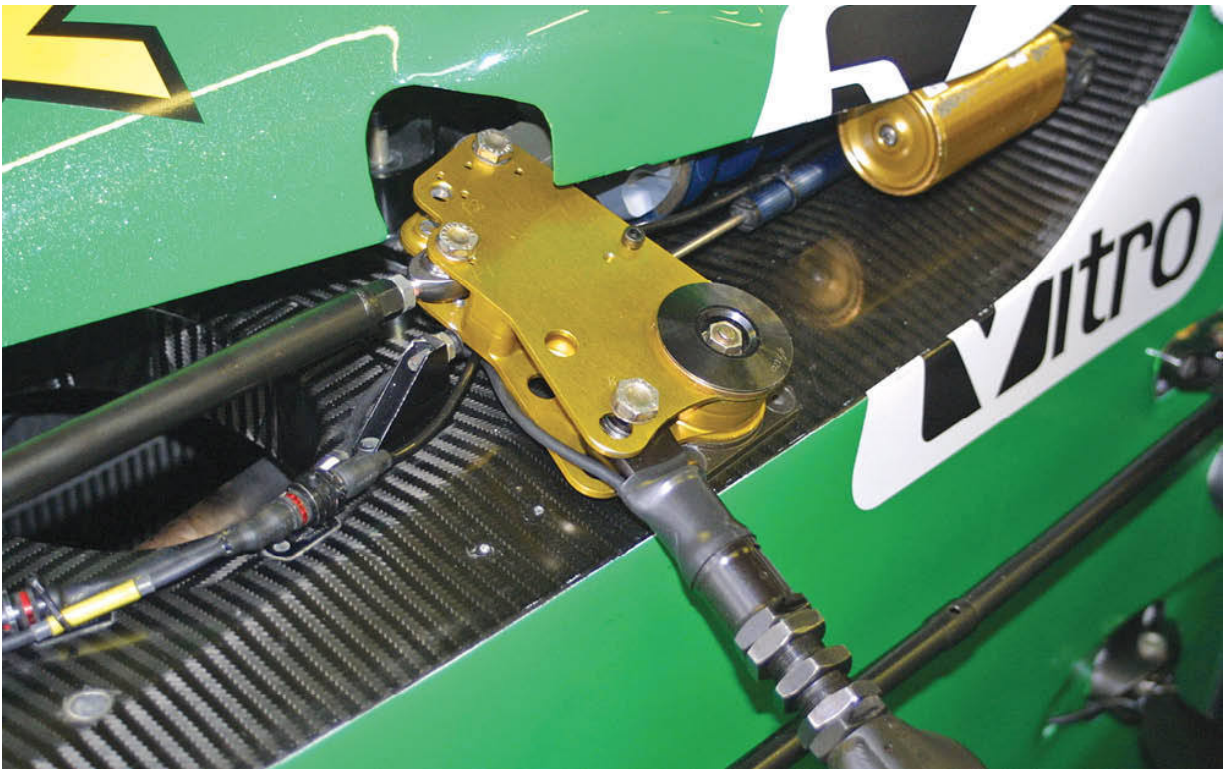
The most commonly used method of attempting to quantify downforce is to measure suspension deflection at speed, which more often than not would be done with linear potentiometers rigged to measure damper travel. Running the car at a constant, fairly high speed enables the deflections arising from aerodynamic suspension compression at front and rear to be logged. And these deflections are calibrated back in the garage by measuring the deflection with a known mass on each axle, throughout the range of travel if non-linear wheel rates are employed. Naturally the ‘noise’ produced by track surface irregularities needs filtering out, but a reasonable assessment of the download acting through the suspension can be attained.

Once more, van Valkenburgh has suggested that suspension deflections could be measured with some form of visual deflection indicator, perhaps attached to the centre of anti-roll bars to measure movement at each axle, or via some form of index mark on the suspension bell cranks for example.

Equipped with a camera to record the readings, this may well provide adequate information if data logging is not available. Needless to say, the ease with which suspension measurement can be performed will also depend on spring stiffness and available suspension travel, and also on friction within the suspension system.



*A linear potentiometer measured the suspension deflection on this spring/damper unit.*



*A load cell at the top of the pushrod could be used to directly measure downforce from the wings and body.*

Other options for measuring downforce include using strain gauge load cells to measure directly the download through the spring/damper units or the pushrods or pullrods that actuate them. The important thing to remember about measuring either suspension deflection or loads is that they do not include the vertical aerodynamic forces generated by the wheels themselves. And with open wheel cars in particular, but even on closed cars, these forces can be significant.

A possibly more precise (depending on the amplitude of suspension travel) but indirect means of assessing download is to use laser ride-height sensors, although this includes tyre deformation too, but a basic ride-height versus vertical load calibration will take this into account. The really well-heeled team might have the budget to use wheel force transducers that are capable of including the wheel-generated loads, but the aim here is to examine the more accessible options.

The precision with which downforce can be measured will still be affected by environmental factors, like wind and track irregularities, as well as the precision of the sensors themselves. But if downforce is greater than drag, we ought to be able to measure it more accurately. And in such cases there is also

the possibility that downforce increments resulting from configuration changes will not only be detectable but quantifiable too. However, if we accept that our repeatability is going to be of the order of plus or minus a few per cent, we'll have to be looking for increments in excess of this to be able to quantify them. Nevertheless, it should be possible to map some balanced options ranging from low to high downforce levels. Then it will be necessary to correlate these settings, which account for body-generated downforce only, with on-track handling characteristics at 'aero speeds' so that a truer picture of what constitutes a balanced set-up may be obtained.

### **Professional methods**

Alex Somerset was formerly chief engineer at front-running British Touring car team Triple Eight Racing, working on the Vauxhalls, and also worked at Team Dynamics in 2004 and its championship-winning 2005 season with the Hondas. He also had previous experience with other well-known touring car and single-seater teams. As a proponent of the importance of aerodynamics even in a category like the British Touring Car Championship, which severely restricts freedoms in this area, he has devised his own methodologies for both coastdown testing to measure drag and straight-line testing to measure downforce. 'Straight-line testing is still considered the most useful tool in aerodynamic testing, and is still employed by F1 teams,' he says. So his thoughts on how to carry out downforce measurements are therefore well worth noting:

'First you have to look at the car set-up. I have noted that as drivers attempt to maintain 100mph or 120mph, minor throttle changes can alter the attitude of the car. Therefore, a method of maintaining a fixed engine speed aids the driver in maintaining a constant car attitude. One solution involves a steering wheel-operated engine [rpm] limiter that can be activated when the driver reaches the required speed in a certain gear.'



*Alex Somerset engineered Fabrizio Giovanardi to multiple British Touring Car Championship titles while at Triple Eight Race Engineering.*

'In terms of the chassis set-up, you can run softer springs – that still prevent the car from bottoming out – to maximise the deflection for a given load and improve resolution. But don't take this to extremes, because the ride height will be affected and this can affect the downforce generated.' Indeed, with softer springs the dynamic change in ride height with increasing speed will differ on softer springs, so as Alex advises 'it's best to come up with a consistent set-up that you use for all your aerodynamic test work. This will usefully include the same set of dampers whose loads are accurately known. Disconnect the anti-roll bars to isolate the effects of one-wheel bumps or any binding up or hysteresis in the system. And have four damper potentiometers that use as much of their available travel as possible. These are then calibrated to reflect spring displacement, and you can then write a maths channel in your data acquisition system (DAS) software for spring displacement times spring constant to give a direct reading of spring force [which can then be factored via the 'known mass' calibration into a direct reading of downforce].'

To supplement the damper potentiometers, Alex Somerset has also used load cells and laser ride-height sensors. 'Measuring loads at the damper tops allows you to correlate with the damper displacement method. And lasers take

account of suspension and tyre compression, but are prone to “contamination” when it’s wet. Nevertheless they can provide some indication of total [body-generated] downforce.

‘If you don’t use a Pitot tube then testing will only be meaningful on a still day. Typically the Pitot tube should be positioned approximately one metre above or two metres in front of a body. Also calibration of the Pitot tube should ideally be performed in a wind tunnel.’ If wind tunnel time was unavailable, calibration against vehicle speed on a still day would presumably be a reasonable substitute. ‘Another problem with the Pitot tube involves the alignment of the tube with the flow. However, an investigation into the yaw sensitivity of the Pitot tube has revealed that for [effective] aerodynamic yaw angles of up to 12° the error is less than 0.5%. With this in mind it can be said that where there is a constant aerodynamic yaw angle less than 12° the error associated with the Pitot tube can be ignored.’ For reference, a (90°) side wind of 20mph and a vehicle velocity of 90mph result in an aerodynamic yaw angle of about 12°. ‘It’s useful too to have a small weather station that records temperature and barometric pressure so that the actual air density can be calculated.

‘The way I work,’ continued Alex Somerset, ‘is to set up two beacons at half and three-quarter-mile marks on our chosen test straight to enable steady state readings to come from the same section of track each time. This gives about seven seconds of data. If the car is capable of getting to a steady 120mph before the quarter-mile mark then you can get a half-mile test section and about 15 seconds of data. The driver is instructed to accelerate his car up to 120mph before the first beacon and hold the speed constant until he passes the second beacon. We do two passes up and down to give good error cancellation. You could use any section of straight on a circuit too, with the driver instructed to hold a steady speed between two markers. As long as the information is dissected from the same section of track then reasonably accurate analysis can be made. In any case, absolute values are not vital; it’s the gains [or losses] that are important.

With two beacons the data is split into convenient chunks. The readings taken are the average of the damper displacements (DAS software often gives you an average of any channel between two markers). And pressure, temperature and Pitot pressures can all be incorporated into the calculations. A simple Excel spreadsheet can then be written where you input all these values and it outputs downforce.’

So the extent to which you go with instrumentation and so forth depends on the precision and reliability of the data you require. But once you’ve

obtained a data acquisition system and some or all of the sensors discussed here, the cost of additional testing is restricted to the cost of getting to and from, and hiring a suitable straight length of track. This can make it pretty good value. So long as it's not windy...’

## Wind tunnels

It is a measure of the importance of efficient aerodynamics that so many competition car manufacturers making cars for motorsport categories, from Formula 1 down to Formula Ford use wind tunnel testing as a part of their design and development process. The amount of testing that can be done is, naturally, budget related, and in the case of the very best funded teams, nothing less than their own wind tunnels – allowing constant access and a continuous test programme (if permitted by series regulations) – will do.

It might seem reasonable to assume then that wind tunnel time does not come cheap, and that most likely it is well beyond the reach of the small manufacturer, let alone the amateur garagiste or clubman competitor.

Fortunately, this is not necessarily the case. It is possible to hire a wind tunnel on a day or even part-day basis, enabling a reasonable number of tests to be carried out, and to gain a basic picture of the aerodynamics of your particular competition car. One such facility is the full-scale wind tunnel at MIRA, in Warwickshire, England. It is possible for a small group of people to book the tunnel for a day between them, and take three or four cars along, spending a part of the session on each car. Providing the team is organised and has made sensible preparations, it should be possible to test several different configurations on each car, depending on the time taken to change from one set-up to the next. Let’s take a closer look at wind tunnel types, and how to select and use them.

Wind tunnels are precision laboratory instruments that create a controlled simulation of simplified real world conditions. In our context they enable evaluations of the aerodynamics of our strange and variously shaped ground proximity projectiles. But like all simulation tools they have imperfections. So what are the pros and cons of the different types?

There are various ways in which wind tunnels might be categorised, the most important being whether they are for hire or for the sole use of the teams that built them! We’ll look shortly at some features of tunnels you can’t hire because it’s useful to know why they incorporate them. But we’ll major on what’s offered by commercially available types for the obvious reason that they are available. Some of the technical distinctions are somewhat academic in nature, and some are of more practical import when it comes to the type and

quality of data provided. But it will help if we briefly cover the basic types of wind tunnel because of the practical implications of their design on operating characteristics.

From the viewpoint of providing a moving airflow, there are two fundamental types of wind tunnel; open-return and closed-return, as shown in Figures 8-2 and 8-3 respectively. Both types of tunnel use a fan (or fans) to generate a steady airflow; both (usually) suck the air through a 'flow straightening' screen, and then through the crucial contraction section to accelerate the airflow prior to entering the test section; and both then have diffuser sections to slow the airflow prior to encountering the fan. The closed-return type has an obvious energy-saving advantage, though it entails greater initial cost and can suffer from exhaust product or flow visualisation smoke build-up and temperature increases during long sessions. The open-return is probably much cheaper to build and can be more easily purged of smoke or exhaust fume build-up, although to isolate it from external environmental fluctuations and to contain noise it needs housing within a suitably sized building.

These distinctions will be of no more than passing interest unless the intention is to construct a wind tunnel. Of more importance to most users is the configuration of the test section, and again there are different types, with variations. The two basic types of test section are 'open jet' and 'closed jet'. In Figures 8-2 and 8-3 the test section is of closed jet type. A simplified open jet configuration is shown in Figure 8-4.

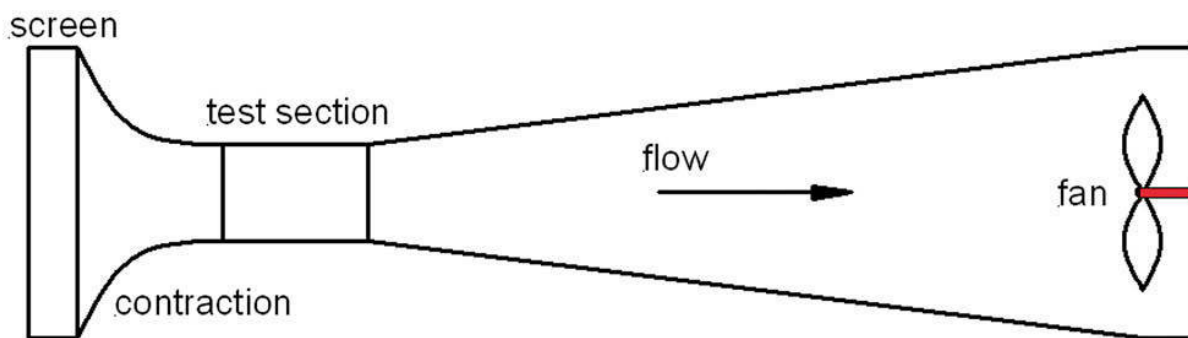


**Figure 8-2** Schematic diagram of an open return wind tunnel.

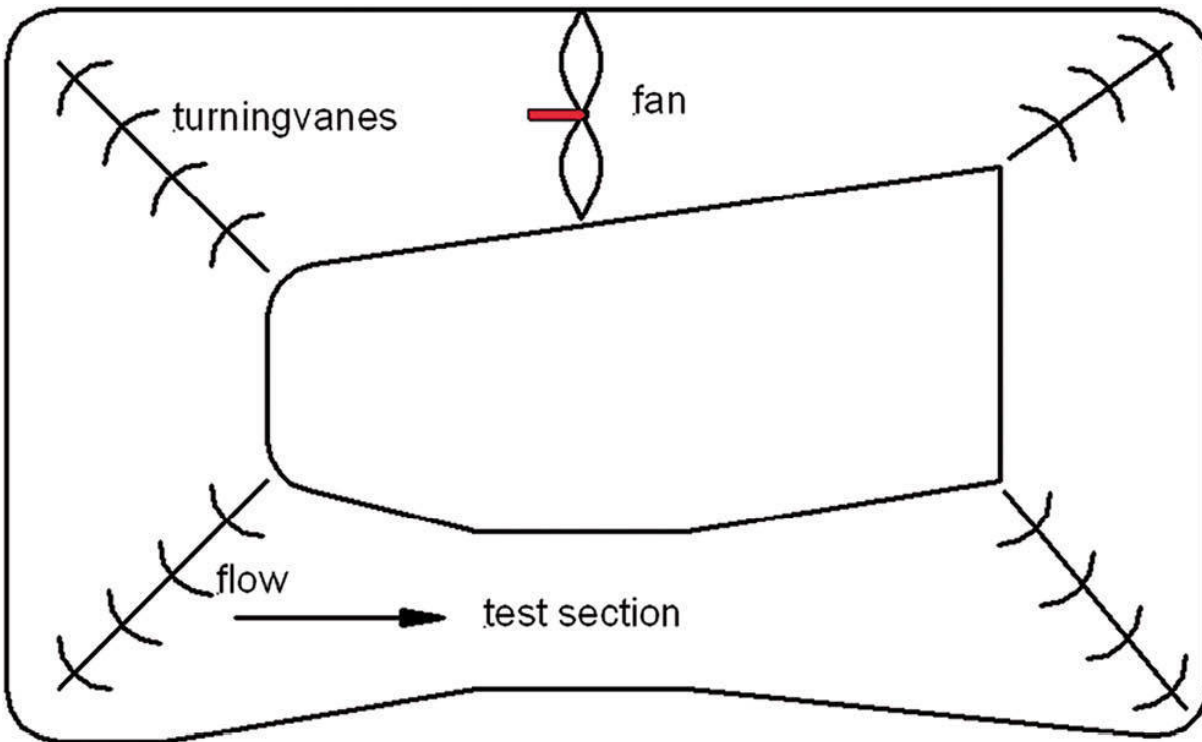


**Figure 8-3** Schematic diagram of a closed return wind tunnel.

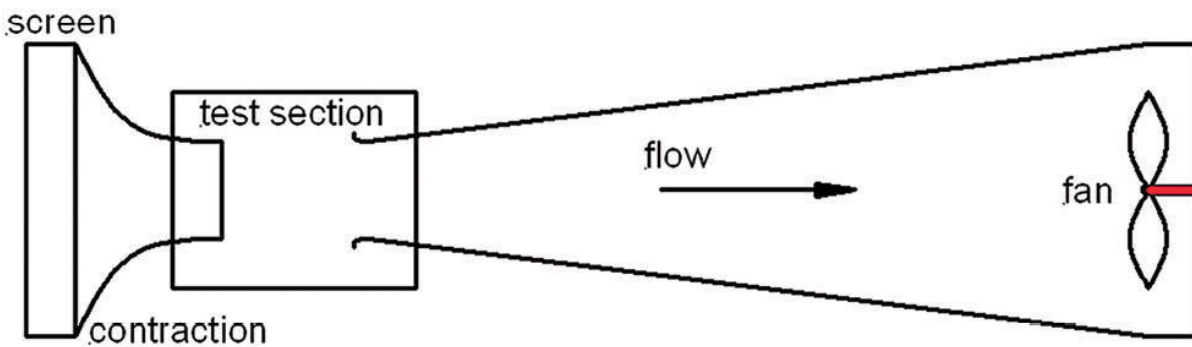


**Figure 8-4** Schematic diagram of an open jet wind tunnel.

An open jet test section allows better visibility and access for vehicle/model configuration adjustments. It also has positive and negative influences on the airflow around the test vehicle; on the negative side the flow can dissipate and mix with the surroundings, which puts a practical limit on the length of the test section, and also means more power is required to maintain air speed; on the positive side the flow around the model is not constrained by walls and is

more akin to that which occurs out on the track. We'll look at this effect in more detail shortly.

But the most obvious selection criterion involves the vehicle to be tested. Does it already exist as a full-size vehicle? Or do you plan on building a less costly (to make and modify) reduced scale model for ongoing aerodynamic development?

For the majority contemplating wind tunnel testing, the car will already exist. So the choice of type of facility is simple – you need a tunnel that can accommodate a full-size vehicle. But the physical dimensions required to fit around the car are one thing; the volume through which the air flows around the car is quite another. Any wind tunnel needs to be large enough to accommodate not just the model/vehicle but also, as far as is practicable, the airflow disruptions caused by the vehicle. The extent to which the tunnel walls interfere with the flow patterns around the vehicle is dependent on the size of the test section relative to the vehicle. The effect is known as 'blockage', expressed as the ratio in percentage terms of the frontal area of the body under test to the cross-sectional area of the test section of the wind tunnel.

Numbers variously quoted for the maximum acceptable blockage range from around 5% to 10%. This figure will also depend on the manner in which the vehicle modifies the airflow. In practical terms a degree of blockage is unavoidable within a closed jet test section, and 'blockage corrections', derived from correlations with real world or possibly CFD data, are generally applied.

The smaller the blockage, the smaller the required corrections, and open jet test sections require smaller corrections. So why aren't all wind tunnels of the open jet variety? It seems they can be prone to pressure and velocity pulsations, an effect that does not afflict closed jets. Thus most motorsport wind tunnels are closed jet. We'll revisit the issue of blockage later because circumventing the problem has led to some interesting developments in motorsport wind tunnels.

For now, though, consider that if a typical full-size vehicle frontal area is in the range  $1\text{m}^2$  to  $2\text{m}^2$ , then a minimum wind tunnel test section area of  $20\text{m}^2$  would be needed, and preferably nearer  $40\text{m}^2$ . This instantly restricts the choice of facility because there are not very many commercially available wind tunnels with test sections this large. An incomplete list would include MIRA's FSWT ( $35\text{m}^2$  test section) in the UK, the German/Dutch DNW facility (max  $90.3\text{m}^2$  test section in one of their tunnels), the huge Langley full-scale tunnel ( $161\text{m}^2$ ), the Lockheed Georgia Low Speed wind tunnel ( $34.7\text{m}^2$ ) and the sophisticated Windshear facility in the States ( $16.7\text{ m}^2$  but three-quarter open jet). Another full-scale USA-based tunnel that is also somewhat smaller than

most full-scale examples is the AeroDyn tunnel ( $20.9\text{m}^2$ ) in Mooresville, North Carolina. We'll come back to that interesting facility again later. (See Appendix 4 for a longer list of wind tunnels.)

One factor that, aerodynamically speaking, distinguishes racecars is that they always operate close to the ground. This has a profound influence on the airflow around them that becomes still more significant on lower ground clearance cars. But when passing airflow over a racecar (model) in a wind tunnel, the airflow also moves relative to the ground. And as air passes over any fixed surface it develops a boundary layer, where viscous effects sap energy and momentum from the airflow near the surface. This affects the airflow under a car in a wind tunnel, and can cause underestimates of (negative) lift and drag coefficients.

So wind tunnels are also categorised according to whether they have fixed or moving floors. With a fixed floor the boundary layer potentially exists over the whole floor. Some fixed-floor wind tunnels adopt methods to lessen the effect of the boundary layer. For example, MIRA's boundary layer 'fence' creates a rolling vortex that draws energetic flow back down to floor level, reducing the boundary layer ahead of the vehicle. The boundary layer then starts to re-form, but is much thinner at the front of the vehicle than it would otherwise be. Other tunnels apply suction ahead of the car to remove the boundary layer so that, again, a fresh boundary layer starts at the front of the car. And the idea of sitting the car on an elevated platform above the tunnel's boundary layer achieves much the same result – a boundary layer begins at the start of the platform, where the front of the car is also positioned.

Other fixed-floor wind tunnels apply 'distributed suction' or 'tangential blowing' through the test section floor ahead of, beneath and beyond the car to attempt to eradicate the boundary layer altogether. Suction can correlate well with road measurements, and tangential blowing is another step forward because it can reinstate lost momentum in the boundary layer, though it is not without problems.

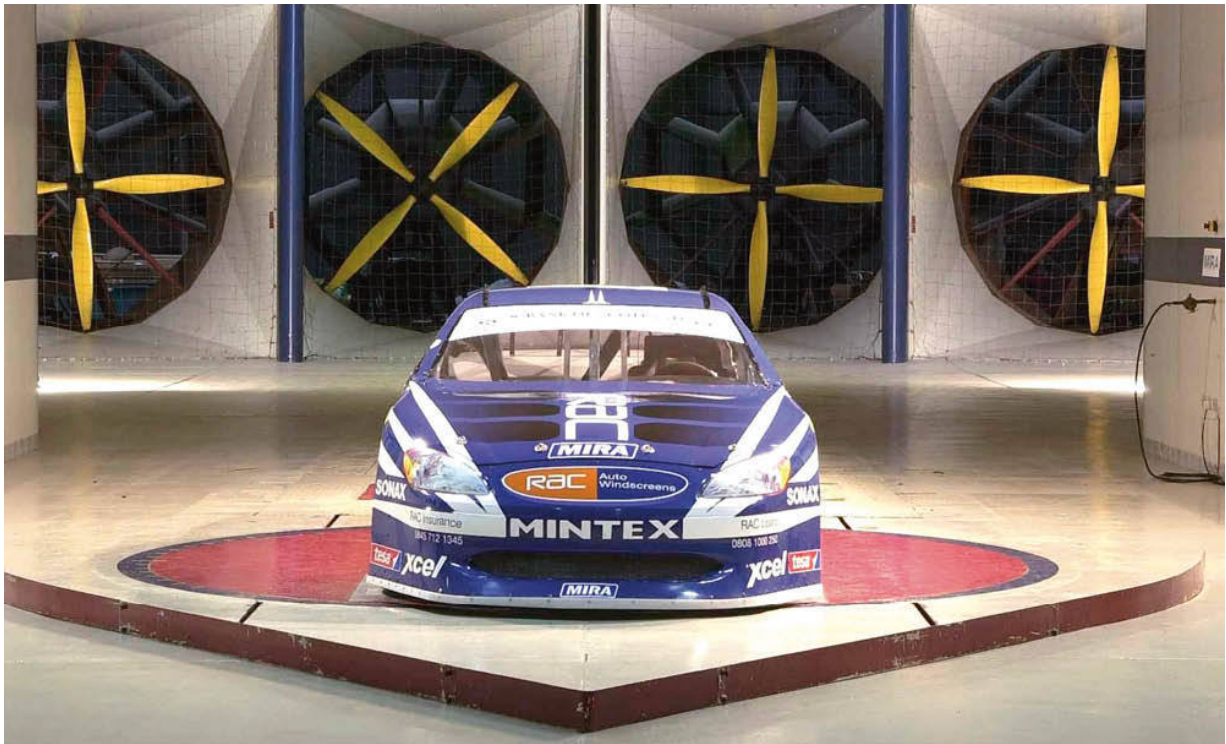
The limitation of the boundary layer does compromise the proper simulation of under-car airflow, especially with low ground clearances. But this doesn't stop these fixed-floor tunnels from providing incredibly useful information on upper surface and internal flows, and the effects of configuration changes. A degree of caution is needed, however, where under-car flow is involved.

A moving-floor – or moving-ground – tunnel uses a type of conveyor belt running beneath the test vehicle at the same speed as the airflow, which at first glance overcomes the problem of the boundary layer at 'ground' level. But the

boundary layer still develops ahead of the moving-ground belt, and therefore still needs dealing with if the expense and complexity of the moving ground belt is not to be squandered.



*The sophisticated full-scale, moving ground, rotating wheels wind tunnel at Windshear, North Carolina, USA. (Windshear)*



*MIRA's boundary layer fence. (MIRA)*

There are few moving-ground full-scale facilities (see Appendix 4). And even in a smaller tunnel designed for testing scale models, other complexities include: applying boundary layer suction ahead of the belt; running the belt over a platen and applying suction to keep it flat and prevent it being sucked upwards by the low pressure developed beneath racecar models; supporting the model, controlling its position and attitude, and acquiring force, moment and pressure data; accurately locating and supporting the wheels to run (and rotate) on the belt; keeping the belt cool; and enabling yaw adjustment for car/model and belt. Careful engineering solves these problems, so moving-ground wind tunnels appear to be the perfect answer for aerodynamic testing of low ground clearance racecars whose performance is in part governed by under-car airflow...

But there are still problems simulating the real world. As mentioned, full-scale tunnels with moving ground are rare because of cost. So, historically, smaller tunnels have been used. Thus, blockage limits the size of the models that can be tested. Consider that a typical single-seater frontal area might be  $1.5\text{m}^2$ , then even allowing for 10% blockage being acceptable in a closed jet tunnel it would require a  $15\text{m}^2$  test section for reliable full-scale work, or 6.0 to  $7.5\text{m}^2$  for 40–50% scale models. Figures quoted for the scale of models that

can be accommodated in some tunnels suggest that blockages in excess of 10% have been used...

To reduce blockage problems, models need to be small relative to tunnel cross-section. But reductions in model size lead to two types of errors. If manufacturing tolerances are thought of as fixed, then making a half-scale model means that imperfections are, relatively, twice as large as at full-scale. And reduced scale brings problems of ‘flow similarity’.

As we saw earlier in this book, the type of flow (laminar or turbulent) prevailing in the boundary layer depends, among other factors, on the distance over which the flow has passed on the surface, and on the mainstream airflow speed. If density and viscosity remain constant, the Reynolds Number is proportional to the product of distance and speed. (Surface roughness also affects boundary layer development, and is clearly also relevant to model manufacture.) So, to achieve flow similarity between scale and full size, air speed should ideally be increased in inverse proportion to the scale. Thus, for the same Reynolds Number on a 50% scale model as a full-size car, real world air speeds should be doubled in the tunnel. This has not been achievable with most ‘scale’ wind tunnels because of air movement and moving-ground belt speed limitations, and so there are flow dissimilarities with the real world. This is the main reason top echelon wind tunnel models increased in size from 40% to 50% and now to 60% or more. And, as investment cycles come and go, the commercial market is slowly following the trend.

On a practical level, if flows are fully attached to all surfaces on a scale model then the same ought to be true on the full size version. But where flow separations occur on a model, it is actually difficult to predict not only where but IF separation will occur at full size. And designing shapes from flows that are fully attached at scale can lead to too conservative a design at full scale. So ‘pushing the performance envelope’ using scale testing is not easy. There are corrections and ‘fudges’ that can be applied, but caution is again the watchword here.

So, bigger models are preferable, but cause greater blockage, yet suitably bigger moving-ground tunnels and much faster speeds have been generally unattainable...The next step in tunnel sophistication used one of the benefits of the open jet test section. Recall that the open jet lessens wall interference, permitting larger models to be tested. Three further techniques utilised this benefit in rather different ways.

‘Slotted wall’ test sections allow some air to bleed through the test section walls. These enable lower correction factors to be used for a given vehicle size or yaw orientation, yet they don’t suffer the inherent unsteadiness found with

open jet sections. Thus, larger models can be used in nominally the same size tunnel. Minor downsides include worsened visibility and access to the model.

A variation on this theme is the ‘contoured wall’ test section. Here the walls are solid, but the shape of the walls (and ceiling) is designed to ‘fit’ to the ‘far field’ flow streamlines. This lessens interference with flow close to the model and greatly reduces the blockage caused by the model. The required shape of the walls would probably come from CFD simulations of the flow field around a car, so this method is only going to be absolutely right for a given model shape and scale. The Honda Wind Tunnel at Imperial College, London, was modified in this way and optimised for 50% scale open wheel racecars (corrections still enable other car types/scales to be tested).

With the aforementioned AeroDyn wind tunnel in Mooresville, NC, the test section was built specifically to suit NASCAR racecars. The shape was defined with help from Advantage CFD (now TotalSim) in the UK, who evaluated the flow field around a generic NASCAR model to aid the AeroDyn design. The test section originally had adjustable slotted walls, but closing up the slots had no adverse effects on flow quality, such was the benefit of the contoured wall approach. Thus, full size models of the type around which the tunnel was designed can be reliably tested in a section quite a bit smaller than in other full-scale tunnels.

More recently in Formula 1 came the expensive extension of the contoured wall concept, christened ‘adaptive wall’. Here pressures and velocities sensed around the model are fed back through control mechanisms to actuators that alter movable panels to change the test section shape to maintain a constant pressure along the test section. It is said that adaptive walls permit acceptable blockage to be increased by as much as a factor of four or five, which ought to enable a full-size vehicle to be tested in a test section size recently thought only big enough for scale models.

One of the simpler dynamic effects to have been beneficially incorporated into wind tunnel testing was mentioned earlier – rotating the wheels. Generally, isolated (exposed) rotating wheels produce less lift and drag because the flow separates earlier than on a stationary wheel. So the forces on an open wheel car will be less accurately predicted by a wind tunnel that does not enable rotating wheels. Suitably shaped wedges or ‘trip strips’ that cause flow separation at a more realistic location on non-rotating exposed wheels have been used when wind tunnel testing open wheelers in fixed-ground full-scale wind tunnels. One method of rotating the wheels is used at AeroDyn – electrically powered rollers (sitting atop the load cells) drive the wheels at the

appropriate speed. Thus, even on closed wheel cars the effect of non-rotating wheels is perceived as significant.



*The AeroDyn wind tunnel was designed with the help of CFD! (AeroDyn)*

Another aspect mentioned earlier is the ability to alter the yaw angle of a car under test. Many tunnels, full- or reduced-scale, have turntable facilities enabling testing across a range of static yaw angles to better simulate cornering situations. Similarly there are methods for altering pitch angle, ground clearance and roll angle. But generally it is only possible to make measurements with these parameters fixed. And the truth is that this only allows us to scratch the surface of possibilities here because the aerodynamics during rapid dynamic changes to yaw, pitch, heave and roll will be very different to simplified steady state measurements.

That's the drawback of using any simplified model, be it physical or computational. We might gain a sufficiently improved grasp of what's happening to allow us to make improvements, but our simulations fall short of reality. A proper understanding of these transient states will probably provide the next substantial 'unfair advantage' in motorsport aerodynamics, but the problems are also considerable.

So what you can expect from wind tunnel testing depends fundamentally on the type and size of car/model and tunnel available, and how sophisticated an aero R&D programme you require. Very useful indicative data and trends can often be obtained from some fairly simple full-scale or model testing, even if absolute correlation with the real world is less than perfect. It's all about where you are now, and where you want to be. And above all, it's about understanding the strengths and limitations of the facility you decide to use. Remember – Peter Wright and his Lotus colleagues ‘discovered’ ground effect using far less sophisticated, smaller facilities than are now available for hire...

### **How to approach wind tunnel testing**

Full-scale wind tunnel time isn't cheap, so maximising the benefits is all about preparation. But for the first-time visitor to the wind tunnel the initial approach at least may need to be more basic, as David Wain, manager at the UK's only commercially available full-scale wind tunnel at MIRA, suggested: ‘Until baseline figures are established you may not know where to concentrate your efforts. So we suggest that new customers with no data come in for a couple of hours to measure this. After they've gone away and analysed the baseline data they can then make parts to try out, and come back for a development session.’

Once you know the total forces, and especially the front to rear split of vertical forces, you are then in a better position to design a development programme. But it isn't always going to be viable or possible to make two visits, in which case you just have to prepare for all eventualities. The key at the outset is to define what you hope to achieve, prepare a plan, and gather the requisite materials and tools. But before you head off to the wind tunnel, there's a lot more useful preparation to be done.

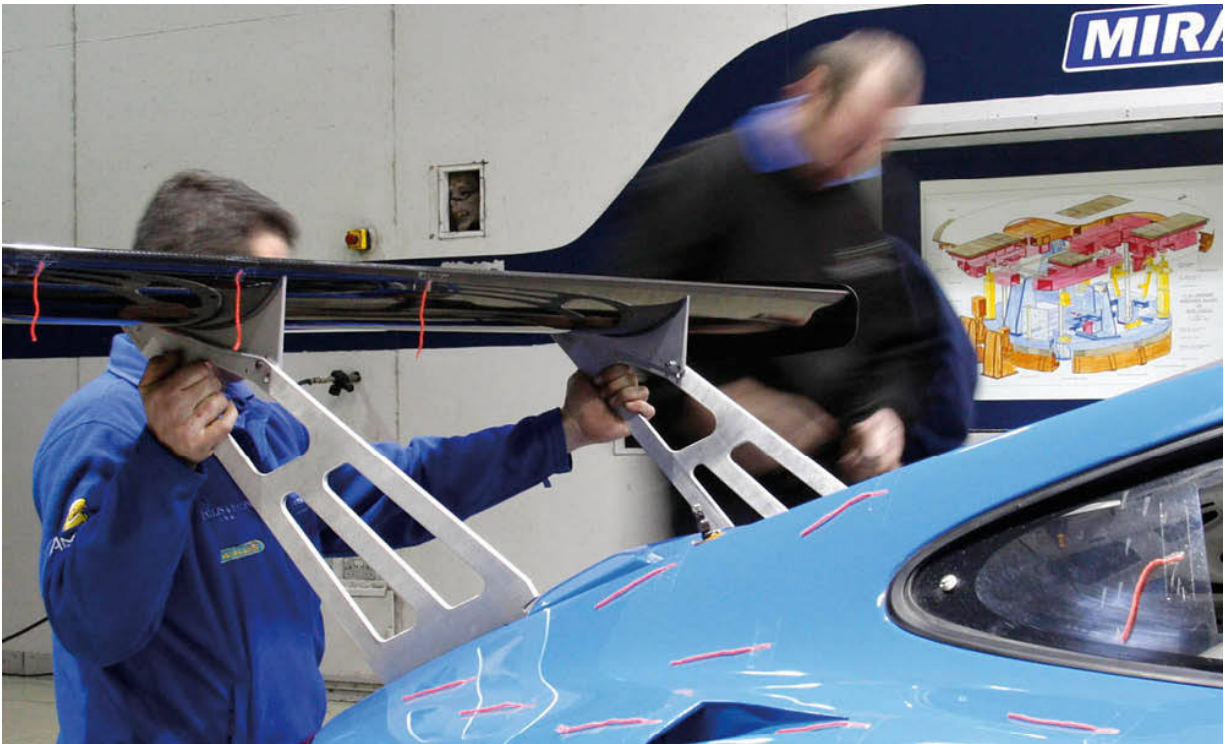
First, prioritise the configurations you want to evaluate, and then work out how many runs you hope to fit in to the allotted session duration. One of the first questions is how long does a run take? At MIRA, for instance, it takes about a minute to accelerate and stabilise the airflow, a minute to sample data, and a further minute to decelerate the air again before entering the test section to make a configuration change. An allowance of five minutes per run is therefore a good basis for planning.

But of more significance to the number of tests that can be performed in a given time is the time it takes to make the configuration changes themselves, and this is key to optimising your session. If possible, install as many test parts as you can on the car beforehand, because removing them will almost certainly be faster than fitting them. If for experimental reasons this can't be done, if

strong interaction between parts is likely for example, then spend time ahead of the session pre-fitting parts to minimise fitting time in the tunnel. The professionals suggest rehearsing changes and timing how long they take so you can refine your schedule, adding a time contingency of 50% for each change, especially if they involve jacking the car up. Chances are some modifications will be made up on the day too, so take plenty of suitable materials (see the list below). Once you've prepared your schedule in this way, bear in mind that you may have to deviate from it in response to the results too. If something particularly interesting needs further investigation, do it. Conversely, if you sense you're going up a blind alley, stop and move on to the next configuration.

Plan-in time for 'flow visualisation' too, using smoke if available; wool tufts (which will have been stuck on previously of course...) and test fluid if applicable. Time spent recording this with still and video cameras can be very worthwhile, but eats into your allotted test period all too quickly.

There is some basic information that the wind tunnel team will require from you in advance, depending on how the forces on your car are to be measured in the wind tunnel you are visiting. At MIRA, for example, the maximum and minimum track widths (to the inside and outside of the tyres) and the wheelbase enable the pads that sit atop the load cells to be pre-adjusted to fit. And a value for the frontal area will enable the data acquisition software to calculate coefficients from the forces measured by the load cells. And coefficients are often easier to work with in making quick assessments of changes. See Figures 8-5 and 8-6 for a guide on working out a reasonable estimate of frontal area.



*Rehearsing configuration changes can save valuable time in the wind tunnel.*



*Allow time during your wind tunnel session for flow visualisation and photography.*

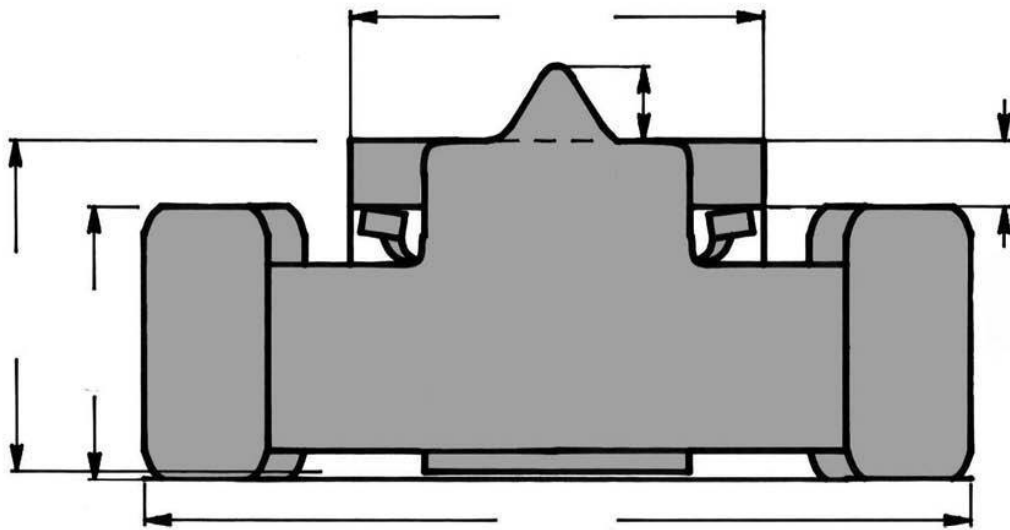


**Figure 8-5** Add up the frontal areas of the grey shaded parts to estimate the overall frontal area of an open-wheeler.

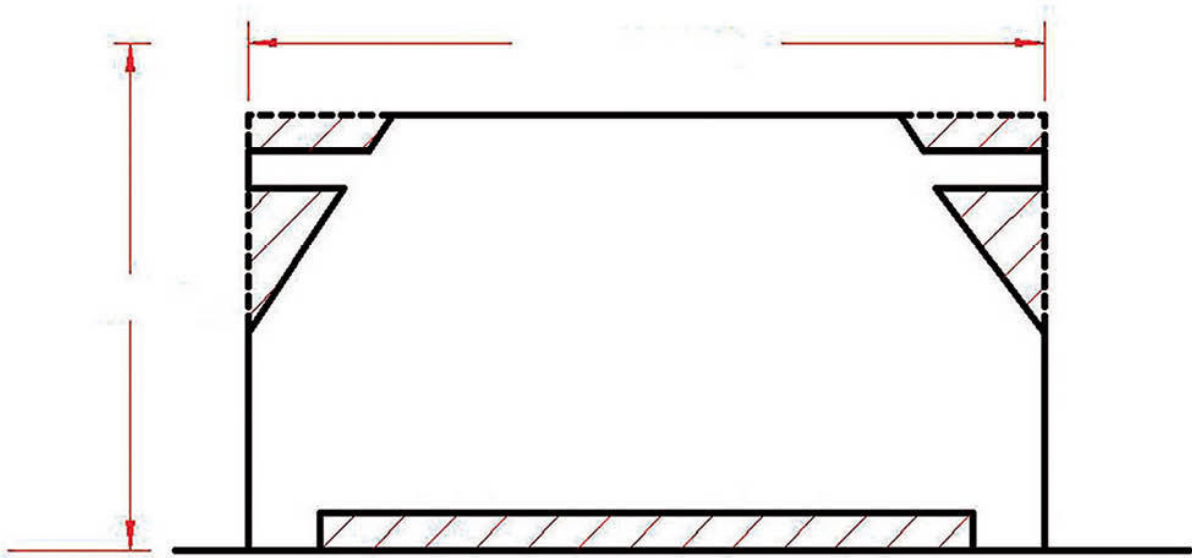


**Figure 8-6** Multiply the width by the height, then subtract the area of the hatched sections for an estimate of the overall frontal area of a closed-wheeler.

Other measurements usefully done ahead include the front and rear ride heights, ideally at easily accessed reference points that enable rapid verification

in the tunnel. Another time-saver is to work out what effect a turn on the spring platforms or push/pull rods has on ride height so that predetermined incremental changes can be quickly made. If ride height is not easily adjustable in this way an alternative, if the tunnel floor under the wheels is fixed, is to preset the car to its lowest envisaged ride heights and prepare some tyre contact patch-sized ‘shims’ from plywood, say 3mm to 5mm thick, so that a range of ride heights and rakes may be tested, if appropriate. Check with your tunnel team to see if they can provide weights to simulate the driver aboard (if relevant) and that if it’s an open car, a suitable crash helmet-wearing dummy is available to put in the cockpit!

Another way of dealing with the ride heights is to replace the spring/damper units with something like tube or bar, with suitable end fittings enabling attachment where the spring/damper units normally bolt, that hold the car solidly at pre-determined ride heights, and which are quickly adjustable or interchangeable to cover the range of relevant ride heights. This will give you control of the ride height and prevent the tunnel’s airflow actually altering it through downforce compressing the suspension, thus enabling you to ‘map’ the aerodynamic results across a relevant dynamic working range with greater precision, remembering to deduct tyre compression later...

One last important preparation task is to have a means of holding the brake pedal firmly down to render the car immovable, if it doesn’t have an efficient parking brake that is.

A small team is required to perform a test session, with a designated leader/decision maker; a configuration notes maker/photo taker (possibly the leader); and a well-organised small group (probably two to four people, as appropriate) to carry out configuration changes. The session leader may well be a team aerodynamicist, but if your team does not have one available, your wind tunnel can probably provide one if pre-booked. Although an accessible, qualified aerodynamicist will probably incur an extra fee, he/she is a valuable asset, especially in the early stages of base lining and development.

Different wind tunnels have different methods of dealing with the boundary layer that develops along the wind tunnel floor as we have seen. The important thing with racecars with generally low ground clearances is to specify the best boundary layer control that’s available. And if rotating wheels is an option, then it’s clearly better to utilise that facility too.

At MIRA it’s usual to start a session with a couple of baseline runs at different speeds to establish whether there are any ‘Reynolds effects’, which is to say, whether there is any significant difference in the calculated coefficients at different air speeds. Such differences might arise, for example, if a particular

car shape creates flow separations in different locations at the different speeds. If not, then it's more economical to run at the slower speed, and it also takes less time to accelerate and decelerate the airflow.

These initial runs also serve to indicate what level of repeatability is to be expected. Coefficients are generally reported to three decimal places, and one would expect duplicate readings from a single run to be within 1%. For example, on a GT car tested at MIRA the drag coefficient was around 0.500, so on any pair of duplicate results from a run, variation between results should be no greater than 0.005, or 'five counts'. In practice, duplicates from this session were nearly all within two or three counts. If variation consistently exceeds this level, stop to look for reasons – something may be loose on the car and interfering with the airflow.

Once under way, it's then a case of running through scheduled configuration changes, taking notes and photos, and logging results. The wind tunnel data acquisition system generates an electronic file or paper printout at session's end. But it helps the results to 'sink in' at the time if the team's note-taker writes down the key data or types them into a laptop-based spreadsheet. It helps too, where appropriate, to plot the results of parameters mapped over a range of angles, heights or distances, and this again can be done with pencil and paper or spreadsheet at the time. Trends – and deviations from trends – are much easier to spot using graphs.

BTC engineer Alex Somerset advises that 'should a configuration lead to suspect, contradictory or just plain surprising results, if time permits then flow visualisation using a smoke generator can help indicate what the flow in the area of interest is doing, and increase understanding.' In any case, on a first visit with a car it helps enormously to allot 10 to 15 minutes during the session to run the smoke plume all over the car and video and/or photograph the results for later study. Note that if ambient temperature is below 'comfortable', then standing in a wind tunnel at 25–30mph for flow visualisation runs will cause major wind chill, so take a securely fitting hat and a warm coat!

Sometimes an idea doesn't work as hoped, so if some parts show poor results, be prepared to abandon that development route. It is no less valuable to discover which ideas don't work, and negative results shouldn't necessarily be disappointing.

As a final task during a session return to a baseline configuration for the last run if time and practicality permit. This will increase confidence in the results – as long as the baseline is more or less the same as it was earlier!

On that first visit to the wind tunnel it can take a while to home in on the numbers that matter on the data acquisition PC screen. MIRA provides a

printout of the results that appear on screen during the session, and examples are shown in Figures 8-7 and 8-8. There are two basic formats, displaying either forces or coefficients, and each has its uses.

MIRA Full-Scale Wind tunnel Aerodynamic Forces and Moments															
FIRM:			MEASUREMENTS STARTED 13Apr2007 09:23:49												
VEHICLE MAKE															
MODEL												OVERALL LENGTH			
TYPE												3785 mm (12.42 ft)			
CONFIGURATION 9												OVERALL WIDTH			
TRIM HEIGHT												1719 mm (5.64 ft)			
FRONT 0.0												OVERALL HEIGHT			
REAR 0.0												1163 mm (3.82 ft)			
FRONTAL AREA												WHEELBASE			
FRONT 1510 mm (4.95 ft)												2300 mm (7.55 ft)			
TRACK REAR 1570 mm (5.15 ft)												FRONTAL AREA			
FRONT 1.74 Sq.m (18.73 Sq.ft)												GROUND BOARD HT.			
REAR 0.0 mm												B. L. FENCE			
INSTALLED															
MEASURED VEHICLE WEIGHT 996.4 kg (2196.7 lb)															
FRONT AXLE LOAD: 405.7 kg (894.4 lb), REAR AXLE LOAD: 590.7 kg (1302.3 lb),															
MEASURED CENTRE OF GRAVITY 214 mm (0.70 ft) Behind Reference Centre															
No Moment Ref. offsets. Vehicle Position Offsets: X= 25.0 mm, Y= 0.0 mm.															
RUN/CONF	WIND	YAW	FORCES			MOMENTS			AXLE LOADS			DRAG	Lift/	FRONTAL	
NO.	SPEED	ANGLE	Newtons			Newton.m			POWER			POWER	Drag	AREA	
ALL SCALED TO A WINDSPEED OF: 67.10 m/s (150.10 mph, 241.56 kph)															
m/s	Deg	DRAG	SIDE-F	LIFT	MX	MY	MZ	YF	YR	LF	LR	kW	L:D	Sq.m	
1/ 1	27.50	0.0	2691.1	-39.3	-3031.8	-27.0	1323.9	-36.3	-35.4	-3.9	-940.3	-2091.5	179.1	-1.127	1.740
2/ 1	27.50	0.0	2687.1	-34.0	-3026.5	-22.6	1335.1	-39.5	-34.2	0.2	-932.8	-2093.7	178.9	-1.126	1.740
3/ 2	27.52	0.0	2625.0	-27.2	-2903.7	-9.3	1085.7	-52.0	-36.2	9.0	-979.8	-1923.9	174.7	-1.106	1.740
4/ 2	27.51	0.0	2637.3	-25.4	-2912.1	2.7	1096.6	-49.8	-34.3	8.9	-979.3	-1932.9	175.5	-1.104	1.740
5/ 3	27.42	0.0	2793.6	-42.2	-3164.4	-27.2	1603.1	-23.5	-31.3	-10.9	-885.2	-2279.2	186.0	-1.133	1.740
6/ 3	27.43	0.0	2785.7	-44.8	-3158.1	-35.4	1602.8	-24.6	-33.1	-11.7	-882.2	-2275.9	185.5	-1.134	1.740
7/ 4	27.50	0.0	2644.2	-27.3	-2947.2	-2.7	1248.6	-51.8	-36.2	8.9	-930.8	-2016.5	176.0	-1.115	1.740
8/ 4	27.50	0.0	2647.1	-33.8	-2944.8	-9.2	1250.0	-49.2	-38.3	4.5	-928.9	-2015.9	176.2	-1.112	1.740
9/ 5	27.51	0.0	2541.3	-44.3	-2519.6	-18.0	386.4	-24.2	-32.7	-11.6	-1091.8	-1427.8	169.1	-0.991	1.740
10/ 5	27.50	0.0	2551.4	-48.3	-2530.0	-24.9	390.1	-22.9	-34.1	-14.2	-1095.4	-1434.7	169.8	-0.992	1.740
11/ 6	27.48	0.0	2715.5	-40.6	-2874.7	-18.0	1023.6	-32.3	-34.3	-6.3	-992.3	-1882.4	180.8	-1.059	1.740
12/ 6	27.46	0.0	2720.0	-43.0	-2881.2	-16.5	1019.8	-29.3	-34.2	-8.8	-997.2	-1884.0	181.1	-1.059	1.740
13/ 7	27.44	0.0	2705.8	-34.4	-2828.9	-2.4	985.1	-26.9	-28.9	-5.5	-986.2	-1842.8	180.1	-1.046	1.740
14/ 7	27.45	0.0	2699.1	-36.2	-2824.6	-19.5	986.0	-28.9	-30.7	-5.5	-983.6	-1841.0	179.7	-1.046	1.740
15/ 8	27.38	0.0	2695.0	-54.8	-2839.2	-31.5	1042.5	-11.1	-32.2	-22.6	-966.3	-1872.9	179.4	-1.053	1.740
16/ 8	27.44	0.0	2675.6	-51.4	-2814.0	-38.2	1029.9	-19.0	-33.9	-17.5	-959.2	-1854.8	178.1	-1.052	1.740
17/ 9	27.38	0.0	2377.0	-68.6	-3334.2	-119.9	1448.5	56.7	-9.7	-58.9	-1037.3	-2296.9	158.1	-1.403	1.740
18/ 9	27.32	0.0	2419.6	-64.5	-3350.9	-120.2	1458.0	51.1	-10.0	-54.4	-1041.5	-2309.4	160.9	-1.385	1.740

Figure 8-7 Force data from MIRA.

## MIRA Full-Scale Wind tunnel Aerodynamic Coefficients

FIRM:				MEASUREMENTS STARTED 13Apr2007 09:23:49																	
VEHICLE	MAKE	MODEL	RACE CAR	OVERALL LENGTH			13785 mm (12.42 ft)			OVERALL WIDTH			1719 mm (5.64 ft)			OVERALL HEIGHT			1163 mm (3.82 ft)		
TYPE	CONFIGURATION 9			WHEELBASE			2300 mm (7.55 ft)			TRACK FRONT			1510 mm (4.95 ft)			TRACK REAR			1570 mm (5.15 ft)		
TRIM HEIGHT	FRONT 0.0			FRONTAL AREA			1.74 Sq.m (18.73 Sq.ft)			GROUND BOARD HT.			0.0 mm			B. L. FENCE INSTALLED					
FRONT	REAR 0.0																				
MEASURED VEHICLE WEIGHT	996.4 kg (2196.7 lb)			FRONT AXLE LOAD: 405.7 kg (894.4 lb), REAR AXLE LOAD: 590.7 kg (1302.3 lb),			CD has been reduced by 0.004 due to HBL factor of 0.700			MEASURED CENTRE OF GRAVITY 214 mm (0.70 ft) Behind Reference Centre			No Moment Ref. offsets. Vehicle Position Offsets: X= 25.0 mm, Y= 0.0 mm.								
RUN/CONF	WIND	YAW	FORCE COEFFICIENTS				MOMENT COEFFICIENTS			AXLE LOAD COEFFICIENTS			CENTRE OF PRESSURE			Lift% Front			FRONTAL AREA		
NO.	SPEED	ANGLE	CD(-CX)	CY	CL(-CZ)	CMX	CMY	CMZ	CYF	CYR	CLF	CLR	XCP	%	Sq.m						
m/s	Deg																				
1/ 1	27.50	0.0	0.556	-0.008	-0.632	-0.002	0.120	-0.003	-0.007	-0.001	-0.196	-0.436	0.0	31.0	1.740						
2/ 1	27.50	0.0	0.555	-0.007	-0.630	-0.002	0.121	-0.004	-0.007	0.000	-0.194	-0.436	0.0	30.8	1.740						
3/ 2	27.52	0.0	0.543	-0.006	-0.605	-0.001	0.098	-0.005	-0.008	0.002	-0.204	-0.401	0.0	33.7	1.740						
4/ 2	27.51	0.0	0.545	-0.005	-0.607	0.000	0.099	-0.005	-0.007	0.002	-0.204	-0.403	0.0	33.6	1.740						
5/ 3	27.42	0.0	0.578	-0.009	-0.659	-0.002	0.145	-0.002	-0.007	-0.002	-0.184	-0.475	0.0	28.0	1.740						
6/ 3	27.43	0.0	0.576	-0.009	-0.658	-0.003	0.145	-0.002	-0.007	-0.002	-0.184	-0.474	0.0	27.9	1.740						
7/ 4	27.50	0.0	0.547	-0.006	-0.614	0.000	0.113	-0.005	-0.008	0.002	-0.194	-0.420	0.0	31.6	1.740						
8/ 4	27.50	0.0	0.547	-0.007	-0.613	-0.001	0.113	-0.004	-0.008	0.001	-0.193	-0.420	0.0	31.5	1.740						
9/ 5	27.51	0.0	0.525	-0.009	-0.525	-0.002	0.035	-0.002	-0.007	-0.002	-0.227	-0.297	0.0	43.3	1.740						
10/ 5	27.50	0.0	0.527	-0.010	-0.527	-0.002	0.035	-0.002	-0.007	-0.003	-0.228	-0.299	0.0	43.3	1.740						
11/ 6	27.48	0.0	0.561	-0.008	-0.599	-0.002	0.093	-0.003	-0.007	-0.001	-0.207	-0.392	0.0	34.5	1.740						
12/ 6	27.46	0.0	0.562	-0.009	-0.600	-0.001	0.092	-0.003	-0.007	-0.002	-0.208	-0.392	0.0	34.6	1.740						
13/ 7	27.44	0.0	0.559	-0.007	-0.589	0.000	0.089	-0.002	-0.006	-0.001	-0.205	-0.384	0.0	34.9	1.740						
14/ 7	27.45	0.0	0.558	-0.008	-0.588	-0.002	0.089	-0.003	-0.006	-0.001	-0.205	-0.383	0.0	34.8	1.740						
15/ 8	27.38	0.0	0.557	-0.011	-0.591	-0.003	0.094	-0.001	-0.007	-0.005	-0.201	-0.390	0.0	34.0	1.740						
16/ 8	27.44	0.0	0.553	-0.011	-0.586	-0.003	0.093	-0.002	-0.007	-0.004	-0.200	-0.386	0.0	34.1	1.740						
17/ 9	27.38	0.0	0.491	-0.014	-0.695	-0.011	0.131	0.005	-0.002	-0.012	-0.216	-0.478	0.0	31.1	1.740						
18/ 9	27.32	0.0	0.500	-0.013	-0.698	-0.011	0.132	0.005	-0.002	-0.011	-0.217	-0.481	0.0	31.1	1.740						

**Figure 8-8 Coefficient data, calculated from the forces shown in Figure 8-7.**

The load cells under the wheels measure absolute aerodynamic forces exerted horizontally, vertically and laterally at the tyre contacts. The coefficients are calculated using the basic aerodynamic force equations, which include the frontal area of the car, hence a reasonably accurate estimate of frontal area makes the coefficients meaningful. Let's run through the printout to see what each column means and determine which numbers you are most likely to focus on.

Looking at the force printout, from left to right, the run/configuration number, wind speed and yaw angle are self-explanatory. The next three columns are the basic total forces, drag, side force and lift (negative when it's downforce). Here the major forces are drag and downforce, with small side force being logged. Side force arises either from a yaw angle or from vehicle asymmetry. In this case side force is very small compared to the drag and downforce, and can be ignored.

The moments MX, MY and MZ arise from the distribution of the aerodynamic forces around the centre of gravity. Here there's a large pitching moment (about the y-axis) arising from more downforce at the rear.

The axles loads YF and YR are the side forces measured at each axle, and are negligibly small here. The vertical loads LF and LR are important though, showing the split of downforce on the front and rear wheels ( $LF + LR =$  total lift, and  $LF/\text{total lift} = \%$  front lift as a proportion of the total, a handy measure of aerodynamic balance).

Drag is often more comprehensible in terms of horsepower absorbed, and the next column shows this in kilowatts (divide by 0.746 to convert to bhp). And aerodynamic efficiency is frequently expressed as lift divided by drag ( $L/D$ ). The final column indicates that it is possible to amend the frontal area used to calculate the coefficients should a configuration significantly alter the area.

Although coefficients (Figure 8-8) are just a mathematical treatment of forces, they can make it easier to quickly spot trends and quantify gains or losses. Note that as with the forces,  $CYF + CYR = CY$ , total side force, and  $CLF + CLR = CL$ , total lift.

This printout format also offers to calculate the Centre of Pressure, which is the point at which the total of the aerodynamic forces is effectively exerted. But the lift % front is perhaps a more useful way of expressing the aerodynamic balance, calculated from the coefficients as  $[CLF / (CLF + CLR)] \times 100$ .

Of all these figures, the ones to concentrate on in most cases will be lift and drag, whether as forces or coefficients,  $L/D$  and balance as % front lift. Balance is key in just about every case where cornering is concerned, whereas the trade off between downforce (if it can be generated in your category) and drag (generated by every racecar) is very much down to your racecar and its competition arena.

Rest assured, once you've started generating data from the wind tunnel the next questions will centre on what those trade-offs should be, and on what aerodynamic configurations you plan to test in your next session!

There are some essential materials to take into the wind tunnel for making configuration changes:

- Heavy gauge card.
- Medium to low-density tooling block or builders PU insulation foam panel.
- Aluminium foil tape (various widths and gauges).
- Race tape, lots of.
- Quick-set superglue gel.
- Foam sealing tape, lots of.
- Fasteners.
- Aluminium sheet.

- GFRP sheet.
- MDF, plywood.
- ‘Flow vis fluid’, which can comprise paraffin coloured with a little copper grease or talc.
- Tools to work with the above. Check your wind tunnel workshop has band saws, guillotines, folders etc.

Summing up some wind tunnel Dos and Don’t then:

Do:

- Plan and prepare well.
- Forward track and wheelbase dimensions to the wind tunnel in advance.
- Pre-fit parts where possible.
- Have a means of clamping the brakes on.
- Ensure all temporary parts are securely affixed.
- Predetermine exact effects of ride-height adjustments.
- Have packs of ‘tyre shims’ to alter ride height if required.
- Be methodical, work through your schedule a step at a time.
- Have one person to take notes and photos.
- Have one person to make decisions.
- Have a small group to make changes.
- Always have materials and tools ready for the next configuration change.
- Test a baseline set-up periodically.
- Allow time for flow visualisation.
- Run repeats on key or suspect tests.
- Investigate the cause of poor duplicate results.
- Use the best floor boundary layer control available.
- Analyse data fully after the session.
- Be prepared to track-test to validate conclusions.

But don’t:

- Turn up without a plan.
- Squander valuable tunnel time in discussion or decision making.
- Change more than one thing at a time.
- Place absolute faith in the results from parts near the ground in a fixed-floor tunnel, especially if there’s no boundary layer removal. Trends can still be useful if treated with caution, however.

## Scale-model testing

Among the techniques gradually filtering down from top-level motorsport and being used even at national level now is model wind tunnel testing. Racecar

manufacturers like Lola, Dallara and others have, of course, been using such facilities for design and development for years. But independent teams in Formula 3 and the British Touring Car Championship are now building their own models and running aerodynamic development programmes. So, what is involved in starting a model wind tunnel test programme, why would you do it, and what can you realistically expect in return for the not insubstantial investment in a racecar model and associated test parts, not to mention the hire costs of the tunnel?

The primary consideration is the racecar model; how it's to be made, and what the cost will be. If a 3D CAD model of the racecar is available then this can be suitably scaled, and simplified as appropriate, to create a downsized digital model of the external and internal 'wetted' surfaces. Where no CAD data is available there is a choice of scanning techniques. These can be applied to a full-scale racecar and, probably with some additional CAD work to 'fill in' inaccessible areas, they enable the relatively cost effective and relatively rapid generation of a digital model. Then, however the digital model is created, a combination of (probably computer-aided) manufacturing methods including machining, moulding, fabricating and rapid prototyping is used to construct the various components that are assembled into a – hopefully – faithful scale model of the racecar.

Some numbers from 2008 on the BTCC-winning Triple Eight Race Engineering Vauxhall Vectra model are illustrative of cost contributors. Vauxhall/GM provided CAD data to Triple Eight but it took 180 man-hours to just create the model of the bodyshell, although this included translation from one CAD platform to another (Unigraphics to Autodesk Inventor). Fortunately the digital models of the wheels and the real model wheels were available from the previous car, which in part dictated that Triple Eight stayed at 30% scale for the Vectra, even though the chosen wind tunnel (ACE in France) could accommodate a larger model. Nevertheless, the CAD for the rest of the model's air-licked components still had to be generated.

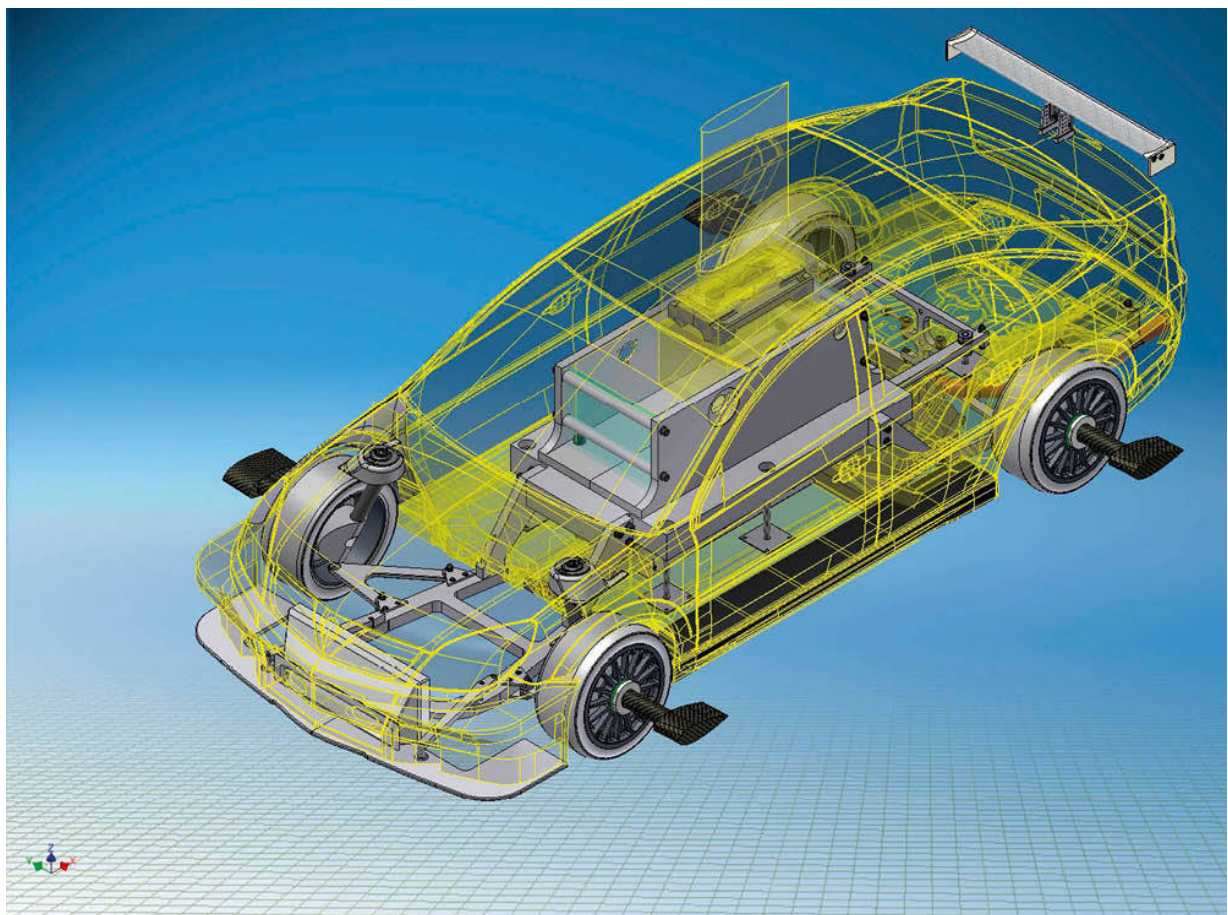


*Figure 8-9 The CAD model of Triple Eight Race Engineering's 2008 BTCC Vectra model. (Triple Eight Race Engineering)*

The pattern for the body shell, underfloor and front and rear bumpers then needed machining from epoxy tooling block, which took 120 hours of machining time. From this, moulds were then made, taking two people five days, and finally the carbon shell was made. Add to this the wheels, suspension, under-bonnet details like radiator ducting, the suitably porous radiator matrix, engine and transmission and so forth, and it becomes clear why model costs quickly add up, even if much of the work is done in-house as at Triple Eight.

Ex-Red Bull Racing aerodynamicist Simon Smart runs an aerodynamics consultancy called Velo Science that has managed wind tunnel programmes in categories like F3. He reckoned that 'the cost of contracted-out model manufacture starts at a sum just in six figures (pounds sterling) for a good quality 50% model with basic functionality. This would not include any instrumentation, which lower-budget teams tend to hire from the wind tunnel.'

Provision must also be made at the design stage for the containment of the load-measuring ‘balance’ that in most cases resides inside the model. And of course the model must attach to the wind tunnel’s ‘sting’ (the support strut from which the model is suspended), so this requirement also needs to be incorporated into the design, along with any other provisions required to achieve the model’s positional control and movement. The wheels will most likely be supported on horizontal stings. This is known as ‘wheels off’, because the wheels are not actually connected to the car. It is easier to take aerodynamic force measurements from the wheels this way than it is from a ‘wheels on’ model, and the wheel forces can then be added to the body forces to get total figures.

One of the reasons model wind tunnel test programmes have become viable for some teams in F3, for example, is that there is a three- to four-year cycle between major rule and chassis amendments over which to amortise the capital costs. This was also the case with the multiple championship-winning Triple Eight BTCC Vectra. But against this, in a sense, is that three years’ worth of development parts are also needed. Again, Simon Smart’s take on this is instructive: ‘Parts costs depend very much on what area of the car you are working on, and also on manufacturing methods. But for a low-budget wind tunnel session you’d be looking to allow on average £1,000 to £2,000 per day on parts. Just as an example, bargeboards would cost £350 to £600 each depending on manufacturing process.’

Hiring time in one of the suitable wind tunnels does not come cheap either, and although different tunnels have different pricing structures, budget figures in the order of £3,000 per day should be considered par for the course.

But although initial and ongoing costs are high, there are benefits to using a model rather than a full-scale car. There are also downsides to be considered. So let’s take a closer look at the pros and cons.

Among the principal advantages of a scale model programme is that test parts are cheaper, quicker and easier to manufacture than the equivalent full-scale parts, particularly where the parts are designed in CAD and can then be directly made using rapid prototyping methods like 3D printing. So a given budget can cover more configurations than at full-scale.

Also many tunnels offer automatic control of at least some degrees of movement of the model, further accelerating data acquisition. Ride height and chassis rake maps, for instance, can be generated automatically using the control and data acquisition software found in many tunnels, making it possible to evaluate a configuration change across the full dynamic ride-height range in a matter of tens of minutes.

The fact that a model wind tunnel programme can proceed independently of any other use to which the full-scale car is being put, be that racing, testing or undergoing a rebuild, could also make good operational sense. So there are several benefits to be had, and what value these might offer any given team really depends on the nature of the operation.

But there are also downsides other than the financial outlay. What is crucial is that the model is scaled and manufactured as accurately as possible, including the detail of the underside of the racecar, any ducting, and the porosity (or resistance) of model cooling matrices. Regarding the almost universal use of ‘moving ground’ belts in model tunnels in particular, Triple Eight Race Engineering’s former aerodynamics design engineer Alex Somerset remarked: ‘The argument for having a moving floor is mainly centred around the interaction of the airflow between the ground and the underfloor of the model. So there’s no point in having accurate ground conditions and an inaccurate underfloor.’



*A 30% scale model needs to be very accurately made. (Triple Eight Race Engineering)*

Then there are the geometric as well as the aerodynamics problems discussed earlier in this chapter associated with scale. The geometric scaling

issues relate to the accuracy of the model mentioned above, and also to the accuracy of its positioning. For example, at full scale an error of  $+/-1\text{mm}$  on a 80mm touring car ride height represents a 2.5% error range. At 30% scale the ride height becomes 24mm, and to achieve the same error range requires the accuracy to be  $+/-0.3\text{mm}$ , perhaps not so easy to achieve...

The problem of model support structures interfering with the flow over the vehicle has no easy solution either. In reality, as in a full-scale wind tunnel it is still possible to see the effects of many different types of configuration changes. But correlation with full-scale testing either on track or, if relevant, in a full-scale wind tunnel, should be the order of the day, especially with components that might be influenced by model stings.

So if a model wind tunnel programme looks right for your team, what can you expect to measure? Naturally the basic loads and moments: drag, downforce (front and rear to balance) and side force, plus roll, pitch and yaw moments are all measurable to high levels of accuracy and repeatability. In addition, pressure-tapping instrumentation can provide surface pressure distributions along key surfaces if desired. And various forms of flow visualisation are possible, including on-surface flows using fluids or wool tufts, and off-surface flows using smoke or possibly one of the ‘particle seeding’ techniques. And as mentioned, depending on your chosen wind tunnel you may have the facility to automatically or manually control heave (ride height), pitch, roll, yaw and steer angle, and control software may permit the rapid acquisition of an aero map for each configuration tested.

Once you’ve committed to a programme and a tunnel, you will probably spend some time in the early stages evaluating configurations for which you already have a good feel on track, just to put hard data to those settings, and also to enable some sort of correlation between full-scale and model. If you already have aerodynamic data derived from track testing or straight-line testing, this will make this correlation all the more valuable. But Alex Somerset sounded a cautionary note: ‘Relating full-scale data to model data will give you a scale factor, but be warned, this can vary from tunnel to tunnel. However, once you have a scaling factor you are happy with, further validate it with some alternative set-ups. Then always judge your progress as percentage improvements from this baseline and don’t focus too much on absolute values. Repeat baseline tests as often as your budget allows to ensure that improvements are genuine and not the result of errors.’

Once you are confident of the correlation between model and full-scale, then the development programme can commence and, as Alex Somerset suggested, this might initially involve taking existing ideas to the extremes that

the rules permit. This will give a good idea of the aerodynamics at the boundaries of the rules, and you can then work from there to seek whatever is your target, be that maximum downforce, best efficiency ( $-L/D$ ), minimum drag, or all of the above, depending on circuit configuration. All of this will generate a much better idea of what works and what does not, leading to a clearer understanding of the flows around the racecar, and this in turn will point at other directions worth trying. Eventually you will be looking for ever-smaller performance increments until you resemble a Formula 1 team!

Of course, it would be really useful to relate the time and expense of a projected model wind tunnel programme to expected performance gains on track. Simon Smart reckoned ‘the old rule of thumb in Formula 1 was 10% efficient downforce gain per year, which was worth approximately a second per lap. But it depends so much on how refined the car already is when you start your programme, how much scope there is in the regulations for aero development and ultimately the tyres’ ability to handle aerodynamic load. Starting with something already pretty refined by the manufacturer, you would do well to find three-tenths on lap time a year, assuming say 40 days’ testing per year. But three-tenths would be huge in some categories. With something fairly unrefined I could imagine finding one or two seconds per lap. But as the development programme progresses the returns quickly begin to diminish.’

Alex Somerset referred back to his time at Team Dynamics, working on the BTCC Honda Civic in the full-scale wind tunnel to try to answer this question: ‘The first aero kit we did moved the car from typically eighth or ninth on the grid to second or third, with one pole. And it’s safe to say that by the end of 2004 the Honda Civic was the fastest car. I think we found about 0.15 seconds at some tracks.’

We’ll round off this section with some more sound advice from our advisers to anyone contemplating a model wind tunnel programme. Alex Somerset: ‘Do it well or not at all. And an experienced aerodynamics designer will save you the costs of going up blind alleys.’ Simon Smart echoed that last remark: ‘When testing on a limited budget you can’t test everything, therefore you need aerodynamic experience to choose development areas that will be responsive. Equally significant, choose areas where it is feasible to manufacture full-size parts within the budget and timescales. Above all, be accurate and realistic on the medium- to long-term costs. Many people think that just building a model and doing a few tests gives all the answers. But it takes time to accumulate knowledge and understanding before worthwhile gains can be translated to the track.’ And, remarked Alex Somerset, ‘after settling on a final configuration get

a proper kit made, with no temporary parts, plasticine etc, then baseline the car again. This is your new baseline, and you then generate your aero map on that.'

And then you need to transfer all this hard-won data and knowledge on to the racecar and make it work for you on track...

### Computer simulations

We looked at CFD in some detail earlier in this book, and used its output to illustrate numerous examples along the way. So how else can computers be used to model the effects of aerodynamics on competition car performance? The answer is, by carrying out 'performance simulation', another form of mathematical modelling made practical by computers. Whereas the calculations for the performance of a car at a given instant could be done fairly easily with pen, paper and pocket calculator, it is not the work of a moment. It follows then that to investigate varying configurations would take an extremely long time, and that contemplating analysing an entire lap, never mind a whole race, is not something a sane race engineer would contemplate. Once the mathematical methods for this type of analysis have been written, that is, the computer program has been written, a computer will happily, and pretty rapidly churn out solutions for various configurations, such as different aerodynamic set-ups, enabling a race team to predict the probable best aerodynamic set-up for a circuit long before they get there. This has to be a vital advantage when practice and qualifying time is limited, and there just isn't enough time to work through a range of aero configurations as well as the mechanical variables on a car while at the track.

Performance simulation doesn't necessarily need to predict precise lap times for a given track, interesting though that may be. What really matters is that the relative effects of changes can be analysed, and with sufficient iterations, an idealised set-up can be derived. For example, in general terms, it is obvious that increasing the front and rear wing angles on a car will generate more downforce, and allow corners to be taken faster and braking to be delayed until a bit later. It is also obvious that straight-line speed will be reduced because of the increased induced drag. By feeding in different downforce and drag values, a performance simulation program will predict lap times in each case, and, theoretically, allow the ideal compromise to be selected, at least from the range of possibilities that were fed into the computer in the first place. What the simulation model cannot do is to take account of uncontrollable variables that might be encountered at a circuit, such as changing track temperature, or dust build up, which will affect available grip. Rather in the same way that a wind tunnel does not take account of gusty side winds that

may be encountered in real life, this is actually of benefit to the analysis in that it allows changes to be tested out in equal conditions, something that rarely happens out on the track.

Performance prediction is done by modelling a variety of aspects that influence vehicle performance, and integrating them onto a ‘map’ of the track or circuit being studied. Fairly detailed knowledge of the venues of interest as well as the car is therefore required. Things like the mass, dimensions and roll stiffness of the car are needed to calculate the forces and accelerations involved, and to work out the loadings on each tyre at any one instant (see Figure 8-10). An aerodynamic model is incorporated, probably based on CFD and/or wind tunnel data, so that the influences on the tyre loadings and on straight-line performance can be worked out. Then there are models to calculate the accelerative performance of the car, using data on power and torque curves and gearing, braking performance, and perhaps most importantly, the tyres and their ability to transmit power, cornering forces and braking effort to the road surface under constantly changing circumstances. Clearly, the downforce to drag compromise plays a large role in this analysis, especially for high downforce formulas like the top single-seater categories, but also categories where aerodynamic efficiency is key, such as Le Mans prototype sports cars.

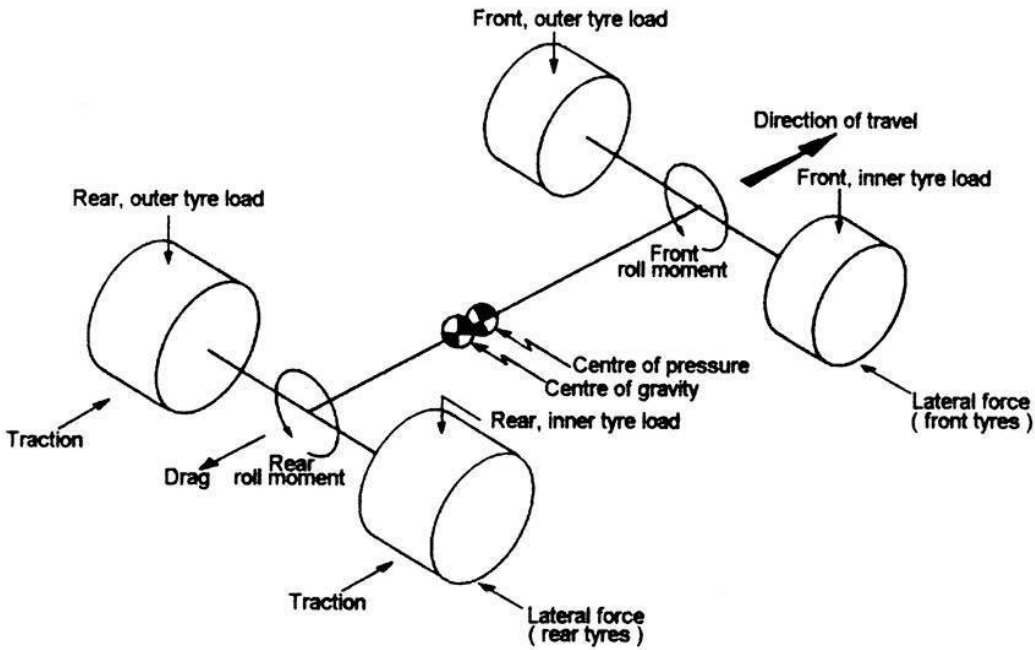


**Figure 8-10** Some of the variables used in computer performance simulation. (Dr Rob Dominy)

In essence, the model might look first at a corner, calculating the theoretical maximum speed that could be carried around it, given that the corner radius is known, and the level of grip is fixed, perhaps, at some value measured on a previous visit to the venue. A very simple analysis might assume steady state cornering with little or no tractive effort being fed into the driven wheels. Then, as the track straightens out, the model has as its corner exit speed the steady speed at which the car came off the previous corner, which is the speed that acceleration is assumed to begin from. By calculating the acceleration that is achievable from that speed, it is then possible to work out the speed at the end of the straight. All of this naturally takes into account the changing aerodynamic forces involved. The distance required to brake to corner entry speed can be worked out, and then the next corner follows like the first, and so on. The entire lap is built up in this way, and the calculation of lap time is very simply achieved by adding together the sector times.

A race team equipped with this type of analysis tool can then feed in various aerodynamic configurations, and get the computer to work out the relative lap times achieved with each set-up, thus allowing it to arrive at a circuit with

pretty much the right settings to begin practice (see Figure 8-11). Hopefully, all that will be needed from there is fine-tuning to suit the prevailing conditions. Once again, the use of this particular tool is, predominantly, the privilege of the moneied professionals, but it is now possible to obtain some pretty affordable programs that will run on a home computer. All are necessarily based on a lot of assumptions that have variable validity. So, like any simulation tool, these programs have their limitations, but at least they allow the testing of some basic configuration changes.

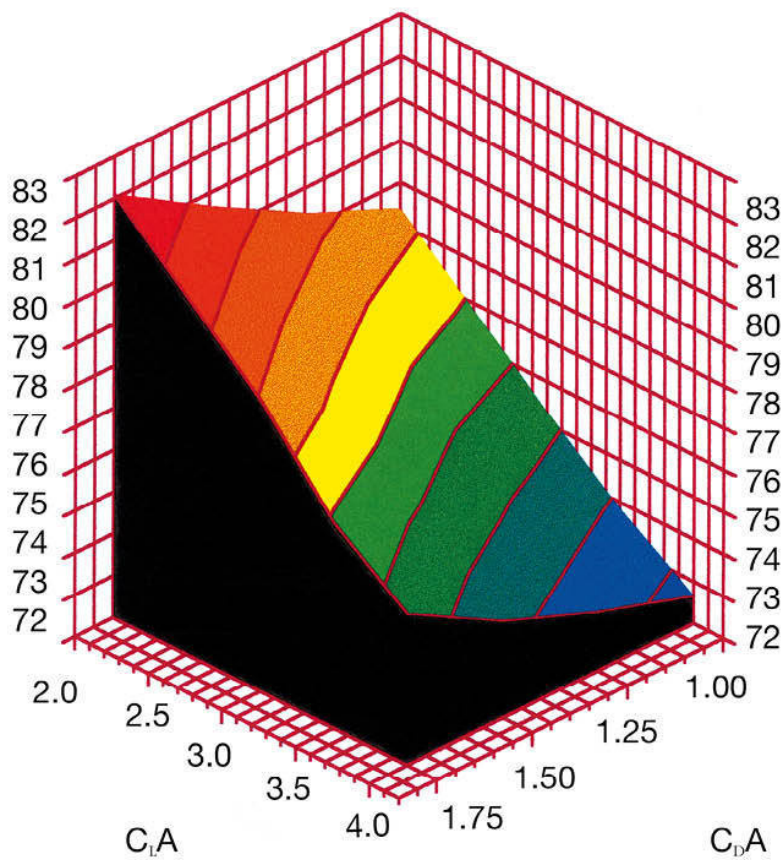


**Figure 8-11** Downforce and drag values versus lap time (in seconds) predicted by a performance simulation. (Dr Rob Dominy)

This chapter has looked at a wide range of analysis tools, from the simple and affordable, to the complex and exotic. But it doesn't matter what your budget is, and which type of tools you are accordingly obliged to rely on. The

prerequisite in all cases is to use the tools carefully, with common sense, and you will be able to improve your understanding of your competition car's aerodynamics in ways that will help to improve its performance.

## Chapter 9

# A few case studies

IT GOES WITHOUT SAYING that it is extremely useful to study cars that have been the subject of thorough aerodynamic design and development. However, it is just as important to keep in mind that all competition cars are designed and built to a set of technical regulations that are often very specific to the category. Thus a degree of caution must be exercised when scanning a particular car or category for ideas that you might think about exploiting on your own machine, especially if you compete in a different category. A design that has been optimised for one set of rules may be entirely inappropriate for another. Having said that, it is fun and informative to try to figure why a designer (or design team) has produced certain shapes, devices and other trickery. So this chapter will take a brief tour of a few interesting and informative cases from a variety of competition categories.

### **Formula 1**

No book on competition car aerodynamics could be considered anywhere near complete without taking a look at what goes on in Formula 1 because this is where the most aerodynamic development work takes place. That said, the above caveat about the rules applying to a specific category is especially pertinent here, where tweaks to the permitted dimensions and locations of aerodynamic surfaces is an on-going process, and as such the rules now bear little resemblance to any other category.

The rule changes brought in for 2009 are a case in point, where the latest efforts of Formula 1's Overtaking Working Group were implemented, some of which saw quite radical alterations to the bodywork and aerodynamic devices. Front wings went from 1,400mm overall span to 1,800mm; rear wings were narrowed but allowed to run higher; diffusers were altered; and most of the ugly protuberances that had sprouted all over the cars were banned. The purpose of these changes, we were told, was to cut downforce and to make the cars aerodynamically less sensitive when closely following another car. And this was intended to make overtaking a bit easier. Leaving aside for the

moment any judgements on whether the aims were achieved or not, the imposition of these sweeping new rules meant that all the teams on the Formula 1 grid had to virtually start afresh on their aerodynamic design. And this presented a unique opportunity to gain a little bit of an insight into that process.

The 2009 Formula 1 season was very different from preceding ones in many respects, and most people agreed that this was largely because of the major changes to the technical regulations. Considering that all the teams had to adapt to these changes, and also that roughly a year's worth of development was done away from the public – and the other teams' – gaze, one of the biggest surprises was the remarkable closeness of the cars' performance. The general perception was that the field had never been so tight, in terms of the lap time difference between the fastest and slowest cars, prompting the remark that there are no weak teams in F1 nowadays.

While this closeness in performance between the cars was in part responsible for the 'usual' order being shuffled, it also meant that any team introducing a successful upgrade could make significant progress within the order. This however may simply have been a reflection of the state of play during that particular season, and it was not long before much the usual status quo seemed to reassert itself. But it provided a welcome degree of unpredictability for a time. And one team to make a notable impact through the 2009 season, with a thoroughly deserved pole position and second in the race at the Belgian GP, was Force India F1. Just days prior to that race the technical director at Force India at the time, James Key, offered his thoughts on the team's approach to developing its cars under the new regulations.

The FIA's Overtaking Working Group (OWG) presented its recommendations to the Technical Working Group (TWG) in autumn 2007 so that the 2009 regulations could be discussed and ultimately formalised. This meant that the first draft that the teams could begin working to became available in late 2007, although the detailed wording was being worked on for another six months or so before the regulations were finally published in July 2008.



*With limited pre-season testing possible thanks to a late engine switch, Force India started 2009 with a fairly simple aerodynamic package. (Force India F1 Team)*

James Key picked up on the timeline: "The fundamentals presented in late 2007 covered the dimensions of the car, where the front wing had to sit in relation to the front wheel centreline, and all the other "architectural points", so that allowed us to start. I set up a programme at an external wind tunnel separate to the team's Brackley facility and the one in Italy that was being used (Aerolab). We did a two-week on, two-week off programme from January 2008 getting all the fundamentals sorted out with a target of, by just before the middle of the year, having something which balanced, cooled, had good directions on it, and had basic bodywork. The basics were all nailed down so that the fundamental questions were answered. And this gave us directions for what turned out to be the really important development areas so we could hit the ground running in Brackley after we'd finished the 2008 programme with a kind of a half developed car if you like, rather than starting from scratch."

This is perhaps where the main protagonists in the 2008 F1 World Championship got left behind because of the need to continue focussing their development resources on what was a very close and tense title fight that season. But the flip side of this was that it allowed teams not embroiled in the 2008 battle to focus more on the even larger task involved in preparing for 2009, and this was clearly the other reason behind the shake-up in the established order in F1. However, Force India also had to deal with a fairly late switch from a Ferrari to a Mercedes drivetrain, which clearly took its toll on

resources for a time. But its ongoing aerodynamic development programme saw Force India make significant progress with its performance relative to the rest of the field through the season.

James Key again picked up the early development tale: ‘We did a fair bit of CFD early on just to begin to understand some of the basic flow structures. And it was clear, looking at the CFD, that it was just fundamentally different to 2008. We also used CFD for the cooling, so we understood where we were with that. So CFD played a part in getting the fundamentals pinned down early, and beginning to really understand what we needed to do. But it was a bit of a staircase really, because there were so many fundamental changes compared to what we were used to; the wind tunnel was telling us directions and what was good and bad, and the CFD was helping us understand why. But it was showing us this very new set of flow structures coming off the front wing and other areas of the car that we had to get our heads around. We took a long time getting the front wing to work in the way that we wanted it to because it was just totally different to what we’d seen before.’

Making the front wings (now as wide as the car) work well, with the extra width ahead of and the proximity to the front tyres, was not simple, as James Key continued: ‘It was quite easy to have a lot of separations going on but once we got it working, for us the front wing proved to be very powerful. And the more you could use it the better, because it is upstream of the rest of the car and therefore affects various development directions (and it was helpful balancing the diffuser changes that came later). I think pretty much every team had similar development direction around the front wing, much of which was to get the wing to work in front of a big, bluff, rotating tyre.

‘And then the “spinners” [the devices that sprouted on the outside of the front wheels for a time] have developed on the front wheels; ours pushed forward as some teams’ did, others had very curvaceous features, cut-outs and so on, and that was all very different to how they’d been used in 2008. There’s a lot of stuff going on there, they were far more advanced in 2009 than anything we saw the previous year, because we now had airflow that goes outboard of the car from the wide front wings. Previously it all went inboard, and you controlled that airflow with bargeboards and devices under the chassis.’

The two main changes to the rear wing regulations saw the span reduced from 1,000mm to 750mm, and the maximum permitted height increased from 800mm to 950mm. So, plan area was reduced by 25% but the wing was shifted up into somewhat cleaner air. James Key: ‘The new wing was less powerful, and more prone to letting go [stalling] if you pushed it too hard. But you

needed to push it reasonably hard because it's not that powerful, and it's still the primary "drag adjuster". There are not many components with the 2009 regulations that can be used to adjust drag levels so the rear wing range became more important.'

While raising the wing put it into cleaner air, this also moved it further away from the diffuser, weakening the interaction between these two important devices. James Key: 'Yes, that was certainly a different scenario. The width changed things too – we now had a wide diffuser and a narrow rear wing so that was not so good, previously they were more equal. The fore-and-aft position inevitably also meant that they were less coupled than they were; for 2009 there was effectively a vertical line down at the back whereas before you had almost a cascade comprising the beam wing, the track rod, diffuser and rear wing, but that was all eradicated. So although those interactions were still valid for development, they were quite different compared to previously.'



*Modified front wheel fairings and front wing end plates appeared in Malaysia. (Force India F1 Team)*

The surprise that Brawn, Toyota and Williams sprang when the 2009 cars first appeared in testing in late 2008 was the so-called double-diffuser, so were Force India already aware of the potential 'loophole' but just steered clear of it? James Key: 'Yes and no! There were actually two parts to this; there was the

interpretation of the inlet, which is the floor, and is where all the uncertainty arose about the step plane, the reference plane; and then there was the outlet, and actually the double deck diffuser is the outlet. Now around August 2008 we realised that you could have a double outlet to the diffuser because the “legality boxes” permit a diffuser low down and a diffuser high up. So the outlet side of things for us was clear, but we couldn’t really get it to work. Clearly it had a lot of potential but it needed a different inlet condition. And this is where the other teams cottoned on to a loophole, or an interpretation, however you want to put it, which allowed that double-decker outlet to work. So we were pretty familiar with it really but it wasn’t until the other teams launched their cars that we could see what everyone else had been doing. And after that it was a case of making your own interpretation and putting it on the car. And that then prompted another completely new development because it was effectively a change of regulation for the teams who hadn’t [already] done a double-deck diffuser. So a fresh, very powerful development thread popped out of that for the guys who hadn’t done it.’

Much was made of the effect of the double-diffusers, especially by some of those that didn’t initially fit them but ‘sought clarification over their legality’, for which read ‘protested their legality’. Force India simply dug in and developed theirs in time for the fourth race of the season in Bahrain, but was there a significant gain in downforce? James Key: ‘Yes, definitely. It’s hard to quantify because [other] development kept going. But two things came from it; it opened up a load of parameters we didn’t have before, so you had to look at all of those, and that kept going right through the season. The other thing was that because it is such a powerful device it modified the flow around the rest of the car, so it sparked life into areas that you maybe hadn’t found much potential in, or you’d tried things out and they [previously] didn’t work. We introduced ours in Bahrain, and it came with other developments arising from the fact that the diffuser changed the way the car worked so much. It’s a very powerful thing to have on. Quantifying exactly what the benefit was is difficult, but you’re talking about tenths of a second per lap from the whole development.’



*In Turkey a modified front wing upper flap was introduced. (Force India F1 Team)*

There was some necessary minor rebalancing that came with the double-deck diffuser, but as James Key said: 'We gained a big chunk [of downforce] when we put it on, as I'm sure everyone did. But although it wasn't something that unbalanced the car, for our second upgrade [for race 8, Britain] we did have to do some front wing work to facilitate getting a balance because we were finding we were right at the very top end of the front wing [adjustment] by the time we'd got the diffuser on the car and established.'

Referring to the list of upgrades below, the double-deck diffuser (race 4, Bahrain) coincided with an immediate modest gain in performance relative to the rest of the field, based on times set in the first qualifying session at each race, a session in which all the teams were in similar 'mode' and which therefore makes an interesting basis for comparison. And with the exception of race 8 (Silverstone) – where a crash in Q1 put Adrian Sutil out and ironically hampered team-mate Giancarlo Fisichella's progress too, despite this being where a major front wing upgrade was introduced – the team steadily reduced its lap time deficit relative to the fastest car in Q1 on almost a race by race basis. The rolling average position in the pack also showed an improving trend, with particularly strong performance at race 9 (Germany) and of course race 12 (Belgium) and race 13 (Italy), where the team had its best results of the season. A backward step in Q1 position in race 10 (Hungary) probably

reflected how close the field was there, combined with a compromising practice crash for Sutil and a car struggling somewhat on the low-grip track. After that, the next major aerodynamic upgrade was at race 11 (European GP, Valencia), which again saw immediate relative performance gains leading up to the highly competitive showings in Belgium, where Giancarlo Fisichella grabbed pole position and was second in the race, and Italy, where Adrian Sutil qualified second and finished fourth.



*A new front wing mainplane was introduced at the British GP, along with a revised front end plate. (Force India F1 Team)*



*The final major revision came along for Valencia, with more front wing modifications. (Force India F1 Team)*

The performance at Spa and Monza highlighted the Force India's strengths, as this forecast by James Key related: 'Our top speeds were quite competitive, and Spa's obviously an efficiency circuit, it has more sweeps and high speeds and our car had been better at the high-speed stuff than the low-speed stuff, so Spa should have been a better circuit for us.'

So, following a season's learning with the new regulations, was the emphasis different in relation to the development challenge as originally perceived?

James Key: 'Yes, simply because everyone got to know what the big-hitting areas are, whereas you didn't know how much you could exploit a front wing or a diffuser initially. You could have a dry couple of weeks and then suddenly a quarter of a second would pop in through a development on something. So it was a very jagged development rate to begin with and that was a case of learning where the big-hitting stuff was and trying to connect everything together as well. Your development philosophy was building up at that point. Once that was better understood, we could then say "this is the sort of approach we need to take to this part of the car", so the finer detail began appearing. So the emphasis did change as we've got to know much more about it.'

Force India's major aerodynamic developments during the 2009 season were as follows:

- Australia/Malaysia: new wheel fairings and front wing end-plate turning vanes.
- Bahrain: new double-diffuser.
- Spain: new 'cascade' front wing plus modified sidepod 'vane'.
- Monaco: small winglet above rear wing.
- Turkey: revised front wing flap and wheel fairings.
- Britain: major upgrade to front wing comprising modified end plates, different wing profile, different front wishbone fairings.
- Germany: modified floor ahead of rear wheels.
- Europe (Valencia): second major upgrade including revised front wing and slimmed down sidepods; package said to be worth 0.7s per lap.

So 2009 did produce a season with a number of differences in Formula 1, but whether the aerodynamic rule changes actually did contribute to more overtaking is debatable. It was said that the cars were able to run more closely together, so perhaps the changes were a partial success.

It's not hard to imagine that a similar process to the foregoing occurred ahead of the 2014 regulation changes as front wings were narrowed again, and other changes at the rear were implemented. The next section is a case study that goes back several iterations of Formula 1 rule changes, but it still offers an interesting insight into the aerodynamic changes encountered by single-seater racing cars running close together.

## Overtaking in Formula 1

As soon as they raced nose to tail, racers knew about the drag reductions in the wake of the car in front that enabled 'slip streaming' or 'drafting'. Later, when downforce became exploited, the loss of downforce on a closely following car also became clear. Whether these effects are perceived as beneficial or detrimental depends fundamentally on whether you're in front or behind.

Some think the effects are crucial. There is a commonly held perception that 'downforce ruins racing because it lessens the opportunities for overtaking'. This is highly debatable, and examples could be cited of poor racing in categories where downforce is outlawed, and excellent racing where downforce plays a big part in racecar performance. Also, let us not forget, as was stated earlier in this book, that overtaking frequency is influenced by other

factors such as track design, driver ability (and mentality) and electronic driver aids.

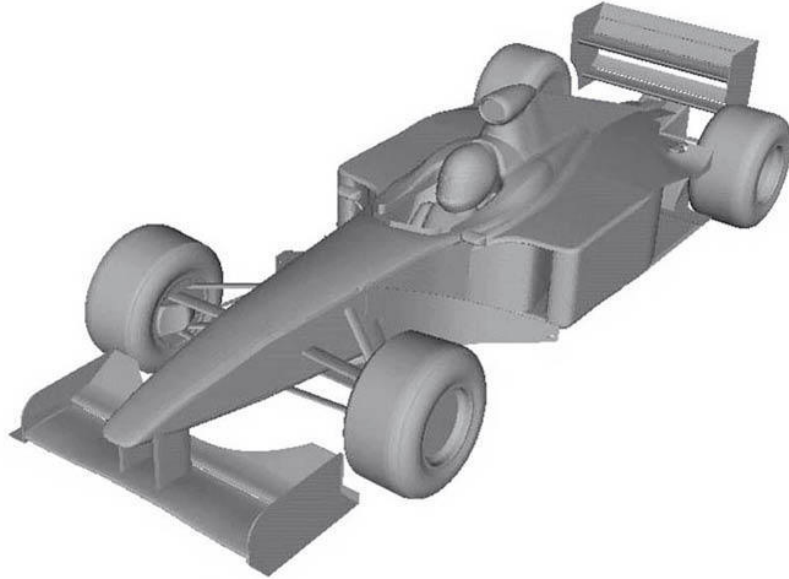


**Figure 9-1** The virtual model of the BAR Honda used to evaluate line-astern interactions using CFD. (Advantage CFD)

However, what is not arguable is that racecars interact aerodynamically in ways that can both improve and worsen performance. Overtaking opportunities may be affected in positive and negative ways. So, to determine just what the aerodynamic effects were, and how big they were, BAR Honda commissioned Advantage CFD, their then semi-autonomous CFD department, to carry out a CFD study on the interaction between two cars running line astern using the virtual model of one of its earlier cars. Although car configurations have changed quite a bit, as we can see, the general trends will still be present.

The cases of two cars running at separation distances, ranging from a half car's length to eight car lengths, were evaluated against a baseline single car, all at the equivalent of 200mph (320km/h). The graph in Figure 9-2 summarises the percentage changes to the overall forces felt by the following car, and the results are plain to see. There was a reduction in drag and overall downforce, and the magnitude of these reductions increased with decreasing car separation, the more so at closer separations. Thus, even at eight-car lengths separation the following car sensed a 13% reduction in drag, but also

experienced nearly 18% reduction on downforce. These values rose to 28% and 45% respectively at half a car's length separation.

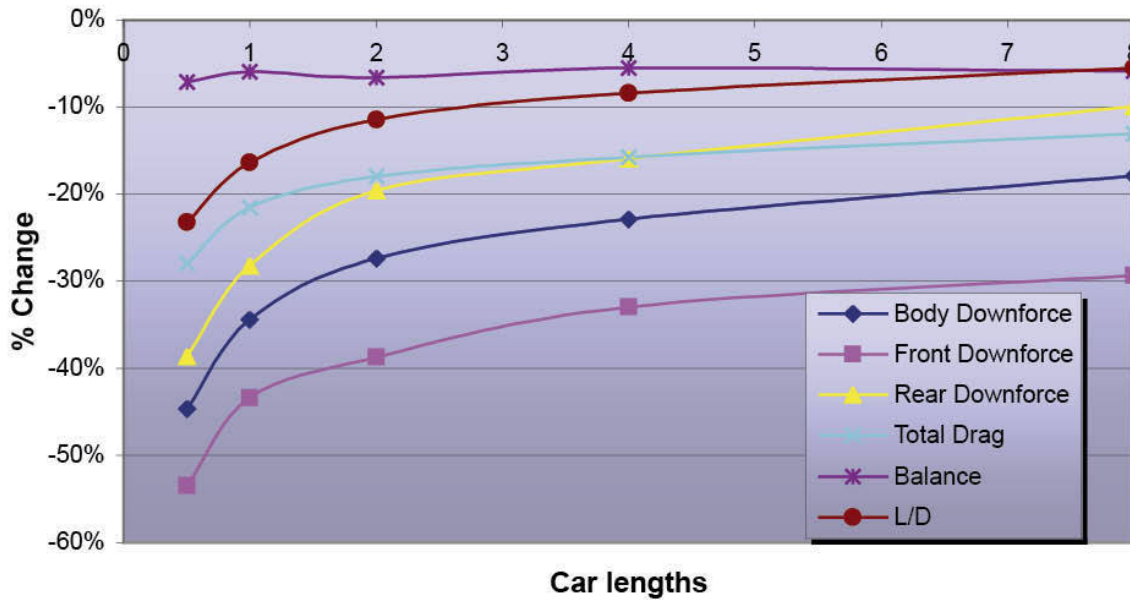


**Figure 9-2** Percentage changes to the forces felt by the following car, relative to the single car case. (Advantage CFD)

Looking a little more closely at this graph, the relative changes to the front and the rear of the following car are also shown. Clearly, both ends of the car saw a drop in downforce, but the reduction at the front was considerably bigger, resulting in a significant rearward shift of the aerodynamic balance. Interestingly, this rearward balance shift was actually pretty consistent across the range of separations investigated, averaging around 6% shift to the rear. The magnitude of the reduction at the front was as high as 29% even at eight car lengths, rising to over 53% loss of downforce at half a car's separation, while at the rear the reduction was just 10% at eight car lengths rising to nearly 39% at half a car's separation.

It doesn't take a huge mental leap to connect these substantial aerodynamic changes felt by the following car to the real-world ability to close the gap to the car in front along fast straights, or to the visually reduced braking capacity and understeer experienced by the following car in braking zones and corners where aerodynamic loads are significant.

Now look at Figure 9-3, which shows what the *leading* car experienced. First, it is apparent that the lead car experienced the effects of interactions, but they

produced much smaller percentage changes than those felt by the following car. Secondly, the effects were potentially significant, the change most likely to affect handling being the loss of rear downforce that increased with decreasing car separation, with a 5% loss at half a car's separation. There was also a loss of front downforce but this was very much smaller, and the overall balance shifted slightly to the front in line with the greater loss at the rear. Total drag decreased slightly too, by up to almost 4% at the closest separation, this being an effect reportedly sometimes exploited by team-mates (not necessarily in single-seater categories) to extract better lap times from each others' cars.

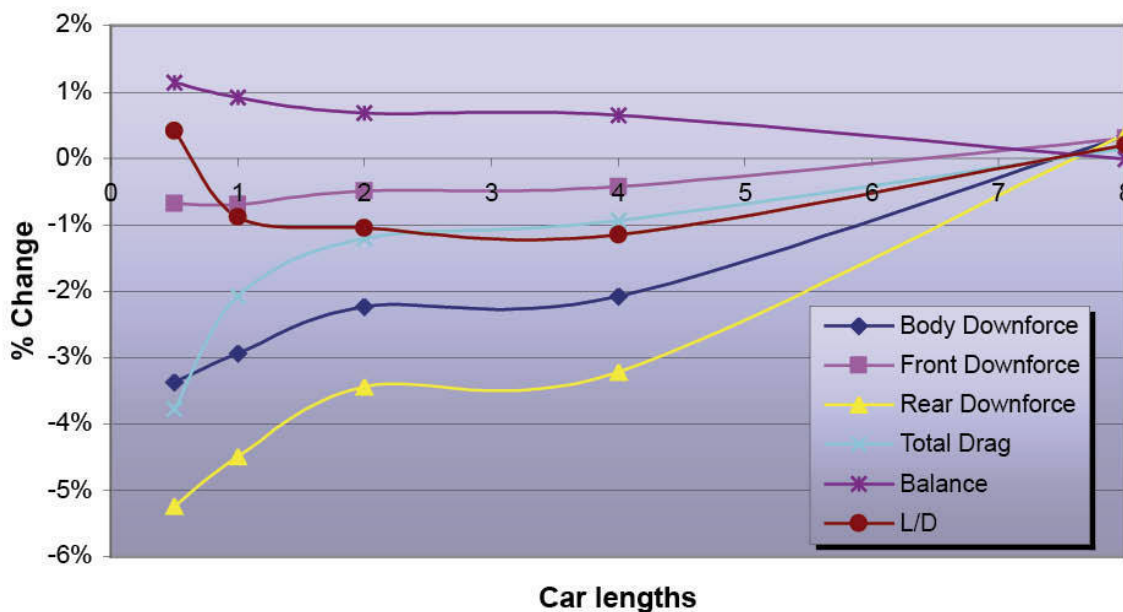
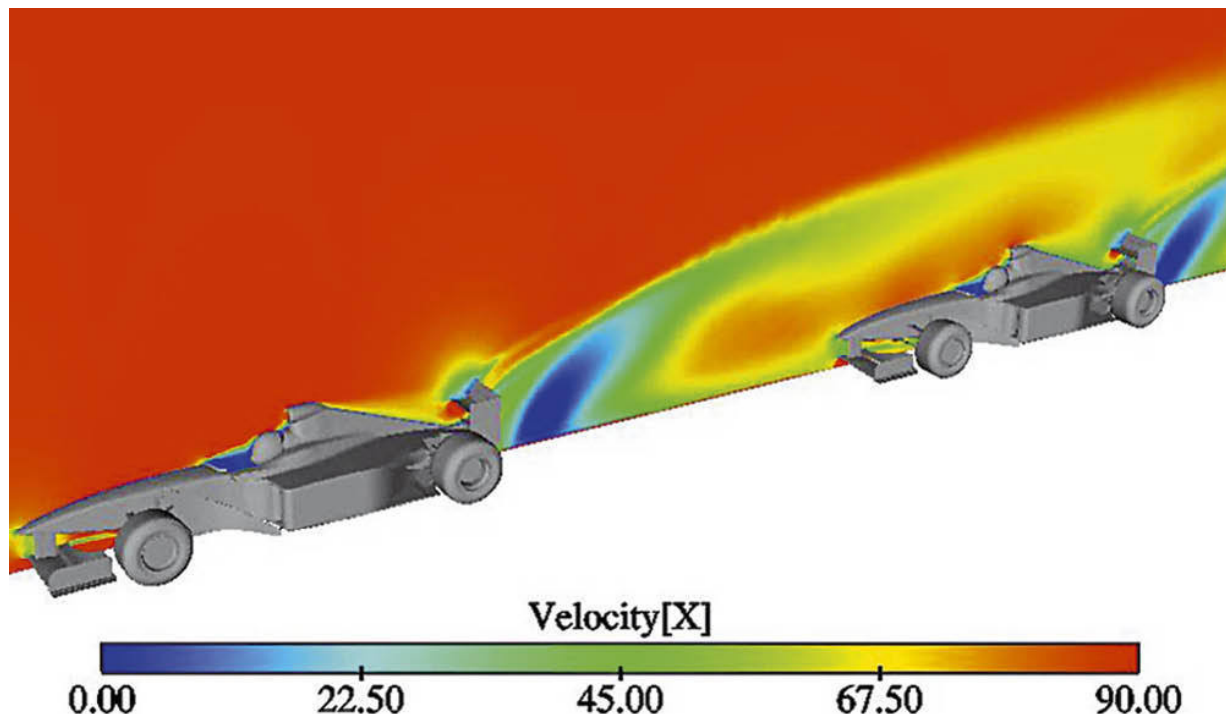


**Figure 9-3** Percentage changes to the forces felt by the leading car, relative to the single car case. (Advantage CFD)

So, the interactions can be summarised as: reductions in drag for the leading and, more significantly, the following car; a big reduction in downforce on the following car, especially at its front end, and a small but significant reduction in rear downforce for the leading car.

CFD visualisation techniques help to show what's going on at a detailed level as well as overall. Figure 9-4 gives a clearer idea of the 'big picture' along the car centrelines at one car's length separation. Here the colours represent air velocity, red showing the unimpeded 'freestream' airflow while greens and blues show areas of reduced velocity. It is immediately evident that the airflow had slowed down greatly in the leading car's wake (no surprise there), and it

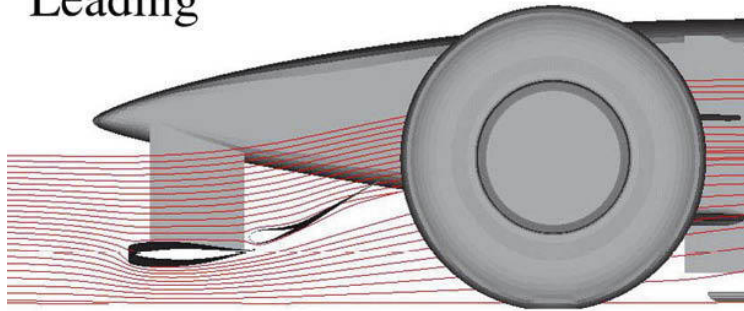
will be obvious too that this reduction of the flow velocity on the following car contributed to the reduction in both drag and downforce it feels.



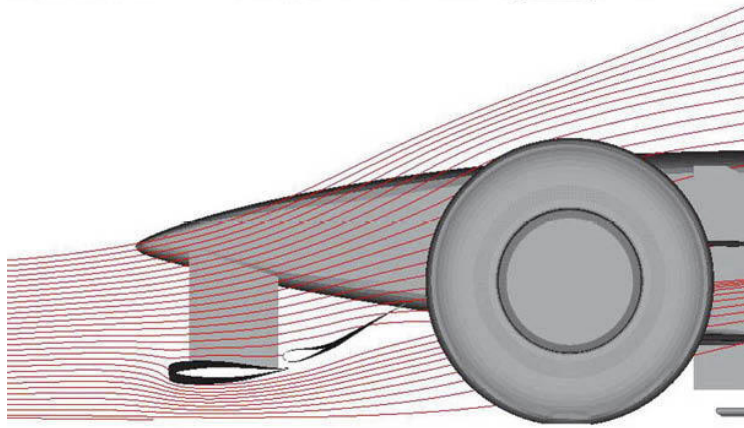
**Figure 9-4** Velocities at one car length's separation. (Advantage CFD)

Figure 9-5 provides an explanation for some of the loss of front wing downforce. The streamlines showed a noticeable difference in the angle at which the approaching air hit the front of the following car. This has the same effect as reducing the angle of attack of the front wing, resulting in a reduction in downforce. Thus, as well as a reduction in air velocity on the front of the following car, the airflow also changed direction in a way that reduced its downforce.

Leading



Following



**Figure 9-5** Streamlines on the front wings of the leading and following cars at half a car's length separation. (Advantage CFD)

Looking at the following car again, Figure 9-6 shows how the upper surface static pressures changed, relative to a car running on its own. Negative colours (greens and blues) demonstrate a reduction in static pressure on the upper surface corresponding to decreases in downforce. Figure 9-7 shows how the lower surface static pressures changed, with positive colours (reds and yellow) indicating increased static pressure on the underbody, also corresponding to decreases in downforce.

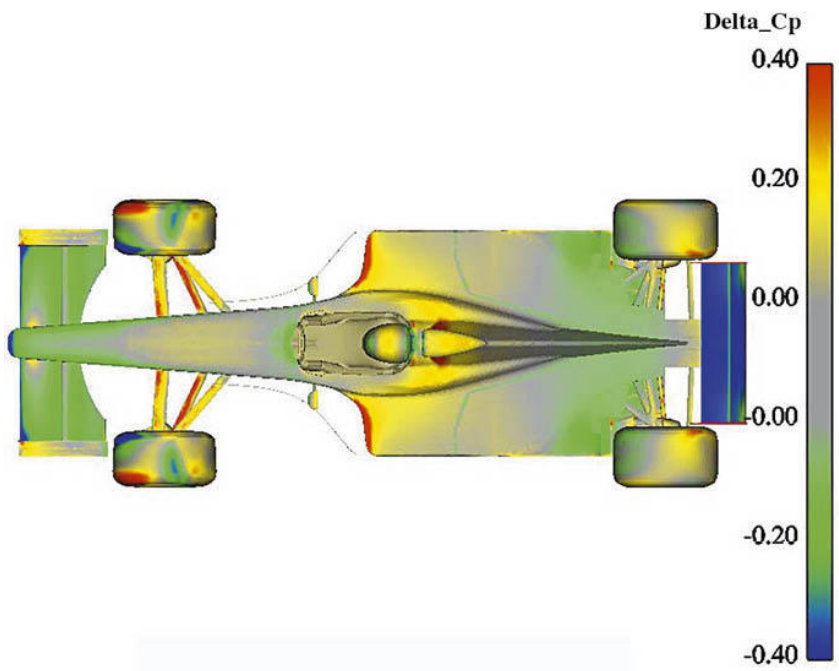


**Figure 9-6** Changes to upper surface static pressures on the following car at half a car's length separation. (Advantage CFD)

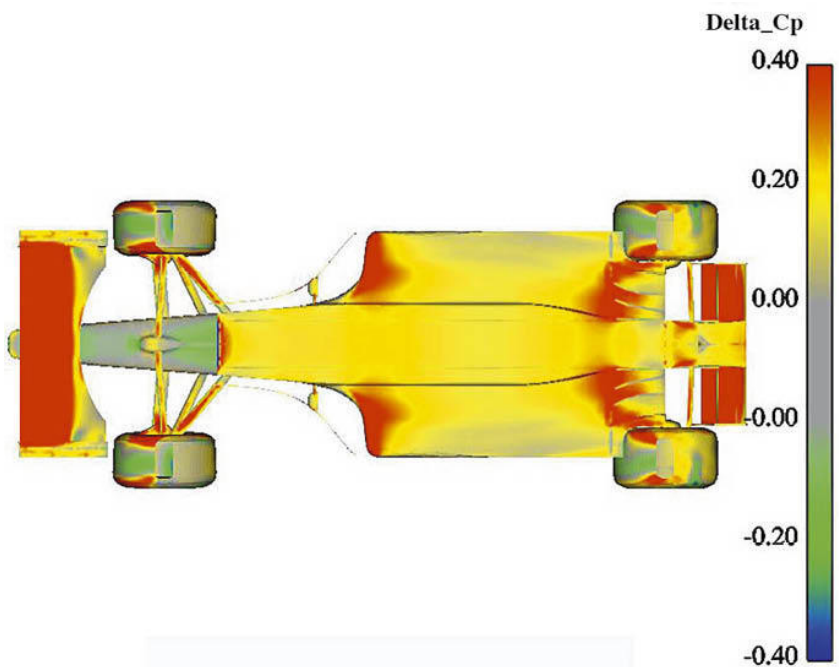


**Figure 9-7** Changes to lower surface static pressures on the following car at half a car's length separation. (Advantage CFD)

While there was an obvious loss of downforce from the upper wing surfaces in particular, large losses also accrued from increases to the pressure on the entire underside of the car, with the effects concentrated on the wing undersides and the sidepod inlet and diffuser inlet sections of the underbody. Again, the reduction in velocity of the incoming airflow to the following car would explain this. So it is not just wing downforce that is ‘robbed’, but underbody downforce too.

The changes in surface pressures felt by the leading car were more subtle, as Figures 9-8 and 9-9 show. Figure 9-8 illustrates very small upward acting pressure changes to the upper sidepod and rear deck surfaces only, while Figure 9-9 shows more significant upward-acting changes to the underbody, especially around the diffuser inlet area, and the rear wing undersides. Obviously, these changes were concentrated at the rear end of the car, corresponding with the reduction in rear downforce. There was also a small but definite change to the front wing underside, corresponding to the small drop in front end downforce mentioned previously. Thus, the ‘bow wave’ effect of the following car was slightly modifying the airflow over the whole of the leading car, be that by affecting the direction and/or the velocity of the airflow.

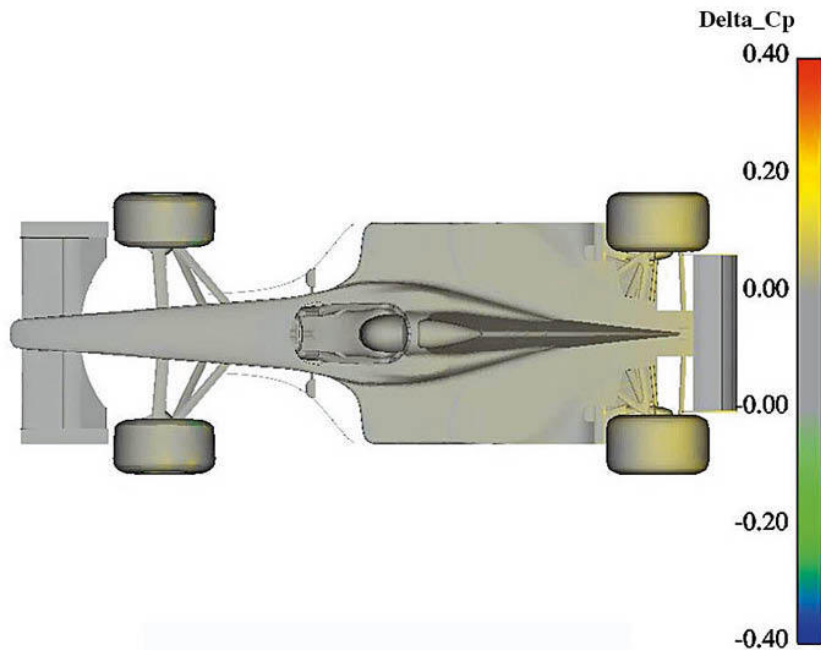


**Figure 9-8** Changes to upper surface static pressures on the leading car at half a car's length separation. (Advantage CFD)

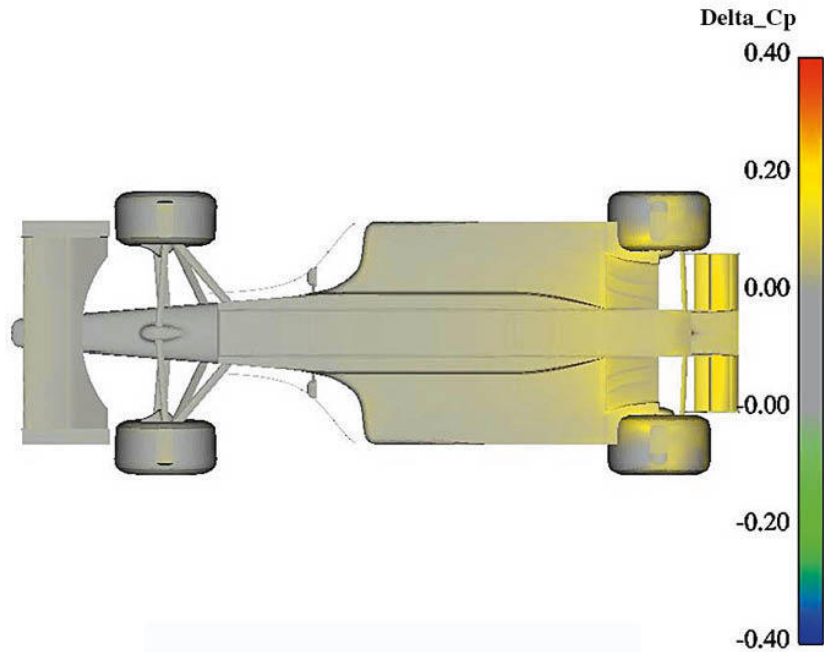


**Figure 9-9** Changes to lower surface static pressures on the leading car at half a car's length separation. (Advantage CFD)

At its simplest level this study demonstrated changes that are well known. By putting some numbers on the effects though it is abundantly evident that these are highly significant. But an analysis of cars running line astern necessarily only looks at the earliest phase of the overtaking scenario. There would, ideally, be a detailed study of the interaction between two such cars in all phases of an overtaking manoeuvre, with differing lateral offsets at various longitudinal separations, and at various 'alongside' phases, again at differing lateral offsets. Proximity to walls and multi-car scenarios represent other possible fields of study.

There is only one certainty here. Whatever influences the regulators may have, as long as racecars run in close proximity there will be aerodynamic interactions. The team that pays closest attention to these will have less difficulty passing its opposition, or staying in front.

A quote from Peter Wright in *Racecar Engineering* (April 2000) demonstrates how the powers that be of Formula 1 apparently, but briefly, showed great common sense: '*on the table for 2001 is less pitch sensitive and reduced downforce aerodynamics using venturi sidepods but no diffuser, a raised front wing and limits on the number of elements making up the rear wing. These rules are somewhat similar to those used in CART (ChampCar), where it has been found that not only do venturi sidepods encourage longer impact structures, but also help to maintain the aerodynamic balance in the wake of another car on high speed ovals.*'

Well, a few regulation changes down the road, somehow these changes still have not happened, and Formula 1 still has regulations that didn't improve safety perhaps as much as they could have, or which might have benefited overtaking opportunities by reducing the balance shift on following cars. The logic of reduced balance shift with underbody-generated downforce is simple enough – the downforce is generated nearer to the car's centre of gravity, so when downforce reduces when close behind another car, the aerodynamic balance is not overly affected. If, however, front wing downforce constitutes a large proportion of the car's total downforce (and it does – over 30% of the total on 2009 Formula 1 cars) then the balance is going to change markedly in another car's wake. This loss of balance, when following closely, is a bigger problem than the loss of downforce itself. Since 2011, Formula 1 has employed the 'Drag Reduction System' (DRS) to artificially improve the cars' ability to overtake, rendering the foregoing largely academic in that category, but it does seem rather to be admitting defeat, so we can but hope that logic may eventually prevail. Smaller front wings, controlled venturi sidepods with low pitch and ground clearance sensitivity, and a modest rear wing to balance the front shouldn't, in theory, be difficult to mandate.

### Drafting stock cars

Having looked in detail at a CFD study on F1 cars running line astern, we can now take a brief tour of a study MIRA did in the full-scale wind tunnel; but this project had a number of key differences, one of which was obviously the use of real, full-size racecars instead of digital models (although that is merely an observation and shouldn't be taken as any kind of comment on the relative merits of the two techniques). Another distinction to note is that the CFD studies simulated a moving ground whereas the MIRA full-scale wind tunnel has a fixed floor, albeit with boundary layer control. The cars used, however, were not low ride-height 'ground-effect' single-seaters or sports cars, but SCSA racers, subsequently known as European Late Model Series cars (Europe and the UK's rough equivalent of NASCAR stock cars), so the less

sophisticated ground plane simulation will have been less critical. The ‘bumper-to-bumper’ separations used were much smaller than in the CFD studies, and left and right lateral offsets were also examined. First we’ll look at the changes to drag on the lead and following cars, and compare the results to the F1 CFD study for interest.



*A drafting study was carried out by MIRA on SCSA stock cars. (MIRA)*

The least surprising observations on the SCSA racecars are highlighted in Figure 9-10, showing the expected reductions in drag coefficient felt by the following car. At zero lateral offset (the red line) we can see that the drag reduction at both 3,390mm and 2,290mm separation was 19%, rising to 28% at 1,290mm and 48% at 290mm separation.

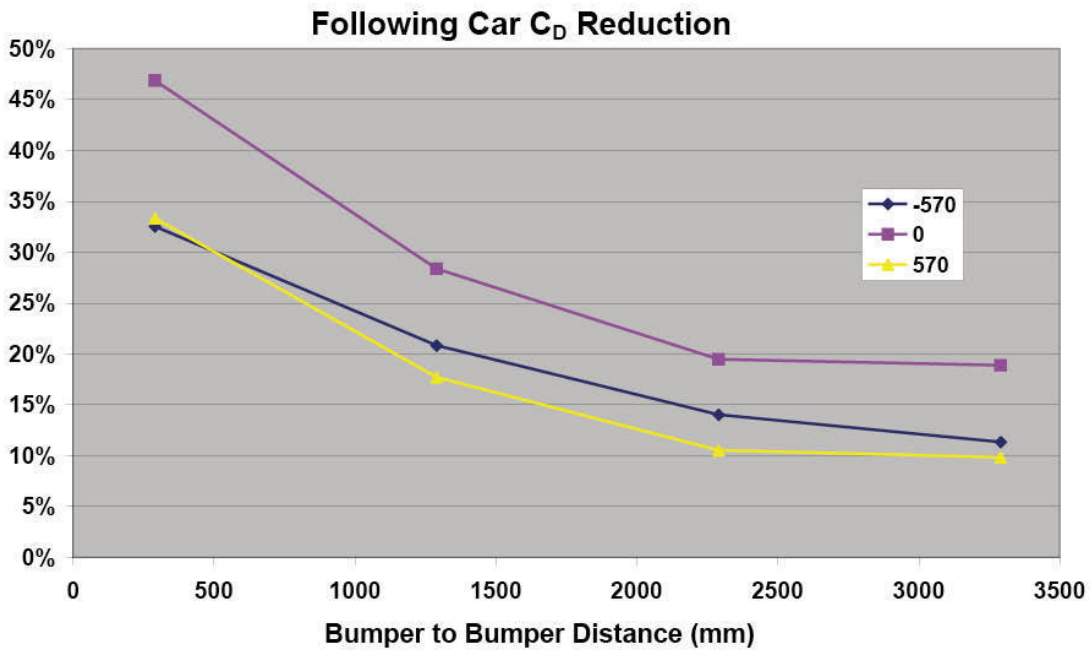


**Figure 9-10** The effect on the drag coefficient of the following car.

Lateral offset of the following car by  $\pm 570\text{mm}$  (approximately one-third car's width) produced a similar general pattern but the reductions in  $C_D$  were of lower magnitude, again as might reasonably be expected, given that less of the following car was in the wake of the lead car. There were small differences in the results at left and right offset, and these may be due to the asymmetry of the cars (the driver's window is always open, for example).

The F1 CFD numbers make for interesting comparison here. In this case the following car saw  $C_D$  reductions of 21% and 28% at 1.0 and 0.5 car lengths respectively. Half a car's length in the case of the SCSA cars would be about 2,550mm, where a 19% reduction was seen. Thus, the digital F1 car apparently experienced a somewhat greater reduction in drag at similar separation, and maybe this could be attributed to its considerably higher drag coefficient, and the way in which the drag was produced. Thus, running behind a similarly high-drag lead car, with its exposed wheels, and rear wing upwash and vortices, may have had a bigger effect.

If the general pattern and the magnitude of the changes to the drag of the following car were perhaps as expected, then certainly the extent of the effect on the *leading* car in the MIRA study was pretty surprising. The plot in Figure 9-11 summarises. Generally, running closer produced a greater reduction in the  $C_D$  of the lead car except at the closest distance measured here, when a

maximum 20% reduction at 1,290mm separation changed to an 18% reduction at just 290mm separation. It would seem likely that there are two interacting mechanisms at work here; firstly, the wake of the lead car is probably being progressively modified to an extent that depends on how close the following car is, with attendant effects on the wake's drag; and secondly, at closer proximity what we might think of as the 'bow wave' of the following car will be affected such that it doesn't push the car in front to the same extent. Then as lateral offset is introduced it appears that the combined effect is further reduced.

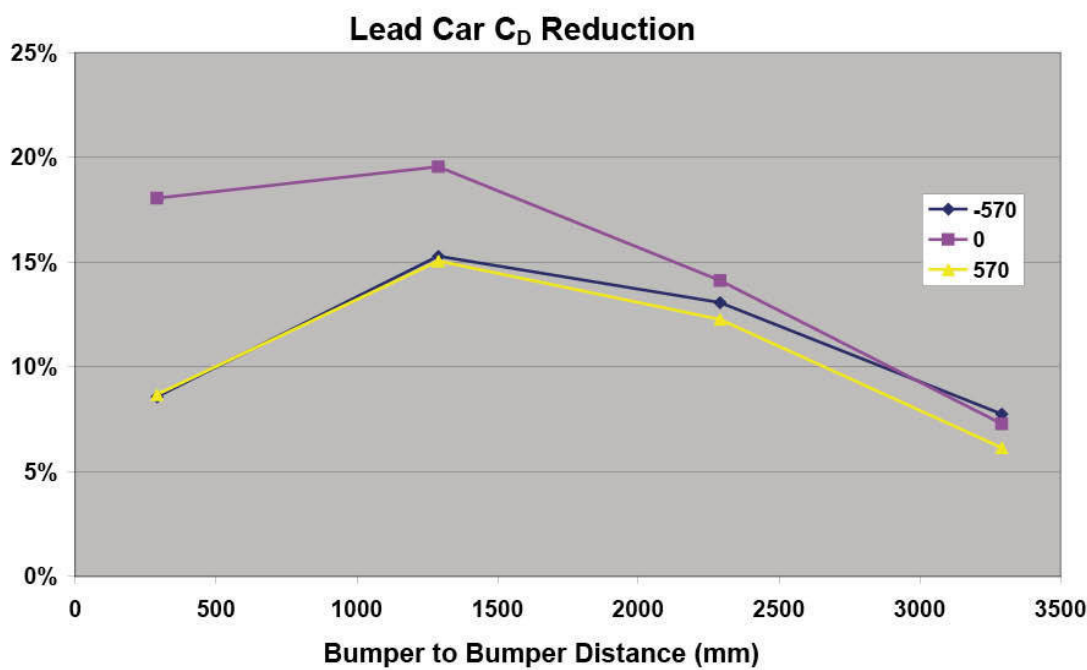


**Figure 9-11** The effect on the drag of the leading car.

So, looking at Figures 9-10 and 9-11 together, for a following driver to maximise his drag-reducing drafting benefit and yet not hand his leading competitor too big a drag reduction, it looks like he would need to stay line astern and get about as close as he can! All the lead driver can really do to try and minimise the following driver's benefit is to create a lateral offset, though he loses some of his own advantage in so doing. He might also get penalised for weaving were he to frequently repeat the move...

Comparing these data to the F1 CFD data again is also interesting. At 1.0 to 0.5 car lengths separation, the lead F1 car saw just 2% and 4% drag reductions respectively. This was a much smaller effect than was measured on the SCSA

cars that, at 0.5 car lengths' vseparation (interpolating from Figure 9-11), saw a 13%  $C_D$  reduction. Taking the general shape of an F1 car into account along with this data, we might reasonably conclude that the 'bow wave' ahead of an F1 car is a less developed effect than it is ahead of the bluff shape of an SCSA car. And maybe also the wake of the lead F1 car is so large and complex (compared to that of a lower drag, closed-wheel car) that it is less affected by the close proximity of a following car.

Looking at downforce, Figure 9-12 shows the reductions in overall downforce ( $-C_L$ ) felt by the following car. It can be seen that in the line astern case (the red line) the reduction in downforce was more or less linear, going from a 16.4% loss of downforce at 3,390mm bumper-to-bumper separation to 29.3% loss at 290mm separation. However, with positive (to the driver's right, the yellow line) or negative (left, blue line) lateral offset of just one third of a car's width, these losses of overall downforce were substantially reduced. In fact, the losses were only around 5%, give or take a little, until the cars are extremely close.

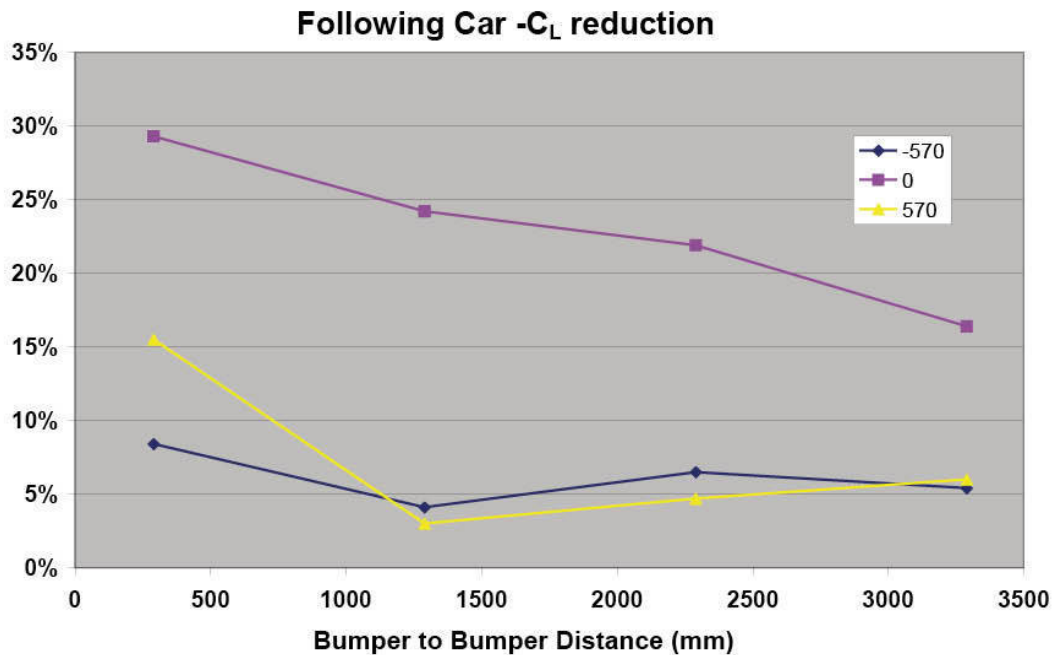


**Figure 9-12** The effect on the downforce of the following car.

The comparable numbers in the F1 two-car CFD study showed 34% to 45% loss of overall downforce at 1.0 and 0.5 car-length separations, rising steeply with closer proximity if we were to extrapolate the plots. At the

equivalent of half a car's separation (around 2,550mm) the SCSA following car lost 20% of its downforce, so this effect was a lot smaller than on the F1 car.

So, coming back to the SCSA cars, if the driver of a following car were to try to lessen the loss of downforce and grip, which he might well want to do when following through a corner, it would appear that the best thing to do is to laterally offset his car slightly from the car in front. We saw above that the best position for the following car to be in to achieve the maximum drag reduction was line astern and as close as possible. So, here we have aerodynamic data that provide an explanation for why this type of racecar might be expected to follow line astern on the straights but to try to run offset through the turns. Of course the driver of the lead car may have other ideas about that...

But what about aerodynamic balance in these situations? Figure 9-13 provides some answers. What we have here is the percentage reduction in the proportion of downforce felt at the front end of the following car. As a guide, the front to rear aerodynamic balance measured in isolation was 26.5% front and 73.5% rear. Figure 9-13 shows the percentage change to that baseline front-end figure as the result of that car's proximity to the lead car, and what we see are significant balance changes on the following car, but with big differences at the different lateral offsets.

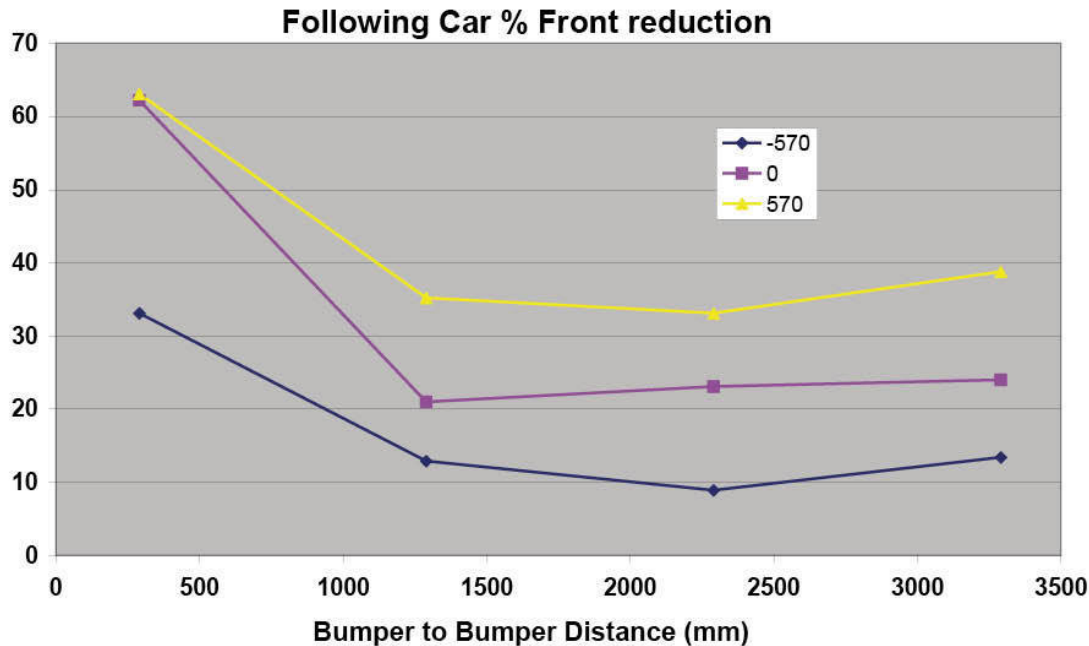


**Figure 9-13** The effect on the aerodynamic balance of the following car.

Looking first at the line astern plot (the red line again), we see a substantial rearward aerodynamic balance shift at all the separations measured, and this became very marked when the cars were at their closest. This shift is dominated by the similar pattern and the significant magnitude of the change to the front-end downforce, which reduces markedly at the closest separation, while the more modest rear downforce reductions actually peak at 1,290mm. Comparing with the F1 CFD study, changes in balance there showed that roughly a 6% rearward shift occurred even at eight car-lengths' separation, but this only rose to just over 7% at half a car length separation. So although this represents a big balance change for a high downforce car, by contrast closer proximity didn't make matters so much worse.

Returning to the SCSA cars, when taking the lateral offsets into account, the plot lines are strikingly different. The blue (negative) line represents offset of the following car to the driver's left, as shown in the photo, and demonstrates less of a change in aerodynamic balance than the line-astern case. The dominant underlying causes are lesser reductions to front downforce at this offset, combined with very small changes to rear downforce.

In the case of the yellow (positive) line that represents offset to the driver's right, there was a much greater rearward shift in aerodynamic balance at the three largest separations than in the line-astern case, and much the same balance change at the closest separation. Again, two factors contributed to this; the front downforce reduces to a very similar extent to the line-astern case; and the rear downforce actually *increased* slightly rather than reducing.

The big differences according to whether lateral offset is to the right or the left presumably arise from the cars' asymmetry in respect of open drivers' windows on the upper, left side of the vehicle, and in the location of components like the exhaust system in the (generally very rough) underbody region.

So once again, from the viewpoint of the driver of a following car, the way to mitigate losses of downforce and grip is to not only offset the car laterally from the car in front, but to do so to the left, which coincidentally and usefully will also give the best view from a left-hand-drive position. Naturally this would assume that the cars had the same overall configuration as the ones tested here...

So these two very different case studies have demonstrated very clearly that when competition cars run close together, they unavoidably interact with each other, and although it might be possible to modify the effects to a limited extent, the existence of those interactions is just a fact of life.

## Sports prototypes at small yaw angles

We frequently hear how Formula 1 teams nowadays do much of their scale wind tunnel testing with the car at yaw angles representative of cornering conditions as well as in the straight ahead position. They do this because there are significant differences in aerodynamic performance between the two conditions. Straight-ahead testing is good for basic mapping, optimising drag and, for example, the aerodynamics for the braking phase from high speed in a straight line, which requires a sound knowledge of the distribution of downforce and how it shifts throughout that phase. But generally speaking more lap time is spent in corners. So it makes good sense to spend a proportionate amount of time optimising a racecar's aerodynamics at attitudes that represent cornering.



*Aerodynamic interactions are a fact of life when cars are racing. (MIRA)*



*The Eco Racing Radical SR10 LMP1 sports prototype was tested at small yaw angles in the MIRA full-scale wind tunnel.*

F1 teams will therefore run through large numbers of ‘cornering’ variations, setting the racecar model up at a variety of yaw and roll angles to cover as many eventualities as possible. The leading sports car manufacturer teams like Audi and Peugeot will surely do the same, whether in the wind tunnel or using CFD, or both. So one of the things that was keenly anticipated during a day-long MIRA full-scale wind tunnel session on the Eco Racing Radical SR10 LMP1 prototype racer was to set it up at a range of yaw angles that covered what might be regarded as more or less normal cornering attitudes. There wasn’t time to incorporate different roll angles as well, but the yaw data alone produced much food for thought.

The SR10 was set up in a medium downforce configuration (based on the range of downforce levels explored on the day) and swept through a range of yaw angles up to 10° degrees, in 2° increments. The results are shown in the table below and graphically in Figure 9-14.

*Changes to the basic aerodynamic parameters over a range of yaw angles, forces in N at 100mph*

Yaw: 0

Total Df: 3242.7  
Front Df: 1285.4  
Rear Df: 1957.4  
% front: 39.64%

Yaw: 2

Total Df: 3317.2  
Front Df: 1368.4  
Rear Df: 1948.8  
% front: 41.25%

Yaw: 4

Total Df: 3331.2  
Front Df: 1415.1  
Rear Df: 1916.2  
% front: 42.48%

Yaw: 6

Total Df: 3327.5  
Front Df: 1482.3  
Rear Df: 1845.2  
% front: 44.55%

Yaw: 8

Total Df: 3278.1  
Front Df: 1486.2  
Rear Df: 1791.9  
% front: 45.34%

Yaw: 10

Total Df: 3203.7  
Front Df: 1455.4  
Rear Df: 1748.4  
% front: 45.43%

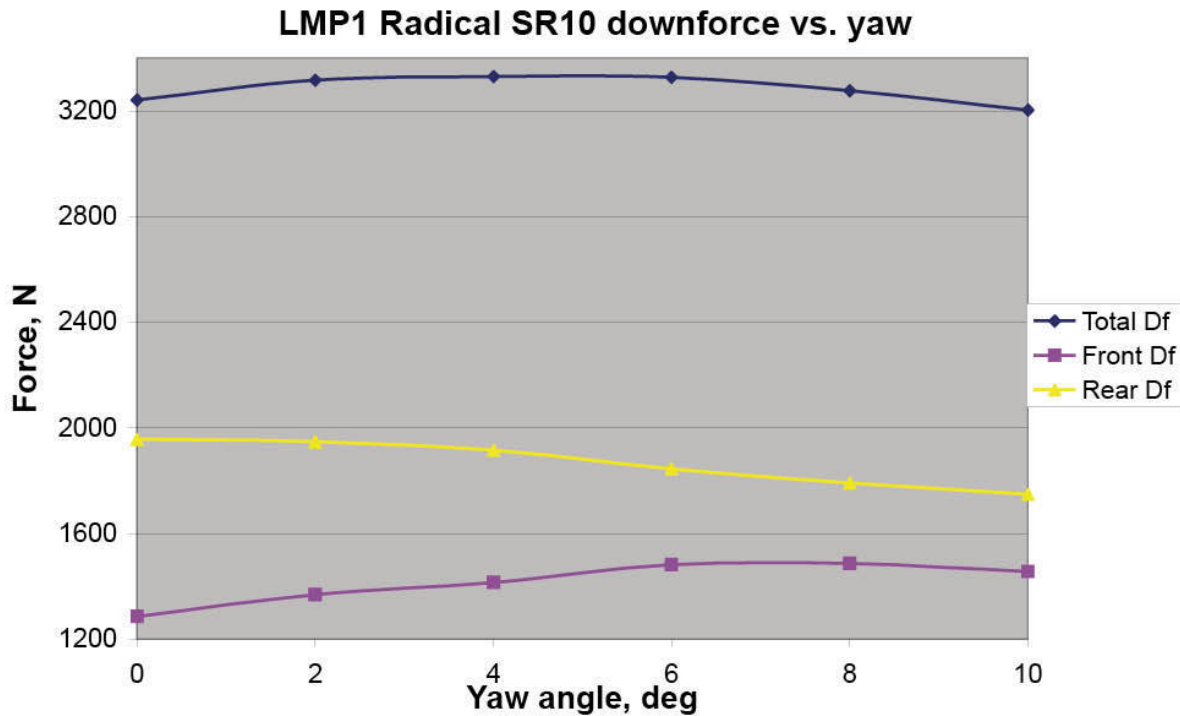


**Figure 9-14** At yaw angles representative of cornering situations, downforce levels were quite different to those at zero yaw.

Clearly then, as yaw angle increased to between  $4^\circ$  and  $6^\circ$ , total downforce increased. But this came about because the downforce at the front end increased at these modest yaw angles (up to  $8^\circ$ ) before then declining again, whereas at the rear the downforce decreased as soon as yaw was applied.

This increase in front downforce at small yaw angles, whatever the mechanisms involved, has important implications for the ideal set up of the car. It can be seen from the table above and figure 9-15 below that at zero yaw the aerodynamic balance wasn't bad, perhaps a bit too forward-biased with 39.64% of the downforce on the front (the static weight split saw 39.26% of the car's weight on the front). But as yaw angle was increased, the gain in front downforce that accompanied this clearly created a balance that was too forward biased. This got progressively worse as yaw increased and the decline in rear downforce added to the increase at the front so that at  $6^\circ$  to  $10^\circ$  yaw the balance had shifted to approximately 45% of the total downforce on the front end.

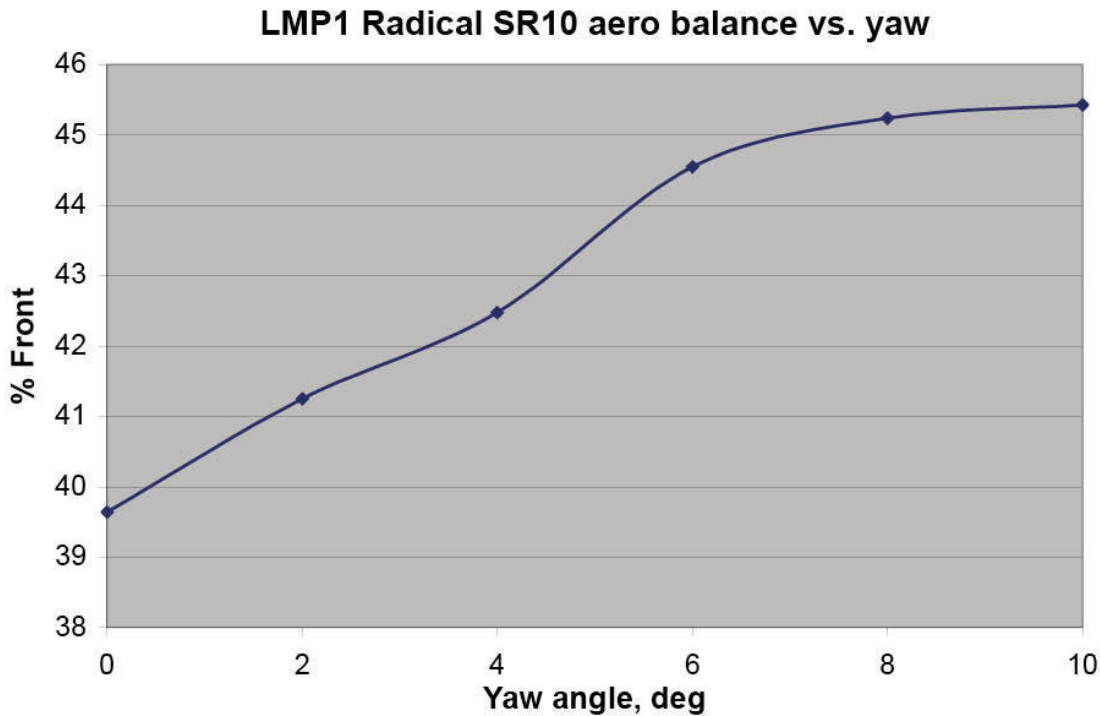


**Figure 9-15** Aerodynamic balance altered markedly when at small yaw angles too.

Some obvious thoughts inevitably arise from this finding. An initial and perhaps simplistic conclusion would be to look for a set-up that gave a straight-line balance with around 35–36% of the downforce on the front in the knowledge that once the car was cornering, and therefore at around 4° or so yaw (a basic assumption based on the approximate slip angle at which peak grip apparently occurs on the tyres in use on this car) its aerodynamic balance would move closer to the static front:rear weight split, give or take a little according to car and driver preference. This ought to ensure the car was better balanced for cornering, at least in the mid-corner phase.

But the reality is clearly more complex, for a number of things obviously happen when approaching a corner and turning in; first, under braking the probable reduction in front ride height as a result of the forward weight transfer would also shunt a bigger proportion of the total downforce on to the front, helping to maximise the front tyres' grip; second, assuming turn-in was initiated before the front had come up too much again, this extra increment of front downforce would add to turn-in grip; and third, the forward shift in aerodynamic balance as yaw angle increases during turn-in could be helping initially too, given that the car would be encouraged to rotate into its cornering attitude by virtue of increasing grip at the front and reducing grip at the rear.

What ideally would then be needed would be a stabilisation of that balance in mid-corner, requiring that the shift of downforce to the front should halt as yaw angles approached those achieved in mid-corner. However, the SR10 saw that forward shift continuing until much higher yaw angles than this, which doesn't look like a stable condition.

Also, although not shown in the data presented here, the SR10 exhibited practically zero restorative yaw moment (intrinsic straightening effect) that would tend to stabilise the car as yaw angle increased. So could there be a way of tuning what happens in yaw to stabilise the initial forward shift in downforce with yaw sooner, so that as the car reached its peak yaw angle in mid-corner it was balanced and stable? This would require further study to determine the causes of the forward balance shift at modest yaw angles so that it might possibly be better exploited. But it's interesting to note that new rules for 2011 imposed by the Auto Club de l'Ouest (ACO), the Le Mans regulator, and the FIA included a large 'dorsal fin' over the engine cover. This would surely add yaw stability at small angles, though it remains to be seen as this is written what might happen at much larger yaw angles, such as when a car gets fully sideways...

## 2011 LMP2 Zytek

An early 2012 wind tunnel session saw the opportunity to work on the 2011 LMP2 Le Mans 24 Hours-winning and 2011 LMP2 Le Mans Series-winning Zytek Z11 SN-Nissan of UK-based Greaves Motorsport. This also provided some glimpses into how a top professional team goes about testing in MIRA's full-scale wind tunnel facility.

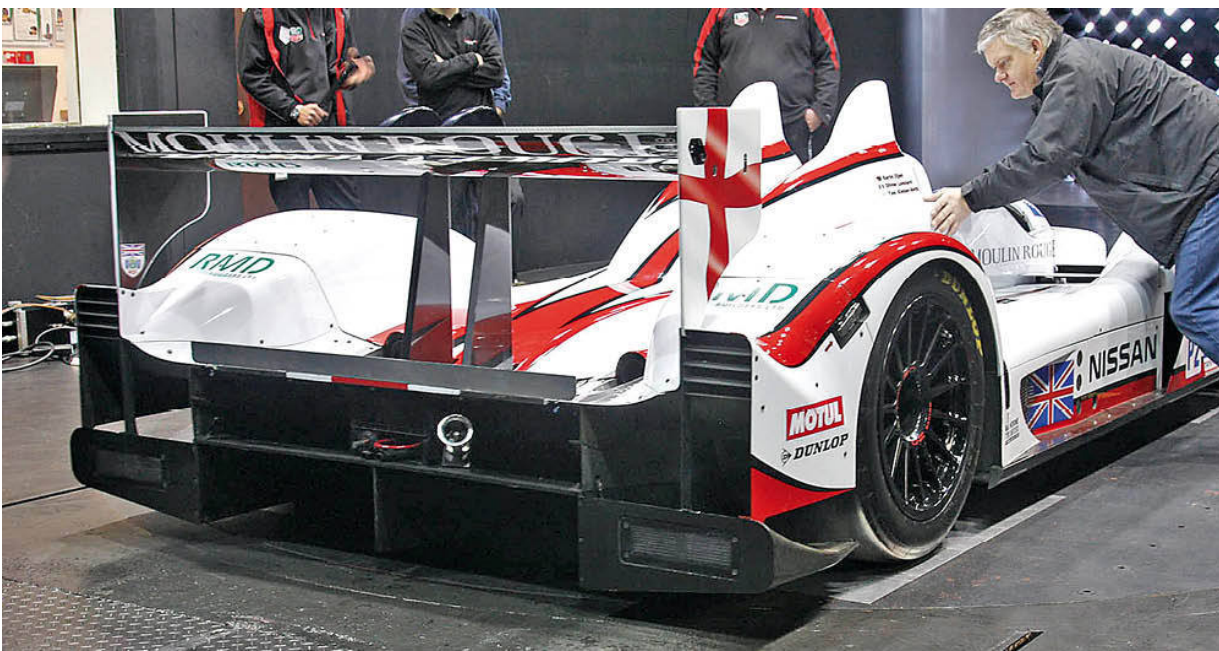
Let's look first at the Zytek's baseline data, and make comparisons with slightly earlier Radical SR10 in the previous section. Then we'll take a look at the effects of some of the mandatory modifications imposed in LMP2 for 2012, including an engine cover fin, wheel arch top apertures and larger mirrors, with the car straight ahead and at meaningful yaw angles.

Most of the main aerodynamic appendages are readily visible in the photos, with the large regulation-governed splitter, double dive planes, and louvred wheel arches. Not visible, of course, was the curvaceous, broad front diffuser under the front bodywork. Behind the front wheels were apertures in the side panel to allow some of the air to exit from under the front diffuser, and these apertures were fitted with turning vanes just outboard of the apertures and attached to the running boards. At the rear the wheel arches were again louvred, and the regulation boxes behind the wheels outboard of the controlled, but still fairly voluminous, diffuser can be seen. The wing was a

well cambered dual-element device, limited to the 1600mm span imposed at the time and supported on ‘swan neck’ mounts. A large Gurney sat on the trailing edge of the rear bodywork.



*The 2011 LMP2 Zytek Z11 SN-Nissan of UK-based Greaves Motorsport yielded some fascinating information.*



*Preparing the Zytek for its wind tunnel runs.*

The car came into the wind tunnel in what was described as the 2011 ‘preferred specification’. By way of comparison, the data for the Eco Racing

LMP1 Radical SR10 (a modified variant of the SR9 LMP2 car) in its highest downforce, best balanced configuration are also given in the following table, and CD.A and -CL.A values are given to enable direct comparison, given that the cars had different – and only roughly estimated – frontal areas.

Radical

CD.A: 1.130

-CL.A: 3.262

%front: 37.20

-L/D: 2.887

Zytek

CD.A: 1.048

-CL.A: 3.439

%front: 41.72

-L/D: 3.281

$\Delta$ , counts

CD.A: -82

-CL.A: +177

%front: +4.52

-L/D: +394

$\Delta$ , percent

CD.A: -7.3%

-CL.A: +5.4%

%front: absolute

-L/D: +13.5%

In simple terms, then, the Zytek generated 7.3% less drag than the Radical, and also generated over 5% more total downforce, leading to a 13.5% greater efficiency (-L/D) figure. The Zytek's downforce was also more forward-biased.

One of the most interesting aspects was that, despite running with the narrower (1.6m) span, reduced (250mm) chord rear wing mandated from the beginning of 2009, as well as the control floor and diffuser of course, the Zytek nevertheless achieved over 8% more rear downforce than the Radical. Another key difference between the cars was the level of front end downforce, the Zytek generating an impressive 30%+ more than the Radical. However these numbers must be viewed in relation to the cars' static front to rear weight splits, which were roughly 39% front for the Radical and 45% for the Zytek. So the Radical's aerodynamic balance was actually somewhat closer to

its static weight split than was the Zytek, but given that the Zytek was in its well-honed preferred specification, whereas the Eco Racing Radical was much under-developed, we can perhaps assume that the Zytek's '%front' value in relation to its static weight split represented a balanced condition out on track. This assertion has two codicils: firstly, with the fixed floor and non-rotating wheels this wind tunnel underestimates the downforce of devices like front splitters and floors that are very close to the ground; and secondly, a car that has slightly less front aerodynamic percentage than static weight percentage is more likely to have a little understeer at high speed, rather than the inherently less stable alternative. So the '%front' values should be looked at with this in mind and the Zytek provides a useful yardstick in this respect.

One of the things that emerged with the Radical was how the balance shifted as a range of realistic yaw angles was applied. The Zytek was also tested at up to  $6^\circ$  yaw angle (in each configuration evaluated, which we will look at in more detail in shortly). This maximum yaw angle was used because the slip angle at which the tyres generated maximum grip was  $6^\circ$  according to Greaves Motorsport. The effect on the balance of the two cars from  $0^\circ$  to  $6^\circ$  in  $2^\circ$  increments is shown in table below.

'%front' at yaw angle:  $0^\circ$

Radical SR10: 39.6

Zytek Z11 SN: 41.7

'%front' at yaw angle:  $2^\circ$

Radical SR10: 41.3

Zytek Z11 SN: 40.6

'%front' at yaw angle:  $4^\circ$

Radical SR10: 42.5

Zytek Z11 SN: 40.9

'%front' at yaw angle:  $6^\circ$

Radical SR10: 44.6

Zytek Z11 SN: 41.4

Clearly the two cars showed a quite different response to increasing yaw angle over this range. The Radical's aerodynamic balance became markedly more front biased as yaw increased, which one would think would be a potentially unstable response. The Zytek, on the other hand, showed an initial shift away from the front at  $2^\circ$  yaw, but the balance then moved more to the front with the remaining yaw increments, until at  $6^\circ$  yaw the balance was quite similar to the straight ahead position. This seemed like an altogether more

stable response. It must be remembered, though, that these numbers were recorded as steady state readings with data averaged over minute long sampling intervals, and the actual dynamic transient response may not be the same. Nevertheless, the Zytek looked to have more benign characteristics when tested in steady state across this yaw range.

So, what was the overall effect of the 2012 mandatory modifications, that is, fitting the ‘new to LMP2’ engine cover fin, opening up the newly mandatory wheel arch tops to the maximum, and fitting the larger mirrors? Figures 9-16 to 9-18 illustrate the changes across the working yaw range. Unfortunately, it was not possible to test the car at very high yaw angles, which is the condition that the engine cover fin and wheel arch apertures were devised for in order to reduce the lift that can be generated when an LMP-type car gets sideways. Nevertheless it was important for the team to establish the effect of these new modifications on the aerodynamic parameters during normal running.

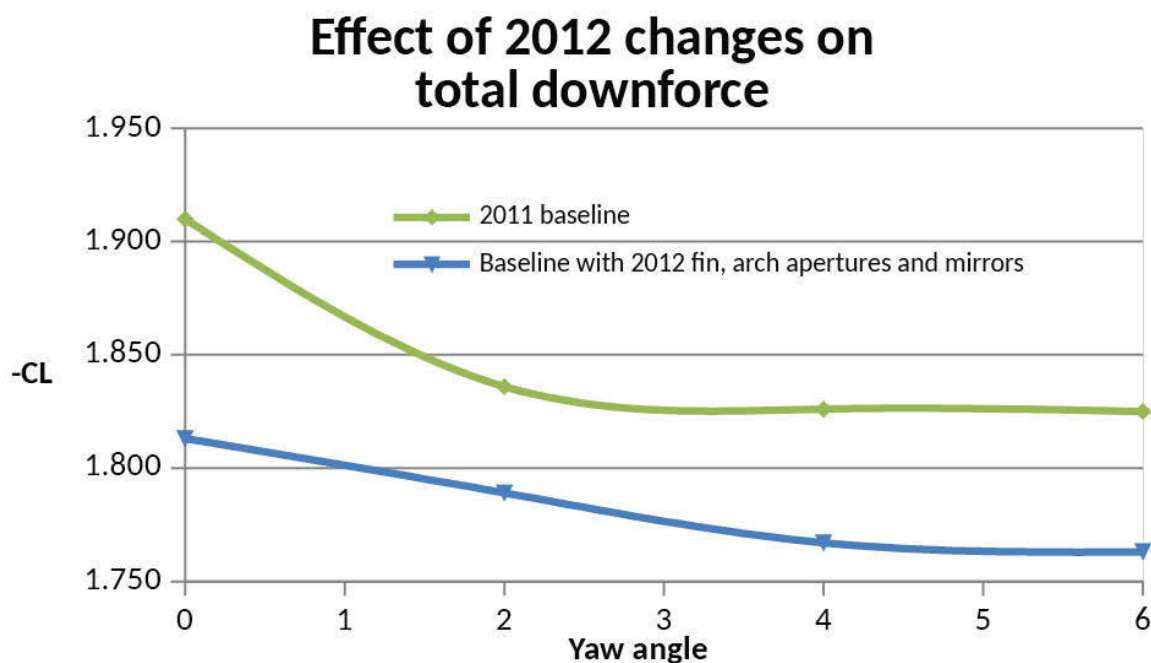


**Figure 9-16** Total downforce versus yaw angle on the Greaves Motorsport Zytek LMP2 in 2011 configuration and initial 2012 configuration.

## Effect of 2012 changes on aerodynamic balance

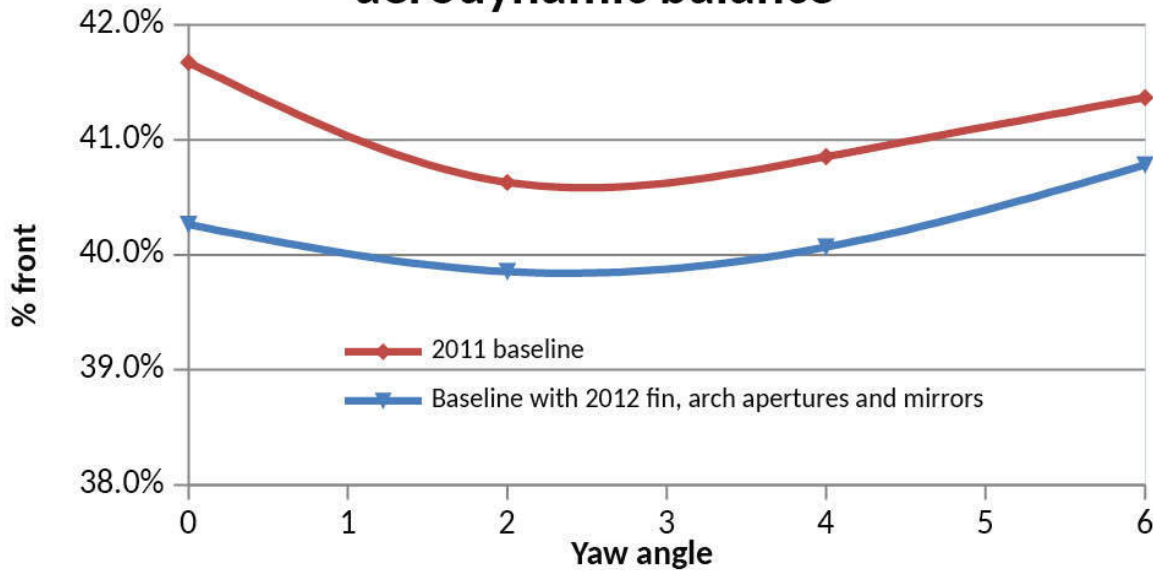


**Figure 9-17** The Zytek's balance versus yaw angle in 2011 and initial 2012 configurations.

## Effect of 2012 changes on drag

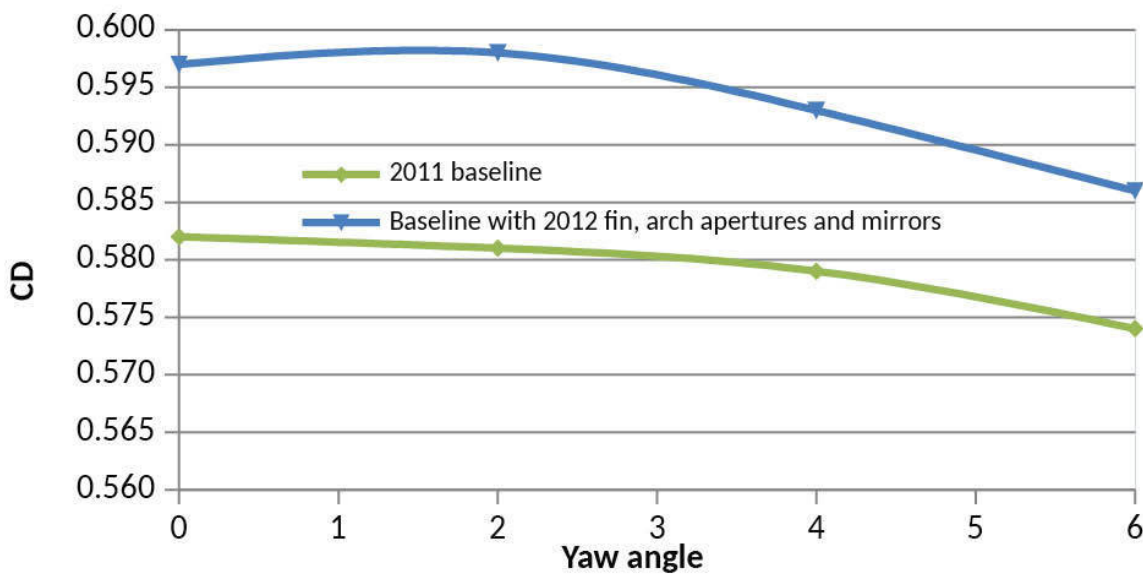


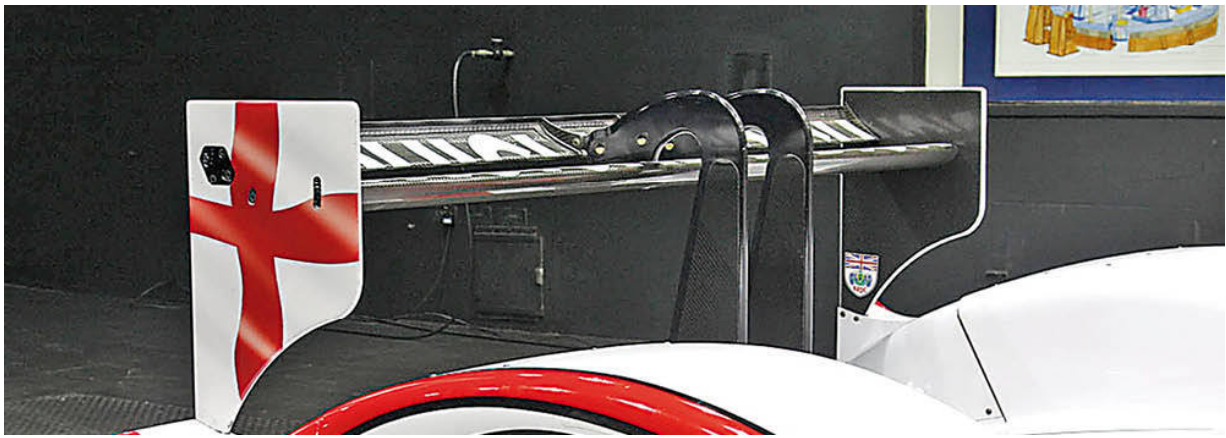
**Figure 9-18** Drag versus yaw angle for the 2011 and initial 2012 configurations on the Greaves Motorsport Zytek.

So we can see that total downforce was reduced across the whole yaw range, between 3.4% and 5.1% at 6° yaw and zero yaw respectively, although the effect of yaw on the 2012 specification was less than it was on the 2011 specification car. In terms of aerodynamic balance, the 2012 modifications shifted the balance somewhat rearwards across the yaw range, but the effect of yaw on the 2012 specification car was rather greater, with the '%front' value actually higher at 6° yaw than at zero yaw. And drag was higher in 2012 specification, between 2.1% and 2.6% at 6° and zero yaw respectively.

So whatever else the 2012 modifications were intended to achieve, on the basis of this initial look-see evaluation they made the cars less aerodynamically efficient, with less downforce and more drag over a typical working yaw range. This would obviously have decreased corner speeds as well as straight line speeds, but Greaves Motorsport and all the other teams were very soon able to devise ways of mitigating and even reversing those aerodynamic losses.

### **'Swan neck' wing mountings**

In 2009 the Auto Club de L'Ouest (ACO), the ruling body at Le Mans, mandated that rear wings should be reduced in width from 2000mm to 1600mm (78.7in to 63.0in) and in chord dimension from 300mm to 250mm (11.8in to 9.8in) in an effort to reduce the cornering speeds of the cars. As a direct response to this, it was no surprise to see more aggressive wing profiles and angles being used by the teams in order to recoup some of the lost downforce and address the inherent balance changes that had also occurred. But an interesting development that also appeared at this time was what became known as 'swan neck' rear wing mountings, as seen on the 2011 Greaves Motorsport Zytek LMP2. Interestingly, these two new developments – more aggressive wings and swan neck top mounts – were related.



*The Greaves Motorsport Zytek sported 'swan neck' top mounts for its rear wing*

Following the appearance of these new wing mounts, Mike Fuller of [www.mulsannescorner.com](http://www.mulsannescorner.com) fame contacted the writer to see if a simple CFD study on wing models in isolation (neither of us having full CAD models of LMP prototypes, nor the resources on which to carry out the CFD) could determine what the connection was between aggressive wings and swan neck mounts. Mike provided the CAD models, based on profiles from a named but anonymous team, and the writer carried out the CFD. The sequence in which the CAD and CFD was performed started with a model of a 2008 vintage, 2000mm span by 300mm chord wing as the baseline. This produced downforce and drag values at 200mph of 7754N (1739lb) and 1009N (226lb) respectively, which resulted in a -L/D value of 7.68.

Next, the profile was scaled down to 250mm chord, and 400mm was lopped off the span to meet the 2009 regulations. This saw downforce fall by 34% to 5110N (1146lb), drag by 31% to 696N (156lb) and -L/D to 7.34, values that were apparently in broad agreement with those found by the teams when they confronted the rule change. And the general approach of the teams was initially to address this with increases in main element angle and camber, so that was the next step in our exercise. Interestingly this produced less downforce, 4544N (1019lb) and more drag, 954N (214lb), -L/D dropping to 4.76, and the reason for this was plain to see when surface streamlines were plotted on the wing's suction surface, as seen in figure 9-19. Flow separation from the conventional lower surface wing mounts was disturbing the flow across a wide expanse of the main element.

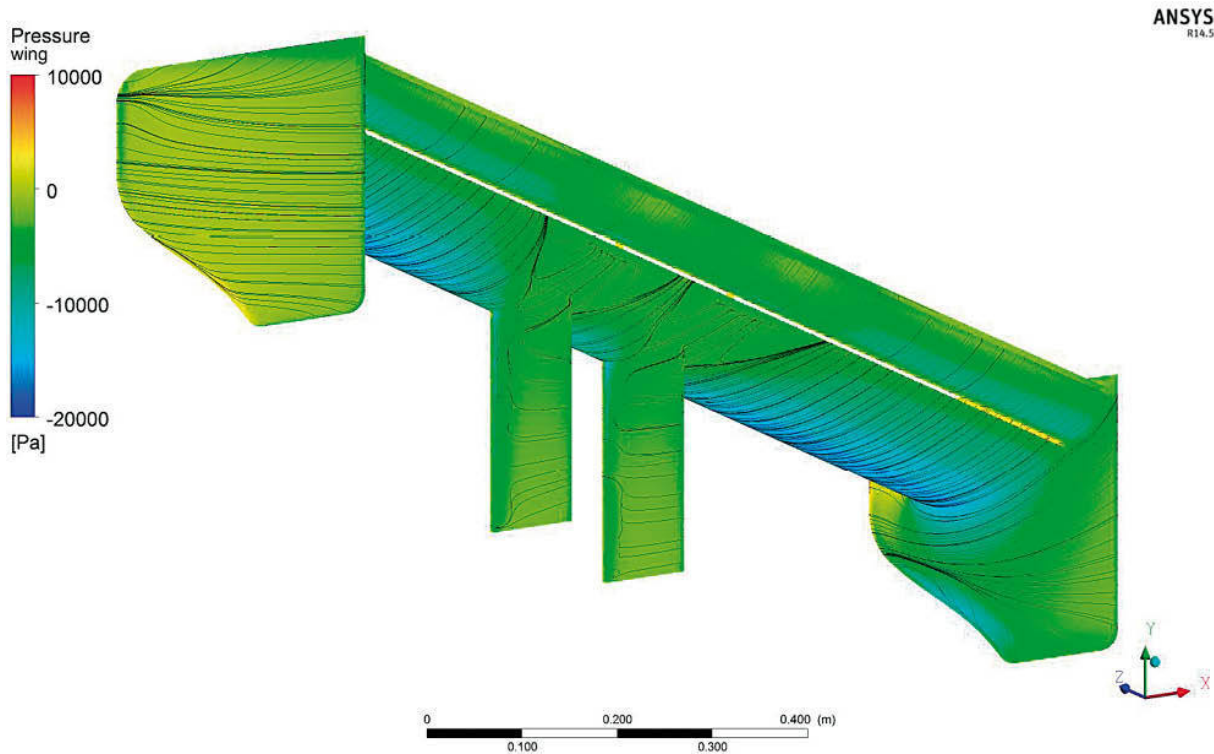


**Figure 9-19** Making the 2009-specification wings more aggressive saw the appearance of flow separation from the lower wing mounts

As a response to this flow separation, the angle of the main element was reduced by 3° by pivoting it at its trailing edge, thus leaving the flap and end plates in the same places, and the wing was rerun in CFD again. This saw downforce jump up to 5471N (1227lb) and drag was 798N (179lb), -L/D climbing back up to 6.86, and the streamlines showed full flow attachment on the main element. So there was clearly a limit to how far the main element angle could be pushed before the combination of the steep adverse pressure gradient and the presence of the wing mountings created a conflict.

And this is where the original clever leap of imagination came (more or less simultaneously at Audi and Acura), although with 20-20 hindsight it seems obvious now; instead of backing off the wing to reduce the pressure gradient, the wing mountings were moved to the top surface in the expectation that the conflict would be eradicated. And so it was on our model, as figure 9-20 clearly demonstrates; full flow attachment was now visible with the steeper main element angle, and there was much reduced static pressure right across the suction surface compared to figure 9-19. Downforce had climbed once more to 5792N (1299lb) with drag at 829N (186lb), making -L/D 6.99.

Indeed a flap angle increase of  $8^\circ$  was then applied and downforce climbed further to 6301N (1413lb) with drag rather higher at 968N (217lb).

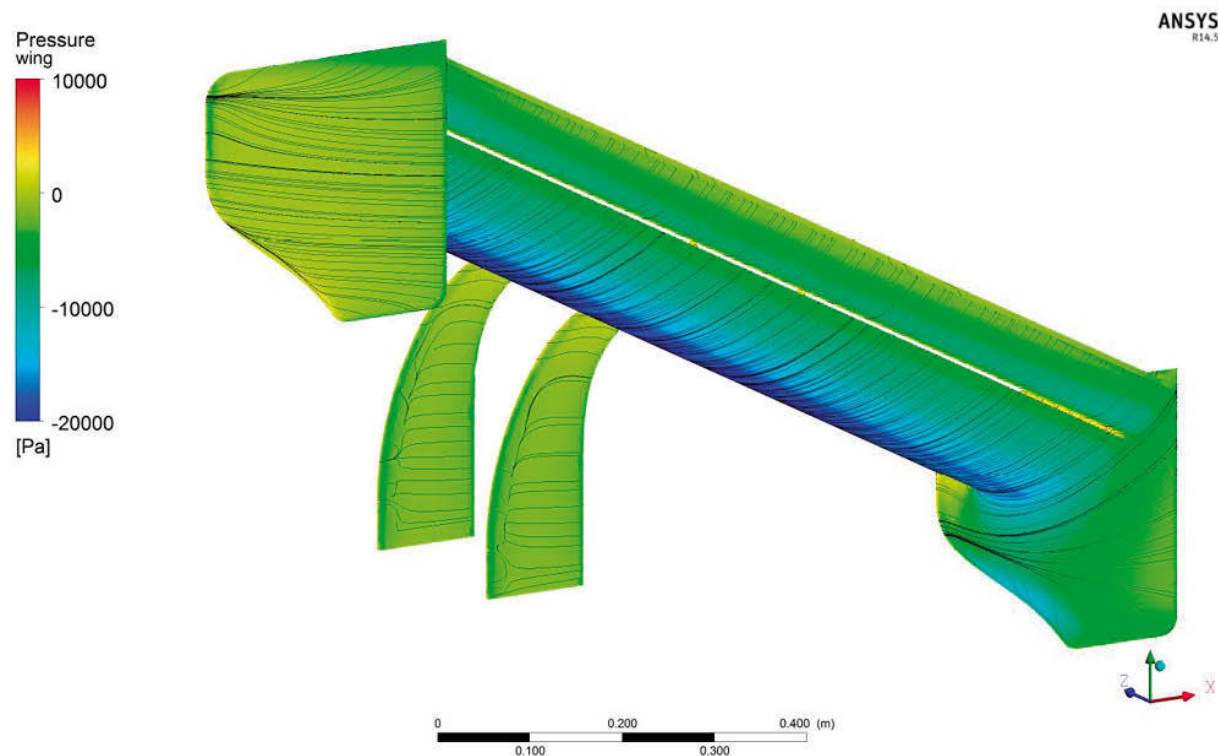


**Figure 9-20** Upper surface 'swan neck' mounts enabled aggressive wing design without the flow separation seen with lower surface mounts

So with just a very few quick and basic changes the original 34% reduction in downforce compared to 2008 levels had been reduced to 18.7% on our wing model, and not surprisingly the teams did even better in time, possibly even getting back to pre-2009 levels of downforce and efficiency in the space of a year, although this involved more than just rear wing development.

Another result of these developments was a legacy where swan neck mounts have become a preferred option for an increasing number sports prototype and related cars, although it's worth keeping in mind that the problem with lower surface mounts only arises when pushing the main element very hard to extract maximum downforce. In many applications lower mounts work satisfactorily.

As a final note to this section, 'reverse swan neck' mounts were also evaluated in the CFD exercise above, with the mounting plates coming up behind the wing to pick up on the upper surface from behind (although this may fall foul of many regulation sets that stipulate a maximum rearwards

location for body and aerodynamic parts). The results were almost identical to the more elegant forward swept swan necks, giving no tangible advantage.

### Formula 3

January 2012 saw Dallara Automobili in the midst of supplying its then new F312 Formula 3 car to its customers, and at that time the author was fortunate to be able to evaluate the new car and compare it to its predecessor, the F308 in 2011 specification, thanks to British and European F3 contender Fortec Motorsport, who brought their new steed into MIRA's full-scale wind tunnel in order to do some benchmarking with the previous car. The new car featured cleaner bodywork with less aerodynamic paraphernalia, a higher nose, a larger front wing (with no raised centre section) mounted slightly further forward, and a sharply terminated engine cover with a gearbox top shroud below.



*The 2011 specification Dallara F308 of Fortec Motorsport.*



*Brand new at the time of this wind tunnel session, Fortec Motorsport's Dallara F312 performed better than its predecessor.*

With an F3 car's ultra-low front ground clearance (typically 10mm to the front splitter under the driver), MIRA's fixed floor would not enable fully realistic data to be generated, especially on downforce from the floor and to a lesser extent from the front wing. But this would still enable comparison between the 2011 and 2012 cars and also examination of the effects of configuration changes in relative terms. Both cars were brought to the wind tunnel with maximum front and rear wing settings. And during the cars' set up, each was fitted with 'trip strips' on the tyres to better simulate rotating wheels, these angled aluminium strips serving to cause flow separation on the tyres more closely to where it would naturally occur if the wheels were rotating (the flow stays attached further around a stationary wheel and creates a different flow field downstream). The baseline aerodynamic data on the two cars is shown in the table below, together with the differences ( $\Delta$  or 'delta' values) between the two cars.

2011 car  
CD.A: 0.794

-CL.A: 1.850

%front: 38.6

-L/D: 2.330

2012 car

CD.A: 0.788

-CL.A: 1.989

%front: 44.7

-L/D: 2.524

$\Delta$ , counts

CD.A: -6

-CL.A: +139

%front: +6.1%

-L/D: +194

$\Delta$ , percent

CD.A: -0.8%

-CL.A: +7.5%

%front: absolute

-L/D: +8.3%

So, with maximum wing angles and the same chassis rakes both cars generated much the same drag level, but the new car generated 139 counts (7.5%) more overall downforce, with all the gains at the front end. Given that exactly the same adjustment ranges were provided on the front and rear wings of both cars, the new front wing was clearly a significantly more potent device. According to Andi Scott, Fortec's chief race engineer at the time, the static weight split of the old car of around 41% to 42% on the front meant that it was always hard to generate enough front end downforce to obtain an aerodynamic balance. It would appear that the F312 would not have this problem (and it also appeared to have slightly less weight on the front end too).

The F312 front wing differed in a number of respects from the previous car's, but with the same range of available adjustment provided on its larger and more complex flap, figure 9-21 illustrates how the new car's aerodynamic balance altered across the range of front wing adjustment relative to the previous car, the front wing design of which had changed little over the years. Because the F312's wing was a more potent device, the changes in downforce between the same adjustment increments were somewhat larger. Fortunately, Dallara provides a wide range of adjustments in between the settings

illustrated here, and it is clear that there was plenty of scope to span the likely preferred range of front downforce percentage.

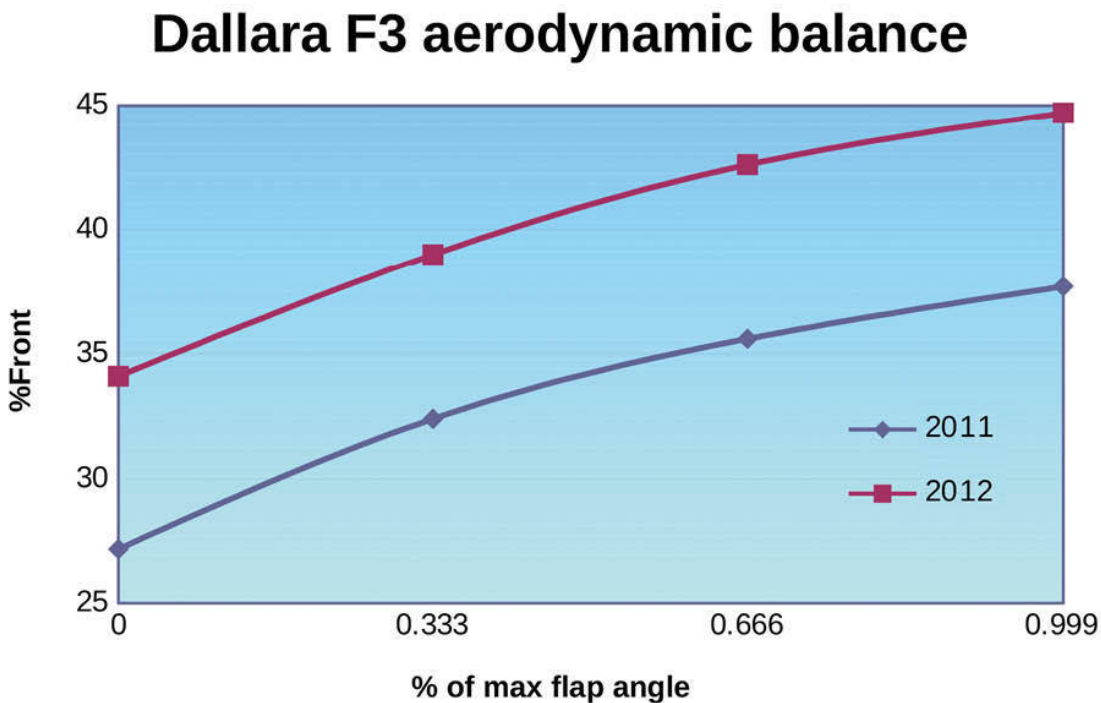
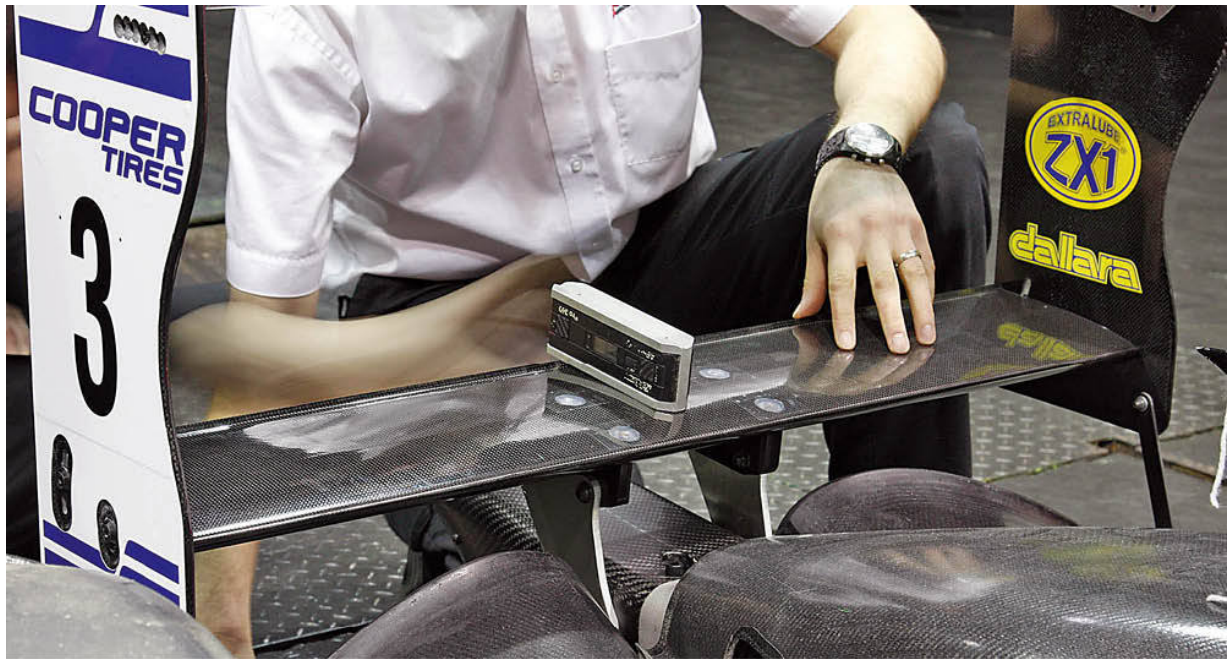


**Figure 9-21** The aerodynamic balance of the 2011 specification Dallara F308 and 2012 F312 covered different ranges, the newer car offering more forward-biased balance options.

Another interesting study performed during this session was to look at the effects of adjusting the lower rear wing beam, which together with the tall end plates also serves as the mount for the upper wing tier. The adjustment ranges available on the two cars' lower wing beams were not the same so direct comparison wasn't possible, but nevertheless the data proved illuminating. The changes to the aerodynamic coefficients are shown in tables below to highlight points of interest. The first table shows data from the 2011 car and the second from the 2012 car.

0 to 8.2deg  
 $\Delta CD$ : +21  
 $\Delta CL$ : +62  
 $\Delta CL_f$ : -1  
 $\Delta CL_r$ : +62  
 $\Delta \%front$ : -1.6

$\Delta\text{-L/D}$ : +18  
 6 to 14deg  
 $\Delta\text{CD}$ : +16  
 $\Delta\text{-CL}$ : +49  
 $\Delta\text{-CLf}$ : +4  
 $\Delta\text{-CLR}$ : +45  
 $\Delta\%$ front: -0.9  
 $\Delta\text{-L/D}$ : +12



*Adjusting the angle of the lower beam wing on both cars yielded some interesting data.*

Looking first at the 2011 car's data in the upper table, we can see that over the angle range tested (the maximum available was just  $8.2^\circ$  on this car) there was a reasonably efficient downforce gain of 62 counts for 21 counts of drag (a ratio of 2.952:1, better than the car's overall  $-\text{L/D}$  ratio). With the steeper angle range tested on the 2012 car, the overall downforce gain was less at 49 counts but the drag increase was commensurate at 16 counts (3.063:1, also better than the car's overall  $-\text{L/D}$ ).

The 2011 car showed effectively no off-loading at the front for the 62 counts of extra rear downforce. This is interesting because if we compare an adjustment to the upper rear wing tier which yielded 64 counts of extra rear downforce for 21 counts of drag, it showed the  $-\text{CLf}$  to reduce by 7 counts. Thus we might reasonably assume that the lower rear wing beam was also

helping the underbody to add a little more downforce, some of which was felt at the front end, thus offsetting the mechanical offloading seen with an adjustment to the upper rear wing tier. The 2012 car actually saw a small increase in  $-\text{CL}_f$  with increased lower wing beam angle despite the smaller rear downforce increment achieved from the wing beam adjustment, perhaps suggesting that the 2012 car's underfloor was working better than the 2011 car's.

Prior to the new Dallara's appearance the previous model had sprouted a profusion of 'off-body' devices in much the same way that pre-2009 Formula 1 cars had done. We saw in chapter 5 how the turning vanes or strakes under the front wing of the Dallara F308 affected the aerodynamic data, and during the last few minutes of the wind tunnel time on the F308, a few other bodywork devices removed from the car, one at a time, so we could actually measure their effect on the car's aerodynamic numbers. The first of these were the devices known to the team as the 'front sidepod fenders', the vertical vanes attached just outboard of the front of the sidepods. The results, shown as the effects of adding these devices are shown in the table below, and we can see that adding them produced a quite efficient, forward biased downforce increment of 31 counts of downforce for 10 counts of drag.

+ 'fenders'
$\Delta C_D$ : +10
$\Delta C_l$ : +31
$\Delta -C_{L_f}$ : +27
$\Delta -C_{L_r}$ : +4
$\Delta \%_{\text{front}}$ : +1.1
$\Delta L/D$ : +11

Finally the 'rear wheel flip-ups' were removed from the sidepods, and the results of adding them are shown in the table below. Once again an efficient downforce benefit was gained with the flip ups, and this time the bias was towards the rear although there was also a gain in front downforce. The mechanism here would most likely be of the flip ups acting as conventional inverted but very thin wings

+ flip ups
$\Delta C_D$ : +10
$\Delta C_l$ : +45
$\Delta -C_{L_f}$ : +10

$\Delta\text{-CLr}$ : +36

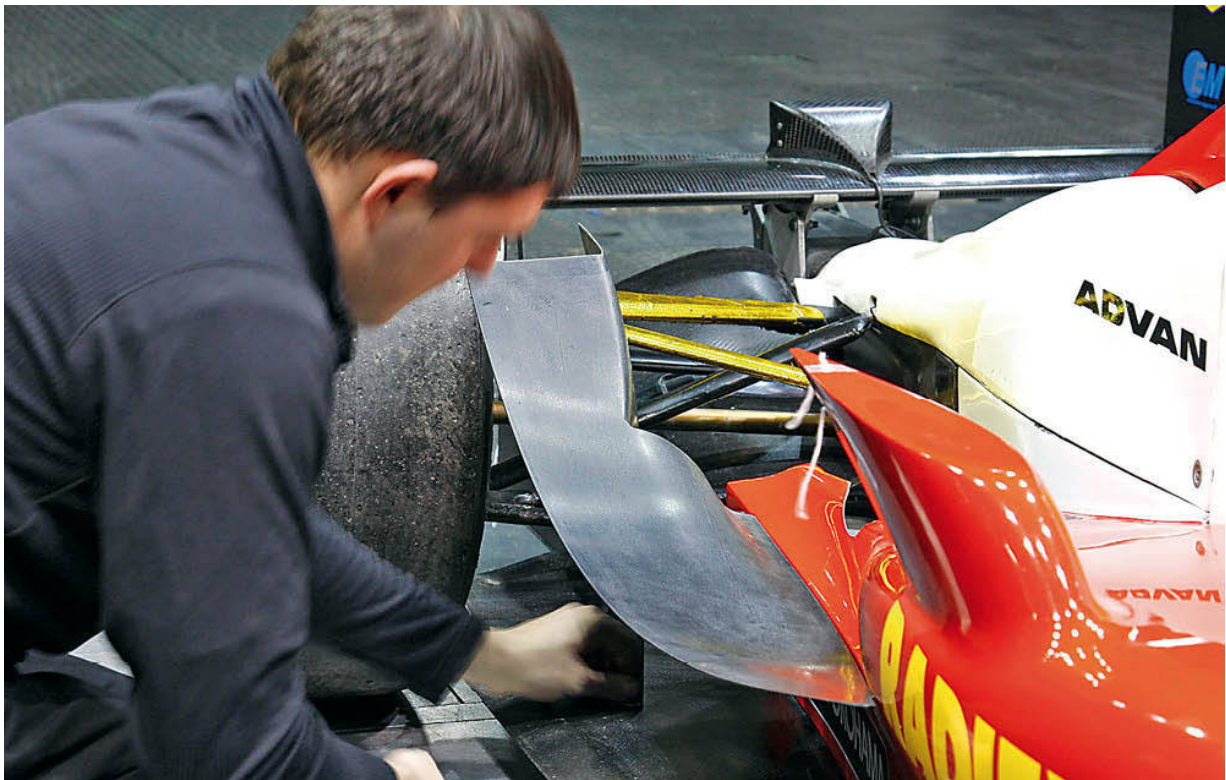
$\Delta\%$ front: -0.5

$\Delta\text{-L/D}$ : +37

This gives some idea of the extent of the benefits achieved by these carefully designed and crafted parts. In the great scheme of things the benefits are modest and in many categories there may be lower hanging fruit to pick before it becomes appropriate or necessary to search for gains of this order. But in a competitive arena like Formula 3 and of course Formula 1, small gains can make big differences in grid or race position.



*The front 'sidepod fenders' on the Fortec Dallara F308 provided forward-biased benefit.*



*'Flip ups' on the sidepods produced gains at the front and the rear ...*

### **Low speed aerodynamics on a hillclimb car**

An oft-asked question is ‘at what speed do aerodynamics start to play a role?’ There are two main influences on the answer. First, the flows on downforce-generating (and drag-inducing) surfaces do not fully develop and ‘attach’ until speed is high enough, which in practical terms means that vehicle speed needs to exceed the stall speed of downforce generating devices. Secondly, the speed also needs to be sufficiently high for the aerodynamic forces thus generated to be tangible, meaning that useful additional grip is generated. (Drag is also governed by these same factors, but at low speeds it has very little relevance.) An opportunity to attempt to answer the initial question arose with a visit to the MIRA full-scale wind tunnel with the DJ Firestorm, which competes in the top echelon of UK hillclimbing. Two separate trials were performed on the Firestorm at different speeds.

The first trial was carried out, as usual at the start of a session, to see at what air speed the remainder of the session would need to be run. Generally this involves running in the configuration as delivered to the wind tunnel at 60mph (26.8m/s) and then at 80mph (35.7m/s), and analysing the results. Sometimes the lift coefficients on racecars can be significantly smaller at 60mph than at 80mph, when ideally the coefficients would be the same at

either speed; such differences then can be an indication that flows are not fully attached to the downforce-generating devices at the lower speed, and so subsequent tests are performed at the MIRA tunnel's maximum air speed of 80mph. In this case the DJ Engineering team, who constructed the Firestorm, and its owner/driver Wallace Menzies also wanted to see how the aerodynamics worked at lower speeds, and so another run was done at 50mph. The results are shown below.

21.7m/s (~50mph)

CD: 0.767

-CL: 1.466

-CLfront: 0.583

-CLrear: 0.883

%front: 39.8

-L/D: 1.911

26.4m/s (~60mph)

CD: 0.768

-CL: 1.481

-CLfront: 0.589

-CLrear: 0.892

%front: 39.8

-L/D: 1.928

35.1m/s (~80mph)

CD: 0.759

-CL: 1.456

-CLfront: 0.583

-CLrear: 0.873

%front: 40.0

-L/D: 1.918



*Smoke and wool tufts seem to show attached flow on the DJ Firestorm's usual rear wing configuration, even at the 25mph speed used for the flow visualisation session.*

Although there was a wider spread of results than might ordinarily be expected between runs in the same configuration, the lowest lift coefficients actually occurred at the highest test speed. Had there been flow separations occurring at lower speeds, then the lowest lift coefficients would be expected to have been at the lowest test speed. And the differences in the coefficients at 50mph and 60mph were very small too. So it appears that the flows were fully attached at 50mph, and that the aerodynamic devices were already working efficiently at this speed.

A second trial was carried out with a four-element rear wing installed, and runs were done at 40mph and 60mph to see whether the flow was attached to this aggressive device. The results are shown below.

18.3m/s (~40mph)

CD: 0.919

-CL: 1.805

-CLfront: 0.772

-CLrear: 1.033

26.4m/s (~60mph)

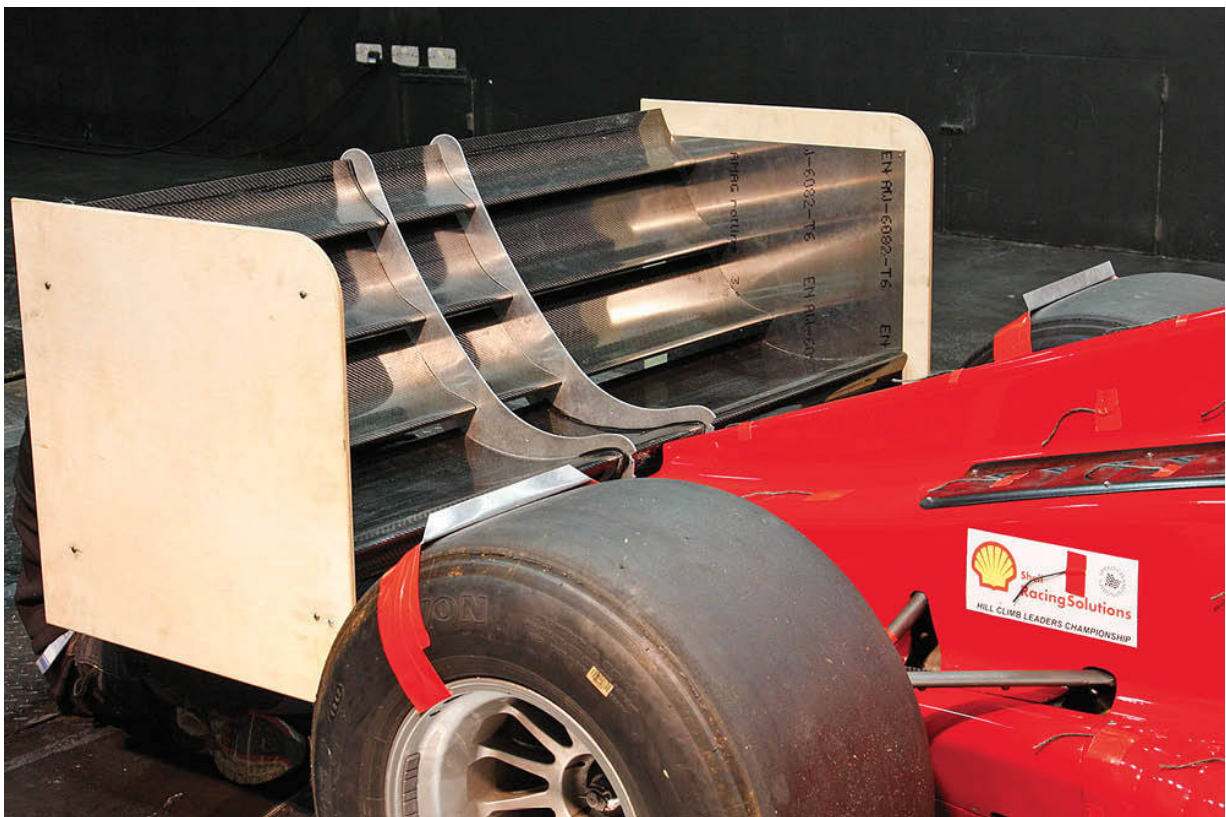
CD: 0.932

-CL: 1.904

-CLfront: 0.881

-CLrear: 1.024

Interestingly, the rear wing performed as well at 40mph as it did at 60mph, suggesting that flow was already fully attached to the wing at the lower speed. But the front wing showed a reduced coefficient at the lower speed, and combining this with the results of the first trial, we can say that the front wing started to work fully between 40mph and 50mph. The apparently greater speed sensitivity of the front wing can probably be attributed to a steeper adverse pressure gradient on its underside, thanks to its ground proximity.



*This four-element rear wing showed attached flow at 40mph, even though the feed to its main element must have been compromised by its low position.*

But levels of downforce were being generated at 50mph? Were they enough to make any difference to performance? Using the downforce equation  $F = 1/2\rho Av^2C_L$ , the overall downforce at 50mph was approximately 570N. With an

estimated weight including driver of around 560kg (5494N), this downforce represented just over 10% of car weight, which would correspond approximately to 10% additional grip. So even at 50mph, the level of downforce here was already pretty significant in relation to additional grip developed for acceleration, braking and cornering.

Clearly this car had potent downforce-generating devices, and the answer to the original question might be different for cars generating less downforce. But the exercise served to illustrate that flow attachment to the devices that generated the downforce here was happening at speeds as low as 40mph, and seemingly fully developed by 50mph such that very useful levels of downforce could be exploited from that speed.

## Formula Student

The phenomenon that is Formula Student has flourished and impressed around the world, and wings and other downforce-inducing paraphernalia have blossomed in the category. We take a brief tour here of two UK-based entries to whom *Racecar Engineering* provided half-day sessions in the MIRA full-scale wind tunnel in 2013 (the University of Hertfordshire) and 2014 (the University of Bath).

2013 was the first year that the University of Hertfordshire, which had been involved in the competition since 1998, had entered a car with a full aerodynamics package, although aerodynamics designs had been worked on in previous years. Analysing the overall performance of its 2012 contender, UH15, the team decided that the only way to make up the three-second lap time deficit to other teams in the sprint competition was with aerodynamics.

The first iteration aerodynamics package devised for the 2013 competitions comprised front and rear high downforce wings. It was decided to utilise pre-existing aerofoil profiles with coordinates in the public domain, rather than spend time on bespoke profile design, and a short list of candidates was whittled down with the help of Star CCM+ CFD software to the Selig1223 ‘high lift’ profile for the main elements and flaps, front and rear. The decision to run with dual-element wings front and rear for this first iteration was taken on the practical basis that this configuration required optimising just one slot gap over the wide adjustment range needed to suit the sprint, endurance and acceleration phases of the competition, even though a triple-element (or more) configuration offered greater downforce potential. CFD was utilised to establish the optimal relative positions and angles of the main elements and flaps, and also end plate size and shape. Cost and time considerations were

also involved in the choice of configuration and overall package design, as indeed were overall car design changes simultaneously underway.

The planned quarter scale wind tunnel test of UH16 with wing package in the University' of Hertfordshire's own wind tunnel unfortunately didn't happen because of time constraints, apart from some runs on the wing sections only, which compared reasonably favourably with the CFD data. So the MIRA test was the first opportunity to derive some hard data on the first integrated aero package.



*The 2013 Formula Student car from the University of Hertfordshire. Notice the front wing's wake impacting on the rear wing's flow field...*

As ever we should restate that MIRA's full-scale wind tunnel has a fixed floor and the test car's wheels are stationary; the fixed floor tends to lead to underestimates of downforce generated by ground-effect devices, including front wings. However, with the 'boundary layer control fence' installed and with no downforce-inducing underbody on the car, overall under-estimates would be relatively minor. And rear downforce and drag would have been accurately determined. So how did the car perform? The car was run in the baseline configuration (maximum wing angles all round) at just 40mph and 60mph. As usual, and of especial interest in this application because of the very relevant speed range of the Formula Student competition's dynamic phases, the car was run at two speeds to see if there were differences in the coefficients, and the data are shown in the table below together with the differences between the two speeds.

40mph

CD: 1.158

-CL: 1.758

-CLfront: 0.980

-CLrear: 0.778

%front: 55.7

-L/D: 1.518

60mph

CD: 1.146

-CL: 1.797

-CLfront: 1.055

-CLrear: 0.742

%front: 58.7

-L/D: 1.568

Difference

CD: -12

-CL: +39

-CLfront: +75

-CLrear: -36

%front: +3.0

-L/D: +50

The first observations to make then are that although the drag coefficient was rather high, the overall negative lift coefficient was even higher, producing an efficiency figure, -L/D, of over 1.5. Of significance though are the differences between the coefficients at 40mph and 60mph. Aerodynamic forces normally increase with the square of speed so, all other things being equal, the calculated coefficients derived from the logged force data would be the same at the two different speeds. For the coefficients to vary with speed, all other things were not equal. This is not an unusual situation, with the flows over (or more often, under) downforce-inducing surfaces not being fully developed at speeds as low as 40mph. In this instance what we saw in the results was that the front lift coefficient increased by 7.7% from 40mph to 60mph, leading to the conclusion that the flow was better developed (for which read ‘better attached’) at the higher speed. Remember all the flaps were at their maximum angles in this baseline configuration, and this may have been too steep for the flow to be adequately attached to the front flaps at 40mph. Wool tufts on the flap undersides confirmed that these flows were not fully attached and that the higher speed showed improved attachment.

It will also be noted in the results that the rear lift coefficient decreased slightly at the higher speed. This could have been the result of any improvements there may have been in flow attachment at the rear being small enough to be masked by the increased mechanical leverage ahead of the front wheels arising from the improved front wing performance, this slightly offloading the rear wheels. Or it could have been the consequence of the increased upwash arising from improved front wing flap attachment leading to its wake encountering the rear wing more than previously and slightly reducing the rear wing's performance aerodynamic performance. The actual mechanisms are best left to CFD; the wind tunnel simply reports the results measured at the tyre contacts. But the fact that the drag coefficient also decreased, something that is known to occur when a rear wing angle is reduced for example, suggests there may have been an actual aerodynamic interaction here as well as a mechanical one.

The net result of the front gains and rear losses was a 3% shift in balance to the front from 40mph to 60mph, something that might be felt by the driver if the track contained corners or braking areas taken at the two different speeds. Of more significance though would probably be that for a car with a 50/50 static weight balance, the aerodynamic balance was rather forward biased even at 40mph, this aspect worsening at 60mph, which would tend to make the rear more skittish as speeds increased, possibly provoking some instability when braking from the highest speeds encountered, or oversteer in faster corners if the chassis was mechanically balanced at lower speeds.

A year later and the University of Bath team was invited to the wind tunnel. The team had been contending Formula Student for over 10 years and 2014 was the third year that Team Bath Racing (TBR) had run with wings on the car. Clearly a great deal of design and manufacturing time had gone into this aspect, especially where the front wing was concerned. TBR was therefore expecting high levels of grip enhancement from its 2014 aerodynamics. What would the wind tunnel results say?

First, a brief tour of TBR 14's aerodynamics package is in order. The car was dominated by its large plan area wings. The rear wing was a straightforward large chord three-element design with no span-wise deviation in the selected profiles, mounted high and just aft of the rear axle line. The front wing however was something of a work of art, featuring a tapering span, variable span-wise ground clearance, a complex end plate with vertical openings just ahead of the flaps and, underneath, a sculpted chord-wise inverted channel just inboard of the end plate's footplate. One might surmise that some Formula 1 influence was exerted here!



*The 2014 Formula Student car from the University of Bath, with an extremely potent wing package.*

As above, the first runs were conducted at different test speeds to check for any changes in the aerodynamic performance. The results as coefficients at approximately 40mph (17.9m/s) and 60mph (26.0m/s) are given in table 1, with the changes shown in counts.

40mph

CD: 1.446

-CL: 2.430

-CLf: 0.900

-CLR: 1.530

%front: 37.02

-L/D: 1.701

60mph

CD: 1.389

-CL: 2.355

-CLf: 0.970

-CLR: 1.385

%front: 41.20

-L/D: 1.695

Difference

CD: -57

-CL: -75

-CLf: +70

-CLR: -145

%front: +4.18

-L/D: -6

The first observation to make is that in baseline trim TBR 14 set two new Aerobytes wind tunnel session records; the highest drag coefficient and highest negative lift coefficient seen in our MIRA sessions. It would go on to achieve even greater heights during the session! Facetious remarks aside though, the aim with TBR 14 was to generate high downforce with wings, and this it most certainly did. The inevitable penalty for that was high drag, but the team's approach was to not be concerned about drag; downforce was the target.

The coefficient changes brought about by changing speed initially looked puzzling in some respects. The drag coefficient reduced slightly at the higher speed, as is often seen; but the overall negative lift coefficient decreased in magnitude at the higher speed, and this is not what is usually seen. The front 'downforce' coefficient (-CLf) certainly followed the usual pattern of increasing at the higher speed, this again most likely down to improved flow attachment under the front wing's suction surface as speed increased. But for the rear downforce coefficient to reduce significantly at the higher speed was unusual.

We have seen more modest 'speed sensitive' losses of -CL magnitude due entirely to aerodynamic and related mechanical effects in the past, as for example happened on the University of Hertfordshire Team's UH16 car above on which a 75 count gain at the front combined with a loss of 36 counts at the rear. The primary cause in TBR 14's case however appeared to be that the rear mounts in the rear wing were (inadvertently...) allowing the wing to pivot to a reduced angle as air speed increased. Although the difference in wing angle between 40mph and 60mph was not measured, and most of the angle reduction appeared to be at quite low speed, the difference in the -CL values would seem to be most reasonably explained this way, accompanied too as it was by a significant drop in drag.

For simplicity the comparative baseline run data on the pair of Formula Student shown here can be seen in the table below. The fundamental

difference between the two cars' aerodynamic configurations was that the University of Hertfordshire's car featured a dual-element rear wing compared to TBR 14's triple-element rear wing.

#### UH16

CD: 1.146  
-CL: 1.797  
-CLf: 1.055  
-CLR: 0.742  
%front: 58.70  
-L/D: 1.568

#### TBR 14

CD: 1.389  
-CL: 2.355  
-CLf: 0.970  
-CLR: 1.385  
%front: 41.20  
-L/D: 1.695

#### Difference

CD: +243  
-CL: +558  
-CLf: -85  
-CLR: +643  
%front: -  
-L/D: +127

While the two cars did not have the same aerodynamic balance in their respective baseline configurations, they both had maximum wing and flap angles set at front and rear, so in that sense the comparison is valid. The main difference was obviously due to TBR 14's triple-element rear wing, which required that it needed more front downforce to attain the desired balance (45-50% front) whereas UH16 needed less front downforce to attain a balance.

The extent of the influence of aerodynamics on handling and grip does depend though on the magnitude of the aerodynamic forces relative to the car's weight, so let's look at the actual forces in that context against two other cars tested in the MIRA wind tunnel for comparison. The table below shows downforce at 60mph as a proportion of all-up vehicle weight including driver on two high downforce single seaters and on the two Formula Student cars we have tested. Clearly any comparison between cars running to different

regulation sets has little technical validity, but it is of more than passing interest!

Car: Honda RA107 Formula 1, best configuration

Downforce at 60mph as % of all-up weight: 18%

Car: DJ Firestorm hillclimber, best configuration

Downforce at 60mph as % of all-up weight: 26%

Car: UH16, baseline configuration

Downforce at 60mph as % of all-up weight: 28%

Car: TBR 14, baseline configuration

Downforce at 60mph as % of all-up weight: 46%

The F1 Honda's relatively high minimum weight clearly hampered its downforce to weight ratio, whereas the hillclimber, with no minimum weight limit, weighs considerably less. Both however developed a significant proportion of their downforce with their underbodies, and so downforce values will have been underestimated by the MIRA fixed floor wind tunnel. The Formula Student cars' front wings may have been held back to an extent by the fixed floor, but their total downforce readings would have been closer to reality on track.

For all that though, UH16's downforce to weight ratio at 60mph was very respectable, and that of TBR 14 was well ahead, the car generating almost half its own weight in downforce at just 60mph. It should be added that this was partly due to its commendably low vehicle weight, but aerodynamics certainly played the major role. The inevitable calculation immediately follows, which is to establish the speed at which TBR 14 could drive across the ceiling, if it were able to get there, and 'Vceiling' works out at a remarkably low 86.8mph (38.74m/s).

### **Wing location on sports racing cars**

If the technical regulations allow the requisite freedom, just where do you locate your rear wing? At the rear of course; but just exactly where? Rear wing location on sports racing cars is, perhaps, a topic to which there is no single answer. Looking at such cars around the world a huge range of wing location solutions is on display, from high up and far back, to low down over the rear deck, to – most intriguingly of all – apparently tucked so low and far back that at first glance the wing appears to be in the wake of the main body. So, with the aid of Ansys CFD software and a sports racer CAD model, a closer examination was undertaken. And the author was also privileged to speak with

a well-known adherent of the low rear wing concept, Rennie Clayton at Dauntless Racing in the USA, who shared some fascinating insights on the development of his company's aerodynamic package for the Stohr WF1 sports racer.

The basis for the CFD exercise was one of the simple CAD models the writer had produced for 'Project Pipedream', a long-running back-burner – fast (?) becoming 'retirement' – project to design and build his own 'sports libre' hillclimb car, the Vortex. Examining rear wing location on this model was thus another short step on the long road towards that project eventually becoming a solid object...

The model (see figure 9-22) was deployed in a brief preliminary CFD exercise that showed that while the wing's downforce reduced as its height was reduced, the downforce produced by the body initially increased as height was reduced. And although total downforce nevertheless declined as wing height was reduced, balance shifted markedly forwards as the wing was lowered.

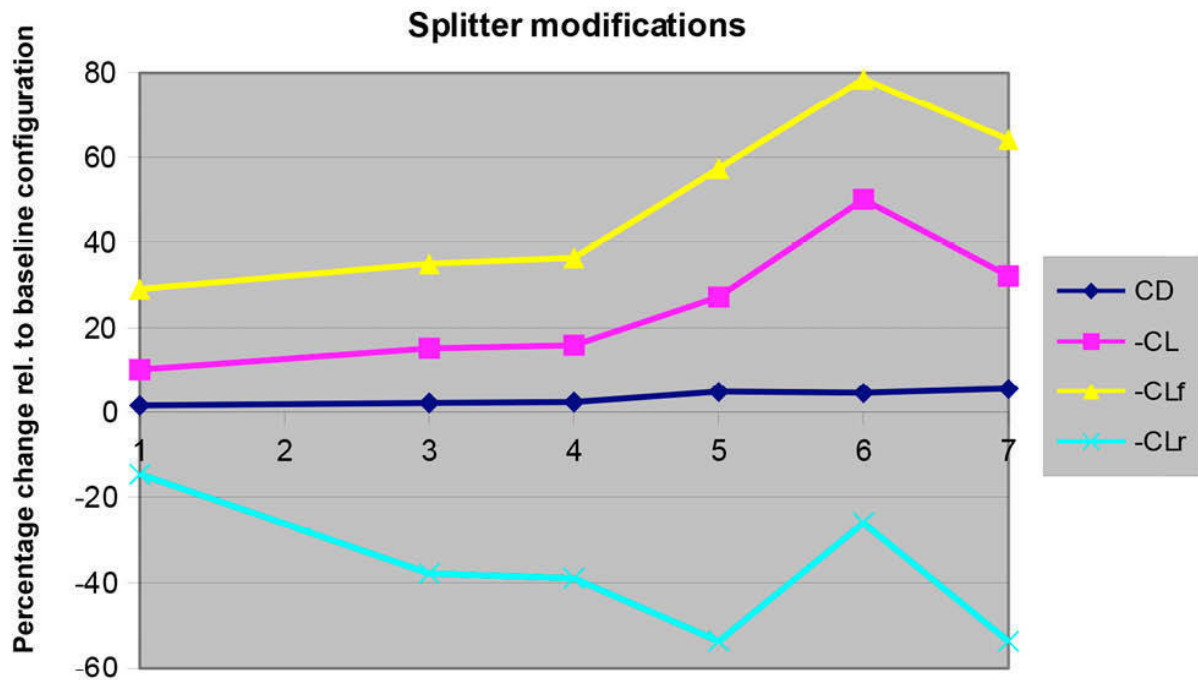


**Figure 9-22** The CAD model for this wing location exercise in CFD.

This only depicted the situation at one fore/aft, or x-location of the wing, which had been selected using the time-honoured index-finger-in-the-air process that has to be applied in the absence of any better information. This

saw the wing's leading edge overlapping the rear deck's trailing edge by about 50mm (2in), with the datum height putting the highest part of the wing assembly at the permitted maximum in UK hillclimbing of 900mm (35.4in) above the ground plane. The reasoning behind this particular x-location was that it was hoped it would put the wing's region of maximum suction directly above the diffuser exits, and that this ought to help to drive the flow through the underbody and diffusers in a manner analogous to the relationship between the flap and the main element of a dual-element wing layout. But in making this choice it was also in mind that the initial vertical separation between the wing and the diffuser exit might better see the wing further aft as well as lower.

So, the next phase of work thus saw the wing moved to two additional x-locations, 150mm (5.9in) and 300mm (11.8in) further aft, and the model was evaluated once again at six different wing heights, ranging from maximum height to 500mm (19.7in) below maximum, in 100mm (3.9in) increments to create a matrix of data points, all at the datum static ride height of 40mm and with zero rake.

Available time often restricts wind tunnel evaluations to just a few variations of something relatively time-consuming like a wing location change. By way of illustrating how easy it is to miss a useful development direction with just a few variations, let's look initially at the CFD comparisons between the three x-locations at just the datum maximum wing height of 900mm. The table below shows the basic aerodynamic parameters.

#### x-location: Datum

Total Df, N: 3330.6

Drag, N: 839.2

-L/D: 3.97

%front: 17.5%

#### x-location: x+150mm

Total Df, N: 3332.0

Drag, N: 808.6

-L/D: 4.12

%front: 15.4%

#### x-location: x+300mm

Total Df, N: 3172.3

Drag, N: 798.3

-L/D: 3.97

%front: 13.1%

Clearly, if this was the extent of a toe-in-the-water glimpse at the effect of changing wing location then that data wouldn't look too promising. Downforce had barely changed at  $x+150\text{mm}$ , and although drag decreased and efficiency ( $-L/D$ ) improved, these benefits were offset by an unsurprising rearwards shift in aerodynamic balance (%front). At  $x+300\text{mm}$  downforce actually declined and although  $-L/D$  remained as at  $x=\text{datum}$ , balance had shifted still further rewards. However the data in the next table showing wing and body downforce separated out, offered more hope...

x-location: Datum

Wing Df, N: 1491.6

Body Df, N: 1027.0

x-location:  $x+150\text{mm}$

Wing Df, N: 1448.1

Body Df, N: 1089.9

x-location:  $x+300\text{mm}$

Wing Df, N: 1431.0

Body Df, N: 928.5

Although wing downforce declined with each rearward increment, probably because the onset angle of the airflow to the wing reduced with each rearward step, body downforce increased at  $x+150\text{mm}$ , reinforcing the suggestion from the  $-L/D$  improvement in the first table that there was a positive interaction at this x-location. Moving on then to the data from the whole test matrix, figure 9-23 shows the plot of total downforce at the three x-locations and six heights evaluated.

### The effect of wing location on a sports racer model

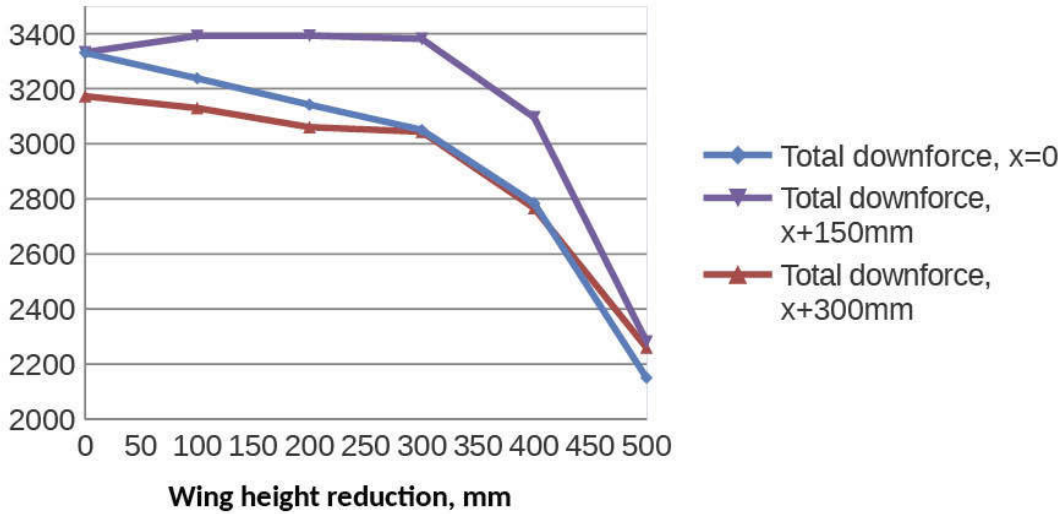


**Figure 9-23** Total downforce at three wing  $x$ -locations and six heights.

A totally different pattern becomes visible from figure 9-23, and the first thing to stand out is that downforce at  $x+150\text{mm}$  actually increased slightly compared to the datum location at the first reduction in wing height,  $h=100\text{mm}$ , and then pretty much levelled out until  $h=300\text{mm}$  rather than declining with each height reduction as it did at the other  $x$ -locations. Common to each  $x$ -location though was the rapid decline in total downforce as the height reduction exceeded  $300\text{mm}$ . So the total downforce plot confirms that there was something important happening at  $x+150\text{mm}$ . What happened to the other aerodynamic parameters?

Figure 9-24 shows  $-L/D$  versus wing location and the pattern is similar to the total downforce plot, with the  $x+150\text{mm}$  location standing out as the most efficient across the whole range of wing heights. In fact efficiency at  $x+150\text{mm}$  remained pretty much at the same level from  $h=\text{datum}$  to  $h=300\text{mm}$  before declining, whereas at the other two  $x$ -locations  $-L/D$  reduced as soon as height was reduced.

## The effect of wing location on a sports racer model

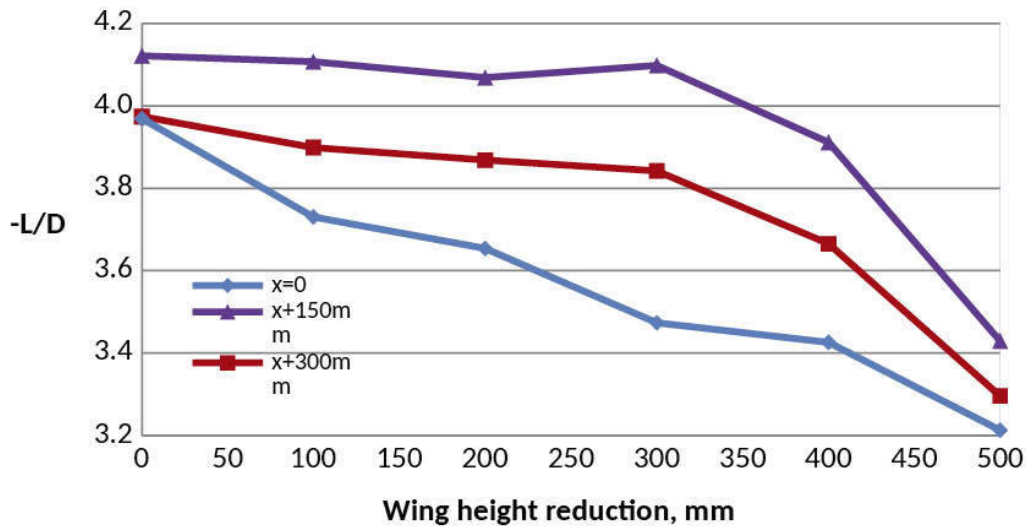


**Figure 9-24**  $-L/D$  at the three wing  $x$ -locations and six heights.

Aerodynamic balance (%front) showed a slightly different pattern. All three  $x$ -locations saw a forward shift in balance as wing height was reduced, but repeating the pattern we saw in the first table, where balance unsurprisingly shifted more rearwards with each rearwards shift of the wing at the datum height, the datum  $x$ -location produced the highest forward balance across the range evaluated. Nevertheless at  $x+150\text{mm}$  and  $h=200\text{mm}$  and  $h=300\text{mm}$  the %front value was quite close to the %front values at  $x=\text{datum}$ .

Next, an overall view of ‘wing only’ downforce is instructive, as figure 9-25 illustrates. Clearly the downforce generated by the wing declined with each height reduction in all three  $x$ -locations. But the pattern shown in the second table, where the highest wing downforce was produced at the datum  $x$ -location, downforce then declining with each rearward increment, was reversed with the first reduction in height. And this reversal persisted across the rest of the range, with  $x+300\text{mm}$  yielding the highest wing downforce at each height. Perhaps the most likely explanation for this is that there was more room for reasonably energetic flow to reach the wing the further back it was shifted. But importantly, the values at  $x+150\text{mm}$  were not far behind those at  $x+300\text{mm}$ ...

### The effect of wing location on a sports racer model

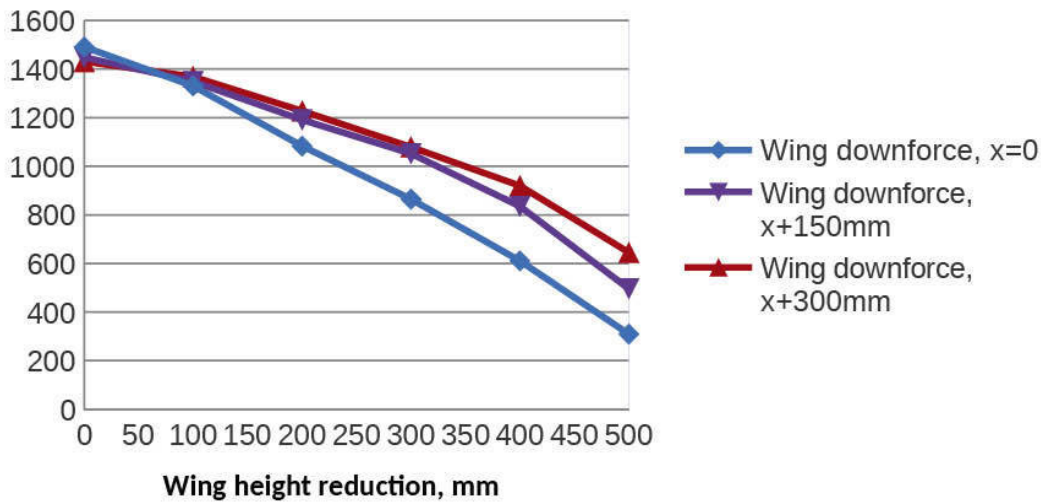


**Figure 9-25** Wing downforce at the three wing x-locations and six heights.

Finally, body downforce (not including splitter downforce, which showed only minor changes across the range) produced the most interesting plot, as shown in figure 9-26. Here we can see that the body produced peak downforce when the wing was at h-300mm in all three x-locations, but that the clear overall winner was with the wing at a fore/aft location of x+150mm. The second best fore/aft position was the initial datum location, and x+300mm was obviously the least effective across the range for body downforce.

## The effect of wing location on a sports racer model

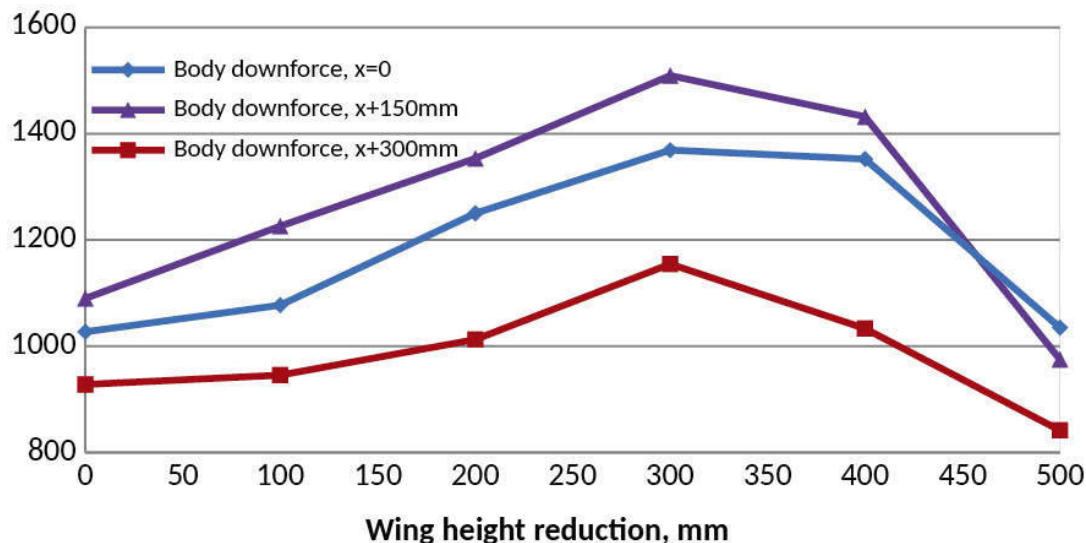


**Figure 9-26** Body downforce at the three wing x-locations and six heights.

So, given that there is clearly plenty room for optimisation to the simple shape of this model's body, and its underbody in particular, potentially also the span-wise and chord-wise profiles of the wing too, there was every reason to think that in this instance the x+150mm, h-300mm location for this wing was the best of the positions evaluated here, with its combination of peak downforce, efficiency and aerodynamic balance. Equally clear is that there would need to be a continuation of this exercise to better refine the wing's position, concentrating on locations close to x+150mm and h-300mm.

Having said that, there may well be applications where minimum drag is of more interest than maximum downforce or maximum efficiency, and the x+300mm location achieved the lowest drag across most of the wing height range. Assuming minimum drag with useful downforce and aerodynamic balance was the aim then the preferred low drag wing location might be x+300mm and h-300mm, this generating about 4% less drag than the x+150mm, h-300mm location. And addressing the slightly lower %front value this lower drag position achieved might involve a reduction in rear wing flap angle, which in turn would produce a further reduction in drag.

Interested readers may now be expecting a more specific definition of the optimum wing's location with respect to the rear bodywork of the racecar in this exercise! Well, apart from the model being far from optimised at this juncture, the optimum location on any other car is also sure to be dependent

on the exact shaping of the rear deck upper surfaces, the underbody and diffuser exit locations and shapes, and the rear wing's potency, profile(s) and plan-form shape. However, the  $x+150\text{mm}$ ,  $h-300\text{mm}$  location put the tip of the wing's leading edge, relative to the upper deck's trailing edge, at  $x+185\text{mm}$ ,  $y+145\text{mm}$ . This may or may not put you in the right ballpark with your sports racer!

At the favoured location the one parameter that was not what it would need to be was the aerodynamic balance. However, the trials were all conducted at zero rake and static ride height, and as both these parameters are means of addressing balance (and total downforce) a few changes to both were made, culminating in the results in the table below, which shows the comparison at zero rake and static ride height.

Condition: Zero rake, static ride height

Total Df, N: 3380.7

Drag, N: 825.0

-L/D: 4.10

front: 22.2%

Condition: 0.5deg rake, -10mm ride height

Total Df, N: 3805.8

Drag, N: 858.9

-L/D: 4.43

front: 36.3%

Not only did balance shift markedly forwards and well towards an ideal value but total downforce increased by 12.5% and -L/D by 8%. Separating out the sources of the forces, splitter downforce rose by 21.9%, body downforce by 15.9% and rear wing downforce increased by 0.9%. Of course the whole wing location exercise ought now to be repeated across a range of rakes and ride heights...

Above all, this exercise showed that it is most definitely worthwhile trying a matrix of wing locations on this type of racecar, because making the basic aerodynamic elements work together as effectively as possible in an integrated package can bear fruit.

One man who would definitely agree with this philosophy, and who has already implemented it in the development of what became a real world aerodynamic package, is Rennie Clayton at Dauntless Racing. Dauntless purchased the Stohr Cars business in summer 2014, and now owns all of the design and production rights to the WF1 sports racer and F1000 single seater

racecar lines. New cars are produced in their Bay Area, California facilities, and support for the existing ‘ecosystem’ of 120+ cars comes from there. Prior to that, although separate from and independent of Stohr Cars, Dauntless designed and produced their WF1 update kits.

Rennie Clayton takes up the tale: ‘The design work for the WF1 aero kit started in late 2007, and we always took a holistic approach to the design challenge. Eventually this culminated in three distinct updates to the WF1 which could be applied separately, but were designed from the start to work together for best effect: splitter, undertray, and rear wing. Of note, our basic constraint was that the core mechanical elements and body surfaces of the car were to be left largely intact, so we had to work around such things as radiator placement and orientation with the undertray, and assume that the top – fenders, cockpit surround, engine cover, etc. – were as delivered from the factory. Our pieces needed to be bolt-on, inasmuch as that could be achieved in a car like this.

We decided very quickly to design holistically for best overall effect rather than trying to focus on areas in succession. We didn’t want to be stuck in a position where we’d designed a mega rear wing, only to have our new front splitter not be capable of maintaining balance or worse, mucking up the flow to the rear of the car! So we designed it all at once and of course needed to isolate interaction effects as quickly as possible. Our solution to that was a DOE / factorial process with a rather large number of factors in the mix to achieve the best combination of overall downforce, overall drag, pitch sensitivity, and dynamic range of operation. No small challenge, that... it took the better part of a year to arrive at the proper combination of configurations and features.



*The Dauntless Stohr WF1 with fully integrated aerodynamics package including a low-mounted rear wing (Pepper Bone)*

'Our working hypothesis at the time was to try to treat the rear wing as the secondary element to the "wing" of the main body of the car; use the rear wing to activate the tunnels and front diffuser, rather than using the rear wing as a "trim" device for aero balance. In particular, we started from the classic NACA studies on optimum flap gap positioning and distances – this turned out to not be quite correct in our application, but very illuminating nonetheless. The airfoils (four sections, all told) and basic layout of the rear wing were guided by CFD and track testing of the car without a rear wing to gain a better understanding of airflow patterns over and around the car. That got us into the ballpark for orientation and local wind speed / turbulence factors for choosing airfoils. The exact placement was driven by more factorial experiments for height and setback from the trailing edge of the bodywork – one to establish interaction with the undertray / splitter, and another one to narrow down the precise placement. We could quite readily get better results for the rear wing in isolation by placing it up in clear airflow 300-400mm above the tail of the car, but this always had a negative effect on overall performance numbers for the car. Since our guiding principle was a holistic approach, optimising the car as a package won out.'

'CFD was followed by instrumented track testing, and we eventually managed to get a day in the Ford wind tunnel with a WF1 to test our rear wing assembly. As one might expect, the numbers did not match exactly with CFD, but the behavioural patterns were quite predictable and correlated nicely with the virtual work that we'd done on the car. Very gratifying!'

And so to the nub of the matter: how did the aerodynamic data alter between the earlier conventional wing location package and the new, low wing integrated package? Clayton was refreshingly open with some comparisons and hard data, commenting that 'the comparisons vary depending on downforce configuration.' See the table below for the key data.

Specification: 2007 spec factory WF1

Total downforce, N (lb), 100mph: ~2280 – 2380 (511 – 534)  
-L/D: ~3.2  
%front: 41%

Specification: Low Df Dauntless WF1

Total downforce, N (lb), 100mph: ~3170 – 3270 (710 – 733)  
-L/D: ~5.1

%front: 45%

Specification: High Df Dauntless WF1

Total downforce, N (lb), 100mph: ~3765 (844)

-L/D: ~4.9

%front: 44%

It's clear from these numbers that the Dauntless aero package represented a considerable advance over the 'pre-low wing' integrated package. And although it plainly isn't sensible to ascribe that entire advance to the low wing per se, it obviously played a large part in the integrated whole.

The last word then to Rennie Clayton: 'It should be noted that our raised splitter (to avoid pitch sensitivity) also creates knock-on effects for the undertray and rear wing – and the philosophy behind the undertray design plays into the airflow patterns around the car, in turn influencing how the rear wing behaves. We've found that there is no "one-size fits all" approach frankly because they can all be made to work to a reasonable degree. The question is: can you put them together in a beneficial way where all of the interactions reinforce each other positively?'

### A saloon car case study

This is another study from the MIRA archives, which looked at the wind tunnel programme they carried out for 2005 BTCC winners Team Dynamics prior to that winning season. Some years prior to this, when 'Super Touring' rules prevailed in the BTCC, one or two teams utilised front airdam/splitters that exposed the lower portion of the front tyres to view – and to the oncoming airflow. This seemed counter-intuitive; we know that exposed tyres/wheels cause drag and positive lift. However, Scibor-Rylski and Katz show us that on the forward, lower portion of exposed tyres there is a stagnation zone, where the static pressure is raised. So it's possible that the idea behind cutaway airdams was to allow the creation of a raised static pressure stagnation zone ahead of the exposed portion of the tyre, and to then 'tap' this with the splitter to gain an increment of front downforce. But would this not also expose the part of the tyres of a production car that creates lift? Furthermore if, as seems likely, straight-line track testing was used to evaluate this idea, then neither lift nor drag created by the exposed tyres themselves would have been captured by data acquisition sensors measuring suspension loads or deflections. This may have led to an exaggerated, if not completely erroneous, view of the effectiveness of this design...

However, a full-scale wind tunnel measures aerodynamic loads through the tyre contacts, and as such lift and drag generated by the tyres is measured. A full-scale wind tunnel is therefore a much better tool to evaluate such a cutaway airdam/splitter on a racecar. And as the pressure distribution on the lower, front face of an exposed tyre does not apparently alter significantly between rotating and non-rotating wheel cases, the fact that the wheels are stationary in MIRA should not have made too much difference here.



*The last of a set of airdam and splitter arrangements evaluated on the 2005 BTCC Honda.  
(MIRA)*

So MIRA and Team Dynamics set about a short programme of modifications to change the geometry of these cutaway sections, which were based on a design ‘inherited’ with the Honda Civics they ran in 2004, as follows. The baseline configuration (number 2) was with a flat splitter and an airdam cut away to the wheel centre height to reveal the outer portion of the front tyres. The three alternative configurations (numbers 1, 3 and 4) featured increasing height rising ramps on the outermost top surfaces of the splitter on each side. Then a short vertical fence was fitted to infill the gap between the top of the steepest ramp and the wheelarch (configuration 5). Next the ramps were removed completely and full-height vertical fences were installed between

the splitter and the wheelarches (configuration 6). And finally, the shallowest ramps were added in front of the vertical fence (configuration 7). This last configuration is shown in the photograph.

Figure 9-27 shows the percentage changes each configuration made to four aerodynamic parameters, compared to the baseline. For confidentiality reasons we cannot reveal actual forces, so to put some form of perspective on the absolute force magnitudes, drag was the largest force by some margin. And it is well known that the drag coefficients of small and medium production cars car are typically in the range 0.35 to 0.45. The sleek-looking coupé shape of the Honda Integra could reasonably be assumed to be in the lower reaches of that range. The measured changes to the drag coefficient amounted to a maximum increase of 4.8%, which with the frontal area involved adds up to a fairly significant force change on a moderate power racecar like this.

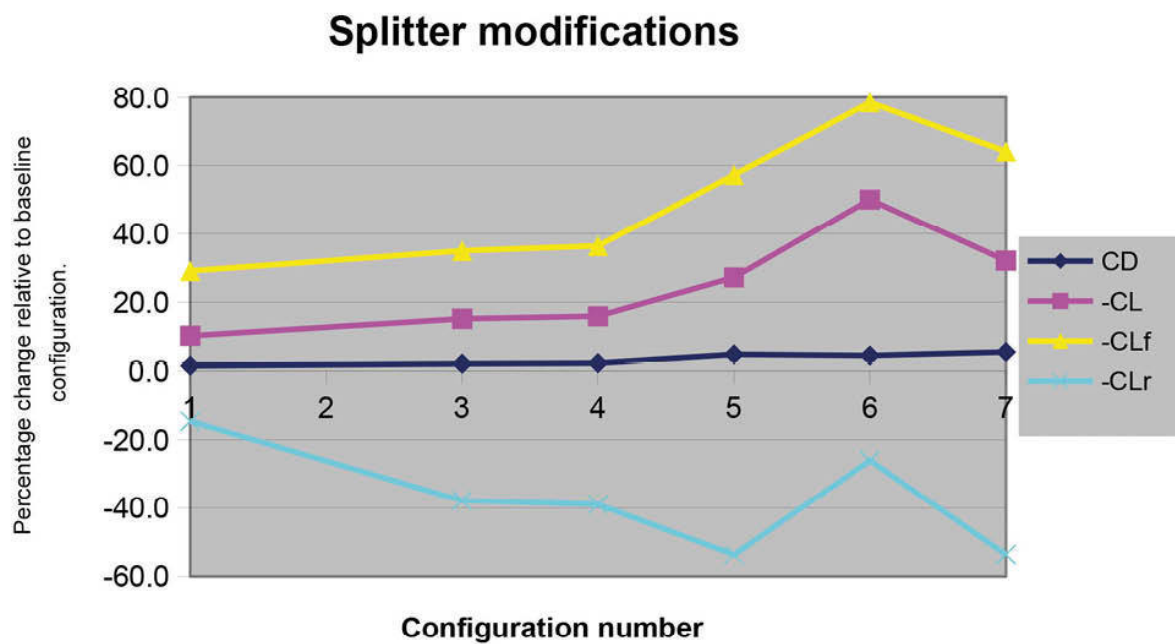


**Figure 9-27** The proportional changes to the coefficients arising from airdam and splitter modifications.

However, of greater significance were the changes to downforce, with incremental increases in the magnitude of the overall and front-end negative lift coefficients at each configuration change except the last one. The increasing ramp sizes generated increments of additional downforce at the front end, with the rear downforce, which was very modest to start with, also

declining at each step. The addition of the short vertical fence to the top of the steepest ramp (configuration 5) produced bigger changes.

But removing the ramps altogether and adding a full-height vertical fence between the splitter and the wheelarch (configuration 6), produced the largest gain in downforce – total downforce went up by 50.1%, with front downforce increasing by 78.5%. Rear downforce, of course, declined as the pitching moment arising from gains in a region with a large front overhang had its effect. But clearly there was more to this balance shift than just the pitching moment, because the decline in rear downforce in configuration 6 was much smaller than in all but the first change from the baseline configuration. Also interesting was the increase in drag in configuration 6, which, curiously, at 4.5% was smaller than the drag increase from configuration 5.

The final configuration showed further that the splitter ramps had a perhaps unexpected detrimental effect on efficiency. Adding small ramps again in front of the full-height vertical fences not only reduced downforce at front and rear but also increased drag. Oddly then, what looked like a device that might have made the vertical fences more efficient in fact had the opposite effect.

Conversely, vertical fences might have looked as if they would add drag for little benefit, and although there was an increase in drag, taking into account the downforce gain this was a very efficient configuration. The increase in downforce, presumably arising from a region of high static pressure ahead of the vertical fences that then acted on the upper surface of the splitter, was substantial. And unlike the high pressure that forms on the lower, front portion of the tyres, which has a positive lift component, the pressure on these fences has only a horizontal component, while the splitter taps the stagnation zone ahead of the fences to generate a negative lift (downforce) component.

## Zero downforce single-seaters

Not every category is allowed to use downforce-inducing bodywork and appendages, and it is instructive to take a look at a couple that specifically ban such things: Formula Ford and Formula Vee.

Formula Fords have become much sleeker-looking over the years, but do the aerodynamic numbers bear out the perception? Like its junior cousin Formula Vee, Formula Ford has been around a long time all around the world. And whereas wings and overt downforce-generating devices are similarly outlawed, FFords are patently sleeker despite being outwardly larger in terms of overall width than FVees. So let's take a look at the aerodynamic data derived in a session in the MIRA full-scale wind tunnel on the Spectrum FFord, manufactured by Australian-based Borland Racing Developments. The

car featured here was jointly provided by UK agent Mark Bailey Racing and Wiltshire College (Castle Combe), the latter being responsible for much of the trackside engineering on this particular car.

In ‘straight from the racetrack’ trim, the aerodynamic forces on the Spectrum were as shown in the table below, compared to baseline data of the Challenger FVee car evaluated in an earlier session, all calculated at 100mph (160km/h).

*The basic aerodynamic forces on the Spectrum FFord and Challenger FVee*

At 100mph: Spectrum FF

Drag, N: 526.7

Lift, N: 342.5

Front lift, N: 203.3

Rear lift, N: 139.2

% front: 59.4%

At 100mph: Challenger FVee

Drag, N: 698.5

Lift, N: 331.9

Front lift, N: 199.6

Rear lift, N: 132.3

% front: 60.1%



*The Spectrum Formula Ford.*



*The AHS Challenger Formula Vee.*



*Small, well ducted sidepods can help with effective cooling at little cost in drag. The rear of the Spectrum FF is also very sleek.*

So the wider track, seemingly larger FFord produced nearly 25% less drag than the FVee, but quite similar levels of lift front and rear, with a similar aerodynamic balance. The lesser drag of the FFord is evidently the result of sleeker shaping, not just of the body in general, but in terms of what connects the wheels to the chassis. FVees are compelled to run those aerodynamically disruptive front suspension beams, whereas FFords use slim-section wishbones and pushrods. Some FVees feature outboard rear spring damper units too, and this particular car also used bulky-looking outboard carburettors.

Another significant difference between the two car types is the method of cooling – the FVee engine is air-cooled whereas the FFord engine is water-cooled. The former is almost inevitably going to generate greater drag if it involves scooping air into the engine bay to wash over and interact with the requisite parts of the engine, before making its exit to the rear of the car. The latter can be done with ducts that feed air to fairly small heat exchangers. If well executed these duct arrangements can cause minimal drag, offsetting the apparent addition to frontal area from even small sidepods like the ones used in FFord, and exemplified by those on the Spectrum here.

It can be illuminating to calculate the drag in terms of the engine power required to overcome it, and this is easily done if the drag force at a given speed is known, using the approximation:

$$\text{BHP absorbed} = [\text{Drag force} \times 2 \times V]/1,500, \text{ with force in N and } V \text{ in m/s.}$$

Thus at 100mph (44.7m/s) the FFord absorbed 31.4bhp. The FVee absorbed 41.6bhp at 100mph, 10bhp more than the FFord when it already has a lot less available in the first place.

Meanwhile, what of the generation of positive lift on these cars, and its distribution? The exposed wheels and tyres of open-wheelers generate a fair proportion of the total lift, and we can see that the front generated more lift than the rear on these two cars, the rear wheels being in the wakes of the front wheels of course. But we have to be careful when taking data from non-rotating wheel measurements, such as currently generated in the MIRA wind tunnel. The textbooks tell us that the lift measured on a non-rotating wheel will be greater than that measured on a rotating wheel because the flow separates on a rotating wheel nearer to the top of the tyre, thereby lessening

the cumulative static pressure reduction over the whole of the top of the tyre. And the drag from rotating wheels would likewise be expected to be less than from non-rotating wheels, though generalising on the magnitude of these differences seems not to be possible.



*The air-cooled Formula Vee also suffers from other drag-creating mechanical protuberances.*

However, it is possible to better simulate the flow separation of rotating wheels in the wind tunnel using ‘trip strips’. Mention can be found in references of triangular wedge shapes attached to non-rotating tyres for this purpose, with the ‘peak’ of the wedge at about the ten o’clock position (where the flow comes from three o’clock). Equally effective are small right-angle strips – like Gurneys – that can be taped to the tyres in roughly the same location.

Trip strips were tried out on both the FVee and the FFord on the front tyres only to enable a quick look at the extent of the effect, and the results are shown in the tables below. The photographs show that without a trip strip on the FVee wheel, the flow still seems to be attached quite well around the rear face of the tyre, whereas with the trip strip on the FFord tyre, the flow has separated at the strip, and this is more akin to what happens with a rotating wheel.

*The effects of front-tyre trip strips on the Spectrum FFord*

FFord: Without trip strips

CD: 0.507

CL: 0.323

CLF: 0.218

CLR: 0.104

% front: 67.5%

FFord: With trip strips

CD: 0.502

CL: 0.299

CLF: 0.197

CLR: 0.102

% front: 65.9%

*The effects of front-tyre trip strips on the FVee*

FVee: Without trip strips

CD: 0.620

CL: 0.322

CLF: 0.233

CLR: 0.089

% front: 72.4%

FVee: With trip strips

CD: 0.621

CL: 0.302

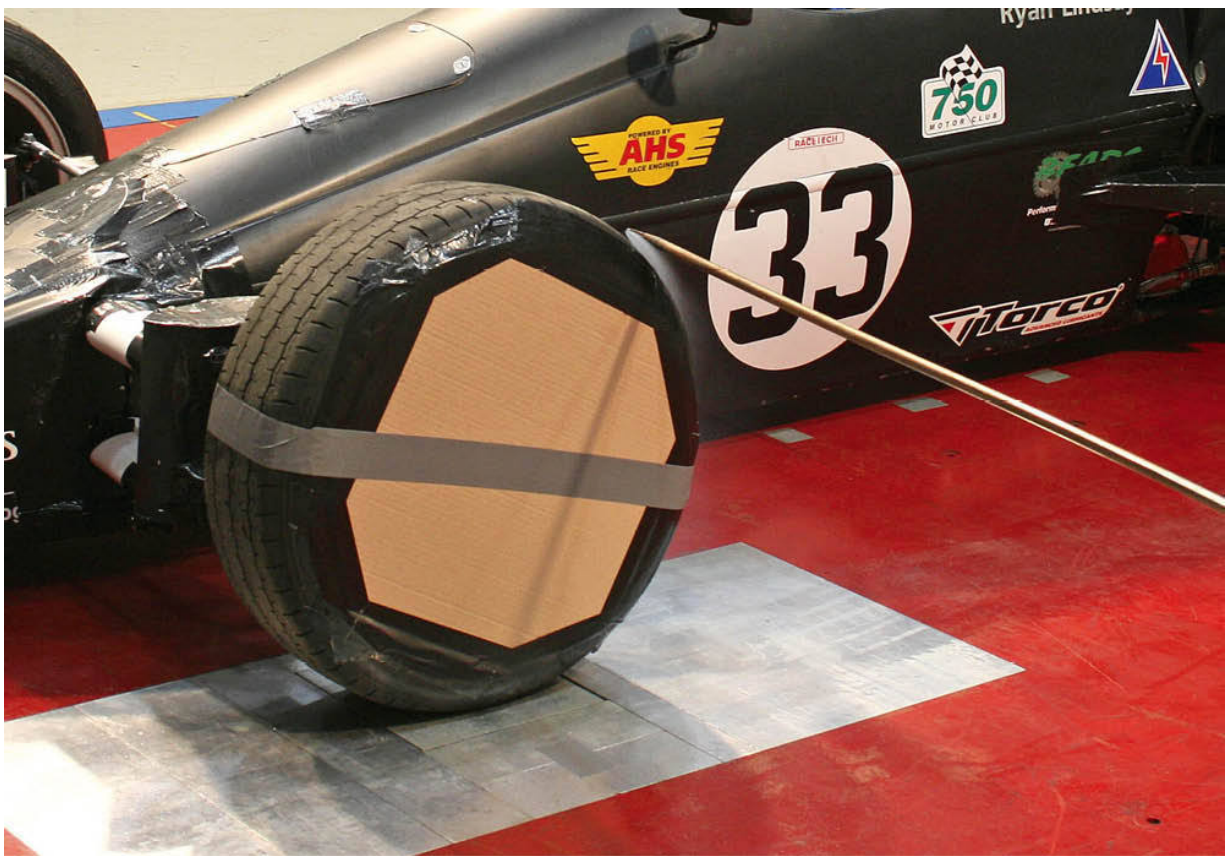
CLF: 0.219

CLR: 0.083

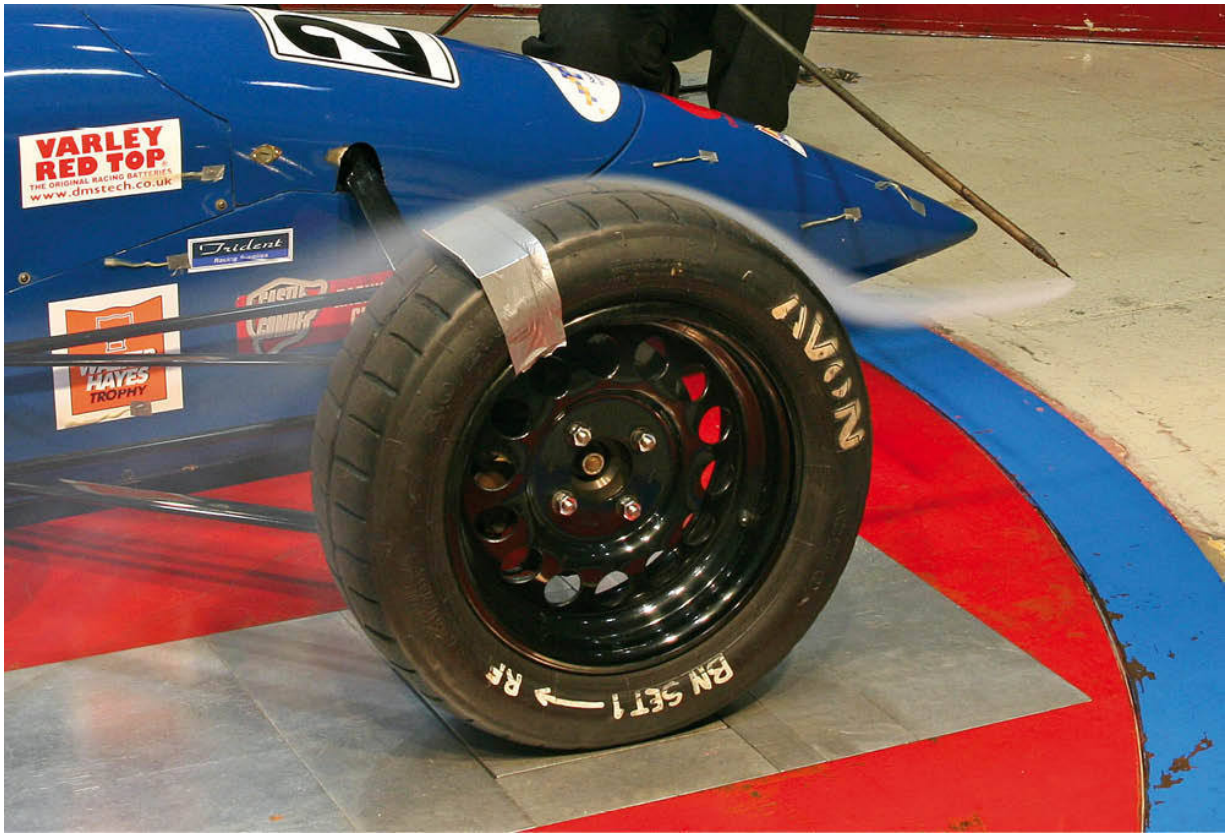
% front: 72.5%

Note that the configurations before these tests were not the same as those measured in the previous table, and that the frontal areas used to calculate the coefficients were rather approximate; hence the coefficients are also rather approximate. Nevertheless, the changes arising from the trip strips are meaningful. And it would appear that on these similar-sized wheels and tyres that drag was barely affected by the trip strips whereas lift was reduced by approximately similar amounts overall, by 20 to 24 ‘counts’ in fact, a reasonably significant proportion of the total lift. One difference between the cars is that the FFord saw a balance shift whereas the FVee did not.

But the main point here is that the lift values using non-rotating wheels should not be regarded as absolute on open-wheeled racecars.



*The flow stays attached well around the periphery of a non-rotating wheel.*



*A 'trip strip' causes the flow to separate roughly where it would if the wheel were rotating.*

## Superkarts

An important rung on the career ladder for drivers, karts are technically fascinating machines in their own right. So we decided to put a selection in the MIRA full-scale wind tunnel to see how they stacked up aerodynamically. Here we take a brief look at the baseline aerodynamic data of our test subjects and attempt to put that data into some kind of context.

Three karts were made available for this session: an Anderson 125 Open Superkart; an Anderson Division 1 250 Superkart; and a Raider Division 1 250 Superkart. The 125 Open karts feature, obviously, 125cc engines with six-speed sequential gearboxes and bodywork that excludes rear wings. The Division 1 250 Superkarts feature 250cc engines producing about 100bhp, and bodywork regulations that permit rear wings. Both categories feature flat underbodies and restricted diffusers, nose fairings with a radiused leading edge but not splitters, and sidepods or fully-enveloping side panels.

MIRA had tested superkarts in the past in the full-scale wind tunnel, and thus had the necessary adaptors available on which to mount the karts, with their narrow tracks and short wheelbases, to connect the tyre contact patches

to the in-floor load cells. A ‘false floor’ raised the floor level so it was flush with the top surface of the wheel pad adaptors. However, the very low ground clearance of the karts in this fixed-floor wind tunnel meant that caution would need to be applied to the results arising from altering the ground clearance.

Another practical issue was whether to use the usual MIRA dummy driver or the ‘real thing’. As it happened we had the three regular drivers of these karts available, and it was felt that repeatability would be better with real drivers, with what one might call their innate autonomous closed loop stability control, than with a dummy that was liable to move about because of buffeting at speeds up to 80mph. So, suitably briefed on keeping as still as possible during runs, the drivers got to experience live wind tunnel testing. Interestingly the comment was made that this put more strain on the neck muscles than is ordinarily felt out on track at considerably higher speeds, perhaps because there are more distractions when racing than when just sitting still for minutes at a time!

So, without further ado, let’s take a look at the baseline data from each of the karts ‘as delivered’ in the table below.

#### Baseline aerodynamic coefficients of the three karts

##### Anderson Open 125

CD: 0.409

CL: 0.035

CL front: 0.031

CL rear: 0.004

% front: 88.6%

L/D: 0.086

##### Anderson Div 1 250

CD: 0.479

CL: -0.330

CL front: -0.010

CL rear: -0.320

% front: 2.9%

L/D: 0.689

##### Raider Div 1 250

CD: 0.475

CL: -0.177

CL front: 0.069

CL rear: -0.246

% front: -39.0%

L/D: 0.373

Taking the 125 Open kart first, a drag coefficient of 0.409 is lower than the wingless single-seaters we have tested in the MIRA tunnel, and no doubt the faired-in wheels help in this regard. It was also virtually neutral in terms of aerodynamic lift too, that 0.031 front lift coefficient amounting to 22N (2.2kg or 4.9lb) of lift at 100mph.



*Ben Willshire in his Anderson 125 Open Superkart.*

On the Division 1 Anderson kart the drag was some 70 counts (17%) higher than the wingless 125 Open kart, and rear downforce was up by some 300 or so counts (where one ‘count’ = 0.001 on a coefficient). Some of the extra drag will have come from the rear wing, but the 250 kart also featured an exposed exhaust and large rear oil cooler. Offsetting that was the slightly taller driver in the 125 Anderson kart. But it looks as though the rear wing was pretty efficient. Removing the rear wing from the Raider 250, with constant driver size of course, saw 88 counts of drag reduction and 375 counts of rear downforce reduction.

So the wingless kart generated a small amount of lift, and the winged karts generated significant rear-biased downforce in these initial configurations. But

how significant were these levels of lift and downforce? There are two ways in which we can put the data into comparative context: by comparing the data with other cars; and by comparing the forces with the weights of the cars in question.

In the table below are aerodynamic data from a small range of racecars tested at MIRA. As well as giving the CD and CL values, the more useful CD.A and CL.A values are also quoted, where A is the frontal area. CD.A and CL.A are directly proportional to the actual measured forces of course, as given by the basic drag and lift equations.

*Aerodynamic comparisons between a small range of racecars*

2005 BTCC

CD: 0.35 to 0.43  
CD.A: 0.74 to 0.90  
CL: -0.15 to -0.23  
CL.A: -0.32 to -0.48

Formula Ford

CD: 0.507 to 0.536  
CD.A: 0.406 to 0.429  
CL: 0.309 to 0.366  
CL.A: 0.247 to 0.293

LMP3

CD: 0.529 to 0.636  
CD.A: 0.741 to 0.890  
CL: -1.318 to -1.667  
CL.A: -1.845 to -2.334

125 Open kart

CD: 0.400 to 0.417  
CD.A: 0.240 to 0.250  
CL: -0.021 to 0.047  
CL.A: -0.013 to 0.028

250 Div 1 kart

CD: 0.470 to 0.516  
CD.A: 0.282 to 0.310  
CL: -0.330 to -0.432  
CL.A: -0.198 to -0.259

We can now see that because of the small size of the karts, their CD.A and CL.A values are relatively small compared to the other cars in this table. This is not at all surprising – the smaller frontal area helps create less drag force, and by virtue of their small plan areas they have smaller surfaces with which to generate downforce. So another way to evaluate how significant the aerodynamic forces are, and especially lift or downforce, is to relate it to the vehicle's static weight, which is what the table below does.

*Downforce (or lift) at 100mph related to vehicle weight*

2005 BTCC

Weight, kg: 1,150

Downforce, kg: 38.9 to 61.9

Downforce/weight: 3.4% to 5.4%

LMP3

Weight, kg: 605

Downforce, kg: 230.2 to 291.1

Downforce/weight: 38.0% to 48.1%

Formula Ford

Weight, kg: 510

Downforce, kg: 30.8 to 36.6 *lift*

Downforce/weight: 6.0% to 7.2% *lift*

250 Div 1 kart

Weight, kg: 224

Downforce, kg: 24.7 to 32.3

Downforce/weight: 11.0% to 14.4%

125 Open kart

Weight, kg: 191

Downforce, kg: 1.6 (Df) to 3.5 (lift)

Downforce/weight: 0.8% (Df) to 1.8% (lift)



*The Anderson Division 1 250 Superkart of European Champion Gavin Bennett.*



*The Raider Division 1 250 Superkart with owner/driver/constructor Phil Featherstone aboard.*

In crude terms, the percentage of downforce over weight is the same as the extra grip obtained by virtue of that downforce at the speed at which the calculation was done. So we can see that the 2005 BTCC car would have gained between 3.4% and 5.4% extra grip from the downforce generated at 100mph, depending on the configuration used, and even seemingly modest percentages like this translate into tenths in lap time.

Looking at the numbers for the 125 Open kart then, although the forces measured in the wind tunnel were quite small, there is still a 2.6% spread in potential grip at 100mph from a configuration that generated a little bit of downforce compared to one that generated a little bit of lift. This perhaps puts these small forces into better perspective. For the 250 Division 1 karts there is no question that, relative to their weight, the downforce potential is very definitely significant.

# Chapter 10

## Final thoughts

WE HAVE SPENT quite a while looking at aerodynamics and the effects of airflow on competition cars, and what devices are used in various competition categories in order to exploit the forces involved. So, by now, you may well have designed some new, improved (you hope) aerodynamic parts, and maybe even made them and fitted them to your competition car. Before rushing into that first race, or run, or stage, whatever it might be in your chosen branch of the sport, think about spending some time testing, if at all possible. This will enable you to compile a database of reference settings that you can use wherever you compete, whether you've been to the venue before or not, and whatever weather and track conditions you encounter. It will not be possible to get the set-up for a given course right first time, every time, but if you take the trouble to establish a table of settings, from low downforce to high downforce, which you know gives you a balanced set-up, you will be one step nearer to doing better than your competitors who haven't bothered. The assumption here is that your aerodynamic aids are adjustable, and that the chassis can deal with the downforce you have decided to put on it.

### A balancing act

Perhaps one of the most sensible things you can try to do is to separate the mechanical balance of your car from the aerodynamic balance. It is a regular cause of surprise how many people try to overcome a mechanical chassis imbalance by making an aerodynamic change, or vice versa. This doesn't necessarily refer to the upper echelons here, where the race engineering practices seem to be a law unto themselves. But, for example, there wouldn't seem to be any logical reason, in any category, for trying to cure a low-speed chassis imbalance by making aerodynamic changes. You might mask the effects of the imbalance at higher speeds, and this might give the illusion of a good set-up on a fast course. However, wouldn't it be better to have a chassis that was mechanically balanced first, *then* aerodynamically optimised as well? OK, life is never so simple or convenient that such a state of affairs is always

going to be possible, and there are, undoubtedly, branches of motorsport, and particular venues and occasions when it is advantageous to have a car that, say, oversteers at low speed, but is neutral at high speed, and this might well constitute a ‘good set-up’. For the sake of compiling a set of aerodynamic data that can be called upon to cover different venues and conditions, and which enable a ballpark first guess at what will be needed, it is better to get the aerodynamically unaided chassis balanced first.

So how about starting that first or next test session with the downforce inducing appendages removed? This might be difficult in the case of an underbody on which the radiators and so forth are mounted, so this simplistic approach isn’t going to work for a lot of cars that rely heavily on underbody downforce. It will be effective for a lot of others though, so go on, take off the front and rear wings, and go and see if the chassis is balanced and if it isn’t, then fiddle with the springs, dampers, tyre pressures, suspension geometry and anti-roll bars until it is balanced. Hopefully, adjustments needed from venue to venue will be relatively minor after this exercise. Then, you have a baseline from which to start assembling aero data, because any changes you make now to the car’s balance at medium and high speed will be due to downforce adjustments.

With front and rear downforce aids now fitted, there are different ways in which you can approach the first test run. It depends on how confident you are about the probable balance that the wings, or spoilers, are going to give you, but a ‘safe’ starting point is one which will create a dynamically stable handling condition, which is to say, medium and high-speed understeer. Start by setting the front to ‘minimum downforce’, and the rear to whatever setting you believe will outperform the front. If this means putting the rear to ‘maximum downforce’, then do that. Now go out and try the car. If you encounter understeer, and hopefully you will in the faster corners, you can then back off the rear downforce until you get the car balanced. Once you have done this, you have established your minimum downforce and the aerodynamically balanced setting. Should the understeer still be present with the rear wing or spoiler at its minimum setting, then you will need to increase the front downforce setting until the understeer is eradicated. If you are timing your laps or runs, and it would be much more valuable if you did, keep the times in your records too. If you are logging data, then to an extent the data logging system will record most of what’s required, but you will probably need to add notes and times to these records.

Now you can increase the rear wing or spoiler, run the car to sense the understeer again, and then adjust the front until the car is once again balanced.

This provides you with another point of balance which is giving more downforce than the first set-up. Keep reiterating this process until you reach the maximum rear downforce setting you can practically achieve so that you will then have your reference table of balanced settings from minimum to maximum downforce, and a set of times to enable you to assess which is the quickest set-up for the test venue at least. This will give you a good idea of the level of downforce that will be needed at other tracks you go to. If you have been able to do some data logging as well, even better, because you will be able to study the changes in cornering and straight line speeds, and compare segment and lap/run times. Many people get hung up on achieving the highest top speed they can. The aerodynamic set-up that achieves this will rarely coincide with that which achieves the best lap time, as those who ‘discovered’ downforce proved. It depends on the competition category and venue of course, but while attaining a higher top speed than your competitors might boost your ego, it probably won’t boost your finishing position.

This is a pretty simplistic, not to say time-consuming approach to aerodynamic tuning, which also puts wear and tear on the car, but the information compiled in this way will avoid the need for guesswork later. This can be particularly useful when, say, you come back to the same track that you tested on, but it’s raining and you want to put on all the downforce you can. All you have to do now is look up the relevant front wing or spoiler setting that balances the maximum rear setting, set it, and you’ve saved precious practice time, which can now be used for learning the track in the wet, instead of searching for a balance. In reality there isn’t always time to separate mechanical from aerodynamic balance tuning, but hopefully it will be possible to isolate the effect of each if the test venue has low and higher speed corners in which to analyse mechanical and aerodynamic performance.

Of course this is a very basic approach to the complex topic of aerodynamic balance. We have seen how downforce and balance can be markedly affected by changes in car attitude in yaw, and especially with pitch (rake change), and also with ride height. But we have only examined those parameters in the ‘static’ sense in our CFD and wind tunnel studies whereas vehicle attitude out on track is, in reality, transient and alters constantly with dynamic changes in mechanical and aerodynamic loads. Add to that the transient nature of airflow around our competition cars. All the simulations and wind tunnel data in this book have been taken using ‘time averaged’ data sampling methods, and yet the reality is that flows are also unsteady, even around a stationary vehicle... Hence, aerodynamic balance can – and will – change every time a competition

car alters speed and goes from straight running, to braking, to cornering and to accelerating again. Finding the best compromise set-up is very challenging!

## **Research and development**

There are two reasons why you might want to try out new ideas on your competition car – one is natural curiosity, and the other is that you perceive the need to improve. Both are entirely valid justifications for experimenting, and it is only by actually doing so that you will find out what works and what does not work on your particular car. You *can* rely on others with the same model of car trying things out first, and you can then copy their successes and ignore their failures, but this won't ever get you in *front* – following never does. The only way to get ahead is to find that elusive 'unfair advantage', which means thinking about what might work, making it and trying it. On the other hand, don't ever burn your bridges, or be too proud to revert to your old set-up if things don't work out – there are far more blind alleys than yellow brick roads in motorsport! Remember too, that 'it is good to talk'. Discussing ideas is one of the best-known ways for expanding your knowledge.

## **In conclusion**

Hopefully, this book has pooled sufficient information and ideas, based as it is on the experience of the engineers, academics and fellow competitors who have helped in its compilation, to be of some value to anyone with an interest in motorsport, but especially to those who, like the author, are interested in how you can 'work the wind' to help you go faster! Above all though, I hope it is now evident that it is very difficult to generalise on a great many aspects of competition car aerodynamics. What works on one car may not work on another, apparently similar car. Trial and error are essential parts of the development process, at any level of the sport. So if, having read this book, you discover something that makes you go quicker, then that's great. If however, you go slower, don't blame me. Just say: 'That's motorsport', and try something else! Good luck.

# Appendix 1

## MIRA wind-tunnel test data

Data from some of the competition cars tested in the MIRA full-scale wind tunnel for the Aerobytes series in Racecar Engineering magazine are listed below. The data have been given as the product of the relevant coefficients multiplied by the frontal area, since this is directly proportional to the actual forces at any given speed, and the force equations may therefore be used to work out the range of forces at any chosen speed. Using CD.A and CL.A values also eliminates the need to incorporate the sometimes rather approximate estimates of frontal area that were used to calculate the coefficients from the measured forces.

The data have been arranged in order of increasing peak downforce, starting with those that generated positive lift.

Car: AHS Challenger

Category: Formula Vee

CD.A: 0.54 to 0.58

CL.A: +0.26 to +0.31

Car: Spectrum

Category: Formula Ford

CD.A: 0.40 to 0.45

CL.A: +0.24 to +0.30

Car: Classic Mini

Category: UK Hillclimb

CD.A: 0.78 to 0.84

CL.A: -0.04 to +0.30

Car: Anderson 125

Category: 125 Open Kart

CD.A: 0.24 to 0.25

CL.A: -0.01 to +0.03

Car: Anderson 250

Category: 250 Div 1 Kart

CD.A: 0.28 to 0.31

CL.A: -0.20 to -0.26

Car: 2005 Honda Integra

Category: BTCC

CD.A: 0.74 to 0.90

CL.A: -0.32 to -0.48

Car: 2010 Honda Civic Type R

Category: BTCC

CD.A: 0.71 to 0.94

CL.A: -0.48 to -0.71

Car: Noble M400

Category: Britcar

CD.A: 0.94 to 0.97

CL.A: -0.94 to -1.03

Car: Lotus Exige S2

Category: Britcar etc

CD.A: 0.87 to 0.97

CL.A: -0.92 to -1.22

Car: Ford Taurus

Category: SCSA (European Late Model)

CD.A: 0.92 to 1.10

CL.A: -0.95 to -1.23

Car: Porsche 997

Category: ALMS GT2 (plus...)

CD.A: 0.72 to 0.86

CL.A: -0.97 to -1.35

Car: ADR3

Category: Bikesports/CN

CD.A: 0.65 to 0.87

CL.A: -1.04 to -1.52

Car: Tiga A (formerly Chiron)

Category: CN

CD.A: 0.74 to 0.81

CL.A: -1.32 to -1.67

Car: Arachnid

Category: Bikesports

CD.A: 0.57 to 0.75

CL.A: -1.15 to -1.78

Car: Ferrari F430 Scuderia

Category: GT3

CD.A: 0.97 to 1.13

CL.A: -1.53 to -1.81  
Car: Subaru Impreza  
Category: Time Attack Pro (2013)  
CD.A: 1.38 to 1.62  
CL.A: -1.59 to -1.85  
Car: Dallara F308 (2011 spec)  
Category: Formula 3  
CD.A: 0.66 to 0.80  
CL.A: -1.32 to -1.92  
Car: Uni. Of Hertfordshire UH16  
Category: Formula Student (2013)  
CD.A: 0.66 to 1.29  
CL.A: +0.16 to -2.00\*  
Car: Dallara F312 (2012 spec)  
Category: Formula 3  
CD.A: 0.64 to 0.80  
CL.A: -1.42 to -2.09  
Car: Force LM  
Category: UK Hillclimb Sports Libre  
CD.A: 0.91 to 1.08  
CL.A: -1.65 to -2.17  
Car: Tiga B (formerly WFR)  
Category: CN  
CD.A: 0.71 to 0.88  
CL.A: -1.77 to -2.20  
Car: Lotus Exige  
Category: Time Attack Pro class (2013)  
CD.A: 0.78 to 1.30  
CL.A: -1.08 to -2.42  
Car: Ligier JS49  
Category: CN  
CD.A: 0.74 to 0.90  
CL.A: -1.86 to -2.42  
Car: Mannic sports libre  
Category: UK Hillclimb Sports Libre  
CD.A: 0.99 to 1.38  
CL.A: -2.10 to -2.59  
Car: Benetton B198  
Category: BOSS Formula

CD.A: 1.18 to 1.26

CL.A: -2.32 to -2.70

Car: Honda RA107

Category: Formula 1, 2007

CD.A: 1.12 to 1.28

CL.A: -1.86 to -2.70

Car: DJ Firestorm

Category: UK Hillclimb Racing

CD.A: 1.02 to 1.29

CL.A: -1.95 to -2.85

Car: Radical SR10

Category: LMP1

CD.A: 1.01 to 1.13

CL.A: -2.14 to -3.08

Car: Uni. Of Bath TBR14

Category: Formula Student (2014)

CD.A: 0.96 to 1.70

CL.A: -1.48 to -3.09

Car: Zytek Z11 SN Nissan

Category: LMP2

CD.A: 0.99 to 1.13

CL.A: -3.08 to -3.44

Car: Jaguar XJR-16

Category: Group C / IMSA GTP

CD.A: 1.39 to 1.62

CL.A: -5.00 to -5.88

\*Note: Included testing without wings, hence positive CL.A lower limit.

## Appendix 2

# Some wing profile suggestions

Just where *do* you start if you want to make a wing of your own? Disregarding the manufacturing aspects, such as whether sheet metal or fibre reinforced moulded construction is best for your needs, finding a suitable profile is not always easy. There are a couple of references in Appendix 5 that will provide a whole range of profiles to choose from. They are essentially aeronautical references, but at least the profiles and their ordinates are published. Most racecar wing manufacturers jealously guard their designs, and the author speaks as one of them! However, having obtained an aeronautical profile, a) it will do a pretty good job, b) you can always hire some CFD time to optimise the profile's characteristics for your application, and c) you can apply changes to it in a way that will be briefly described here.

First, let's check out a couple of aeronautical profiles that might be worth considering. In Chapter 5 we concluded that for low drag applications we would probably pick a section thickness of around 14% to 16% with camber of 4% to 6%, and for higher downforce we might go for, say, 18% thickness and quite probably more than 6% camber. Looking in the listings in Martin Simons excellent book *Model Aircraft Aerodynamics*, the Wortman FX 63-137 profile has approximately 14% thickness and 6% camber, so that might do as a low downforce wing to run at low angles. The NACA 63(3)-618 has 18% thickness and just over 3% camber which might make a reasonable higher downforce wing, and perhaps one that could be supplemented with a flap or two for greater downforce.

Here are the wing ordinates for these two profiles, starting at the trailing edge, but the zero point (origin) is at the leading edge. Both profiles are given as if their chord dimension were 100 units long. To scale to any other chord dimension, multiply by your proposed chord (ie if you want to draw a 250mm chord wing, multiply the ordinates by 2.5).

Other useful sources of wing profiles can be found on the Internet, and specifically in some of the aerofoil simulation packages to be found there. Some basic ones can be used at no cost, more advanced ones must be

purchased. And while they generally also appear to concentrate on two-dimensional aeronautical profiles, some show simulated flows and allow limited interactive manipulation of fundamental parameters such as thickness and camber, while displaying the changes to forces or coefficients. And very usefully, ordinates of the shape you decide upon can be plotted and used for manufacturing your own wing. See the references list in Appendix 5 for a small selection of websites offering these facilities.

*Wortman FX 63-137*

X: 1.000, Y: 0.000  
X: 99.893, Y: 0.082  
X: 99.572, Y: 0.249  
X: 99.039, Y: 0.501  
X: 98.296, Y: 0.818  
X: 97.347, Y: 1.189  
X: 96.194, Y: 1.601  
X: 94.844, Y: 2.043  
X: 93.301, Y: 2.516  
X: 91.573, Y: 3.018  
X: 89.668, Y: 3.553  
X: 87.592, Y: 4.114  
X: 85.355, Y: 4.711  
X: 82.967, Y: 5.323  
X: 80.438, Y: 5.962  
X: 77.779, Y: 6.605  
X: 75.000, Y: 7.273  
X: 72.114, Y: 7.927  
X: 69.134, Y: 8.590  
X: 66.072, Y: 9.204  
X: 62.941, Y: 9.804  
X: 56.526, Y: 10.823  
X: 53.270, Y: 11.221  
X: 50.000, Y: 11.578  
X: 46.730, Y: 11.833  
X: 43.474, Y: 12.042  
X: 40.245, Y: 12.137  
X: 37.059, Y: 12.191  
X: 33.928, Y: 12.128

X: 30.866, Y: 12.024  
X: 27.886, Y: 11.792  
X: 25.000, Y: 11.522  
X: 22.221, Y: 11.122  
X: 19.562, Y: 10.704  
X: 17.033, Y: 10.165  
X: 14.645, Y: 9.622  
X: 12.408, Y: 8.961  
X: 10.332, Y: 8.313  
X: 8.472, Y: 7.555  
X: 6.699, Y: 6.836  
X: 5.156, Y: 6.005  
X: 3.806, Y: 5.248  
X: 2.653, Y: 4.480  
X: 1.704, Y: 3.625  
X: 0.961, Y: 2.740  
X: 0.428, Y: 1.750  
X: 0.107, Y: 0.900  
X: 0.000, Y: 0.000  
X: 0.107, Y: -0.232  
X: 0.428, Y: -0.566  
X: 0.961, Y: -0.995  
X: 1.704, Y: -1.254  
X: 2.653, Y: -1.537  
X: 3.806, Y: -1.698  
X: 5.156, Y: -1.887  
X: 6.699, Y: -1.992  
X: 8.427, Y: -2.122  
X: 10.332, Y: -2.180  
X: 12.408, Y: -2.256  
X: 14.645, Y: -2.263  
X: 17.033, Y: -2.277  
X: 19.562, Y: -2.220  
X: 22.221, Y: -2.161  
X: 25.000, Y: -2.034  
X: 27.886, Y: -1.895  
X: 30.866, Y: -1.688  
X: 33.928, Y: -1.460  
X: 37.059, Y: -1.167

X: 40.245, Y: -0.848  
X: 43.474, Y: -0.486  
X: 46.730, Y: -0.103  
X: 50.000, Y: 0.307  
X: 53.270, Y: 0.716  
X: 56.526, Y: 1.112  
X: 59.755, Y: 1.475  
X: 62.941, Y: 1.813  
X: 66.072, Y: 2.098  
X: 69.134, Y: 2.345  
X: 72.114, Y: 2.530  
X: 75.000, Y: 2.668  
X: 77.779, Y: 2.745  
X: 80.438, Y: 2.768  
X: 82.967, Y: 2.729  
X: 85.355, Y: 2.631  
X: 87.592, Y: 2.479  
X: 89.668, Y: 2.284  
X: 91.573, Y: 2.052  
X: 93.301, Y: 1.794  
X: 94.844, Y: 1.514  
X: 96.194, Y: 1.219  
X: 97.347, Y: 0.921  
X: 98.296, Y: 0.630  
X: 99.039, Y: 0.373  
X: 99.572, Y: 0.169  
X: 99.893, Y: 0.040  
X: 100.000, Y: 0.000

*NACA 63(3)-618*

X: 100.000, Y: 0.000  
X: 94.952, Y: 0.603  
X: 89.897, Y: 0.571  
X: 79.897, Y: -0.297  
X: 69.813, Y: -1.702  
X: 59.875, Y: -3.241  
X: 50.000, Y: -4.633  
X: 45.081, Y: -5.197

X: 40.171, Y: -5.630  
X: 35.266, Y: -5.906  
X: 30.360, Y: -5.990  
X: 25.451, Y: -5.903  
X: 20.531, Y: -5.642  
X: 15.596, Y: -5.181  
X: 10.633, Y: -4.484  
X: 8.132, Y: -3.998  
X: 5.607, Y: -3.372  
X: 3.035, Y: -2.500  
X: 1.703, Y: -1.849  
X: 1.139, Y: -1.458  
X: 0.844, Y: -1.211  
X: 0.000, Y: 0.000  
X: 0.156, Y: 1.511  
X: 0.361, Y: 1.878  
X: 0.797, Y: 2.491  
X: 1.965, Y: 3.616  
X: 4.393, Y: 5.268  
X: 6.868, Y: 6.542  
X: 9.367, Y: 7.586  
X: 14.404, Y: 9.219  
X: 19.469, Y: 10.418  
X: 24.549, Y: 11.273  
X: 29.640, Y: 11.822  
X: 34.734, Y: 12.086  
X: 39.829, Y: 12.056  
X: 44.919, Y: 11.767  
X: 50.000, Y: 11.251  
X: 60.125, Y: 9.667  
X: 70.187, Y: 7.534  
X: 80.178, Y: 5.073  
X: 90.103, Y: 2.531  
X: 95.048, Y: 1.293  
X: 100.000, Y: 0.000

These ordinates can be drawn out on graph paper, scaled appropriately, and joined with smooth curves. They can also be entered in a spreadsheet and then graphed into an x-y scatter plot with smoothed curve fitting, the x and y scales

set to the same values. With some fiddling you could plot or photo enlarge the profiles to your desired chord dimension, or they can be entered into a suitable drawing or CAD package, again using an appropriate smooth curve, such as a spline curve, to fit between the points. The drawings shown here were done in Autosketch®, the ‘cut down’ version of Autocad®, with which you can do 2D draughting.

Clearly, these ordinates create a shape with an infinitely thin trailing edge – not a very practical notion. The fact is the trailing edge is going to end up at around 1.5mm to 2mm (0.06 to 0.08in) thick whether a wing is made from sheet metal or it is moulded. It may even be structurally desirable to make it thicker than this, although thin is nice, aerodynamically speaking. In this respect therefore, it isn’t possible to exactly match the profile dictated by the numbers here.

To graphically ‘morph’ these, or any wing profiles to a different camber, try this method. Draw the camber line on your profile, and then draw circles that just fit the profile, centred on the camber line. Now draw your new camber line, and translate the circles onto this new line. Then, draw new fitted curves tangential to the circumference of the circles (note that some ‘fiddling’ was needed in the example here to produce a smooth curve ...) to generate your new profile. There’s a reasonable chance the new profile will work satisfactorily if it’s based on a proven one, and providing the morphing isn’t taken too far.

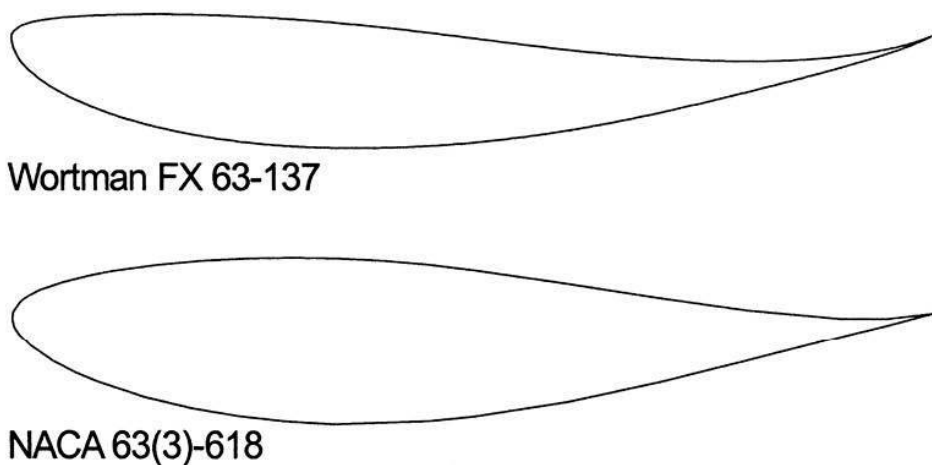


**Figure App2-1** Two potentially useful wing profiles.

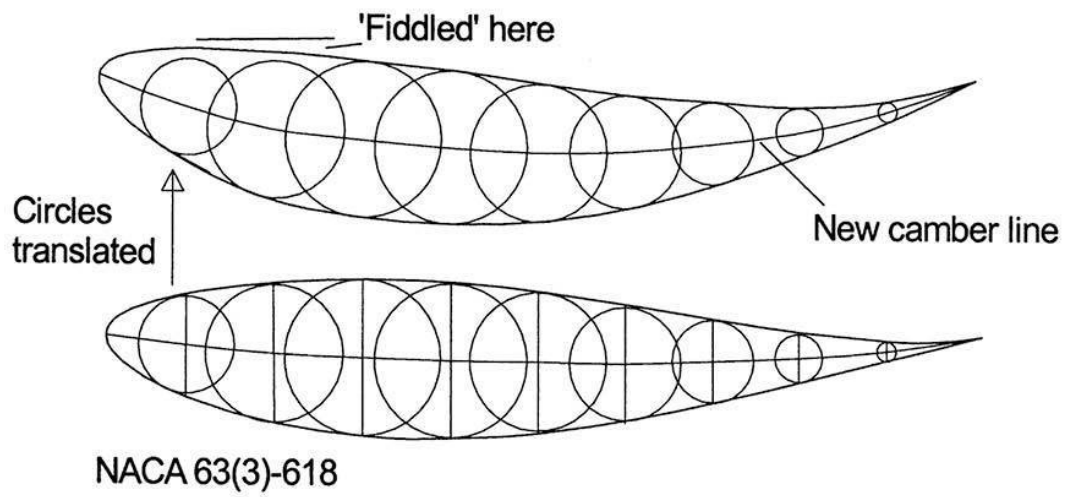


**Figure App2-2** Modifying an existing profile's camber curve to generate a new profile.

# Appendix 3

## Flow visualisation fluid

Using ‘flow visualisation fluid’ can help determine the local flow directions adjacent to body panel surfaces. A ‘recipe’ is given below.

- To 1 litre of paraffin or diesel oil add:
- Titanium dioxide powder; enough to make a thin slurry that’s in between paraffin and lubricating oil in consistency.
- Half a teaspoonful of fluorescein colour indicator (or other suitable pigment powder to contrast with the car or body panel colour).
- A few drops of oleic acid or linseed oil, which is high in oleic acid, to act as a ‘wetting agent’ to help the fluid flow on surfaces.

The above chemicals can be obtained from laboratory supplies companies.

A few small-scale trials will determine the ideal consistency, amount of colouring powder etc needed. Alternatively, paraffin with a few spots of copper grease added works OK too.

Small spray bottles or dropper bottles are useful for applying the fluid to the area of interest. Spray or spot the fluid on to the car immediately before setting off on a run and, if relevant, accelerate immediately up to the speed of interest. How long the fluid takes to dry depends on ambient temperature, so some experimentation is needed here too. Then simply examine and photograph the evidence.

# Appendix 4

## Commercially available full-scale wind tunnels

This is by no means a complete list, but these wind tunnels should be big enough or ‘smart’ enough to accept a full size racecar without undue ‘blockage’ of the test section by the car’s frontal area – see chapter 9.

Name (country): AeroDyn A1 (USA)

Test section area, m<sup>2</sup>: 21.0

Maximum speed, m/s: 209km/h

Remarks: Closed jet, contoured wall (option for slotted wall), boundary layer suction, rotating wheels. [www.aerodynwindtunnel.com](http://www.aerodynwindtunnel.com)

Name (country): DNW LLF (Germany/Netherlands)

Test section area, m<sup>2</sup>: 90.25 max, configurable

Maximum speed, m/s: 547km/h (depending on config)

Remarks: Closed or open jet configurations, various boundary layer controls including moving ground, tripping, blowing. [www.dnw.aero](http://www.dnw.aero)

Name (country): Langley FST (USA)

Test section area, m<sup>2</sup>: 167.0

Maximum speed, m/s: 130km/h

Remarks: 3/4 open jet, fixed ground, ‘ground board’ or ‘active secondary boundary layer control’ [www.lfst.com](http://www.lfst.com)

Name (country): Langley ‘14 x 22’ (USA)

Test section area, m<sup>2</sup>: 29.3

Maximum speed, m/s: 370km/h (270km/h in open jet config)

Remarks: Closed jet or 3/4 open jet, single belt moving ground in late 2008.

[www.lfst.com](http://www.lfst.com)

Name (country): Lockheed Martin (USA)

Test section area, m<sup>2</sup>: 35.1

Maximum speed, m/s: 321km/h

Remarks: Closed jet, fixed floor with tangential blowing boundary layer control. [www.lockheedmartin.com/aeronautics/windtunnel/index.html](http://www.lockheedmartin.com/aeronautics/windtunnel/index.html)

Name (country): MIRA FSWT (UK)

Test section area, m<sup>2</sup>: 35.0

Maximum speed, m/s: 133km/h

Remarks: Closed jet, fixed ground, boundary layer trip fence.

[www.mira.co.uk](http://www.mira.co.uk)

Name (country): Monash University (Australia)

Test section area, m<sup>2</sup>: 45.0 (open) 20.0 (closed)

Maximum speed, m/s: 180km/h

Remarks: Open or closed jet. [www.eng.monash.edu.au](http://www.eng.monash.edu.au)

Name (country): NRC (Canada)

Test section area, m<sup>2</sup>: 82.8

Maximum speed, m/s: 198km/h

Remarks: Closed jet, boundary layer removal by upstream suction, moving central ground belt plus wheel rollers. [www.nrc.ca/iar](http://www.nrc.ca/iar)

Name (country): Pininfarina (Italy)

Test section area, m<sup>2</sup>: 40.3

Maximum speed, m/s: 250km/h

Remarks: 3/4 open jet, moving ground ‘T-belt’ comprising long central belt plus short belts under front wheels. [www.arc.pininfarina.com](http://www.arc.pininfarina.com)

Name (country): SAA GIE S2A (France)

Test section area, m<sup>2</sup>: 24.0 at nozzle

Maximum speed, m/s: ‘>240km/h’

Remarks: 3/4 open jet, moving ground central belt plus driven wheels (max speed 200km/h). [www.gies2a.fr](http://www.gies2a.fr)

Name (country): Windshear (USA)

Test section area, m<sup>2</sup>: 16.7 at nozzle

Maximum speed, m/s: 289km/h

Remarks: 3/4 open jet, single belt moving ground; came on line during 2008. [www.windshearinc.com](http://www.windshearinc.com)

### **Commercially available scale model wind tunnels (not including many others at academic institutions around the world)**

Name (country): ACE (France)

Test section area, m<sup>2</sup>: 5.0

Maximum speed, m/s: 40

Remarks: Up to 60%, closed jet, yaw, pitch, roll, steer control, EOLE VIEW software. [www.aero-ce.com](http://www.aero-ce.com)

Name (country): ARC Indianapolis (USA)

Test section area, m<sup>2</sup>: 6.0

Maximum speed, m/s: 50

Remarks: 50%, open jet, 5-axis model control. [www.arcindy.com](http://www.arcindy.com)

Name (country): Aerolab (Italy)

Test section area, m<sup>2</sup>: 7.5

Maximum speed, m/s: 45

Remarks: 50%, closed jet, slotted wall, heave, pitch, yaw, roll control, variable wheel pre-load, own software. [www.fondmetal.com](http://www.fondmetal.com)

Name (country): BMT (UK)

Test section area, m<sup>2</sup>: 3.6

Maximum speed, m/s: 55

Remarks: 50%, closed jet, adaptive wall, height and pitch control.

[www.bmtfm.com](http://www.bmtfm.com)

Name (country): Carlin Advanced Technologies (UK)

Test section area, m<sup>2</sup>: 2.5

Maximum speed, m/s: 30

Remarks: 33%, closed jet. [www.carlin.co.uk](http://www.carlin.co.uk)

Name (country): Cranfield (UK)

Test section area, m<sup>2</sup>: 4.3

Maximum speed, m/s: 45

Remarks: 30–50%, closed jet, auto heave and pitch control automotive.

[www.cranfield.ac.uk/](http://www.cranfield.ac.uk/)

Name (country): Dallara (Italy)

Test section area, m<sup>2</sup>: 3.6

Maximum speed, m/s: 50

Remarks: 40–50%, closed jet, slotted wall, auto heave and pitch control.

[www.dallara.it](http://www.dallara.it)

Name (country): Dallara (Italy)

Test section area, m<sup>2</sup>: 7.5

Maximum speed, m/s: 67

Remarks: 50–60%, closed jet, slotted wall, 4-axis model control.

[www.dallara.it](http://www.dallara.it)

Name (country): DNW NWB tunnel (Germany)

Test section area, m<sup>2</sup>: 9.1

Maximum speed, m/s: 70–85

Remarks: Closed, slotted wall or open jet. [www.dnw.aero](http://www.dnw.aero)

Name (country): Dome (Japan)

Test section area, m<sup>2</sup>: 6.9

Maximum speed, m/s: 60

Remarks: 50%, closed jet, 3 axis plus heave control, auto data acquisition and processing. [www.dome.co.jp](http://www.dome.co.jp)

Name (country): Durham University (UK)

Test section area, m<sup>2</sup>: 2.0

Maximum speed, m/s: 30

Remarks: 40%, open jet, auto heave and pitch control. [www.dur.ac.uk](http://www.dur.ac.uk)

Name (country): Imperial College 'Honda' (UK)

Test section area, m<sup>2</sup>: 4.6

Maximum speed, m/s: 40

Remarks: 50%, closed jet, contoured wall, auto heave and pitch control, manual yaw and roll, auto data acquisition. [www3.imperial.ac.uk](http://www3.imperial.ac.uk)

Name (country): Lola (UK)

Test section area, m<sup>2</sup>: 6.7

Maximum speed, m/s: 65

Remarks: 50%, closed jet, pitch, heave, roll, yaw, own software.

[www.lolacars.com](http://www.lolacars.com)

Name (country): Monash University (Australia)

Test section area, m<sup>2</sup>: 4.0

Maximum speed, m/s: 50

Remarks: 50%, closed jet, yaw. [www.eng.monash.edu.au](http://www.eng.monash.edu.au)

Name (country): NRC (Canada)

Test section area, m<sup>2</sup>: 5.1

Maximum speed, m/s: 140

Remarks: 50% (?), closed jet, moving belt available, auto pitch and yaw; Labview and Aerotech software. [www.nrc.ca/iar](http://www.nrc.ca/iar)

Name (country): Oreste Berta (Argentina)

Test section area, m<sup>2</sup>: ?

Maximum speed, m/s: 40

Remarks: 25%. [www.oresteberta.com](http://www.oresteberta.com)

Name (country): RUAG (Switzerland)

Test section area, m<sup>2</sup>: 3.8

Maximum speed, m/s: 60

Remarks: 50%, 3/4 open jet, 5-axis auto model positioning. [www.ruag.com](http://www.ruag.com)

Name (country): Scott Flow (UK)

Test section area, m<sup>2</sup>: 5.4

Maximum speed, m/s: 60

Remarks: 50%, closed jet, yaw control. [www.eng.gla.ac.uk/sflow](http://www.eng.gla.ac.uk/sflow)

Name (country): Shrivenham (UK)

Test section area, m<sup>2</sup>: 3.9 (at nozzle)

Maximum speed, m/s: 50

Remarks: 50%, open jet. [www.cranfield.ac.uk/automotive](http://www.cranfield.ac.uk/automotive)

Name (country): Southampton University (UK)

Test section area, m<sup>2</sup>: 9.1

Maximum speed, m/s: 45

Remarks: 50%, closed jet, yaw, heave, pitch; Pi Mistral software.

[www.windtunnel.soton.ac.uk](http://www.windtunnel.soton.ac.uk)

Name (country): Swift Engineering (USA)

Test section area, m<sup>2</sup>: 6.7

Maximum speed, m/s: 62.6

Remarks: 40–50%, closed jet, auto pitch & heave, manual yaw, roll, steer; custom software by Random Computing. [www.swiftengineering.com](http://www.swiftengineering.com)

Name (country): Tokyo R&D, Japan

Test section area, m<sup>2</sup>: ?

Maximum speed, m/s: ?

Remarks: 25%, open jet

# Appendix 5

## References

\* Indicates books which catalogue wing profiles

- Abbott, I. H. and von Doenhof, A. J., *The Theory of Wing Sections\**, Dover, 1959
- Aird, F., *Aerodynamics for racing and performance cars*, HP Books, 1997
- Allen, J. E., *Aerodynamics. The Science of Air in Motion*, Allen Bros & Father, 1986 Ed
- Althaus, D. & Wortmann, F. X., *Stuttgarter Profilkatalog\**, Vieweg, 1981
- Anderson, J. D., *Fundamentals of Aerodynamics*, McGraw Hill, 1991
- Benzing, E., *Ali/Wings\**, Automobilia, 1991
- Campbell, C., *Design of Racing Sports Cars*, Chapman and Hill, 1976
- Cimarosti, A., *The Complete History of Grand Prix Motor Racing*, Guild, 1990
- Dymock, E., *The Guinness Guide to Grand Prix Motor Racing*, Guinness Superlatives, 1980
- Henry, A., *Brabham – The Grand Prix Cars*, Hazleton, 1985
- Henry, A., *Grand Prix Car Design and Technology in the 1980s*, Hazleton, 1988
- Herbert, P. & Harvey, D., *750 Racer*, Patrick Stephens, 1996
- Houghton, E. L. and Carpenter, P. W., *Aerodynamics for Engineering Students*, Edward Arnold, 4th Ed, 1993
- Howard, G., *Automobile Aerodynamics*, Osprey, 1986
- Hucho, W. H., *Aerodynamics of Road Vehicles*, Butterworth, 1987
- Katz, J., *Race Car Aerodynamics – Designing for Speed*, Bentley, 1995
- Kermode, A. C., (updated by Gunston, B.), *Flight without Formulae*, Harlow: Longman, 5th Ed, 1989
- Kermode, A. C., (revised and updated by Barnard, R. H. and Philpott, D. R.) *Mechanics of Flight*, Harlow: Longman, 10th Ed, 1996
- McCormick, B. W., *Aerodynamics, Aeronautics and Flight Mechanics*, Wiley, 1995
- Milliken, W. F. & Milliken, D. L., *Race Car Vehicle Dynamics*, SAE, 1995
- Muto, S., *Automotive Aerodynamics*, Kaneko Enterprises Inc (sole subscription agent), 2001
- Nye, D., *McLaren – The Grand Prix, CanAm and Indy Cars*, Hazleton, 1988
- Rudd, T., *It was Fun!*, Patrick Stephens, 1993
- Scibor-Rylski, A. J., *Road Vehicle Aerodynamics*, Osprey, 2nd Ed, 1984

Simons, M., *Model Aircraft Aerodynamics\**, Argus, 3rd Ed, 1989  
Smith, C., *Tune to Win*, Osprey, 1987  
Smith, C., *Engineer to Win*, Osprey, 1985  
Staniforth, A., *High Speed, Low Cost*, Patrick Stephens, 2nd Ed, 1973  
Staniforth, A., *Race & Rally Car Source Book*, Haynes, 2nd Ed, 1989  
Terry, L. & Baker, A., *Racing Car Design and Development*, Motor Racing Publications, 1973  
Tremayne, D., *The Science of Speed*, Haynes, 1997 & 2000  
Van Valkenburgh, P., *Race Car Engineering and Mechanics*, pub. by author, 2000  
Versteeg, H. K. & Malalasekera, W., *An introduction to Computational Fluid Dynamics – The finite volume method*, Prentice Hall, 1995  
Yeager, J. et al, *Voyager*, Knopf, 1986

## Websites

(A small selection to try. More thorough research should yield others)

[www.pdas.com/aerosoft.htm](http://www.pdas.com/aerosoft.htm) – Public Domain Aeronautical Software (PDAS).  
[www.aerologic.com](http://www.aerologic.com) – design and analysis of streamlined bodies  
[www.compufoil.com](http://www.compufoil.com) – airfoil design software  
[www.dreesecode.com](http://www.dreesecode.com) – DesignFOIL design and analysis of simple wings  
[www.grc.nasa.gov/WWW/k-12/airplane/foil3.html](http://www.grc.nasa.gov/WWW/k-12/airplane/foil3.html) – FoilSim II, version 1.5 now available, simplified 2D computational models allowing visualisation of the effects of parameter changes, and plotting of ordinates  
[www.tdmsoftware.com/afd](http://www.tdmsoftware.com/afd) – ‘Airfoil Design Workshop’  
[http://m-selig.ae.illinois.edu/ads/coord\\_database.html](http://m-selig.ae.illinois.edu/ads/coord_database.html) – a database with the coordinates of over 1,500 aerofoils collated by Professor Michael Selig and his UIUC Applied Aerodynamics Group at the University of Illinois at Urbana Champaign  
[www.grc.nasa.gov/WWW/K-12/airplane/bernnew.html](http://www.grc.nasa.gov/WWW/K-12/airplane/bernnew.html) – discussion on the theories of wing lift  
<http://www.grc.nasa.gov/WWW/K-12/airplane/index.html> – some really good comprehensible explanations of aerodynamics basics  
<http://web.mit.edu/drela/Public/web/xfoil/> – XFOIL is described as ‘an interactive program for the design and analysis of subsonic isolated airfoils’; it is released at no cost under the GNU General Public License  
<http://www.profil2.com/> – a relatively low cost software package to aid the design and manufacture of wing profiles.  
<http://www.aerospaceweb.org/question/planes/q0176.shtml> – a fascinating article on vortex enhanced lift creation, with reference to the phenomenon of

‘vortex bursting’

<http://www.avweb.com/news/reviews/182564-1.html> – a commercial site, but some thought-provoking material on the use of vortex generators on wings

[www.f1technical.net](http://www.f1technical.net) – Technical discussions on Formula 1 including aerodynamics

[www.mulsannescorner.com](http://www.mulsannescorner.com) – Technical discussions on Le Mans and related sports prototypes including aerodynamics

# Glossary of terms and abbreviations

Words in italics within definitions have their own entries in the glossary.

**Aerodynamics** The study of the interaction between air and solid bodies moving through it. In the context of this book, the ‘solid bodies’ are competition cars and their ancillary components.

**Aerodynamic force** The force created by a vehicle’s movement through the air. It is the combination of aerodynamic *drag* and aerodynamic *lift*.

**Aerofoil** Synonymous with ‘airfoil’, strictly speaking an aerofoil is the transverse cross-section of a *wing*, but in motorsport it is usually regarded as just another word for a wing.

**Airdam** A device to block off some of the airflow to a vehicle’s underside region.

**Angle of attack** The angle between an aerofoil’s *chord line* and the incident airflow.

**Anhedral** The angle between a wing’s span and the horizontal when the *wing* is inclined downwards from its mounting.

**Aspect ratio** The arithmetic ratio of the *span* dimension divided by the *chord* dimension.

**Attached flow** A regime in which the airflow follows the contours and surfaces of the body it is flowing around.

**Bargeboard** A generally vertical, curved plate positioned behind and between the front wheels of an open-wheeled competition car, whose purpose is to steer and control the airflow.

**Bernoulli’s Theorem (or Equation)** In essence, where an airflow accelerates, for example around a body, the *dynamic pressure* increases so the local *static pressure* decreases. Assuming there are no losses, the sum of the local dynamic pressure and static pressure will be constant, following the Conservation of Energy, which states that energy cannot be created or destroyed, just converted from one form to another (possibly reversibly).

**Boundary layer** A layer of static to slow moving air adjacent to the surfaces of a moving body. Friction between the body and the surrounding air holds back the flow nearest the surfaces, while the air further from the body in the *freestream* flows past at unabated speed.

**Camber** An aerofoil with one surface curved more than the other is said to have camber.

**Centre of pressure** The point at which the aerodynamic forces on a body appear to act, and at which there is no aerodynamic moment. It is analogous to the centre of gravity in mechanical terminology.

**Chord** The distance between an aerofoil's leading edge and its trailing edge.

**Chord line** A line joining the leading edge to the trailing edge.

**Computational fluid dynamics (CFD)** The use of computers to calculate complex fluid dynamic equations to solve theoretical flow problems around bodies.

**$C_D$**  Abbreviation for *drag coefficient*.

**$C_L$**  Abbreviation for *lift coefficient*.

**$C_P$**  Abbreviation for *pressure coefficient*.

**Data acquisition** Also known as data logging, the electronic sensing and recording of engine and chassis parameters to provide information on car and driver responses and behaviour.

**$\Delta$  ('delta')** The Greek letter 'delta', used to represent an incremental change in a parameter: for example,  $\Delta CP$  would be a change to a *pressure coefficient*.

**Density** The mass per unit volume of a substance. In the case of air, this book uses the convention that the density of air is 0.00238 pounds per cubic foot ( $\text{lb}/\text{ft}^3$ ) or 1.225 kilograms per cubic metre ( $\text{kg}/\text{m}^3$ ).

**Diffuser** The divergent section of a duct which slows down an airflow. On a competition car it is an upswept panel or panels at the rear of the *underbody*, or at the rear of *tunnels*.

**Dive plate, or dive plane** An inclined plate, usually attached to the front of a vehicle, to modify and adjust the airflow.

**Downforce** The opposite of aerodynamic *lift*, sometimes referred to as negative lift.

**Downwash** The part of the airflow turned downwards by an aerofoil. In the case of a downforce inducing aerofoil, the downwash occurs just in front of the aerofoil.

**Drag** That component of the *aerodynamic force* which is parallel to, but opposes the movement of a body through air. *Form drag*, *induced drag* and *skin friction drag* are all components of drag which can affect vehicles.

**Drag coefficient, or  $C_D$**  A 'dimensionless' value (one without units) that allows the comparison of drag incurred by different sized and different shaped bodies.

**Dynamic pressure** Dynamic pressure can be thought of as the kinetic energy or movement energy of a moving fluid, which in our context is air flowing

past a competition car. It is given by  $1/2\rho V^2$ , where  $\rho$  is the fluid density and  $V$  is the fluid (or body) velocity.

**End plate** Also sometimes known as a spill plate, a more or less flat and vertical sheet of rigid material attached to the ends of an aerofoil.

**FIA** The Federation International d'Automobile, the Paris-based ruling body of worldwide motorsport.

**Flap Part** of a multi-element aerofoil, set just above and behind the main element (on a racecar), for the purpose of supplementing aerodynamic downforce.

**Flow visualisation** General term for methods by which the airflow around a body is made visible.

**Fluid** Usually a gaseous or liquid substance which is capable of flowing. Air is a fluid under normal conditions.

**Form drag** That portion of a body's *drag* caused by the horizontal component of the overall *pressure distribution*. So, form drag results from higher pressure occurring on the front of a body than on the rear.

**Form drag** is sometimes called *pressure drag*.

**Freestream** That part of the airflow around a body which is far enough away to remain undisturbed by the body's passage. Thus, the freestream velocity will always be equal, although opposite in direction, to the body's velocity.

**Frontal area** Generally taken to be the area of the front view 'silhouette' of a vehicle, but sometimes simplified as width multiplied by height.

**Ground effect** The aerodynamic modification of the airflow beneath a vehicle caused by its close proximity to the ground. All cars operate in ground effect, although not all exploit the effect beneficially.

**Gurney flap** A small right-angled strip attached to the top of the trailing edge of a wing assembly's rearmost element, or to another part of the body, with its upright perpendicular to the upper surface, for the purpose of supplementing aerodynamic downforce.

**Induced drag** That portion of drag caused by the generation of lift (or downforce). Also known as *vortex drag*.

**Laminar flow** Flow in which layers of air adjacent to a body slide smoothly over each other.

**Lift** That component of the *aerodynamic force* which is perpendicular to the direction of a body's travel, directed vertically upwards or downwards.

**Lift coefficient, or  $C_L$**  A dimensionless value that allows the comparison of lift incurred by different-sized and different-shaped bodies. A positive lift coefficient represents *lift*, while a negative lift coefficient represents *downforce*.

**Lift-to-drag ratio** The arithmetic ratio of lift divided by drag, often used as a measure of a vehicle's aerodynamic efficiency.

**Moving ground wind tunnel** A *wind tunnel* equipped with a belt which simulates the ground passing beneath a car. This allows the simulated air speed to be matched to the simulated ground speed, allowing the realistic modelling of airflows adjacent to the ground, and underneath vehicles.

**NACA** National Advisory Committee for Aeronautics, the predecessor of NASA, the USA's aerospace agency. Among other things, the NACA catalogued a vast number of aerofoil profiles.

**NASCAR** National Association for Stock Car Auto Racing Inc., the regulatory body for the USA's premier racing series.

**Pitch** That motion of a vehicle about the transverse, horizontal axis in which the front or rear move up and down relative to the static position.

**Pitch sensitivity** The magnitude of aerodynamic forces can markedly alter as the result of *pitch* movements. This can affect the vehicle's performance and 'feel'.

**Plan area** The area of a vehicle (or a wing) defined by an overhead view 'silhouette'.

**Pressure** Air pressure is all around us, and results from collisions between air molecules and bodies that the air surrounds. When a body is stationary, and there is no air flowing past it, the sum of the pressures on a body balance out. However, when a body moves through the air, the pressures can change and, for example, in the case of an aerofoil, *lift* and *drag* forces occur as the result of changes to *pressure distribution*.

**Pressure coefficient** A dimensionless value which acts as a means of indicating the local *static pressure* at some point of interest around a body, and which is independent of air velocity.

**Pressure distribution** The representation of local pressures at points all over a body moving through the air. The sum of all the pressures felt by a body is the *aerodynamic force*.

**Pressure drag** The same as *form drag*.

**Pressure gradient** As air is accelerated over, say, the forward part of a vehicle, the *dynamic pressure* increases and the *static pressure* reduces (*Bernoulli's Theorem*). A region of falling static pressure constitutes a 'favourable pressure gradient'. Where the airflow starts to slow again, the local static pressure rises again, constituting an 'adverse pressure gradient'.

**Profile drag** The sum of *form*, or *pressure drag* and *viscous*, or *skin friction drag*.

**Rake** The inclination of the underside of a vehicle. A positive rake would generally be thought of as the front being lower than the rear.

**Reynolds Number** A dimensionless value which is proportional to the air speed of a body multiplied by some ‘characteristic length, such as a vehicle’s overall length, or for an aerofoil being studied in isolation, the aerofoil chord dimension. The Reynolds Number is used to indicate scale effects.

**Ride height** Synonymous with ground clearance in this book, the ride height can be taken as the size of the gap between a vehicle underside and the ground.

**Roughness** Describes the variation of, for example, the underside of a vehicle from an ‘average surface’. Thus, a production vehicle with cavities and protrusions has a rough underside, while a panelled-in racecar has a smooth underside.

**Separated flow** A regime in which the flow no longer follows the contours and surfaces of the body it is flowing around.

**Skin friction drag** That portion of drag caused by friction between the air and the surface of a body. In the case of vehicles, it is generally a very small contributor to overall drag. Also known as *viscous drag*.

**Skirt** A device for bridging the gap between a vehicle’s sides and the ground for the purpose of controlling the airflow under the car, and sealing it from the flow outside.

**Slat** Part of a multi-element aerofoil, set just ahead of and below the leading edge of the main element (on a racecar), for the purpose of supplementing aerodynamic downforce.

**Slot** The gap between aerofoil elements, eg between the main element and a *flap*.

**Span** The side-to-side dimension of an aerofoil; its width.

**Splitter** A flat (generally), horizontal, forward-protruding extension to an airdam.

**Spoiler** Any device whose purpose is to ‘spoil’ a fast, low-pressure flow over a vehicle in order to reduce or reverse positive lift.

**Static pressure** Static pressure can be thought of as the ‘pressure energy’ or ‘potential energy’ of a fluid to do work, which in our context is air exerting forces on body surfaces.

**Stagnation point** A point, usually near the front of a moving body, where the air velocity is zero, and the static pressure is high. (The pressure coefficient is 1.0.)

**Strake** A flat plate attached to a vehicle to modify and adjust the airflow.

**Streamline** The mean flow path of an air particle past a moving body.

Streamlines are often depicted graphically as a set of curves around an object defining the flow directions.

**Throat** The narrowest part of a *venturi*.

**Total pressure** The sum of *static pressure* + *dynamic pressure* + any losses that may occur in a system. When an airflow is accelerated around a vehicle its *dynamic pressure* increases and its *static pressure* decreases, but the total pressure remains constant, as long as no losses occur. Losses can however arise, for example where *flow separation* occurs, in which case energy is converted into sound and heat.

**Turbulent flow** Flow in which layers of air adjacent to a body do not slide smoothly over each other, but instead, mix and swirl. The overall average speed of the flow may be the same as in a laminar case, but the streamlines within a turbulent flow are much more complex.

**Turning vanes** Flat or curved plates, usually mounted vertically, whose purpose is to steer and control an airflow.

**Tunnel** A generic name for three-dimensional underbody *venturi* sections, especially when mounted in pairs, one either side of a central chassis/engine/transmission unit.

**Tyre shelf** A flat, horizontal low-mounted plate extending in front of the rear tyres of an open-wheel racecar, sometimes also referred to as *skirt*, and usually an extension to the *underbody*.

**Underbody** General term for the underside of a competition car.

**Upwash** The part of the airflow deflected upwards by an aerofoil. In the case of a downforce inducing aerofoil, the upwash occurs behind the aerofoil.

**Venturi** Strictly, a narrow tube joining two wider sections of tube, whose purpose is to accelerate flow and cause a reduction in pressure. In a competition car context, venturi is used synonymously with *tunnel*.

**Viscosity** Resistance to flow, or to motion through a fluid, and analogous to mechanical friction.

**Viscous drag** The same as *skin friction drag*.

**Vortex** A rotatory motion in a parcel of air.

**Vortex drag** The same as *induced drag*.

**Wake** The disturbed air behind a body moving through the air, where *total pressure* is low. The air within the wake tends to move along with the body.

**Wicker** Another term for a *Gurney flap*.

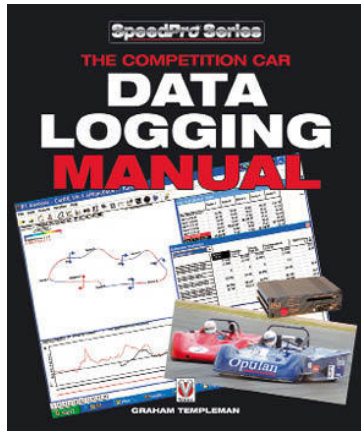
**Wind tunnel** A room or chamber through which a fast airflow is pulled over a car or a scale model of a car, for the purpose of aerodynamic data gathering.

**Wing** In motorsport, a synonym for *aerofoil*. It is a device for creating *downforce* – and displaying sponsors' names!

**Yaw** That motion of a vehicle about a vertical axis where the front or rear may swing out of line, for example during steering.

More great eBooks from Veloce Publishing

**The Competition Car Data Logging Manual**  
Graham Templeman



Aimed at amateur racers, this book will no doubt find its way onto the bookshelves of many professionals because of its no-nonsense direct approach to the use of data logging to improve the performance of both car and driver.

It includes a buying guide to ensure that you buy a system that suits your present and future needs, and deals with installing and calibrating the system to give useful results. Contains practical advice that will minimize problems with the system, and It deals with strategies to extract the maximum amount of useful information to help mechanics, engineers and drivers. Reveals the secrets of the professionals: what is possible and what is worthwhile.

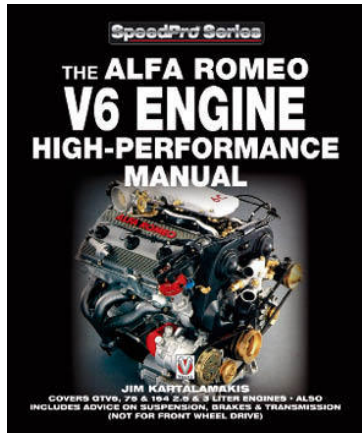
eBook ISBN - 978-1-845846-65-7

Print ISBN - 978-1-845841-62-1

[digital.veloce.co.uk/ebooks/eV4665.html](http://digital.veloce.co.uk/ebooks/eV4665.html)

## Alfa Romeo V6 Engine High-performance Manual

Jim Kartalamakis



Following in the tracks of the author's well-known and hugely successful Alfa DOHC tuning manual, Jim Kartalamakis describes all kinds of useful information and techniques to increase power, performance and reliability of V6 Alfias and their engines.

eBook ISBN - 978-1-845848-57-6  
Print ISBN - 978-1-845840-21-1

[digital.veloce.co.uk/ebooks/eV4857.html](http://digital.veloce.co.uk/ebooks/eV4857.html)